# SOLVENT EXTRACTION OF SOME TRIVALENT LANTHANIDES AND ACTINIDES IN ALKYLDIGLYCOLAMIDES AND THE AGGREGATION AND SPECTROSCOPIC INVESTIGATIONS ON THE EXTRACTED PHASE

*By*

**K. RAMA SWAMI**

**Enrolment No: CHEM02201504004**

**Indira Gandhi Centre for Atomic Research**

**Kalpakkam**

*A thesis submitted to the*

*Board of Studies in Chemical Sciences*

*In partial fulfillment of requirements*

*for the Degree of*

**DOCTOR OF PHILOSOPHY**

*of*

**HOMI BHABHA NATIONAL INSTITUTE**

**December 2020**

# Homi Bhabha National Institute

## Recommendations of the Viva Voce Committee

As members of the Viva Voce Committee, we certify that we have read the dissertation prepared by **K. Rama Swami** entitled **"Solvent extraction of some trivalent lanthanides and actinides in alkyldiglycolamides and the aggregation and spectroscopic investigations on the extracted phase"** and recommend that it may be accepted as fulfilling the thesis requirement for the award of Degree of Doctor of Philosophy.

| | | |
|---|---|---|
| Chairman – Prof. N. Sivaraman | N. Sivaraman | **Date:** 27/04/2021 |
| Guide / Convener – Prof. K.A.Venkatesan | K.A. Venkatesan | **Date:** 27/4/21 |
| Co-guide - Prof. V. Jayaraman | V. Jayaraman | **Date:** 27/04/2021. |
| Examiner - Prof. Siddarth Pandey | Siddharth Pandey | **Date:** 27/4/21 |
| Member 1- Prof. S. Jeyakumar | | **Date:** 27/4/21 |
| Member 2- Prof. R.V. Subba Rao | | **Date:** 27/4/21 |
| Member 3- Prof. A. Suresh | | **Date:** 27/4/2021 |
| Member 4- Prof. K. Ananthasivan | | **Date:** 27/4/21 |

Final approval and acceptance of this thesis is contingent upon the candidate's submission of the final copies of the thesis to HBNI.

I/We hereby certify that I/we have read this thesis prepared under my/our direction and recommend that it may be accepted as fulfilling the thesis requirement.

**Date:** 27/4/21

**Place:** **Kalpakkam**

V. Jayaraman 27/04/2021.
**Dr. V. Jayaraman**
**Co-guide (if any)**

K.A. Venkatesan 27/4/21
**Dr. K.A. Venkatesan**
**Guide**

# STATEMENT BY AUTHOR

This dissertation has been submitted in partial fulfillment of requirements for an advanced degree at Homi Bhabha National Institute (HBNI) and is deposited in the Library to be made available to borrowers under rules of the HBNI.

Brief quotations from this dissertation are allowable without special permission, provided that accurate acknowledgement of source is made. Requests for permission for extended quotation from or reproduction of this manuscript in whole or in part may be granted by the Competent Authority of HBNI when in his or her judgment the proposed use of the material is in the interests of scholarship. In all other instances, however, permission must be obtained from the author.

K. Ramaswamy

K. Rama Swami

# Chapter 8: Conclusions and Future directions

This chapter summarizes the conclusions of the studies reported in various chapters of the thesis. It also discusses about the studies that can be carried out in future.

## 8.1 Aggregation behaviour of tetraalkyl diglycolamides in *n*-paraffins

The self-aggregation behaviour of various symmetrical diglycolamides in different *n*-paraffins and the aggregation behavior of extracted phase containing nitric acid and Nd(III) was probed by DLS, ATR-FTIR spectroscopy. The results were compared with MD simulation studies.

### 8.1.1 Extraction and aggregation behavior of various symmetrical diglycolamides in *n*-paraffins

Initially, The extraction behavior of nitric acid and Nd(III) was studied in a solution of 0.2 M alkyl DGAs in the *n*-DD. The alkyl moiety in DGA was varied from hexyl to dodecyl groups. The dissolution of alkyl DGAs in *n*-DD resulted in the formation of reverse micelles or self-aggregates, with the average aggregate size of 2 nm in *n*-DD medium. The tendency of self-aggregation increased in the order THDGA < TODGA < TDDGA < TDdDGA. In contrast to this, the aggregation tendency of acid or Nd(III) extracted organic phase increased in the order TDdDGA < TDDGA < TODGA < THDGA. The presence of nitric acid and $Nd(NO_3)_3$ in the core of the aggregates increased the polarity of the organic phase and facilitated the formation of newer aggregates and merger of existing aggregates. Since such polar-polar interactions and inter-aggregate interactions were predominant in case of DGAs with smaller alkyl chain length, the aggregate size and their distribution increased in the order TDdDGA < TDDGA < TODGA < THDGA. In addition to polar-polar interactions, the aggregates were also interacting with *n*-DD that led to dispersion and homogenous distribution of aggregates in the *n*-DD medium. In the view of this, the aggregates were soluble in the *n*-DD medium. The dispersive interaction of acid or Nd(III) extracted DGAs increased in the order of THDGA < TODGA < TDDGA < TDdDGA. The increase in the concentration and size of aggregates upon extraction continued until the aggregates were dispersed and distributed homogenously in *n*-DD phase.

The tendency of third phase formation was dependent on the nature of alkyl group attached to the diglycolamide. The DGAs with longer alkyl chain showed lesser tendency to form aggregates and third phase formation, owing to the predominant dispersive interaction of the aggregates with *n*-DD. As a result, the tendency of third phase formation increased in order TDdDGA < TDDGA < TODGA < THDGA. Among the DGAs, TDDGA and TDdDGA did not form the third phase even with concentrated nitric acid and with the solution of Nd(III) ( 7 g/L) in 5 M nitric acid. However, the third phase was observed in TDDGA when the concentration of nitric acid was increased to 8 M at the initial Nd(III) concentration of 7 g/L.

To understand the aggregation behavior of same symmetrical diglycolamide, the extraction behavior of nitric acid in different DGAs dissolved in various *n*-paraffins was studied and subjected organic phase to dynamic light scattering experiments. The *n*-paraffin was varied from *n*-octane to *n*-tetradecane. The extraction of nitric acid into all DGAs in *n*-paraffins was quite similar. The aggregate size and their distribution of DGAs in any diluent increased in the order TDdDGA < TDDGA < TODGA < THDGA, which was also confirmed by MD simulation studies. As a result, the third phase formation tendency of DGAs also increased in order of TDdDGA < TDDGA < TODGA < THDGA. In addition, the aggregates were also interacting with *n*-paraffins in organic phase, which was responsible for the dispersion of aggregates in *n*-paraffin phase. For a particular DGA, the aggregate size and their distribution in organic phase increased in the order *n*-octane < *n*-decane < *n*-dodecane < *n*-tetradecane, which was the order of third phase formation tendency also. To verify the aggregation behavior of DGAs in *n*-paraffins, the MD simulations of different organic phases were performed at the given experimental conditions. It was noted that the cluster size obtained after simulation showed the results in line with those obtained by DLS. It was observed that the cluster size obtained from MD simulation increased with increase in the extraction of nitric acid in the organic phase. The size of cluster was bigger in tetrahexyl diglycolamide and *n*-tetradecane containing systems at a particular nitric acid**.** The pair-correlation calculated from MD simulation showed that the interaction between water and nitric acid in the core of the cluster was more in the DGA with lower alkyl chain and in the *n*-paraffins with longer alkyl chain. Since the dodecyl group attached to the DGA interacted efficiently with *n*-DD, the third phase was not observed for TDdDGA, even after contacting the 0.2 M solution of TDdDGA/*n*-DD with 7 g/L in 10 M.

### 8.1.2. Aggregation behavior in tetra (2-ethylhexyl)diglycolamide (TEHDGA) in *n*-dodecane

The aggregation behaviour of TEHDGA reverse micelles formed during the extraction of neodymium nitrate and nitric acid was investigated by DLS, ATR-FTIR and Raman spectroscopic methods. The extraction of nitric acid and neodymium nitrate in organic phase resulted in the formation of reverse micellar aggregates. The DLS studies showed that a large number of aggregates of different sizes were formed in organic phase. Broadening of amidic transmittance bands in the ATR-FTIR spectra of the organic phase below third phase formation showed that there were several protonated (acid-solvates) species of TEHDGA present in organic phase. Since the core of these reverse micelles was polar nature and they were dispersed in a non-polar *n*-dodecane medium, they tend to exert an inter-aggregate interaction among the various aggregates leading to swelling of aggregates and these interactions increased with increase in the extraction of neodymium, nitric acid and water. However, average aggregate size decreased with increase in the temperature of the system. The amidic carbonyl bonds were strongly affected by the extraction of nitric acid and Nd(III) below third phase formation and etheric bonds were not significantly affected under these conditions.

Third phase formation was observed when 0.2 M TEHDGA/*n*-DD was contacted with 4 M nitric acid, or when the concentration of neodymium nitrate exceeded 6g/L at 1 M nitric acid, 2g/L at 2 M nitric acid and 0.5g/L at 3 M nitric acid. The DLS studies of third phase showed that there was a significant increase in the concentration and size of aggregates upon third phase formation. This observation was supported by a dramatic increase in the intensity of amidic and etheric transmittance bands of TEHDGA upon third phase formation. Even though the average aggregate size was more in third phase as compared to the organic phase before third phase formation, the aggregate distribution was narrow in third phase, possibly due to the merger of aggregates in third phase due to strong inter-aggregate interaction. In addition, the concentration of nitric acid present in the third phase was significantly higher than the 1:1 stoichiometry of TEHDGA and $HNO_3$, and this observation was supported by ATR-FTIR and Raman studies.

In contrast to third phase, the concentration of aggregates, size and distribution of aggregates in diluent phase were lower than that observed for the third phase. The ATR-FTIR studies also confirmed that the aggregates formed upon loading of neodymium and nitric acid in organic phase tends to migrate towards third phase possibly due to inter-aggregate interactions.  As a result, the size and distribution of aggregates in diluent phase was small.

## 8.2 Role of phase modifiers in controlling the third phase formation in TEHDGA+ phase modfier in *n*-dodecane medium

The conclusions on the role of phase modifiers in 0.2 M TEHDGA+ phase modifier/*n*-DD in controlling the third phase formation during the extraction of Nd(III) from nitric acid medium has been detailed in this section.

### 8.2.1 Role of neutral extractants as phase modifiers

To understand the role of neutral extractants as phase modifiers, the extraction behaviour of nitric acid and Nd(III) was studied in a binary solution of 0.2 M TEHDGA + TBP in *n*-dodecane, and 0.2 M TEHDGA+ DHOA in *n*-dodecane. The organic phase obtained after extraction was subjected to DLS measurements. Since LOC and CAC of nitric acid in 1.1 M TBP/*n*-DD and 0.5 M DHOA/*n*-DD were significantly higher than the concentration of nitric acid prevailing HLLW, these reagents were, in fact, capable of performing the role of phase modifiers during the extraction of trivalent actinides. The average size of aggregate and the aggregate distribution in organic phase increased with increase in the concentration of nitric acid in aqueous phase. The average aggregate size for these aggregates increased in the order TBP < DHOA < TEHDGA, which was the increasing order of basicity of these extractants. The critical aggregates size for third phase formation with nitric acid in these ligands increased in the order of TBP < DHOA < TEHDGA. Since the mole ratio of extractant to $HNO_3$ was about 1:1.3 at LOC for all these extractants, the study indicated that strongly basic extractants facilitate the formation of newer aggregates, merge the existing aggregates and occlude large quantity of water molecules in aggregates upon nitric acid extraction in the organic phase.

The study revealed that phase modifiers play multiple roles in minimizing or preventing the third phase formation. The results showed that the formation TEHDGA acid-solvates above

1:1.3 (extractant: $HNO_3$) mole ratio could result in the splitting of the organic phase. However, the formation of TEHDGA acid-solvates can be minimized by adding phase modifiers to the binary solution as the phase modifiers can also coordinate with nitric acid. In fact, the phase modifier served as the protecting agent for the other extractant, which was susceptible to acid-solvates formation and third phase formation. Since, it was necessary to achieve complete acid-solvate formation of both extractants present in the binary solution (with extractant to nitric acid mole ratio above 1:1.3) for third phase formation, the LOC and CAC values increased with increase in the concentration of phase modifier in the binary solution.

The study also showed that the phase modifiers can decrease the average size of aggregates and their distribution in binary solution, below the critical aggregate size for third phase formation, owing to the dispersive nature of these phase modifiers in *n*-dodecane medium. The presence of TBP or DHOA phase modifier in fact diluted the inter-aggregate interaction and minimised the merger of aggregates below the critical aggregate size. Since the dispersive tendency of these phase modifiers was more than TEHDGA in the binary solution, the average aggregate size decreased with increase in the concentration of phase modifier in the binary solution.

### 8.2.2 Role of long-chain alcohols as phase modifiers

The extraction behavior of Nd(III) from nitric acid medium in a solution of 0.2 M TEHDGA in *n*-DD containing long chain aliphatic alcohols such as *n*-octanol, *n*-decanol and isodecanol was studied and the organic phase obtained after extraction was subjected to dynamic light scattering studies to understand the role of alcohols in controlling the third phase formation. The extraction of Nd(III) or $HNO_3$ in all organic phases increased with increase in the initial amount of Nd(III) or nitric acid in aqueous phase, and therefore, the aggregate size obviously increased with increase in the amount of Nd(III) or $HNO_3$ in organic phase. However, the organic phase in the absence of alcohol showed the formation of third phase when the concentration of nitric acid or Nd(III) in organic phase exceeded the LOC values. Addition of alcohol phase modifiers controlled the aggregate size to a much lower value than the limiting aggregate size (LAS) for third phase formation, minimized the aggregate distribution and the aggregate concentration. The polar nature of alcohol seems to interact with polar acid- and metal-solvates by solvation and prevents these solvates undergoing aggregation in organic phase. The investigations also revealed that *n*-decanol was superior to other alcohol phase modifiers.

## 8.3. The aggregation behavior of irradiated solvent

The aggregation behavior of the organic phase containing radiolytically degraded TEHDGA and *n*-DD was studied by dynamic light scattering technique. The organic phases were irradiated from 10 kGy to 500 kGy absorbed dose in a $^{60}$Co gamma irradiator. The radiolytic degradation of TEHDGA and *n*-DD produced a number of degradation products and the aggregation behavior observed in the radiolytically degraded solution, 0.2 M TEHDGA/*n*-DD, was due to the combined effect of all degradation products. The production of polar degradation products minimized the aggregation, and the formation of higher homologs of paraffins enhanced the aggregation. The results revealed the following.

Case 1. The irradiated sample was a solution of 0.2 M TEHDGA dissolved in *n*-dodecane medium. The irradiation of 0.2 M TEHDGA/*n*-DD produced significant amount of radiolytic degradation products resulting from the degradation of TEHDGA due to sensitization effect. The dispersion of aggregates observed in the irradiated solution was attributed predominantly to the formation of smaller homologs of *n*-dodecane and the branched hydrocarbons. Even though the tendency of third phase formation could not be avoided in the unirradiated 0.2 M TEHDGA/*n*-

DD, when contacted with nitric acid solution of concentration 4 M and above, interestingly no third phase formation was observed in the irradiated solution at the absorbed dose of 50 kGy and above, when contacted with 4 M nitric acid, showing the spin-off merit of gamma irradiation.

Case 2. Since TEHDGA was irradiated alone in this case, the radiolytic degradation of TEHDGA due to sensitization effect was absent. Eventually, the overall degradation of TEHDGA was quite lower than those observed in case 1, and the behavior of aggregation in the organic phase containing irradiated TEHDGA in unirradiated *n*-dodecane was similar to those observed in the solution containing unirradiated TEHDGA present in unirrdiated *n*-dodecane. However, the aggregation tendency was marginally lower in the irradiated solution. The aggregate size and their distribution in organic phase decreased with increase of absorbed dose.

Case 3. In this case, the *n*-dodecane was irradiated and mixed with TEHDGA for aggregation studies. In contrast to the above two cases, interestingly, the average size of aggregates formed in organic phase at a particular concentration of nitric acid increased with increase of absorbed dose. This behavior was attributed to the formation of the higher homologs of *n*-paraffins, which seems to control the aggregation behavior of the solution containing 0.2 M unirradiated TEHDGA in irradiated *n*-dodecane.

Case 4. This case involved irradiation of TEHDGA and *n*-dodecane independently to various absorbed dose levels and mixed together to obtain 0.2 M solution of irradiated TEHDGA in irradiated *n*-dodecane for DLS measurements. The studies showed that the average aggregate size and their distribution in organic phase in this case were intermediate between cases 2 and 3 which is applicable at all dose levels and at all nitric acid concentrations.

Case 5. The organic phase composed of 0.19 M extracted nitric acid in 0.2 M TEHDGA/*n*-DD was irradiated to different gamma absorbed dose levels. The aggregate size, aggregate distribution and the intensity of aggregates in the irradiated solution decreased significantly with increase of absorbed dose, in this case. The FTIR analysis of the irradiated organic phase confirmed the presence of strongly polar nitroalkanes, derivatives of alcohol etc., in the irradiated solution that dispersed the aggregates to a significant extent. In view of this, the third phase formation was not observed in the irradiated organic phase at all absorbed dose levels when contacted with 4 M nitric acid.

In addition to nitric acid extraction studies in the irradiated solvent system, the extraction of Nd(III) in organic phase at 1 M nitric acid was studied in irradiated solvent also. The third phase formation in the irradiated 0.2 M TEHDGA/*n*-DD (500 kGy) was observed above 12 g/L of Nd(III) in aqueous phase as compared to 5 g/L in the unirradiated system, showing the unexpected merit of radiolytic degradation of organic phase. Aggregation results revealed that the phase splitting was observed when the average aggregate size reached the value of ~30 nm in both irradiated and unirradiated organic phases. However, the 30 nm aggregate size was achieved in the irradiated and unirradiated systems at 12 g/L and 5 g/L Nd(III) in 1 M nitric acid. Under these conditions only the critical amount of Nd(III) in organic phase (~3.52 g/L) was achieved, above which the organic phase underwent splitting.

When TEHDGA was irradiated alone the sensitization effect was absent. The loading of Nd(III) in the irradiated organic phase decreased in the order of case 3 > case 2 ~ case 4 > case 1, which was also the order of aggregate distribution in organic phase. When *n*-dodecane was irradiated alone and mixed with an unirradiated TEHDGA (i.e. case 3), the loading behaviour of Nd(III) was nearly comparable with the unirradiated organic phase. As a result, the aggregate distribution of case 3 organic phase was comparable with unirradiated 0.2 M TEHDGA/*n*-DD. However, the irradiation of TEHDGA alone (case 2) showed the Nd(III) loading behavior in between the behavior observed for case 1 and case 3 organic phases. The Nd(III) loading in case 4 was similar to case 2, and therefore, their aggregate distribution in organic phases were comparable. Since the radiolytic degradation of TEHDGA in case 2 was lower than that observed in case 1, the aggregate distribution of case 2 organic phase was more than that observed for case 1. In contrast to the assumption of deteriorating effect of gamma radiation on organic phases, the studies showed that the radiolytic degradation of diglycolamide/*n*-dodecane produced polar degradation products, and these polar products benefits the organic phase by preventing the third phase formation.

## 8.4 Effect of pKa of acidic extractants on the extraction of trivalent actinides in combined solvent system containing TEHDGA and acidic extractant

The role of pKa of acidic extractants on the extraction behaviour of Am(III) and Eu(III), and the spectroscopic investigations of the extracted organic phase was reported in this chapter.

### 8.4.1 Effect of $pK_a$ of acidic extractant

The dependence TEHDGA and the $pK_a$ of HDEHP, PC88A and CYANEX-272 on the distribution ratio of Am(III) in the binary solvent system was investigated to understand the role of acidic extractant in the extraction of Am(III) from nitric acid medium. The $pK_a$ value of the acidic extractant played a profound role in enhancing the distribution ratio of Am(III) especially at lower nitric acid. The distribution ratio of Am(III) increased with decrease in the $pK_a$ value of the acidic extractant in the combined solvent system at a particular acidity. Slope analysis of the extraction data revealed the synergic extraction of Am(III) when TEHDGA was mixed with HDEHP and antagonistic effect when TEHDGA was mixed with PC88A and CYANEX-272 at lower acidities. In contrast to this, synergistic extraction of Am(III) was observed at higher acidity irrespective of the $pK_a$ value of the acidic extractant. Among the various solvent formulations investigated 0.1 M TEHDGA+0.25 M HDEHP/*n*-DD provided appreciable separation of Am(III) over Eu(III) from FR-SHLLW by using DTPA and CA.

### 8.4.2 FTIR investigations in the binary solvent system

The extraction behavior of Eu(III) from nitric acid medium was studied in a binary solution of TEHDGA and HA (HDEHP, PC88A and CYANEX-272) present in *n*-DD. The changes in the amidic C=O and etheric C-O stretching bands of TEHDGA and phosphoryl P=O stretching bands of HA were monitored before and after the extraction of Eu(III) from nitric acid medium, and correlated the peak shits observed in the FTIR spectrum to the distribution ratio of Eu(III) as well as to the $pK_a$ value of the acidic extractant. The red shift of amidic carbonyl stretching bands from 1663 $cm^{-1}$ to 1610 $cm^{-1}$ and the blue shift of etheric C-O stretching bands from 1117 $cm^{-1}$ to 1125 $cm^{-1}$ showed the coordination of these oxygen donor ligands with Eu(III) and extraction of Eu(III) from aqueous phase. Similarly, the shift of P=O stretching bands to lower wavenumber region observed only in case of HDEHP/*n*-DD and PC88A/*n*-DD showed that these ligands were strongly involved in the extraction of Eu(III).

At 3 M nitric acid, a binary solution showed a marginal broadening of P=O stretching bands upon Eu(III) extraction when HDEHP and PC88A acted as acidic extractant. The distribution ratio of Eu(III) in the binary solution at 3 M nitric acid increased in the order TEHDGA ~ (TEHDGA + CYANEX-272) < (TEHDGA + PC88A) ~ (TEHDGA + HDEHP). At lower nitric acid concentration, the relative intensity of the amidic C=O stretching bands of TEHDGA at the shifted position (1627 $cm^{-1}$) decreased in the order HDEHP > PC88A > CYANEX-272, when HA acted as co-extractant. Therefore, the extraction of Eu(III) in combined solvent system at lower nitric acid concentration range decreased in the order (TEHDGA + HDEHP) > (TEHDGA + PC88A) > (TEHDGA + CYANEX-272).

### 8.4.3 Effect of pKa of organophosphorus acidic extractants on the aggregation behavior of TEHDGA + phase modifier in *n*-dodecane

The aggregation behavior of the organic phase containing 0.2 M TEHDGA+0.25 M organo phosphorous acid in *n*-DD was investigated by dynamic light scattering technique The added acidic extractant seems to form an adduct with TEHDGA in the order TEHDGA…. CYANEX-272 < TEHDGA…..PC88A < TEHDGA…..HDEHP, which was the decreasing order of the pKa of acidic extractants namely CYNAEX-272 (6.37) < PC88A (4.57) < HDEHP (3.24). In view of the adduct formation, the extraction of nitric acid in organic phase decreased in the order (TEHDGA+CYANEX-272) > (TEHDGA+PC88A) > (TEHDGA+HDEHP). As a result, the reverse micellar aggregates produced in organic phase increased in the order (TEHDGA+HDEHP) < (TEHDGA+PC88A) < (TEHDGA+CYNEX-272) < TEHDGA.

The addition of acidic extractant to TEHDGA/*n*-DD increased the limiting concentration of nitric acid required for organic phase splitting. The limiting aggregate size determined for phase splitting decreased in the order of (TEHDGA+CYANEX-272) > (TEHDGA+PC88A) > (TEHDGA+HDEHP), which is decreasing order of pKa of acidic extractant. The extraction of Nd(III) in the organic phase increased in the order of TEHDGA < (TEHDGA+CYNEX-272) < (TEHDGA+PC88A) < (TEHDGA+HDEHP), but average aggregate size increased in the reverse order (TEHDGA+HDEHP) < (TEHDGA+PC88A) < (TEHDGA+CYNEX-272) < TEHDGA. The acidic extractant with lower pKa minimized the average size of aggregates produced in the binary solution to a larger extent. The addition of HA to TEHDGA favored synergic extraction of Nd(III) from nitric acid medium and liberated the TEHDGA molecules from coordination sphere of Nd(III). Since coordination of TEHDGA with Nd(III) was responsible for aggregation in organic phase, the average aggregate size decreased in the order TEHDGA > (TEHDGA+CYANEX-272) > (TEHDGA+PC88A) > (TEHDGA+HDEHP).

## 8.5 Single-cycle separation of trivalent actinides from nitric acid medium using hydoxyacetamide-acidic extractant systems and aggregation behavior of the binary solutions

The extraction and stripping behaviour of Am(III) and Eu(III) from the organic phase composed of DOHyA-HDEHP or DOHyA- HDEHDGA in *n*-DD was reported in this chapter. In addition, the results on the aggregation of the organic phase obtained after the extraction of nitric acid and Nd(III) ion was also reported.

### 8.5.1 The extraction behavior of Am(III) and Eu (III) in DOHyA-HDEHP solvent system

The extraction behavior of Am(III) and Eu(III) from nitric acid medium was studied in a binary solution composed of 0.2 M DOHyA+0.25 M HDEHP in *n*-DD and the results were compared with those obtained in the individual solvent system. Synergic extraction of Am(III) and Eu(III) was observed in the binary extractant system and the number of molecules of DOHyA and HDEHP involved in the extraction of Am(III) and Eu(III) in the combined solvent decreased (as compared to the individual solvent system) to accommodate to the involvement of the other extractant in the binary solution. The synergic coefficient obtained in the binary solution increased with increase in the concentration of nitric acid reached a maximum at 1 M nitric acid. The synergic participation of both extractants in the binary solution was confirmed by the slope analysis of the extraction data and ATR-FTIR spectroscopy. The extraction behavior of Am(III), lanthanides and other metal ions present in the FR-SHLLW was studied to understand the feasibility of using the combined solvent for single-cycle separation of Am(III) from FR-SHLLW. The results revealed the possibility of such separations with a separation factor of ~10 for Am(III) over Eu(III).

### 8.5.2 The extraction behavior of Am(III) and Eu(III) in DOHyA-HDEHDGA solvent system

The extraction behaviour of Am(III) and Eu(III) was studied in a completely incinerable binary solution of DOHyA + HDEHDGA in *n*-DD to explore the possibility of single-cycle separation of Am(III) from Eu(III) present in 3 M nitric acid medium. Comparing the extraction of Am(III) and Eu(III) in the binary solution with those obtained in the individual extractants, the study revealed that the group extraction of Am(III) and Eu(III) was controlled by DOHyA present in organic phase and the stripping of Am(III) was controlled by the differences in the coordinating ability of HDEHDGA present in organic phase and DTPA present in aqueous phase.

The mechanism of Am(III) and Eu(III) extraction in the binary solution was determined by the slope analysis of the extraction data. Interestingly, synergic extraction of Am(III) and Eu(III) was observed at nitric acid concentrations above 0.5 M, where both the ligands present in organic phase co-ordinate to trivalent metal ion for facilitating the extraction of Am(III) and Eu(III). However, the stoichiometry of the ligand coordinated to Am(III) and Eu(III) was dependent on the aqueous phase nitric acid concentration. Even though HDEHDGA did not extract Am(III) and Eu(III) at nitric acid concentration above 0.5 M, HDEHDGA participated in the extraction of these metal ions when combined with DOHyA in the binary solution. The participation of HDEHDGA in the extraction of Am(III) and Eu(III) decreased, whereas the participation of DOHyA increased with increase in the concentration of nitric acid. In contrast to the synergic extraction of Am(III) and Eu(III) observed at nitric acid concentrations above 0.5 M nitric acid, antagonistic extraction of Am(III) and Eu(III) was observed at lower acidities.

The selective stripping of Am(III) from loaded organic phase was facilitated by the adding DTPA to aqueous phase. A separation factor of ~ 13 and 86 were respectively obtained for the mutual separation of Eu(III) over Am(III) and Nd(III) over Am(III). Even though the separation factor achieved in batch mode was not very high, but it would be quite sufficient for the separation of Am(III) from other lanthanides when a continuous counter current mixer-settler was employed for mutual separations.

### 8.5.3 Aggregation and organic phase splitting behavior in DOHyA-HDEHDGA synergistic system

The ligands, DOHyA and HDEHDGA, undergo reverse micellar aggregation in *n*-dodecane and the self- aggregate size increased in the order DOHyA< DOHyA + HDEHGA < HDEHDGA in *n*-dodecane medium. The extraction of nitric acid in organic phase containing either DOHyA or HDEHDGA or the binary ligands in *n*-dodecane increased with increase in the concentration of nitric acid and the average size of aggregates formed in organic phase at a particular concentration of nitric acid increased in the order DOHyA < DOHyA + HDEHGA << HDEHDGA. As a result, the tendency of third phase formation increased in the same order when the organic phase was contacted with nitric acid. Interestingly, all these ligands in *n*-dodecane resulted in a third phase when the average aggregate size exceeded the limiting value of about 10-15 nm. However, the limiting aggregate size was achieved at different concentrations of nitric acid in aqueous phase for these organic solutions.

Similarly, the extraction of Nd(III) in DOHyA or a binary solution in *n*-dodecane increased with increase in the concentration of Nd(III) and nitric acid in aqueous phase. The average aggregate size and their distribution in organic phase was significantly more in case of binary solution as compared to that observed in DOHyA/*n*-DD. The aggregates formed in binary solution easily exceeded the LAS of 15 nm at 5 M nitric acid solution containing 4 g/L of Nd(III). However, at 1 M and 3 M nitric acid, the aggregate size was much lower than the LAS, even at higher Nd(III) loadings. As a result, the third phase formation was not observed in the binary solution at 1 M and 3 M nitric acid. Moreover, the binary solution did not form third phase when it was contacted with simulated waste containing ~4 g/L of trivalents (lanthanides and actinides) in 3 M nitric acid in addition to other metal ions. In all the cases discussed above, the aggregate size and distribution was much lower in DOHyA as compared to the binary solution. Finally, the binary solution composition 0.2 M DOHyA+0.1 M HDEHDGA/*n*-DD was suitable for the extraction of trivalent metal ions from SHLLW without third phase formation

## 8.6 Scope for future studies

The aggregation behavior of symmetrical diglycolamides in *n*-paraffins during the extraction of nitric acid and Nd(III) ion was studied. The extracted organic phase was probed by using dynamic light scattering, ATR-FTIR and MD simulation studies. All the these studies revealed that the extraction behavior of nitric acid and trivalent metal ion increased with increase in the concentration of nitric acid and metal ion in aqueous phase, which subsequently increased the aggregates size and their distribution in organic phase. In addition, the aggregate size and third phase formation tendency was more in longer alkyl chain diluents and DGAs containing smaller alkyl chain length. These studies can be further investigated by other complementary techniques such as the small angled X-ray scattering (SAXS), small angle neutron scattering, thermodynamic approach, NMR tensiometry and vapor pressure osmometry etc. to understand the other parameters that influences the aggregation behavior of the organic phase. The present study was restricted only to the aggregation and third phase formation behavior of the organic phase containing DGA and *n*-paraffin. The studies can be extended to the aggregation behavior of DGA system present in various polar, aromatic diluents by different spectroscopic techniques.

The aggregation of behavior of TEHDGA in the presence of various phase modifiers was studied using dynamic light scattering and ATR-FTIR spectroscopy. Even though, the neutral extractants such as TBP, DHOA were regarded as inert phase modifiers, they extract significant amount of nitric acid and unwanted metal ions coexisting with trivalent metal ions in high-level liquid waste. As a result, the scrubbing of organic phase was required, before stripping of trivalents, to remove the unwanted metals from organic phase. Moreover, the presence of nitric acid in organic phase increased the number of contacts required for stripping of trivalent metal ions. Therefore, instead of TBP and DHOA, the neutral extractants namely DOHyA etc. can be added to the diglycolamides to understand the behavior of third phase formation and the aggregation behavior in these binary solvent systems. The present study showed that the addition of acidic extractant phase modifiers to the organic phase containing diglycolamides offered dual advantages such as lowering of the aggregate size, prevention of third phase formation and enhancement in the extraction of trivalent metal ions. The aggregation behavior was investigated only by dynamic light scattering studies in the present study. The other advanced spectroscopic methods such as SAXS, SANS, tensiometry, thermodynamic, VPO, MD simulation studies can be employed for the better understanding the aggregation behavior in organic phase.

The effect of gamma radiation on the radiolytic degradation of TEHDGA was studied in the present work. The results revealed that formation of polar degradation products upon irradiation shifted the third phase formation limits to higher concentrations. The aggregate size decreased with increase of the absorbed dose at particular concentration of nitric acid. A similar study can be conducted by irradiating organic phase to α-radiation, since the solvents are proposed for the separation of alpha emitting radionuclides such as Am and Cm from HLLW.

The extraction behavior of metal ions present in FR-SHLLW was studied in the combined solvent formulation composed of TEHDGA-HA, DOHyA-HDEHP and TEHDGA-HDEHDGA. All these studies were conducted in batch mode experiments. Since results were promising, a continuous counter current mixture settler studies can be conducted for the separation of Am(III) from simulated as well as real waste by using TEHDGA-HA, DOHyA-HDEHP and DOHyA - HDEHDGA solvent systems.

The ATR-FTIR spectroscopic studies were conducted for understanding the interaction of metal with ligand in organic phase. Reasonably good information was obtained from these studies. To understand further, advanced spectroscopic techniques such as $^{1}$H , $^{13}$C , $^{31}$P NMR, ESI -MS, EXAFS studies can be employed to obtain more insights into the coordination behavior of metal and ligand in organic phase.

# ABSTRACT

Solvent extraction of trivalent actinides (Am and Cm) from high-level liquid waste (HLLW) and transmutation of them into stable products is a viable option for minimizing the radiotoxicity of HLLW. Diglycolamides (DGAs) are proven candidates for partitioning of trivalent lanthanides and actinides from HLLW. However, the DGAs have several drawbacks such as third phase formation, extraction of unwanted metal ions etc, during the course of solvent extraction. The alkyl group attached to DGAs plays a pivotal role in deciding the extraction of metals and third phase formation behaviour in organic phase. To prevent the third phase formation, significant amount of organic phase modifiers have been added to the organic phase containing DGAs in *n*-DD. However, the exact role of alkyl group attached to DGA and the function of phase modifiers have not been understood, unambiguously. In view of the absence of these vital informations, the solvent extraction behaviour of the trivalent representative ions such as Am(III), Nd(III) and Eu(III) from nitric acid solution was studied into the organic phase composed of (DGA+phase modifier) in *n*-DD and the organic phase obtained after extraction was probed by FTIR, dynamic light scattering and MD simulations etc., to bring out the insights of aggregation and third phase formation. For investigations, the alkyl chain attached to DGA was varied from hexyl to dodecyl moiety, the nature of diluent was varied from octane to tetradecane, the phase modifiers added to DGA/*n*-DD phase were grouped in to neutral ligands such as TBP and DHOA, acidic ligands such as HDEHP (pKa = 3.24), PC88A (pKa = 4.57) and CYANEX-272 (pKa =6.31), and long chain alcohol modifiers. The outcome of these investigations identified the best DGA for modifier-free separation of trivalent metal ions from nitric acid solution representing HLLW, unveiled the role of phase modifiers, mechanism of third phase formation and the best phase modifier for trivalent actinide partitioning. As a spin-off, the study also opened up a new method for partitioning of trivalent actinides in a single processing cycle.

# CONTENTS

## CHAPTER 1: Introduction

## CHAPTER 2: Experimental

## CHAPTER 3: Aggregation behaviour of tetraalkyl diglycolamides in *n*-paraffins medium during the extraction of nitric acid and Nd(III)

**Part I.** Extraction and aggregation behavior of various symmetrical diglycolamides in *n*-paraffins

Part II. Aggregation behavior in tetra (2-ethylhexyl)diglycolamide (TEHDGA) in *n*-dodecane

## CHAPTER 4: Role of phase modifiers in controlling the third phase formation

**Part I.** Role of neutral extractants as phase modifiers in controlling the third phase formation

**Part II.** Role of alcohol phase as modifiers during the extraction of Nd(III) from nitric acid medium in tetra(2-ethylhexyl)diglycolamide in *n*-dodecane

## CHAPTER 5: Effect of gamma irradiation on the aggregation behaviour of tetra (2-ethylhexyl)diglycolamide in *n*-dodecane

## Chapter 6: Effect of pKa on the extraction of trivalent actinides in combined solvent system

phosphorus acid and diglycolamide solvent system

**Part II.** FTIR investigations on the extraction of Eu(III) in diglycolamide-organophosphorous acid binary solvent system

**Part III.** Effect of pKa of organophosphorus acidic extractants on the aggregation behavior of TEHDGA in *n*-dodecane

## CHAPTER 7: Single-cycle separation of minor actinides from nitric acid medium with hydoxyacetamide-acidic extractant solvent system and aggregation behavior in binary solution

**Part I.** The extraction behavior of Am(III) and Eu (III) in DOHyA-HDEHP solvent system

**Part II.** The extraction behavior of Am(III) and Eu(III) in DOHyA-HDEHDGA solvent system

**Part III.** Aggregation and organic phase splitting behavior in DOHyA-HDEHDGA synergistic system

## CHAPTER 8: Summary and conclusions

## List of Figures

# List of Tables

# Chapter 1: Introduction

## 1.1 Nuclear energy

Electricity is required for the welfare of human beings. It plays a vital role in the sustained development of a mankind. The economic growth of the country heavily relies on the demand, supply and consumption of electricity. At present, the electrical energy is produced from various resources such as fossil fuels (70%), natural gas (21.4%), nuclear power (11%), and hydroelectric power (5%) [1]. The use of fossil fuels for the production of electricity releases considerable amount of greenhouse gases, which are identified to be the major factor for global warming and climate changes happening all over the world [2,3]. Moreover, the consumption of these non-renewable fossil fuels for the production of electricity decreases the availability of valuable energy resources in the earth crust [3,4]. Therefore, there is a need to look into the alternative resources that produces electricity without emitting the greenhouse gases. In this context, the production of energy from renewable resources and nuclear reactors have evolved as promising alternatives to fossil fuels [5,6].

Among these resources, the nuclear option for the production of energy received much attention owing to the attractive features such as zero-emission of greenhouse gases, small space, less fuel requirement for the production of energy and breeding of fuel etc [7]. Currently, there are 448 nuclear reactors operating worldwide, 58 reactors are under construction and 158 nuclear reactors are planned in the near future [8]. In India, there are 22 nuclear reactors operating for the production of electricity contributing about 4% of the total electricity generation and it is planned to increase its share to 30 % by the year 2050 [9,10]. The nuclear reactors employ uranium (natural or enriched) oxide and uranium-plutonium mixed oxide as a fuel for the generation of nuclear power. The fissile isotopes $^{235}$U and $^{239}$Pu present in the nuclear fuel undergoes nuclear fission reaction producing nearly 200 MeV of energy per fission. The heat energy liberated during fission reaction is converted into electrical energy and depending upon the type of fuel employed in a reactor, there are several types of nuclear reactors operating across the globe.

## 1.2 Nuclear power programme in India

Homi Jehangir Bhabha is an architect of atomic energy programme in India proposed a three-stage nuclear power programme by considering the limited availability of uranium resources and vast deposits of thorium resources in India, in early 1950. The natural uranium resource available in India is estimated to be ~1,72,000 tons and that of thorium is ~6,50,000 tons, which is the second largest deposit as compared to that available all over the world[11,12]. The aim of the three-stage programme was to maximize the utilization of thorium resources available in India for production of energy. According to the visionary of Homi Bhabha, it was proposed to use natural uranium as a fuel in the first stage of nuclear power programme. Currently, there are 18 pressurized heavy water reactors (PHWR), 2 boiling water reactors (BWR), 2 Voda Voda Energo Reactor (VVER) type nuclear reactors are operating with the power generation of 6780 MWe capacity and six more reactors are under construction, which are likely to generate additional 4,300 MWe. The second stage of the nuclear energy program envisages the deployment of fast breeder reactors (FBRs) that utilizes the fissile plutonium ($^{239}$Pu) produced from first stage for fueling FBRs and the depleted uranium containing $^{238}$U as blanket, for breeding $^{238}$U to $^{239}$Pu [13]. A Fast Breeder Test Reactor (FBTR) was built at Kalpakkam, Tamil Nadu for gaining the operational experience of fast breeder programme and it is operating since 1985 [14]. The India's first commercial fast reactor namely the 500MWe Prototype Fast Breeder Reactor (PFBR) is in the advanced stage of completion. In the second stage, once sufficient nuclear power capacity is built through plutonium-based FBRs, thorium-232 will be introduced as a blanket material to convert the thorium-232 to uranium-233. The third stage of the programme will be using $^{233}$U fueled reactors for producing energy. A 30 kwt reactor, namely KAlpakkam MINI reactor (KAMINI) at kalpakkam, India is the only reactor operating in the world that uses $^{233}$U as fuel [14,15].

### 1.3 Nuclear fuel cycle

The number of processing steps involved in the production of electricity from mining to waste management are collectively known as nuclear fuel cycle. It starts right from mineral exploration, mineral processing, and purification of uranium/thorium, fuel fabrication, reactor operation, spent fuel reprocessing, radioactive waste management and recycling of fissile material [12,16,17]. The steps involved in nuclear fuel cycle are depicted in Figure 1.1. Starting from mining of uranium resources to reactor operation, the different processing steps are called as “front end nuclear fuel cycle” and the remaining steps starting from discharging of the fuel to waste management are called as “back end nuclear fuel cycle”. The fuel discharged after the production of energy is called as “used nuclear fuel (UNF)” or “spent nuclear fuel (SNF)”. It mainly contains unreacted uranium (depleted uranium) and plutonium, along with several fission products formed during fission reaction. In addition, small amount of activation products such as neptunium, americium and curium are also produced in the spent nuclear fuel due to neutron capture reactions of uranium and plutonium [18]. There are two approaches to process the spent nuclear fuel discharged from the reactor. They are once-through fuel cycle (or open fuel cycle) and closed fuel cycle. In the once-through fuel cycle, the spent nuclear fuel is directly disposed as waste in deep geological repositories without any treatment [19]. In closed fuel cycle, the spent nuclear fuel is reprocessed for the recovery of valuable elements such as depleted uranium and plutonium, which can be used as fuel for future reactor operation. Therefore, the closed fuel cycle makes efficient utilization of the fuel resources [12,20].

**Figure 1.1.** Schematic representation of Nuclear fuel cycle[17].

## 1.4 Reprocessing of spent nuclear fuel

Reprocessing of spent nuclear fuel can be carried out in two ways namely, aqueous and non-aqueous reprocessing methods. The non-aqueous reprocessing is the high temperature pyrochemical method preferred for the recovery of metals from metallic fuels. In this method, the irradiated fuel is dissolved in electrolytic medium at high temperatures ($400^{0}$C- $500^{0}$C) and separated into individual components by electrodeposition method [21]. It has certain attractive features such as less number of processing steps, lower volumes of waste generation etc. However, it also has several limitations such as difficultly in handling, lower separation factors, requirement high purity inert atmosphere and high-temperature operation etc. In contrast to this, the aqueous reprocessing involves a solvent extraction process which is easier, continuous and technologically advanced than the non-aqueous process.

Several solvent extraction processes have been proposed for the separation of uranium and plutonium from the spent nuclear fuel. Among them the Plutonium Uranium Recovery by Extraction (PUREX) process has been industrially adopted for reprocessing of spent nuclear fuel all over the world[22]. In PUREX process, the solvent phase composed of tri-*n*-butyl phosphate (TBP) dissolved in *n*-dodecane (*n*-DD) is employed for the separation of uranium and plutonium from the SNF dissolver solution. The PUREX process is carried out in three major steps. They are (i) initial step including decladding of fuel, dissolution, and feed preparation, (ii) solvent extraction step involving the co-extraction of uranium and plutonium by 1.1 M TBP/*n*-DD and partitioning of uranium and plutonium, and (iii) final purification and conversion of uranium and plutonium to their respective oxides[23]. The flow sheet for PUREX process is shown in Figure 1.2.

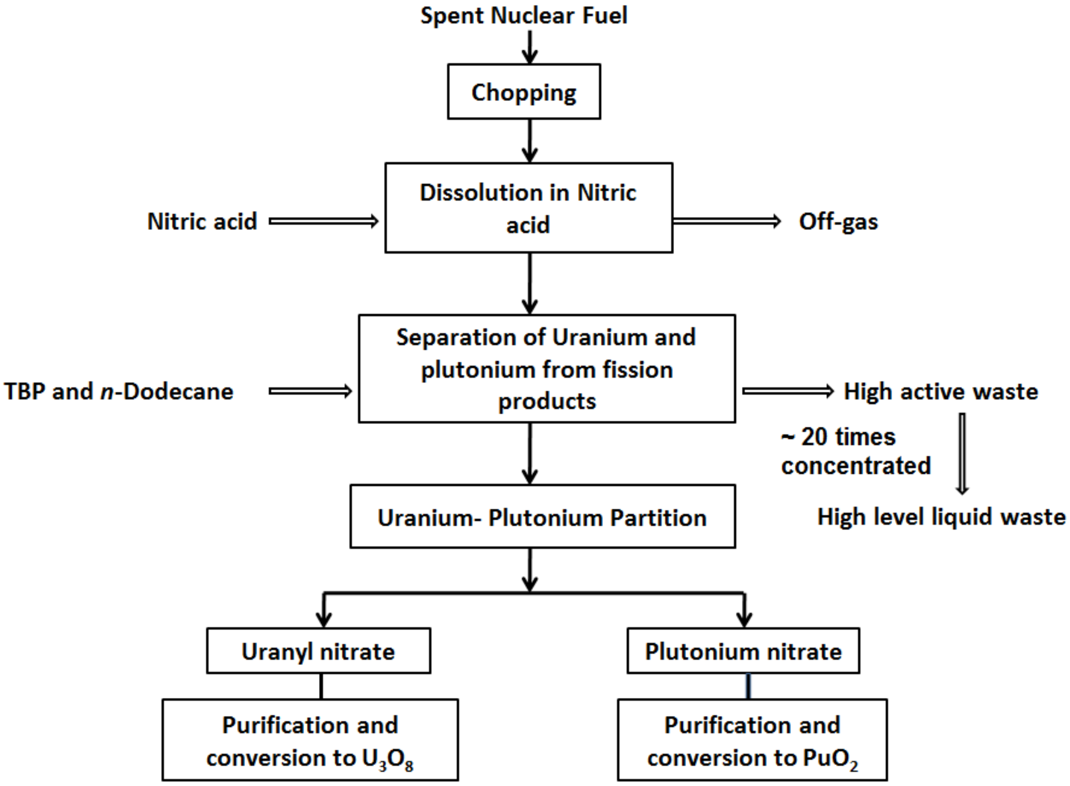

**Figure 1.2.** Flow sheet of PUREX process

### 1.5 Partitioning and Transmutation strategy

The aqueous raffinate rejected after the separation of uranium and plutonium by PUREX process is called as high-level liquid waste (HLLW). The HLLW contains a mixture of fission products, activation products, lanthanides, and corrosion products in 3-4 M nitric acid medium. Many fission products and activation products produced in the spent nuclear fuel are radioactive with half-lives varying from few seconds to several hundred years[24,25]. Therefore, the HLLW poses a long-term risk to the public health and safety of environment. The radiotoxicity of SNF is mainly due to the presence of plutonium, fission products, and minor actinides. Once the uranium and plutonium are removed by reprocessing, the long-term radiotoxicity of the remaining HLLW is essentially due to activation products of heavier actinides and fission products. The fission products such as cesium and strontium ($^{137}$Cs, $t_{1/2}$= 30.2 yrs, $^{90}$Sr, $t_{1/2}$= 28.8 yrs) are beta gamma emitting that radionuclides requires few hundred of years for the decay. The other fission products present in the HLLW have long half-lives and therefore they are regarded as less radiotoxic[26]. In addition, the long-term radiotoxicity of HLLW is mainly due to the small fraction of long-lived actinides present in HLLW. They are $^{241}$Am ($t_{1/2}$ = 433 yrs), $^{243}$Am ($t_{1/2}$ = 7380 yrs), $^{245}$Cm ($t_{1/2}$ = 8500 yrs) and $^{237}$Np ($t_{1/2}$ = $2.14*10^6$yrs). These radionuclides are known as minor actinides owing to the low level of concentration present in HLLW, however, they contribute maximum to the total alpha activity. The radiotoxicity of HLLW decays to near background level only after$10^5$-$10^6$ years in the presence of these minor actinides[27].

At present, immobilization of HLLW into a suitable ceramic or glass matrix, followed by the deposition in deep geological repositories is being practiced for the management of HLLW[28]. However, it demands the long-term surveillance due to the presence of these minor actinides owing to the long half-live, which makes the current disposal option very expensive. To resolve this issue, the partitioning and transmutation (P&T) strategy has been proposed for the management of HLLW, which envisages the selective separation of minor actinides from HLLW followed by transmutation of them into stable and short lived products. The transmutation of minor actinides can be accomplished in fast reactors or in acceleration driven system (ADS) [26,29]. After partitioning of minor actinides, the radiotoxicity of HLLW is mainly contributed by fission products, which decays to the background level within ~ 300 years. Therefore, the remaining waste can be vitrified and buried in subsurface repositories at a much-reduced risk and at economical cost. If required, these fission products ($^{137}$Cs and $^{90}$Sr) can also be separated from HLLW and transmuted them into stable products. Several countries in the world have proposed to adopt P&T strategy to reduce the radiotoxicity of the waste[30]. Figure 1.3 shows advantages of P&T strategy in minimizing the radiotoxicity of HLLW. It is interesting to note that the average radiotoxicity of HLLW can be dramatically reduced to few hundred years, by partitioning of minor actinides and transmutation. Therefore, P&T is an inevitable option for the safe management of HLLW. Table 1.1 explains the natural half-lives of actinides before and after transmutation.

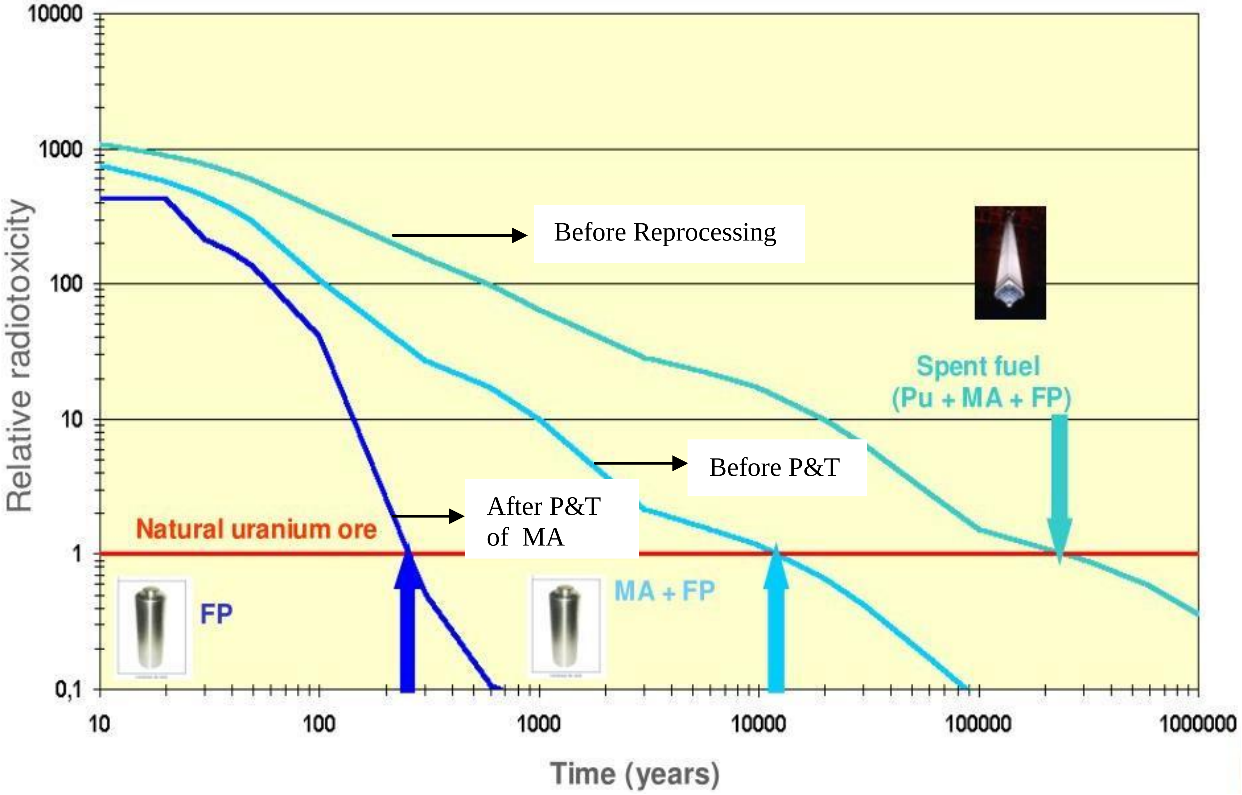

**Figure 1.3.** The pictorial representation of advantage of partitioning and transmutation for reprocessing of spent nuclear fuel [31].

**Table 1.1.** Half lives (Y) of actinides present in SNF due to natural decay and after transmutation with fast neutrons. The fission half-life was calculated using the relation $\tau_{½} = 2/(\sigma, \Phi)$ where $\sigma$ and $\Phi$ are the fission cross section and the neutron flux respectively. The neutron flux was assumed to be $5 \times 10^{15}$ $cm^{-2}$ $s^{-1}$[32].

| **Actinide** | **$t_{1/2}$ (natural decay) in years** | **$\tau_{1/2}$ (transmutation) in years** |
|---|---|---|
| $^{237}Np$ | $2.14 \times 10^6$ | 2.46 |
| $^{238}Pu$ | 88 | 1.61 |
| $^{239}Pu$ | $2 \times 10^4$ | 1.76 |
| $^{240}Pu$ | $6 \times 10^3$ | 2.35 |
| $^{241}Pu$ | 14 | 1.95 |
| $^{242}Pu$ | $4 \times 10^5$ | 2.83 |
| $^{241}Am$ | 433 | 2.40 |
| $^{242m}Am$ | 152 | 1.72 |
| $^{243}Am$ | $7 \times 10^3$ | 2.89 |
| $^{242}Cm$ | 0.44 | 1.93 |
| $^{243}Cm$ | 30 | 1.46 |
| $^{244}Cm$ | 18 | 1.97 |
| $^{245}Cm$ | $8 \times 10^3$ | 1.60 |

## 1.6 Partitioning of minor actinides from HLLW

The success of partitioning and transmutation strategy depends on the efficient separation of minor actinides from HLLW. The Am and Cm present in HLLW generally exist in +3 oxidation state. But neptunium exists in various oxidation states from +4 to +6. In advanced PUREX flow-sheets, the neptunium present in the dissolver solution is routed along with uranium and plutonium by adding suitable processing steps [33]. Therefore, the HLLW generated after reprocessing contain trivalent actinides such as americium and curium, which are the main contributors for the long-term radiotoxicity of HLLW, in addition of fission products in 3-4 M nitric acid medium. The separation of trivalent actinides from HLLW is usually carried out by a solvent extraction process [34]. However, it involves huge challenges. This is essentially due to the similarity in the solution and extraction chemistry of both trivalent actinides and lanthanides. In view of this, the trivalent lanthanides along with actinides are co-extracted together into the organic phase during solvent extraction. Since lanthanide elements are efficient neutron absorbers, transmutation of trivalent actinides in the presence of lanthanides is tedious or difficult [30,35]. Therefore, it is essential to separate lanthanide from actinides prior to transmutation.

The choice of ligands/extractants employed for the separation of minor actinides in a solvent extraction process depends up on a number of factors involving physical, chemical, and economic aspects. The key points for choosing the ligands for the extraction of metal ions including trivalent metal ions are shown below [36]:

- The extractant should have reasonable distribution ratios for the extraction of target metal from nitric acid medium.
- It should have very less aqueous solubility and high solubility in organic diluent such as *n*-dodecane
- Good selectivity on the trivalent metal ions than others.
- Ease of stripping of metal ions after extraction at moderate acidic solutions
- It should have low toxicity, low volatility, non- flammability and incinerability.
- Ease of synthesis and availability
- Optimum viscosity and interfacial tension of the solutions for fast phase disengagement.
- It should have good hydrolytic and radiolytic stability.

The literature survey on the separation of trivalent actinides from nitric acid solution representing HLLW, indicates that these trivalent metal ions (Ln$^{+3}$ and An$^{+3}$) require a bidentate or tridendate type ligands for efficient extraction. In this context, several methods and ligands have been developed and studied for the extraction of lanthanides and actinides from nitric acid solution for the past 4-5 decades. The structures of extractants employed for trivalent actinide separation reported in the literature, are shown in Figure 1.4. The experimental and demonstration studies related to these ligands can be found in references [29,30,37–43]. Among the various ligands, the alkyl diglycolamide derivatives are regarded as promising extractants for trivalent actinide separation from nitric acid solution and HLLW.

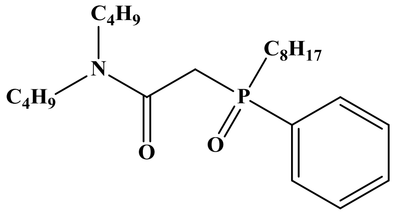

**Octyl(phenyl)-diisobutyl carbamoylmethylphosphine oxide (CMPO)**

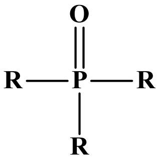

**R= Hexyl or octyl**

**TRPO**

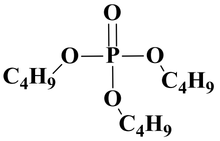

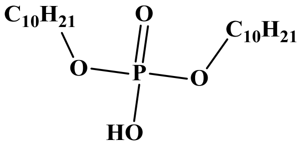

**Tributylphosphate (TBP) Di-isodecyl phosphoric acid (DIDPA)**

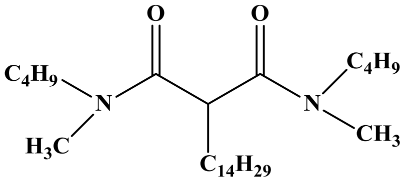

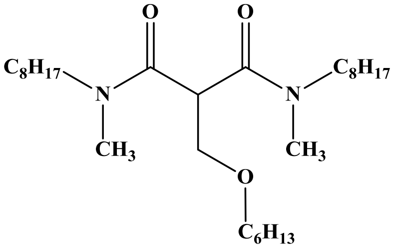

**Dibutyl-dimethyltetradecylmalonamide (DBDMTDMA) Dimethy-dioctylhexylethoxymalonamide (DMDOHEMA)**

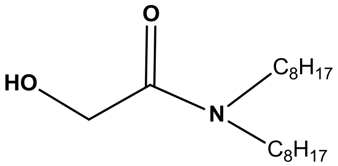

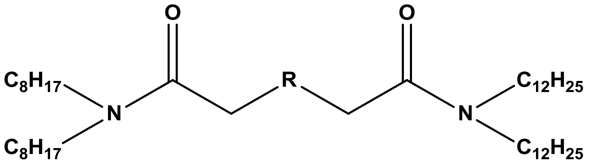

**N,N-dioctylhydroxyacetamide (DOHyA) Dioctyl-ditetradecyldiglycolamide ($D^3$DODGA)**

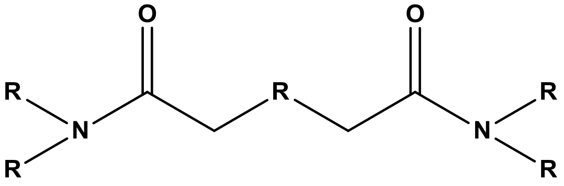

**Symmetrical Diglycolamides**

R=$C_6H_{13}$ = THDGA
R=$C_8H_{17}$ = TODGA
R=$C_8H_{17}$ = TEHDGA (2-ethyl hexyl)
R=$C_{10}H_{21}$ = TDDGA
R=$C_{12}H_{25}$ =TDdDGA

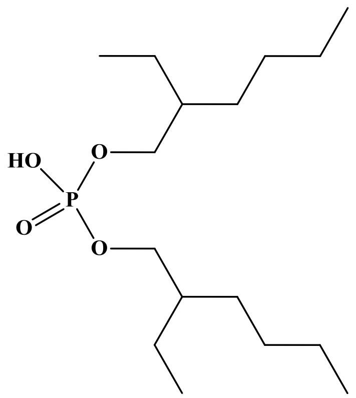

**Bis(2-ethylhexyl)phosphoric acid (HDEHP)**

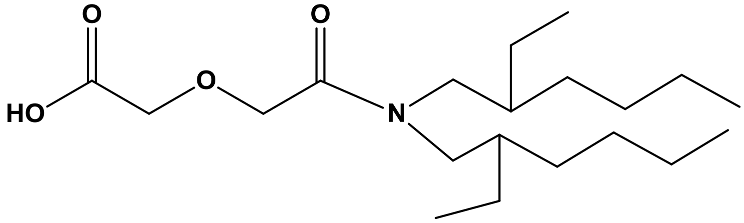

**Bis(2-ethylhexyl)diglycolamic acid (HDEHDGA)**

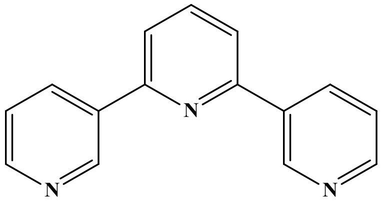

**Terpyridine (terpy)**

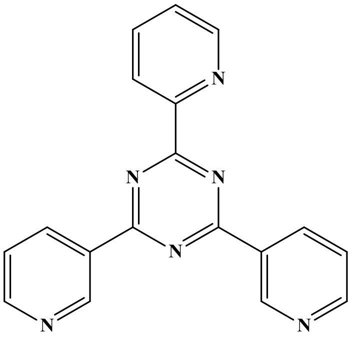

**2,4,6-tripyridyl-1,3,5-triazine (TPTZ)**

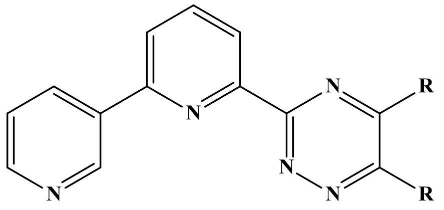

**6-(1,2,4-triazinyl)-2,2'-bipyridine (TiBpy)**

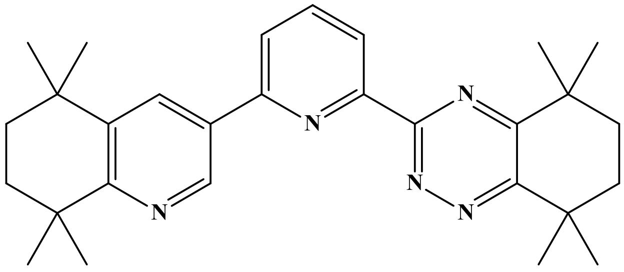

**2,6-bis-(5,5,8,8-tetramethyl-5,6,7,8-tetrahydro-benzo-1,2,4-triazine-3-yl)pyridine (CyMe$_4$-BTP)**

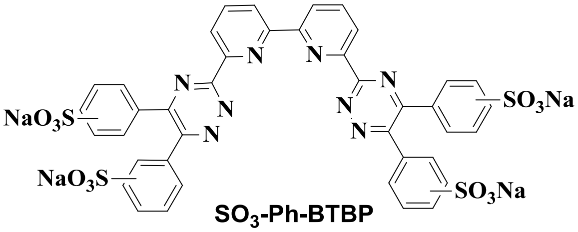

**SO$_3$-Ph-BTBP**

**Figure 1.4.** The structure of various extractants employed for partitioning of minor actinides.

### 1.6.1 Diglycolamides

Alkyl diglycolamides are introduced by the researchers at Japan Energy Research Institute (JAERI) in late 1990's [44–49]. Diglycolamides (DGAs) contain a couple of amidic carbonyl group and an etheric group as shown in Figure 1.4 for coordination with metal ions. Sasaki *et al.,* extensively studied the extraction behavior of trivalent metal ions in various diglycolamides and their physicochemical properties. It was observed that the alkyl chain attached to the amidic nitrogen atom played a crucial role in the determining the solubility of DGAs in non-polar diluents (e.g. *n*-dodecane) and distribution ratio of trivalents in organic phase [45,46,50,51]. Among the DGAs, tetraoctyldiglycolamide (TODGA) was found to be the most promising extractant with respect to the extraction of trivalent metal ions. However, TODGA in *n*-dodecane diluent undergoes organic phase splitting when contacted with HLLW or with trivalent metal ions present in nitric acid solution [29,52,53]. For instance, the solvent system composed of 0.1 M TODGA/*n*-DD undergoes organic phase splitting (i.e third phase formation, to be discussed below) when the Nd(III) concentration reaches 8 mM in 3 M nitric acid medium. Therefore, the solvent phase (TODGA/*n*-DD) requires organic phase modifier for maneuvering the organic phase splitting during the extraction of these metal ions from HLLW. In this context, the phase modifiers such as TBP, DHOA or long chain alcohol have been added to TODGA/*n*-dodecane for preventing the organic phase splitting [54,55] . The TODGA solvent containing different phase modifiers have been employed in many of the demonstration runs with real waste in Germany, Japan, USA and India [29,48,56–59]. Apart from organic phase splitting, the co-extraction of troublesome fission products such as Zr(IV), Pd(II), Mo(VI) and Ru(III) from HLLW into the organic phase is also another drawback of TODGA. In view of this, the branched isomer of TODGA, namely *N,N,N’,N’*-tetra-2-ethylhexyldiglycolamide (TEHDGA) was developed and studied for the extraction of trivalent metal ions from HLLW. It showed a better selectivity towards trivalent metal ions over TODGA[50,60–62]. Large-scale studies on the extraction of various metal ions from real radioactive waste solution using TEHDGA have been reported at BARC, India [63]. However, both these symmetrical diglycolamdies (the alkyl group attach to both sides of DGA are same) showed several drawbacks such as organic phase splitting and secondary waste generation [64].

To overcome the limitations of symmetrical diglycolamides, unsymmetrical diglycolamides (UDGAs) have been developed and reported for the extraction of trivalent metal ions from nitric acid solution. In UDGAs, the alkyl groups attached to the two amidic nitrogen atoms are different. The UDGAs showed good distribution ratios for the extraction trivalent metal ions and higher third phase limits (organic phase splitting) as compared to symmetrical diglycolamides[64,65]. In this context, didodecyl-dioctyl-diglycolamide ($D^3$DODGA) was identified as a promising candidate for the separation of trivalent actinides from HLLW. This diglycolamide does not require organic phase modifier for the separation of trivalent actinides [65–67]. In addition to this, several other kinds of diglycolamides were synthesized and studied the extraction studies of trivalent metal ions from nitric acid solution by researchers across the world [43]. In the recent past, *N*,*N*-dialkyl hydroxy acetamides have been developed and investigated for the extraction of trivalent lanthanides and actinides. The hydroxyacetamide derivatives have several advantages such as less nitric acid extraction, higher selectivity towards trivalents, no third phase formation etc [68–70]. Prathibha *et al.* demonstrated the separation of Am(III) and Eu(III) from Fast reactor (FR) - simulated high-level liquid waste (SHLLW) using octylhydroxyacetamide/*n*-DD in a 20 stage mixer-settler[71].

### 1.7 Organic phase splitting or Third phase formation during liquid-liquid extraction

Third phase formation is a matter of concern during the solvent extraction of trivalent lanthanides and actinides from HLLW. It is the splitting of organic phase into two phases during the course of solvent extraction. The lighter phase is known as the “diluent rich” phase and the heavier phase is called as “third phase”. The third phase is a dense viscous organic phase, rich in metal-solvates, acid-solvates and extractant. The diluent-rich phase is less dense than third phase with little extractant, and metal ion. The third phase is sandwiched between the aqueous bottom and diluent rich phase. The third phase can be dissolved by diluting the concentration of metal or nitric acid present in aqueous or organic phase. The concentration of metal ion in organic phase obtained after the disappearance of third phase is known as limiting organic phase concentration (LOC) and corresponding metal ion or acid concentration in aqueous phase is known as critical aqueous phase concentration (CAC)[72,73].

Third phase formation leads to large variations in the physicochemical properties of the solvent phase such as changes in density, poor phase disengagement accompanied by flooding etc. during industrial scale solvent extraction procedure. Moreover, the accumulation of fissile elements in the third phase causes criticality concerns[74–77]. Various parameters such as concentration of metal ion and acid, nature of the diluent, phase modifier, and extractant, and temperature can influence the third phase formation[36,72,73,78,79]. Several reports and review articles are available in the literature regarding the third phase formation behavior in different solvent systems [36,71–77]. The third phase formation phenomenon was successfully explained by the combination of coordination chemistry and colloidal chemistry (reverse micellar approach)[80,81] .

### 1.7.1 The colloidal approach for the third phase formation

In reverse miceller approach, the extractants or ligands employed for the extraction of metal ions are considered as amphiphiles, in which the polar part of the ligand coordinates with the target metal ion and the non-polar group interacts with the non-polar diluent (especially n-DD) for the solubilization of ligand in organic phase [82]. The pioneering work on the reverse micellar aggregation behavior of TBP in *n*-DD was studied by Osseo-Asare in 1991. It was reported that TBP undergoes self-aggregation in *n*-DD and the quantity of reverse micellar aggregates increases upon water, acid, and metal ion extraction in *n*-DD phase[80,83]. Erlinger *et al.* proposed that the occurrence of third phase formation was due to the extensive aggregation of reverse micelles in organic phase arising from the attractive interactions among the reverse micelles, as predicted by Baxter-hard sphere model[84,85].

When the amphiphilic ligands is dissolved in *n*-dodecane, they tend to undergo reverse micellar self-aggregation in *n*-dodecane due to polar-polar interaction between the polar groups of the ligand. In addition, the reverse micelles also undergo Van der Waals interactions with *n*-dodecane and facilitate the dispersion of reverse micellar aggregates in *n*-dodecane [83,86,87]. Any factor that increases the polar-polar interactions facilitates aggregation and any factor that increase Van der Waals interaction facilitates dispersion of ligands in *n*-dodecane medium. As a result of polar-polar interaction, a large number of aggregates of different sizes are formed in organic phase and they undergo distribution in organic phase [88–90]. For instance, the extraction of nitric acid or metal ion in organic phase results in the coordination of the metal ion with ligand or protonation of ligand. These protonated (acid-solvates) and coordinated metal-solvates impart more polarity to the organic phase. As the extraction of nitric acid and metal ion into organic phase increases, a large number of new aggregates are formed in the organic phase. In addition, the interaction between the aggregates results in the merger of aggregates in organic phase [70,86,91–93]. It should be noted that the aggregates distributed in organic phase also interact with *n*-dodecane and undergo dispersion in organic medium. This kind of dispersion of aggregates continues until the interaction between the aggregates and *n*-dodecane is stronger than the polar-polar interaction among the aggregates. However, at a particular loading of metal ion or acid in the organic phase, the polar-polar interactions among the aggregates become much stronger than the dispersive interactions. Under such conditions, the majority of the aggregates distributed in organic phase merge together and undergo demixing or disengagement from bulk of the organic diluent phase. The event of demixing of polar aggregates from the bulk of the organic phase is known as third phase formation. The aggregate rich phase is known as "third phase" and the diluent rich phase is known as "diluent phase"[70,88,94].

Several researchers have carried out extensive studies on the aggregation behavior of various ligands in *n*-DD phase, and probed the aggregation by various different experimental methods. The techniques such as interfacial tensiometry and conductivity have been employed for determining the critical micellar concentration (CMC) in organic phase. In addition, Small Angle X-ray and Neutron Scattering (SAXS and SANS), vapour pressure osmometry (VPO), dynamic light scattering (DLS), nuclear magnetic resonance (NMR) spectroscopy, mass spectrometry etc. techniques have also been used to probe third phase formation [77-94] . These spectroscopic techniques have been successfully used for determining the size of reverse micellar aggregates and their interaction parameters. Molecular dynamic simulations, DFT calculations and FT-IR spectroscopy techniques have been employed to bring out the insights of aggregation in various extractant systems used in nuclear fuel cycle [95–100].

## 1.8 Mutual separation of lanthanides and actinides

After the group separation of trivalent lanthanides and actinides, the mutual separation of lanthanides and actinides is necessary for transmutation of actinides. Since lanthanides act as neutron poisons, the presence of lanthanides in actinide fraction dramatically reduces the efficiency of transmutation of actinides. However, the mutual separation of trivalent actinides and lanthanides is a challenging job, owing to the close similarity in the chemical behavior of the lanthanides and actinides. Both lanthanides and actinides exist in trivalent oxidation state in nitric acid solution. The methods explored for the mutual separation of lanthanides and actinides are based on the small differences in the chemical binding property of lanthanides and actinides. According to Pearson's HSAB principle, the trivalent actinides are classified as soft acids as compared to lanthanides, due to the covalent bond forming tendency of spatially extended 5f-orbitals of actinides[101,102]. However, the 4f-orbitals of lanthanides are buried inside and shielded by the outermost 5d–orbital. As a result, the 4f-orbitals do not take part in bond formation with ligands during solvent extraction, and they prefer to exhibit ionic interaction with ligands as compared to trivalent actinides. Trivalent actinides form strong complexes with nitrogen based soft donor ligands, and lanthanides with oxygen donor ligands. Based on these preferences, several methods have been reported in literature on the mutual separation of lanthanide and actinides. Among the various methods, the most efficient method is known as Trivalent Actinide Lanthanide Separation with Phosphorus-Reagent Extraction from Aqueous Komplexes (TALSPEAK) process. In this method the An(III) selective diethylenetriaminepentaaceticacid (DTPA) with lactate buffer has been added to aqueous phase to hold An(III) in aqueous phase, while allowing the extraction of lanthanides in organic phase containing oxygen donor ligand namely the bis-(2-ethylhexyl)phosphoric acid (HDEHP)[103]. However, maintaining the pH of aqueous phase is very difficult during this process and it also takes more time for phase disengagement.

In order to overcome the problems encountered in TALSPEAK process, researchers have developed a reverse TALSPEAK process, in which both trivalent actinides and lanthanides are co-extracted from dilute nitric acid solution into the HDEHP phase, and the trivalent actinides alone from organic phase is stripped to the aqueous phase using DTPA and lactic acid-citric acid solution leaving the lanthanides in organic phase. The lanthanides are then recovered at higher nitric acid concentration. The advanced TALSPEAK process developed at Argonne national laboratory, USA, uses bis(2-ethylhexyl) phosphonic acid (HEH(EHP) or PC88A) ligand for the extraction of Ln(III) and *N*-(2-hydroxyethyl)-ethylenediamine-*N*,*N'*,*N'*-triacetic acid (HEDTA) for holding An(III) in aqueous phase. The method of Ln-An separation was demonstrated in a 24 stage counter current centrifugal contactor with a decontamination factor of >1000. In recent past, Suneesh *et al.,* developed a completely incinerable ligand namely diglycolamic acid for the mutual separation of lanthanide and actinides. Bis(2-ethylhexyl)diglycolamic acid (HDEHDGA) showed superior selectivity for Eu(III) over Am(III) under stripping conditions [104,105].

### 1.9 Single-cycle separation of minor actinides

The two-cycle process discussed above, for partitioning of trivalent actinides showed some drawbacks such as the generation of large volume of aqueous and organic waste, third phase formation, hydrodynamic problems etc. To minimize these problems, the processes based on single-cycle separation of trivalent actinides from HLLW have drawn the attention of researchers across the world. This can be achieved by a couple of approaches. The first approach is the direct separation of trivalent metal ions from HLLW using actinide selective ligands. Various methods such as Selective ActiNide Extraction (SANEX) such as r-SANEX, i-SANEX, and 1-cycle SANEX concept have been developed for direct separation of actinides[106–108]. The second approach envisages the separation of trivalent metal ions using combination of neutral and acidic extractants. In this method, the trivalent actinides and lanthanides are co-extracted together from HLLW in to the organic phase followed by selective stripping of actinides alone from the loaded organic phase. In this approach, several methods such as TRUSPEAK, PALADIN, and ALSEP have been reported [109–114]. The schematic illustration of single-cycle and two-cycle process is shown in Figure 1.5. The various methods proposed for single cycle separation are described in references [106-114].

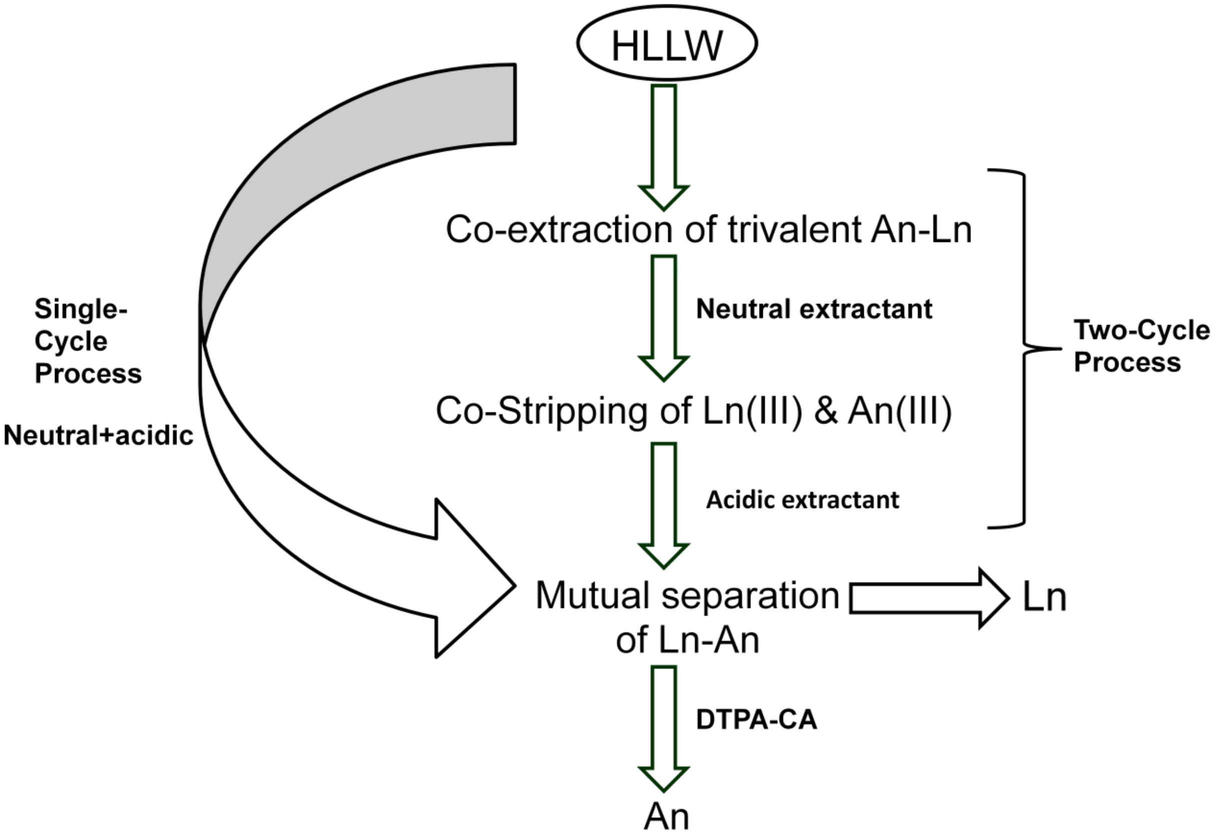

**Figure 1.5.** Schematic representation of two cycle and single cycle process.

## 1.10 Radiolytic stability

The radiolytic stability of the solvent system is an important parameter in deciding the utility of solvent, when proposed for separation of trivalent actinides from HLLW. During the solvent extraction procedure, the solvent phase is exposed to the high energitic α, β and γ radiations[115,116]. Due to the absorption of radiation energy by the solvent phase, the chemical bonds present in the solvent system undergo cleavage and produces a number of chemically active species such as free radicals and ions. These free radical or ions recombines or reacts with other molecules generating a number of chemical products, collectively called as radiolytic degradation products. On an average, the radiation dose felt by the organic solvent during the treatment of HLLW is about 100 kGy for the HLLW arising from thermal reactor fuel reprocessing and 250kGy for fast reactor fuel reprocessing[61,117,118].

The radiolytic degradation of the system is usually expressed in terms of G-value, which is the number of molecules produced or degraded by the absorption of 100 eV of energy [115]. The radiolytic degradation of solvent decreases the distribution ratio of metal ions, and alters in physical properties such as viscosity and density of the solvent system. In addition, the degradation also decreases the selectivity and recovery of target metal ions[119–121]. Therefore, it is essential that the solvent system proposed for the separation of minor actinides should have good radiolytic stability.

## 1.11 Scope of the present work

The literature survey showed that the diglycolamides (DGAs) are regarded as promising reagents for the separation of trivalent actinides and lanthanides from nitric acid solution. The alkyl group attached to DGA plays a pivotal role in deciding the extraction and third phase formation behavior of trivalents in organic phase. However, the exact role of the alkyl group attached to DGA in deciding the third phase formation is not known, unambiguously. To prevent the undesirable third phase formation during the course of solvent extraction, organic phase modifiers have been usually added to the organic solvent phase. For instance, the phase modifiers such as tri-*n*-butyl phosphate (TBP), or dihexyloctanamide (DHOA), or long chain alcohols have been added as phase modifiers during the extraction of trivalent actinides in a solution of tetra octyl diglycolamide in *n*-dodecane. However, the knowledge on how the addition of phase modifiers controls the aggregation and third phase formation is very limited. Moreover, the behavior of reverse micellar aggregation of the radiolytically degraded diglycolamides in *n*-DD is not known so far, even though the effect of degradation products on the solvent extraction of actinides is well documented.

A combination of neutral and acidic extractants has been proposed for the single-cycle separation of trivalent actinides from HLLW. The neutral extractant in the binary solution governs the extraction of lanthanides and actinides as a group, and the acidic extractant controls the stripping of actinides alone from the organic phase. For efficient separation of lanthanides and actinides, it is necessary to understand the role of acidic extractant and its pKa value on the extraction and stripping behaviour of lanthanides and actinides from the binary solvent system. Apart from this, the behavior of acidic extractants in controlling the third phase formation and the mechanism of aggregation in the presence of acidic extractant has not been reported so far.

In view of the absence of vital information on the issues discussed above, it is proposed to address them in the present thesis. Therefore, the objective of the thesis is many fold and they are highlighted in below.

1. The role of alkyl chain length attached to DGA (varied from hexyl to dodecyl derivatives) in determining the tendency of aggregation and third phase formation of alkyl diglycolamides in *n*-DD was investigated by dynamic light scattering technique. The aggregation behavior of a particular alkyl diglycolamide in different *n*-paraffins was also investigated. The extraction behavior of nitric acid in various organic phases was studied and the organic phase obtained after extraction was subjected to dynamic light scattering and MD simulations to understand the aggregation and organic phase splitting behaviour.
2. To examine the role of phase modifiers, the solvent extraction of Nd(III) from nitric acid medium was carried out in a solution of tetra(2-ethylhexyl)diglycolamide (TEHDGA) dissolved in *n*-dodecane in the presence of TBP, DHOA and long chain alcohols. The

organic phase obtained after extraction was again subjected to dynamic light scattering studies to bring out the role of these modifiers in minimizing the third phase formation.

3. Similarly, the role of degradation products on the aggregation behavior of organic phase containing tetra(2-ethylhexyl) diglycolamide and *n*-dodecane was studied by irradiating the organic liquid to various absorbed dose levels in a gamma irradiation chamber. The irradiated organic phases were subjected to solvent extraction and the organic phase obtained after the extraction of nitric acid and Nd(III) was investigated by dynamic light scattering. The results were compared with those obtained for the un-irradiated organic phases.
4. Towards the development of single-cycle separations, the effect of pKa of the acidic extractant in the binary solution was investigated by studying the extraction behavior of Am(III) in a solution of tetra(2-ethylhexyl)diglycolamide and acidic extractant (HA) present in *n*-dodecane. The acidic extractants investigated were bis(2-ethylhexyl)phosphoric acid (HDEHP), bis(2-ethylhexyl)phosphonic acid (PC88A) and bis(2,4,4-trimethylpentyl)phosphinic acid (CYANEX-272) and whose pKa values decreased in the order CYANEX-272 (6.37) > PC88A (4.51) > HDEHP (3.24). The extraction results obtained in the combined solvent system was further probed by ATR-FTIR spectroscopy to understand the interactions between metal ion and solvent system. Moreover, the organic phase was probed by dynamic light scattering to examine the reverse micellar aggregation in the binary solution.
5. Similarly, a binary solution composed of *N*,*N*-2-dioctylhydroxyacetamide (DOHyA) and HDEHP or bis(2-ethylhexyl)diglycolamic acid (HDEHDGA) was evaluated for the mutual separation of Am(III) from Eu(III) containing nitric acid solution for the development of a

method for single-cycle separation. The feasibility of selective stripping of Am(III) alone from loaded solvent system containing both Am(III) and Eu(III) was investigated. In addition, the reverse micellar aggregation behavior of the binary solution containing DOHyA+ HDEHDGA dissolved in *n*-dodecane was also studied.

[1] V.S. Arunachalam, E.L. Fleischer, The global energy landscape and materials innovation, MRS Bull. 33 (2008) 264–276.

[2] P.A. Kharecha, J.E. Hansen, Prevented mortality and greenhouse gas emissions from historical and projected nuclear power, Environ. Sci. Technol. 47 (2013) 4889–4895.

[3] S. David, Future scenarios for fission based reactors, Nucl. Phys. A. 751 (2005) 429–441.

[4] S. Shafiee, E. Topal, When will fossil fuel reserves be diminished?, Energy Policy. 37 (2009) 181–189.

[5] N. Armaroli, V. Balzani, The future of energy supply: Challenges and opportunities, Angew. Chemie - Int. Ed. 46 (2007) 52–66.

[6] J. Parikh, K. Parikh, India’s energy needs and low carbon options, Energy. 36 (2011) 3650–3658.

[7] B. van der Zwaan, The role of nuclear power in mitigating emissions from electricity generation, Energy Strateg. Rev. 1 (2013) 296–301.

[8] P. Bolton, Nuclear Energy Statistics, Libr. House Commons. (2013).

[9] A. Mohan, The Future of Nuclear Energy in India, Obs. Res. Found. . (2016).

[10] I.E.A. IEA, India Energy Outlook, World Energy Outlook Spec. Rep. (2015).

[11] S. Banerjee, H.P. Gupta, The evolution of the Indian nuclear power programme, Prog. Nucl. Energy. 101 (2017) 4–18.

[12] R. Chidambaram, R. Sinha, Importance of closing the nuclear fuel cycle, Nucl. Energy. (2006) 90–91.

[13] A. Gopalakrishnan, Evolution of the Indian nuclear power program, Annu. Rev. Energy Environ. 27 (2002) 369–395.

[14] B. Raj, S.L. Mannan, P.R. Vasudeva Rao, M.D. Mathew, Development of fuels and structural materials for fast breeder reactors, Sadhana - Acad. Proc. Eng. Sci. 27 (2002) 527–558.

[15] S.C. Cheta, P. Chellapandi, P. Puthiyavinayagam, S. Raghupathy, V. Balasubramaniyan, P. Selvaraj, P. Mohanakrishnan, B. Raj, Current status of fast reactors and future plans in

India, in: Energy Procedia, 2011: pp. 64–73.

[16] H. Feiveson, Z. Mian, M.V. Ramana, F. von Hippel, Spent Fuel from Nuclear Power Reactors: An Overview of a New Study by the International Panel on Fissile Materials, Int. Panel Fissile Mater. (2011) 1–21.

[17] Nuclear Energy Agency, Advanced Nuclear Fuel Cycles and Radioactive Waste Management, Oecd. (2006) 244.

[18] J. Bruno, R.C. Ewing, Spent nuclear fuel, Elements. 2 (2006) 343–349.

[19] M. Bunn, J.P. Holdren, S. Fetter, B. Van Der Zwaan, The economics of reprocessing versus direct disposal of spent nuclear fuel, Nucl. Technol. 150 (2005) 209–230.

[20] J.M. Gras, R. Do Quang, H. Masson, T. Lieven, C. Ferry, C. Poinssot, M. Debes, J.M. Delbecq, Perspectives on the closed fuel cycle - Implications for high-level waste matrices, J. Nucl. Mater. 362 (2007) 383–394.

[21] A. V. Bychkov, O. V. Skiba, Review of Non-Aqueous Nuclear Fuel Reprocessing and Separation Methods, in: Chem. Sep. Technol. Relat. Methods Nucl. Waste Manag., 1999: 71–98.

[22] V.A. Drake, W.W. Schulz, L.L. Burger, J.D. Navratil, K.P. Bender, W.D. Bond, W.W. Schulz, L.L. Burger, J.D. Navratil, K.P. Bender, Science and Technology of Tributyl Phosphate, 1990.

[23] D.D. Sood, S.K. Patil, Chemistry of nuclear fuel reprocessing: Current status, J. Radioanal. Nucl. Chem. 203 (1996) 547–573.

[24] G.M. Gasparini, G. Grossi, Long chain disubstituted aliphatic amides as extracting agents in industrial applications of solvent extraction, Solvent Extr. Ion Exch. 4 (1986) 1233–1271.

[25] J. Veliscek-Carolan, Separation of actinides from spent nuclear fuel: A review, J. Hazard. Mater. (2016).

[26] C. Madic, N. Ouvrier, EUROPART: EUROpean research program for the PARTitioning of minor actinides from high active wastes arising from the reprocessing of spent nuclear fuels, Radiochim. Acta. 96 (2008) 183–185.

[27] M. Salvatores, G. Palmiotti, Radioactive waste partitioning and transmutation within advanced fuel cycles: Achievements and challenges, Prog. Part. Nucl. Phys. 66 (2011) 144–166.

[28] C. McCombie, Nuclear waste management worldwide, Phys. Today. 50 (1997) 56–62.

[29] S.A. Ansari, P. Pathak, P.K. Mohapatra, V.K. Manchanda, Aqueous partitioning of minor actinides by different processes, Sep. Purif. Rev. 40 (2011) 43–76.

[30] J.N. Mathur, M.S. Murali, K.L. Nash, Actinide partitioning-A review, Solvent Extr. Ion Exch. 19 (2001) 357–390.

[31] C. Den Bonin, B., E. Abonneau, I. Bisel, Le traitement-recyclage du combustible nucléaire usé : La séparation des actinides, application à la gestion des déchets, CEA. Editions (2008).

[32] J.M. L. Koch, J. P. Glatz, R. J. M.Konings, Partitioning and transmutation studies at ITU, ITU Annual report 1999 (EUR-19504) 34–49.

[33] R.J. Taylor, C.R. Gregson, M.J. Carrott, C. Mason, M.J. Sarsfield, Progress towards the Full Recovery of Neptunium in an Advanced PUREX Process, Solvent Extr. Ion Exch. 31 (2013) 442–462.

[34] G.M. Ritcey, Solvent extraction in hydrometallurgy: Present and future, Tsinghua Sci. Technol. 11 (2006) 137–152.

[35] S. Bourg, A. Geist, J.-M. Adnet, C. Rhodes, B.C. Hanson, Partitioning and transmutation strategy R&D for nuclear spent fuel: the SACSESS and GENIORS projects, EPJ Nucl. Sci. Technol. 6 (2020) 35.

[36] A. Suresh, T.G. Srinivasan, P.R.V. Rao, Parameters influencing third-phase formation in the extraction of Th(NO3)4 by some trialkyl phosphates, Solvent Extr. Ion Exch. 27 (2009) 132–158.

[37] E.P. Horwitz, D.R. McAlister, A.H. Bond, J.E. Barrans, Novel extraction of chromatographic resins based on tetraalkyldiglycolamides: Characterization and potential applications, Solvent Extr. Ion Exch. 23 (2005) 319–344.

[38] X. Liu, J. Liang, J. Xu, Simplified Chinese TRPO process to extract and recover

transuranium elements from high-level liquid waste, Solvent Extr. Ion Exch. 22 (2004) 163–173.

[39] S. Tachimori, H. Nakamura, Extraction of Some Elements by Mixture of DIDPA-TBP and Its Application to Actinoid Partitioning Process, J. Nucl. Sci. Technol. 19 (1982) 326–333.

[40] M.R. Antonio, R. Chiarizia, B. Gannaz, L. Berthon, N. Zorz, C. Hill, G. Cote, Aggregation in solvent extraction systems containing a malonamide, a dialkylphosphoric acid and their mixtures, Sep. Sci. Technol. 43 (2008) 2572–2605.

[41] O. Courson, M. Lebrun, R. Malmbeck, G. Pagliosa, K. Römer, B. Sätmark, J.P. Glatz, Partitioning of minor actinides from HLLW using the DIAMEX process. Part 1 – Demonstration of extraction performances and hydraulic behaviour of the solvent in a continuous process, Radiochim. Acta. 88 (2000) 857.

[42] M.S. Murali, J.N. Mathur, Use of a mixture of trpo and tbp for the partitioning of actinides from high-level waste solutions of purex origin and its comparison with cmpo and other phosphorus-based extractants, Solvent Extr. Ion Exch. 19 (2001) 61–77.

[43] A. Leoncini, J. Huskens, W. Verboom, Ligands for f-element extraction used in the nuclear fuel cycle, Chem. Soc. Rev. 46 (2017) 7229–7273.

[44] Y. Sasaki, G.R. Choppin, Solvent extraction of Eu, Th, U, Np and Am with N,N′-dimethyl-N,N′-dihexyl-3-oxapentanediamide and its analogous compounds, Anal. Sci. 12 (1996) 225–230.

[45] Y. Sasaki, Y. Sugo, S. Suzuki, S. Tachimori, The novel extractants diglycolamides for the extraction of lanthanides and actinides in $HNO_3$-*n*-dodecane system, Solvent Extr. Ion Exch. 19 (2001) 91–103.

[46] Z.X. Zhu, Y. Sasaki, H. Suzuki, S. Suzuki, T. Kimura, Cumulative study on solvent extraction of elements by N,N,N′,N′-tetraoctyl-3-oxapentanediamide (TODGA) from nitric acid into *n*-dodecane, Anal. Chim. Acta. 527 (2004) 163–168.

[47] H. Suzuki, Y. Sasaki, Y. Sugo, A. Apichaibukol, T. Kimura, Extraction and separation of Am(III) and Sr(II) by *N,N,N′,N′*- tetraoctyl-3-oxapentanediamide (TODGA), Radiochim. Acta. 92 (2004) 463–466.

[48] Y. Sasaki, Z.X. Zhu, Y. Sugo, H. Suzuki, T. Kimura, Extraction capacity of diglycolamide derivatives for Ca(II), Nd(III) and Zr(IV) from nitric acid to *n*-dodecane containing a solvent modifier, Anal. Sci. 21 (2005) 1171–1175.

[49] E.A. Mowafy, H.F. Aly, Synthesis of some N,N,N′,N′-tetraalkyl-3-oxa-pentane-1,5-diamide and their applications in solvent extraction, Solvent Extr. Ion Exch. (2007).

[50] Y. Sasaki, Y. Sugo, K. Morita, K.L. Nash, The Effect of Alkyl Substituents on Actinide and Lanthanide Extraction by Diglycolamide Compounds, Solvent Extr. Ion Exch. 33 (2015) 625–641.

[51] Y. Sasaki, Y. Kitatsuji, Y. Tsubata, Y. Sugo, Y. Morita, Separation of Am, Cm and lanthanides by solvent extraction with hydrophilic and lipophilic organic ligands, Solvent Extr. Res. Dev. 18 (2011) 93–101.

[52] S.A. Ansari, P.N. Pathak, V.K. Manchanda, M. Husain, A.K. Prasad, V.S. Parmar, Solvent Extraction and Ion Exchange N,N,N′,N′-Tetraoctyl Diglycolamide (TODGA): A Promising Extractant for Actinide-Partitioning from High-Level Waste (HLW)Tetraoctyl Diglycolamide (TODGA): A Promising Extractant for Actinide-Partitioning from High-Level , (2006) 463–479.

[53] S.A. Ansari, P.N. Pathak, V.K. Manchanda, M. Husain, A.K. Prasad, V.S. Parmar, N,N,N’,N’-Tetraoctyl diglycolamide (TODGA): A promising extractant for actinide-partitioning from high-level waste (HLW), Solvent Extr. Ion Exch. 23 (2005) 463–479.

[54] S.A. Ansari, P. Pathak, P.K. Mohapatra, V.K. Manchanda, Chemistry of diglycolamides: Promising extractants for actinide partitioning, Chem. Rev. 112 (2012) 1751–1772.

[55] R.B. Gujar, S.A. Ansari, D.R. Prabhu, P.N. Pathak, A. Sengupta, S.K. Thulasidas, P.K. Mohapatra, V.K. Manchanda, Actinide Partitioning with a Modified TODGA Solvent: Counter-Current Extraction Studies with Simulated High Level Waste, Solvent Extr. Ion Exch. 30 (2012) 156–170.

[56] G. Modolo, H. Asp, C. Schreinemachers, H. Vijgen, Development of a TODGA based process for partitioning of actinides from a PUREX raffinate part I: Batch extraction optimization studies and stability tests, Solvent Extr. Ion Exch. 25 (2007) 703–721.

[57] D. Magnusson, B. Christiansen, J.P. Glatz, R. Malmbeck, G. Modolo, D. Serrano-Purroy,

C. Sorel, Demonstration of a TODGA based extraction process for the partitioning of minor actinides from a PUREX raffinate part III: Centrifugal contactor run using genuine fuel solution, Solvent Extr. Ion Exch. 27 (2009) 26–35.

[58] S.A. Ansari, D.R. Prabhu, R.B. Gujar, A.S. Kanekar, B. Rajeswari, M.J. Kulkarni, M.S. Murali, Y. Babu, V. Natarajan, S. Rajeswari, A. Suresh, R. Manivannan, M.P. Antony, T.G. Srinivasan, V.K. Manchanda, Counter-current extraction of uranium and lanthanides from simulated high-level waste using N,N,N′,N′-tetraoctyl diglycolamide, Sep. Purif. Technol. 66 (2009) 118–124.

[59] D. Whittaker, A. Geist, G. Modolo, R. Taylor, M. Sarsfield, A. Wilden, Applications of Diglycolamide Based Solvent Extraction Processes in Spent Nuclear Fuel Reprocessing, Part 1: TODGA, Solvent Extr. Ion Exch. 36 (2018) 223–256.

[60] P. Deepika, K.N. Sabharwal, T.G. Srinivasan, P.R. Vasudeva Rao, Studies on the use of N,N,N’,N’-Tetra(2-ethylhexyl) diglycolamide (TEHDGA) for actinide partitioning. I: Investigation on third-phase formation and extraction behavior, Solvent Extr. Ion Exch. 28 (2010) 184–201.

[61] P. Deepika, K.N. Sabharwal, T.G. Srinivasan, P.R. Vasudeva Rao, Studies on the use of N,N,N′,N′-Tetra(2-Ethylhexyl) Diglycolamide (TEHDGA) for Actinide Partitioning II: Investigation on Radiolytic Stability, Solvent Extr. Ion Exch. 29 (2011) 230–246.

[62] R.B. Gujar, S.A. Ansari, M.S. Murali, P.K. Mohapatra, V.K. Manchanda, Comparative evaluation of two substituted diglycolamide extractants for “actinide partitioning,” J. Radioanal. Nucl. Chem. 284 (2010) 377–385.

[63] S. Manohar, J.N. Sharma, B. V. Shah, P.K. Wattal, Process development for bulk separation of trivalent actinides and lanthanides from radioactive high-level liquid waste, Nucl. Sci. Eng. 156 (2007) 96–102.

[64] J. Ravi, K.A. Venkatesan, M. Antony, T.G. Srinivasan, P.R. Vasudeva Rao, New unsymmetrical digycolamide ligands for trivalent actinide separation, Radiochim. Acta. 102 (2014) 609–617.

[65] J. Ravi, K.A. Venkatesan, M.P. Antony, T.G. Srinivasan, P.R. Vasudeva Rao, Tuning the diglycolamides for modifier-free minor actinide partitioning, J. Radioanal. Nucl. Chem.

295 (2013).

[66] J. Ravi, K.A. Venkatesan, M.P. Antony, T.G. Srinivasan, P.R. Vasudeva Rao, Feasibility of Using Di-Dodecyl-Di-Octyl Diglycolamide for Partitioning of Minor Actinides from Fast Reactor High-Level Liquid Waste, Solvent Extr. Ion Exch. 32 (2014) 424–436.

[67] P.K. Nayak, R. Kumaresan, S. Chaurasia, K.A. Venkatesan, G.G.S. Subramanian, S. Rajeswari, M.P. Antony, P.R. Vasudeva Rao, B.M. Bhanage, Demonstration of trivalent actinide partitioning from simulated high-level liquid waste using modifier-free unsymmetrical diglycolamide in n-dodecane, Radiochim. Acta. 103 (2015) 359–368.

[68] S. Kannan, B.G. Vats, I.C. Pius, D.M. Noronha, P.S. Dhami, P.W. Naik, M. Kumar, Extraction and structural studies of an unexplored monoamide, N,N′-dioctyl, α-hydroxy acetamide with lanthanide(III) and actinide(III) ions, Dalt. Trans. 43 (2014) 5252–5255.

[69] T. Prathibha, R. Kumaresan, B.R. Selvan, K.A. Venkatesan, M.P. Antony, P.R.V. Rao, N,N-dialkyl-2-hydroxyacetamides for modifier-free separation of trivalent actinides from nitric acid medium, Radiochim. Acta. 104 (2016) 173–181.

[70] T. Prathibha, K.A. Venkatesan, M.P. Antony, Comparison in the aggregation behaviour of amide extractant systems by dynamic light scattering and ATR-FTIR spectroscopy, Colloids Surfaces A Physicochem. Eng. Asp. 538 (2018) 651–660.

[71] T. Prathibha, R. Kumaresan, P.K. Nayak, K.A. Venkatesan, G.G.S. Subramanian, S. Rajeswari, T. Kalaiyarasu, R. Karunakaran, M.P. Antony, Modifier-free separation of trivalent actinides and lanthanides from fast reactor simulated high-level liquid waste using N,N-di-octyl-2-hydroxyacetamide, J. Radioanal. Nucl. Chem. 314 (2017) 2365–2375.

[72] P.R. Vasudeva Rao, Z. Kolarik, A review of third phase formation in extraction of actinides by neutral organophosphorus extractants, Solvent Extr. Ion Exch. 14 (1996) 955–993.

[73] J. Ravi, T. Prathibha, K.A. Venkatesan, M.P. Antony, T.G. Srinivasan, P.R. Vasudeva Rao, Third phase formation of neodymium (III) and nitric acid in unsymmetrical N,N-di-2-ethylhexyl-N′,N′-dioctyldiglycolamide, Sep. Purif. Technol. 85 (2012).

[74] K. Benadict Rakesh, A. Suresh, N. Sivaraman, V.K. Aswal, P.R. Vasudeva Rao,

Extraction and third phase formation behaviour of tri-iso-amyl phosphate and tri-n-butyl phosphate with Zr(IV) and Hf(IV): A comparative study, J. Radioanal. Nucl. Chem. 309 (2016) 1037–1048.

[75] S. Sarkar, A. Suresh, N. Sivaraman, V.K. Aswal, An insight into third-phase formation in the extraction of thorium nitrate by tris(2-methylbutyl) phosphate and tri-n-alkyl phosphates, Sep. Sci. Technol. 54 (2019) 970–984.

[76] S. Mallick, A. Suresh, T.G. Srinivasan, P.R. Vasudeva Rao, Comparative studies on third-phase formation in the extraction of thorium nitrate by tri-n-butyl phosphate and tri-n-amyl phosphate in straight chain alkane diluents, Solvent Extr. Ion Exch. 28 (2010) 459–481.

[77] T.G. Srinivasan, S. Vijayasaradhi, R. Dhamodaran, A. Suresh, P.R. Vasudeva Rao, Third phase formation in extraction of thorium nitrate by mixtures of trialkyl phosphates, Solvent Extr. Ion Exch. 16 (1998) 1001–1011.

[78] S. Tachimori, Y. Sasaki, S.I. Suzuki, Modification of TODGA-n-Dodecane solvent with a monoamide for high loading of lanthanides(III) and actinides(III), Solvent Extr. Ion Exch. 20 (2002) 687–699.

[79] P.R.V. Rao, R. Dhamodaran, T.G. Srinivasan, C.K. Mathews, The effect of diluent on third phase formation in thorium nitrate - tbp system: Some novel empirical correlations, Solvent Extr. Ion Exch. 11 (1993) 645–662.

[80] K. Osseo-Asare, Volume changes and distribution of HCl and H2O in the tri-n-butyl phosphate-H2O-HCl liquid-liquid system: A reversed micellar phenomenological model, Colloids and Surfaces. 50 (1990) 373–392.

[81] M.R. Antonio, R. Chiarizia, B. Gannaz, L. Berthon, N. Zorz, C. Hill, G. Cote, Aggregation in solvent extraction systems containing a malonamide, a dialkylphosphoric acid and their mixtures, in: Sep. Sci. Technol., 43 (2008) 2572-2605.

[82] M.P. Jensen, T. Yaita, R. Chiarizia, Reverse-micelle formation in the partitioning of trivalent f-element cations by biphasic systems containing a tetraalkyldiglycolamide, Langmuir. 23 (2007) 4765–4774.

[83] K. Osseo-Asare, aggregation, reversed micelles, and microemulsions in liquid-liquid

extraction: the tri-n-butyl phosphate- diluent-water-electrolyte system, 37 (1991) 123–173.

[84] C. Erlinger, L. Belloni, T. Zemb, C. Madic, Attractive interactions between reverse aggregates and phase separation in concentrated malonamide extractant solutions, Langmuir.15 (1999) 2290-2300.

[85] C. Erlinger, D. Gazeau, T. Zemb, C. Madic, L. Lefrançois, M. Hebrant, C. Tondre, Effect of nitric acid extraction on phase behavior, microstructure and interactions between primary aggregates in the system dimethyldibutyltetradecylmalonamide (DMDBTDMA) / n-dodecane / water: A phase analysis and small angle X-ray scattering (SAXS) char, Solvent Extr. Ion Exch. 16 (1998) 707–738.

[86] T. Yaita, A.W. Herlinger, P. Thiyagarajan, M.P. Jensen, Influence of extractant aggregation on the extraction of trivalent f-element cations by a tetraalkyldiglycolamide, Solvent Extr. Ion Exch. 22 (2004) 553–571.

[87] P.N. Pathak, S.A. Ansari, S. Kumar, B.S. Tomar, V.K. Manchanda, Dynamic light scattering study on the aggregation behaviour of N,N,N′,N′-tetraoctyl diglycolamide (TODGA) and its correlation with the extraction behaviour of metal ions, J. Colloid Interface Sci. 342 (2010) 114–118.

[88] T. Prathibha, K.R. Swami, S. Sriram, K.A. Venkatesan, Interference of zr(IV) during the extraction of trIValent nd(III) from the aqueous waste generated from metallic fuel reprocessing, Radiochim. Acta. 108 (2020) 543-554.

[89] T. Prathibha, K.A. Venkatesan, M.P. Antony, Comparison in the aggregation behaviour of amide extractant systems by dynamic light scattering and ATR-FTIR spectroscopy, Colloids Surfaces A Physicochem. Eng. Asp. 538 (2018) 651-660.

[90] P.N. Pathak, S.A. Ansari, P.K. Mohapatra, V.K. Manchanda, A.K. Patra, V.K. Aswal, Role of alkyl chain branching on aggregation behavior of two symmetrical diglycolamides: Small angle neutron scattering studies, J. Colloid Interface Sci. 393 (2013) 347–351.

[91] S. Nave, C. Mandin, L. Martinet, L. Berthon, F. Testard, C. Madic, T. Zemb, Supramolecular organisation of tri-n-butyl phosphate in organic diluent on approaching

third phase transition, Phys. Chem. Chem. Phys. 6 (2004) 799-804.

[92] E.L. Campbell, V.E. Holfeltz, G.B. Hall, K.L. Nash, G.J. Lumetta, T.G. Levitskaia, Nitric Acid and Water Extraction by T2EHDGA in n-Dodecane, Solvent Extr. Ion Exch. 35 (2017) 586–603.

[93] R. Chiarizia, D. Stepinski, M.R. Antonio, Sans study of HCl extraction by selected neutral organophosphorus compounds in n-octane, Sep. Sci. Technol. 45 (2010) 1668-1678.

[94] M.P. Jensen, R. Chiarizia, J.S. Ulicki, B.D. Spindler, D.J. Murphy, M.M. Hossain, A. Roca-Sabio, A. de Blas, T. Rodríguez-Blas, Solvent Extraction Separation of Trivalent Americium from Curium and the Lanthanides, Solvent Extr. Ion Exch. 33 (2015) 329-345.

[95] M.B. Singh, S.G. Nayak, A.D. Kanthe, R.B. Patil, V.G. Gaikar, Insight into acidity driven third phase formation of TBP in organic solutions by MD simulation, J. Mol. Liq. 232 (2017) 1–8.

[96] A.G. Baldwin, M.J. Servis, Y. Yang, N.J. Bridges, D.T. Wu, J.C. Shafer, The structure of tributyl phosphate solutions: Nitric acid, uranium (VI), and zirconium (IV), J. Mol. Liq. 246 (2017) 225–235.

[97] M. Baaden, M. Burgard, G. Wipff, TBP at the water - Oil interface: The effect of TBP concentration and water acidity investigated by molecular dynamics simulations, J. Phys. Chem. B. 105 (2001) 11131–11141.

[98] R. Motokawa, T. Kobayashi, H. Endo, J. Mu, C.D. Williams, A.J. Masters, M.R. Antonio, W.T. Heller, M. Nagao, A Telescoping View of Solute Architectures in a Complex Fluid System, ACS Cent. Sci. 5 (2019) 85–96.

[99] A. Paquet, O. Diat, L. Berthon, P. Guilbaud, Aggregation in organic phases after solvent extraction of uranyl nitrate: X-ray scattering and molecular dynamic simulations, J. Mol. Liq. 277 (2019) 22–35.

[100] M. Borkowski, J.R. Ferraro, R. Chiarizia, D.R. McAlister, FT-IR study of third phase formation in the U(VI) or Th(IV)/$HNO_3$ TBP/alkane systems, Solvent Extr. Ion Exch. 20 (2002) 313–330.

[101] R.G. Pearson, Hard and Soft Acids and Bases, J. Am. Chem. Soc. 85 (1963) 3533–3539.

[102] G.R. Choppin, Comparative solution chemistry of the 4f and 5f elements, J. Alloys Compd. 223 (1995) 174–179.

[103] M. Nilsson, K.L. Nash, Review article: A review of the development and operational characteristics of the TALSPEAK process, Solvent Extr. Ion Exch. 25 (2007) 665–701.

[104] A.S. Suneesh, K.A. Venkatesan, K. V. Syamala, M.P. Antony, P.R. Vasudeva Rao, Mutual separation of americium(III) and europium(III) using glycolamic acid and thioglycolamic acid, Radiochim. Acta. 100 (2012) 425–430.

[105] A.S. Suneesh, R. Kumaresan, S. Rajeswari, P.K. Nayak, K. V. Syamala, K.A. Venkatesan, M.P. Antony, P.R.V. Rao, Development and Demonstration of Americium (III)-Europium (III) Separation Using Diglycolamic Acid, Sep. Sci. Technol. 48 (2013) 1998–2006.

[106] Z. Kolarik, Complexation and separation of lanthanides(III) and actinides(III) by heterocyclic N-donors in solutions, Chem. Rev. 108 (2008) 4208–4252.

[107] M.J. Hudson, Some new strategies for the chemical separation of actinides and lanthanides, Czechoslov. J. Phys. 53 (2003) A305–A311.

[108] A. Bhattacharyya, P.K. Mohapatra, Separation of trivalent actinides and lanthanides using various “N”, “S” and mixed “N,O” donor ligands: A review, Radiochim. Acta. 107 (2019) 931-949.

[109] G.J. Lumetta, A. V. Gelis, G.F. Vandegrift, Review: Solvent systems combining neutral and acidic extractants for separating trivalent lanthanides from the transuranic elements, Solvent Extr. Ion Exch. 28 (2010) 287–312.

[110] A. V. Gelis, G.J. Lumetta, Actinide lanthanide separation process - ALSEP, Ind. Eng. Chem. Res. 53 (2014) 1624-1631.

[111] G. Modolo, R. Odoj, Synergistic selective extraction of actinides(III) over lanthanides from nitric acid using new aromatic diorganyldithiophosphinic acids and neutral organophosphorus compounds, Solvent Extr. Ion Exch. 17 (1999) 33–53.

[112] P.K. Nayak, R. Kumaresan, S. Chaurasia, K.A. Venkatesan, G.G.S. Subramanian, T.

Prathibha, K. V. Syamala, B.R. Selvan, S. Rajeswari, M.P. Antony, P.R. Vasudeva Rao, B.M. Bhanage, Studies on the feasibility of using completely incinerable reagents for the single-cycle separation of americium(III) from simulated high-level liquid waste, Radiochim. Acta, 103 (2015) 265–275.

[113] P.K. Nayak, R. Kumaresan, K.A. Venkatesan, M.P. Antony, P.R. Vasudeva Rao, A New Method for Partitioning of Trivalent Actinides from High-Level Liquid Waste, Sep. Sci. Technol. 48 (2013) 1409–1416.

[114] P.K. Nayak, R. Kumaresan, K.A. Venkatesan, M.P. Antony, P.R. Vasudeva Rao, Extraction Behavior of Am(III) and Eu(III) from Nitric Acid Medium in Tetraoctyldiglycolamide-Bis(2-Ethylhexyl)Phosphoric Acid Solution, Sep. Sci. Technol. 49 (2014) 1186–1191.

[115] B.J. Mincher, G. Modolo, S.P. Mezyk, Review article: The effects of radiation chemistry on solvent extraction 3: A review of actinide and lanthanide extraction, Solvent Extr. Ion Exch. 27 (2009) 579–606.

[116] Y. Sugo, Y. Sasaki, S. Tachimori, Studies on hydrolysis and radiolysis of N,N,N′,N′-tetraoctyl-3-oxapentane-1,5-diamide, Radiochim. Acta. 90 (2002) 161–165.

[117] R.B. Gujar, S.A. Ansari, A. Bhattacharyya, A.S. Kanekar, P.N. Pathak, P.K. Mohapatra, V.K. Manchanda, Radiolytic Stability of N,N,N′,N′-Tetraoctyl Diglycolamide (TODGA) in the Presence of Phase Modifiers Dissolved in *n*-Dodecane, Solvent Extr. Ion Exch. 30 (2012) 278-290.

[118] B.J. Mincher, G. Modolo, S.P. Mezyk, Review article: The effects of radiation chemistry on solvent extraction 3: A review of actinide and lanthanide extraction, Solvent Extr. Ion Exch. 27 (2009) 579–606.

[119] J.N. Sharma, R. Ruhela, K.K. Singh, M. Kumar, C. Janardhanan, P. V. Achutan, S. Manohar, P.K. Wattal, A.K. Suri, Studies on hydrolysis and radiolysis of tetra(2-ethylhexyl)diglycolamide (TEHDGA)/isodecyl alcohol/*n*-dodecane solvent system, Radiochim. Acta. 98 (2010) 485–491.

[120] Y. Sugo, Y. Izumi, Y. Yoshida, S. Nishijima, Y. Sasaki, T. Kimura, T. Sekine, H. Kudo, Influence of diluent on radiolysis of amides in organic solution, Radiat. Phys. Chem. 76

(2007) 794–800.

[121] R.B. Gujar, S.A. Ansari, A. Bhattacharyya, P.K. Mohapatra, A.S. Kanekar, P.N. Pathak, V.K. Manchanda, Studies on the radiolytic stability of N,N,N′,N′-tetra-2- ethylhexyl diglycolamide in n-dodecane solution containing different phase modifiers, J. Radioanal. Nucl. Chem. 288 (2011) 621–627.

# Chapter 2: Experimental

The present chapter deals with the description of materials, methods and experimental conditions employed in the present study. The experimental procedures involved in the synthesis of extractants and preparation of reagent solutions for the liquid-liquid extraction as well as aggregation studies are discussed. The synthesized extractants were purified and characterized by various analytical techniques to ascertain the purity. The details of instrumental techniques employed for the studies such as dynamic light scattering (DLS), HPGe detector, NaI(Tl) detector, ATR-FTIR, inductively coupled plasma - optically emission spectrometry (ICP-OES) etc. are explained briefly.

## 2.1 Chemicals and reagents

All the chemicals and reagents used in the study were of analytical grade (AR, purity > 98%) and they were used as received unless otherwise it is mentioned.

### 2.1.1 Inorganic and organic salts

**Citric acid**

Anhydrous Citric acid was obtained from Loba Chemi Private Limited, Mumbai, India.

**Disodium hydrogen phosphate**

Disodium hydrogen phosphate (AR grade) was received from M/s. Sarabhai Chemicals, India and used as received.

**Diethylenetriaminepentaaceticacid (DTPA)**

Diethylenetriaminepentaacetic acid was purchased from Sigma Aldrich, Mumbai, India. The solution of DTPA was prepared by dissolving desired amount DTPA in Millipore water followed by adding the required quantity of NaOH pellets then the pH of the solution was adjusted using $HNO_3$ to desired value.

**Europium oxide ($Eu_2O_3$)**

$Eu_2O_3$ was obtained from M/s. SD Fine Chemicals and used for the preparation of europium nitrate in concentrated nitric acid solution.

**EDTA**

EDTA (ethylenediaminetetraacetic acid) was purchased from Aldrich, Mumbai, India and used for complexmetric titrations.

**Hexamethylenetetramine (HMTA)**

HMTA of analytical grade supplied by Sigma Aldrich, Mumbai, India was used as received. It was employed for the estimation of concentration of trivalent lanthanides in aqueous and organic phases.

**Methylthymolblue sodium salt**

Methylthymolblue sodium salt (ACS grade) was obtained from M/s. Merck, India

**Neodymium nitrate**

$Nd(NO_3)_3.6H_2O$ was procured from Sigma Aldrich, Mumbai, India and it was used for the preparation of stock solutions.

***N*-(2-hydroxyethyl)ethylenediamine-*N,N′,N′*-triacetic acid tri-sodium salt (HEDTA)**

*N*-(2-hydroxyethyl)ethylenediamine-*N,N′,N′*-triacetic acid tri-sodium salt (HEDTA) was obtained from Sigma Aldrich, Mumbai, India.

**Oxalic Acid**

Oxalic acid was procured from Sigma Aldrich, Mumbai, India.

**Phenolphthalein**

Phenolphthalein indicator was purchased from Merck, Mumbai, India and was prepared by dissolving the required quantity of solid in a 1:1 solution of distilled water and ethanol.

**Potassium dihydrogen phosphate**

Potassium dihydrogen phosphate (AR grade) was purchased from Sigma Aldrich, Mumbai, India and it was used for the preparation of buffer solution.

**Potassium hydrogen phthalate (KHP)**

Potassium hydrogen phthalate (KHP) of analytic grade was procured from M/s. Glaxo Laboratories, India and it was used for standardization of sodium hydroxide solution.

**Potassium oxalate**

Potassium oxalate (AR grade) obtained from M/s. Loba Chemie Private Limited, Mumbai, India and it was used for the estimation of free acidity (concentration of nitric acid) of aqueous and organic phases containing hydrolysable metal ions.

**Silica gel**

Silica gel (60-120, 100-200 and 120-240 mesh) for column chromatography was obtained from SD Fine chemicals Limited, Chennai, India and it was dried at 373 K for one hour prior to use.

**Sodium hydroxide**

Sodium hydroxide of analytical grade was procured from Sigma Aldrich, Mumbai,, India.

**Sodium Nitrite**

Sodium Nitrite was obtained from S.D. fine Chemicals, Mumbai, India.

**Trans-1,2-diaminocyclohexane-*N,N,N'N'*-tetraacetic acid (CyDTA)**

Trans-1,2-diaminocyclohexane-*N,N,N'N'*-tetraacetic acid (CyDTA) was obtained from M/s TCI Chemicals, Japan and it was employed for the rentetion of unwanted metal ions such as Zr(IV), Pd(II) etc. in aqueous phase during solvent extraction.

### Triethylamine

Triethylamine of analytical grade (> 95 %) was purchased from Merck, Mumbai, India and it was further purified by distillation over calcium hydride before each use.

### 2.1.2 Organic chemicals and solvents

### Diglycolic chloride and dialkyl amines

Diglycolic chloride (> 90%) dihexylamine, dioctylamine, didecyl amine, didodecyl amine and di-2-ethylhexylamine were procured from Sigma Aldrich, India.

### Acetoxyacetyl chloride

Acetoxyacetylchloride (97%) was purchased from M/s Thermo Fischer Scientific, India and it was used without any purification.

### Tributylphosphate (TBP)

TBP (> 99%) was obtained from M/s. Sigma Aldrich. It was washed with dilute sodium carbonate solution or sodium hydroxide followed by distilled water and then dried in a rotary evaporator.

### *N, N*-dihexyloctanamide (DHOA)

N, N-dihexyloctanamide **(**DHOA) was obtained from Heavy Water Board, Tuticorin, India.

### *N,N,N’,N’*-tetra (2-ethyl hexyl) diglycolmide (TEHDGA)

*N,N,N’,N’*-tetra(2-ethylhexyl)diglycolamide (TEHDGA) procured from Orion Chemicals, Mumbai, India and it was purified by column chromatography. In some cases it was synthesized by the procedure described elsewhere [1].

### Diluents

*n*-Dodecane (> 98%) was purchased from Alfa Aesar, Mumbai, India. The *n*-parafiins such as *n*-hexane, *n*-octane, *n*-decane, *n*-tetradecane were obtained from Ranbaxy Fine Chemicals Limited, New Delhi.

### Alcohols

The long chain aliphatic alcohols namely *n*-octanol, *n*-decanol and isodecanol of purity > 98% were purchased from Loba Chemi Private Limited, Mumbai, India, and they were used without any purification

### Bis (2-ethylhexyl)phosphoric acid (HDEHP)

Bis(2-ethylhexyl)phosphoric acid (HDEHP) was obtained from M/s. Fluka Chemie GmbH, Buche, Switzerland and it was further purified by copper (II) precipitation method, described elsewhere [2].

### Bis (2-ethylhexyl)phosphoric acid (PC88A)

Bis(2-ethylhexyl)phosphonic acid (PC88A) was received from Heavy Water Board, Tuticorin, Tamil Nadu. The chemical was purified by method as reported in the literature [3,4].

### Bis(2,4,4-trimethylpentyl)phosphinic acid (CYANEX-272)

Bis(2,4,4-trimethylpentyl)phosphinic acid (CYANEX-272) was procured from Shanghai Bojing Chemical Co. Ltd., China. It was was purified by the procedure described elsewhere [3].

### Dichloromethane

Dichloromethane was obtained from Fischer Inorganics and Aromatics Limited, Chennai, India.

### Chloroform

Chloroform solvent was procured from Alfa Aesar, India

### Ethylacetate

Ethylacetate was obtained from Fischer In organics and Aromatics Limited, Chennai, India.

### 2.1.3 Acid solutions

The acid solutions such as $HNO_3$ and HCl (AR grade) were purchased from E. Merck Private Limited, Mumbai, India. The stock solutions of desired concentrations were prepared by the dilution of concentrated acid. The concentration of acid was estimated by standard NaOH solution with phenolphthalein as indicator.

### 2.1.4 Radioactive tracers

The radio isotope $^{(152+154)}$Eu(III) in the form of $EuCl_3$ was purchased from Board of Radiation and Isotope Technology, Mumbai. The HCl was evaporated off and the tracer solution was prepared by re-dissolving in dilute nitric acid. The radio isotope $^{241}$Am(III) was procured from Bhabha Atomic Research Centre, India. It was dissolved in dilute nitric acid of desired concentration.

## 2.2 Instrumentation

### 2.2.1 High Pure Gamma Spectrometer (HpGe Detector)

The gamma emitting radioactive species were characterized and estimated by gamma spectrometry. A planar high pure germanium (HpGe) crystal semiconductor detector obtained from Baltic Scientific Instruments, Latvia was used. It was coupled with multichannel analyzer (MCA).

### 2.2.2 Gamma counter

The gamma radioactivity of $^{241}$Am, $^{(152+154)}$Eu was estimated NaI(Tl) detector coupled with single channel analyzer. The NaI(Tl)-photo multiplier tube (PMT) integral assembly was procured from Harshaw, U.S.A and other electronic modules were obtained from Electronic Corporation of India Limited (ECIL), Hyderabad, India.

### 2.2.3 Gamma chamber for irradiation

An indigenous, compact, self-shielded (Gamma Chamber 5000, BRIT) gamma chamber was used in the present study. The radiation field was provided by a set of stationary cobalt-60 gamma sources placed in a cylindrical cage. The samples were placed in an irradiation chamber (5 litre) located in the gamma irradiator and kept in a static condition during irradiation. The gamma chamber was calibrated using Fricke dosimeter before placing the samples for irradiation.

### 2.2.4 Rotary evaporator

A rotary evaporator (Model : IKA RV 10 Digital) was used for distilling the volatile solvents from the reaction mixtures and from the fractions collected during the column chromatography.

### 2.2.5 pH meter

All pH adjustment and measurement was made using Cyberscan 500 pH, Metrohm. The pH meter was calibrated at 298 K with standard buffers of pH 4, 7 and 10.

### 2.2.6 Karl Fischer titrator

The concentration of water present in the organic phase before and after the extraction was determined by Karl Fischer titration (Metrohm KF-831 Karl Fischer titrator). Double distilled water or Millipore water was used to calibrate the instrument. Known weights of the samples were taken for the determination of water content. The values obtained for the water analysis were within the error range of ±5%.

### 2.2.7 Inductively coupled plasma-optical emission spectrometer

Ultima C spectroanalyser (Jobin Yvon, France) equipped with inductively coupled plasma (ICP) excitation source was used for analysis of several non-radioactive elements present in the fast reactor-simulated high-level liquid waste. The spectrometer provides a resolution of 0.015 nm with a poly scan facility of ±2 nm. RF generator of 40.68 MHz with a maximum output power of 1550 W was used for plasma generation. Samples were injected into using peristaltic pump at the flow rate of 1.5 mL/min. The emission lines chosen for the given metal analysis were the most sensitive lines having negligible interference from other elements in the group.

### 2.2.8 Dynamic light scattering

Dynamic light scattering (DLS) technique is a well-recognized method for determining the size of aggregates (reverse micelles) and their distribution in the liquid phase. The schematic diagram of dynamic light scattering technique is shown in Figure 2.1. The principle of DLS technique for the measurement of size and distribution of aggregates is described elsewhere [5-7]. The DLS technique determines average hydrodynamic diameter of the particle suspension by measuring the fluctuations in the intensity of scattered photons. It is well recognized that the reverse micelles (or aggregates) suspended in a liquid are under constant Brownian motion due to the interactions and random collisions with neighboring molecules or aggregates. When a monochromatic and coherent beam of light falls on such a suspension, the light is scattered at various angles and the scattered photons carry information about the size and distribution of aggregates intensity. The DLS technique measures the time dependent fluctuations in the scattering intensity to determine the translational diffusion coefficient (D), and subsequently the hydrodynamic diameter ($D_h$). The apparent hydrodynamic diameter of the species can be calculated by using a Stokes–Einstein equation with the assumption that the scattering species as hard sphere, is given in equation 2.1. The algorithm employed for the determination of average aggregate size, and distribution of aggregates was based on the cumulant analysis, which extracts the data from auto correlation function generated by the autocorrelator built-in the equipment. Poly dispersive Index (PDI) in dynamic light scattering studies describes that the width of peak is a Gaussian distribution. The PDI of 0.2 or less indicates that the sample is mono dispersive and the PDI of more than 0.7 is not suitable for the DLS analysis. In the present study the PDI of self-aggregation of samples was determined to be less than 0.1, and those with acid and Nd(III) extracted samples ranged from 0.2 to 0.5.

$$d_h = \frac{k_B T}{3\pi\eta D} \qquad (2.1)$$

Where $d_h$ is hydrodynamic diameter of the aggregate, $k_B$ is the Boltzmann constant, T is the temperature of the measurement and η is the viscosity of the dispersion medium or solvent.

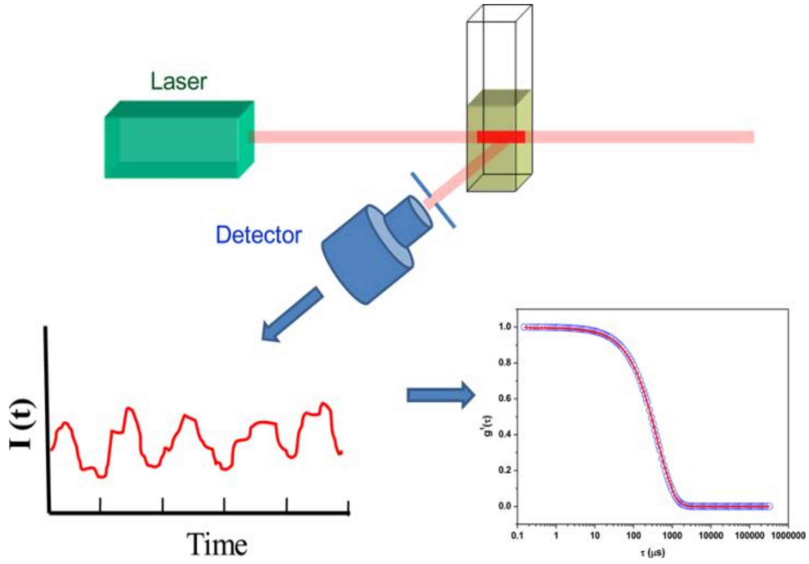

**Figure 2.1.** Schematic diagram of dynamic light scattering

For DLS measurements, the organic phase sample was equilibrated with the aqueous solution containing either nitric acid or Nd(III) nitrate solution in nitric acid taken in a stoppered glass tube immersed in a constant temperature water bath. The concentration of the nitric acid in aqueous phase was varied from 1 M to ~16 M and the initial amount of Nd(III) in nitric acid was varied from 1 g/L to 15 g/L. The test tubes were rotated in an up-side-down manner for one hour. After completion of equilibration, the stoppered test tubes were kept aside for 30 minutes in order to settle the organic and aqueous phases. The organic phase was taken and subjected for DLS measurements. Zetasizer- nano ZS90 (Malvern Instrument Company, UK) with a 4 mW He–Ne laser beam at a wavelength of 632.8 nm at a scattering angle of 90° was used for measuring the aggregate size. The experiments were carried out in a 4 mm or 10 mm path length cell at 298 K depending upon the experimental conditions. Before the measurements, the cuvettes were washed twice with methanol, acetone followed by Millipore water and dried in oven. The accuracy in the measurement of particle size was verified using NIST standard polystyrene Latex colloidal suspension (Duke cooperative private limited, USA) of size 60 nm before and after measurement of samples. One mL or sometimes 0.5 mL of sample was taken in transparent and well-cleaned glass cuvette was used for DLS measurements to obtain accurate aggregate size. Before each measurement, the liquid sample filtered into a 0.3 μm disposable polypropylene membrane filter (Aldrich make) to remove the dust, if present. The measurements were carried out for five times to obtain the reproducibility of the data. The average standard deviation of measured data was ± 5%.

### 2.2.9 NMR spectrometer

A Brucker Avance III 500 MHz (AV 500) multi nuclei solution NMR spectrometer was used for recording proton and $^{13}C$ NMR of synthesized samples. $CDCl_3$ or DMSO-$d_6$ containing 0.03 % of TMS was used as the solvent.

### 2.2.10 FT-IR spectrometer

The Fourier transformed infrared (FTIR) spectrum of the sample was recorded using BRUKER TENSOR II FT-IR spectrometer equipped with an ATR (attenuated total reflectance) diamond crystal. Few micro litres of sample was placed on the diamond disk and the spectrum was recorded from 600 $cm^{-1}$ to 4000 $cm^{-1}$. For each sample the data was acquired for about 16 scans with a resolution of 4 $cm^{-1}$. The acquired data was corrected to the background spectrum (without sample) and presented as ATR-FTIR spectrum of the sample.

### 2.2.11 Raman spectrometer

Raman spectrum of the organic phase was recorded using an Renishaw (Gloucestershire, UK) inVia Raman microscope system containing with a Leica microscope. It contained a 785 nm excitation laser with a power of 300 mW and charge couple device (CCD) detector. A 20X or 10 X objective lens was used and the laser exposure time was 10 s.

### 2.2.12 Molecular Dynamic Simulations

In molecular dynamics (MD) simulations, SPC/E [8] water model was used for water, whereas OPLS-AA (all–atom optimized potential for liquid simulation) force field [9] was applied for all diglycolamides and long chain alkanes. The initial converged coordinates at the B3LYP/SVP level of theory were further subjected to single point energy calculation for the generation of Mulliken partial atomic charges at the B3LYP/TZVP level of theory [10, 11] using TURBOMOLE program [12]. The Lorentz -Berthelot mixing rule was considered for all the non-bonded pair interactions using cut off of 12Å. Particle mesh Ewald (PME) [13-15] method was applied to calculate long range electrostatic interactions with an order of 6 and with a cut off distance of 12Å.

All liquid state simulations (single and two phase systems) have been conducted using GROMACS [16-19] MD simulation package in the simulation box with varying nitric acid concentration. The simulation details of diglycolamides, water, $HNO_3$, *n*-alkanes are tabulated in Table 2.1. The initial coordinates of the filled simulation box was allowed to relax via steepest descent energy minimization technique followed by equilibration in NPT ensemble for 10ns simulation length with a time step of 2 fs. Berendsen like weak coupling methods for thermostat and Parrinello-Rahman coupling method for barostat were employed to maintain the temperature and pressure at 300K and 1 atm respectively. The periodic boundary conditions are applied in three directions. Further, the 10ns production run was performed using NVT ensemble and then this production data were analyzed for the determination of various structural properties and cluster analysis.

**Table 2.1.** Details of simulation box for *n*-paraffis-Ligand-$HNO_3$-water system

| System | Acidity (M) | Box dimension x, y,z ($nm^3$) | $N_{Ligand}$ | $N_{diluent}$ | $N_{Water}$ | $N_{HNO3}$ |
|---|---|---|---|---|---|---|
| Octane-THDGA | 1.2 | 4.905, 4.905, 4.905 | 10 | 400 | 12 | 3 |
| Octane-THDGA | 2 | 4.918, 4.918, 4.918 | 10 | 400 | 20 | 5 |
| Octane-THDGA | 3.5 | 4.921, 4.921, 4.921 | 10 | 400 | 48 | 12 |
| Octane-THDGA | 6 | 4.934, 4.934, 4.934 | 10 | 400 | 60 | 15 |
| Octane-THDGA | 8 | 4.946, 4.946, 4.946 | 10 | 400 | 80 | 20 |
| Octane-THDGA | 10 | 4.959, 4.959, 4.959 | 10 | 400 | 100 | 25 |

| | | | | | | |
|---|---|---|---|---|---|---|
| Octane-TODGA | 1.2 | 4.919, 4.919, 4.919 | 10 | 400 | 12 | 3 |
| Octane-TODGA | 2 | 4.939, 4.939, 4.939 | 10 | 400 | 20 | 5 |
| Octane-TODGA | 3.5 | 4.950, 4.950, 4.950 | 10 | 400 | 48 | 12 |
| Octane-TODGA | 6 | 4.959, 4.959, 4.959 | 10 | 400 | 60 | 15 |
| Octane-TODGA | 8 | 4.983, 4.983, 4.983 | 10 | 400 | 80 | 20 |
| Octane-TODGA | 10 | 4.989, 4.989, 4.989 | 10 | 400 | 100 | 25 |
| Octane-TDDGA | 1.2 | 4.967, 4.967, 4.967 | 10 | 400 | 12 | 3 |
| Octane-TDDGA | 2 | 4.960, 4.960, 4.960 | 10 | 400 | 20 | 5 |
| Octane-TDDGA | 3.5 | 4.992, 4.992, 4.992 | 10 | 400 | 48 | 12 |
| Octane-TDDGA | 6 | 4.983, 4.983, 4.983 | 10 | 400 | 60 | 15 |
| Octane-TDDGA | 8 | 5.003, 5.003, 5.003 | 10 | 400 | 80 | 20 |
| Octane-TDDGA | 10 | 5.009, 5.009, 5.009 | 10 | 400 | 100 | 25 |
| Octane-TDdDGA | 1.2 | 4.988, 4.988, 4.988 | 10 | 400 | 12 | 3 |
| Octane-TDdDGA | 2 | 4.993, 4.993, 4.993 | 10 | 400 | 20 | 5 |
| Octane-TDdDGA | 3.5 | 5.019, 5.019, 5.019 | 10 | 400 | 48 | 12 |
| Octane-TDdDGA | 6 | 5.012, 5.012, 5.012 | 10 | 400 | 60 | 15 |
| Octane-TDdDGA | 8 | 5.030, 5.030, 5.030 | 10 | 400 | 80 | 20 |
| Octane-TDdDGA | 10 | 5.041, 5.041, 5.041 | 10 | 400 | 100 | 25 |
| Decane-THDGA | 1.2 | 5.162, 5.162, 5.162 | 10 | 400 | 12 | 3 |
| Decane-THDGA | 2 | 5.187, 5.187, 5.187 | 10 | 400 | 20 | 5 |
| Decane-THDGA | 3.5 | 5.206, 5.206, 5.206 | 10 | 400 | 48 | 12 |
| Decane-THDGA | 6 | 5.209, 5.209, 5.209 | 10 | 400 | 60 | 15 |
| Decane-THDGA | 8 | 5.215, 5.215, 5.215 | 10 | 400 | 80 | 20 |

| | | | | | | |
|---|---|---|---|---|---|---|
| Decane-THDGA | 10 | 5.244, 5.244, 5.244 | 10 | 400 | 100 | 25 |
| Decane-TODGA | 1.2 | 5.197, 5.197, 5.197 | 10 | 400 | 12 | 3 |
| Decane-TODGA | 2 | 5.204, 5.204, 5.204 | 10 | 400 | 20 | 5 |
| Decane-TODGA | 3.5 | 5.232, 5.232, 5.232 | 10 | 400 | 48 | 12 |
| Decane-TODGA | 6 | 5.234, 5.234, 5.234 | 10 | 400 | 60 | 15 |
| Decane-TODGA | 8 | 5.242, 5.242, 5.242 | 10 | 400 | 80 | 20 |
| Decane-TODGA | 10 | 5.268, 5.268, 5.268 | 10 | 400 | 100 | 25 |
| Decane-TDDGA | 1.2 | 5.233, 5.233, 5.233 | 10 | 400 | 12 | 3 |
| Decane-TDDGA | 2 | 5.233, 5.233, 5.233 | 10 | 400 | 20 | 5 |
| Decane-TDDGA | 3.5 | 5.259, 5.259, 5.259 | 10 | 400 | 48 | 12 |
| Decane-TDDGA | 6 | 5.263, 5.263, 5.263 | 10 | 400 | 60 | 15 |
| Decane-TDDGA | 8 | 5.278, 5.278, 5.278 | 10 | 400 | 80 | 20 |
| Decane-TDDGA | 10 | 5.278, 5.278, 5.278 | 10 | 400 | 100 | 25 |
| Decane-TDdDGA | 1.2 | 5.251, 5.251, 5.251 | 10 | 400 | 12 | 3 |
| Decane-TDdDGA | 2 | 5.266, 5.266, 5.266 | 10 | 400 | 20 | 5 |
| Decane-TDdDGA | 3.5 | 5.283, 5.283, 5.283 | 10 | 400 | 48 | 12 |
| Decane-TDdDGA | 6 | 5.289, 5.289, 5.289 | 10 | 400 | 60 | 15 |
| Decane-TDdDGA | 8 | 5.296, 5.296, 5.296 | 10 | 400 | 80 | 20 |
| Decane-TDdDGA | 10 | 5.315, 5.315, 5.315 | 10 | 400 | 100 | 25 |
| Dodecane-THDGA | 1.2 | 5.443, 5.443, 5.443 | 10 | 400 | 12 | 3 |
| Dodecane-THDGA | 2 | 5.480, 5.480, 5.480 | 10 | 400 | 20 | 5 |
| Dodecane-THDGA | 3.5 | 5.458, 5.458, 5.458 | 10 | 400 | 48 | 12 |
| Dodecane-THDGA | 6 | 5.470, 5.470, 5.470 | 10 | 400 | 60 | 15 |

| | | | | | | |
|---|---|---|---|---|---|---|
| Dodecane-THDGA | 8 | 5.484, 5.484, 5.484 | 10 | 400 | 80 | 20 |
| Dodecane-THDGA | 10 | 5.499, 5.499, 5.499 | 10 | 400 | 100 | 25 |
| Dodecane-TODGA | 1.2 | 5.459, 5.459, 5.459 | 10 | 400 | 12 | 3 |
| Dodecane-TODGA | 2 | 5.480, 5.480, 5.480 | 10 | 400 | 20 | 5 |
| Dodecane-TODGA | 3.5 | 5.482, 5.482, 5.482 | 10 | 400 | 48 | 12 |
| Dodecane-TODGA | 6 | 5.484, 5.484, 5.484 | 10 | 400 | 60 | 15 |
| Dodecane-TODGA | 8 | 5.500, 5.500, 5.500 | 10 | 400 | 80 | 20 |
| Dodecane-TODGA | 10 | 5.533, 5.533, 5.533 | 10 | 400 | 100 | 25 |
| Dodecane-TDDGA | 1.2 | 5.482, 5.482, 5.482 | 10 | 400 | 12 | 3 |
| Dodecane-TDDGA | 2 | 5.485, 5.485, 5.485 | 10 | 400 | 20 | 5 |
| Dodecane-TDDGA | 3.5 | 5.514, 5.514, 5.514 | 10 | 400 | 48 | 12 |
| Dodecane-TDDGA | 6 | 5.514, 5.514, 5.514 | 10 | 400 | 60 | 15 |
| Dodecane-TDDGA | 8 | 5.536, 5.536, 5.536 | 10 | 400 | 80 | 20 |
| Dodecane-TDDGA | 10 | 5.551, 5.551, 5.551 | 10 | 400 | 100 | 25 |
| Dodecane-TDdDGA | 1.2 | 5.512, 5.512, 5.512 | 10 | 400 | 12 | 3 |
| Dodecane-TDdDGA | 2 | 5.523, 5.523, 5.523 | 10 | 400 | 20 | 5 |
| Dodecane-TDdDGA | 3.5 | 5.544, 5.544, 5.544 | 10 | 400 | 48 | 12 |
| Dodecane-TDdDGA | 6 | 5.544, 5.544, 5.544 | 10 | 400 | 60 | 15 |
| Dodecane-TDdDGA | 8 | 5.556, 5.556, 5.556 | 10 | 400 | 80 | 20 |
| Dodecane-TDdDGA | 10 | 5.564, 5.564, 5.564 | 10 | 400 | 100 | 25 |
| Tetdecane-THDGA | 1.2 | 5.666, 5.666, 5.666 | 10 | 400 | 12 | 3 |
| Tetdecane-THDGA | 2 | 5.680, 5.680, 5.680 | 10 | 400 | 20 | 5 |
| Tetdecane-THDGA | 3.5 | 5.687, 5.687, 5.687 | 10 | 400 | 48 | 12 |

| | | | | | | |
|---|---|---|---|---|---|---|
| Tetdecane-THDGA | 6 | 5.705, 5.705, 5.705 | 10 | 400 | 60 | 15 |
| Tetdecane-THDGA | 8 | 5.709, 5.709, 5.709 | 10 | 400 | 80 | 20 |
| Tetdecane-THDGA | 10 | 5.720, 5.720, 5.720 | 10 | 400 | 100 | 25 |
| Tetdecane-TODGA | 1.2 | 5.688, 5.688, 5.688 | 10 | 400 | 12 | 3 |
| Tetdecane-TODGA | 2 | 5.697, 5.697, 5.697 | 10 | 400 | 20 | 5 |
| Tetdecane-TODGA | 3.5 | 5.714, 5.714, 5.714 | 10 | 400 | 48 | 12 |
| Tetdecane-TODGA | 6 | 5.705, 5.705, 5.705 | 10 | 400 | 60 | 15 |
| Tetdecane-TODGA | 8 | 5.717, 5.717, 5.717 | 10 | 400 | 80 | 20 |
| Tetdecane-TODGA | 10 | 5.733, 5.733, 5.733 | 10 | 400 | 100 | 25 |
| Tetdecane-TDDGA | 1.2 | 5.722, 5.722, 5.722 | 10 | 400 | 12 | 3 |
| Tetdecane-TDDGA | 2 | 5.722, 5.722, 5.722 | 10 | 400 | 20 | 5 |
| Tetdecane-TDDGA | 3.5 | 5.719, 5.719, 5.719 | 10 | 400 | 48 | 12 |
| Tetdecane-TDDGA | 6 | 5.735, 5.735, 5.735 | 10 | 400 | 60 | 15 |
| Tetdecane-TDDGA | 8 | 5.737, 5.737, 5.737 | 10 | 400 | 80 | 20 |
| Tetdecane-TDDGA | 10 | 5.765, 5.765, 5.765 | 10 | 400 | 100 | 25 |
| Tetdecane-TDdDGA | 1.2 | 5.734, 5.734, 5.734 | 10 | 400 | 12 | 3 |
| Tetdecane-TDdDGA | 2 | 5.523, 5.523, 5.523 | 10 | 400 | 20 | 5 |
| Tetdecane-TDdDGA | 3.5 | 5.761, 5.761, 5.761 | 10 | 400 | 48 | 12 |
| Tetdecane-TDdDGA | 6 | 5.761, 5.761, 5.761 | 10 | 400 | 60 | 15 |
| Tetdecane-TDdDGA | 8 | 5.781, 5.781, 5.781 | 10 | 400 | 80 | 20 |
| Tetdecane-TDdDGA | 10 | 5.781, 5.781, 5.781 | 10 | 400 | 100 | 25 |

### 2.2.13 Electronic single pan balance

A calibrated electronic single pan balance with a sensitivity of 0.01 mg was used for weighing the reagents.

### 2.2.14 Density, viscosity and refractive index measurements

The density and viscosity of the organic phase was determined using Anton Paar Lovis 2000ME rolling ball viscometer. It measures the rolling time of a ball through transparent liquids using Höppler’s principle. The refractive index of the organic solutions was measured using Anton Paar Abbemat 200 refractometer.

## 2.3 Preparation of Fast Reactor Simulated High-Level Liquid Waste (FR-SHLLW)

The typical composition of FR-SHLLW of the fuel with burn-up of 80,000 MWd/Te and cooled for two years was shown in Table 2.1[21]. For the preparation of FR-SHLLW solution, stock solution of different metal ions of was prepared by taking known concentrations. The stock solution for metal nitrate salts was prepared by dissolving of individual metal ion in nitric acid (≤ 1 M). The oxide salts were initially dissolved in nitric acid twice under IR lamp and finally the stock solutions were prepared using desired nitric acid solution. The concentration of metal ion in its stock solution was estimated using ICP-OES and complexometric titration. Simulated HLLW was prepared by adding the appropriate amount of stock solution of each metal ion together in nitric acid. Finally the nitric acid concentration was adjusted to 3M using nitric acid. The final acidity was determined by standard acid-base titrations using standard NaOH and phenolphthalein indicator. During titration saturated potassium oxalate solution was added to prevent interfaces from hydrolysable ions.

**Table 2.2.** The simulated composition of fast reactor high-level liquid waste (FR-SHLLW). The composition is based on the HLLW arising from reprocessing of spent fast reactor fuel with a burn-up of 80,000 MWd/Te and 2 year cooling [21].

| Element | Concentration [g/L] | Element | Concentration [g/L] | Element | Concentration [g/L] |
|---|---|---|---|---|---|
| La | 0.342 | Mo | 1.092 | Cs | 1.125 |
| Ce | 0.684 | Cr | 0.101 | Rb | 0.055 |
| Pr | 0.339 | Te | 0.163 | Se* | 0.002 |
| Nd | 1.125 | Cd | 0.038 | Na | 3.000 |
| Sm | 0.306 | Ni | 0.1 | Ag | 0.109 |
| Pm* | 0.053 | Sr | 0.147 | Tc* | 0.262 |
| Eu | 0.032 | Ba | 0.414 | Sb* | 0.007 |
| Gd | 0.065 | Ru | 0.813 | $^{241}$Am | 0.218 |
| Tb* | 0.011 | Pd | 0.600 | $^{(152+154)}$Eu | Tracer |
| Dy | 0.006 | Zr | 0.822 | [$HNO_3$] | ~ 3 M |
| Y | 0.074 | Rh | 0.262 | | |
| Fe | 0.5 | Sn* | 0.163 | | |

* Sb, Sn, Se – were not added due to they are sparingly soluble. La was added instead of Tb, and Pm. Mo was added for Tc.

## 2.4 Experimental procedures

### 2.4.1 Distribution ratio measurements

All equilibration experiments were conducted in duplicate at 298 K using an aqueous to organic phase ratio of unity. All the distribution ratio values were measured in duplicate, after pre-equilibration of organic phases with the required concentration of nitric acid. The organic phase was composed of TEHDGA/*n*-DD or TEHDGA-HA/*n*-DD or HA/*n*-DD or DOHyA/*n*-DD or DOHyA-HDEHP/*n*-DD or DOHyA-HDEHDGA/*n*-DD or HDEHDGA/*n*-DD. The aqueous phase was composed of nitric acid solution or FR-SHLLW spiked with desired radioactive tracer

($^{(152+154)}$Eu(III) or $^{241}$Am(III)). The nitric acid concentration in aqueous phase was varied from 0.001M to 4 M. The organic phase was pre-equilibrated with desired aqueous phase. The extraction experiments involved mixing of aqueous and organic phases (1 mL each) in a 5 mL capacity test tube and rotated in up-side-down manner for about an hour. After equilibration, the radioactivity present in organic and aqueous phases was measured by using a well-type NaI(Tl) scintillation detector. The distribution ratio ($D_M$) of metal ion was determined using equation 2.2.

$$D_M = \frac{[M]_{org}}{[M]_{aq}}, \ M = {}^{241}\text{Am(III)}, \ {}^{(152+154)}\text{Eu(III)} \qquad \text{............ (2.2)}$$

The distribution ratio of various elements present in FR-SHLLW was determined by equilibrating an organic phase composed of TEHDGA+HA/*n*-DD or DOHyA+HDEHP/*n*-DD or DOHyA+ HDEDHDGA/*n*-DD with an aqueous phase consisted of FR-SHLLW spiked with $^{241}$Am, $^{152+154}$Eu, and $^{137}$Cs tracers. Experiments were carried out in presence and absence of aqueous complexing agent (CyDTA) to hold back unwanted metal ions. After equilibration, the concentration of various elements in aqueous phase was analyzed by ICP-AES. The concentration of radioactive nuclides in FR-SHLLW was analyzed by high purity germanium coupled with multichannel analyzer. The distribution ratio ($D_M$) of non radioactive metal ions in organic phase was calculated by using an equation 2.3.

$$D_M = \frac{[M^{n+}]^{aq.}_{ini.} - [M^{n+}]^{aq.}_{fin.}}{[M^{n+}]^{aq.}_{fin.}} \qquad \text{... ... ... ... (2.3)}$$

$[M^{n+}]^{aq.}_{ini.}$ is the initial metal ion concentration in aqueous phase and $[M^{n+}]^{aq.}_{fin.}$ is the final metal ion concentration in aqueous phase.

### 2.4.2 Stripping experiments

Batch equilibration was performed to obtain the number of contacts needed for the recovery of Am(III) and Eu(III) from the loaded organic phase. The organic phase composed of TEHDGA/*n*-DD or TEHDGA-HA/*n*-DD or HA/*n*-DD or DOHyA/*n*-DD or DOHyA-HDEHP/*n*-DD or DOHyA-HDEHDGA/*n*-DD or HDEHDGA/*n*-DD was pre-equilibrated with 3 M nitric acid. About 3 mL of pre-equilibrated organic phase was equilibrated with the aqueous solution of 3 M nitric acid or FR-SHLLW spiked with required radioactive tracer $^{(152+154)}$Eu(III) and $^{241}$Am(III). The percentage extraction of Am(III) and Eu(III) into organic phase was determined by measuring the radioactivity of organic and aqueous phases using High Purity Germanium (HPGe) detector coupled with a multichannel analyzer. The recovery of Am(III) and Eu(III) from the organic phase was studied by contacting equal volume of the organic phase with aqueous formulation containing various complexing agents such DTPA and CA, HEDTA, EDTA, $SO_3$-Ph-BTP at various pH values. The radioactivity of $^{(152+154)}$Eu(III) and $^{241}$Am(III) present in the aqueous phase was measured and therefore the amount of Eu(III) or Am(III) back-extracted into aqueous phase was determined. The aqueous phase was then removed completely and the organic phase was contacted again with equal volume of fresh aqueous formulation for subsequent back-extraction. The percentage back-extraction was measured in each contact from the radioactivity measurements. This procedure was repeated until the aqueous phase and organic phase radioactivity of $^{241}$Am(III) and$^{(152+154)}$ Eu(III) was negligible.

### 2.4.3 Third phase formation studies

For equilibration studies the organic and aqueous phases were taken in a stoppered test tube and mixed at 298 K. The equilibration experiments were performed by immersing the stoppered test tube in a double walled glass jacket at a constant temperature of 298 K, and rotated for about one hour. The nitric acid concentration was varied from 1 M to ~16 M and the nitric acid distributed between the organic and aqueous phases was determined by standard acid-base titration to phenolphthalein endpoint. In some cases, the third phase formed in organic phase at a particular concentration of nitric acid was dissolved by adding distilled water, drop wise, to the organic and aqueous phases under stirring. The addition of water was continued until the third phase was dissolved completely. The organic and aqueous phases were allowed to settle, and the concentration of nitric acid in organic phase, known as the limiting organic concentration (LOC) of nitric acid, and the aqueous phase concentration of nitric acid known as critical aqueous phase concentration (CAC) of nitric acid were determined.

For the Nd(III) extraction studies, The organic phase was composed of a solution of TEHDGA/*n*-DD or TEHDGA-HA/*n*-DD or HA/*n*-DD or DOHyA/*n*-DD or DOHyA-HDEHP/*n*-DD or DOHyA-HDEHDGA/*n*-DD or HDEHDGA/*n*-DD and the aqueous phase was composed of Nd(III) solution in nitric acid. The concentrations of nitric acid was varied from 1 M to 10 M, and the Nd(III) concentration in aqueous phase was varied from 1 g/L to 15 g/L. The organic phase was pre-equilibrated with desired concentration of nitric acid before Nd(III) extraction. Then the pre-equilibrated organic phase was mixed with an aqueous phase in a 15 mL capacity test tube for third phase formation studies. The mixing of organic and aqueous phases results in the extraction of nitric acid and Nd(III). The third phase formation studies were performed by the procedure, as discussed above. However, the third phase was dissolved by adding the nitric acid pre-equilibrated organic phase to the triphasic system. The limiting organic phase concentration (LOC) and the critical aqueous phase concentration of Nd(III) for third phase formation was determined by complexometric EDTA titration and methyl thymol blue used as indicator

## 2.5 Synthesis of extractants

### 2.5.1 Synthesis of *N, N*-di octyl hydroxyacetamide

The synthesis of *N*,*N*-di-octyl-2-hydroxyacetamides was carried out by the procedure described elsewhere [22]. The schematic procedure for the synthesis of DOHyA is shown in Figure 2.2.

**Step 1. Synthesis of acetoxy acetamide from acetoxyacetyl chloride.**

A 250 mL three neck round bottom flask taken and filled around 50-60 mL dry chloroform and acetoxy acetyl chloride (one eq) and the RB flask containing solution is immersed in an ice-bath maintained at 0-5$^0$C. A solution of tri-ethylamine (1.2 eq) and the corresponding *N*,*N*-dioctylamine (one eq) in dry chloroform (50 mL) taken in dropping funnel and then added drop wise to acetoxy acetyl chloride solution under inert atmosphere. The reaction mixture was stirred for four to five hours at room temperature and then the chloroform was removed under high pressure vaccum. The crude was then extracted with *n*-hexane then two times washed with water to remove all the precipitated triethylamine hydrochloride and unreacted amine. The hexane extracted solution was then successively twice washed with 1 M HCl and with water then saturated sodium bi-carbonate solutions. Finally, the compound was dried over anhydrous sodium sulphate and removed the *n*-hexane from the compound by rotary evaporator to get the corresponding acetoxy aceatamide. The characterization data for the N,N-dioctyl hydroxyacetamide is given below. The yield obtained was 85-90 %.

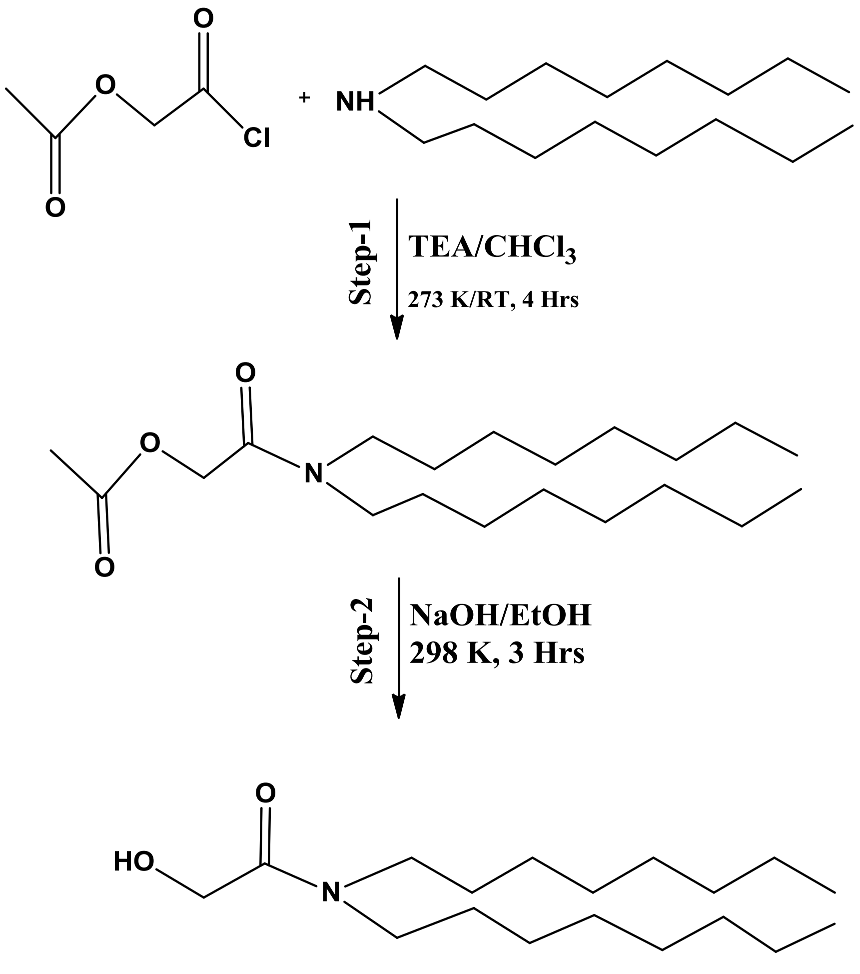

***N,N*-dioctyl-2-hydroxyacetamide (DOHyA)**

**Figure 2.2**. Schematic representation of synthesis of DOHyA

**Step 2. Hydrolysis of acetoxy acetamide**

The product obtain from the step 1 was taken into single neck flask and dissolved in methanol. The desired amount of sodium hydroxide was dissolved in 50 mL of methanol at room temperature. The sodium hydroxide solution was added to the RB flask and stirred for the two hour at room temperature. After completion of the reaction, the methanol was removed from the reaction mixture by using rotatary evaporator. The mixture was dissolved in n-hexane and transferred to the separating funnel for the workup. The mixture was washed as mentioned in above in successive manner of water, 1 M HCl and sodium carbonate and finally dried over anhydrous sodium sulphate and the hexane removed under high vaccum. The crude product was then purified by column chromatography over silica gel using 10% ethyl acetate-petroleum ether as eluent.

***N*,*N*-di-octyl-2-hydroxy acetamide(DOHyA):** (pale yellow liquid, yield: 95%)

$^1$H NMR ($CDCl_3$, δ relative to TMS): 4.138 (d, 2H, J=4Hz), 3.706 (t, 1H, J=4Hz), 3.361 (t, 2H, J=8Hz), 3.047 (t, 2H, J=8Hz), 1.538 (m,4H), 1.286 (m,20H), 0.883 (m, 6H). $^{13}$C NMR ($CDCl_3$, δ relative to TMS): 171.01, 59.71, 46.11, 45.82, 31.77(d), 29.31, 29.22(d), 29.12, 28.52, 27.54, 26.96, 26.81, 22.60(d), 14.03(d).

IR (neat, ν $cm^{-1}$): 3410 (medium, broad, O-H stretch), 2926, 2858 (strong, C-H stretch), 1652 (very strong, C=O stretch), 1462 (medium, -$CH_2$-scissoring), 1402 (medium, C-N stretch), 1278 (medium, -$CH_2$-wagging), 1090 (strong, C-O stretch of hydroxyl group).

### 2.5.2 Synthesis of Bis(2-ethylhexyl) diglycolamic acid (HDEHDGA)

Diglycolic anhydride (1eq.) was dissolved in chloroform (30 mL) and the solution was taken in a three neck round bottom flask. A solution of bis(2-ethyhexyl)amine (1eq.) and tri-ethylamine (1.2 eq) in chloroform solution was taken in a dropping funnel and added drop-wise to diglycolic anhydride solution about an hour. The reaction mixture was stirred at room temperature for six hours to obtain bis (2-ethyl hexyl) diglycolamic acid. After completion of reaction, the chloroform was removed from the reaction mixture and dissolved in *n*-hexane. The dissolved solution was transferred into the separating funnel then washed with distilled water followed by ~1 M HCl and again by distilled water in order to remove the unreacted reactants, if any. The diglycolic anyhydride is water soluble and can be washed out. The organic phase was dried with anhydrous sodium sulphate, and the solvent was removed under vacuum. The structures of diglycolamic acids synthesized in the present study are shown in Figure 2.3. The characterization detail of the compound is given below.

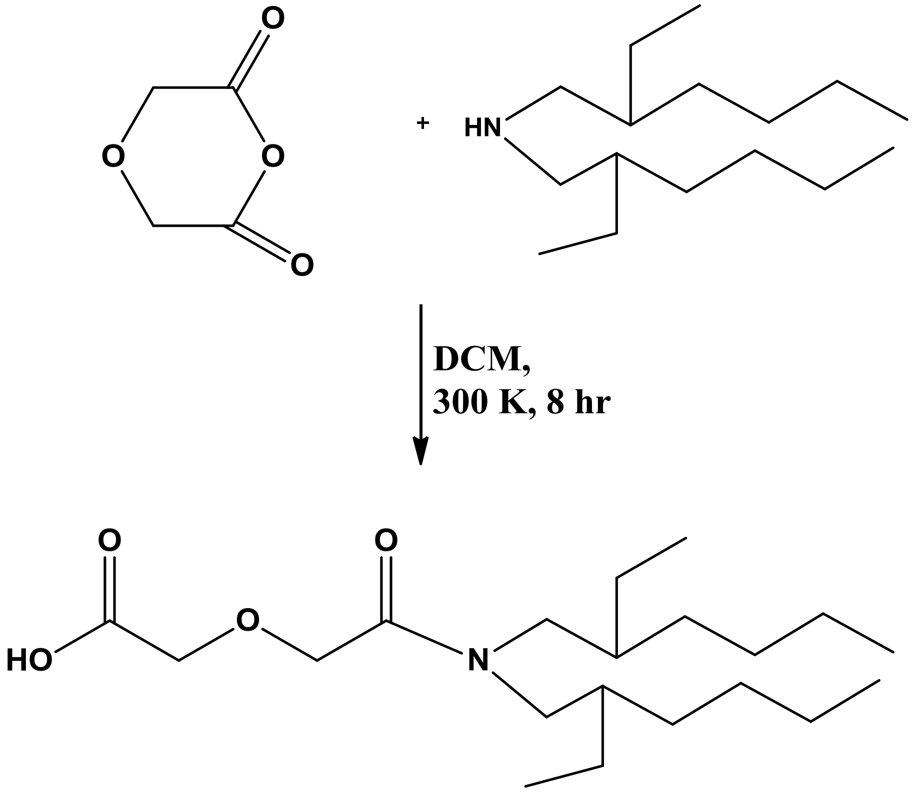

**Bis(2-ethylhexyl)diglycolamic acid**

**Figure 2.3.** The synthetic procedure of Bis(2-ethyhexyl)diglycolamic acid

**Bis(2-ethylhexyl) diglycolamic acid (HDEHDGA)** (pale yellow viscous liquid, yield 95 %) **:** $^1$H-NMR (500 MHz, DMSO-d$_6$, TMS, 298 K), δ 10.67 (s, 1H, COO$\underline{H}$), 4.32 (s, 2H, -OCH$_2$-), 4.11(s, 2H, $^-$C$\underline{H}_2$O$^-$), 3.17-3.31 (m, 4H, 2 C$\underline{H}_2$ - N ), 2.96-2.98 (m, 2H, C$\underline{H}$ ), 1.15-1.24 (m, 16H, C$\underline{H}_2$-R), 0.77-0.84(m, 12H, C$\underline{H}_3$ ). $^{13}$C NMR (500MHz, CDCl$_{3,}$ TMS $_,$ 298K): 172.22 , 172.14 ,77.21(-OCH$_2$), 71.1,49.34, 37.16 ,30.35, 28.47, 23.58 , 22.86, 13.93 ,10.47. IR spectrum showed the transmittance bands at the following frequencies (cm$^{-1}$): 3454 (COOH), 1739 (-CO in COOH), 1622(-CO in –CON).

### 2.5.3 Synthesis of symmetrical diglycolamides

The synthesis of symmetrical diglycolmides was carried out in single step as described elsewhere [1]. Diglycolic chloride (1eq.) was mixed with dichloromethane (30 mL), in a round bottom flask equipped with a $CaCl_2$ guard tube. A solution of desired di-alkylamine (1eq.) in dichloromethane (10 mL) was added drop-wise to diglycolic anhydride solution under inert atmosphere at 0-5$^0$C temperature. The reaction mixture was stirred at room temperature for four to eight hours depending upon the nature of the dialkyl amine, to obtain the corresponding dialkyl-diglycolamic acid. The crude solution was then washed with distilled water followed by ~1 M HCl and again by distilled water in order to remove the unreacted reactants, if any. The organic phase was dried with anhydrous sodium sulphate, and the solvent was removed under vacuum. The final product was purified by column chromatography using silica gel using 20% ethyl acetate-petroleum ether as mobile phase. The final products were then characterized by IR and NMR spectroscopic techniques. The schematic procedure for the synthesis of symmetrical diglycolamides is shown in Figure 2.4. The characterization details of the compounds are given below.. The characterization details of the compounds are given below.

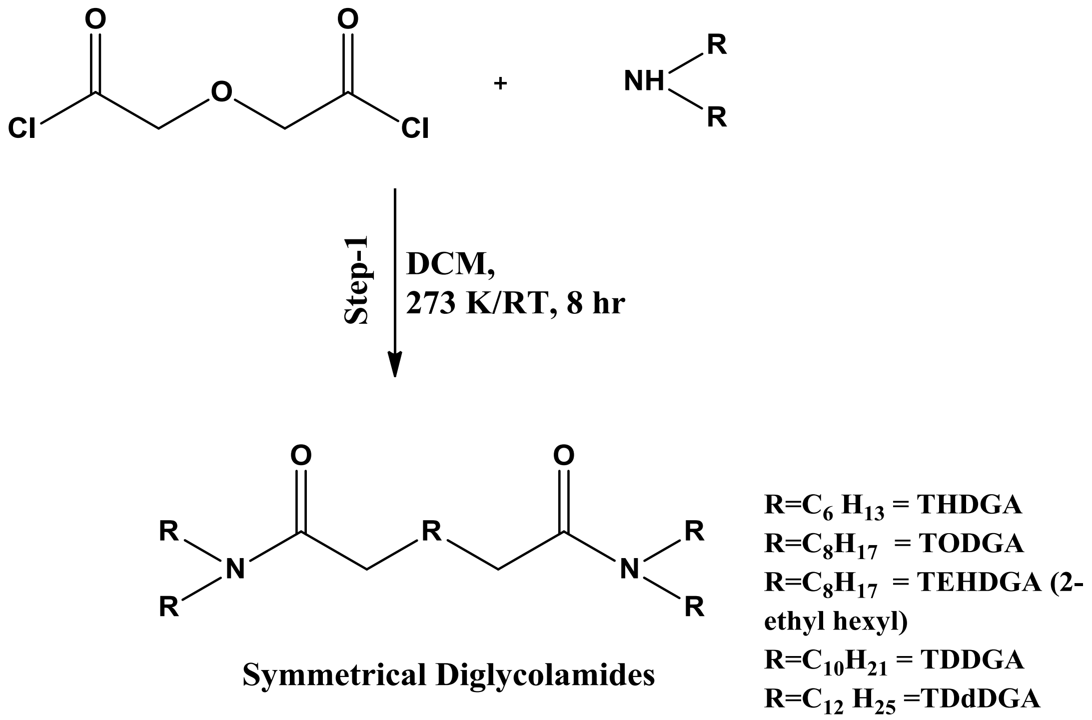

**Figure 2.4.** Schematic representation of synthesis of symmetrical diglycolamides

**Characterization studies of tetraalkyl digycolmides**

***N,N,N'N'*-Tetrahexyldiglycolmide** (pale yellow liquid, yield: 90-95%):

$^1$H-NMR (500 MHz, $CDCl_3$, TMS, 298 K), $\delta$ 0.88 (t, 12H, N-$(CH_2)_5$-$CH_3$), 1.27, 1.56 (m, 32 H, -N-$CH_2$-$(CH_2)_4$-$CH_3$), 3.22 (t, 8 H, -N-$CH_2$-$(CH_2)_4$-$CH_3$), 4.26 (s, 4H,-N-CO-$CH_2$-O-). The IR spectrum showed the transmittance bands at the following frequencies (cm$^{-1}$) 2918, 2849 (-$CH_3$-stretching), 1658 (C=O stretching), 1465 ($CH_2$-bending), 1355 (–C-N- stretching), 1360 (–$CH_3$-bending), 1117 (C-O-stretching). The mass spectrum showed a peak at m/z 468.4.

***N,N,N'N'*-Tetraoctyldiglycolmide** (pale yellow liquid, yield: 90%)**:**

$^1$H-NMR (500 MHz, CDC13, TMS, 298 K), $\delta$ 0.88 (t, 12H, N-$(CH_2)_7$-$CH_3$), 1.27, 1.56 (m, 48 H, N-$CH_2$-$(CH_2)_6$-$CH_3$), 3.22 (t, 8 H, -N-$CH_2$-$(CH_2)_6$-$CH_3$), 4.26 (s, 4H,-N-CO-$CH_2$-O-). The IR spectrum showed the transmittance bands at the following frequencies (cm$^{-1}$) 2918, 2849 (-$CH_3$-

stretching), 1658 (C=O stretching), 1465 ($CH_2$-bending), 1355 (–C-N- stretching), 1360 (–$CH_3$-bending), 1117 (C-O-stretching). The mass spectrum showed a peak at m/z 580.6.

***N,N,N'N'*-Tetradecyldiglycolmide** (pale yellow liquid, yield: 90-92%)**:**

$^1$H-NMR (500 MHz, CDCl3, TMS, 298 K), δ 0.88 (t, 12H, N-$(CH_2)_9$-$CH_3$), 1.27, 1.56 (m, 64 H, - N-$CH_2$-$(CH_2)_8$-$CH_3$), 3.22 (t, 8 H, -N-$CH_2$-$(CH_2)_8$-$CH_3$), 4.26 (s, 4 H,-N-CO-$CH_2$-O-). The IR spectrum showed the transmittance bands at the following frequencies (cm$^{-1}$) 2918, 2849 (-$CH_3$-stretching), 1658 (C=O stretching), 1465 ($CH_2$-bending), 1355 (–C-N- stretching), 1360 (–$CH_3$-bending), 1116 (C-O-stretching). The mass spectrum showed a peak at m/z 692.8.

***N,N,N'N'*-Tetradodecyldiglycolmide** (pale yellow liquid, yield: 85-90%)**:**

$^1$H-NMR (500 MHz, CDCl3, TMS, 298 K), δ 0.88 (t, 12H, N-$(CH_2)_{11}$-$CH_3$), 1.27, 1.56 (m, 80 H, --N-$CH_2$-$(CH_2)_{10}$-$CH_3$), 3.22 (t, 8 H, -N-$CH_2$-$(CH_2)_{10}$-$CH_3$), 4.26 (s, 4 H,-N-CO-$CH_2$-O-). The IR spectrum showed the transmittance bands at the following frequencies (cm$^{-1}$) 2918, 2849 (-$CH_3$-stretching), 1659 (C=O stretching), 1465 ($CH_2$-bending), 1355 (–C-N- stretching), 1360 (–$CH_3$-bending), 1117 (C-O-stretching). The mass spectrum showed a peak at m/z 804.8.

## References

1. S.A. Ansari, P.N. Pathak, P.K. Mohapatra, V.K. Manchanda, Chemistry of diglycolamides: Promising extractants for actinide partitioning, Chem.Rev.112 (2012) 1751-1772.
2. J. A. Partridge, R. C. Jensen, Purification of Di-(2-Ethylhexyl)Phosphoric Acid by Precipitation of Copper(II) Di-(2-Ethylhexyl)Phosphate, J. Inorg. Nucl. Chem. 31 (1969) 2587–2589.
3. H. Zhengshui, P. Ying, M. Wanwu, F. Xun, Purification of organophosphorus acid extractants, Solvent Extr. Ion Exch. 13 (1995) 965-976.
4. V. E. Holfeltz, E.L. Campbell, D.R. Peterman, R.F. Standaert, A. Paulenova, G.J. Lumetta, T.G. Levitskaia, Effect of HEH[EHP] Impurities on the ALSEP Solvent Extraction Process, Solvent Extr. Ion Exch. 36 (2018) 22–40.
5. R. Pecora, R. ed., Dynamic light scattering: applications of photon correlation spectroscopy. Springer Science & Business Media.
6. P.A. Hassan, S. Rana, G. Verma, Making sense of Brownian motion: colloid characterization by dynamic light scattering, Langmuir. 31 (2014) 3-12.
7. A. Cao, Light scattering. Recent applications, Anal. Lett. 36 (2003) 3185-3225.
8. Y. Song, L.L. Dai, The shear viscosities of common water models by non-equilibrium molecular dynamics simulations, Mol. Simul. 36 (2010) 560–567.
9. W.D. Cornell, P. Cieplak, C.I. Bayly, I.R. Gould, K.M. Merz, D.M. Ferguson, D.C. Spellmeyer, T. Fox, J.W. Caldwell, P. A. Kollman, A 2nd generation Force –Field for the Simulation of Proteins, Nucleic-Acids and Organic Molecules, J. Am. Chem. Soc.117 (1995*)* 5179 – 5197.

10. A.D. Becke, Density-Functional Exchange-Energy Approximation with Correct Asymptotic Behavior, Phys. Rev. A. 38 (1988) 3098-3100.
11. J.P. Perdew, Density functional approximation for the correlation energy of the inhomogeneous electron gas, Phys. Rev. B. 33 (1986) 8822-8824.
12. R. Ahlrichs, M. Bar, M. Haser, H. Horn, C. Kolmel, Electronic structure calculations on workstation computers: The program system turbomole, Chem. Phys. Lett. 162 (1989) 165-169.
13. J. Mark, M.J. Abraham, J.E. Gready, Optimization of parameters for molecular dynamics simulation using smooth particle-mesh Ewald in GROMACS 4.5, J. Comput. Chem. 32(2011) 2031-2040.
14. B.A. Luty, M.E. Davis, I.G. Tironi, W. F. van Gunsteren, A Comparison of Particle-Particle, Particle-Mesh and Ewald Methods for Calculating Electrostatic Interactions in Periodic Molecular Systems, J. Mol. Simul. 14 (1994) 11-20.
15. A.Y. Toukmaji, J.A. Broad, Ewald summation techniques in perspective: a survey Computer Physics Communications, Phys. Commun.95 (1996) 73-92.
16. E. Lindahl, B. Hess, D. van der Spoel, GROMACS 3.0: a package for molecular simulation and trajectory analysis, J. Mol. Model.7( 2001) 306–317.
17. S. Pronk, S. Pall, R. Schulz, P. Larsson, P. Bjelkmar, R. Apostolov, M. R. Shirts, J. C. Smith, P.M. Kasson, D. van der Spoel, B. Hess, E. Lindahl, GROMACS 4.5: a high-throughput and highly parallel open source molecular simulation toolkit, Bioinformatics. 29 (2013) 845-854.
18. D.van der Spoel, E. Lindahl, B. Hess, G. Groenhof, A.E. Mark, H.J. Berendsen, GROMACS: Fast, Flexible, and Free, J. Comput. Chem. 26 (2005) 1701−1718.

19. M. Abraham, B. Hess, D.van der Spoel, E. Lindahl, USER MANUAL Version 5.0.7. The GROMACS development teams at the Royal Institute of Technology and Uppsala University, Sweden. 2015.
20. J. N. Mathur, M.S. Murali, M.V. Balarama Krishna, R.H. Iyer, R.R. Chitnis, P.K. Wattal, A.K. Bauri, A. Banerji, Recovery of neptunium from highly radioactive waste solutions of PUREX origin using CMPO, J. Radioanal. Nucl. Chem. Lett. 213 (1996) 419-429.
21. T. Prathibha, B.R. Selvan, K.A. Venkatesan, S. Rajeswari, M.P. Antony, Radiolytic stability of N, N-di-alkyl-2-hydroxyacetamides, J. Radioanal. Nucl. Chem. 311(2017).1929-1935.

# Chapter 3*:* Aggregation behaviour of tetraalkyl diglycolamides in *n*-paraffins

The present chapter discusses about the extraction behavior of nitric acid and Nd(III) in various tetraalkyl diglycolamides dissolved in different *n*-paraffins. The extracted organic phase was subjected to dynamic light scattering, ATR-FTIR and MD simulations to understand the aggregation behavior of the organic phase. The chapter is divided into two parts. Part I deals with the extraction behavior of nitric acid and Nd(III) in a solution of 0.2 M tetraalkyl diglycolamide dissolved in *n*-paraffin and the aggregation behavior of organic phase. Part II details the extraction behavior of Nd(III) from nitric acid solution in TEHDGA in *n*-dodecane The organic phase obtained after extraction was probed by various spectroscopic techniques to understand the aggregation and coordination behavior of Nd(III) with TEHDGA.

# Part I. Extraction and aggregation behavior of various symmetrical diglycolamides in *n*-paraffins

## 3.1 Introduction

Diglycolamides (DGAs) are *N,N,N',N'*-tetraalkyl-3-oxapentane-1,5-diamide derivatives regarded as promising reagents for the extraction of trivalent actinides and lanthanides from high-level nuclear waste [1,2]. The extraction and the third phase formation behavior of trivalent metal ions in DGAs are strongly dependent on the nature of alkyl group attached to 3-oxapentane-1,5-diamide. Sasaki *et al.*, [3–5] studied the physicochemical and extraction properties of symmetrical DGAs, and correlated the observed properties to the nature of alkyl group attached to amidic nitrogen atom. Previously, several authors studied the extraction and third phase formation behavior of Am(III) and Eu(III) in alkyl derivates of DGAs present in various *n*-paraffins. It was reported that the distribution ratio Am(III) and Eu(III) decreased with increase in the chain length of alkyl group attached to the DGA [5,6]. In addition, the tendency of third phase formation was reported to decrease with increase in the chain length of alkyl group attached to DGA molecule [4,5] and increase with increase in the chain length of *n*-paraffinic diluent [7,8]. To unravel the role of alkyl chain length attached to DGA in determining the tendency of third phase formation, the aggregation behavior alkyl diglycolamides in *n*-paraffins was studied as a function of extraction parameters in the present work. The alkyl group attached to the DGA was varied from hexyl to dodecyl moeity. Since the DGAs with alkyl group lower than hexyl exhibit significant solubility in aqueous phase [3–5], these alkyl DGAs (alkyl groups lower than hexyl) are unsuitable for solvent extraction studies. The general structure of symmetrical diglycolamide is shown in Figure 3.1. The extraction behavior of nitric acid and Nd(III) was studied in a solution of 0.2 M alkyl DGAs/*n*-DD. The aggregation behavior of alkyl

DGAs in *n*-DD was probed by dynamic light scattering measurements. Since the amount of trivalent metal ions (lanthanides + actinides) present in nuclear waste varies from 1 g/L to 7 g/ L in 3-4 M nitric acid, the concentration of Nd(III) in aqueous phase was varied from 1 g/L to 7 g/L and the concentration of nitric acid was varied up to ~16 M.

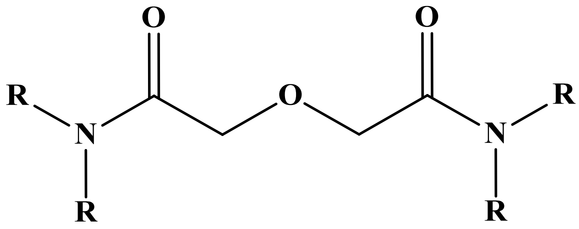

$R=C_6H_{13}$ = THDGA
$R=C_8H_{17}$ = TODGA
$R=C_8H_{17}$ = TEHDGA (2-ethyl hexyl)
$R=C_{10}H_{21}$ = TDDGA
$R=C_{12}H_{25}$ =TDdDGA

**Figure 3.1.** Structure of tetraalkyldiglycolamides

## 3.2 Results and discussion

### 3.2.1 Extraction behaviour of nitric acid

The extraction behavior of nitric acid in 0.2 M alkyl DGAs/*n*-DD is shown in Figure 3.2. The concentration of nitric acid in the aqueous phase was varied from 1 M to concentrated nitric acid (~16 M). It can be seen that the extraction of nitric acid in organic phase increases with increase in the concentration of nitric acid in aqueous phase, in all cases. The concentration of nitric acid extracted in organic phase is quite similar for all DGA derivatives [4,5] . Even though the extraction of nitric was similar, the splitting of organic phase was observed only in case of THDGA and TODGA, after contacting the 0.2 M solution of these diglycolamides in *n*-DD with 2 M and 5 M nitric acid, respectively. However, the third phase was not observed in case of TDDGA and TDdDGA even after contacting the 0.2 M solution of these DGAs in *n*-DD with concentrated nitric acid [4]. The absence of third phase formation in TDDGA and TDdDGA and the formation of the third phase in THDGA and TODGA shows that the alkyl group attached to diglycolamide plays an important role in determining third phase formation.

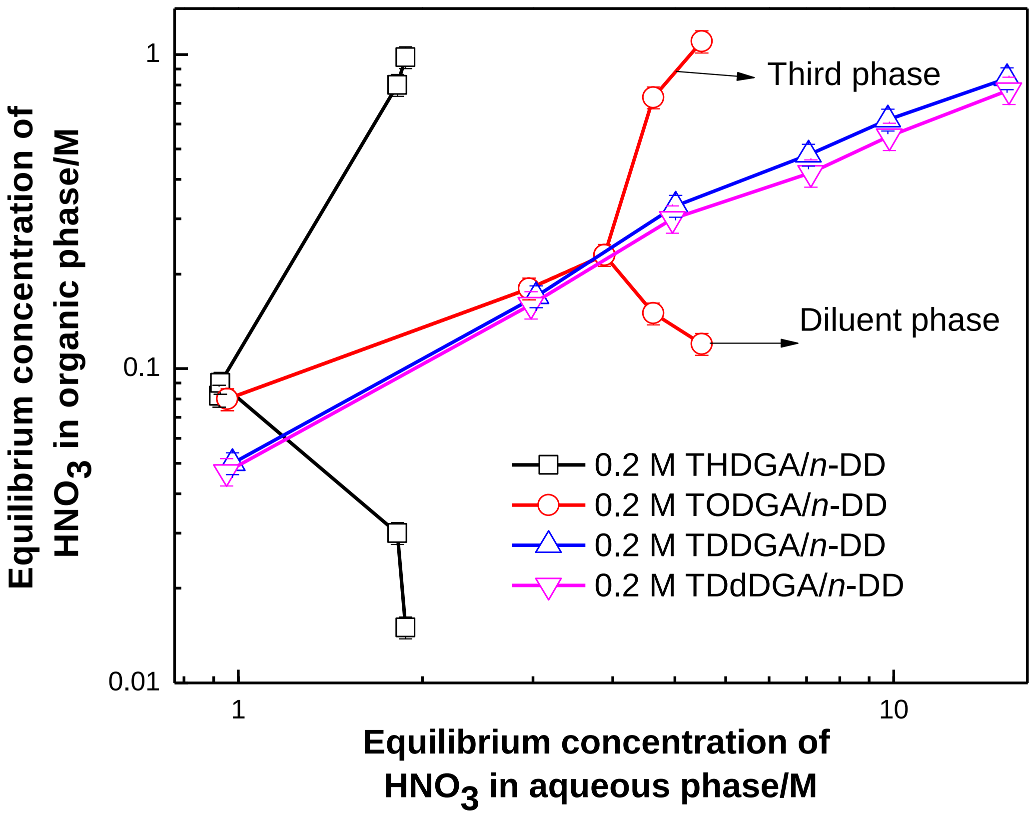

**Figure 3.2.** Extraction behaviour of nitric acid in organic phase as a function of the equilibrium concentration of nitric acid in the aqueous phase at 298 K. Organic phase: 0.2 M alkyl DGA/*n*-DD. Aqueous phase: [$HNO_3$] varied from 1 M to ~ 16 M.

### 3.2.2 Self-aggregation behavior of alkyl DGAs

Third phase formation is due to the aggregation of extractants in *n*-DD medium followed by demixing and expulsion of aggregates from *n*-DD phase at certain conditions. In alkyl diglycolamides, the etheric and amidic functional groups act as polar coordinating sites and the alkyl group attached to this polar moiety serve as a non-polar organophilic group. When such amphiphilic DGAs are dissolved in a non-polar diluent (*n*-dodecane), DGAs tend to undergo self-aggregation in the *n*-dodecane medium due to polar-polar interactions [9–12]. In contrast to this, the alkyl group attached to DGA interacts with *n*-dodecane through Van der Waals forces and such interactions facilitate the dispersion of DGAs in the *n*-DD medium. Therefore, the presence and absence of the third phase is essentially determined by two opposing interactions, one favoring third phase formation and the other favoring dispersion and dissolution of DGAs in *n*-DD [10,13–18].

The self-aggregation of DGAs result in the formation of reverse micellar aggregates, with amidic and etheric group of DGA act as a core and the alkyl group attached to DGA at the periphery of the reverse micelle. The self-aggregation behavior of alkyl DGAs in *n*-DD was investigated by dynamic light scattering studies and the results are shown in Figure 3.3. It can be seen that the relative intensity of aggregates at maximum ($I_{max}$) increases and the full width at half maximum (FWHM) decreases marginally with the increase in the chain length of alkyl group attached to DGA as shown in Table 3.1. The $I_{max}$ represents the relative concentration of aggregates and FWHM represents the size distribution of aggregates in *n*-DD phase. The increase in $I_{max}$ indicates that the concentration of aggregates increases with increase in the chain length of alkyl group attached to DGA. This shows that the DGAs with longer alkyl chain length have the higher tendency to undergo self-aggregation in *n*-DD medium and the self-aggregation increases in order THDGA < TODGA < TDDGA < TDdDGA. The reason for the self-aggregation trend observed in the present system is not clear at present and more studies are needed to understand this behavior. The decrease in FWHM shows that the distribution is narrow in case of DGAs with longer alkyl chain length shown in Table 3.1. It is important to note that the average size of self- aggregates are ~2 nm in all cases, and since these the aggregates are dispersed in *n*-DD, the organic phase is homogeneous. The average aggregate size of 2 nm indicates that it is likely that the DGAs are existing as monomeric form also [14,15,19]. Several authors have determined the size of diglycolamides dispersed in *n*-dodecane as well as in other *n*-paraffins by SANS, SAXS and VPO techniques, and reported a similar size (~ 2 nm) for diglycolamides in *n*-dodecane [14,15,19,20].

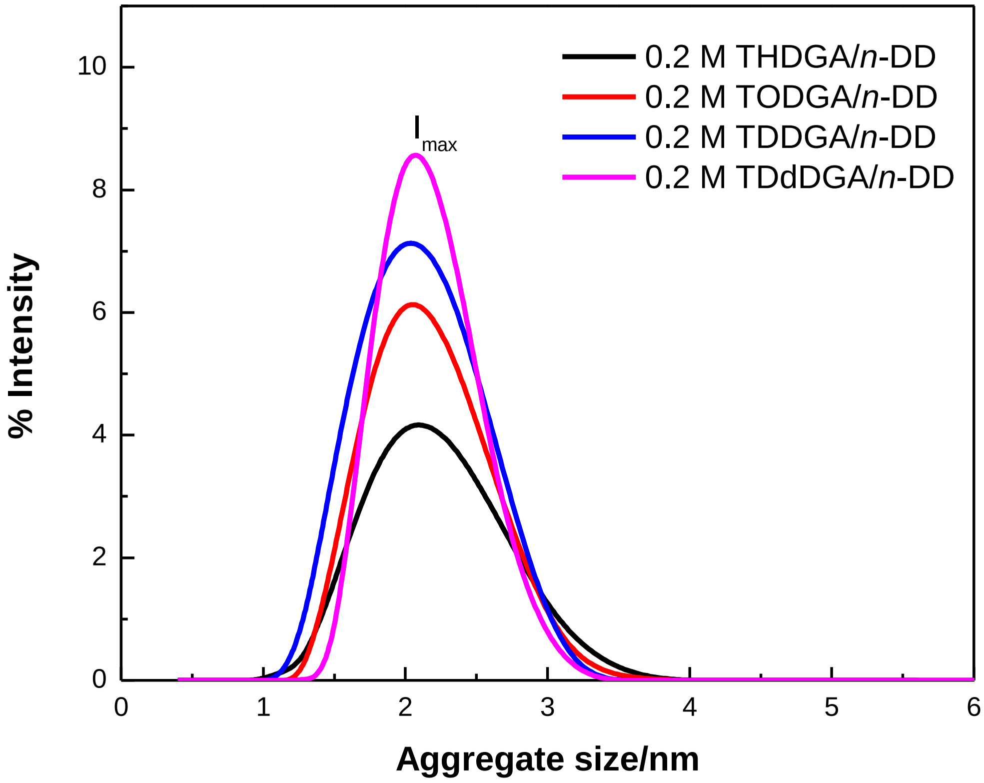

**Figure 3.3.** Self-aggregate distribution of tetraalkyl DGAs in *n*-DD at 298 K.

**Table 3.1.** Full width at half maximum (FWHM)(nm) of aggregate distribution obtained after the extraction of nitric acid in 0.2 M alkyl DGAs/*n*-DD at various concentrations of nitric acid.

| Aqueous phase | 0.2 M THDGA/*n*-DD | 0.2 M TODGA/*n*-DD | 0.2 M TDDGA/*n*-DD | 0.2 M TDdDGA/*n*-DD |
|---|---|---|---|---|
| Neat | 1.2 | 0.96 | 0.88 | 0.78 |
| 1 M $HNO_3$ | 2.36 | 2.25 | 2.1 | 2.05 |
| 3 M $HNO_3$ | - | 8.63 | 2.82 | 2.51 |
| 5 M $HNO_3$ | - | - | 3.8 | 2.8 |
| 10 M $HNO_3$ | - | - | 4.3 | 3.1 |
| ~16 M $HNO_3$ | - | - | 5.8 | 3.6 |

### 3.2.3 Aggregation behavior of acid extracted DGAs

It would be interesting to investigate how the aggregate size of alkyl DGA changes with the extraction of nitric acid in organic phase. When 0.2 M alkyl DGA/*n*-DD was contacted with nitric acid, the DGA present in the organic phase undergoes a protonation reaction leading to the formation of protonated-solvates or acid-solvates (DGA….$(HNO_3)_x$) in organic phase. It should be noted that the nitric acid is extracted into the core of reverse micelles and therefore, the acid extracted aggregates are more polar than the aggregates before extraction [10,21]. As a result, the inter-aggregate interaction among the aggregates present in *n*-DD phase increases and such interaction leads to the formation of bigger and swollen aggregates [19,22]. The degree of aggregation and swelling depends upon the quantity of nitric acid extracted into the organic phase and polarity of acid-solvates in *n*-DD. Figure 3.4 shows aggregation behavior of 0.2 M alkyl DGAs/*n*-DD after equilibrating the organic phase with 1 M nitric acid. The average size of self- aggregates in *n*-DD was determined to be ~ 2 nm for all DGAs, as shown in Figure 3.3 [15,19,20]. However, the average aggregate size obtained after equilibration with 1 M nitric acid increases in the order of TDdDGA < TDDGA < TODGA < THDGA, as shown in 3.4 This shows that DGAs with smaller alkyl group have more tendency to undergo aggregation. This could be due to the relatively predominant polar-polar interactions among the DGA aggregates of smaller alkyl chain length, as compared to the dispersive interactions acting between that DGA and *n*-DD. In contrast to this, the distribution is skewed towards smaller aggregate size in case of DGAs having longer alkyl chain length as shown in Figure 3.4. This shows that these diglycolamides have less tendency to form bigger aggregates. It should be noted that all these aggregates are soluble in *n*-DD irrespective of size and distribution.

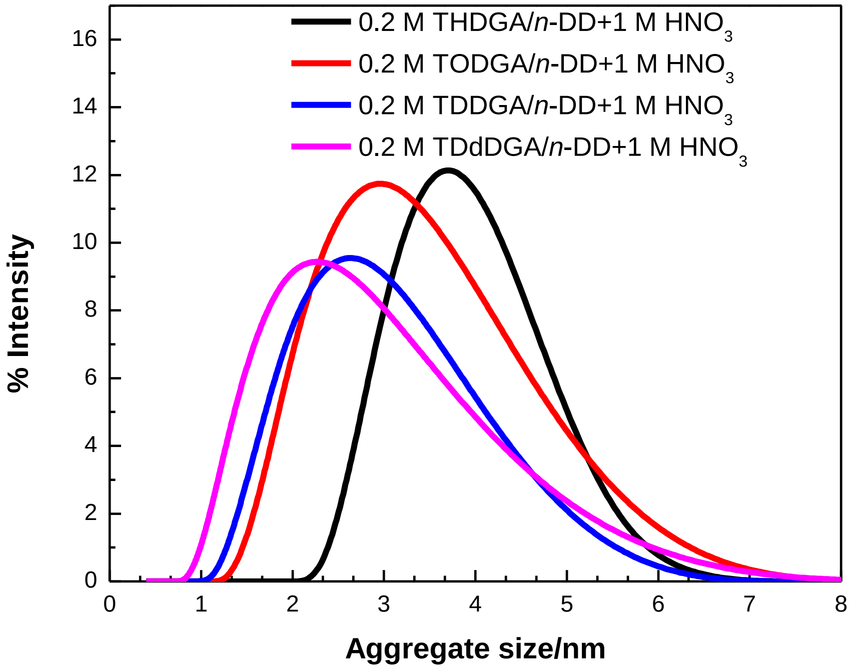

**Figure 3.4.** Aggregate distribution obtained after contacting the 0.2 M alkyl DGAs/*n*-DD phase with 1 M nitric acid at 298 K.

### 3.2.4 Aggregation behavior of third phase

Figure 3.5 shows the aggregation behavior of 0.2 M TODGA in *n*-DD obtained after contacting the organic phase with nitric acid. The nitric acid concentration was varied from 1 M to 5 M. The aggregate distribution was compared with the self-aggregate (without contacting with nitric acid) distribution of 0.2 M TODGA in *n*-DD. It is observed that the average aggregate size and aggregate distribution increases with increase in the concentration of nitric acid from 1 M to 4 M [10,14–16,19]. Increasing the concentration of nitric acid in aqueous phase increases the concentration of protonated-solvates or acid-solvates in organic phase and facilitates the formation of newer and facilitates merger of aggregates. Pathak *et al*. studied the aggregation behavior of 0.1 M TODGA in *n*-DD and 1-octanol. The authors observed that the average aggregate size also increases (1.5 nm at 1 M $HNO_3$ to 10 nm at 6 M $HNO_3$) upon increasing the acid concentration in the aqueous phase [16]. Therefore, the average size of aggregates and FWHM of the distribution increases with increase in the concentration of nitric acid. This trend continues up to 4 M nitric acid. However, when 0.2 M TODGA/*n*-DD was contacted with 5 M nitric acid, the organic phase undergoes splitting into two phases namely the third phase and “diluent rich phase”. The aggregate distribution of third phase and “diluent rich phase” are also shown in Figure 3.5. It can be seen that the average aggregate size of third phase is significantly large (45 nm) as compared to that observed at 4 M nitric acid (25 nm). Since the polar-polar interaction among the aggregates are significantly strong as compared to the dispersive interaction of aggregates at 5 M $HNO_3$, the aggregates are expelled out from bulk *n*-dodecane [12,15,19,20]. The expelled aggregates are concentrated into a small volume of third phase. In the view of this, the value of $I_{max}$ is quite high for third phase than that obtained before third phase formation. Since major quantity of aggregates are transferred to third phase at 5 M nitric acid, the concentration of remaining aggregates in "diluent rich phase" is low. As a result, the aggregate size of "diluent rich" phase is small, as shown in Figure 3.5, as expected.

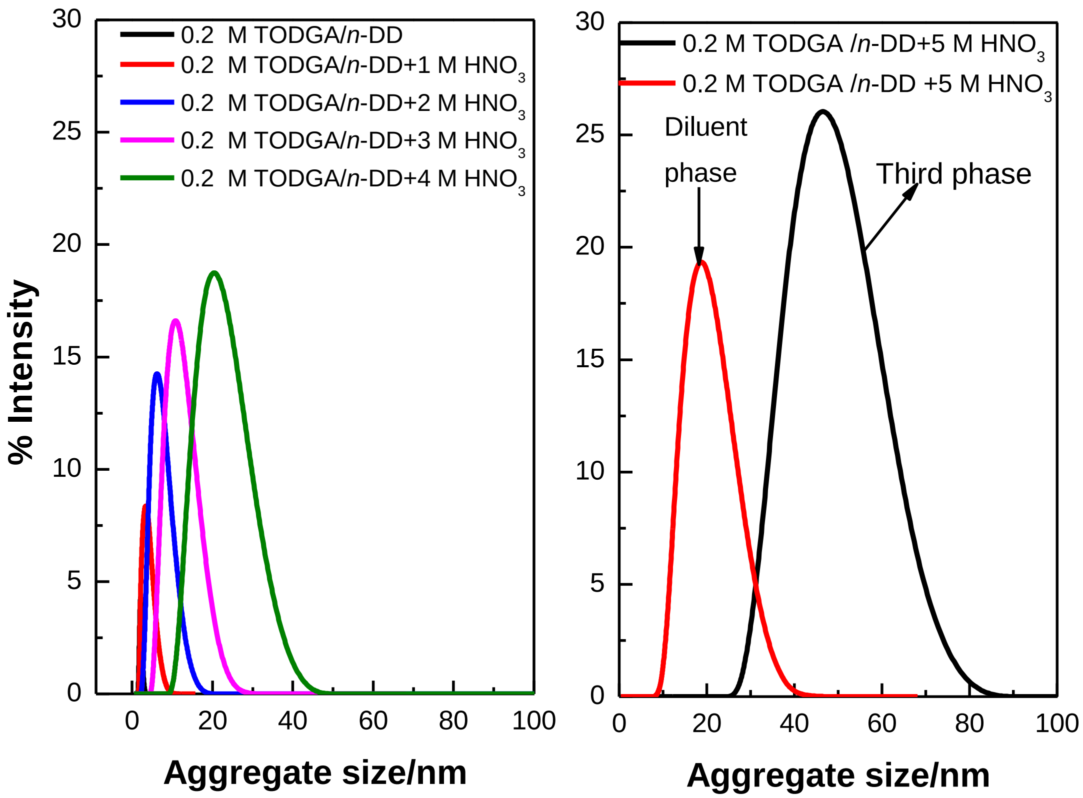

**Figure 3.5.** Aggregate distribution obtained after contacting the 0.2 M TODGA/*n*-DD with different concentrations of nitric acid varied from 1 M to 5 M at 298 K.

### 3.2.5 Comparison of aggregation in different DGAs

Figure 3.6 shows the aggregation behavior of 0.2 M alkyl DGAs/*n*-DD obtained after contacting the organic phase with 3 M nitric acid. Since THDGA forms the third phase with 2 M nitric acid, its aggregation behavior is not shown in the plot. It was noted from Figure 3.2 that the amount of nitric acid extracted into organic phase at 3 M nitric acid was quite similar for all these diglycolamides. However, the aggregation behavior is significantly different, as shown in

Figure 3.6. It can be seen that the intensity and FWHM decrease with increase in the chain length of alkyl group attached to the diglycolamides, as shown in the Table 3.1. This indicates that DGAs with longer alkyl chain length have lesser tendency to undergo aggregation in *n*-DD, and dispersed in *n*-DD to a greater extent.

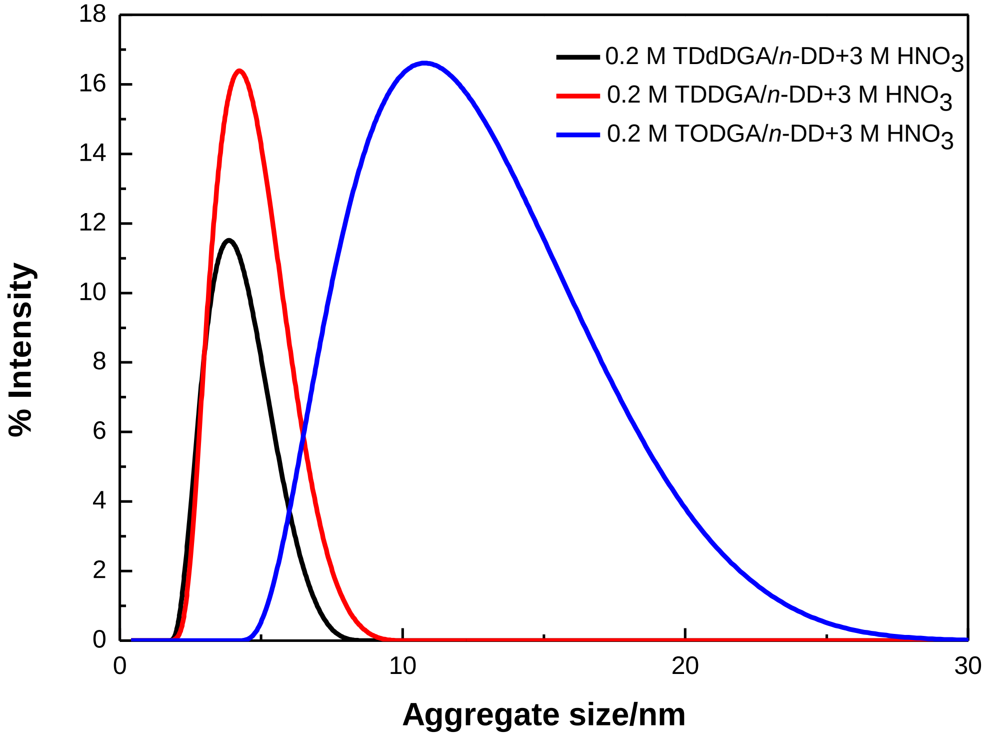

**Figure 3.6.** Aggregate distribution obtained after contacting the 0.2 M alkyl DGAs/*n*-DD with 3 M nitric acid at 298 K.

The aggregation behavior of DGAs with longer alkyl chain length in *n*-DD was studied by recording the aggregate distribution of TDDGA or TDdDGA in *n*-DD at higher nitric acid concentration, wherein the DGA molecules are protonated or acid-solvates formed beyond 1:1 (DGA:$HNO_3$) mole ratios (Figure 3.2). Figure 3.7 shows the aggregation behavior of 0.2 M TDDGA/*n*-DD obtained after equilibrating the organic phase with nitric acid. The concentration of nitric acid in the aqueous phase was varied from 1 M to ~16 M (concentrated $HNO_3$). The distribution was compared with the self-aggregation behavior of 0.2 M TDDGA/n-DD (without contacting with $HNO_3$). It can be seen that the intensity at maximum ($I_{max}$), average aggregate size and FWHM increases with increase in the concentration of nitric acid as expected. The increase in $I_{max}$ is observed up to 3 M nitric acid and thereafter $I_{max}$ remains almost constant. It is important to note that third phase was not observed in the present system even after equilibrating the organic phase (0.2M TDDGA/*n*-DD) with concentrated nitric acid. This confirms that DGAs with higher alkyl chain length has lesser aggregation in the *n*-DD medium. The absence third phase formation in TDDGA also indicates that the aggregates formed at high concentration of nitric acid interacts efficiently in *n*-DD and get dispersed in *n*-DD phase without getting expelled from bulk of *n*-DD phase. A similar behavior was also observed for 0.2 M TDdDGA/*n*-DD after contacting the organic phase with nitric acid concentration varied from 1 M to concentrated nitric acid is shown in Figure 3.8.

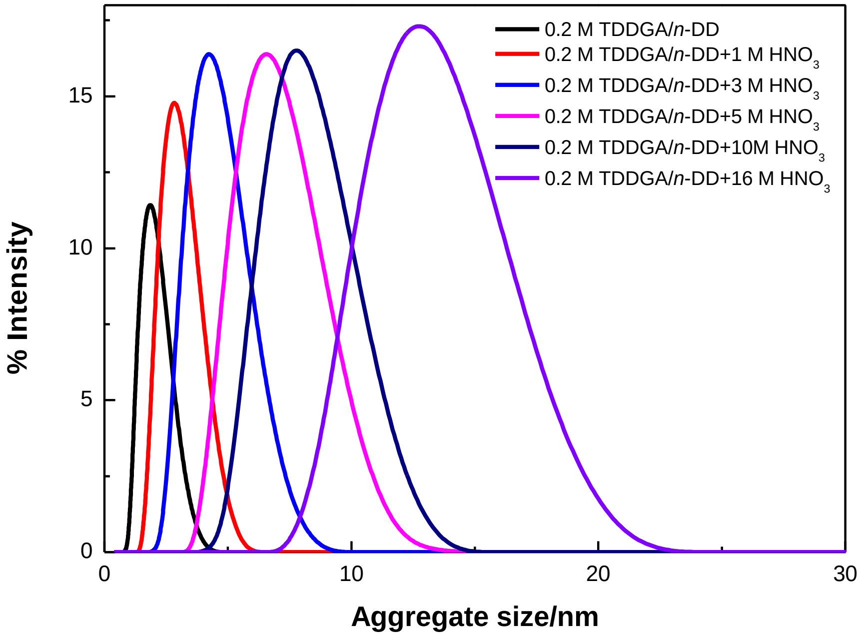

**Figure 3.7.** Aggregates distribution obtained after contacting the 0.2 M TDDGA/*n*-DD with different concentrations of nitric acid varied from 1 M to ~16 M at 298 K.

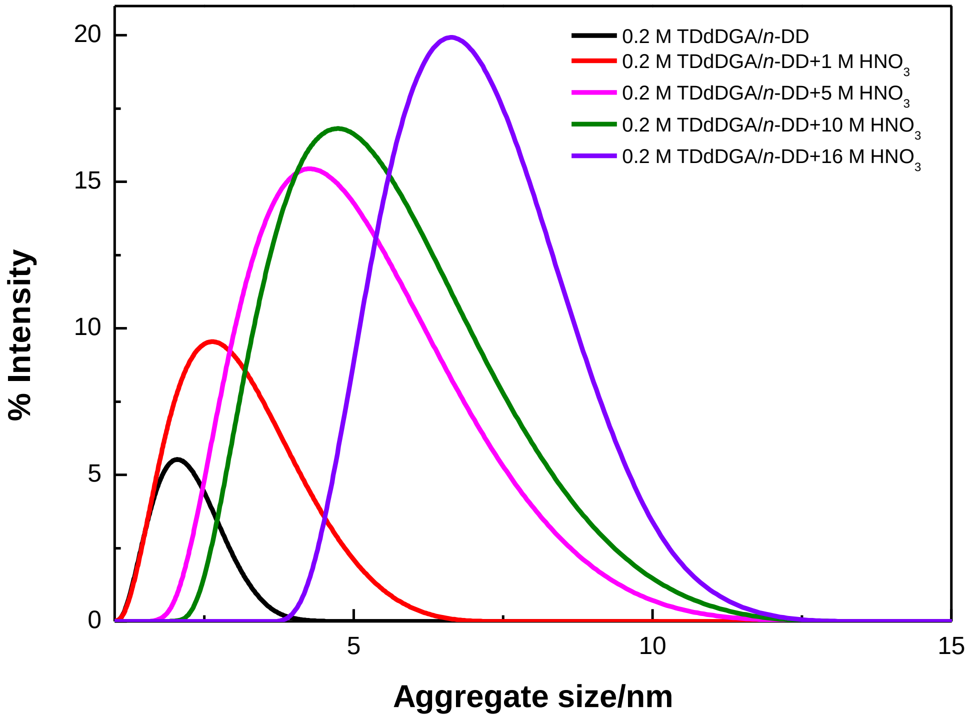

**Figure 3.8.** Aggregates distribution obtained after contacting the 0.2 M TDdDGA/*n*-DD with different concentrations of nitric acid varied from 1 M to ~16 M at 298 K.

### 3.2.6 Nd(III) extraction and aggregation behavior

The extraction behavior of Nd(III) in 0.2 M alkyl DGA/*n*-DD at 1 M nitric acid is shown in Figure 3.9. The initial amount of Nd(III) in aqueous phase was varied from 1 g/L to 7 g/L. Third phase formation was observed in case of 0.2 M THDGA/*n*-DD and 0.2 M TODGA/*n*-DD solutions, when contacted with an aqueous solution of 1 M nitric acid containing 2 g/L and 7 g/L Nd(III) respectively. However, the third phase was not observed in case of TDDGA and TDdDGA. For all DGAs, the extraction of Nd(III) in organic phase increases with increase in the initial amount of Nd(III) in the aqueous phase. The amount of Nd(III) loaded in organic phase increases in the order of TDdDGA < TDDGA < TODGA < THDGA, which is in good agreement with the results reported by Sasaki *et al.* and others [4,5].

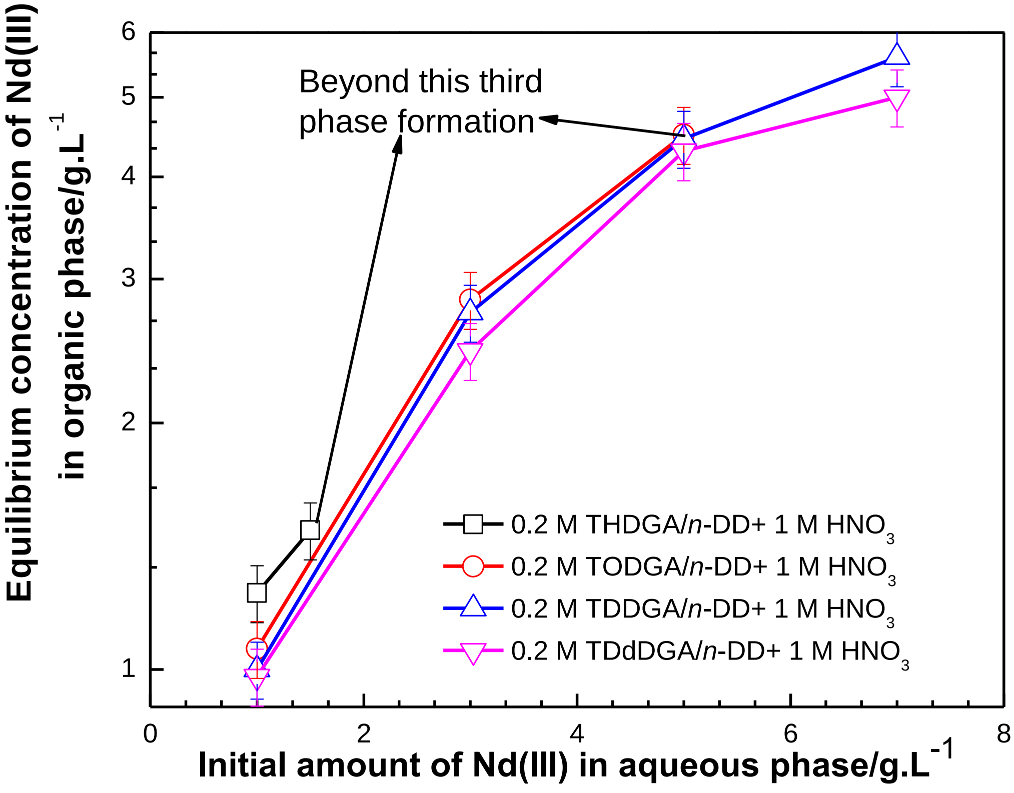

**Figure 3.9.** The extraction behavior of Nd(III) in organic phase as a function of initial concentration of Nd(III) in 1 M nitric acid. Organic phase: 0.2 M alkyl DGAs/*n*-DD. Aqueous phase: $[\mathrm{Nd(III)}]_{\mathrm{initial}}$ varied from 1 g/L to 7 g/L in 1 M nitric acid.

Figure 3.10 and Table 3.2 shows the variation in the average aggregate size and FWHM of the distribution obtained after contacting the 0.2 M alkyl DGAs/*n*-DD with 1 g/L Nd(III) solution in the different concentrations of nitric acid respectively. It can be seen that the average aggregate size and FWHM decreases with increase in the chain length of alkyl group attached to DGA. This shows that, as alkyl chain length of DGAs increases the formation smaller aggregates is facilitated, due to relatively predominant dispersive interactions prevailing in those DGAs. It is also noted from Figure 3.10 and Table 3.2 that the average aggregate size and FWHM increased with increase the concentration of nitric acid respectively, as expected. This could be due to the increase in the extraction of nitric acid and Nd(III) in organic phase with increase in aqueous phase concentration of nitric acid [12,14,20]. Similarly Pathak *et al.*, also reported that aggregate size of the organic phase (0.1 M TODGA/*n*-DD) increases with addition of metal ion in aqueous phase [16]. In case of THDGA and TODGA, third phase formation was observed upon equilibrating 0.2 M solution of these DGAs in *n*-DD with 2 M and 5 M nitric acid respectively. Therefore, the loading behavior of Nd(III) at higher concentrations of nitric acid (up to 10 M) could not studied for these DGAs.

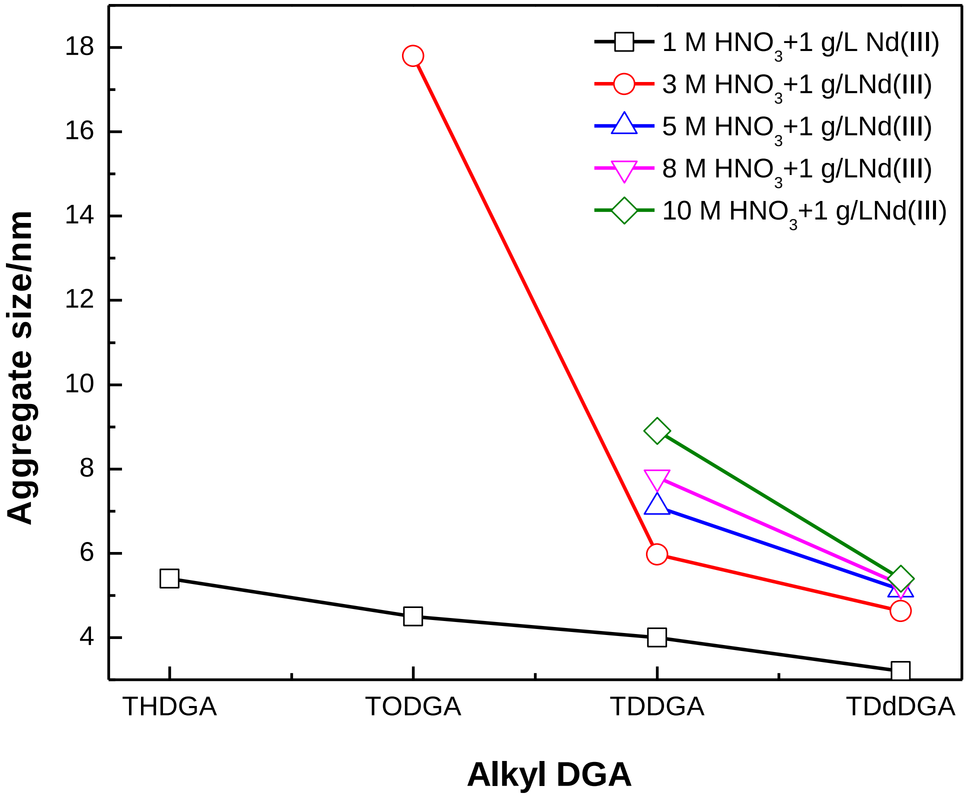

**Figure 3.10**. Variation in the average aggregate size distribution obtained after contacting 0.2 M alkyl DGAs/*n*-DD with the nitric acid solution containing Nd(III) of 1 g/L, at 298 K. The concentration of nitric acid in the aqueous phase was varied from 1 M to 10 M.

**Table 3.2.** Full width at half maximum (FWHM)/nm) of aggregate distribution obtained after the extraction of Nd(III) in 0.2 M alkyl DGAs/*n*-DD at various nitric acid concentrations.

| Aqueous phase | 0.2 M THDGA/*n*-DD | 0.2 M TODGA/*n*-DD | 0.2 M TDDGA/*n*-DD | 0.2 M TDdDGA/*n*-DD |
|---|---|---|---|---|
| Neat | 1.2 | 0.96 | 0.88 | 0.78 |
| 1 M $HNO_3$ +1g/L Nd(III) | 4.1 | 3.4 | 2.8 | 2.6 |
| 3 M $HNO_3$+1g/L Nd(III) | - | 13.6 | 4.5 | 3.1 |
| 5 M $HNO_3$ +1g/L Nd(III) | - | - | 6.5 | 6.4 |
| 8 M $HNO_3$ +1g/L Nd(III) | - | - | 4.1 | 4.2 |

Figure 3.11 shows the variation in the average aggregate size of the organic phase obtained after equilibrating the organic phase of TDDGA and TDdDGA with the solution of Nd(III) in nitric acid. The concentration Nd(III) in nitric acid was varied from 1 g/L to 7 g/L. The nitric acid concentration was varied from 1 M to 10 M. The results indicate that the average aggregate size increases with increase in the initial amount of Nd(III) in the aqueous phase. The splitting of the organic phase was observed in case of 0.2 M TDDGA/*n*-DD when the initial amount of Nd(III) in aqueous phase was 7 g/L at 8 M nitric acid. However, third phase formation was not observed in case of 0.2 M TDdDGA/*n*-DD, even at initial Nd(III) concentration of 7 g/L in 10 M $HNO_3$. All these observations indicate that DGAs with longer alkyl chain length have lesser tendency to undergo aggregation and more tendency to get dispersed in *n*-DD medium.

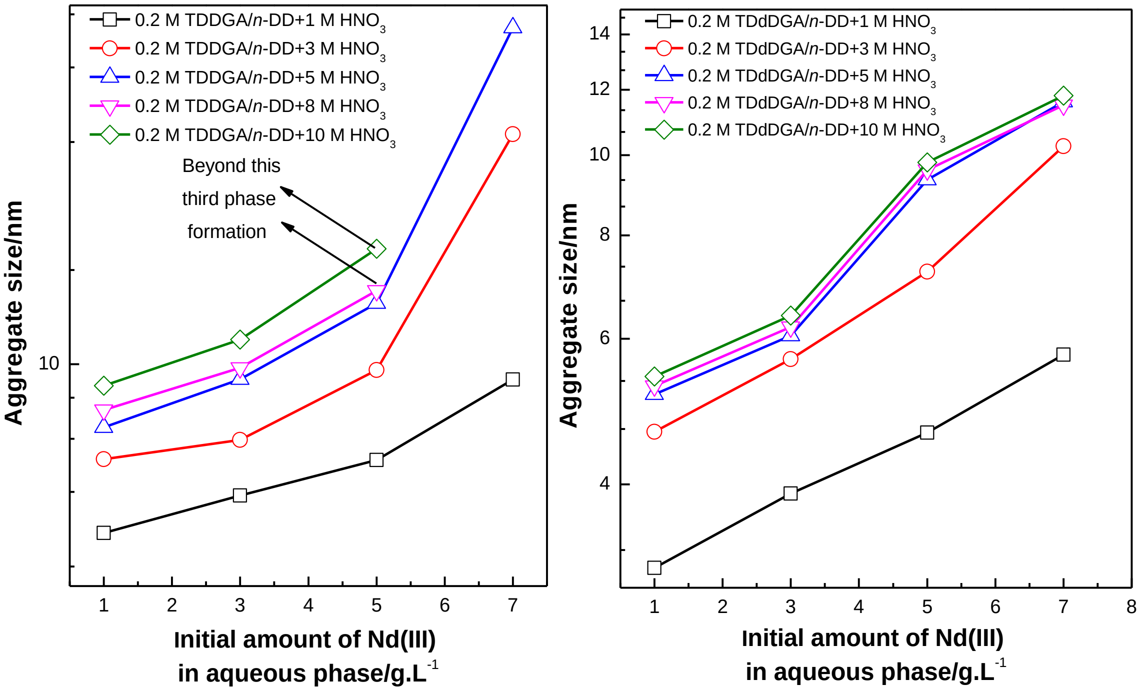

**Figure 3.11.** Variation in the average aggregate size of the organic phase obtained after contacting 0.2 M TDDGA/*n*-DD or 0.2 M TDdDGA/*n*-DD with nitric acid solution containing Nd(III) at 298 K. The initial amount of Nd(III) in nitric acid was varied from 1 g/L to 7 g/L and the concentration of nitric acid in aqueous phase was varied from 1 M to 10 M.

### 3.2.7 Extraction of behavior of nitric acid in different diluents

The previous section discussed about the extraction behaviour of nitric acid in different tetraalkyl diglycolamides in *n*-dodecane medium. It was found that the limiting concentration of nitric acid in organic phase for third phase formation increased with increase in the chain length of alkyl group attached to diglycolamide. In contrast, it would be interesting to understand the behaviour of third phase formation in the same tetraalkyl diglycolamides upon changing the diluent medium from the conventional *n*-dodecane to other *n*-paraffins. This study was necessary to addres the issues associated with scissioning of diluent during gamma irradiation.

Figure 3.12 shows the extraction behaviour of nitric acid in a solution of 0.2 M tetraalkyl DGAs in *n*-octane medium. It can be seen that the extraction of nitric acid in organic phase increases with increase in the concentration of nitric acid in aqueous phase. Similar to those observed in *n*-dodecane medium, the hexyl derivative (THDGA) and the octyl derivative (TODGA) of diglycolamide undergoes third phase formation when they were contacted with the nitric acid of concentration of 3 M and 9 M respectively, whereas no third phase formation was observed in case of decyl (TDDGA) and dodecyl (TDdDGA) derivatives. Figure 3.13 shows the extraction behaviour of nitric acid in 0.2 M tetraalkyl diglycolamide present in *n*-tetradecane. It was observed that the extraction of nitric acid increases with increase in the concentration of nitric acid in aqueous phase, as expected. Comparing these extraction (Figure 3.13) results with those observed in Figure 3.12, it is noted that the initial concentration of nitric acid required for third phase formation decreased upon changing the diluent from *n*-octane to *n*-tetradecane. Table 3.3 shows the limiting organic phase concentration (LOC) and critical aqueous phase concentration (CAC) of nitric acid required for third phase formation in different diglycolamide systems. As expected, the LOC increased with increase in the chain length of alkyl group attached to DGA, whereas the LOC decreased with increase in the chain length of the diluent in organic phase. Similarly, the CAC decreased with increase in the chain length of the diluent.

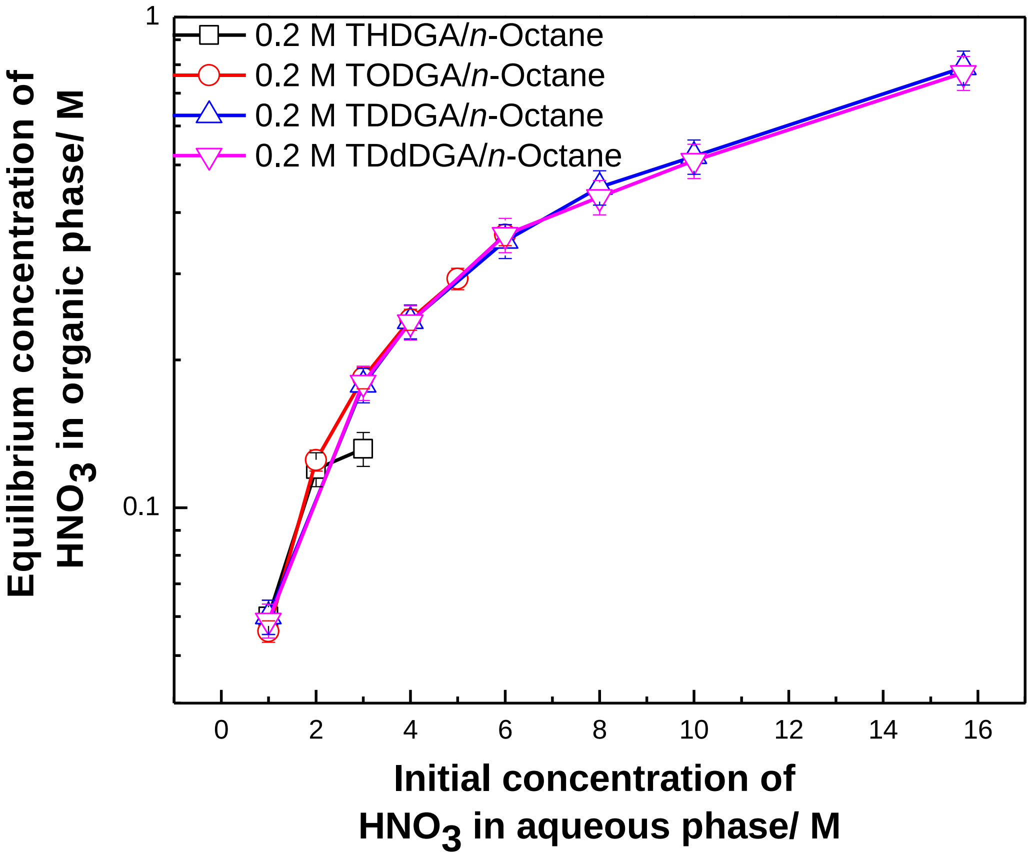

**Figure 3.12.** Variation in the extraction of nitric acid in organic phase as function initial nitric acid concentration in aqueous phase. Organic phase: 0.2 M alkyl diglycolamide/*n*-octane, Aqueous phase: Nitric acid concentration varied from 1 M to 16 M.

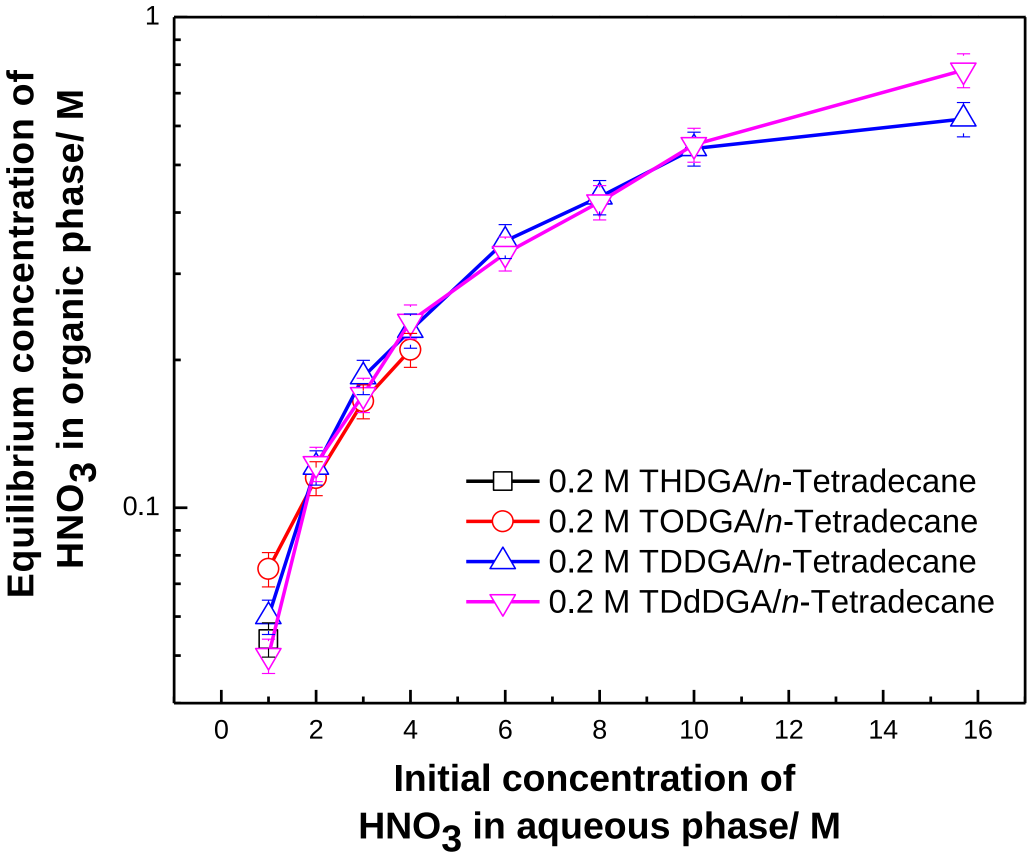

**Figure 3.13.** Variation in the extraction of nitric acid in organic phase as function initial nitric acid concentration in aqueous phase. Organic phase: 0.2 M alkyl diglycolamide/*n*-tetradecane, Aqueous phase: Nitric acid concentration varied from 1 M to 16 M.

**Table 3.3.** LOC and CAC values of nitric at various organic phases.

| Diluent | Ligand | LOC/M | CAC/M | $[HNO_3]_{initial}$ /M for third phase |
|---|---|---|---|---|
| *n*-octane | THDGA | 0.13 M | 2.2 M | 3 M |
| | TODGA | 0.50 M | 7.8 M | 9 M |
| | TDDGA | - | - | No third phase at 16 M |
| | TDdDGA | - | - | No third phase at 16 M |
| *n*-decane | THDGA | 0.11 M | 1.25 M | 2 M |
| | TODGA | 0.43 M | 6.5 M | 7 M |
| | TDDGA | - | - | No third phase at 16 M |
| | TDdDGA | - | - | No third phase at 16 M |
| *n*-dodecane | THDGA | 0.08 M | 1.3 M | 2 M |
| | TODGA | 0.29 M | 4.4 M | 5 M |
| | TDDGA | - | - | No third phase at 16 M |
| | TDdDGA | - | - | No third phase at 16 M |
| *n*-tetradecane | THDGA | 0.07 M | 1.2 M | 2 M |
| | TODGA | 0.21 M | 3.1 M | 4 M |
| | TDDGA | 0.62 M | 12.7 M | 14 M |
| | TDdDGA | - | - | No third phase at 16 M |

### 3.2.8 Aggregation behavior of nitric acid in different diluents

Figure 3.14 shows the aggregate distribution recorded after contacting organic phase with 3 M nitric acid. The organic phase was composed of 0.2 M TODGA present in different diluents, varied from *n*-octane to *n*-tetradecane. It can be seen that the average aggregate size and their distribution in organic phase increases with increase in the chain length of the diluent, indicating that the reverse micellar aggregation is favored upon increasing the chain length of the diluent.

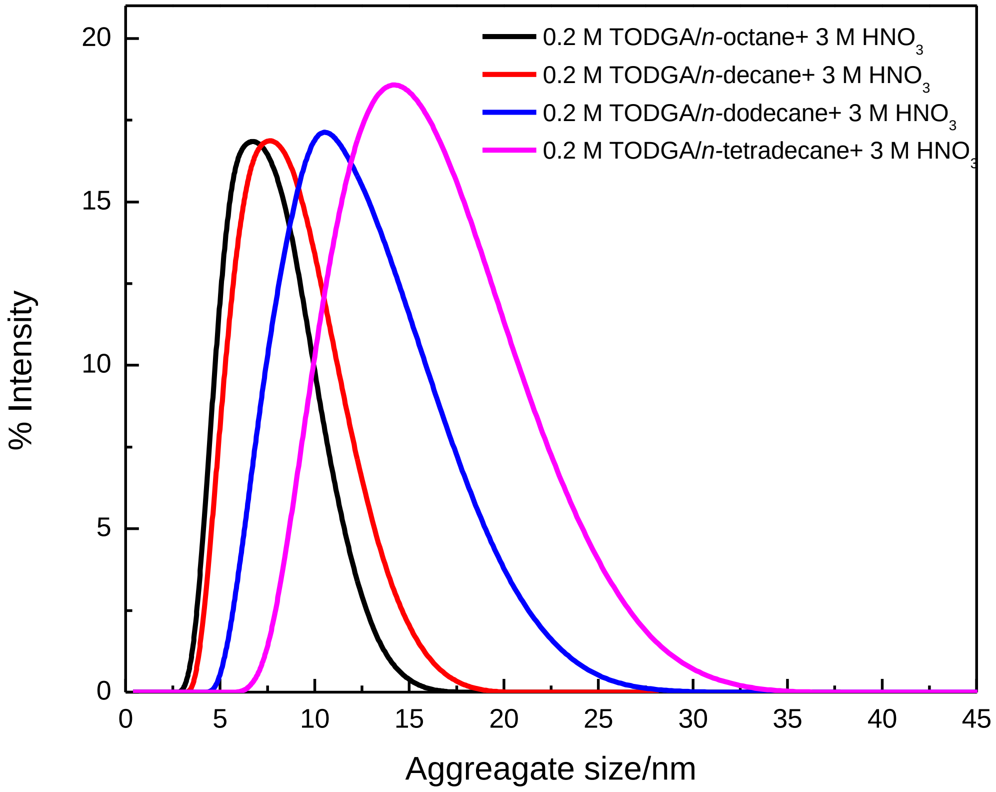

**Figure 3.14.** The aggregate size distribution of organic phase as function of organic phase. Organic phase: 0.2 M TODGA/*n*-octane or 0.2 M TODGA/*n*-decane or 0.2 M TODGA/*n*-dodecane or 0.2 M TODGA/*n*-tetradecane, Aqueous phase: 3 M $HNO_3$.

### 3.2.9 Aggregation behavior by using MD simulations

To understand the insights of aggregation behaviour further, the MD simulation of the organic phase containing 0.2 M TODGA present in different diluents in the presence of the extracted nitric acid was performed and the snapshots of the organic phase at the end of MD simulation (i.e. at equilibrium) is shown in Figure 3.15 (corresponding to aqueous phase equilibrium $HNO_3$ acid concentration of 1.2 M to 10 M). The number of nitric acid molecules in the system was estimated by considering experimental data on transfer of nitric acid from aqueous phase to organic phase. It has been reported that 0.03–0.13 M nitric acid exists in the organic phase, at 0.1 M concentration of TODGA, when corresponding equilibrium aqueous phase acid concentration is in the range of 1–3.5 M [23]. Earlier report suggested that for each molecule of nitric acid, four molecules of water are extracted into the organic phase via hydrogen bonding between nitric acid and water molecules [24]. Therefore, in the present study, the ratio of number of water molecules and nitric acid molecules in the organic phase was taken to be 4:1. It can be seen from Figure 3.15 that the aggregation of TODGA-$HNO_3$- $H_2O$ increases with increase in the alkyl chain length of the diluent in organic phase, which are in line with the experimental results discussed above.

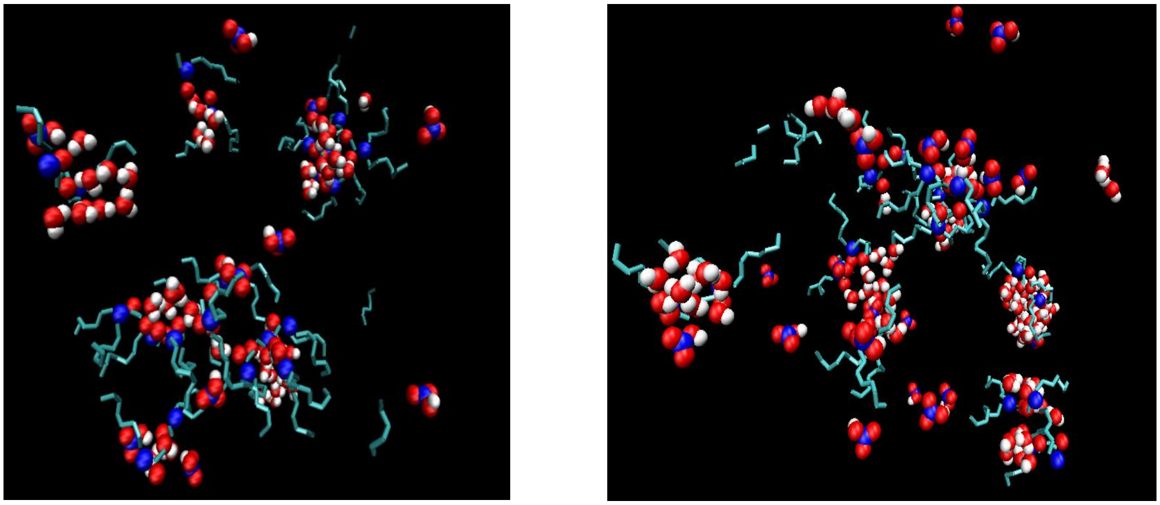

TODGA in *n*-octane TODGA in *n*-tetradecane

**Figure 3.15.** The MD simulated snapshots of aggregates formed after equilibration with nitric acid. Organic phase: 0.2 M TODGA/*n*-octane or 0.2 M TODGA/*n*-tetradecane, Aqueous phase: 3.5 M $HNO_3$.

The MD simulation of organic phase (i.e two phase systems) equilibrated with 6 M nitric acid (i.e third phase formation) was performed and the snapshot of the system after the attainment of equilibrium is shown in Figure 3.16. It can be seen that the organic phase was split into two phases with heavier organic phase (rich in aggregates) sandwiched between the lighter organic phase (rich in diluent) and the bottom aqueous phase containing nitric acid. It is noted that the clusters containing TODGA-$HNO_3$-$H_2O$ are significantly higher in the third phase, and it is very less in diluent rich phase, which is good agreement with results discussed above and those reported elsewhere [25]. In view of this, the third phase is also termed as the aggregate rich phase. This was further supplemented by analyzing the density profile in Figure 3.17. The density reveals the acid-ligand rich phase is sandwiched between water rich aqueous phase and lighter organic phase (rich in diluent).

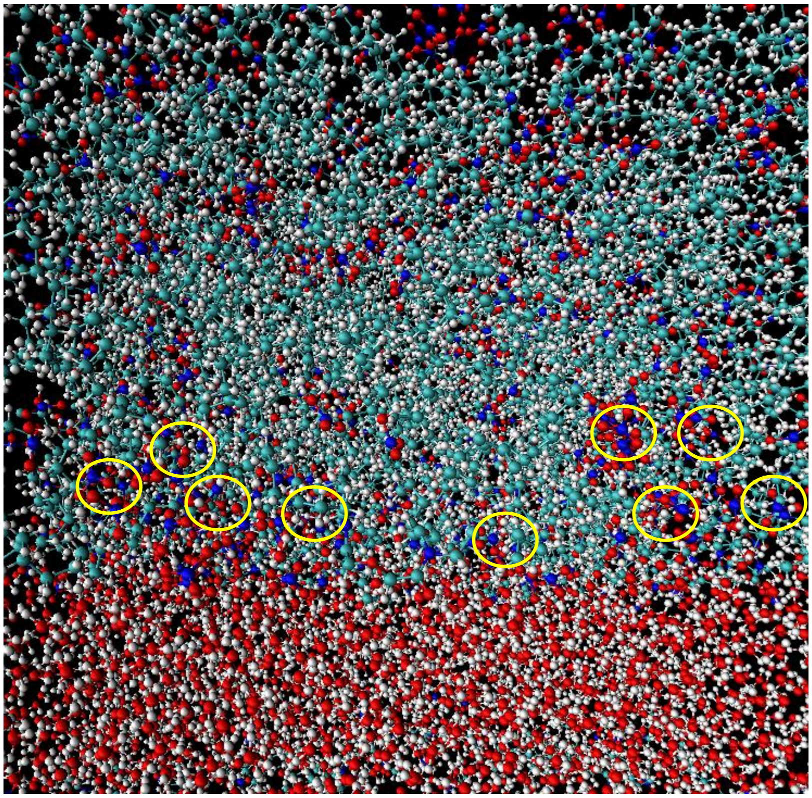

**Figure 3.16**. Snapshot of the system after the attainment of equilibrium. White: H; Red: O; Blue: N; Cyan: C. The bottom side of the snapshot shows the nitric acid aqueous phase (white and red). The top side is the organic phase (cyan and blue). The blue and cyan are not seen in the bulk of aqueous phase indicating that the organic is immiscible in aqueous phase. However, the nitric acid (red and white) is distributed in bulk of organic phase with more concentrated at the interphase existing along with TODGA (blue and cyan), indicating the TODGA…$(HNO_3)_x$. aggregates are more at the interphase. Yellow circles at interphase indicates the formation of acid-rich aggregates of TODGA…$(HNO_3)_x$ that is third phase formation.

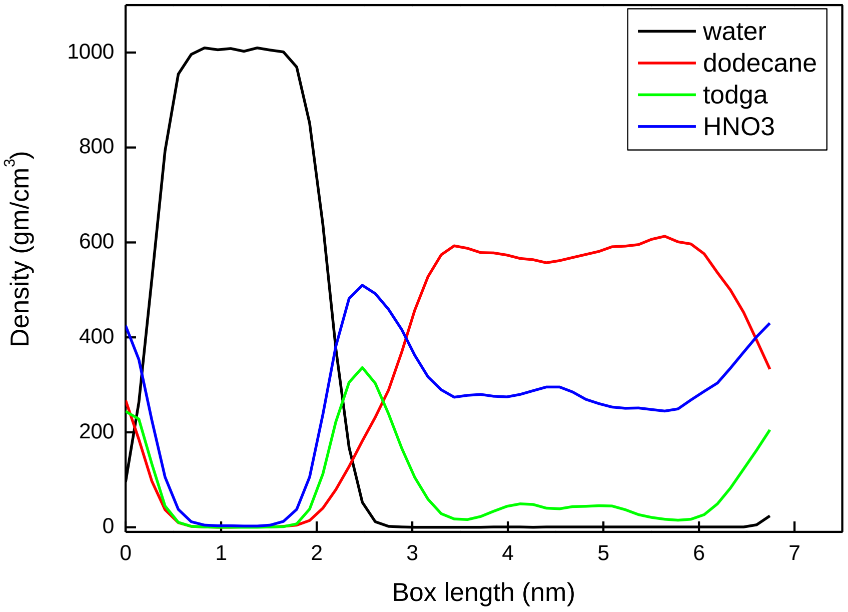

**Figure 3.17.** Plot of density of the chemical species along the box length. The density reveals the acid-ligand rich phase and the lighter organic phase (rich in diluent).

The variation in the average size of aggregates formed in organic phase as a function of nitric acid concentration is shown in Figure 3.18. The organic phase was composed of tetradecyl diglycolamide in different diluents, varied from *n*-octane to *n*-tetradecane. Obviously, the average aggregate size in all cases increases with increase in the concentration of nitric acid. The MD simulation was performed with the organic phase composed of 0.2 M TDDGA in *n*-dodecane and the results were obtained after contacting the organic phase with different concentration of nitric acid varied from 1 M to 10 M. The snapshot of the organic phase obtained after the establishment of equilibrium is shown Figure 3.19. It can be seen that the clusters TDDGA-$HNO_3$-$H_2O$ increases with increase in the concentration of nitric acid in aqueous phase as discussed above [25]. It is also noted from Figure 3.18 that the average size of aggregates formed in organic phase increases with increase in the chain length of the alkyl group present in the diluent at a particular concentration of nitric acid. A similar behaviour was also observed for the 0.2 M TDdDGA in different *n*-paraffins is shown in Figure 3.20. Among the different diluents, the 0.2 M TDdDGA/*n*-tetradecane results in the formation of a third phase upon contacting the organic phase with nitric acid of concentration above 16 M (Table 3.3).

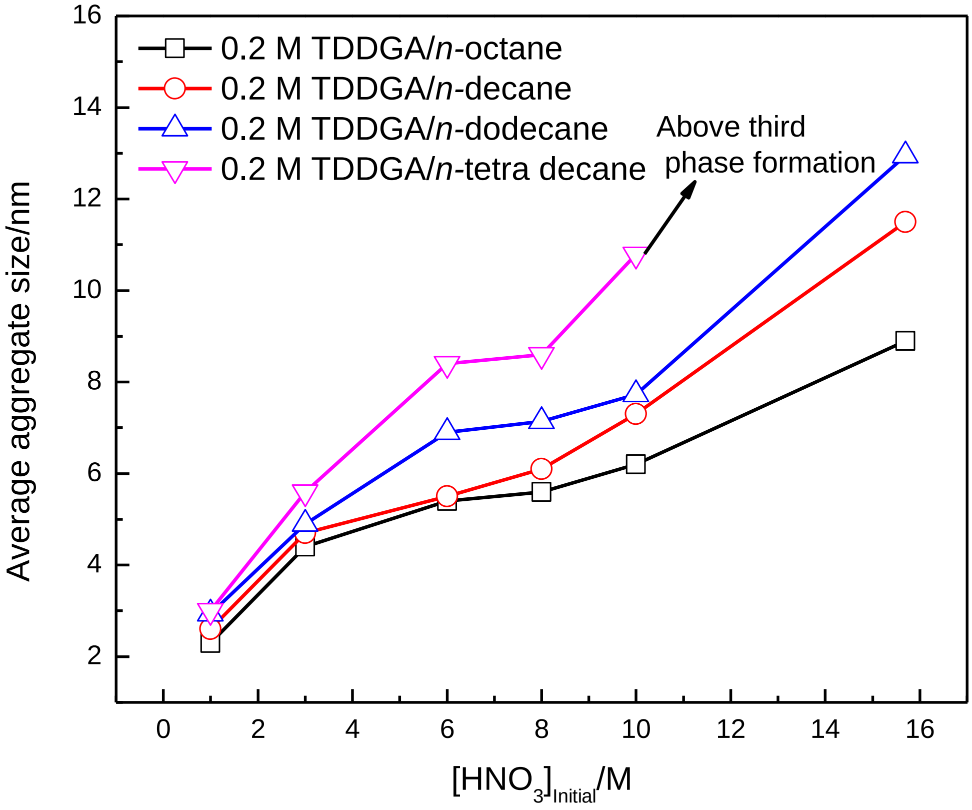

**Figure 3.18.** Variation in the average size of aggregates present in the organic phase at different initial concentration of nitric acid in aqueous phase. Organic phase: 0.2 M TDDGA/*n*-octane or 0.2 M TDDGA/*n*-decane or 0.2 M TDDGA/*n*-dodecane or 0.2 M TDDGA/*n*-tetradecane, Aqueous phase: $[HNO_3]$ = 1 M to 16 M.

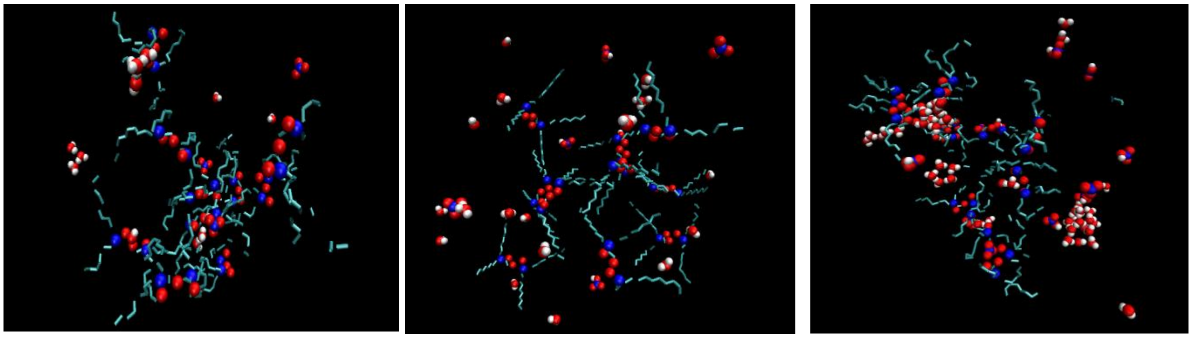

1.2 M $HNO_3$ 2 M $HNO_3$ 3.5 M $HNO_3$

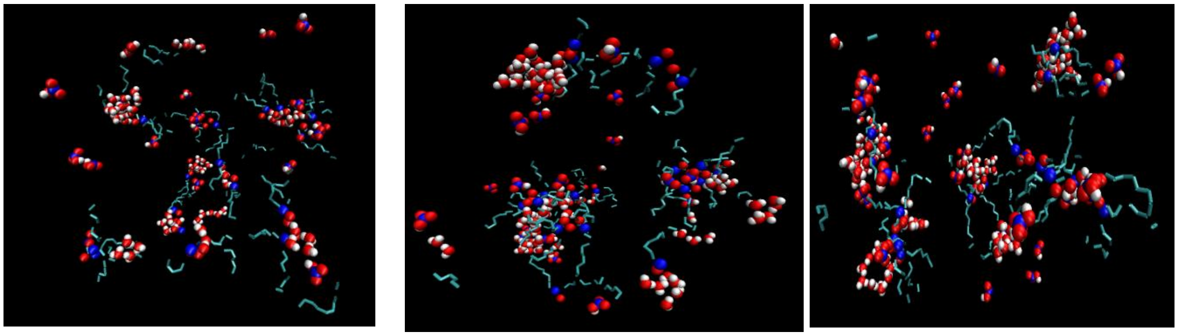

6 M $HNO_3$ 8 M $HNO_3$ 10 M $HNO_3$

**Figure 3.19.** The MD simulated snapshots of aggregates formed after equilibration with nitric acid at various concentrations. Organic phase: 0.2 M TDDGA/*n*-dodecane, Aqueous phase: $HNO_3$ concentration varied from 1 M to 10 M.

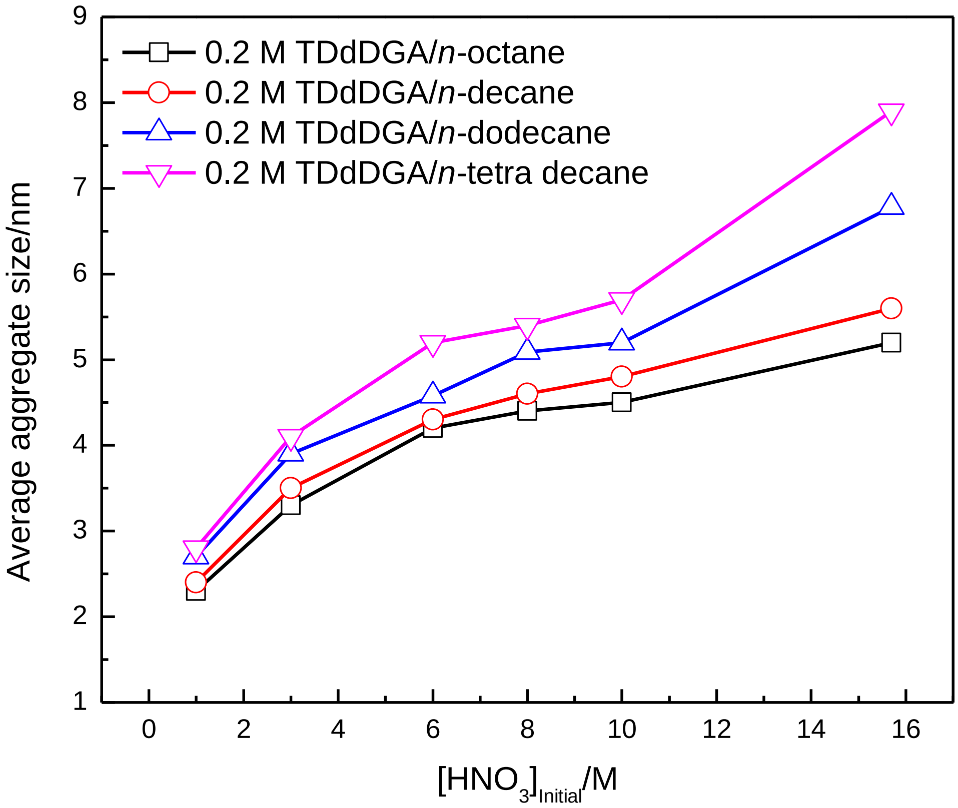

**Figure 3.20.** Variation in the average size of aggregates present in the organic phase at different initial concentration of nitric acid in aqueous phase. Organic phase: 0.2 M TDdDGA/*n*-octane or 0.2 M TDdDGA/*n*-decane or 0.2 M TDdDGA/*n*-dodecane or 0.2 M TDdDGA/*n*-tetradecane, Aqueous phase: $[HNO_3]$ = 1 M to 16 M.

### 3.2.10 Pair correlation function

It is quite important to discern the structural information of the liquid system under investigation. In this perspective, the microstructure of liquid mixtures can be well characterized by analyzing the spatial pair correlation function (PCF) which can also be complemented from X-ray or neutron scattering studies. The calculated PCFs not only provide the microscopic picture of the liquid state but also assist in understanding the macroscopic properties of the liquid mixtures as they are responsible for interaction among molecules in the bulk liquid phase. Diglycolamides contain hydrophilic C=O, group which interacts with $HNO_3$ or $H_2O$ through hydrogen bonding and hydrophobic alkyl group which interacts with hydrophobic alkane molecules. The main interest is on the PCFs of O atom of DGA and H atom of $HNO_3$ and H of $H_2O$ molecule; O atom of $H_2O$ and H atom of $HNO_3$ as the cluster of different molecular species depends on the interplay of interaction between these molecular species. The calculated PCFs of O atom of THDGA and H atom of $HNO_3$; O atom of THDGA and H of $H_2O$ molecule; O atom of $H_2O$ and H atom of $HNO_3$ in *n*-octane, *n* decane, *n*-dodecane and *n*-tetradecane diluents are presented in Figure 3.21 (a-d) respectively. From Figure 3.21a, it is seen that the peak heights of PCF of O atom of THDGA and H atom of $HNO_3$ and that of O atom of THDGA and H of $H_2O$ molecule are much higher than that of O atom of $H_2O$ and H atom of $HNO_3$ in *n*-octane indicating the formation of $HNO_3$ and $H_2O$ mediated cluster. Similar is the case with in *n*-decane (Figure 3.21b). But the interaction of $H_2O$ and $HNO_3$ starts increasing from *n*-dodecane (Figure 3.21c) to *n*-tetradecane (Figure 3.21d) significantly as revealed from the increase in the peak height of the PCF of O atom of $H_2O$ and H atom of $HNO_3$ molecule. The increased interaction among $H_2O$ and $HNO_3$ molecules eventually leads to third phase formation in higher chain alkane as observed in the experiments. Similar trends and characteristics in PCFs were also observed with TDdDGA as displayed in Figure 3.22.

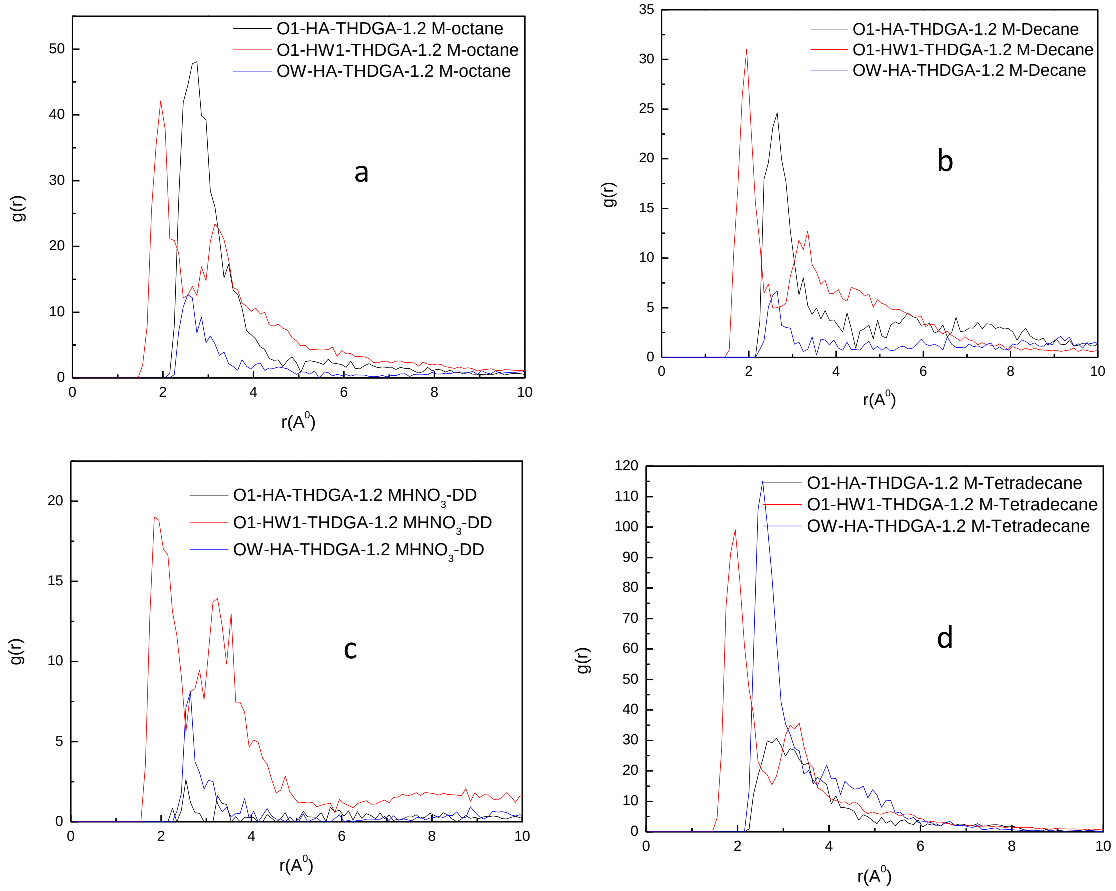

**Figure 3.21.** Computed PCFs among atoms of different molecular species. (a) O atom of THDGA and H atom of $HNO_3$; O atom of THDGA and H of $H_2O$ molecule; O atom of $H_2O$ and H atom of $HNO_3$ in *n*-octane (b) *n*- decane (c) *n*-dodecane and (d) *n*- tetradecane.

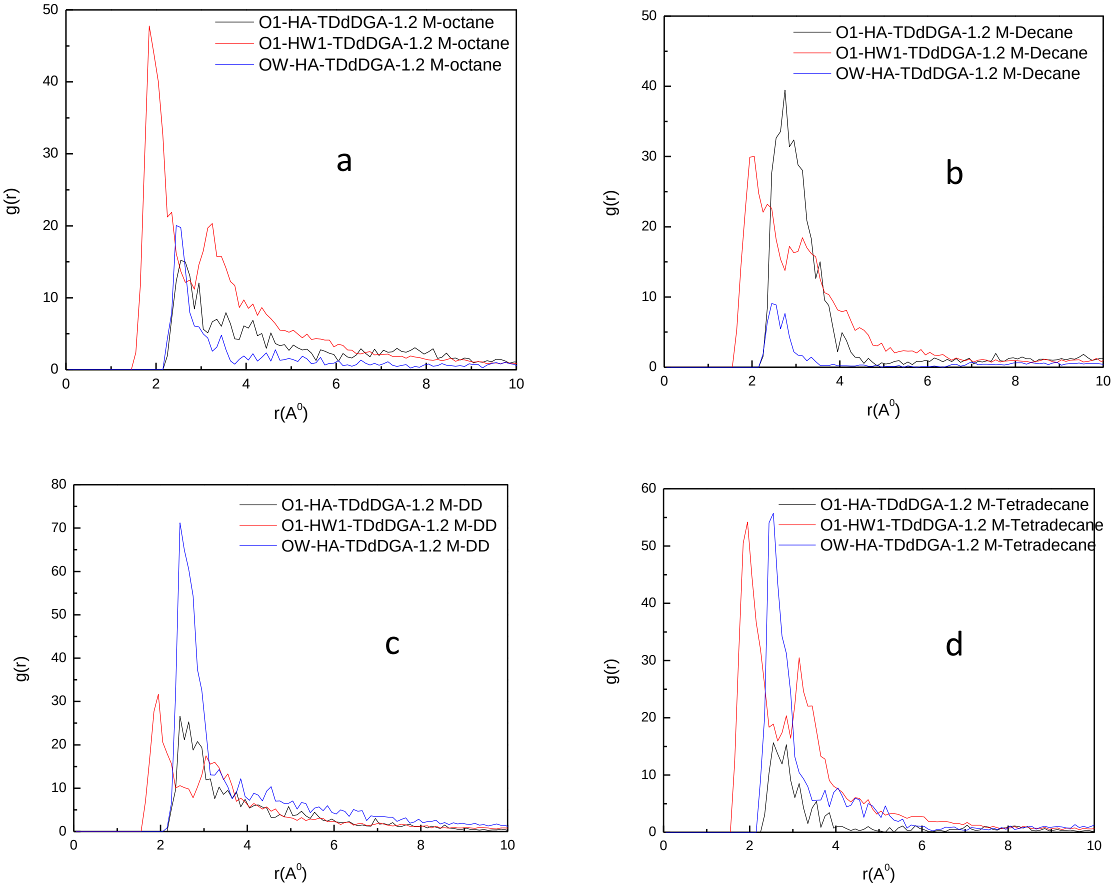

**Figure 3.22.** Computed PCFs among atoms of different molecular species. (a) O atom of TDdDGA and H atom of $HNO_3$; O atom of TDdDGA and H of $H_2O$ molecule; O atom of $H_2O$ and H atom of $HNO_3$ in *n*-octane (b) *n*- decane (c) *n*-dodecane and (d) *n*- tetradecane.

### 3.3 Summary

The extraction behavior of nitric acid and Nd(III) was studied in a solution of 0.2 M alkyl DGAs in the *n*-DD. The alkyl moiety in DGA was varied from hexyl to dodecyl groups. The dissolution of alkyl DGAs in *n*-DD resulted in the formation of reverse micelles or self-aggregates, with the average aggregate size of 2 nm in *n*-DD medium. The tendency of self-aggregation increased in the order THDGA < TODGA < TDDGA < TDdDGA. In contrast to this, the aggregation tendency of acid or Nd(III) extracted organic phase increased in the order TDdDGA < TDDGA < TODGA < THDGA. The presence of nitric acid and $Nd(NO_3)_3$ in the core of the aggregates increased the polarity of the organic phase and facilitated the formation of newer aggregates and merger of existing aggregates. Since such polar-polar interactions and inter-aggregate interactions were predominant in case of DGAs with smaller alkyl chain length, the aggregate size and their distribution increased in the order TDdDGA < TDDGA < TODGA < THDGA. In addition to polar-polar interactions, the aggregates were also interacting with *n*-DD that led to dispersion and homogenous distribution of aggregates in the *n*-DD medium. In the view of this, the aggregates were soluble in the *n*-DD medium. The dispersive interaction of acid or Nd(III) extracted DGAs increased in the order of THDGA < TODGA < TDDGA < TDdDGA. The increase in the concentration and size of aggregates upon extraction continued until the aggregates were dispersed and distributed homogenously in *n*-DD phase.

The extraction behavior of nitric acid in different DGAs dissolved in various *n*-paraffins was also studied. The results were validated with MD simulation studies on the extracted organic phase. The *n*-paraffin was varied from *n*-octane to *n*-tetradecane, to represent the radiolytic degradation products of DGAs and *n*-dodecane respectively. The extraction of nitric acid into all DGAs in *n*-paraffins was quite similar. The aggregate size and their distribution of DGAs in any diluent increased in the order TDdDGA < TDDGA < TODGA < THDGA, which was also confirmed by MD simulation studies. As a result, the third phase tendency of DGAs also increased in order of TDdDGA < TDDGA < TODGA < THDGA. In addition, the aggregates were also interacting with *n*-paraffins in organic phase, which was responsible for the dispersion of aggregates in *n*-paraffin phase. For a particular DGA, the aggregate size and their distribution in organic phase increased in the order *n*-octane < *n*-decane < *n*-dodecane < *n*-tetradecane, which was the order of third phase formation tendency also. To verify the aggregation behavior of DGAs in *n*-paraffins, the MD simulations of different organic phases were performed at the given experimental conditions. It was noted that the cluster size obtained after simulation showed results in line with those obtained by DLS. It was observed that the cluster size obtained from MD simulation increased with increase in the extraction of nitric acid in the organic phase. The size of cluster was bigger in tetrahexyl diglycolamide and *n*-tetradecane containing systems at a particular nitric acid**.** The pair-correlation calculated from MD simulation showed that the interaction between water and nitric acid in the core of the cluster was more in the DGA with lower alkyl chain and in the *n*-paraffins with longer alkyl chain. Therefore, the third phase formation was strongly dependent on the nature of alkyl group attached to the diglycolamide and alkyl chain of the diluent. The studies showed that higher homologs of DGAs containing tetradecyl and tetradodecyl derivatives if formed upon radiolytic degradation could offer advantages in minimizing the third phase formation during the course of solvent extraction. However, the formation of higher homologs of *n*-paraffin, more than *n*-dodecane was not suitable since they facilitate early third phase formation. Since the dodecyl group attached to the DGA interacted efficiently with *n*-DD, the third phase was not observed for TDdDGA, even after contacting the 0.2 M solution of TDdDGA/*n*-DD with 7 g/L in 10 M.

The tendency of third phase formation was dependent on the nature of alkyl group attached to the diglycolamide. The DGAs with longer alkyl chain showed lesser tendency to form aggregates and third phase formation, owing to the predominant dispersive interaction of the aggregates with *n*-DD. As a result, the tendency of third phase formation increased in order TDdDGA < TDDGA < TODGA < THDGA. Among the DGAs, TDDGA and TDdDGA did not form the third phase even with concentrated nitric acid and with the solution of Nd(III) ( 7 g/L) in 5 M nitric acid. However, the third phase was observed in TDDGA when the concentration of nitric acid was increased to 8 M at the initial Nd(III) concentration of 7 g/L. Since, the concentration of Nd(III) and in high-level nuclear waste varies from 1 g/L to 7 g/L and 3-4 M in nitric acid respectively, it is recommended to employ the DGA with longer alkyl chain length, for instance, TDDGA/*n*-DD or TDdDGA/*n*-DD, for the separation of trivalent lanthanides and actinides from high-level liquid waste.

## Part II. Aggregation behavior in tetra (2-ethylhexyl)diglycolamide (TEHDGA) in *n*-dodecane

### 3.4 Introduction

Extensive studies have been carried out for the extraction of trivalent metal ions from nitric acid medium using TODGA and TEHDGA and demonstrated with real waste solutions also [1,2]. The aggregation behaviour of TODGA in *n*-DD was studied by several authors to understand the nature of aggregates and third phase formation. Nave *et al.*, [15] employed tensiometry and small-angle X-ray and neutron scattering methods for characterization of aggregates and showed that the aggregates were spherical reverse micelles consisting of a polar core filled with water and extracted metal ions. The core was surrounded approximately by four extractant molecules. Jensen *et al.*, [19]studied the conditions needed for the reverse micellar formation in a solution of TODGA in alkane diluents, and how the organization of reverse micelles changes extraction of Nd(III) from $HNO_3$ or HCl solution. upon equilibrating the organic phase with aqueous $HNO_3$ or HCl in the presence and absence of $Nd^{3+}$. Small-angle neutron scattering, vapor-pressure osmometry, and tensiometry were employed for probing the structure of reverse micelles. The results showed the formation of TODGA-dimers at lower (< 0.7 M) acidities, and transformed in to a poly dispersed mixture containing TODGA monomers, dimers, and tetramers at aqueous nitric acid acidities above 0.7 M in the absence of Nd. Pathak *et al.*, reported the dynamic light scattering (DLS) studies to investigate the aggregation behaviour of TODGA in *n*-DD and 1-octanol. The aggregation tendency of TODGA with different acids was reported to follow the order $HClO_4 > HNO_3 >$ HCl, which was also similar to the extraction pattern of trivalent actinides/lanthanides in these acids [16]. The literature showed that large numbers of studies were reported for TODGA, even though the extractants TODGA and TEHDGA have been proposed for trivalent metal ion separation from nitric acid medium.

The results reported below were based on the aggregation behavior of organic phase composed of tetra(2-ethylhexyl) diglycolamide (TEHDGA) in *n*-dodecane (*n*-DD). The organic phase was subjected to extraction of Nd(III) from nitric acid medium. Dynamic light scattering (DLS), attenuated total reflectance (ATR)-Fourier transform infrared (FTIR) spectroscopy and Raman spectroscopic methods were employed for characterizing the size, distribution of reverse micelles formed in organic phase upon extraction and the interaction between the metal and ligand.

## 3.5 Results and discussion

### 3.5.1 Extraction behaviour of nitric acid in TEHDGA/*n*-DD

The extraction behaviour of nitric acid in 0.2 M TEHDGA/*n*-DD at 298 K and 323 K is shown in Figure 3.23. It is observed that the extraction of nitric acid in organic phase increases with increase in the equilibrium concentration of nitric acid in aqueous phase. The extraction of nitric acid in organic phase decreases marginally with increase in the temperature of the system. When 0.2 M TEHDGA/*n*-DD was contacted with 4 M nitric acid at 298 K, the organic phase undergoes splitting into two phases, leading to third phase formation [1,27]. The nitric acid concentration in diluent rich phase and third phase was measured and the data were shown in Figure 3.23. It is observed that the concentration of nitric acid in diluent rich phase decreases and that of third phase increases, sharply after third phase formation, with increase in the concentration of nitric acid in the aqueous phase. The nitric acid concentration in third phase is much higher than the stiochiometric requirement of nitric acid for the formation of 1:1 complex with TEHDGA. In contrast to this observation, the third phase formation was not observed in 0.2 M TEHDGA/*n*-DD phase even after contacting the organic phase with 5 M nitric acid at 323 K.

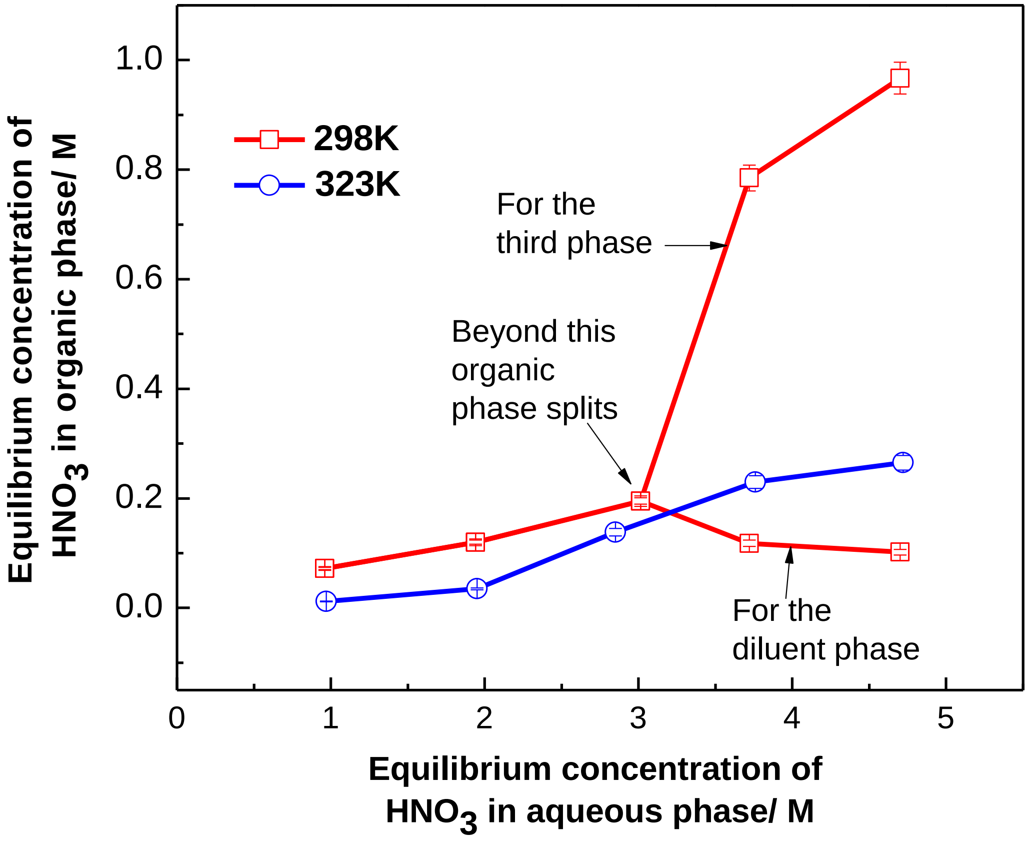

**Figure 3.23.** The extraction behaviour of nitric acid in organic phase as function of equilibrium concentration of nitric acid in aqueous phase at 298 K and 323 K. Organic phase: 0.2 M TEHDGA/*n*-DD. Aqueous phase: [$HNO_3$] varied from 1 M to 5 M.

### 3.5.2 Aggregation behaviour of TEHDGA with nitric acid

It would be interesting to determine the size distribution of aggregates in organic phase at various concentrations of nitric acid in aqueous phase. The organic phase (0.2 M TEHDAGA/*n*-DD) was contacted with desired concentration of nitric acid and dynamic light scattering experiments were performed in the organic phase. The aggregate size distribution is shown in Figure 3.24.

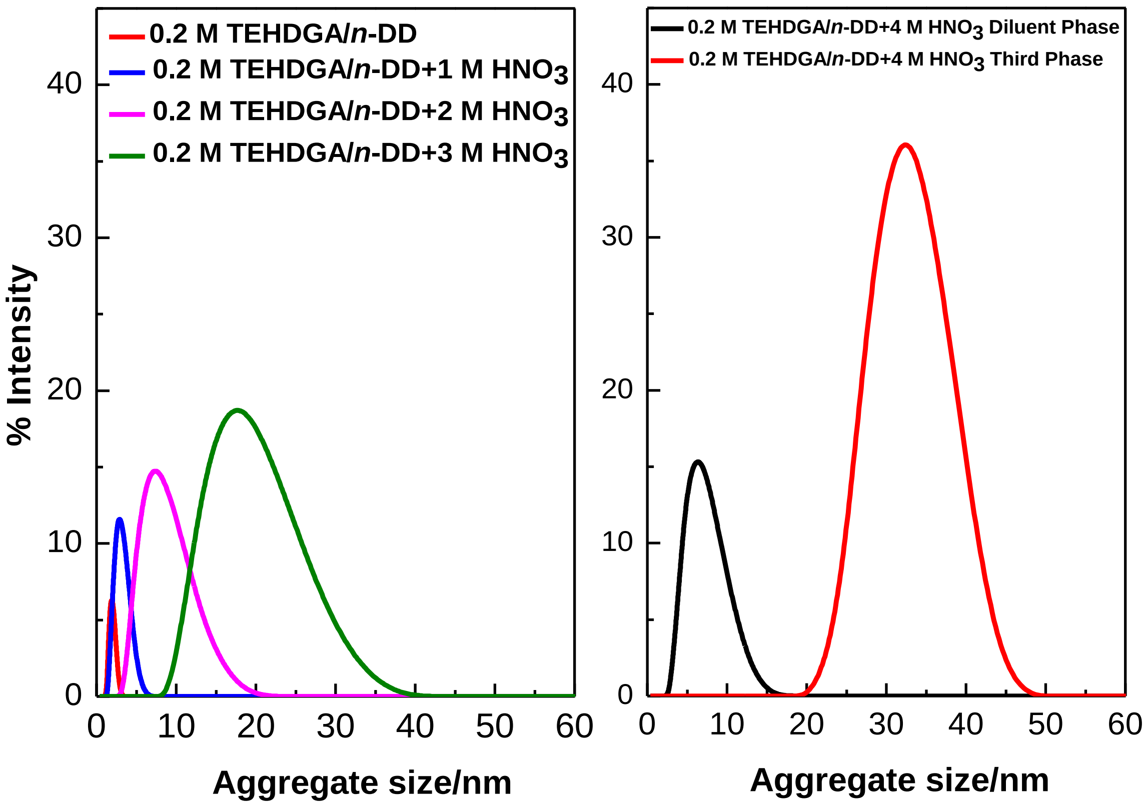

**Figure 3.24.** The aggregate size distribution as a function of nitric acid concentration in aqueous phase. Organic phase: 0.2 M TEHDGA/*n*-DD. Aqueous phase: [$HNO_3$] varied from 1 M to 4 M.

It can be seen that the intensity of distribution and average size of aggregates increases with increase in concentration of nitric acid. This shows that a large number of aggregates of different sizes are formed in organic phase and their concentration increases with increase in the concentration of nitric acid in aqueous phase as discussed in part I of chapter 3 [12]. Table 3.4 shows the data on the average size of aggregates and full width at half maximum (FWHM) determined from the size distribution of aggregates at various nitric acid concentrations. It can be seen that the average aggregate size and FWHM increases with increase in the concentration of nitric acid, as expected. However, the FWHM of third phase is marginally lowered as compared to the FWHM of organic phase before third phase formation. Table 3.4 also shows the average size and aggregate distribution determined as function of temperature at a particular nitric acid concentration. It is observed that the average aggregate size decreases with increase of temperature and as a result the distribution of aggregates (FWHM) also decreases with increase of temperature. This is due to the decrease in the extraction of nitric acid with increase of temperature, as shown in Figure 3.23. Figure 3.25 shows plot of average aggregate size determined as a function of nitric acid concentration at various temperatures. It can be seen that the aggregate size decreases with increase of temperature and increases with increase in the concentration of nitric acid in aqueous phase, as expected.

**Table 3.4.** Aggregate size and FWHM of aggregate distribution at various concentrations of nitric acid.

| Temperature/K | Initial [$HNO_3$]/M | Average aggregate size/nm | Full width at half maximum (FWHM)/nm |
|---|---|---|---|
| 298 | Neat | 1.9 | 1.8 |
| 298 | 0.5 M | 2.6 | 2.4 |
| 298 | 1 M | 3.1 | 2.6 |
| 298 | 2 M | 8.0 | 7.3 |
| 298 | 3 M | 18.4 | 13.8 |
| 298 | 4 M diluent phase | 6.5 | 6.4 |
| 298 | 4 M Third phase | 32.2 | 12.2 |
| 293 | 2 M | 9.2 | 8.7 |
| 303 | 2 M | 6.3 | 5.4 |
| 313 | 2 M | 4.1 | 3.2 |
| 323 | 2 M | 2.3 | 1.9 |

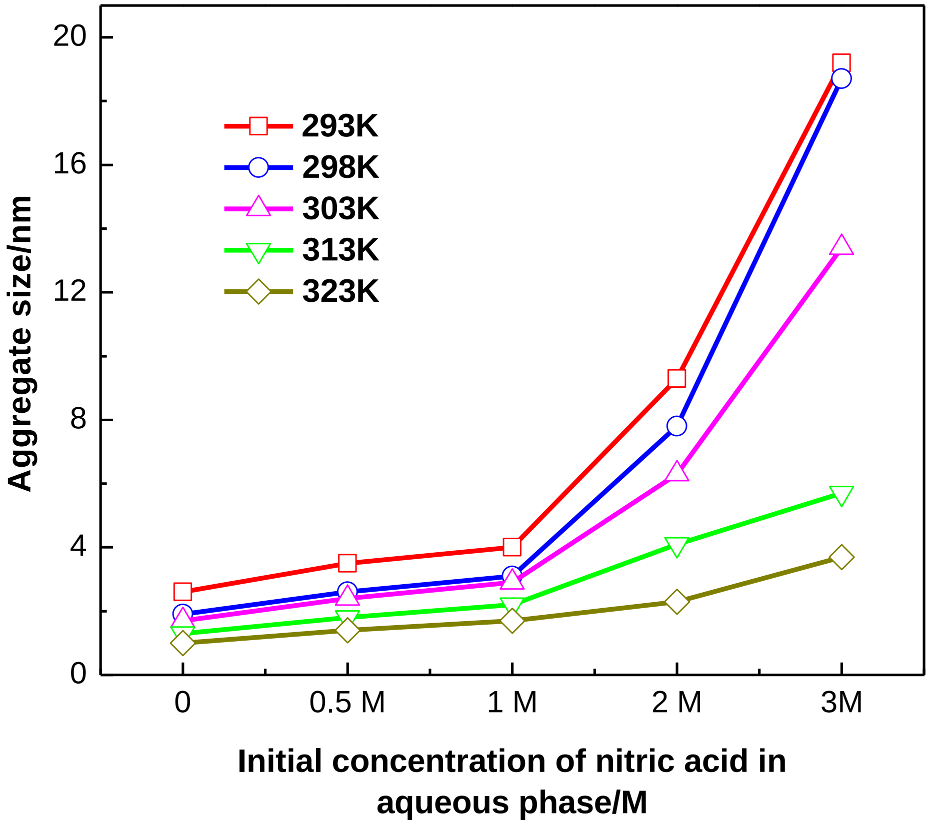

**Figure 3.25.** Average aggregate size as a function of nitric acid concentration at various temperatures. Organic phase: 0.2 M TEHDGA/*n*-DD. Aqueous phase: [$HNO_3$] varied from 1 M to 3 M.

### 3.5.3 ATR-FTIR studies on TEHDGA-$HNO_3$ aggregates

The aggregate formation in the organic phase was investigated by ATR-FTIR spectroscopy. The diglycolamide, TEHDGA, is a tridentate ligand. It contains a couple of amidic carbonyl and an etheric group. The ATR-FTIR spectrum of 0.2 M TEHDGA/*n*-DD recorded after contacting with nitric acid is shown in Figure 3.26. The concentration of nitric acid in the aqueous phase was varied up to 3 M in this case. The ATR-FTIR spectrum of 0.2 M TEHDGA/*n*-DD shows the transmittance bands at 1663 $cm^{-1}$, due amidic carbonyl stretching, and 1117 $cm^{-1}$ bands [28], due to etheric asymmetric (C-O-C) stretching frequencies. The extraction of nitric acid in organic phase could result in protonation of amidic carbonyl or etheric groups. It can be seen from Figure 3.26 that the ATR-FTIR spectrum recorded after contacting with nitric acid results in broadening of amidic transmittance bands and the broadening increases with increase in the concentration of nitric acid in aqueous phase. This observation indicates that the amidic carbonyl groups in TEHDGA are undergoing protonation upon contacting with nitric acid. The broadening of transmittance bands shows that there could be several kinds of protonated species or acid-solavtes (TEHDGA....$(HNO_3)_X$) are formed in organic phase, leading to the distribution species. All these species distributes in organic phase in the form of aggregates. A shoulder observed at 1639 $cm^{-1}$ in the ATR-FTIR spectrum above 2 M $HNO_3$ indicates that the abundance of the aggregate responsible for the 1639 $cm^{-1}$ band is more in the organic phase [28,29]. Since, these aggregates interact efficiently among themselves as compared to the other group of aggregates responsible for broadening (at 1663 $cm^{-1}$), they exhibit a separate transmittance band or a shoulder at 1639 $cm^{-1}$. It is also noted from Figure 5.5 that the changes in the etheric C-O-C transmittance bands are quite less as compared to the changes that occurred in the transmittance band at 1663 $cm^{-1}$. Moreover, the transmittance band at 1117 $cm^{-1}$ is marginally broadened with increase in the concentration of nitric acid. All these observations indicate that the amidic carbonyl bonds are strongly affected by the extraction of nitric acid and etheric bonds are not affected to any significant extent.

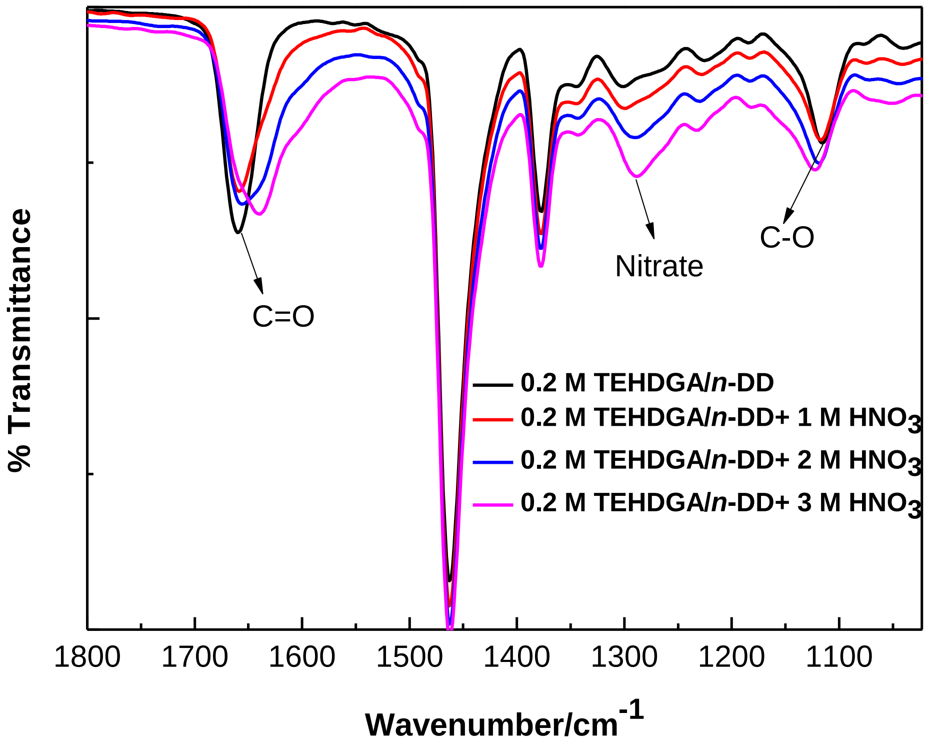

**Figure 3.26.** ATR-FTIR spectra of TEHDGA/*n*-DD recorded after contacting the organic phase with nitric acid solution. Organic phase: 0.2 M TEHDGA/*n*-DD. Aqueous phase: [HNO$_3$] varied from 1 M to 3 M.

### 3.5.4 ATR-FTIR and Raman spectroscopic studies on third phase with nitric acid

Figure 3.27 shows the ATR-FTIR spectrum of third phase and diluent phase formed after contacting 0.2 M TEHDGA/*n*-DD phase with 4 M nitric acid. The spectra were compared with the ATR-FTIR spectrum of 0.2 M TEHDGA/*n*-DD obtained after contacting with 3 M nitric acid, where there was no third phase formation. It is observed that the intensities of all the transmittance bands of third phase are higher. A dramatic 10 fold increase in the intensity of transmittance band at 1639 cm$^{-1}$ (shifted from 1663 cm$^{-1}$) is observed with a shoulder at 1610 cm$^{-1}$ upon third phase formation. This observation indicates that the concentration of aggregates in third phase is quite large, leading to a strong intense peak at 1639 cm$^{-1}$. In fact the increase in the intensity of aggregates determined after third phase formation (see Figure 3.24) also supports this observation.

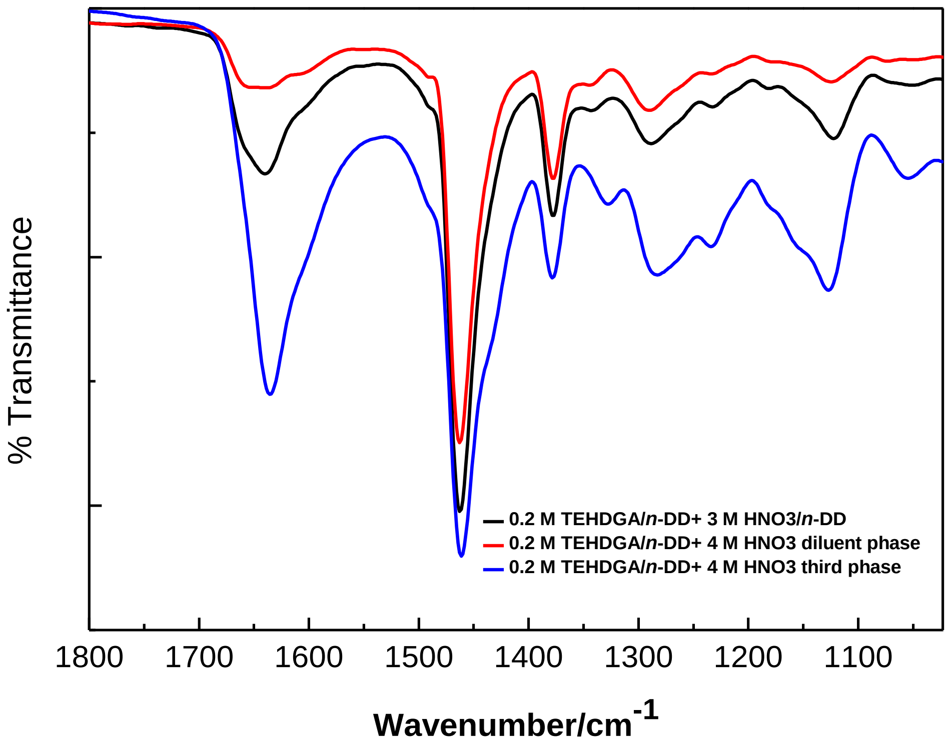

**Figure 3.27.** ATR-FTIR spectra of TEHDGA/*n*-DD recorded after contacting the organic phase with 4 M nitric acid. Organic phase: 0.2 M TEHDGA/*n*-DD. Aqueous phase: [$HNO_3$] = 3 M and 4 M.

The etheric C-O-C transmittance bands are marginally shifted from 1117 cm$^{-1}$ to 1122 cm$^{-1}$ [29] in the third phase with a shoulder at 1160 cm$^{-1}$. These features occur only upon third phase formation. A marginal blue shift of etheric C-O-C transmittance bands and the presence of a shoulder at 1160 cm$^{-1}$ indicate that the etheric oxygen of TEHDGA interacts strongly with nitric acid in third phase. The ATR-FTIR spectrum of third phase also shows the strong transmittance bands at 1287 cm$^{-1}$, which is due to asymmetric $NO_3^-$ stretching frequencies. This shows the presence of nitric acid in third phase in significant concentration.

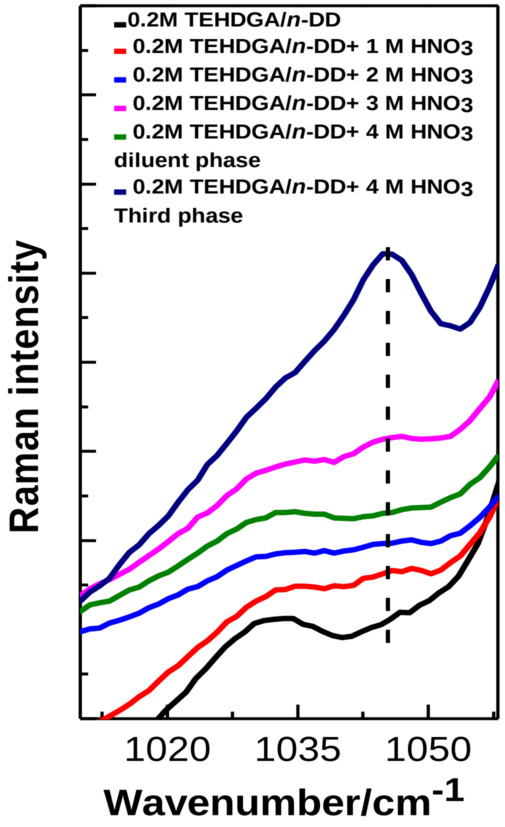

**Figure 3.28.** Raman spectra of the TEHDGA/*n*-DD after contacting organic phase with nitric acid solution. Organic phase: 0.2 M TEHDGA/*n*-DD. Aqueous phase: $[HNO_3]$ varied from 0 M to 4 M.

The Raman spectrum of third phase, plotted in Figure 3.28, also shows a strong intensity at 1044 cm$^{-1}$ confirming the presence of nitric acid in third phase. Such high intense peak in raman spectrum was absent before third phase formation (3 M nitric acid) as well as in the diluent phase. These observations clearly indicate that the concentration of nitric acid is quite significant in third phase. As compared to the features observed in the ATR-FTIR spectrum of third phase, the diluent phase (Figure 3.27) shows that the relative intensities of amidic as well as etheric transmittance bands are quite less, indicating that majority of TEHDGA molecules are moved to the third phase. The amidic transmittance bands at 1663 cm$^{-1}$ shows three weak shoulders one at 1663 cm$^{-1}$ (un protonated amidic) and other two at 1639 cm$^{-1}$ and 1610 cm$^{-1}$. This indicates again a distribution of aggregates of different sizes in diluent phase.

Figure 3.29 shows the ATR-FTIR spectrum of third phase recorded after contacting the organic phase (0.2 M TEHDGA/*n*-DD) with nitric acid of concentration ranging from 4 M to 7 M. It is observed that the intensity of transmittance bands at 1639 cm$^{-1}$ increases with increase in the concentration of nitric acid. The intensity of C-O-C stretching transmittance bands also increases with increase in the concentration of nitric acid. In addition, the C-O-C transmittance bands are shifted from 1122 cm$^{-1}$ to 1160 cm$^{-1}$ with increase in the concentration of nitric acid from 4 M to 7 M. The increase in the intensity of bands at 1287 cm$^{-1}$ indicates that there is an increase in the concentration of nitric acid in third phase. The extracted nitric acid in third phase interacts strongly with amidic carbonyl as well as the etheric oxygen groups of TEHDGA, leading to the red shift and blue shift of these transmittance bands, respectively.

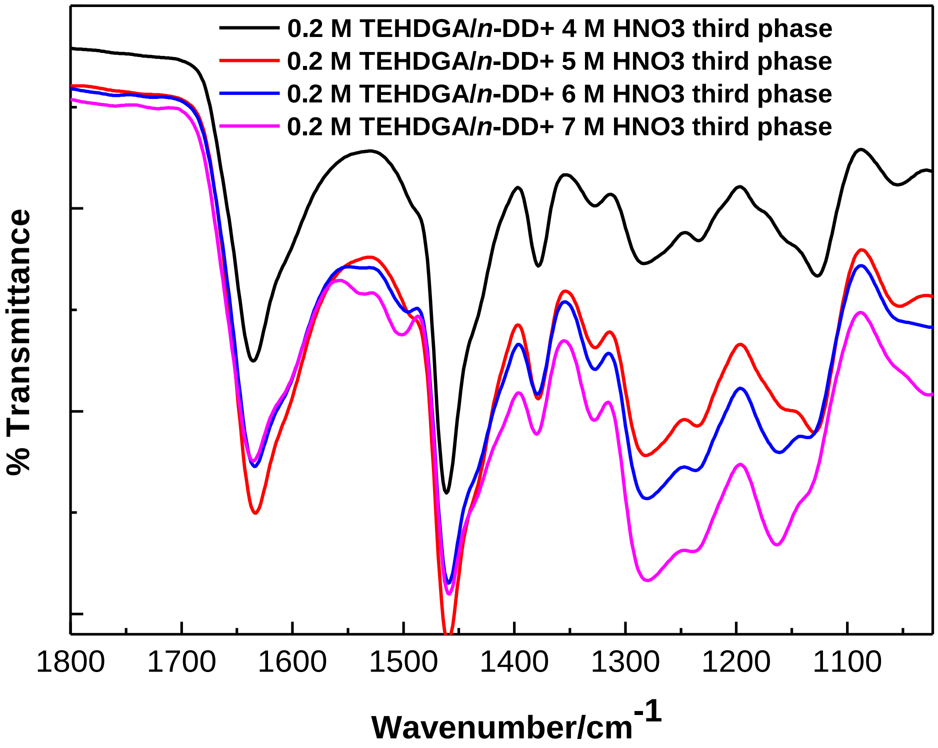

**Figure 3.29.** ATR-FTIR spectra of third phase recorded after contacting the organic phase with nitric acid solution. Organic phase: 0.2 M TEHDGA/*n*-DD. Aqueous phase: [$HNO_3$] varied from 4 M to 7 M.

In contrast to this observation, the ATR-FTIR spectrum of the diluent phase (Figure 3.30) recorded after contacting the organic phase (0.2 M TEHDGA/*n*-DD) with nitric acid of concentration ranging from 4 M to 7 M shows the decrease in the intensity of amidic as well as etheric transmittance bands. This indicates that the concentration of TEHDGA in diluent phase decreases with increase in the concentration of nitric acid in aqueous phase.

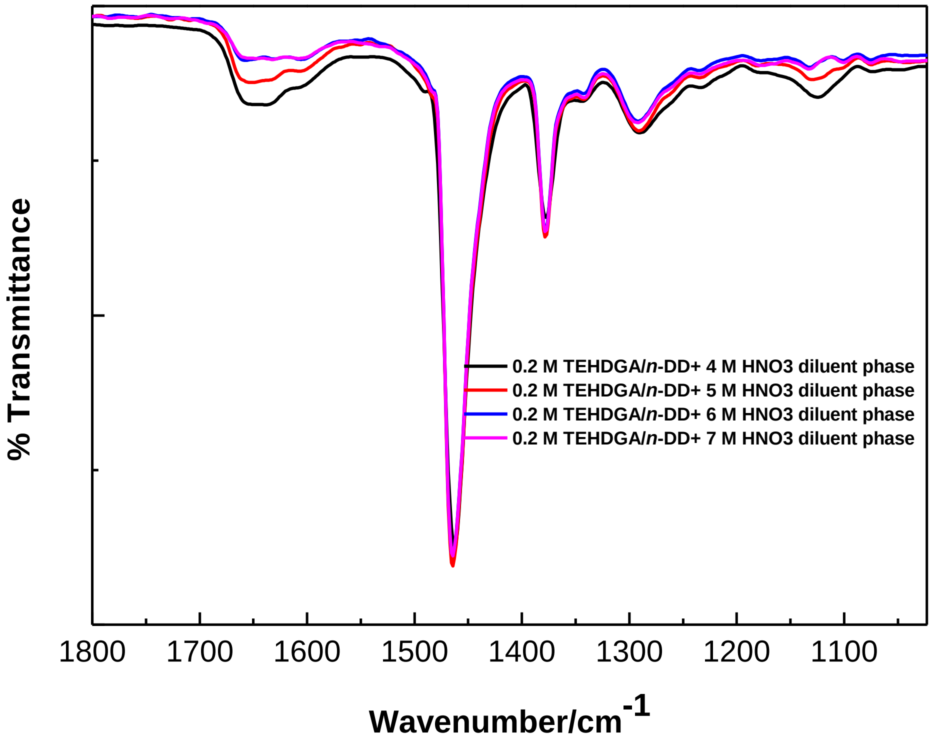

**Figure 3.30.** ATR-FTIR spectra of diluent phase recorded after contacting the organic phase with nitric acid solution. Organic phase: 0.2 M TEHDGA/*n*-DD. Aqueous phase: [$HNO_3$] varied from 4 M to 7 M.

It is also noted from Figure 3.29 that the increase in the intensity of various transmittance bands is more in case of the third phase recorded after contacting with 5 M nitric acid as compared to that observed at 6 M and 7 M nitric acid. This could be due to the higher extraction of nitric acid in third phase when the organic phase was contacted with 5 M nitric acid. Table 3.5 shows the concentration of nitric acid present in the third phase and diluent phase that was obtained after contacting the organic phase (0.2 M TEHDGA/*n*-DD) with various concentrations of nitric acid in aqueous phase. It is observed that the increase in the concentration of nitric acid is more in case of the third phase obtained after contacting with 5 M nitric acid as compared to 6

M and 7 M nitric acids. In view of this, the increase in the intensity transmittance bands is more in case of the third phase recorded after contacting with 5 M nitric acid. Above 5 M nitric acid the increase in the intensity of transmittance bands is gradual, as shown in Figure 3.8. This could be due to the low availability of unprotonated TEHDGA molecules in organic phase, since the concentration of TEHDGA in organic phase is only 0.2 M. In contrast to these observations, the concentration of nitric acid in diluent phase decreases with increase in the concentration of nitric acid in aqueous phase.

**Table 3.5.** The concentration of nitric acid in aqueous and organic phases after third phase formation.

| Initial concentration of $HNO_3$/M | Equilibrium concentration of $HNO_3$/M | | |
|---|---|---|---|
| | Aqueous phase | Organic phase: Diluent phase | Organic phase: Third phase |
| 4.03 | 3.72 | 0.118 | 0.785 |
| 4.99 | 4.7 | 0.102 | 1.15 |
| 6.4 | 5.97 | 0.085 | 1.33 |
| 7.5 | 7.05 | 0.083 | 1.39 |

### 3.5.5 Extraction behaviour of Nd(III) in TEHDGA/*n*-DD

The extraction behaviour of neodymium as a function of initial concentration of Nd(III) in nitric acid phase is shown in Figure 3.31. It can be seen that loading of Nd(III) in 0.2 M TEHDGA/*n*-DD increases with increase in the concentration of neodymium in aqueous phase [27]. When the initial amount of neodymium in aqueous phase exceeds 6g/L at 1 M nitric acid, 2g/L at 2 M nitric acid and 0.5g/L at 3 M nitric acid, the organic phase undergoes splitting in to two phases. It should be noted that nitric acid is also extracted from aqueous phase during the extraction of $Nd(NO_3)_3$ by the neutral extractant TEHDGA. Since nitric acid competes with $Nd(NO_3)_3$ for co-ordination with TEHDGA, the concentration of nitric acid in organic phase was also determined during the extraction of Nd(III). The results are shown in Table 3.6. At 1 M nitric acid in aqueous phase, the concentration of nitric acid extracted into organic phase was determined to be ~0.1 M and at 2 M and 3 M nitric acid, the concentration of nitric acid extracted into organic phase was determined to be ~ 0.17 M and 0.2 M before third phase formation.

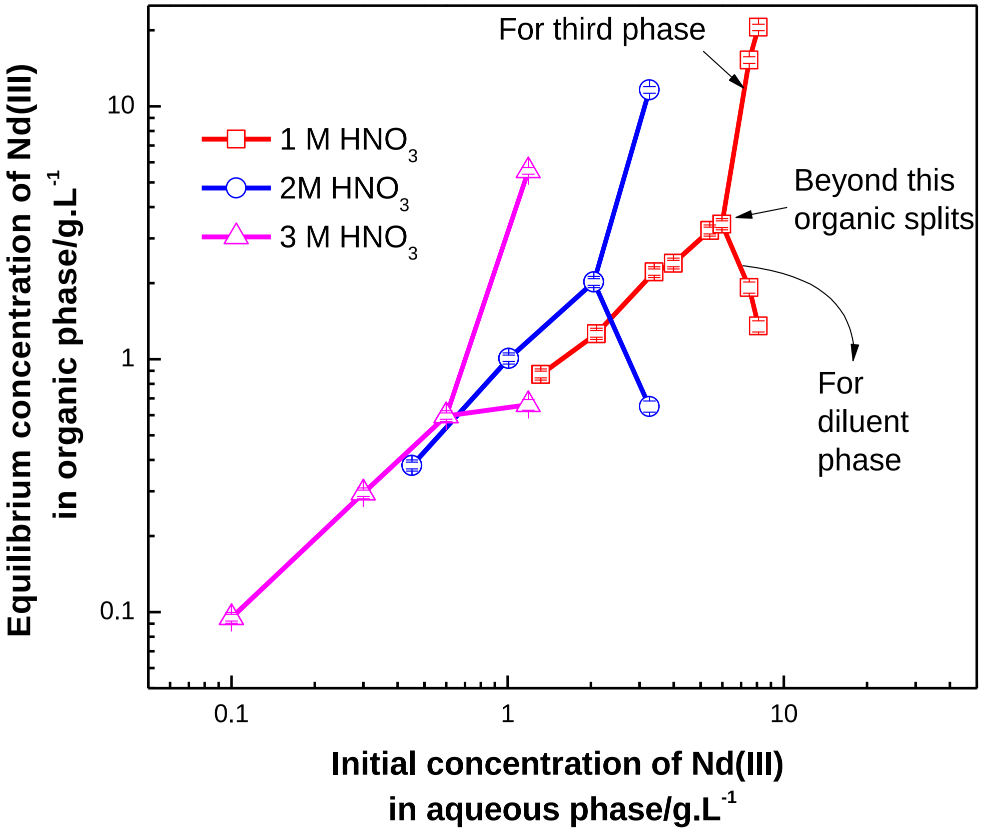

**Figure 3.31.** The extraction behaviour of neodymium(III) in organic phase as function of initial concentration of Nd(III) in aqueous phase after equilibration at 1 M to 3 M $HNO_3$ at 298 K. Organic phase: 0.2 M TEHDGA/*n*-DD. Aqueous phase: : [Nd(III)] varied from 0.5 g/L to 8g/L at 1 M to 3 M nitric acid.

**Table 3.6**. Extraction of nitric acid in the organic phase in the presence of Nd(III) at various nitric acid concentrations. BDL is below detection limit.

| $[HNO_3]$/M | Intial Nd /g.L$^{-1}$ | Initial $[HNO_3]$/M | Equilibrium Nd /g.L$^{-1}$ | | Equilibrium $[HNO_3]$/M | |
|---|---|---|---|---|---|---|
| | | | org | Aq | org | Aq |
| 1 M | 5.4 | 1.16 | 3.23 | 2.21 | 0.10 | 1.06 |
| 2 M | 2.05 | 2.09 | 2.0 | BDL | 0.17 | 1.92 |
| 3 M | 0.6 | 3.06 | 0.59 | BDL | 0.2 | 2.85 |

### 3.5.6 Aggregation behaviour of TEHDGA with Nd(III)

The extraction of Nd(III) in organic phase results in the formation of reverse micelle aggregates. The aggregate size distribution in organic phase as a function of initial concentration of Nd(III) in 1 M nitric acid is shown in Figure 3.32. It is observed that the intensity and size distribution of aggregates increases with increase in the concentration of Nd(III) in aqueous phase. This could be due to the increase in the extraction of Nd(III) and formation of a range of aggregates in organic phase with increase in concentration of Nd(III) in aqueous phase. When the initial concentration of Nd(III) in aqueous phase was 7 g/L the organic phase undergoes splitting into two phases. The aggregate size distribution of third phase and diluent rich phase is also shown in the same figure for comparison. It is observed that there is a significant increase in the intensity of aggregates in third phase, indicating the increase in the concentration of aggregates in third phase [12,21]. Table 3.7 shows the data on the average size of aggregates and FWHM determined from size distribution of aggregates at various nitric acid and Nd(III) concentrations in aqueous phase. It can be seen that the aggregate size and FWHM increases with increase in concentration of Nd(III) in aqueous phase before third phase formation, as expected. However, the FWHM of third phase is marginally lower than the FWHM obtained for the distribution of aggregates below third phase formation i.e. at ~ 6g/L.

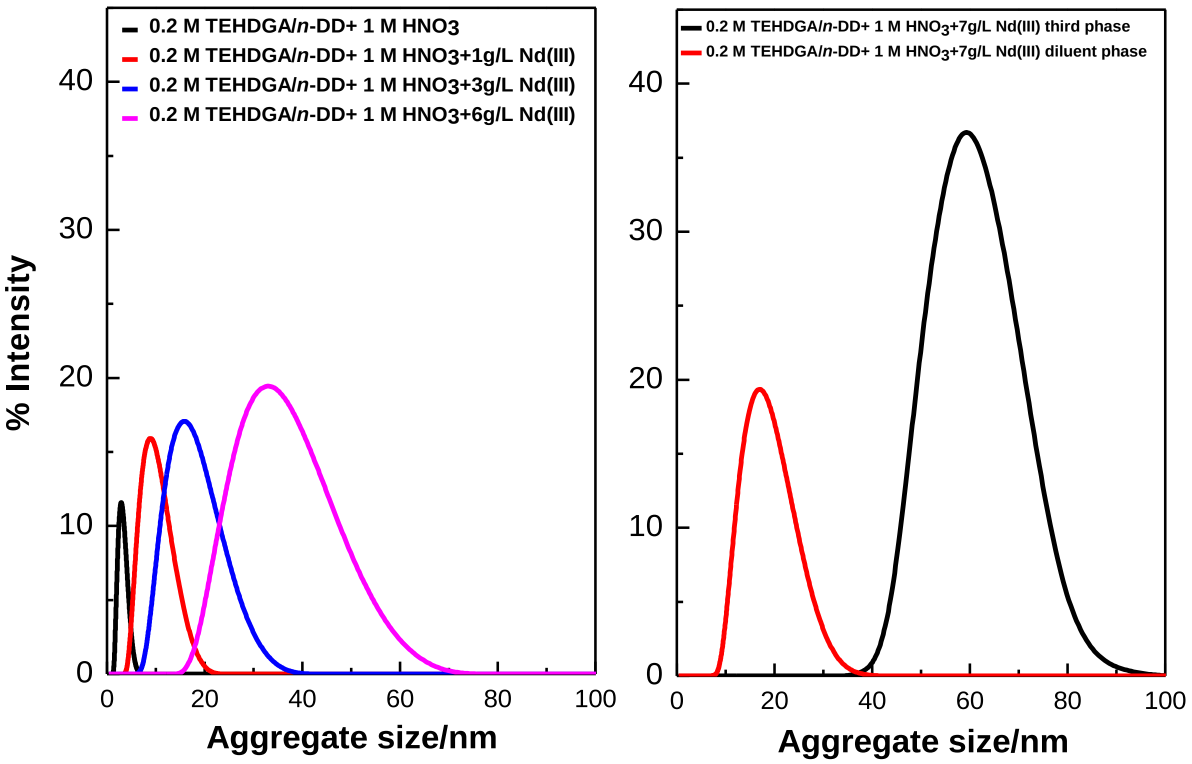

**Figure 3.32.** The aggregate size distribution as a function of neodymium(III) concentration at 1 M $HNO_3$. Organic phase: 0.2 M TEHDGA/*n*-DD. Aqueous phase: [Nd(III)] varied from 1g/L to 7g/L at 1 M $HNO_3$.

**Table 3.7.** Aggregate size and FWHM of aggregate distribution at various concentrations of Nd(III) in aqueous phase.

| $[Nd]_{initial}$ /g.L$^{-1}$ | $[Nd]_{org}$ /g.L$^{-1}$ | $[Nd]_{aq}$ /g.L$^{-1}$ | Average aggregate size/nm | FWHM/nm |
|---|---|---|---|---|
| 1.32 | 0.87 | 0.41 | 9.4 | 7.9 |
| 3.40 | 2.23 | 1.17 | 16.5 | 14.0 |
| 5.40 | 3.32 | 2.21 | 32.3 | 22.4 |
| 5.97 | 3.42 | 2.52 | 34.3 | 24.7 |
| 7.5, diluent phase | 1.92 | 2.95 | 17.6 | 13.5 |
| 7.5, third phase | 15.3 | 2.95 | 61.2 | 21.9 |

### 3.5.7 ATR-FTIR spectroscopy studies on TEHDGA-Nd(III)

The ATR-FTIR spectra of the organic phase (0.2 M TEHDGA/*n*-DD) recorded after containing the organic phase with neodymium(III) nitrate solution in 1 M nitric acid is shown in Figure 3.33. The concentration of Nd(III) in aqueous phase was varied from 1g/L to 6 g/L (i.e. before third phase formation). The spectra was compared with the ATR-FTIR of 0.2 M TEHDGA/*n*-DD recorded after contacting the organic phase with 1 M nitric acid (without Nd(III)). It should be noted that the amidic carbonyl transmittance bands occurs at 1663 cm$^{-1}$ in case of 0.2 M TEHDGA/*n*-DD, when contacted with 1 M nitric acid. However, when the organic phase was contacted with 1 M nitric acid solution contacting Nd(III) nitrate (Nd(III)= 1g/L), a shoulder is observed at 1610 cm$^{-1}$. The intensity of this shoulder increases and that of 1663 cm$^{-1}$ band decreases with increase in the concentration of Nd(III) from 1g/L to 6g/L at 1 M nitric acid. In contrast to this observation, the changes in the etheric (C-O-C) transmittance bands at 1117 cm$^{-1}$ is negligible. In fact, the peak at 1117 cm$^{-1}$ is shifted marginally to 1122 cm$^{-1}$ upon Nd(III) extraction. In addition, the intensity transmittance bands at 1298 cm$^{-1}$ and 1280 cm$^{-1}$ increases with increase in the loading of Nd(III) nitrate from 1 M nitric acid. The 1298 cm$^{-1}$ bands are due to the asymmetric stretching of nitrate ion from nitric acid and 1280 cm$^{-1}$ bands are due to the asymmetric stretching of nitrate ions coordinated to Nd(III) ion Nd($NO_3$)-TEHDGA complex present in organic phase. It should be noted that the intensity of 1280 cm$^{-1}$ band increase more as compared to 1298 cm$^{-1}$ band upon Nd(III) loading. This is due to higher loading Nd(III) nitrate in organic phase with increase in Nd(III) nitrate concentration in aqueous phase at constant $HNO_3$ (1 M) concentration.

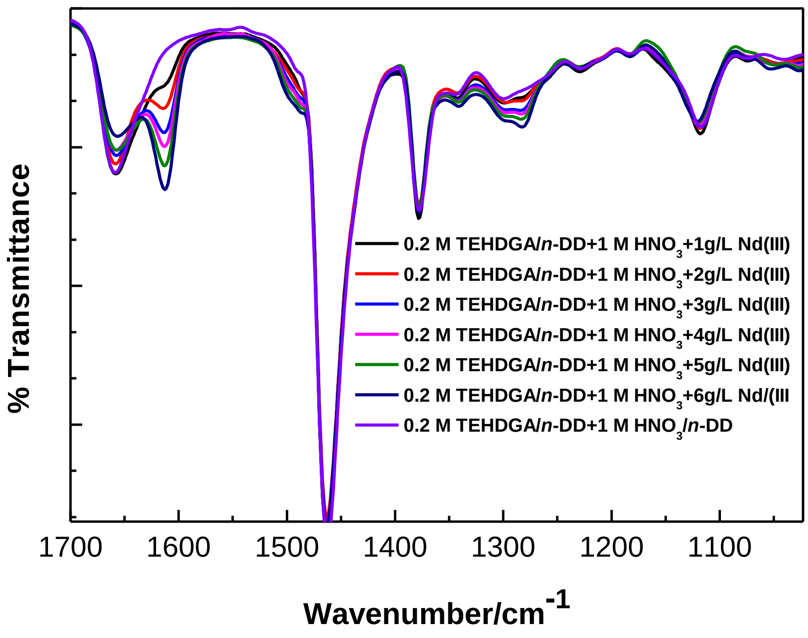

**Figure 3.33.** ATR-FTIR spectra of TEHDGA/*n*-DD recorded after contacting the organic phase with 1 M nitric acid solution containing Nd(III). Organic phase: 0.2 M TEHDGA/*n*-DD. Aqueous phase: [Nd(III)] varied from 1g/L to 6g/L at 1 M nitric acid.

### 3.5.8 ATR-FTIR spectroscopic studies on third phase with Nd(III)

Figure 3.34 compares the ATR-FTIR spectra of organic phase recorded before (Nd = 6g/L) and after (Nd = 7g/L & 8g/L) third phase formation with Nd(III) from 1 M nitric acid. It is observed that the intensity of 1610 cm$^{-1}$ band increases dramatically after third phase formation. In addition, the intensity of etheric transmittance bands at 1122 cm$^{-1}$, and coordinated nitrate bands at 1280 cm$^{-1}$ also increases significantly after third phase formation. These bands continue to increase upon the increasing the concentration of neodymium after third phase formation.

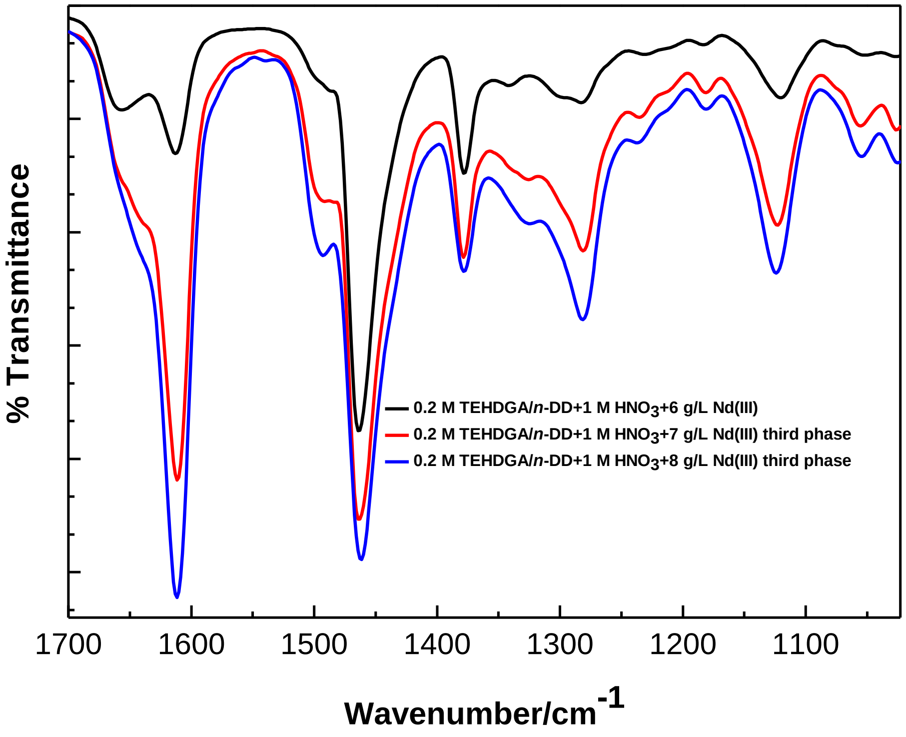

**Figure 3.34.** ATR-FTIR spectra of third phase recorded after contacting the organic phase with 1 M nitric acid solution containing Nd(III). Organic phase: 0.2 M TEHDGA/*n*-DD. Aqueous phase: [Nd(III)] varied from 6g/L to 8g/L at 1 M nitric acid.

The 1663 cm$^{-1}$ band, which is responsible for the amidic carbonyl stretching in TEHDGA, is completely shifted to 1610 cm$^{-1}$ in third phase and the original band at 1663 cm$^{-1}$ appears as a shoulder in the ATR-FTIR spectrum of third phase. In contrast to this observation, the ATR-FTIR spectra of the diluent rich phase, shown in Figure 3.35, indicates that the intensity of the transmittance bands at 1663 cm$^{-1}$, 1610 cm$^{-1}$, 1298 cm$^{-1}$, 1280 cm$^{-1}$ and 1122 cm$^{-1}$ decrease after third phase formation (Nd(III) = 7g/L) and these intensities continue to decrease with increase in the concentration of Nd(III) from 7g/L to 8g/L.

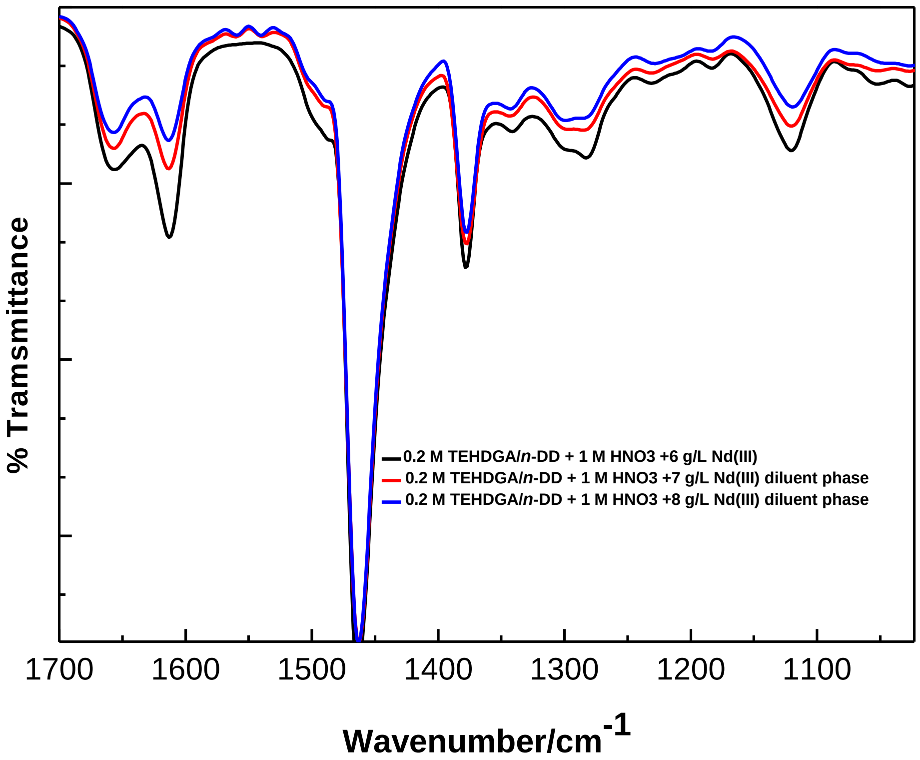

**Figure 3.35**. ATR-FTIR spectra of diluent phase recorded after contacting the organic phase with 1 M nitric acid solution containing Nd(III). Organic phase: 0.2 M TEHDGA/*n*-DD. Aqueous phase: [Nd(III)] varied from 6g/L to 8g/L at 1 M nitric acid.

These observations indicate that the aggregates formed upon loading of neodymium tend to migrate to third phase upon increasing the concentration of neodymium in aqueous phase.

### 3.5.9 Effect of TEHDGA concentration on aggregation behaviour

Figure 3.36 compares that average size aggregates formed in organic phase as a function of TEHDGA concentration in organic phase at various aqueous feed conditions. It can be seen that the aggregate size increases with increase in the concentration of TEHDGA in organic phase, at a particular nitric acid concentration (1 M or 2 M). Deepika *et al*. reported that the extraction of nitric acid in organic phase usually increases with increase in the concentration of TEHDGA in organic phase [27]. Therefore, the increase in the average aggregates size at 1 M or 2 M nitric acid observed in the present study could be attributed to the higher extraction of nitric acid with increase in the concentration of TEHDGA in organic phase. Similarly, at a particular concentration of TEHDGA in organic phase, the increase in the aggregate size with increase in the concentration of nitric acid (1 M and 2 M) could be due to the increased extraction of nitric acid as discussed in section 3.5.1. Comparing the aggregate size obtained at 1 M nitric acid in the presence and absence of Nd(III), the results show that there is a significant increase in the aggregate size due to the extraction of Nd(III) in organic phase. Since the extraction of Nd(III) in organic phase also increases with increase in the concentration of TEHDGA in organic phase at a particular acidity, the average aggregate size also increases in with increase in the concentration of TEHDGA in organic phase.

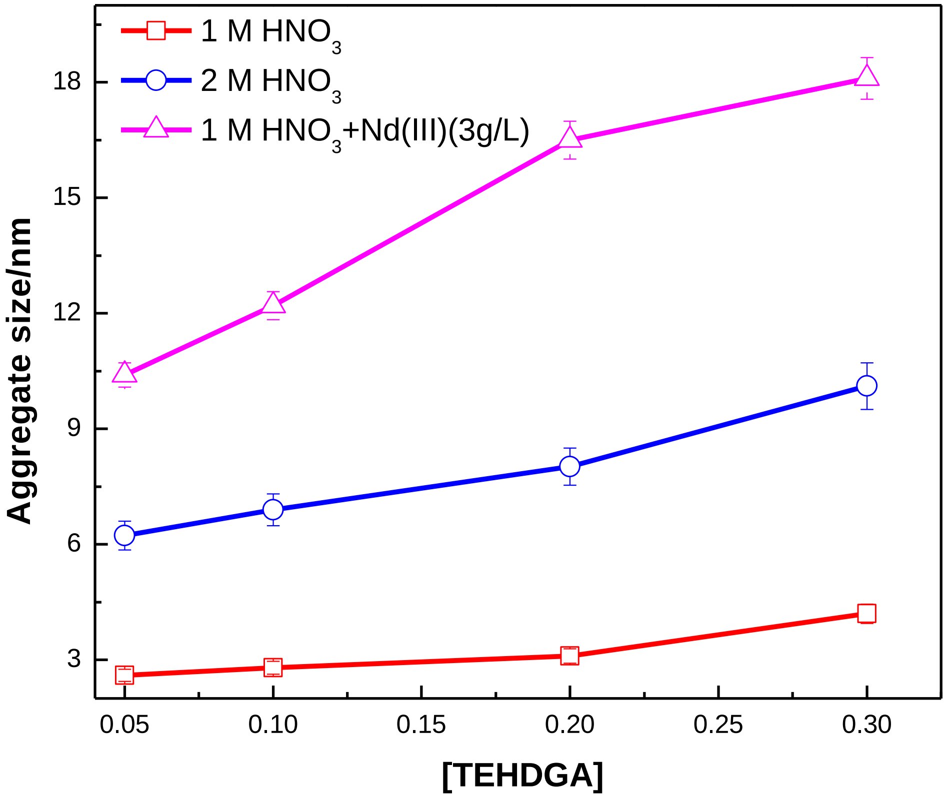

**Figure 3.36.** Variation in the average aggregate sizes as a function of TEHDGA concentration in organic phase. Organic phase TEHDGA/*n*-DD. Aqueous phase: 1 M $HNO_3$ or 2M $HNO_3$.

### 3.6 Summary

The aggregation behaviour of TEHDGA reverse micelles formed during the extraction of neodymium nitrate and nitric acid was investigated by DLS, ATR-FTIR and Raman spectroscopic methods. For this purpose, 0.2 M TEHDGA/*n*-DD organic phase was equilibrated with an aqueous solution of nitric acid in the presence and absence of neodymium nitrate. The extraction of nitric acid and neodymium nitrate in organic phase resulted in the formation of reverse micelles or aggregates. The DLS studies showed that a large number of aggregates of different sizes were formed in organic phase. Broadening of amidic transmittance bands in the ATR-FTIR spectra of the organic phase below third phase formation showed that there were several protonated (acid-solvates) species of TEHDGA present in organic phase, leading to the distribution aggregates. Since the core of these reverse micelles is polar nature and they are dispersed in a non-polar *n*-dodecane medium, they tend to exert an inter-aggregate interaction among the various aggregates leading to swelling of aggregates and these interactions increased with increase in the extraction of neodymium and nitric acid. As a result, the size, concentration and distribution of aggregates increased with increase in the concentrations of neodymium nitrate and nitric acid in aqueous phase. However, average aggregate size decreased with increase in the temperature of the system. The amidic carbonyl bonds were strongly affected by the extraction of nitric acid and Nd(III), below third phase formation and etheric bonds were not significantly affected under these conditions.

At 298 K, when 0.2 M TEHDGA/*n*-DD was contacted with 4 M nitric acid, or when the concentration of neodymium nitrate exceeded 6g/L at 1 M nitric acid, 2g/L at 2 M nitric acid and 0.5g/L at 3 M nitric acid, the organic phase underwent splitting into two phases, leading to third phase formation. The DLS studies showed that there was a significant increase in the concentration and size of aggregates upon third phase formation. This observation was supported by a dramatic increase in the intensity of amidic and etheric transmittance bands of TEHDGA upon third phase formation. Even though the average aggregate size was more in third phase as compared to the organic phase before third phase formation, the aggregate distribution was narrow in third phase, possibly due to the merger of aggregates in third phase due to strong inter-aggregate interaction. In addition, the concentration of nitric acid present in the third phase was significantly higher than the 1:1 stoichiometry of TEHDGA and $HNO_3$, and this observation was supported by ATR-FTIR and Raman studies.

In contrast, the concentration of aggregates, size and distribution of aggregates in diluent phase were lower than that observed for the third phase. The ATR-FTIR studies also confirmed that the aggregates formed upon loading of neodymium and nitric acid in organic phase tends to migrate towards third phase possibly due to inter-aggregate interactions. As a result, the size and distribution of aggregates in diluent phase was small.

## References

[1] S.A. Ansari, P. Pathak, P.K. Mohapatra, V.K. Manchanda, Chemistry of diglycolamides: Promising extractants for actinide partitioning, Chem. Rev. 112 (2012) 1751–1772.

[2] J.N. Mathur, M.S. Murali, K.L. Nash, Actinide partitioning — a review, Solvent Extr. Ion Exch. (2007) 37–41.

[3] Y. Sasaki, G.R. Choppin, Solvent extraction of Eu, Th, U, Np and Am with N,N′-dimethyl-N,N′-dihexyl-3-oxapentanediamide and its analogous compounds, Anal. Sci. 12 (1996) 225-230.

[4] Y. Sasaki, Y. Sugo, K. Morita, K.L. Nash, The Effect of Alkyl Substituents on Actinide and Lanthanide Extraction by Diglycolamide Compounds, Solvent Extr. Ion Exch. 33 (2015) 625-641.

[5] Y. Sasaki, Y. Sugo, S. Suzuki, S. Tachimori, The novel extractants diglycolamides for the extraction of lanthanides and actinides in HNO3-n-dodecane system, Solvent Extr. Ion Exch. 19 (2001) 91–103.

[6] E.A. Mowafy, H.F. Aly, Extraction and separation of Pd(II), Pt(IV), Fe(III), Zn(II), Cu(II) and Ag(I) from hydrochloric acid solutions with selected cyanamides as novel extractants, J. Hazard. Mater. 149 (2007) 465–470.

[7] L. Berthon, L. Martinet, F. Testard, C. Madic, T. Zemb, Solvent penetration and sterical stabilization of reverse aggregates based on the DIAMEX process extracting molecules: Consequences for the third phase formation, Solvent Extr. Ion Exch. 25 (2007) 545–576.

[8] K. Benadict Rakesh, A. Suresh, N. Sivaraman, V.K. Aswal, P.R. Vasudeva Rao, Extraction and third phase formation behaviour of tri-iso-amyl phosphate and tri-n-butyl phosphate with Zr(IV) and Hf(IV): A comparative study, J. Radioanal. Nucl. Chem. 309

(2016) 1037–1048.

[9] K. Osseo-Asare, Aggregation, reversed micelles, and microemulsions in liquid-liquid extraction: the tri-n-butyl phosphate diluent-water-electrolyte system, Adv. Colloid Interface. Sci. 37 (1991) 123-173.

[10] T. Prathibha, B.R. Selvan, K.A. Venkatesan, M.P. Antony, Studies on the radiolytic degradation of N,N-dioctyl-2-hydroxyacetamide using dynamic light scattering and ATR-FTIR spectroscopy, Radiochim. Acta. 107 (2019) 441–448.

[11] K. Osseo-Asare, Volume changes and distribution of HCl and H2O in the tri-n-butyl phosphate-H2O-HCl liquid-liquid system: A reversed micellar phenomenological model, Colloids and Surfaces. 50 (1990) 373–392.

[12] N. Kumari, P.N. Pathak, Dynamic light scattering studies on the aggregation behavior of tributyl phosphate and straight chain dialkyl amides during thorium extraction, J. Ind. Eng. Chem. 20(2014) 1382-1387.

[13] R. Chiarizia, A. Briand, Third phase formation in the extraction of inorganic acids by TBP in n-Octane, Solvent Extr. Ion Exch. 25 (2007) 351–371.

[14] E.L. Campbell, V.E. Holfeltz, G.B. Hall, K.L. Nash, G.J. Lumetta, T.G. Levitskaia, Nitric Acid and Water Extraction by T2EHDGA in n-Dodecane, Solvent Extr. Ion Exch. 35 (2017) 586–603.

[15] S. Nave, C. Mandin, L. Martinet, L. Berthon, F. Testard, C. Madic, T. Zemb, Supramolecular organisation of tri-n-butyl phosphate in organic diluent on approaching third phase transition, Phys. Chem. Chem. Phys. 6 (2004) 799-808.

[16] P.N. Pathak, S.A. Ansari, S. Kumar, B.S. Tomar, V.K. Manchanda, Dynamic light scattering study on the aggregation behaviour of N,N,N′,N′-tetraoctyl diglycolamide

(TODGA) and its correlation with the extraction behaviour of metal ions, J. Colloid Interface Sci. 342 (2010) 114–118.

[17] R. Chiarizia, D. Stepinski, M.R. Antonio, Sans study of HCl extraction by selected neutral organophosphorus compounds in n-octane, Sep. Sci. Technol. 41 (2006) 2075-2095.

[18] R. Chiarizia, M.P. Jensen, M. Borkowski, J.R. Ferraro, P. Thiyagarajan, K.C. Littrell, SANS study of third phase formation in the U(VI)-HNO3/TBP-n-dodecane system, Sep. Sci. Technol. 38 (2003) 3313–3331.

[19] M.P. Jensen, T. Yaita, R. Chiarizia, Reverse-micelle formation in the partitioning of trivalent f-element cations by biphasic systems containing a tetraalkyldiglycolamide, Langmuir. 23 (2007) 4765–4774.

[20] T. Yaita, A.W. Herlinger, P. Thiyagarajan, M.P. Jensen, Influence of extractant aggregation on the extraction of trivalent f-element cations by a tetraalkyldiglycolamide, Solvent Extr. Ion Exch. 22 (2004) 553-571.

[21] T. Prathibha, K.A. Venkatesan, M.P. Antony, Comparison in the aggregation behaviour of amide extractant systems by dynamic light scattering and ATR-FTIR spectroscopy, Colloids Surf. A. 538 (2018) 651-660.

[22] R. Ganguly, J.N. Sharma, N. Choudhury, TODGA based w/o microemulsion in dodecane: An insight into the micellar aggregation characteristics by dynamic light scattering and viscometry, J. Colloid Interface Sci. 355 (2011) 458–463.

[23] K. Bell, A. Geist, F. McLachlan, G. Modolo, R. Taylor, A. Wilden, Nitric Acid Extraction into TODGA, Procedia Chem. 7 (2012) 152–159.

[24] E.S. Shamay, V. Buch, M. Parrinello, G.L. Richmond, At the water’s edge: Nitric acid as a weak acid, J. Am. Chem. Soc. 129 (2007) 12910–12911.

[25] M.B. Singh, S.R. Patil, A.A. Lohi, V.G. Gaikar, Insight into nitric acid extraction and aggregation of N, N, N’, N’-Tetraoctyl diglycolamide (TODGA) in organic solutions by molecular dynamics simulation, Sep. Sci. Technol. 53 (2018) 1361–1371.

[26] S. Nave, G. Modolo, C. Madic, F. Testard, Solvent Extraction and Ion Exchange Aggregation Properties of N,N,N′,N′-Tetraoctyl-3-oxapentanediamide (TODGA) in n-Dodecane Tetraoctyl-3-oxapentanediamide (TODGA) in n-Dodecane, 22 (2007) 257-551.

[27] P. Deepika, K.N. Sabharwal, T.G. Srinivasan, P.R. Vasudeva Rao, Studies on the use of N,N,N’,N’-Tetra(2-ethylhexyl) diglycolamide (TEHDGA) for actinide partitioning. I: Investigation on third-phase formation and extraction behavior, Solvent Extr. Ion Exch. 28 (2010) 184–201.

[28] C. Musikas, H. Hubert, Extraction by N.N’-tetraalkylmalonamides II. extraction of metallic ions, Solvent Extr. Ion Exch. 5 (1987) 877–893.

[29] Y. Cui, J. Yang, G. Yang, G. Xia, Y. Nie, G. Sun, Effect of diluents on extraction behavior of rare earth elements with N,N,N′,N′-tetrabutyl-3-oxy-glutaramide from hydrochloric acid, Hydrometallurgy. 121(2012) 16-21

# Chapter 4: Role of phase modifiers in controlling the third phase formation

Third phase formation is an undesirable event during the extraction of trivalent metal ions from HLLW [1,2]. The third phase formation behaviour and the factors affecting the third phase formation [2-4] have been detailed in chapter 1. The third phase formation in diglycolamide can be prevented in a couple of ways. One method is to modify the structure of ligand or diluent present in the organic phase [5-7] and the other method is to add phase modifiers to the solvent phase, to minimize the aggregation and third phase formation [8-10]. These phase modifiers are nothing but organophilic polar compounds that do not normally participate in the extraction of target metal ion but enhances the compatibility of the polar metal-solvate or acid-solvate formed in organic phase with *n*-dodecane [8,9].

The present chapter describes the role of phase modifiers in controlling the third phase formation. This chapter is divided into two parts. Part I discusses the role of neutral ligand phase modifiers such as TBP and DHOA in controlling the third phase formation in 0.2 M TEHDGA/*n*-DD and Part II describes the role of long chain alcohols in preventing the aggregation and third phase formation.

# Part I. Role of neutral extractants as phase modifiers in controlling the third phase formation

## 4.1 Introduction

The application of diglycolamides in the separation of trivalent actinides and from nitric acid solution has been reviewed by Whittaker *et al*. [8]. The review discussed the importance of different phase modifiers such as TBP, DHOA and long chain alcohols in the solvent phase containing TODGA/*n*-DD for trivalent actinides separation. It was realized that increasing the polarity of the organic phase stabilizes the polar-metal solvates and minimized the aggregation in organic phase [10,11]. This was achieved by adding long-chain alcohol phase modifiers to the organic phase. Moreover, the ligands such as TBP and DHOA have also been suggested as phase modifiers [8]. Several reports are available in literature on the use of TBP and DHOA as phase modifiers for the extraction of trivalent metal ions from nitric acid solutions in the organic phase containing diglycolamides in *n*-DD [8,12]. However, the information on how the addition of TBP or DHOA controls third phase formation in diglycolamide systems is missing in literature.

In view of view of this, studies have been conducted to unravel the role of TBP and DHOA in preventing the third phase formation during the extraction of trivalent metal ions from nitric acid medium. Since TEHDGA has been proposed for group separation of trivalent metal ions from HLLW[12-17], the extraction behavior of the representative trivalent metal ion, Nd(III) from nitric acid medium was studied in a binary solution containing 0.2 M TEHDGA + phase modifier in *n*-dodecane. To understand the insights of the aggregation, the organic phase obtained after extraction was subjected to dynamic light scattering (DLS) measurements.

## 4.2 Results and discussion

### 4.2.1. Extraction behaviour of nitric in TEHDGA, DHOA, TBP alone in *n*-DD

Generally, significant amount of polar extractants such as tri-*n*-butyl phosphate (TBP), and *N*,*N*-dihexyloctanamide (DHOA) have been added to the solution of 0.2 M TEHDGA in *n*-dodecane (*n*-DD) to control the third phase formation, during the extraction of trivalent actinides from HLLW. To understand the role of TBP and DHOA in preventing the third phase formation, it is necessary to understand the aggregation behaviour of the organic solutions containing TEHDGA, TBP, and DHOA in *n*-dodecane alone and that obtained before, and after extraction of nitric acid and Nd(III). The extraction behaviour of nitric acid in 1.1 M TBP/*n*-DD and 0.5 M DHOA/*n*-DD is shown in Figure 4.1. The extraction behaviour was compared with the extraction of nitric acid observed in 0.2 M TEHDGA/*n*-DD [18-20]. In all cases, the extraction of nitric acid in the organic phase increases with increase the concentration of nitric acid in the aqueous phase. When 0.2 M TEHDGA/*n*-DD was contacted with 4 M nitric acid, the organic phase undergoes splitting into “third phase” existing at the bottom of the organic phase which is rich in TEHDGA….$(HNO_3)_x$ complex, and the top phase known as the “diluent rich” phase (see part II of chapter 3). The limiting concentration of nitric acid in organic phase (LOC of $HNO_3$) for third phase formation in 0.2 M TEHDGA/*n*-DD was 0.23 M and critical aqueous phase concentration (CAC) of nitric acid was 3.58 M as shown in chapter 3. In contrast to this, the extraction of nitric acid in both 1.1 M TBP/*n*-DD and 0.5 M DHOA/*n*-DD does not lead to third phase formation even at 9 M nitric acid. However, the third phase formation was observed when 1.1 M TBP/*n*-DD and 0.5 M DHOA/*n*-DD was contacted with 15 M and 10 M nitric acid respectively [18, 19].

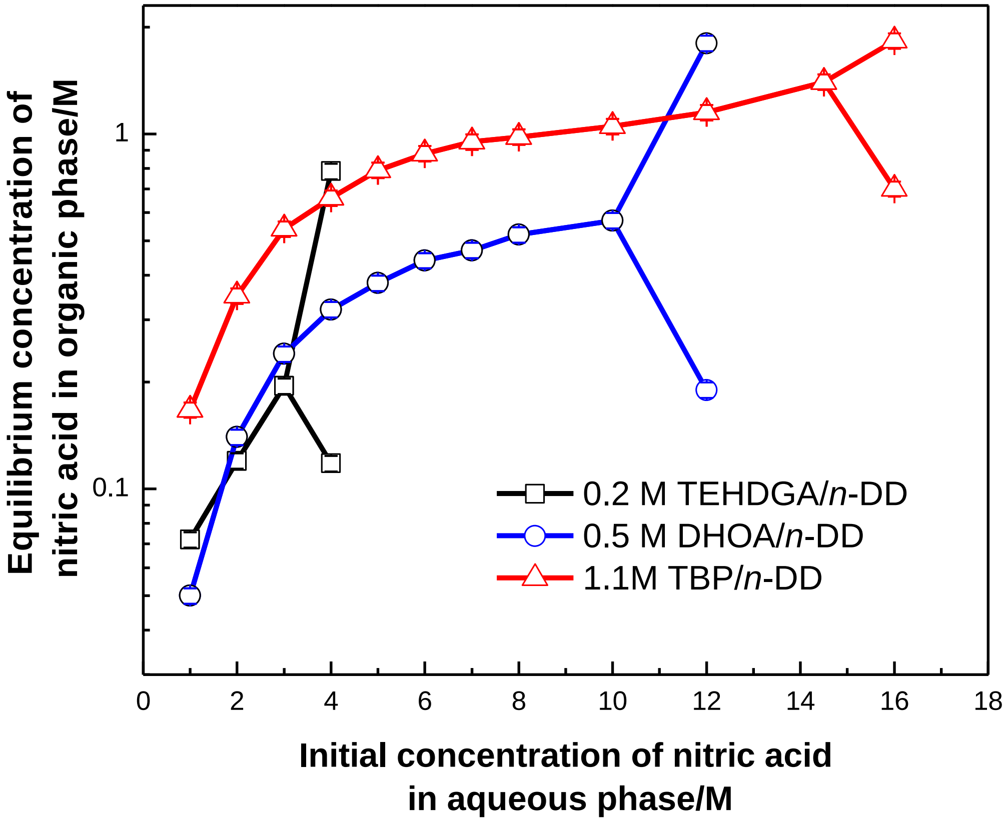

**Figure 4.1**. Extraction behaviour of nitric acid in organic phase as function of initial concentration of nitric acid concentration in aqueous phase. Organic phase: 0.2 M TEHDGA/*n*-DD or 0.5 M DHOA/*n*-DD or 1.1 M TBP/*n*-DD. Aqueous phase: Nitric acid concentration varied from 1 M to ~16 M.

The LOC and CAC were determined for various concentrations of TBP, and DHOA and the results are shown in Table 4.1. It is observed that the LOC and CAC values of nitric acid in TBP/*n*-DD, and DHOA/*n*-DD are much higher than the LOC and CAC values of 0.2 M TEHDGA/*n*-DD system. It should be noted that these values are also higher than the concentration of nitric acid prevailing (3-4 M) in high-level liquid waste (HLLW). Since, higher LOC can avoid the formation of the third phase during the extraction of trivalent metal ions from

HLLW, these reagents (TBP or DHOA) have been chosen as phase modifiers. At LOC, the mole ratio of TBP or DHOA to $HNO_3$ was determined to be 1:1.3. This could be due to complete acid-solvates formation was attained at limiting organic concentration (LOC).

**Table 4.1.** The LOC and CAC value of nitric acid in various systems.

| Organic phase | $[HNO_3]$/ M | LOC/M | CAC/M | [Extractant] to $[HNO_3]$ ratio at LOC |
|---|---|---|---|---|
| 0.2 M TEHDGA/*n*-DD | 4 M | 0.23 | 3.58 | 1:1.2 |
| 0.18 M TBP/*n*-DD | 16 M | 0.20* | 15.4* | 1:1.1 |
| 0.73 M TBP/*n*-DD | 16 M | 0.93 | 13.8 | 1:1.3 |
| 1.1 M TBP/*n*-DD | 15 M | 1.4[18] | 13.2 | 1:1.3 |
| 0.1 M DHOA/*n*-DD | 10 M | 0.12 | 8.3 | 1:1.2 |
| 0.25 M DHOA/*n*-DD | 10 M | 0.29 | 7.8 | 1:1.2 |
| 0.5 M DHOA/*n*-DD | 10 M | 0.57[19] | 7.6 | 1:1.2 |
| 0.2 M TEHDGA+0.18 M TBP/*n*-DD | 5 M | 0.44 | 4.2 | 1:1.2 |
| 0.2 M TEHDGA+0.37 M TBP/*n*-DD | 7 M | 0.76 | 5.9 | 1:1.3 |
| 0.2 M TEHDGA+0.73 M TBP/*n*-DD | 10 M | 1.18 | 8.1 | 1:1.3 |
| 0.2 M TEHDGA+1.1 M TBP/*n*-DD | 12 M | 1.78 | 10.3 | 1:1.3 |
| 0.2 M TEHDGA+0.1 M DHOA/*n*-DD | 5 M | 0.36 | 4.2 | 1:1.2 |
| 0.2 M TEHDGA+0.25 M DHOA/*n*-DD | 6 M | 0.62 | 4.9 | 1:1.3 |
| 0.2 M TEHDGA+0.5 M DHOA/*n*-DD | 8 M | 0.92 | 6.4 | 1:1.3 |

***** The values represent not LOC or CAC

### 4.2.2 Aggregation behaviour of TEHDGA, DHOA, and TBP with nitric acid

The extraction of nitric acid in organic phase results in the formation nitric acid adduct with amidic moiety (O=C-NR$_2$-) of TEHDGA, and DHOA, and phosphoryl (>P=O) group of TBP by nitric acid. Acid-solvates of these extractants leads to the formation of aggregates of different sizes, and they get distributed uniformly into *n*-dodecane phase [21, 22]. The distribution of aggregates in organic phase was probed by dynamic light scattering measurements and results are shown in Figure 4.2. This was recorded after contacting the organic phase, 0.2 M TEHDGA/*n*-DD or 1.1 M TBP/*n*-DD or 0.5 M DHOA/*n*-DD with nitric acid. The concentration of nitric acid was varied from 1 M to 10 M. It can be seen that the average aggregate size and the distribution of aggregates in the organic phase increases with increase in the concentration of nitric acid, in all cases [21]. This could be due to the enhancement in the extraction of nitric acid in the organic phase with the increase in the concentration of nitric acid in the aqueous phase, as shown in Figure 4.1. Extraction of nitric acid results in the formation of newer aggregates and merger of existing aggregates in the organic phase. In view of this, the average aggregate size and aggregate distribution increases with increase in the concentration of nitric acid [21, 23]. Kumari *et al.,* also reported a similar behaviour during extraction of nitric acid with 1.1 M TBP/*n*-DD and 1.1 M DHOA/*n*-DD [20]. At a particular concentration of nitric acid, for instance, 3 M $HNO_3$, the aggregate size and their distribution in the organic phase increases in the order of TBP < DHOA < TEHDGA.

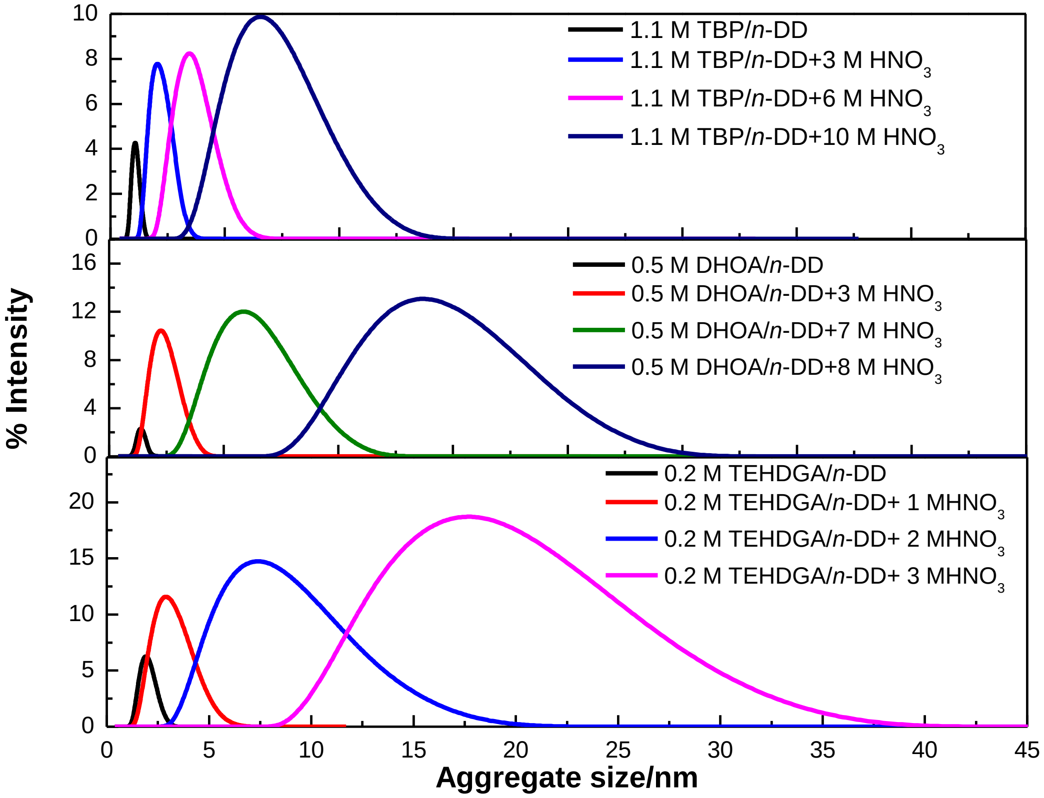

**Figure 4.2.** Comparison in the aggregation behaviour of the organic phase containing 0.2 M TEHDGA/*n*-DD or 0.5 M DHOA/*n*-DD or 1.1 M TBP/*n*-DD, recorded after contacting with nitric acid varied from 1 M to 10 M.

Similarly, the aggregation behaviour of organic phase containing TBP or DHOA in *n*-dodecane as a function of extractant concentration at a fixed acidity of 3 M nitric acid is shown in Figure 4.3. It can be seen that the average aggregate size and the distribution of aggregates in the organic phase increases with increase in the concentration of extractant in organic phase in both cases [21, 22]. This could be again due to the increase in the acid-solvate formation of the extractant with increase in the concentration of extractant in organic phase that leads to more aggregation in organic phase.

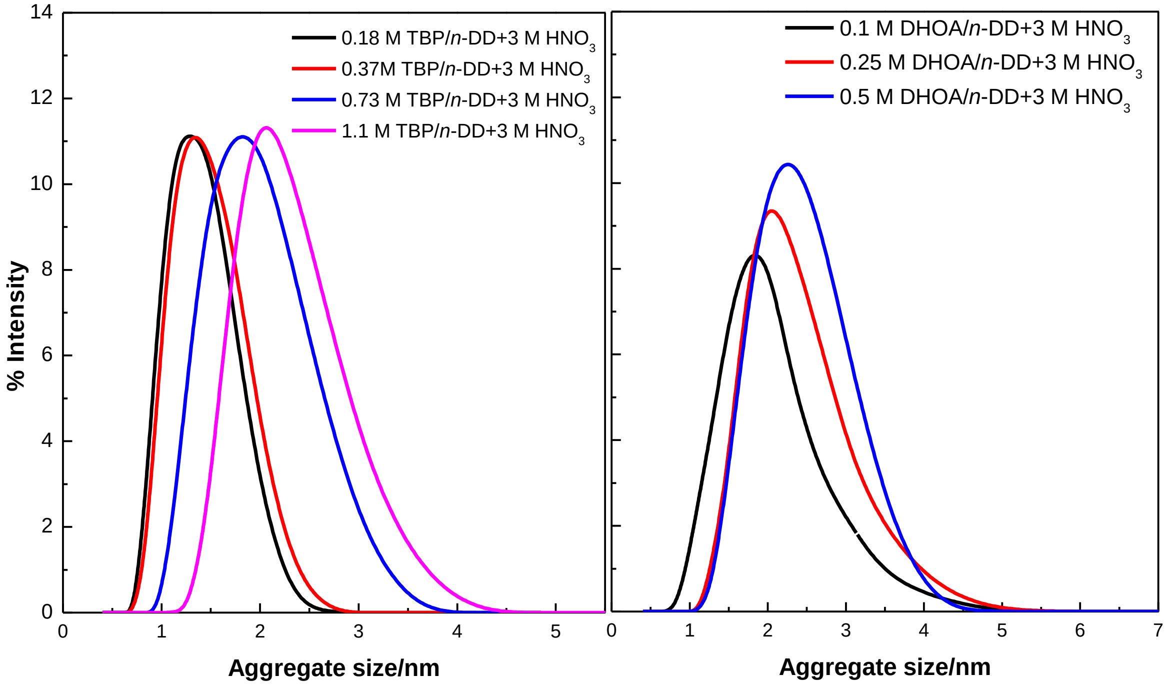

**Figure 4.3.** Aggregate distribution in organic phase as a function of various extractant concentrations recorded after contacting the organic phase with 3 M nitric acid. Organic phase: TBP/*n*-DD or DHOA/*n*-DD. Aqueous phase: 3 M nitric acid.

### 4.2.3 Aggregation behaviour of TEHDGA, DHOA, and TBP at LOC

Figure 4.4 shows the aggregate distribution observed in the organic phase at LOC of nitric acid. This was obtained by equilibrating the organic phase initially with a suitable concentration of nitric acid that could lead to third phase formation. The LOC of organic phase and CAC of aqueous phase was determined, and the organic phase was then subjected to DLS measurements. The results are shown in Figure 4.4. The average aggregate size obtained at LOC represents the limiting aggregate size (LAS) of the system, above which the organic phase undergoes splitting into two phases namely the third phase, and diluent rich phase.

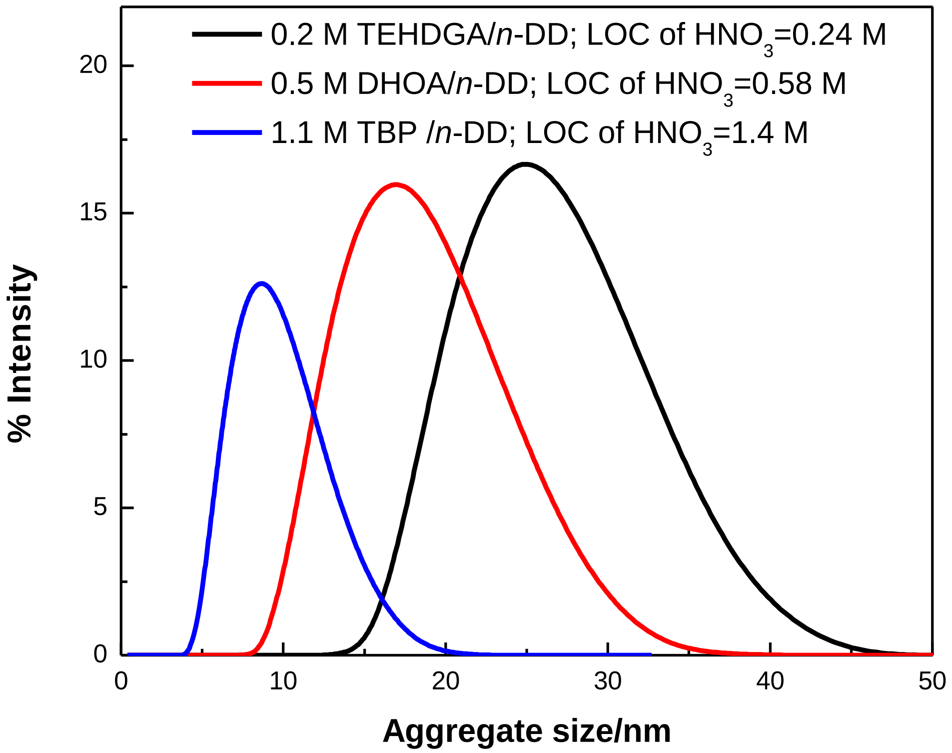

**Figure 4.4.** Aggregate distribution of various organic phases at LOC of nitric acid.

It can be seen from Figure 4.4 that the average aggregate size and FWHM of aggregate distribution at LOC increases in the order TBP (9.2 nm) < DHOA (18.8 nm) < TEHDGA (28 nm), which is the order of increasing polarity of extractants. The values in parenthesis represent the average limiting aggregate size (LAS). It should be noted that DHOA containing an amidic moiety is more polar than the TBP containing a phosphoryl group. Moreover, the TEHDGA containing a couple of amidic and etheric functional groups is obviously more polar than DHOA. Kumari *et al.* reported that the aggregates formed upon extraction of nitric acid in DHOA were larger than those observed in TBP [20]. Therefore, the polarity of the extractants seems to play a predominant role in determining the tendency of aggregation in a non-polar, *n*-dodecane phase.

At LOC the mole ratio of the extractant to $HNO_3$ (Table 4.1) varies from 1:1.15 to 1.1.3 depending upon the nature of extractant. Since the difference between these two ratios is quite less (~10%), it is desirable to take the higher value for assuming complete acid-solvate formation irrespective of the nature of extractant, which is then followed by third phase formation. However, the average aggregate size increases in order TBP < DHOA < TEHDGA. This shows that DHOA and TEHDGA containing strongly polar amidic functional group that facilitates inter-particle interaction among the acid-solvates and also facilitates the merger of aggregates, as compared to TBP. Moreover, the amount of water molecules present in polar aggregates is more (varies from 0.01 M to 0.3 M depending upon the polarity) as compared to the less polar aggregates [18, 22]. As a result, the polar aggregates undergo swelling and the aggregate size at LOC increases in the order TBP < DHOA < TEHDGA.

### 4.2.4 Extraction of nitric acid in binary solution

Since the LOC of nitric acid in TBP and DHOA is higher than the LOC of nitric acid in TEHDGA (See Table 4.1), it is quite likely that the addition of TBP, and DHOA to TEHDGA could increase the third phase formation limits. Therefore, the extraction behaviour of nitric acid in the binary solution composed of 0.2 M TEHDGA+TBP in *n*-dodecane was studied and results are shown in Figure 4.5. The concentration of TBP in the solution was varied from 0.18 M (5% TBP) to 1.1 M (30% TBP). The extraction of nitric acid in the organic phase showed concomitant increase with increase in the concentration of nitric acid in the aqueous phase as expected [16, 18, 24].

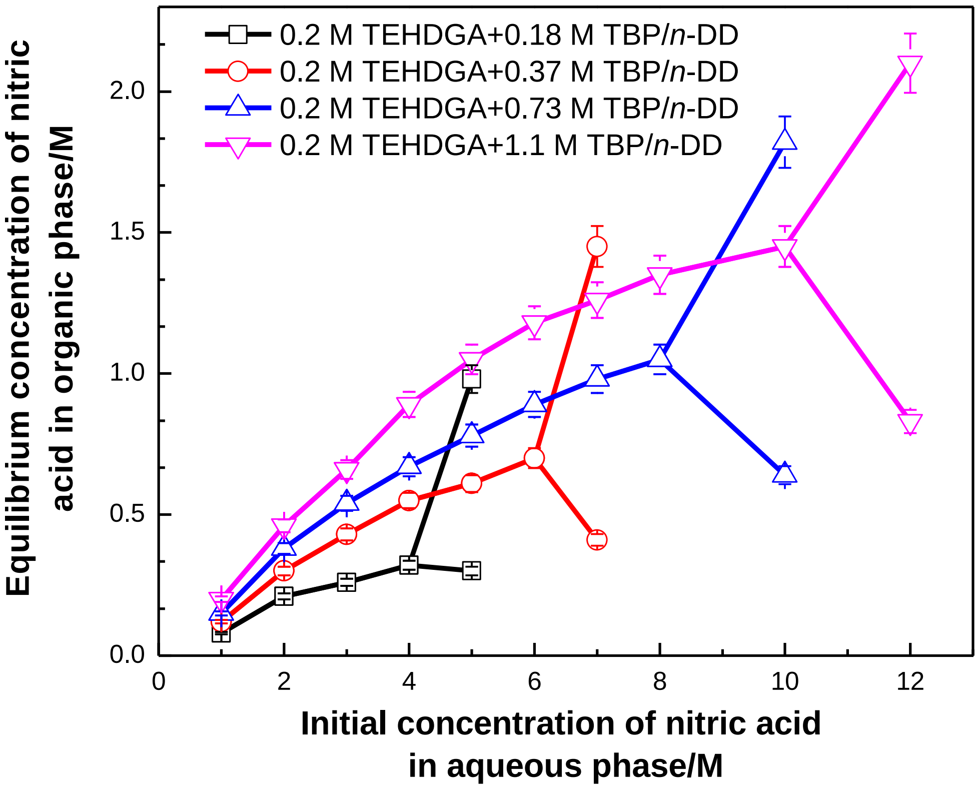

**Figure 4.5.** Extraction behaviour of nitric acid in various organic phases as a function of initial nitric acid concentration in the aqueous phase. Organic phase: 0.2 M TEHDGA+TBP/*n*-DD. Aqueous phase: Nitric acid concentration varied from 1 M to 13 M.

The LOC and CAC values determined at various concentration of TBP in a solution of 0.2 M TEHDGA+TBP/*n*-DD, tabulated in Table 4.1, also increases with increase in the concentration of TBP [24]. This could be possible only when the extracted nitric acid is distributed between TEHDGA and TBP, and the degree of acid-solvate formation with TEHDGA in the solution of TEHDGA+TBP/*n*-DD is minimized to some extent in the presence of TBP. Table 4.2 compares the extraction of nitric acid in TEHDGA, phase modifiers (TBP and DHOA) alone in *n*-dodecane with that obtained in the binary solution at 3 M nitric acid. It can be seen that the concentration of nitric acid extracted in the individual extractants is nearly same when the extractants are combined together. As a result, the LOC and CAC values are shifted to higher nitric acid concentrations, depending upon the concentration of TBP employed in the binary solution.

**Table 4.2**. Extraction behavior of nitric acid in the organic phase as a function extractant concentration at 3 M $HNO_3$.

| Organic phase | $[HNO_3]_{Org}$/M |
|---|---|
| 0.2 M TEHDGA/*n*-DD | 0.19 |
| 0.18 M TBP/*n*-DD | 0.11 |
| 0.37 M TBP/*n*-DD | 0.22 |
| 0.73 M TBP/*n*-DD | 0.33 |
| 1.1 M TBP/*n*-DD | 0.51[18] |
| 0.1 M DHOA/*n*-DD | 0.04 |
| 0.25 M DHOA/*n*-DD | 0.13 |
| 0.5 M DHOA/*n*-DD | 0.22 |
| 0.2 M TEHDGA+0.18 M TBP/*n*-DD | 0.30 |
| 0.2 M TEHDGA+0.37 M TBP/*n*-DD | 0.43 |
| 0.2 M TEHDGA+0.73 M TBP/*n*-DD | 0.52 |
| 0.2 M TEHDGA+1.1 M TBP/*n*-DD | 0.68 |
| 0.2 M TEHDGA+0.1 M DHOA/*n*-DD | 0.24 |
| 0.2 M TEHDGA+0.25 M DHOA/*n*-DD | 0.32 |
| 0.2 M TEHDGA+0.5 M DHOA/*n*-DD | 0.42 |

### 4.2.5 Aggregation behaviour of the binary solution

Figure 4.6 shows aggregate size distribution of the binary solution, 0.2 M TEHDGA+TBP/*n*-DD, obtained after contacting the organic phase with 4 M nitric acid. The concentration of TBP was varied from 0.18 M to 1.1 M in the binary solution. It can be seen from Figure 4.5 that the extraction of nitric acid increases with increase in the concentration of TBP in binary solution. Therefore, it can be expected that the average aggregate size should increase with increase in the concentration of TBP. However, it is observed from Figure 4.6 that the average aggregate size and their distribution in binary solution decreases with increase in the concentration of TBP. This clearly indicates that the extracted nitric acid is distributed between TEHDGA and TBP otherwise TEHDGA acid-solvates alone would have resulted in the third phase at 4 M nitric acid. Since the third phase formation limit for TBP is very high, the acid-solvates of TBP is dispersed in *n*-DD phase at 4 M nitric acid without undergoing aggregation. Moreover, increasing the concentration of TBP increases the acid-solvate formation with TBP and dispersion of TBP acid-solvates in *n*-dodecane phase. Therefore, the average aggregate size of the binary solution decreases with increase in the concentration of TBP. A similar extraction and aggregation size distribution behaviour was also observed in 0.2 M TEHDGA+DHOA/*n*-DD, obtained after contacting the organic phase with 4 M nitric acid.

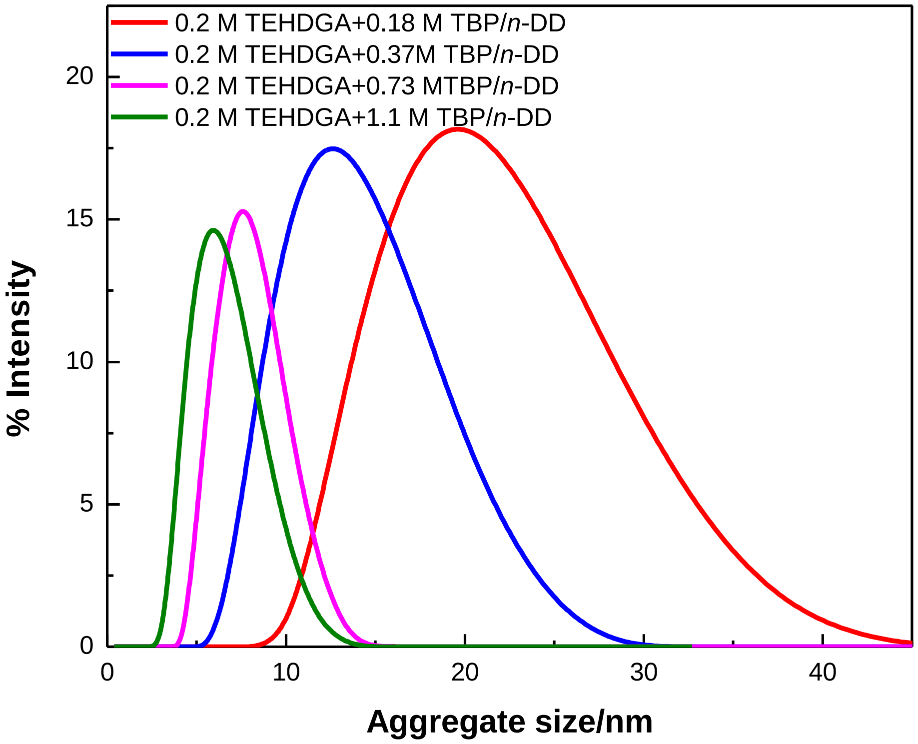

**Figure 4.6.** Aggregate distribution in organic phase at various concentrations of TBP recorded after contacting the organic phase with 4 M nitric acid. Organic phase: 0.2 M TEHDGA+TBP/*n*-DD. Aqueous phase: 4 M nitric acid.

### 4.2.6 Aggregation behaviour of the binary solution at LOC

It would be interesting to understand the aggregation behaviour of the binary solution at the LOC of nitric acid for third phase formation. At LOC, the mole ratio of the binary extractant to $HNO_3$ is 1:1.3, irrespective of the concentration of TBP in the binary solution, as shown in Table 4.1. The third phase formation is facilitated when the mole ratio of nitric acid exceeds the value of 1:1.3 (extractant: $HNO_3$) this means complete acid-solvate formation has achieved. Figure 4.7 shows the aggregate size distribution of the binary solution obtained at LOC of nitric acid. The aggregate distribution is compared with the distribution observed at the LOC of 0.2 M TEHDGA/*n*-DD, and 1.1 M TBP/*n*-DD. It can be seen that the average aggregate size and their distribution in binary solution decreases with increase in the concentration of TBP, even though the mole ratio of extractant: $HNO_3$ (1:1.3) is quite similar, irrespective of the concentration of TBP. This observation clearly indicates that the presence of TBP in the binary solution minimizes the aggregate size possibly by diluting the association of the TEHDGA aggregates and facilitating the dispersion of aggregates in *n*-dodecane phase. As a result, the aggregate size decreases with increase in the concentration of TBP in the binary solution. A similar behaviour has also observed in the case of 0.2 M TEHDGA+DHOA/*n*-DD at LOC, is shown in Figure 4.8.

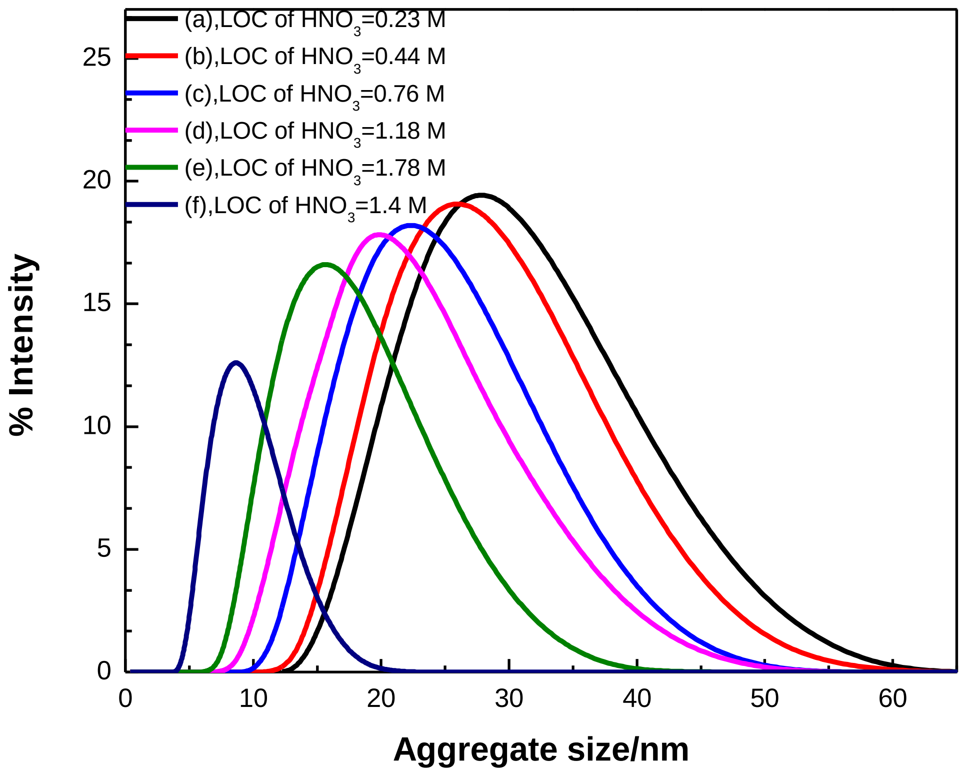

**Figure 4.7.** Aggregate distribution in the organic phase composed of 0.2 M TEHDGA +TBP in *n*-DD at LOC. Organic phase: (a) 0.2 M TEHDGA/*n*-DD, (b) 0.2 M TEHDGA+0.18 M TBP/*n*-DD, (c) 0.2 M TEHDGA+0.37 M TBP/*n*-DD, (d) 0.2 M TEHDGA+0.73 M TBP/*n*-DD, (e) 0.2 M TEHDGA+1.1 M TBP/*n*-DD, (f) 1.1 M TBP/*n*-DD. Aqueous phase: Nitric acid concentrations varied from 1 M to 15 M.

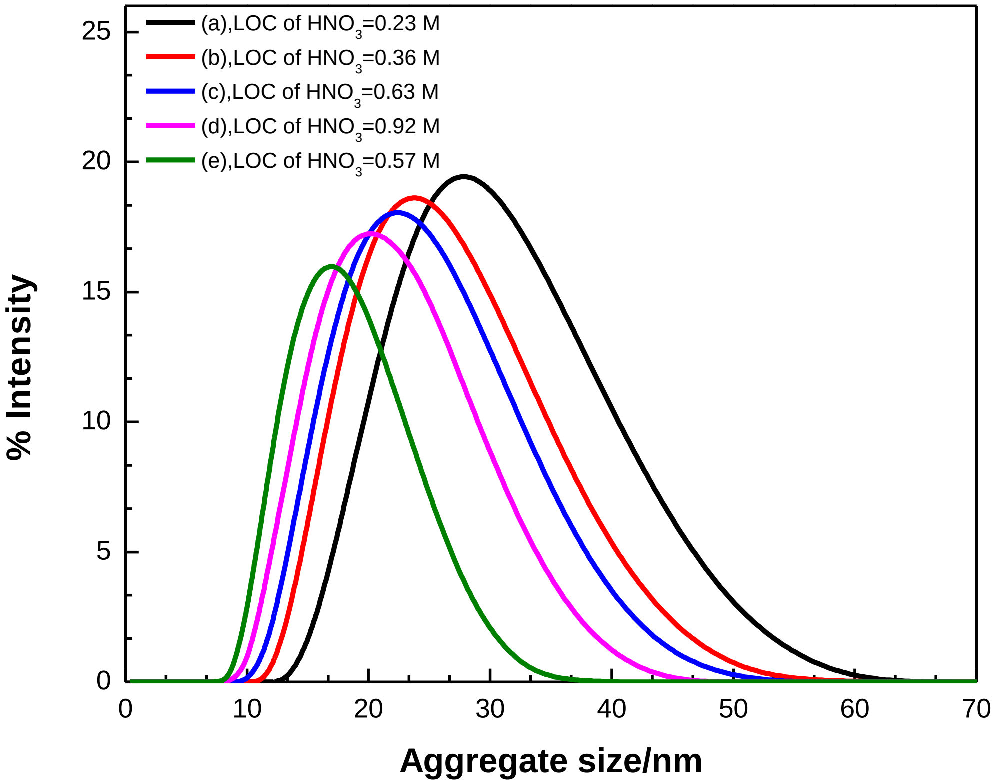

**Figure 4.8.** Aggregate distribution in the organic phase composed of 0.2 M TEHDGA +DHOA in *n*-DD at LOC. Organic phase: (a) 0.2 M TEHDGA/*n*-DD, (b) 0.2 M TEHDGA+0.1 M DHOA/*n*-DD, (c) 0.2 M TEHDGA+0.25 M DHOA/*n*-DD, (d) 0.2 M TEHDGA+0.5 M DHOA/*n*-DD, (e) 0.5 M DHOA/*n*-DD. Aqueous phase: Nitric acid concentrations varied from 1 M to 10 M.

### 4.2.7 Nd(III) extraction isotherm in TEHDGA/*n*-DD

The extraction isotherm of Nd(III) in 0.2 M TEHDGA/*n*-DD at 1 M nitric acid is shown in Figure 4.9. It is observed that the extraction of Nd(III) in organic phase increases with increase in the equilibrium concentration of Nd(III) in aqueous phase. When the equilibrium concentration of Nd(III) in aqueous phase exceeded 2.55 g/L or initial Nd(III) concentration exceeds 6 g/L, the organic phase underwent splitting into two phases. The third phase was dissolved then by the addition 0.2 M TEHDGA/*n*-DD (pre-equilibrated with 1 M $HNO_3$). After dissolution, the concentration of Nd(III) in organic phase was determined to be 3.62 g/L, which is the limiting organic phase (LOC) of Nd(III) at 1 M nitric acid in 0.2 M TEHDGA/*n*-DD. The corresponding initial concentration of Nd(III) in aqueous phase was 6 g/L at LOC. Therefore, the batch equilibrium experiments showed it is desirable to maintain the initial concentration of Nd(III) in 1 M nitric acid at 6 g/L or less to avoid third phase formation.

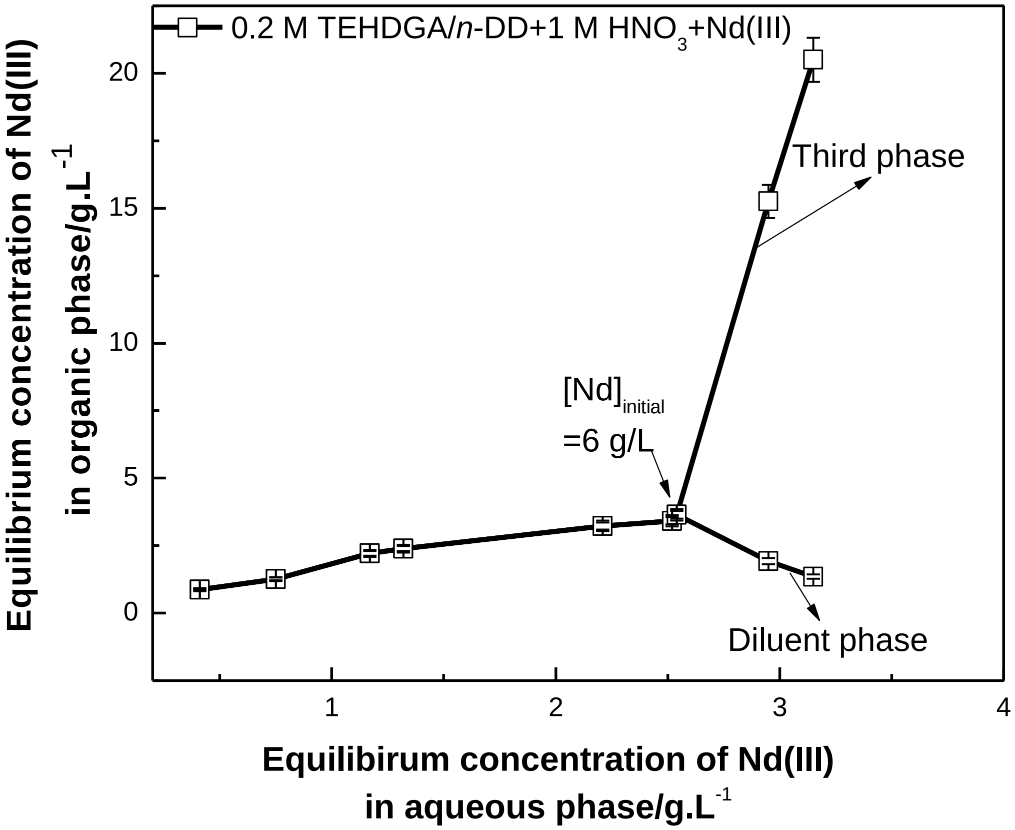

**Figure 4.9.** Variation in the extraction of Nd(III) in organic phase as function of equilibrium concentration of Nd(III) in 1 M nitric acid at 298 K. Organic phase: 0.2 M TEHDGA/*n*-DD. Aqueous phase: : $[Nd(III)]_{initial}$ varied from 1 g/L to 8 g/L in 1 M nitric acid.

### 4.2.8 Aggregation behavior of Nd(III) in TEHDGA/*n*-DD

Figure 4.10 shows the aggregate size distribution in 0.2 M TEHDGA/*n*-DD phase. The organic phase was contacted with 1 M nitric acid solution containing various amounts of Nd(III) before DLS measurements. It is observed that the average aggregate size increases from 3.1 nm to 34 nm with increase in the amount of Nd(III) in 1 M nitric acid from 1 g/L to 6 g/L Nd(III). The details of aggregation behaviour in TEHDGA upon contacting with 1 M nitric acid containing Nd(III) have been discussed in section 3.5.5 of chapter 3. The estimation of Nd(III) in third phase and diluent phase showed that the amount of Nd(III) in third phase and diluent phase were 15.25 g/L and 1.92 g/L respectively. However, after dissolution of third phase (i.e. at LOC), the aggregate size was determined to be 35 nm, as shown in Figure 4.10. Therefore, the DLS studies revealed that the formation of third phase was facilitated when the aggregate size in 0.2 M TEHDGA/*n*-DD exceeds 35 nm after contacting the organic phase with Nd(III) in 1 M nitric acid. Therefore the limiting aggregate size for third phase formation in 0.2 M TEHDGA/*n*-DD is 35 nm at 1 M nitric acid.

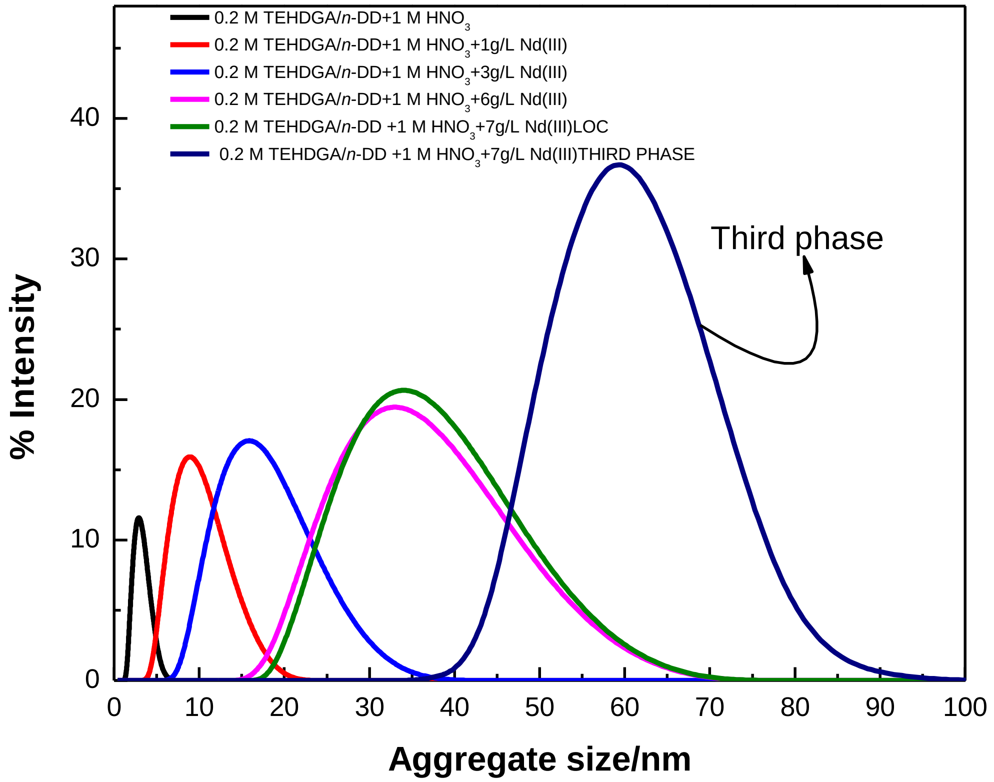

**Figure 4.10.** Variation in the aggregate size distribution as a function of Nd(III) concentration at 1 M $HNO_3$. Organic phase: 0.2 M TEHDGA/*n*-DD. Aqueous phase: [Nd(III)] varied from 1 g/L to 7 g/L at 1 M $HNO_3$.

### 4.2.9 Aggregate size distribution at LOC

The aggregate distribution determined for the 0.2 M TEHDGA/*n*-DD phase at LOC of Nd(III) in different concentration of nitric acid is shown in Figure 4.11. The amount of Nd(III) and concentration of $HNO_3$ in organic phase at LOC are shown in Figure 4.11. It can be seen that the average aggregate size and the aggregate distribution in organic phase decreases with increase in the initial concentration of nitric acid, as against the increase in aggregate distribution expected for the organic phase with increase in the concentration of nitric acid. This observation requires some understanding of the physicochemical changes in organic phase that can occur during the dissolution of third phase. It should be noted that the excess concentration of Nd(III) and $HNO_3$ in organic phase beyond the LOC value, results in the formation of third phase. During this process, the organic phase (composed of third phase and diluent phase) undergoes dilution and the metal ion present in the third phase undergoes redistribution into the newly added organic phase for dissolution. The third phase gradually dissolves and become homogeneous single organic phase after adding a particular volume of acid equilibrated organic phase [1,2]. During this process, the nitric acid and $Nd(NO_3)_3$ coordinated to TEHDGA are diluted, and the associated water also undergoes redistributed into the entire organic phase. The redistribution of extracted water is dependent on the concentration of extracted ions present in organic and aqueous phase [15, 18]. It should be noted that the concentration of ions ($HNO_3$ and $Nd(NO_3)_3$) in organic phase decreased upon dilution during the dissolution of third phase, while the concentration of ions in aqueous phase remains unaffected during the course of the dissolution of third phase. Therefore, it is necessary for the water, which was extracted into organic phase, is transferred into the aqueous phase during the dissolution of third phase. The degree of water movement into aqueous phase is proportional to the concentration of nitric acid present in the aqueous phase. To understand the degree of water movement, the amount of water present in the organic phase was determined by Karl-Fisher titration. The water concentration of the organic phase at LOC decreases in the order of 0.097M water for 1M $HNO_3$ >0.076 M water for 2 M $HNO_3$ > 0.063 M water for 3M $HNO_3$. Therefore, the transfer of water molecules to the aqueous phase is more at higher concentration of nitric acid in aqueous phase. In view of this, the average aggregate size and aggregate distribution observed for the organic phase after dissolution of third phase (i.e. LOC) decreases with increase in the concentration of nitric acid present in aqueous phase at LOC.

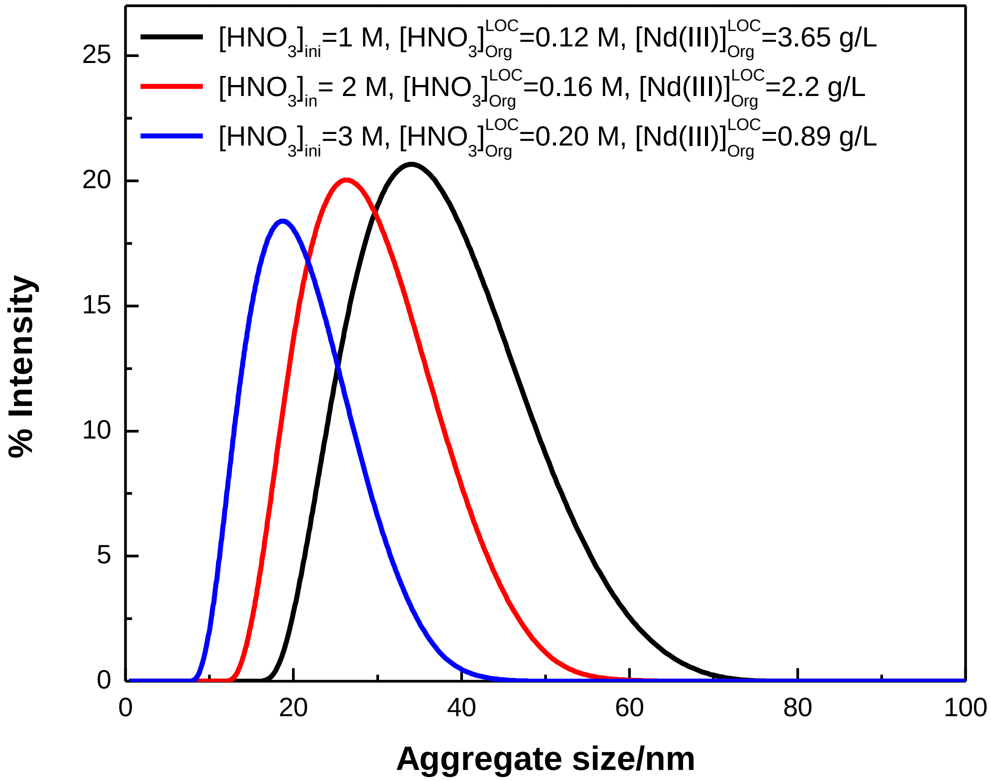

**Figure 4.11.** The aggregate distribution in 0.2 M TEHDGA/*n*-DD at LOC of Nd(III) at different concentrations of nitric acid in aqueous phase. Organic phase: 0.2 MTEHDGA/*n*-DD. Aqueous phase: [Nd(III)] varied from 0.5 g/L to 8g/L in 1 M to 3 M nitric acid.

### 4.2.10 Aggregation behavior of Nd(III) in TEHDGA+TBP/*n*-DD

Figure 4.12 shows the aggregation behaviour of the binary solution obtained after contacting the organic phase with the aqueous solution contacting 5 g/L Nd(III) in 1 M nitric acid. The organic phase was composed of 0.2 M TEHDGA+TBP/*n*-DD and the concentration of

TBP in the binary solution was varied from 0.18 M to 1.1 M. It should be noted that TBP does not extract Nd(III) from nitric acid medium [8, 15] and the extraction is governed only by TEHDGA. Therefore, the concentration of Nd(III) extracted into 0.2 M TEHDGA+TBP in *n*-dodecane is nearly same irrespective of the concentration of TBP present in the binary solution. It can be seen from Figure 4.12 that aggregate size and their distribution in organic phase decreases with increase in the concentration of TBP. This could be possible only when the addition of TBP to 0.2 M TEHDGA/*n*-DD phase minimizes the TEHDGA acid-solvates formation, and instead, the TBP forms acid-solvate in the organic phase. In addition, the presence of TBP in *n*-DD phase dilutes the inter-particle interaction among the aggregates and minimizes the merger of aggregates below the critical size of aggregates for third phase formation. A similar behaviour was also observed in the case of 0.2 M TEHDGA+DHOA/*n*-DD, as shown in Figure 4.13.

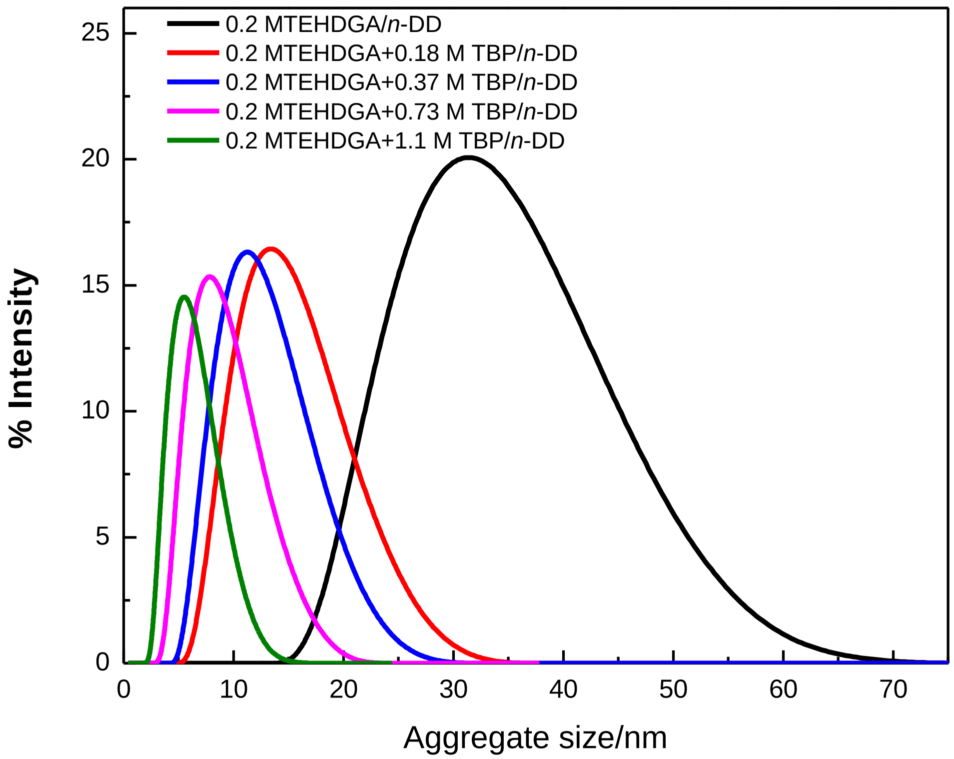

**Figure 4.12.** Aggregate distribution in organic phase at various concentrations of TBP recorded after contacting the organic phase with Nd(III) solution in 1 M nitric acid. Organic phase: 0.2 MTEHDGA+TBP/*n*-DD. Aqueous phase: 1 M nitric acid containing 5 g/L Nd(III).

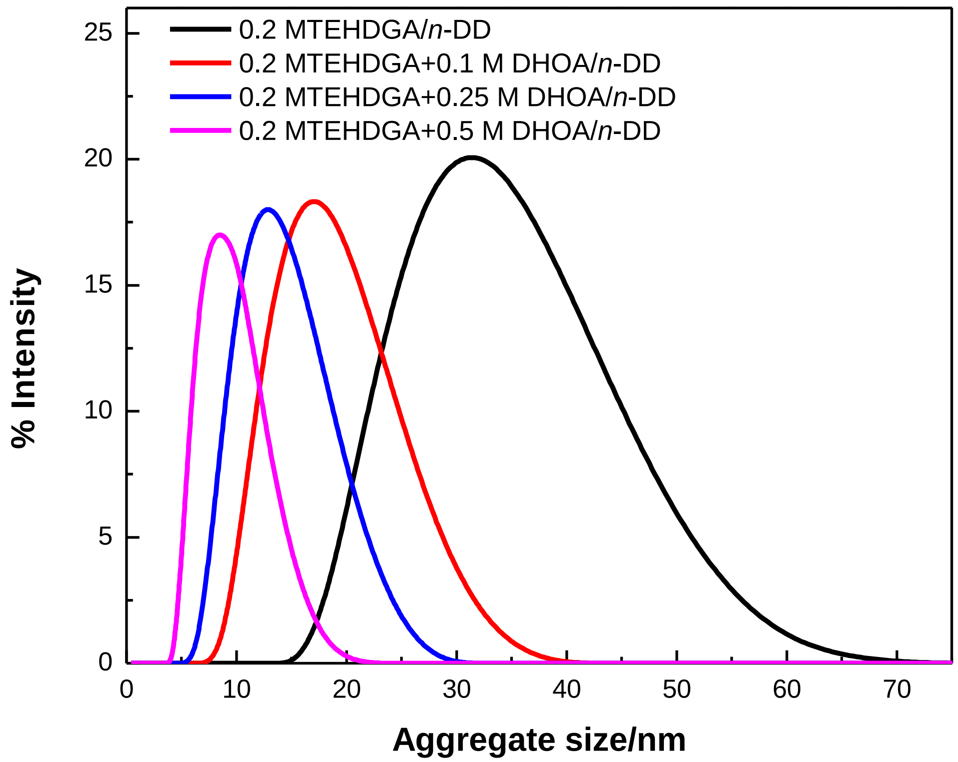

**Figure 4.13**. Aggregate distribution in organic phase at various concentrations of DHOA recorded after contacting the organic phase with Nd(III) solution in 1 M nitric acid. Organic phase: 0.2 M TEHDGA+DHOA/*n*-DD. Aqueous phase: 1 M nitric acid containing 5 g/L Nd(III).

Figure 4.14 shows the variation in the aggregation behaviour of the organic phase, 0.2 M TEHDGA+1.1 M TBP/*n*-DD or 0.2 M TEHDGA+0.5 M DHOA/*n*-DD, obtained after contacting the organic phase with a solution of 5 g/L Nd(III) in nitric acid. The concentration nitric acid in the aqueous phase was varied from 1 M to 10 M. The concentration of TBP, and DHOA was fixed at 1.1 M, and 0.5 M, respectively, since these concentrations have been proposed for the separation of trivalent metal ions from high-level liquid waste (~3-4 M $HNO_3$ medium). It can be seen from Figure 4.14 that the aggregate size in both binary solutions increases with increase in the concentration of nitric acid in the aqueous phase. This could be due to the increase in the extraction of Nd(III) in organic phase, since the distribution ratio of Nd(III) in diglycolamides increases with increase in the concentration of nitric acid as discussed elsewhere [25]. In addition, significant amount of nitric acid is also extracted into organic phase with increase in the concentration of nitric acid in aqueous phase. The amount of $HNO_3$ and Nd(III) extracted into organic phase is indicated in Figure 4.14. The extraction of both Nd(III) and nitric acid in 0.2 M TEHDGA+1.1 M TBP/*n*-DD or 0.2 M TEHDGA+0.5 M DHOA/*n*-DD increases the formation of newer aggregates and facilitates the inter-aggregate interaction among the existing aggregates. As a result, the average aggregate size and their distribution in the organic phase increases with increase in the concentration of nitric acid.

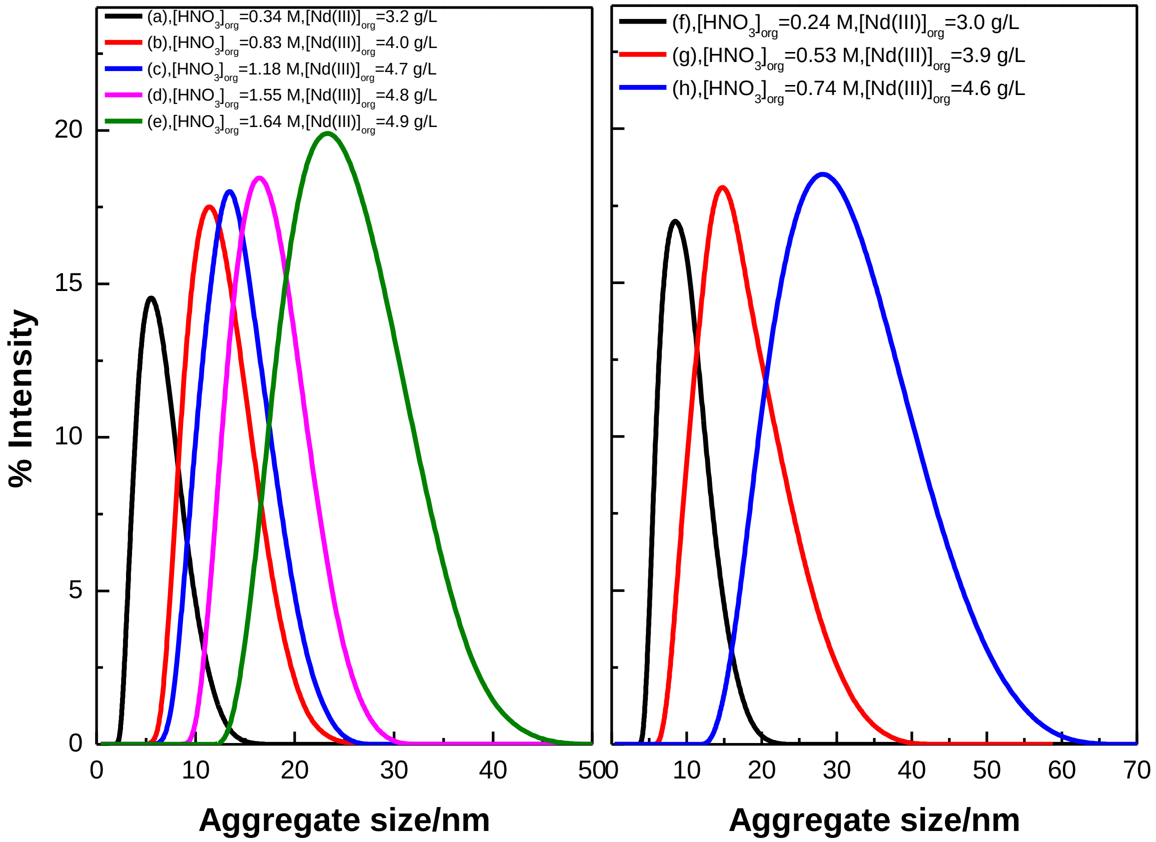

**Figure 4.14.** Aggregate distribution in organic phase at various concentrations of nitric acid recorded after contacting the organic phase with Nd(III) solution in nitric acid. (a) 0.2 M TEHDGA+1.1 M TBP/*n*-DD+1 M $HNO_3$+ 5 g/L Nd(III), (b) 0.2 M TEHDGA+1.1 M TBP/*n*-DD+3 M $HNO_3$+ 5 g/L Nd(III), (c) 0.2 M TEHDGA+1.1 M TBP/*n*-DD+5 M $HNO_3$+ 5 g/L Nd(III), (d) 0.2 M TEHDGA+1.1 M TBP/*n*-DD+8 M $HNO_3$+ 5 g/L Nd(III), (e) 0.2 M TEHDGA+1.1 M TBP/*n*-DD+10 M $HNO_3$+ 5 g/L Nd(III), (f) 0.2 M TEHDGA+0.5 M DHOA/*n*-DD+1 M $HNO_3$+ 5 g/L Nd(III), (g) 0.2 M TEHDGA+0.5 M DHOA/*n*-DD+3 M $HNO_3$+ 5 g/L Nd(III), (h) 0.2 M TEHDGA+0.5 M DHOA/*n*-DD+5 M $HNO_3$+ 5 g/L Nd(III).

Figure 4.15 shows the comparison in the aggregate size distribution of the organic phase, 0.2 M TEHDGA+1.1 M TBP/*n*-DD or 0.2 M TEHDGA+0.5 M DHOA/*n*-DD, recorded after contacting the organic phase with simulated fast reactor high-level liquid waste. The composition of HLLW is discussed elsewhere [26]. It contains trivalent actinides, fission product lanthanides ($Ln^{+3}$), other fission products, corrosion products, etc. present in 3-4 M nitric acid medium. The total concentration of trivalent metal ions (lanthanides and actinides is 3.2 g/L). The average aggregate size of 9.2 nm is observed for 0.2 M TEHDGA+1.1 M TBP/*n*-DD, and 19.3 nm for 0.2 M TEHDGA+0.5 M DHOA/*n*-DD. These aggregate sizes are much lower than the limiting aggregate size of ~ 35 nm for third phase formation for these systems (see part I of chapter 3).

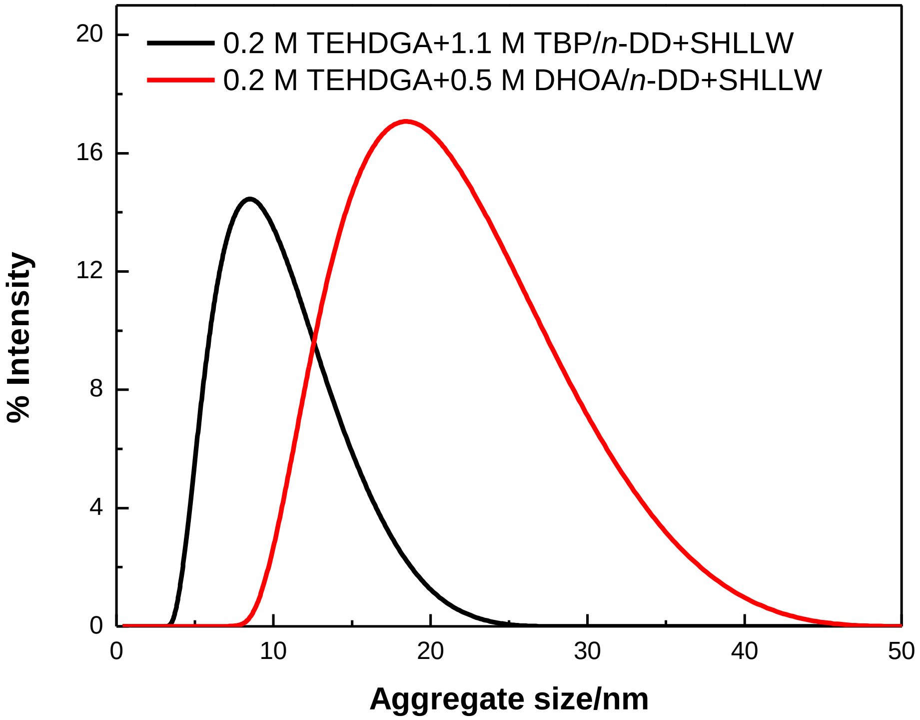

**Figure 4.15**. Aggregate size distribution in organic phase recorded after contacting the organic phase with simulated HLLW. Organic phase: 0.2 M TEHDGA+1.1 M TBP/*n*-DD or 0.2 M TEHDGA+0.5 M DHOA/*n*-DD. Aqueous phase: SHLLW at 4 M $HNO_3$.

## 4.3 Summary

The extraction behaviour of nitric acid and Nd(III) was studied in a binary solution of 0.2 M TEHDGA + TBP in *n*-dodecane, and 0.2 M TEHDGA+ DHOA in *n*-dodecane and the organic phase obtained after extraction was subjected to DLS measurements to understand the role of TBP, and DHOA in controlling the third phase formation during the course of solvent extraction of trivalent actinides from HLLW. Since LOC and CAC of nitric acid in 1.1 M TBP/*n*-DD and 0.5 M DHOA/*n*-DD were significantly higher than the concentration of nitric acid prevailing HLLW, these reagents were, in fact, capable of performing the role of phase modifiers during the extraction of trivalent actinides. The average size of aggregate and the aggregate distribution in organic phase increased with increase in the concentration of nitric acid in aqueous phase. The average aggregate size for these aggregates increased in the order TBP < DHOA < TEHDGA, which was the increasing order of basicity of these extractants. The critical aggregates size for third phase formation with nitric acid in these ligands increased in the order of TBP < DHOA < TEHDGA. Since the mole ratio of extractant to $HNO_3$ was about 1:1.3 at LOC for all these extractants, the study indicated that strongly basic extractants facilitate the formation of newer aggregates, merge the existing aggregates and occlude large quantity of water molecules in aggregates upon nitric acid extraction in the organic phase.

The study revealed that phase modifiers play multiple roles in minimizing or preventing the third phase formation. The results showed that formation TEHDGA acid-solvates above 1:1.3 (extractant: $HNO_3$) mole ratio could result in the splitting of the organic phase because of complete conversion into acid-solvates have attained at LOC. However, the formation of TEHDGA acid-solvates can be minimized by adding phase modifiers to the binary solution as the phase modifiers can also undergo coordination with nitric acid. In fact, the phase modifier can be regarded as the protecting agent for the other extractant, which is susceptible to acid-solvates formation and third phase formation. Since, it was necessary to achieve complete acid-solvates formation of both extractants present in the binary solution above 1:1.3 (extractant: $HNO_3$) mole ratio for third phase formation, the LOC and CAC values increased with increase in the concentration of phase modifier in the binary solution.

The study also showed that the phase modifiers can decrease the average size of aggregates and their distribution in binary solution, below the critical aggregate size for third phase formation, owing to the dispersive nature of these phase modifiers in *n*-dodecane medium. The presence of TBP or DHOA phase modifier in fact diluted the inter-aggregate interaction and minimised the merger of existing aggregates below the limiting aggregate size. Since the dispersive tendency of these phase modifiers was more than TEHDGA in the binary solution, the average aggregate size decreased with increase in the concentration of phase modifier in the binary solution.

As a spin-off, the study also showed that the phase modifiers should have the following properties for preventing third phase formation. They are (i) high LOC values with respect to nitric acid (ii) relatively less polar than the coexisting extractant, and (iii) efficient dispersive interaction with *n*-dodecane. Considering all these properties discussed above and the experiments conducted with simulated waste, the studies point out that TBP is an appropriate choice, as phase modifier, for the separation of trivalent actinides from HLLW using the solvent phase composed of TEHDGA in *n*-dodecane.

# Part II. Role of alcohol phase as modifiers during the extraction of Nd(III) from nitric acid medium in tetra(2-ethylhexyl)diglycolamide in *n*-dodecane

## 4.4 Introduction

The role of phase modifiers such as TBP and DHOA in maneuvering the third phase formation during the extraction of Nd(III) in 0.2 M TEHDGA+TBP or DHOA in *n*-DD has been discussed in the part I of Chapter 4. In this part the role of long chain aliphatic alcohols in preventing the third phase formation during the extraction of trivalent metal ion from nitric acid medium is discussed. The long chain aliphatic alcohols studied were *n*-octanol, *n*-decanol, and isodecanol. The concentration range of alcohol employed in the organic phase varied from 5 % to 15% (0.2 M to 1 M for octanol). The organic phase obtained after extraction was probed by dynamic light scattering (DLS) spectroscopy to understand role of phase modifiers.

## 4.5 Results and discussion

### 4.5.1 Extraction of nitric acid, Nd(III) and aggregate distribution in TEHDGA/*n*-DD

The extraction behavior of nitric acid and Nd(III) in 0.2 M TEHDGA/*n*-DD and the aggregation behaviour of the organic phase as a result of nitric acid extraction and Nd(III) was explained in part II of chapter 3 in detail. The extraction of nitric acid in organic phase increased with increase in the concentration of nitric acid and Nd(III) in aqueous phase. The organic phase (0.2 M TEHDGA/*n*-DD) was reported to undergo phase splitting when the concentration of Nd(III) was 3.62 g/ L, 2.23 g/L and 0.88 g/L at 1 M, 2 M and 3 M nitric acid, respectively. The LAS for third phase formation in nitric acid and metal ion contact found and the values reported in part I of chapter- 4.

### 4.5.2 Extraction of nitric acid and aggregate distribution in TEHDGA-alcohol/*n*-DD

The concentration of alcohol employed in the organic phase containing 0.2 M TEHDGA/*n*-DD varied from 0.2 M to as high a 1 M (i.e. 5% to 19 volume %) [15, 27, 28]. The alcohols reported for preventing third phase formation were *n*-octanol, *n*-decanol and isodecanol. The extraction behaviour of nitric acid in 0.2 M TEHDGA/*n*-DD containing 1 M alcohol is shown in Figure 4.16. The concentration of nitric acid in aqueous phase was varied from 1 M to 12 M. The extraction of nitric acid in alcohol containing phases continued to increase with increase in the initial concentration of nitric acid in aqueous phase, without leading to any phase splitting [4,8]. This indicates that the presence of alcohol stabilizes the polar acid-solvates, TEHDGA….$(HNO_3)_x$ in organic phase, perhaps, the added alcohol is not allowing the formation of reverse micellar aggregates in organic phase.

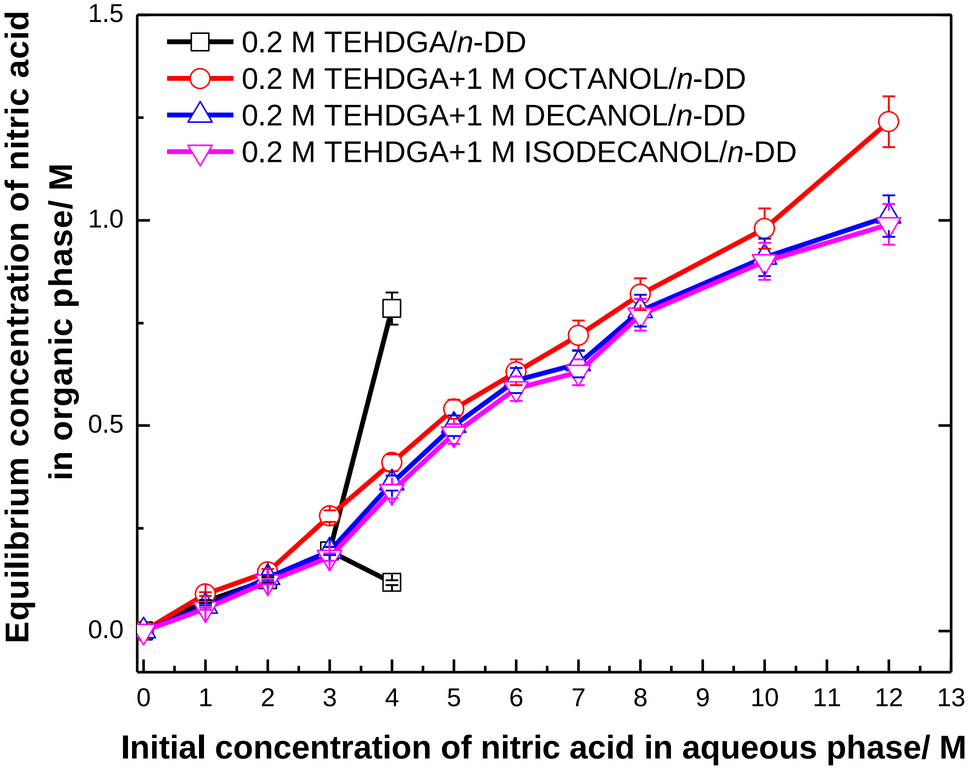

**Figure.4.16.** The extraction behaviour of nitric acid in organic phase as function of initial concentration of nitric acid in aqueous phase. Organic phase: 0.2 M TEHDGA/*n*-DD or 0.2 M TEHDGA+1 M OCTANOL/*n*-DD or 0.2 M TEHDGA+1 M DECANOL/*n*-DD or 0.2 M TEHDGA+1 M ISODECANOL/*n*-DD. Aqueous phase: Nitric acid concentration varied from 1 M to 12 M.

In order to understand the role of alcohols in organic phase, the aggregate distribution of the organic phase was recorded after contacting the organic phase with 3 M nitric acid, and the results are displayed in Figure 4.17. Since 0.2 M TEHDGA/*n*-DD forms third phase when contacted with 4 M nitric acid, the extraction of nitric acid in organic phase was carried out at 3 M nitric acid for all alcohol containing organic phases also. The results shown in Figure 4.17

indicate that the average aggregate size and the aggregate distribution observed in 0.2 M TEHDGA/*n*-DD is significantly large as compared to that observed in case of alcohol containing modifier phases. It is important to note that the average aggregate size observed for the alcohol containing phases (concentration is 1 M in all cases) is about 4 nm as compared to 18.4 nm observed for the organic phase in the absence of alcohol. In addition, the aggregate distribution (FWHM) and the intensity of the aggregate distribution is quite small in case of alcohol containing organic phases. The FWHM was determined to be 3 nm and 13.5 nm for the organic phase in presence and absence of alcohol, respectively. These observations point out that the presence of alcohol in organic phase minimizes the reverse micellar aggregation of acid-solvates in organic phase. The polar nature of alcohol seems to interact with polar acid-solvates by solvation and prevents the acid-solvates undergoing aggregation in organic phase. As a result, the aggregate size, FWHM and the concentration of aggregates (intensity and area) are significantly lowered with the addition of alcohol phase modifiers to the organic phase containing 0.2 M TEHDGA/*n*-DD.

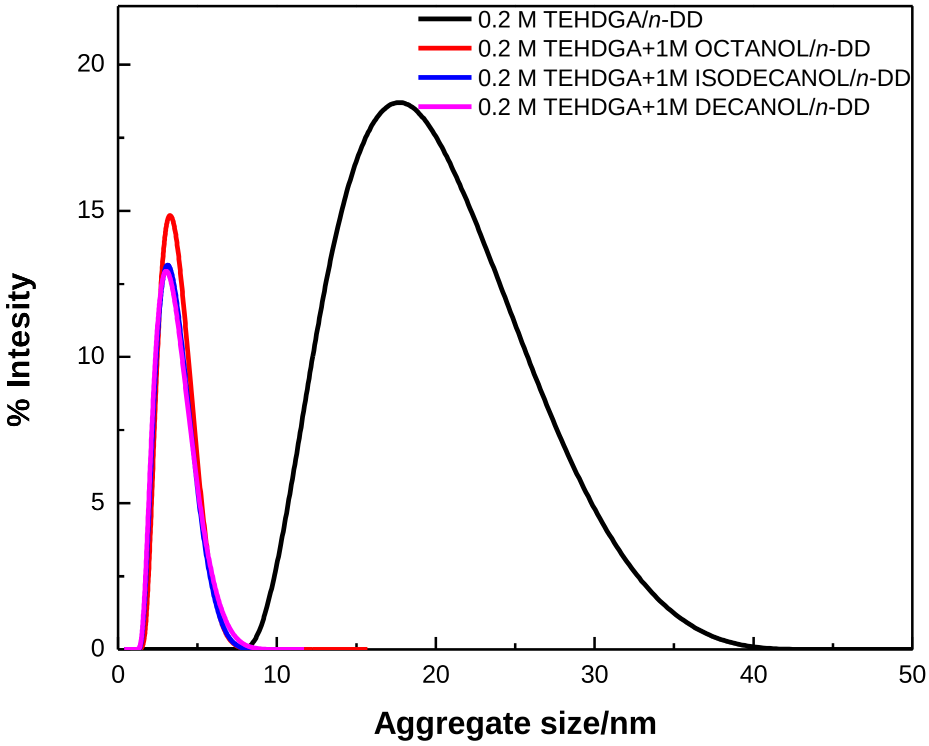

**Figure 4.17.** The aggregate distribution in organic phase as function of nature of alcohol in organic phase. Organic phase: 0.2 M TEHDGA/*n*-DD or 0.2 M TEHDGA+1 M OCTANOL/*n*-DD or 0.2 M TEHDGA+1 M DECANOL/*n*-DD or 0.2 M TEHDGA+1 M ISODECANOL/*n*-DD. Aqueous phase: $[HNO_3]_{Initial}$ =3 M.

### 4.5.3 Effect of nitric acid concentration on aggregation

Figure 4.18 shows the variation in the aggregate distribution obtained in organic phase as a function of nitric acid concentration in aqueous phase. The organic phase was composed of 0.2 M TEHDGA+ 1 M alcohol in *n*-DD and it was contacted with nitric acid of different concentrations before recording the aggregate distribution. It can be seen that the aggregate size in all systems increase with increase in the concentration of nitric acid, due to the extraction of nitric acid, as discussed in Figure 4.16. The extraction of nitric acid results in the formation of TEHDGA……$(HNO_3)_x$ acid-solvates and since these acid-solvates are more polar, they facilitate the formation of newer aggregates, and merger of existing aggregates, as discussed earlier . As a result, the intensity and FWHM of the aggregate distribution increases with increase in the concentration of nitric acid, in all cases, as shown in Figure 4.18. Comparing Figure 4.17 and Figure 4.18, it is important to note that the organic phase (0.2 M TEHDGA/*n*-DD) in absence of alcohol modifier results in the formation of aggregates with average size of 18.4 nm, when the organic phase was equilibrated with 3 M nitric acid. The organic phase (0.2 M TEHDGA/*n*-DD) was found to reach the LAS of 28 nm, when the equilibrium concentration of nitric acid in aqueous phase was 3.58 M. Comparing the LAS (28 nm) with the average aggregate size observed for the organic phase in the presence of alcohol phase modifiers at different nitric acid concentrations (Figure 4.18), the study shows that the presence of alcohol does not seem to allow the acid-solvates to aggregate in organic phase, and form aggregate size equal or above LAS. Moreover, the average aggregate size formed in organic phase containing alcohol phase modifier was much lower than the LAS for third phase formation. Therefore, the organic phase splitting or third phase formation is not observed in 0.2 M TEHDGA/*n*-DD containing alcohol phase modifier, even after contacting the organic phase with 12 M nitric acid.

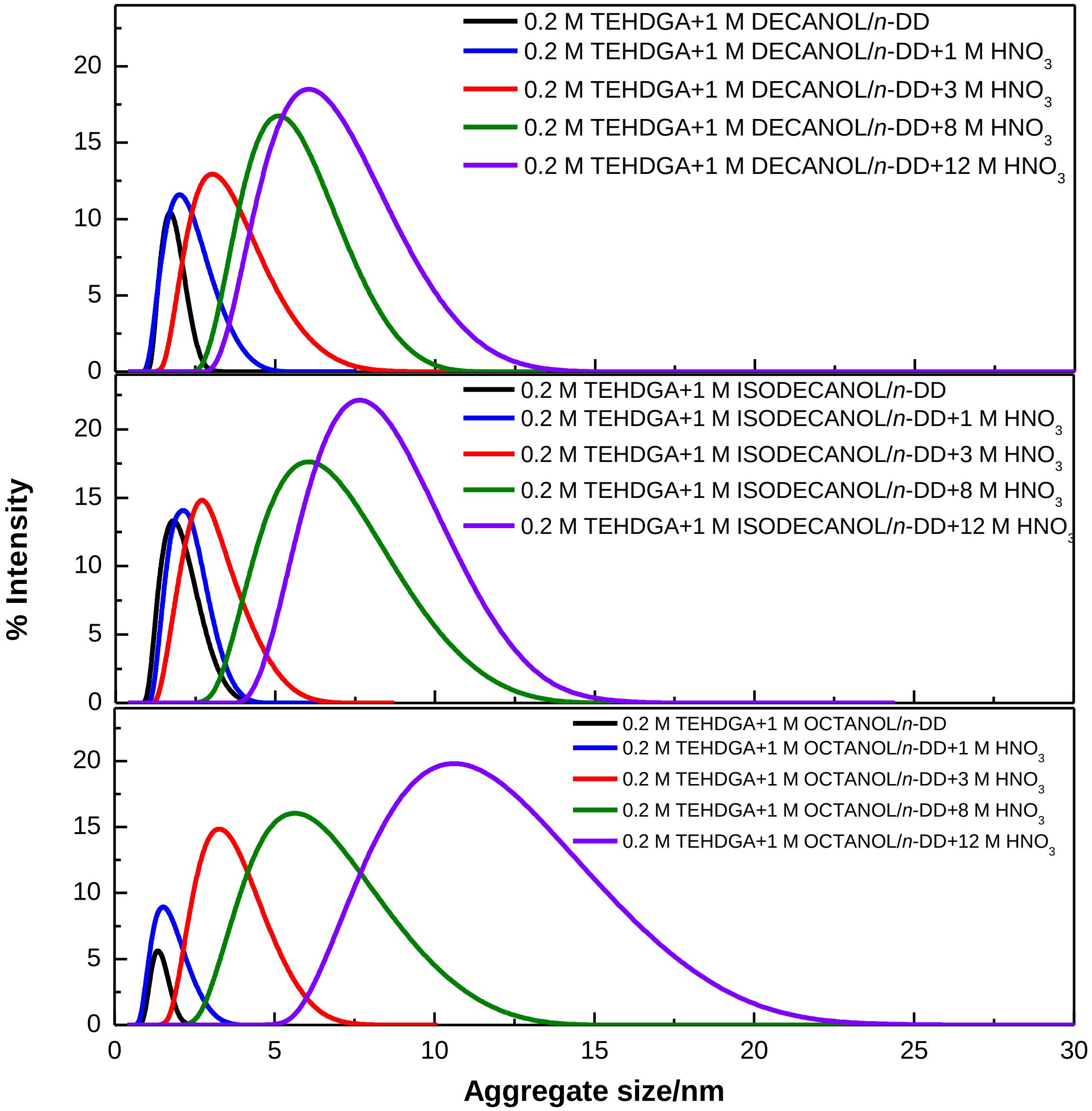

**Figure. 4.18.** Comparison in the aggregation behaviour of the organic phase containing 0.2 M TEHDGA/*n*-DD or 0.2 M TEHDGA+1 M OCTANOL/*n*-DD or 0.2 M TEHDGA+1 M DECANOL/*n*-DD or 0.2 M TEHDGA+1 M ISODECANOL/*n*-DD recorded after contacting the organic phase with nitric acid varied from 1 M to 12 M.

### 4.5.4 Effect of Nd(III) concentration on aggregation

So far, the aggregation behaviour of the alcohol containing organic phase when contacted with nitric acid was discussed. However, the organic phase is in fact employed for the separation of trivalent lanthanides and actinides from high-level liquid waste (HLLW). The concentration of trivalent metal ions in HLLW can vary from 1 g/L to 5 g/L depending upon the burn-up and type of the fuel employed in a nuclear reactor and the concentration of nitric acid in HLLW can vary from 3 M to 4 M [4, 26] as discussed in the chapter 3 and part I of chapter 4. Therefore, it is necessary to study the extraction and aggregation behaviour of a trivalent metal ion from nitric acid medium. For this purpose, Nd(III) was chosen as a trivalent representative. Since, 0.2 M TEHDGA/*n*-DD forms third phase with 3 M nitric acid solution containing a small quantity of Nd(III) (> 0.7 g/L) [15], the extraction experiments were conducted with 1 M nitric acid containing Nd(III) varied up to 7 g/L for better comparison of the extraction systems.

Figure 4.19 shows the comparison in the extraction behaviour of Nd(III) in a solution of 0.2 M TEHDGA/*n*-DD in presence and absence of 1 M alcohol. It can be seen that the extraction of Nd(III) in organic phase increases with increase in the concentration of Nd(III) in aqueous phase, in all cases. The extraction results indicate that the presence of alcohol in organic phase has not altered the extraction of Nd(III) in TEHDGA phase, which is indeed advantages for the employment of alcohol phase modifiers in the extraction process. However, it is important to note that the organic phase in the absence of alcohol modifier, i.e. in 0.2 M TEHDGA/*n*-DD, forms third phase when it is contacted with the aqueous solution of 7g/L Nd(III) in 1 M nitric acid, as discussed in chapter 3. In view of this, the extraction Nd(III) from 1 M nitric acid was carried out at the Nd(III) concentration up to 5 g/L, and the aggregation behaviour of the organic phase is compared in Figure 4.19. It can be seen that the average aggregate size and the aggregate distribution observed in case of alcohol containing organic phases are significantly low as compared to the aggregate size and their distribution observed for 0.2 M TEHDGA/*n*-DD. This shows that the presence of phase modifiers minimized the aggregation, by stabilizing and dispersing the polar metal-solvates in organic phase. The average aggregate size observed in case of 0.2 M TEHDGA/*n*-DD when contacted with 5 g/L Nd(III) in 1 M nitric acid is ~ 33 nm (see chapter 3), which is near the third phase formation limit. Since the organic phase (0.2 M TEHDGA/*n*-DD) already at the verge of LAS, the organic phase undergoes into two phases when contacted with 1 M nitric acid solution containing Nd(III) beyond 5 g/L.

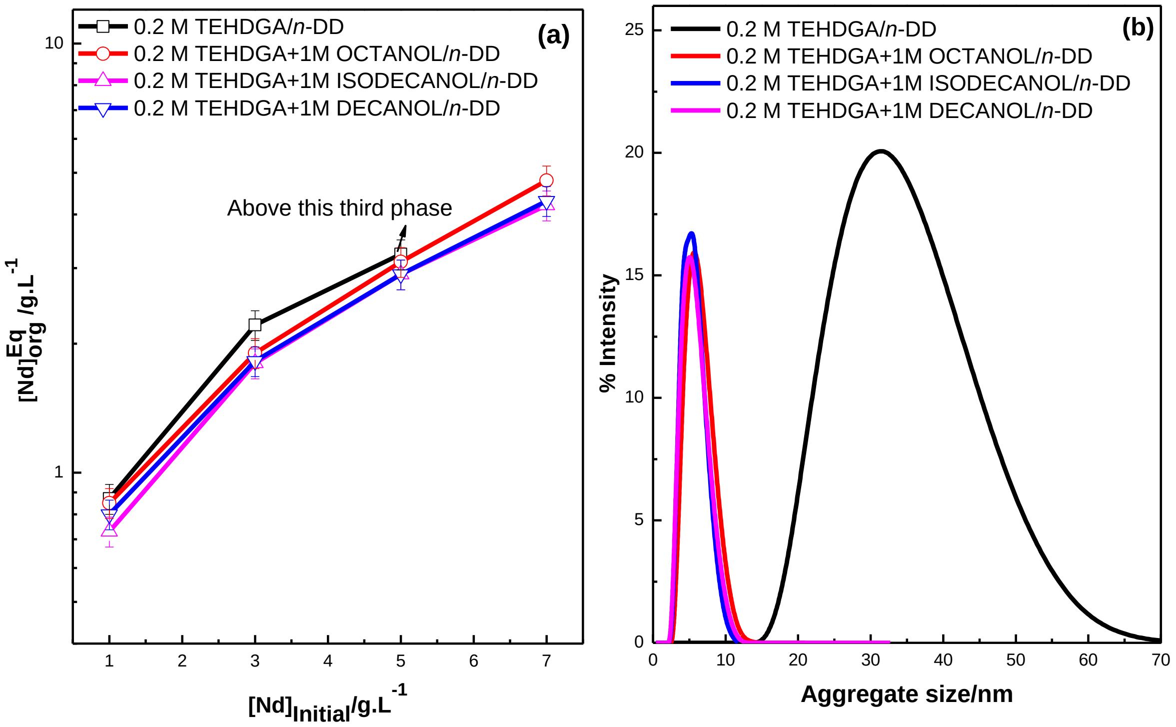

**Figure. 4.19 (a).** The variation in the extraction of neodymium(III) in organic phase as function of initial concentration of Nd(III) in aqueous phase. Organic phase: 0.2 M TEHDGA/*n*-DD or 0.2 M TEHDGA+1 M OCTANOL/*n*-DD or 0.2 M TEHDGA+1 M DECANOL/*n*-DD or 0.2 M TEHDGA+1 M ISODECANOL/*n*-DD. Aqueous phase: [Nd(III)]

varied from 0.5 g/L to 8g/L at 1 M nitric acid.

**Figure 4.19 (b).** The aggregate distribution in organic phase as function of nature of alcohol in organic phase. Organic phase: 0.2 M TEHDGA/*n*-DD or 0.2 M TEHDGA+1 M OCTANOL/*n*-DD or 0.2 M TEHDGA+1 M DECANOL/*n*-DD or 0.2 M TEHDGA+1 M ISODECANOL/*n*-DD. Aqueous phase: $[Nd(III)]_{Initial}$ =5 g/L in 1 M $HNO_3$.

### 4.5.5 Comparison of alcohol modifiers

To identify best modifier among the three different alcohol modifiers employed in the present study, the aggregate distribution of the organic phase was recorded after contacting the organic phase with 10 M nitric acid solution containing 5 g/L Nd(III). The aggregate distribution is shown in Figure 4.20. It can be seen that the average aggregate size and their distribution observed in alcohol containing organic phase modifiers increases in the order of *n*-decanol<isodecanol<*n*-octanol. The aggregate size and their distribution in organic phase is quite low for decanol phase modifier. Moreover, the average aggregate size does not exceed 14 nm even in case of octanol phase modifier, which is much lower than LAS of 35 nm for third phase formation (see chapter 3). Figure 4.20 also shows the aggregation behaviour of the organic phase obtained after contacting the organic phase with simulated high-level waste. It can be seen from Figure 4.20 that the average aggregate size observed in all cases is 7 nm. Therefore, the study shows that alcohol based phase modifiers can be employed for the separation of trivalent actinides from HLLW and without leading to third phase formation in organic phase.

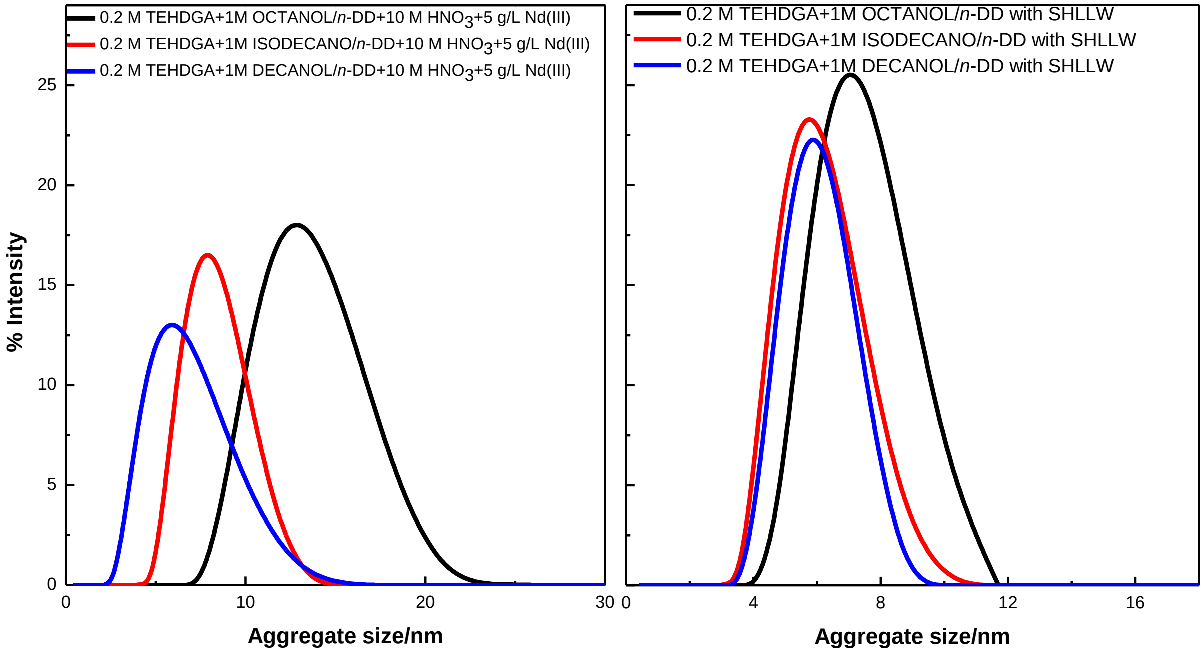

**Figure 4.20.** The aggregate distribution in organic phase as function of nature of alcohol in organic phase. Organic phase: 0.2 M TEHDGA/*n*-DD or 0.2 M TEHDGA+1 M OCTANOL/*n*-DD or 0.2 M TEHDGA+1 M DECANOL/*n*-DD or 0.2 M TEHDGA+1 M ISODECANOL/*n*-DD. Aqueous phase: $[Nd(III)]_{initial}$ =5g/L in 10 M $HNO_3$ or with SHLLW in 4 M $HNO_3$.

The literature shows that different alcohols have been used for maneuvering the third phase formation and the concentration of *n*-octanol was varied from 5%, 10%, and 15%, which corresponds to the concentration of 0.31 M, 0.63 M and 1 M respectively. For practical application point of view and for quick and easy reference, Table 4.3 provides the maximum concentration of nitric acid in aqueous phase, which can be employed for extraction without leading to third phase formation using 0.2 M TEHDGA/*n*-DD maximum concentration of nitric acid employed for extraction studies is 3 M (4 M forms third phase). Addition of 5 % of octanol shifts maximum concentration to 8 M. Similarly increasing volume % of alcohol in organic phase increases the maximum concentration to 11 M and 14 M for 10 % and 15 % octanol addition in 0.2 M TEHDGA/*n*-DD respectively, In all cases, the average aggregate size is ~26 nm which is lower than the 28 nm needed for third phase formation with nitric acid. A similar behaviour is also observed for iso-decanol and *n*-decanol systems. However, the concentration limit of nitric acid increases in the order of *n*-octanol < iso-decanol < *n*-decanol. The third phase could not be determined for the organic phase containing 1 M alcohol, since the organic phase required nitric acid more than 16 M. Moreover, all the organic phases containing alcohol were found to undergo decomposition when nitric acid concentration more than 12 M for 30 minutes to 1 hour. In view of this results reported in Table 4.3 were completed within 10 minutes of equilibration. Based on these observations it can concluded that ~ 5 % alcohol could be adequate for minimizing the third phase formation, since the initial concentration of nitric required for third phase formation is more than 8 M, whereas the concentration of nitric acid prevailing in HLLW is 3-4 M. Among the different alcohols investigated *n*-decanol seems to be a better choice for maneuvering the third phase formation.

**Table 4.3.** The limiting initial concentration of nitric acid and aggregate size values for various systems.

| Organic phase | Molarity of alcohol/M | $[HNO_3]_{Initial}$/M | Aggregate size/nm |
|---|---|---|---|
| 0.2 M TEHDGA/*n*-DD | - | 3 M | 18.4 |
| 0.2 M TEHDGA+5 % octanol/*n*-DD | 0.31 M | 8 M | 26.5 |
| 0.2 M TEHDGA+10% octanol/*n*-DD | 0.63 M | 11 M | 26.7 |
| 0.2 M TEHDGA+15 % octanol/*n*-DD | 1 M | 14 M | 26.8 |
| 0.2 M TEHDGA+5 % Isodecanol/*n*-DD | 0.26 M | 9 M | 25.3 |

| | | | |
|---|---|---|---|
| 0.2 M TEHDGA+10% Isodecanol /*n*-DD | 0.52 M | 12 M | 26.3 |
| 0.2 M TEHDGA+15 % Isodecanol /*n*-DD | 0.78 M | 14 M | 15.6 |
| 0.2 M TEHDGA+5 % decanol/*n*-DD | 0.26 M | 10 M | 26.2 |
| 0.2 M TEHDGA+10% decanol /*n*-DD | 0.52 M | 13 M | 22.3 |
| 0.2 M TEHDGA+15 % decanol /*n*-DD | 0.78 M | 14 M | 15.7 |
| 0.2 M TEHDGA+1 M octanol/*n*-DD | 1 M | 14 M | 26.8 |
| 0.2 M TEHDGA+1 M Isodecanol /*n*-DD | 1 M | 15.7 M | 22.8 |
| 0.2 M TEHDGA+1 M decanol /*n*-DD | 1 M | 15.7 M | 9.2 |

### 4.6 Summary

The extraction behavior of Nd(III) from nitric acid medium in a solution of 0.2 M TEHDGA in *n*-DD containing long chain aliphatic alcohols such as *n*-octanol, *n*-decanol and isodecanol was studied and the organic phase obtained after extraction was subjected to dynamic light scattering studies to understand the role of alcohols in controlling the third phase formation. The extraction of Nd(III) or $HNO_3$ in all organic phases increased with increase in the initial amount of Nd(III) or nitric acid in aqueous phase, and therefore, the aggregate size obviously increased with increase in the amount of Nd(III) or $HNO_3$ in organic phase. However, the organic phase in the absence of alcohol showed the formation of third phase when the concentration of nitric acid or Nd(III) in organic phase exceeded the LOC values. Addition of alcohol phase modifiers controlled the aggregate size to a much lower value than the LAS for third phase formation, minimized the aggregate distribution and the aggregate concentration. The polar nature of alcohol seems to interact with polar acid- and metal-solvates by solvation and prevents these solvates undergoing aggregation in organic phase. The investigations also revealed that *n*-decanol was superior to other alcohol phase modifiers.

## References

1. B.A. Moyer, Ion exchange and solvent extraction: a series of advances, volume 19, chapter 7, CRC Press, 2009
2. S. Tachimori, Y. Sasaki, S.I. Suzuki, Modification of TODGA-*n*-dodecane solvent with a monoamide for high loading of lanthanides (III) and actinides (III), Solvent Extr. Ion Exch. 20 (2002) 687-699.
3. A. Suresh, T.G. Srinivasan, P.V. Rao, Parameters influencing third-phase formation in the extraction of $Th(NO_3)_4$ by some trialkyl phosphates, Solvent Extr. Ion Exch. 27(2009) 132-158.
4. S.A. Ansari, P.N. Pathak, P.K. Mohapatra, V.K. Manchanda, Chemistry of diglycolamides: Promising extractants for actinide partitioning, Chem.Rev.112 (2012) 1751-1772.
5. L. Berthon, L. Martinet, F. Testard, C. Madic, T. Zemb, Solvent penetration and sterical stabilization of reverse aggregates based on the DIAMEX process extracting molecules: consequences for the third phase formation, Solvent Extr. Ion Exch. 25 (2007) 545-576.
6. A. Chandrasekar, N. Sivaraman, T.K. Ghanty, A. Suresh, Experimental evidence and quantum chemical insights into extraction and third phase aggregation trends in Ce (IV) organophosphates, Sep. Purif. Technol. 217 (2019) 62-70.
7. S. Sarkar, A. Suresh, N. Sivaraman, V.K. Aswal, An insight into third-phase formation in the extraction of thorium nitrate by tris (2-methylbutyl) phosphate and tri-n-alkyl phosphates, Sep. Sci. Technol. 54 (2019) 970-984.
8. D. Whittaker, A. Geist, G. Modolo, R. Taylor, M. Sarsfield, A. Wilden, Applications of diglycolamide based solvent extraction processes in spent nuclear fuel reprocessing, part 1: TODGA, Solvent Extr. Ion Exch. 36(2018) 223-256.

9. D. Magnusson, B. Christiansen J.P. Glatz, R. Malmeck, G. Modolo, D.S. Purroy, C. Sorel, Demonstration of a TODGA based extraction process for the partitioning of minor actinides from a PUREX raffinate, Solvent Extr. Ion Exch. 27 (2009) 26–35.
10. S. Manohar, J.N. Sharma, B.V. Shah, P. K. Wattal, Process development for bulk separation of trivalent actinides and lanthanides from radioactive high-level liquid waste, Nucl. Sci. Eng. 156 (2007) 96-102.
11. J.N. Sharma, R. Ruhela, K.K. Singh, M. Kumar, C. Janardhanan, P.V. Achutan, S. Manohar, P.K. Wattal, A.K. Suri, Studies on hydrolysis and radiolysis of tetra (2-ethylhexyl) diglycolamide (TEHDGA)/isodecyl alcohol/*n*-dodecane solvent system, Radiochim. Acta. 98 (2010) 485-49.
12. S.A. Ansari, P. Pathak, P.K. Mohapatra, V.K. Manchanda, Aqueous partitioning of minor actinides by different processes, Sep. Purif. Rev. 40 (2011) 43-76.
13. E.A. Mowafy, D. Mohamed, Extraction behavior of trivalent lanthanides from nitric acid medium by selected structurally related diglycolamides as novel extractants, Sep. Purif. Technol. 128 (2014) 18-24.
14. P.K. Wattal, 2017. Back end of Indian nuclear fuel cycle-A road to sustainability, Prog. Nucl. Energy. 101 (2017) 133-145.
15. P.K. Nayak, R. Kumaresan, K. A. Venkatesan, M.P. Antony, P.R. Vasudeva Rao, 2013. A new method for partitioning of trivalent actinides from high-level liquid waste, Sep. Sci. Technol. 48 (2013) 1409-1416.
16. P. Deepika, K.N. Sabharwal, T.G. Srinivasan, P.R. Vasudeva Rao, Studies on the use of N, N, N, N-tetra(2-ethylhexyl) diglycolamide (TEHDGA) for actinide partitioning. I:

Investigation on third-phase formation and extraction behavior, Solvent Extr. Ion Exch. 28 (2010) 184-201.

17. R.B. Gujar, S.A. Ansari, D.R. Prabhu, D.R. Raut, P.N. Pathak, A. Sengupta, S.K. Thulasidas, P.K Mohapatra, V.K. Manchanda, Demonstration of T2EHDGA based process for actinide partitioning part II: counter-current extraction studies, Solvent Extr. Ion Exch. 28 (2010) 764-777.
18. S. Nave, C. Mandin, L. Martinet, L. Berthon, F. Testard, C. Madic, T. Zemb, Supramolecular organisation of tri-n-butyl phosphate in organic diluent on approaching third phase transition, Phys. Chem. Chem. Phys. 6 (2004) 799-808.
19. K.K. Gupta, V.K. Manchanda, S. Sriram, G. Thomas, P.G. Kulkarni, R. K. Singh, Third phase formation in the extraction of uranyl nitrate by N, N-dialkyl aliphatic amides, Solvent Extr. Ion Exch. 18 (2000) 421-439.
20. N. Kumari, P.N. Pathak, Dynamic light scattering studies on the aggregation behavior of tributyl phosphate and straight chain dialkyl amides during thorium extraction, J. Ind. Eng. Chem. 20 (2014) 1382-1387.
21. P.N. Pathak, S.A. Ansari, S. Kumar, B.S. Tomar, V. Manchanda, Dynamic light scattering study on the aggregation behaviour of N, N, N′, N′-tetraoctyldiglycolamide (TODGA) and its correlation with the extraction behaviour of metal ions, J. Colloid. Interface. Sci. 342 (2010) 114-118.
22. E.L. Campbell, V.E. Holfeltz, G.B. Hall, K.L. Nash, G.J. Lumetta, T.G. Levitskaia, Nitric Acid and Water Extraction by T2EHDGA in *n*-Dodecane, Solvent Extr. Ion Exch. 35 (2017) 586-603.

23. R. Ganguly, J.N. Sharma, N. Choudhury, TODGA based w/o microemulsion in dodecane: An insight into the micellar aggregation characteristics by dynamic light scattering and viscometry, J. Colloid Interface Sci. 355 (2011) 458-463.
24. F. McLachlan, K. Greenough, A. Geist, B. McLuckie, G. Modolo, A. Wilden, R. Taylor, Nitric acid extraction into the TODGA/TBP solvent, Solvent Extr. Ion Exch. 34 (2016) 334-346.
25. M.P. Jensen, T. Yaita, R. Chiarizia, Reverse-micelle formation in the partitioning of trivalent f-element cations by biphasic systems containing a tetraalkyldiglycolamide, Langmuir. 23 (2007) 4765-4774.
26. K.A. Venkatesan, R. Kumaresan, M.P. Antony, T. Kumar, T.G. Srinivasan, P.R. Vasudeva Rao, Characterization of high active waste (155 GWd/Te) arising from fast reactor fuel reprocessing, Radiochim. Acta. 2012, 100(2012) 843–850.
27. P. Deepika, K. N. Sabharwal, T. G. Srinivasan, P. R. Vasudeva Rao, Studies on the use of N, N, N′, N′-tetra (2-ethylhexyl) diglycolamide (TEHDGA) for actinide partitioning II: Investigation on radiolytic stability, Solvent Extr. Ion Exch. 29 (2011) 230-246.
28. R.B. Gujar, S.A. Ansari, A. Bhattacharyya, A.S. Kanekar, P.N. Pathak, P.K. Mohapatra, V.K. Manchanda, Radiolytic stability of N, N, N′, N′-tetraoctyl diglycolamide (TODGA) in the presence of phase modifiers dissolved in *n*-dodecane, Solvent Extr. Ion Exch. 30 (2012) 278-290.

# Chapter 5: Effect of gamma irradiation on the aggregation behaviour of tetra (2-ethylhexyl)diglycolamide in *n*-dodecane

## 5.1 Introduction

The alkyl derivatives of 3-oxapentane-1,5-diamide have been explored extensively for the separation of trivalent lanthanides and actinides, as a group, from the nitric acid medium [1-3] from past two decades. Among the different 3-oxapentanediamides, TODGA and TEHDGA have been suggested for the separation of trivalent actinides (Am and Cm) from HLLW, generated during reprocessing of spent nuclear fuels by the PUREX process [2-4]. The high-level liquid waste contains long-lived α-emitting nuclides, such as $^{241}$Am ($t_{1/2}$ = 432 years), $^{243}$Cm ($t_{1/2}$ = 30 years) and $^{244}$Cm ($t_{1/2}$ = 18 years), long-lived radiotoxic fission products, such as $^{137}$Cs ($t_{1/2}$ = 30 years) and $^{90}$Sr ($t_{1/2}$ = 28.8 years) in addition to the other fission product lanthanides, corrosion products etc., present in 3 to 4 M nitric acid medium as discussed in the previous chapters [5,6].

The separation of Am and Cm from HLLW was achieved by intimately mixing the organic phase with high-level liquid waste during the course of solvent extraction. In this contact, the organic phase is exposed to highly energetic and strongly ionizing alpha and beta-gamma radiations [7, 8]. The organic phase under such condition undergoes a number of changes, both physical and chemical transformations, leading to the formation of a number of chemical compounds, called as radiolytic degradation products that usually degrade the performance of the solvent [9,10]. Extensive damage to the organic phase results in the formation of significant amount of degradation products [9-12]. As a consequence, the physicochemical properties of the solvent are greatly altered, and the recovery of actinides from degraded organic phase is hampered to a significant extent, making the solvent phase unsuitable for further extraction. In view of this, the solvent phase after few cycles is disposed as organic waste [13-15].

The radiolytic degradation behavior of diglycolamides in *n*-dodecane medium has been studied extensively by several researchers [11-18]. The degradation of diglycolamide was reported to increase with increase of absorbed dose leading to the formation of several degradation products such as amines, hydroxyacetamide, acetamide, diglycolamic acid etc. [12-15]. The distribution ratio of americium was reported to decrease with increase of absorbed dose [11, 13-15]. Since diglycolamides produce innocuous degradation products upon radiolytic degradation, the extracted actinides were quantitatively recovered from the degraded organic solvent without any major problem [17-19]. Therefore, the retention of actinides in organic phase was negligible when diglycolamides were employed for extraction [13, 18, 19]. In contrast to these routine studies, the aggregation behaviour of the radiolytically degraded diglycolamides, and how the presence of degradation products in organic phase affect the aggregation and third phase formation behaviour of the organic phase has not been known so far.

In view of this, the studies were taken up to understand the radiolytic degradation behaviour of TEHDGA, *n*-dodecane and the aggregation behaviour of the solution containing 0.2 M TEHDGA in *n*-DD. The liquid phase and the solution obtained after irradiation were subjected to the DLS studies to understand the aggregation behaviour of the radiolytically degraded organic phase. For this purpose, the samples taken for gamma irradiation were classified into five categories, as discussed below. The samples were irradiated from 10 kGy to 500 kGy gamma dose, and the aggregation behavior of the irradiated system, was compared with the unirradiated organic phase.

## 5.2 Irradiation studies and sample preparation

The gamma irradiation of the organic phase was carried out in a $^{60}$Co gamma irradiator facility, available at Indira Gandhi Centre for Atomic Research, Kalpakkam, India. The irradiator provides a gamma dose rate of 2.6 kGy per hour in the gamma chamber, which was calibrated by Fricke's dosimetry before and after irradiation. The organic samples were taken in a stoppered glass tube and kept in the gamma chamber for receiving the required absorbed dose. The samples were irradiated up to 500 kGy under static condition (no stirring of the organic phase). At various intervals of time, the samples were removed from the chamber so that the organic phase receives the gamma absorbed dose of 10 kGy to 500 kGy, and irradiated samples were then subjected to further studies. The samples taken for irradiation were classified into five categories, as discussed below.

**Case 1.** In this case, the sample was a solution of 0.2 M TEHDGA dissolved in *n*-dodecane medium and it was irradiated to various absorbed dose levels. The sample obtained after irradiation was subjected to further studies without any pre-treatment.

**Case 2.** In this case, the ligand, TEHDGA, was irradiated to various absorbed dose levels and mixed with unirradiated *n*-dodecane to obtain 0.2 M TEHDGA in *n*-dodecane. It should be noted that the molecular weight of TEHDGA was assumed to be same before and after irradiation, for preparing the 0.2 M solution of irradiated TEHDGA in unirradiated *n*-dodecane.

**Case 3.** The case 3 involved the irradiation of *n*-dodecane to various absorbed dose levels, and mixed with unirradiated TEHDGA to obtain 0.2 M TEHDGA/*n*-dodecane. Similar to the previous case, the irradiated *n*-dodecane was taken directly (without any pre-treatment) for diluting TEHDGA to obtain the 0.2 M TEHDGA/*n*-DD.

**Case 4.** In this experiment, the organic compounds TEHDGA and *n*-dodecane were taken separately and irradiated to various absorbed dose levels. The irradiated liquids were mixed together to obtain 0.2 M TEHDGA/*n*-DD with assumption that the molecular weight of irradiated and unirradiated TEHDGA were same. The solution, 0.2 M TEHDGA/*n*-DD, thus obtained was subjected to further studies without any pre-treatment.

**Case 5.** The organic phase composed of 0.2 M TEHDGA/*n*-DD was initially equilibrated with 3 M nitric acid in this case. About 0.19 M nitric acid was extracted into organic phase during this equilibration. The organic phase was separated from aqueous phase and it was irradiated to various absorbed dose levels. The organic solution obtained after irradiation was subjected to further studies without any pre-treatment.

## 5.3 Results and discussion

### 5.3.1 Self-aggregation Behaviour of Case 1 of Organic Phase

Tetra(2-ethylhexyl)diglycolamide is a promising candidate for the separation of trivalent actinides and lanthanides from nitric acid medium as explained earlier chapters [2,4,20]. The self-aggregation behavior of 0.2 M TEHDGA in *n*-DD is compared with the self-aggregation behavior of the irradiated solution of 0.2 M TEHDGA/*n*-DD in Figure 5.1. It can be seen that the intensity of aggregates and the distribution of aggregates (FWHM) in *n*-dodecane medium decreases with increase of absorbed dose. This could be possibly due to the decrease in the concentration of TEHDGA or due to the dispersion of the aggregates by the radiolytical degradation products. Sharma *et al.* previously studied the radiolytical degradation of 0.2 M TEHDGA/*n*-DD and reported the variation in the concentration of TEHDGA as function of absorbed dose [21]. It was reported that the concentration of TEHDGA decreased from 0.2 M to ~0.13 M, with the absorption of 500 kGy gamma dose. This accounts for the 30-40 % decrease in the concentration of TEHDGA in *n*-dodecane medium. In contrast, the decrease in the intensity of the aggregates observed in the irradiated samples (see Figure 5.1) is significantly high.

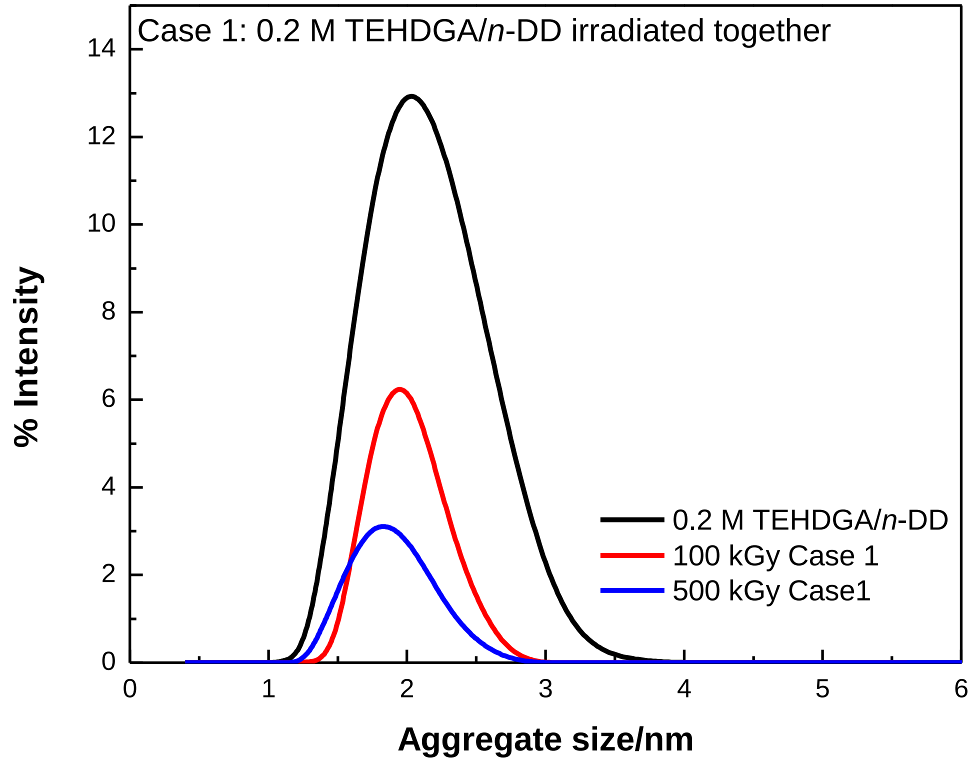

**Figure 5.1.** Self-aggregation behaviour of case 1 organic phase (0.2 M TEHDGA/*n*-DD irradiated together) at different absorbed doses.

It can be seen that the decrease in the intensity is about 80% for the 500 kGy absorbed dose. This indicates that the radiolytic degradation of TEHDGA leading to the decrease in the concentration of TEHDGA alone could not responsible for this observation, but the radiolytic degradation products formed upon irradiation could also be contributing to the decrease in the intensity of aggregates. It is quite likely that scissoning of *n*-DD and the cleavage of alkyl chain attached to amidic nitrogen also could be happening upon irradiation as depicted in the route 3 of Table 5.1. This kind of reaction could lead to the formation of smaller paraffins, and these smaller paraffins might be dispersing the aggregates in organic phase, as discussed elsewhere [13, 16, 21]. The aggregation behavior of the binary solution containing various diluents was studied by several researchers. It was reported that the aggregate size and their distribution in organic phase decreased with decrease in the chain length of *n*-paraffin from tetradecane to the octane [22-24]. Therefore, the significant decrease in the intensity and distribution of aggregates in the irradiated solvent phase could be attributed predominantly to the dispersion of the aggregates by radiolytic degradation products of *n*-DD, which leads to the formation of smaller homologs of *n*-dodecane and the branched hydrocarbons.

**Table 5.1.** Possible routes for the production of radiolytic degradation products upon gamma irradiation on diglycolamides and *n*-dodecane.

| Case | Route | Possible degradation mechanism | Possible degradation products | Remarks |
|---|---|---|---|---|
| Case 1 | 1 | 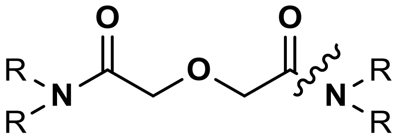 | 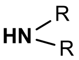 Amine | The aggregation behavior of amine in *n*-DD is not known |
| | | | 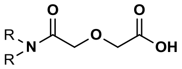 Diglycolamic acid | Diglycolamic acid can increase the aggregate size |
| Case 1 | 2 | 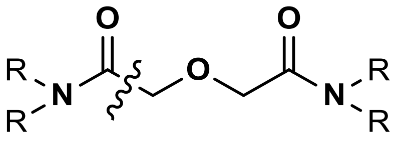 | 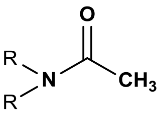 Amide | Amide minimize the aggregate size [27] |
| | | | 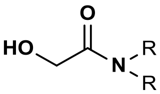 Hydroxy acetamide | Derivatives of Hydroxy Hydroxy acetamide minimizes the aggregate size [27] |

| | | | | |
|---|---|---|---|---|
| Case 1 | 3 | 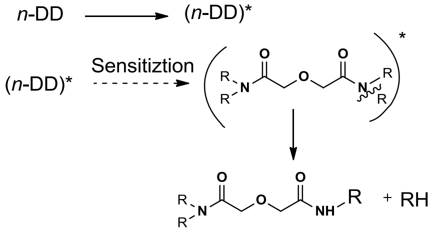 | Amines, Acid, amide, hydroxyl acetamides, smaller paraffins | Activated (*n*-DD)* after transforming the energy to TEHDGA, seem to produce smaller *n*-paraffins, which appear to minimize the aggregate size and other degradation products, which minimizes the aggregate size [16] |
| Case 2 | 4 | Same as discussed in route 1 and 2 | Amines, Acid, amide, hydroxyl acetamides. | Degradation products minimize the aggregate size |
| Case 3 | 5 | *n*-dodecane | Smaller and bigger fragments of *n*-DD | Higher homologs of *n*-dodecane control the aggregation behaviour in case 3. |
| Case 4 | 6 | Same as route 1, 2 and 5 | Same as route 1, 2 and 5 | Intermediate aggregate size obtained between Case 1 and Case 5 |
| Case 5 | 7 | *n*-DD+$HNO_3$ ⟶ alkyl nitrate, alcohols<br>DGA+$HNO_3$ ⟶ nitro derivatives of DGA | Nitroalkanes, alcohols and other polar compounds | Polar degradation products decreases the size of the aggregates by increase in the dispersion of organic phase |

The decrease in the concentration of TEHDGA can also occur due to the scissoning of etheric-O-C bond (see route 2, Table 5.1) and to the cleavage of the alkyl group attached to the amidic nitrogen atom as shown in route 3, Table 5.1. In the first case, the nature of diglycolamide undergoes a radical structural change, whereas the cleavage of alkyl group in the second case results in the formation of smaller homologs of diglycolamide. It should be noted that these smaller homologs of DGA can aggregate efficiently and form bigger aggregates in *n*-DD medium as discussed in part I of chapter 3. A similar behavior of cleavage of TEHDGA upon gamma irradiation (see route 1, 2 and 3, Table 1) has been reported by other authors in the literature [13, 14, 21]. As a result, the aggregate intensity and their distribution in organic phase in such case is expected to increase with increase of absorbed dose. However, such a feature is not reflected in the aggregate distribution of the irradiated solution of 0.2 M TEHDGA/*n*-DD (Figure 5.1). Therefore, it appears that the formation of smaller homologs of diglycolamide upon gamma irradiation is quite less. Nevertheless, it should be noted that all the degradation paths discussed above (shown in Table 5.1) could be occurring upon irradiating 0.2 M TEHDGA/*n*-DD to gamma radiation. The aggregate distribution observed in Figure 5.1 is the resultant of all the degradation possibilities discussed above. However, the substantial decrease in the intensity of the aggregates indicates that the degradation products of *n*-dodecane to smaller *n*-paraffins and branched paraffins seem to be controlling predominantly the distribution and the intensity of aggregates in the irradiated organic phase.

### 5.3.2 Extraction of Nitric Acid in Case 1 Organic Phase

The extraction behavior of nitric acid in the irradiated solution of 0.2 M TEHDGA/*n*-DD is shown in Figure 5.2. The extraction isotherm in the irradiated solution is compared with the extraction behavior of nitric acid in the unirradiated solution of 0.2 M TEHDGA/*n*-DD. It can be seen that the extraction of nitric acid into organic phase increases with increase in the concentration of nitric acid in aqueous phase. The organic phase of the unirradiated 0.2 M TEHDGA/*n*-DD undergoes splitting into two phases (third phase formation), when the concentration of nitric acid in aqueous phase was 4 M and above. The extraction behavior of nitric acid in all the irradiated organic solutions also increases with increase in the aqueous phase concentration of nitric acid. Moreover, the extraction of nitric acid in all the irradiated cases is quite similar to those observed in the unirradiated 0.2 M TEHDGA/*n*-DD. However, it was interesting to note that there was no third phase formation in the case of the organic phases irradiated to 50 kGy and above when contacted with 4 M nitric acid. Moreover, the irradiated organic phase was found to undergo third phase formation only when the 50 kGy, 100 kGy, 250 kGy, and 500 kGy irradiated organic phases were contacted with 5 M, 6 M, 7 M, and 8 M nitric acid solutions, respectively. This observation requires deeper understanding of the irradiated systems, and the results also indicate the merit of irradiating 0.2 M TEHDGA/*n*-DD solution to gamma radiation, even though the radiolytic degradation was regarded as deleterious from the process point of view, so far. However, the aggregation results obtained in the irradiated 0.2 M TEHDGA/*n*-DD shows the benefits of irradiation, as it prevents the undesirable event of third phase formation during the course of solvent extraction.

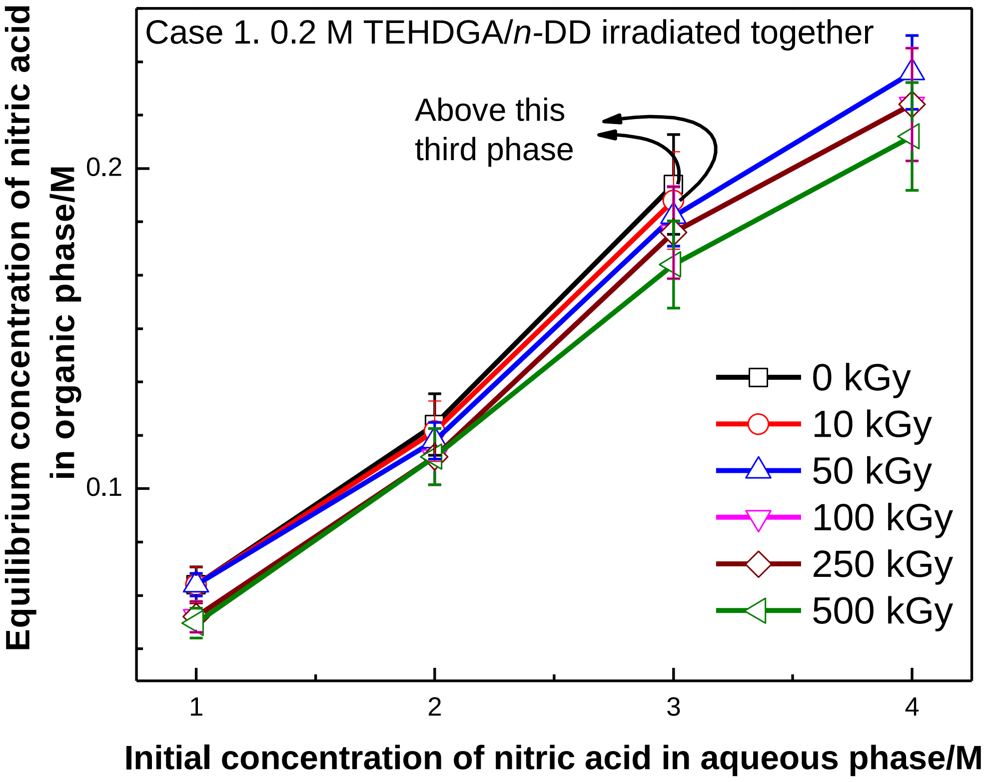

**Figure 5.2.** Variation in the extraction of nitric acid in organic phase as function of initial concentration of nitric acid in aqueous phase at various absorbed dose levels. Organic phase: 0.2 M TEHDGA/*n*-DD irradiated from 0 kGy to 500 kGy (case 1), Aqueous phase: Nitric acid concentration varied from 1 M to 4 M.

Figure 5.3 shows the average size of the aggregates formed in organic phase, upon nitric acid extraction. The organic phase was composed of either unirradiated or irradiated solution of 0.2 M TEHDGA/*n*-DD. It can be seen that the average aggregate size in all cases increases with increase in the concentration of nitric acid in aqueous phase, obviously due to the extraction of nitric acid, as discussed in previous chapters. It is also noted that the average aggregate size decreases upon irradiation.

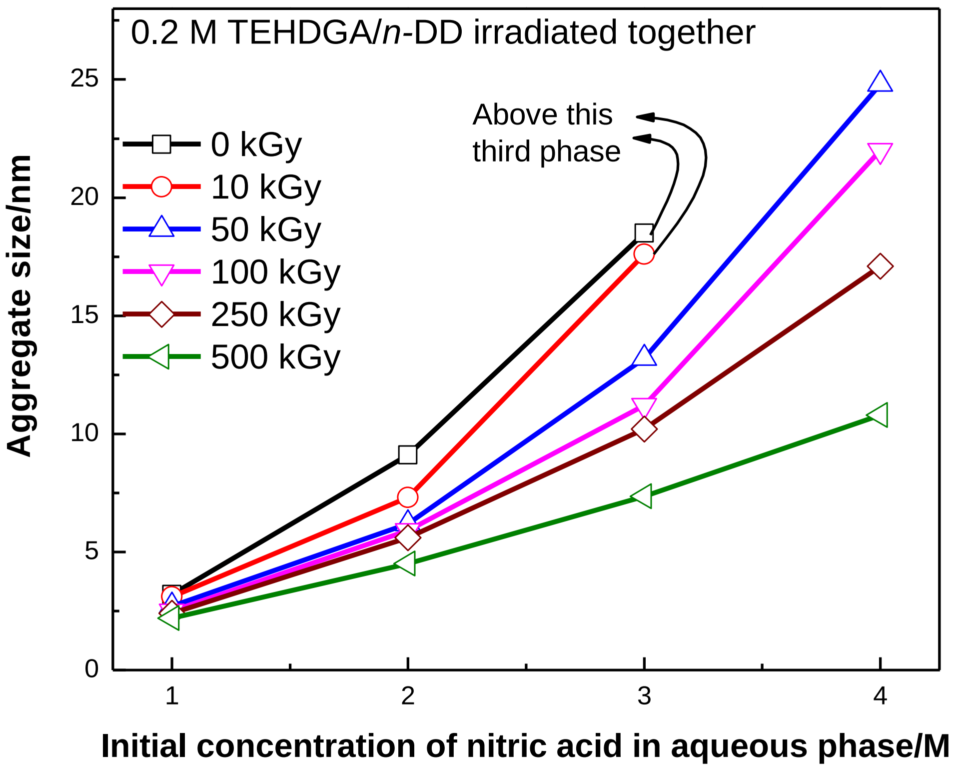

**Figure 5.3.** Variation in the average size of aggregates present in the case 1 organic phase at different initial concentration of nitric acid in aqueous phase. Organic phase: 0.2 M TEHDGA/*n*-DD irradiated from 0 kGy to 500 kGy (case 1), Aqueous phase: Nitric acid concentration varied from 1 M to 4 M.

The aggregate distributions of the irradiated and unirradiated organic phases are shown in Figure 5.4. This was obtained by irradiating the 0.2 M TEHDGA/*n*-DD solution to different absorbed dose levels and equilibrating the irradiated organic phase with 3 M nitric acid. The organic phase obtained after the extraction of nitric acid was subjected to DLS measurements. It is obviously seen from Figure 5.4 that the aggregate distribution (FWHM), average aggregate size, and the intensity of aggregates in organic phase decreased with increase of absorbed dose.

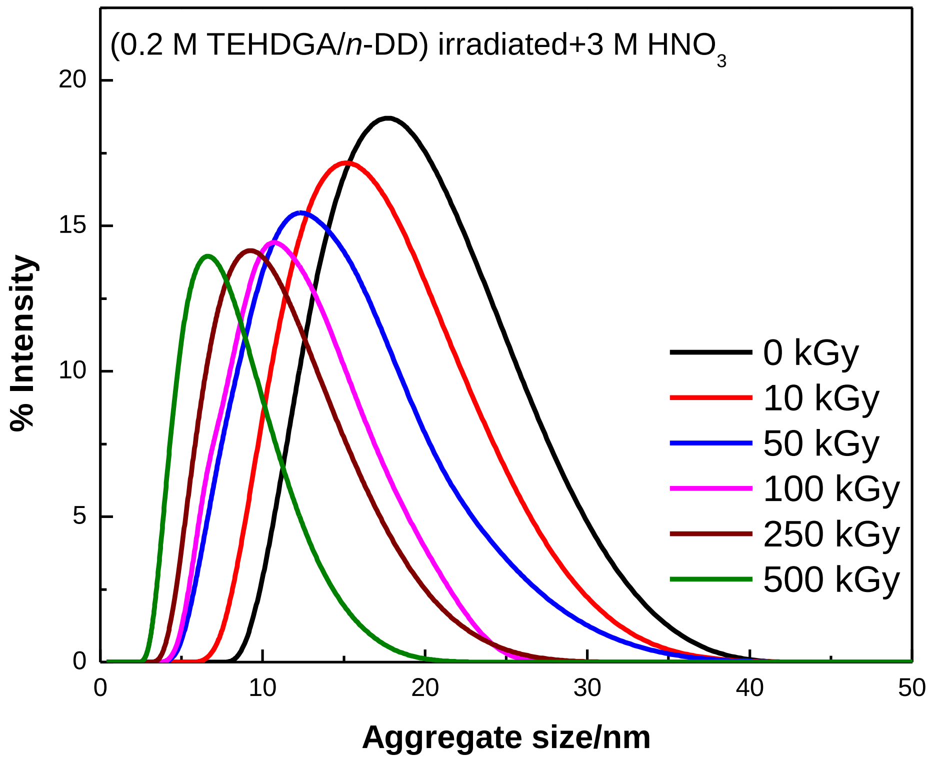

**Figure 5.4.** The aggregation behaviour of case 1 organic phase as a function of various absorbed doses. Organic phase: (0.2 M TEHDGA/*n*-DD) irradiated from 0 kGy to 500 kGy (case 1), Aqueous phase: [$HNO_3$] = 3M.

### 5.3.3 Self-aggregation Behaviour of Case 2 Organic Phase

To understand the role of individual irradiated components present in the solvent phase, the ligand, TEHDGA, was irradiated alone to different absorbed dose levels and the aggregation behavior of the irradiated TEHDGA present in unirradiated *n*-dodecane (0.2 M) is displayed in Figure 5.5. The aggregate distribution is compared with unirradiated 0.2 M TEHDGA/*n*-DD. It can be seen that the intensity of aggregates decreases with increase of absorbed dose, as expected. However, it is important to note that the decrease in the intensity is not significant in this case, as compared to the intensity decrease observed in the irradiated solution of 0.2 M

TEHDGA/*n*-DD (irradiated together) as shown in Figure 5.1. Previously, Ravi *et al.* studied the radiolytic degradation of diglycolamides (DGAs) present in *n*-DD medium, and reported that the radiolytic degradation of DGA was more, when *n*-dodecane was present along with DGA, which was attributed to the sensitization effect (see route 3, Table 5.1) [15-17]. A similar behavior was also reported by others [2, 13, 25]. Therefore, the higher intensity observed for the aggregates formed upon irradiating TEHDGA alone (Figure 5.5) could be due to the absence of sensitization. This observation was supported by the analytical estimation of TEHDGA in the irradiated and unirradiated TEHDGA systems, reported elsewhere [13, 25, 26]. Sharma *et al.* estimated the concentration of TEHDGA in the irradiated solutions. It was reported that the concentration of TEHDGA decreased from 0.2 M to ~ 0.18 M [21], when TEHDGA was irradiated alone, as compared to the decrease in concentration from 0.2 M to ~ 0.13 M, when TEHDGA (0.2 M) and *n*-dodecane were irradiated together.

.

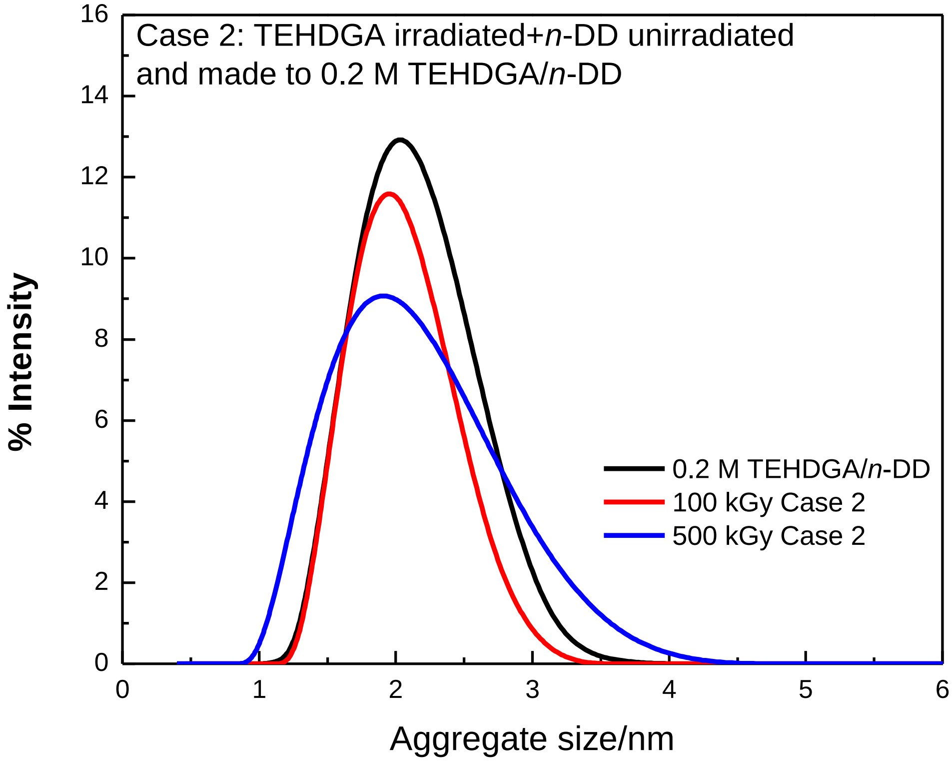

**Figure 5.5.** Self-aggregation behaviour of case 2 organic phase (0.2 M irradiated TEHDGA in unirradiated *n*-DD) at different absorbed doses.

### 5.3.4 Extraction of Nitric Acid in Case 2 Organic Phase

Since the radiolytic degradation was less when TEHDGA was irradiated alone (see Table 5.1), it can be expected that the average size of aggregates formed in organic phase could be more during the extraction of nitric acid in this case. The nitric acid extraction isotherm of the solution containing irradiated TEHDGA present in unirradiated *n*-dodecane is shown in Figure 5.6. The concentration of TEHDGA in the solution was 0.2 M. It can be seen that the extraction of nitric acid in the irradiated and unirradiated organic phases are quite similar. The extraction data presented in Figure 5.6 is also comparable with those presented in Figure 5.2, wherein the

TEHDGA and *n*-dodecane are irradiated together (i.e. case 1). However, the third phase formation behaviour observed in Figure 5.6 differs significantly from those observed only in Figure 5.2. It is interesting to note from Figure 5.6, that the third phase formation was not observed in case of the organic phase containing 500 kGy irradiated TEHDGA present in unirradiated *n*-dodecane. In other irradiated systems namely, 10 kGy to 250 kGy irradiated TEHDGA present in unirradiated *n*-dodecane, the organic phase was found to form third phase, when the organic phase was contacted with nitric acid concentration of 4 M and above. In view of the presence of higher concentration of TEHDGA due to the absence of sensitization, the third phase formation was observed in 10 kGy to 250 kGy irradiated TEHDGA present in unirradiated *n*-DD.

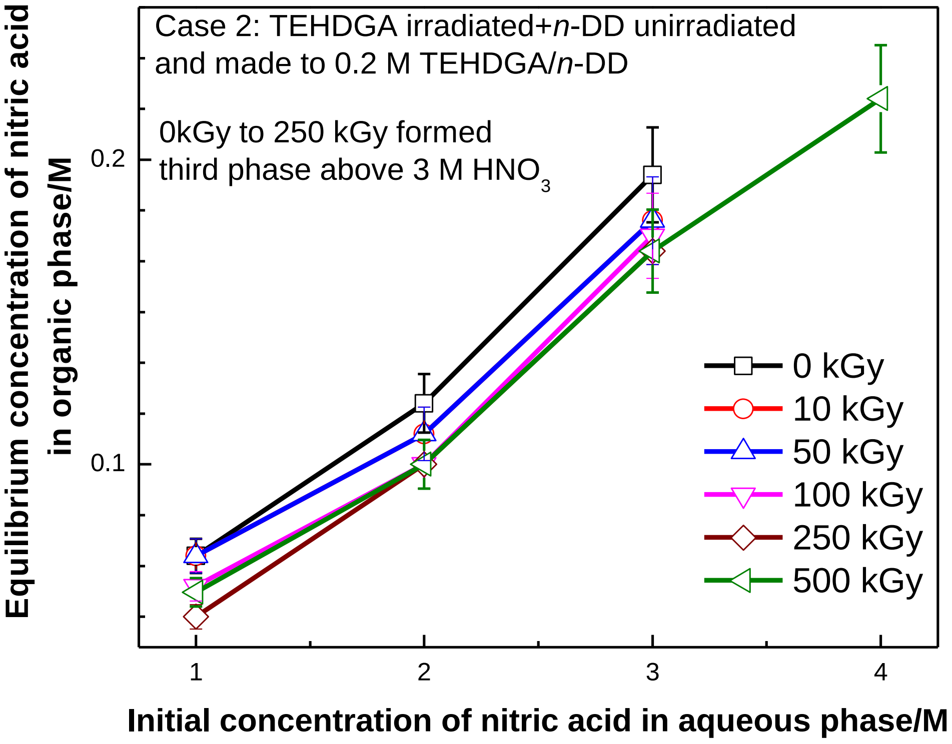

**Figure 5.6.** Variation in the extraction of nitric acid in organic phase as function of initial concentration of nitric acid in aqueous phase at different absorbed doses. Organic phase: 0.2 M TEHDGA irradiated/*n*-DD unirradiated (case 2), Aqueous phase: Nitric acid concentration varied from 1 M to 4 M.

### 5.3.5 Extraction of Nitric Acid in Case 3 Organic Phase

The radiolytic degradation behavior of *n*-dodecane alone and the role of radiolytic degradation products of *n*-DD on the aggregation behaviour of unirradiated TEHDGA dissolved in irradiated *n*-dodecane was studied. For this purpose, the *n*-dodecane alone was irradiated to various absorbed dose levels and mixed with unirradiated TEHDGA to obtain 0.2 M TEHDGA in *n*-dodecane. The self-aggregation behaviour of the solution containing 0.2 M unirradiated TEHDGA in irradiated *n*-dodecane is shown in Figure 5.7. It can be seen that the self-aggregation behaviour of irradiated and unirradiated systems are comparable. The nitric acid extraction behavior of 0.2 M TEHDGA (unirradiated) present in irradiated *n*-dodecane, is shown in Figure 5.8. As expected, the extraction of nitric acid in organic phase increases with increase in the concentration nitric acid present in aqueous phase at all absorbed dose levels. It is important to note that the organic phase splitting (third phase formation) was observed in all cases, when the organic phase was equilibrated with 4 M nitric acid. The nitric acid extraction behavior observed in these cases resembles the behavior observed in unirradiated solution of 0.2 M TEHDGA/*n*-DD, shown in Figure 5.8. However, the third phase formation behavior shown in Figure 5.8 is quite different from the other conditions shown in Figures 5.2 and 5.6.

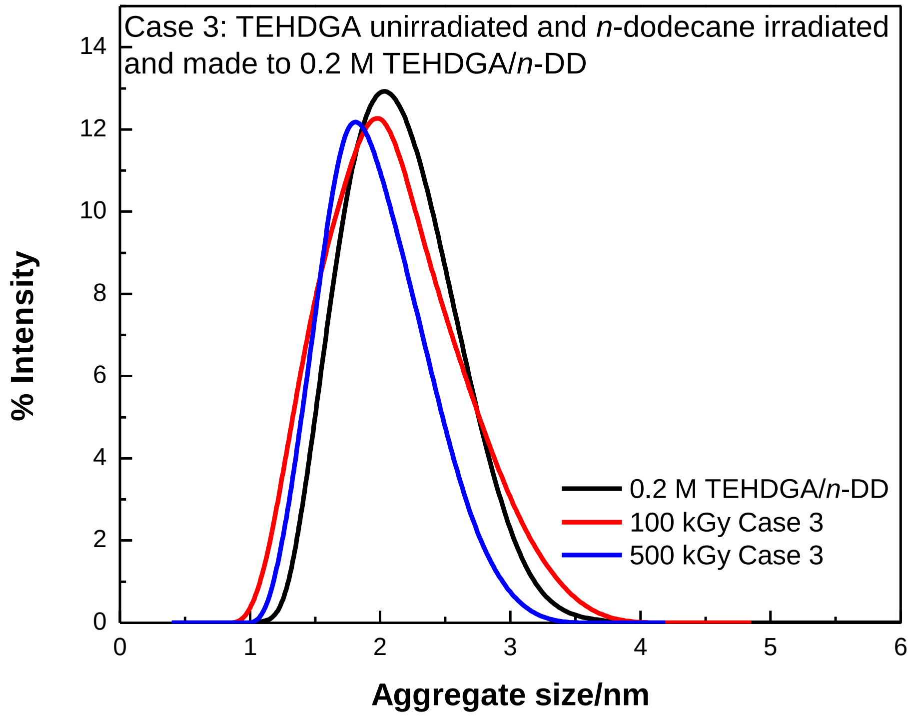

**Figure 5.7.** Self-aggregation behaviour of case 3 organic phase (unirradiated TEHDGA in irradiated *n*-DD) at different absorbed doses.

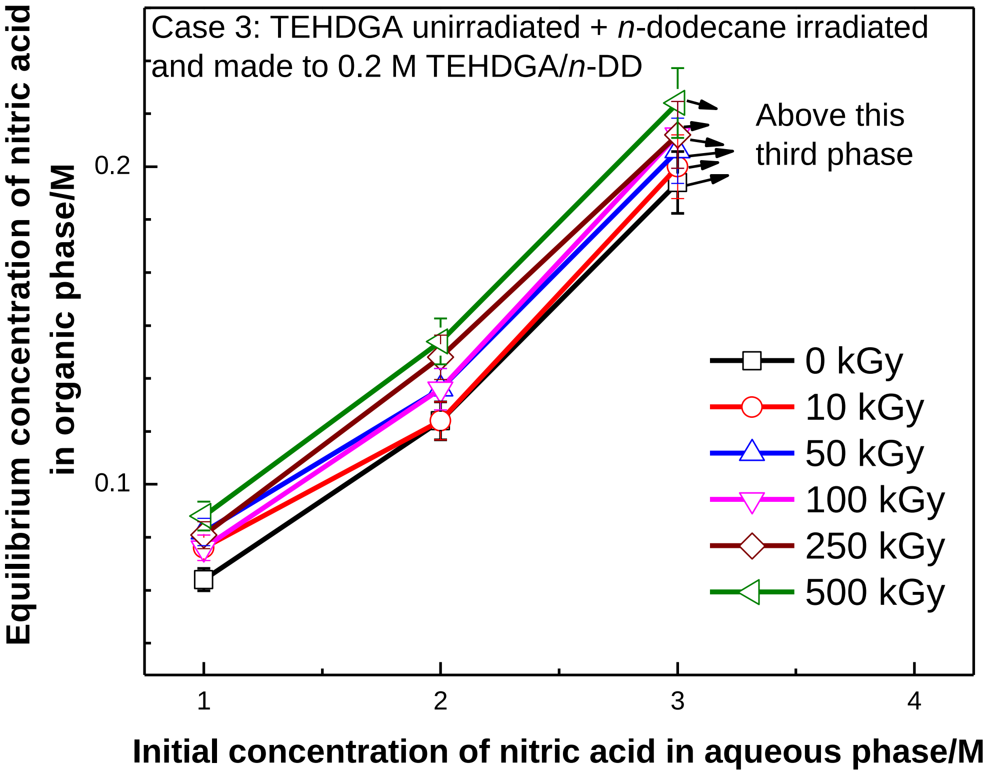

**Figure 5.8.** Variation in extraction of nitric acid in case 3 organic phase as a function of initial nitric acid concentration in aqueous phase at different absorbed doses. Organic phase: 0.2 M TEHDGA unirradiated/*n*-DD irradiated (case 3), Aqueous phase: Nitric acid concentration varied from 1 M to 4 M.

### 5.3.6 Aggregation Behaviour of the Case 3 Organic Phase

The organic phase (case 3) obtained after extraction of nitric acid was subjected to dynamic light scattering studies. The variation in the average aggregate size of the organic phase as function of nitric acid concentration in aqueous phase is shown in Figure 5.9. It should be noted that *n*-dodecane alone was irradiated to various absorbed dose levels and mixed with unirradiated TEHDGA to obtain 0.2 M TEHDGA (unirradiated) in irradiated *n*-dodecane. The organic phase was contacted with different nitric acid concentrations and the average aggregate size was determined for the organic phase. It is interesting to note from Figure 5.9 that the average aggregate size at a particular concentration of nitric acid increases with increase in the absorbed dose of irradiated *n*-dodecane. The increase in aggregate size with increase of absorbed dose reported in Figure 5.9 is likely to occur when the higher homologs of *n*-dodecane are formed upon irradiation of *n*-dodecane as depicted in route 5 of table 1. Similar aggregation behavior was also observed in the chapter 3. It was reported that the average aggregate size increased with increase in the chain length of *n*-paraffin at a particular concentration of nitric acid.

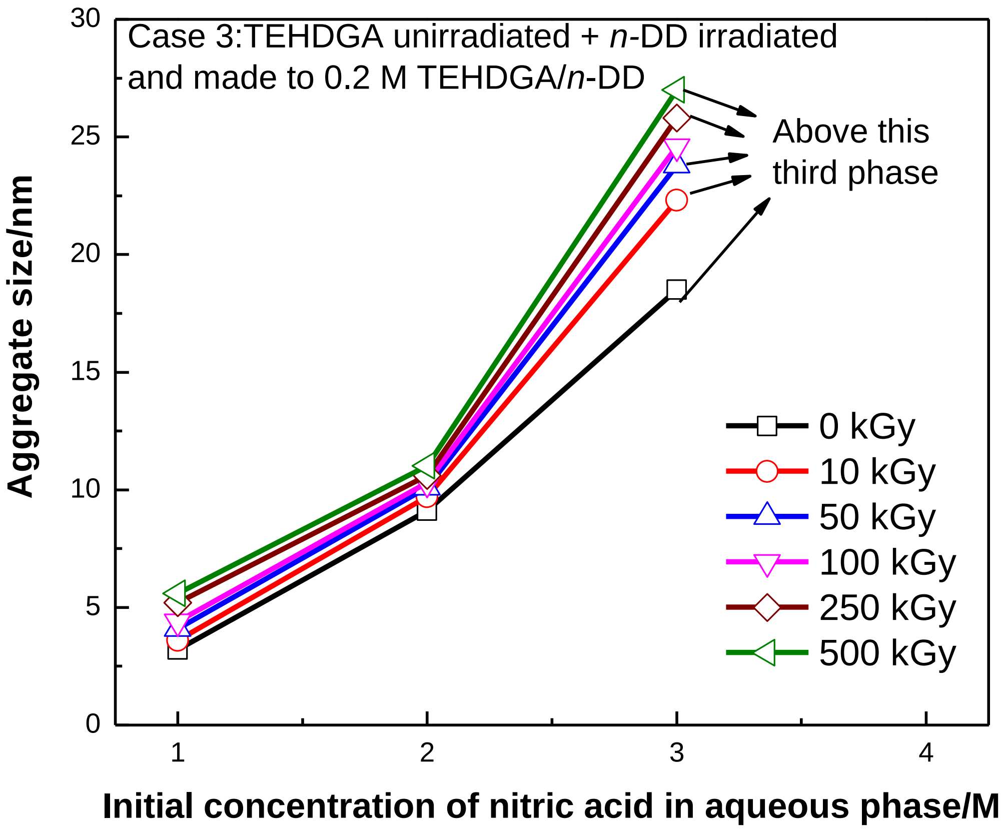

**Figure 5.9.** Comparison in the average size of aggregates present in the organic phase as a function of initial concentration of nitric acid in aqueous phase at different absorbed doses. Organic phase: 0.2 M TEHDGA unirradiated/*n*-DD irradiated (case 3), Aqueous phase: Nitric acid concentration varied from 1 M to 4 M.

It should be noted that the irradiation of *n*-dodecane by gamma radiation can result in the formation of smaller fragments of *n*-DD and branched hydrocarbon, higher homologs of *n*-DD and smaller branched paraffins etc., as discussed elsewhere [16,25]. The smaller homologs of *n*-DD and branched paraffin, when mixed with unirradiated TEHDGA, it is expected to decrease the average aggregate size, as discussed elsewhere [22,23]. In contrast to this, the increase in the average aggregate size upon irradiating *n*-dodecane, as shown in Figure , point out to the fact that the higher homologs of *n*-dodecane especially *n*-paraffins are predominantly controlling the average size of the aggregates formed in a solution of 0.2 M unirradiated TEHDGA present in irradiated n-dodecane. The aggregate distribution recorded in the organic phase containing 0.2 M unirradiated TEHDGA dissolved in irradiated *n*-dodecane after contacting the organic phase with 3 M nitric acid is shown in Figure 5.10. It is clearly seen that the average aggregate size and the aggregate distribution increases with increase of absorbed dose.

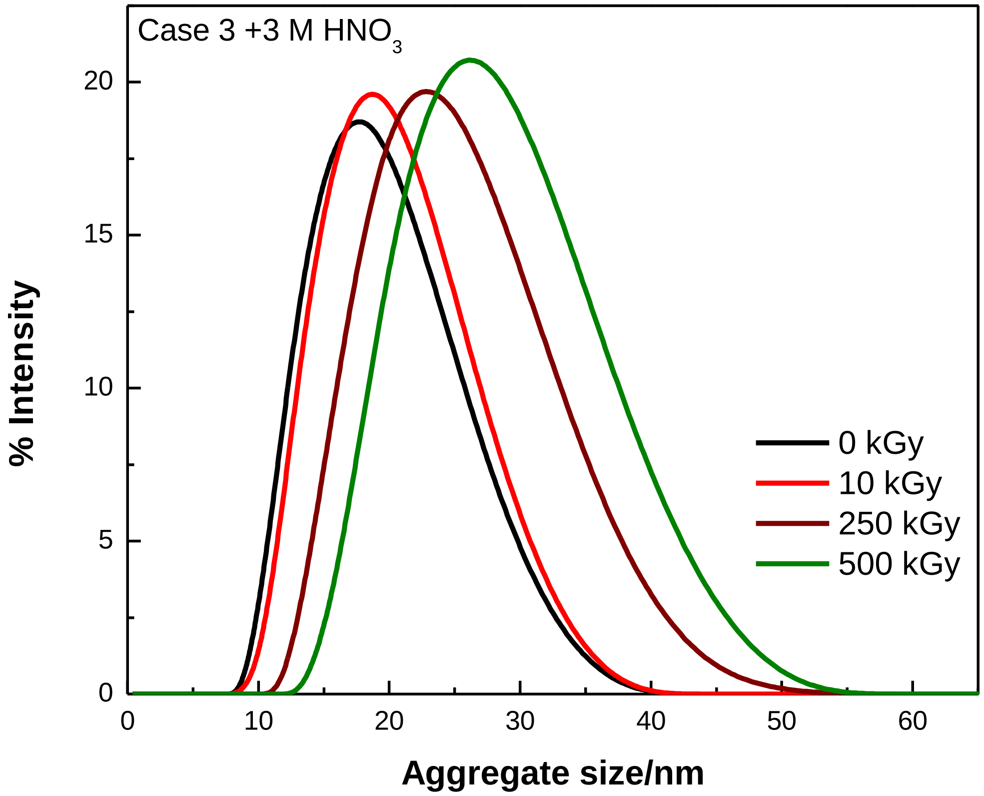

**Figure 5.10.** The aggregate behaviour of case 3 organic phase as a function of different absorbed doses. Organic phase: 0.2 M TEHDGA unirradiated/*n*-DD irradiated (case 3), Aqueous phase: [$HNO_3$] = 3M.

### 5.3.7 Aggregation Behaviour of the Case 4 Organic Phase

The above studies were discussing about the results on the aggregation behaviour of the solution containing either irradiated TEHDGA or *n*-dodecane present either unirradiated *n*-dodecane or unirradiated TEHDGA, respectively, to obtain 0.2 M TEHDGA/*n*-DD. It would be interesting to understand the aggregation behaviour of the organic phase containing irradiated TEHDGA and irradiated *n*-dodecane. To obtain this information the TEHDGA and *n*-dodecane were irradiated independently to 500 kGy and mixed together to obtain 0.2 M solution of

TEHDGA in *n*-dodecane. The organic phase thus obtained was equilibrated with 3 M nitric acid and then subjected to DLS measurements. The aggregation behaviour observed in this case (case 4) is compared with other two cases (case 2 and 3) in Figure 5.11. It can be seen that the average aggregate size and their distribution in organic phase (case 4) is intermediate between other two organic solutions, in which TEHDGA alone or *n*-dodecane alone were irradiated to 500 kGy and mixed with the other component to obtain 0.2 M TEHDGA/*n*-DD. Moreover, the aggregate size and their distribution observed in the organic solution containing irradiated TEHDGA in irradiated *n*-dodecane (case 4) is tending towards the aggregate distribution observed in the irradiated TEHDGA in unirradiated *n*-dodecane (case 2). The intermediate nature of aggregation behaviour observed for case 4 organic phase was found to be applicable at all dose levels and at all nitric acid concentrations.

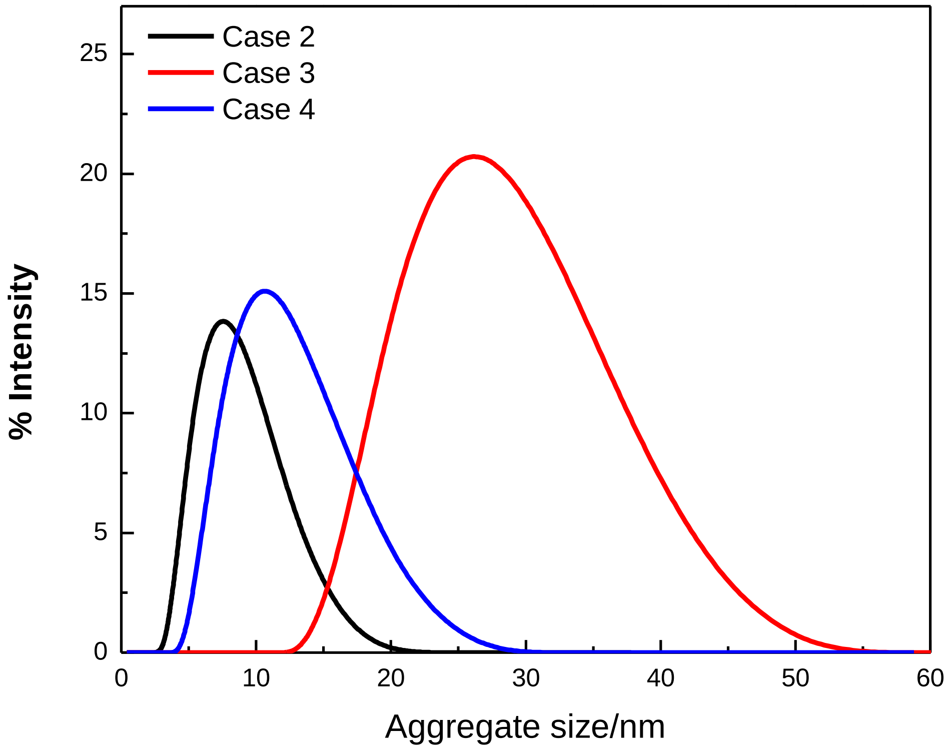

**Figure 5.11.** Aggregate size distribution behaviour of the organic phase containing 0.2 M TEHDGA irradiated/*n*-DD unirradiated (case 2) or 0.2 M TEHDGA unirradiated/*n*-DD irradiated (case 3) or 0.2 M TEHDGA irradiated/*n*-DD irradiated (case 4) at 500 kGy absorbed dose. The aggregation distribution recorded after contacting the organic phase with 3 M nitric acid medium.

### 5.3.8 Aggregation Behaviour of the Case 5 Organic Phase

In the actual extraction of trivalent actinides, the organic phase was contacted with high-level liquid waste containing the actinides present in 3-4 nitric acid medium. During this process, significant amount of nitric acid was also co-extracted into organic phase. The presence of nitric acid in organic phase can induce a large number of transformations in organic phase, both physical and chemical changes, upon gamma irradiation, as discussed elsewhere [9, 10, 26]. It was reported that the radiolytic degradation of organics in the presence of nitric acid can lead to the formation of strongly polar nitro alkanes, alcohols, hydroxamic acid etc [26]. To understand this, the organic solution composed of 0.2 M TEHDGA/*n*-DD was equilibrated with 3 M nitric acid, and subjected the organic phase to gamma irradiation after nitric acid extraction. The organic phase was containing about 0.19 M nitric acid (see chapter 3). After the irradiation, the organic phase was recorded for dynamic light scattering studies without any treatment. The results on the aggregation behaviour of the organic phases are shown in Figure 5.12 It can be seen that the aggregate size, aggregate distribution and the intensity of aggregates decreases with increase of absorbed dose. This observation is significantly different from the other cases (case 1 to 4) discussed above. The results of Figure 5.4 were obtained by irradiating the solution of 0.2 M TEHDGA/*n*-DD to various absorbed doses, whereas the results shown in Figure 5.12 were obtained by irradiating 0.2 M TEHDGA/*n*-DD phase containing extracted nitric acid, which was about 0.19 M. Comparing the results shown in Figures 5.4 and 5.12, it is evident that the presence of nitric acid in organic phase influences the aggregation behaviour of organic phase to a significant extent, due to the formation of polar degradation products of organics (route 7, Table 5.1). The formation of degradation products such as alcohols and nitroalkanes have been reported for radiolytic degradation of acid equilibrated DGA in *n*-DD [13, 26]. It is important to note that the degradation products such as nitro alkanes, alcohols etc. are strongly polar. The aggregation behaviour of 0.2 M TEHDGA/*n*-DD in the presence of octanol, decanol and isodecanol was discussed in Part II of chapter 4. It was reported that the presence of a small concentration of alcohol in organic phase decreased the aggregate size and the distribution of aggregates to a significant extent. Moreover, the presence of any organics containing the polar group can stabilize the polar aggregates formed in organic phase. A similar behavior was also reported by others [28]. In view of this, the significant decrease in the aggregate size of the organic phase obtained upon irradiation of the organic phase in the presence of nitric acid could be attributed to the formation of polar degradation products of the organics present in the organic phase.

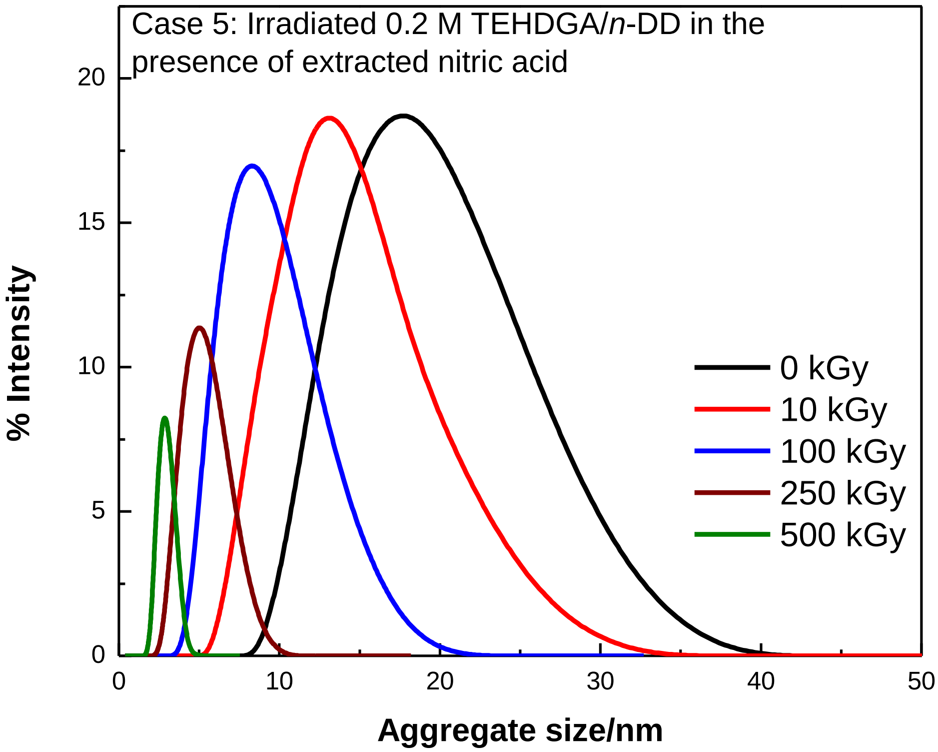

**Figure 5.12.** The aggregation behaviour of the case 5 organic phase (0.2 M TEHDGA/*n*-DD+ extracted nitric acid) irradiated at various absorbed dose levels from 0 kGy to 500 kGy.

The irradiated organic phase was also analyzed by ATR-FTIR spectroscopy. Since, the extracted nitric acid ($NO_3$ or $HNO_3$) and nitrioalkanes ($NO_3$ or $RNO_2$) can give the transmittance bands at 1550 $cm^{-1}$ and 1277 $cm^{-1}$ due to nitrate stretching, it is necessary to remove the extracted nitric acid from organic phase to understand the formation of nitro alkanes. Therefore, the irradiated organic phase (case 5) containing 0.2 M TEHDGA/*n*-DD (irradiated in the presence of extracted nitric acid) was subjected to extensive washing with distilled water. During this process, the extracted nitric acid was back extracted into water phase leaving the water insoluble nitro alkanes in organic phase. The organic phase obtained after water wash was subjected to ATR-FTIR analysis. The results are displayed in Figure 5.13. It is compared with unirradiated 0.2 M TEHDGA/*n*-DD and irradiated 0.2 M TEHDGA/*n*-DD in the absence of nitric acid. The spectrum of 0.2 M TEHDGA/*n*-DD irradiated in the presence of nitric acid, shows the transmittance bands at 1550 $cm^{-1}$ and 1277 $cm^{-1}$, indicating the formation of nitroalkanes in the organic phase. Such a transmittance band is not observed in 0.2 M TEHDGA/*n*-DD irradiated in the absence of nitric acid extraction, confirming the formation of nitroalkanes in organic phase irradiated in the presence of nitric acid.

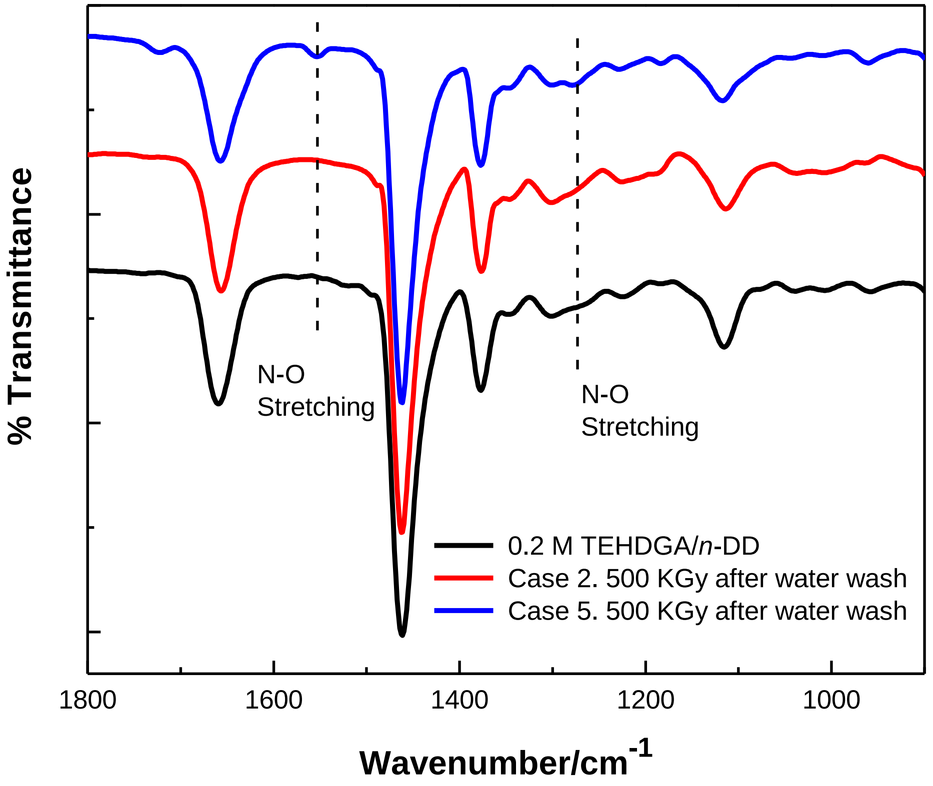

**Figure 5.13.** ATR-FTIR spectrum of the organic phase containing 0.2 M TEHDGA/*n*-DD recorded at different experiment conditions (case 1 and case 5).

### 5.3.9 Extraction behavior of Nd(III) upon irradiation

Figure 5.14 shows that the extraction behavior of Nd(III) from 1 M nitric acid medium in 0.2 M TEHDGA/*n*-DD, studied as a function of initial amount of Nd(III) in aqueous phase. The extraction of Nd(III) in 0.2 M TEHDGA/*n*-DD was carried from 1 M nitric acid solution instead of 3-4 M nitric acid that represents the concentration of nitric acid prevailing in high-level liquid waste, since the extraction of small quantity of Nd(III) (i.e. 0.6 g/L) results in the formation of third phase as shown in section 3.5.5 of chapter 3. In view of this, the concentration of nitric in aqueous phase was reduced to 1 M, and the results on the extraction of Nd(III) in 0.2 M

TEHDGA/*n*-DD was shown in Figure 5.14. It can be seen that the loading of Nd(III) in organic phase increases with increase in the initial amount of Nd(III) in aqueous phase, as expected. It is important to note that when the initial amount of Nd(III) in aqueous phase exceeds 5 g/L, the organic phase undergoes phase splitting, in case of the unirradiated organic phase as discussed in section 3.5.5 of chapter 3. Figure 5.14 also shows the loading behavior of Nd(III) in the irradiated (500 kGy) 0.2 M TEHDGA/*n*-DD (case 1 organic phase) studied as a function of initial amount of Nd(III) in aqueous phase. It can be seen that the loading of Nd(III) in organic phase increases with increase in the initial amount of Nd(III) in aqueous phase in this case also. However, the loading of Nd(III) in the irradiated organic phase is less as compared to the unirradiated organic phase at particular value of Nd(III) in aqueous phase. In addition, it is also important to note that the organic phase undergoes phase splitting only when the initial amount of Nd(III) in aqueous phase exceeds 12 g/L, which is about 2.5 times higher than that observed in the unirradiated 0.2 M TEHDGA/*n*-DD. However, the organic phase undergoes phase splitting only when the concentration of Nd(III) in organic phase reaches about 3.6 g/L (see section 3.5.5 of chapter 3), irrespective of the irradiated or unirradiated system. To achieve 3.6 g/L Nd(III) in organic phase, it is necessary to contact the irradiated organic phase (500 kGy) with aqueous phase containing 12 g/L Nd(III) in 1 M nitric acid.

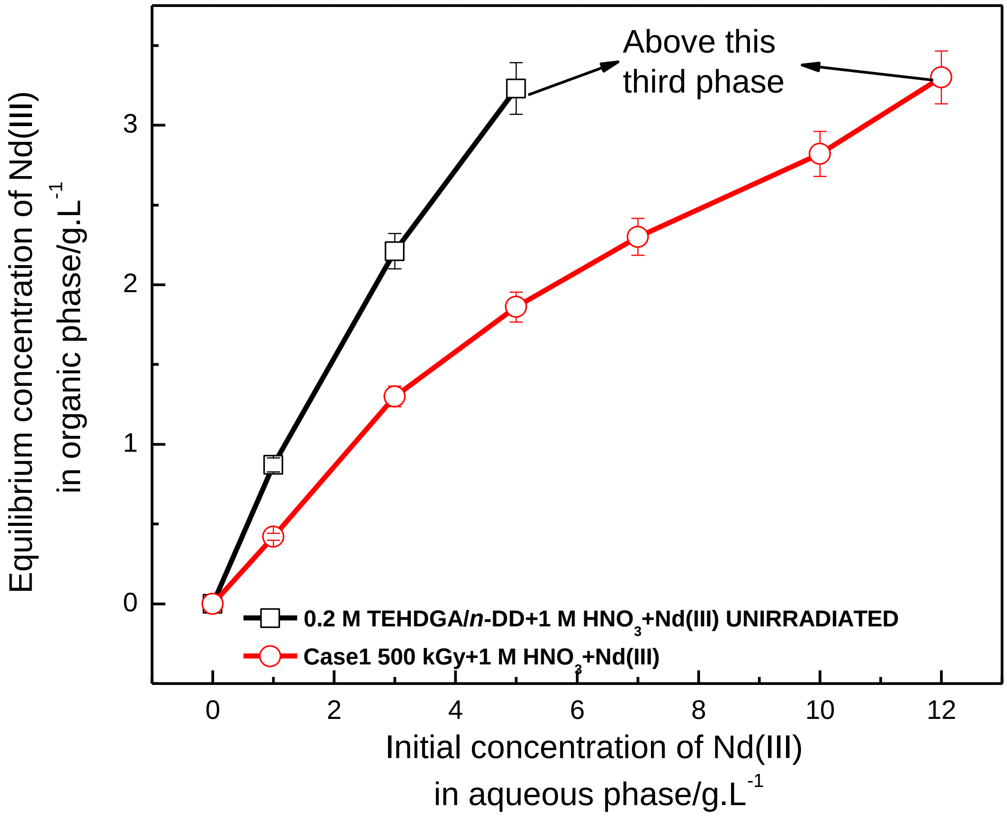

**Figure 5.14.** Variation in the extraction of Nd(III) as a function of initial amount of Nd(III) in aqueous phase. Organic phase: unirradiated 0.2 M TEHDGA/*n*-DD or case 1 organic phase, Aqueous phase: 1 M $HNO_3$+ Nd(III).

In order to understand the loading of Nd(III) and aggregation behavior of the radiolytically degraded organic phase, the TEHDGA and *n*-DD were irradiated together or individually to various absorbed gamma dose levels. Figure 5.15 shows the variation in the loading behavior of Nd(III) studied as a function of absorbed dose, varied from 10 kGy to 500 kGy. It can be seen that the loading of Nd(III) in all the irradiated organic phases decrease with increase of absorbed dose. However, at particular absorbed dose, the loading of Nd(III) in the irradiated organic phase decreases in the order of case 3 > case 2 ~ case 4 > case 1. This indicates that the presence of *n*-dodecane along with TEHDGA during irradiation (i.e. case 1) facilitates the radiolytic degradation of the organic phase and reduces the loading of Nd(III) [13]. In contrast to this, when *n*-dodecane was irradiated alone and mixed with an unirradiated TEHDGA (i.e. case 3), the loading behaviour of Nd(III) in the this case is nearly comparable with the unirradiated organic phase (absorbed dose is zero). It can be seen in Figure 5.15 that the loading of Nd(III) does not vary much with respect to absorbed dose. When TEHDGA alone was irradiated and mixed with unirradiated *n*-dodecane (case 2), the loading behavior of Nd(III) in the irradiated organic phase is in between the behavior observed for case 1 and case 3 organic phases. Since, the *n*-dodecane when irradiated alone does not cause much changes to the loading of Nd(III) in the organic phase, the loading behavior of 0.2 M irradiated TEHDGA in irradiated *n*-dodecane (case 4) is similar to case 2.

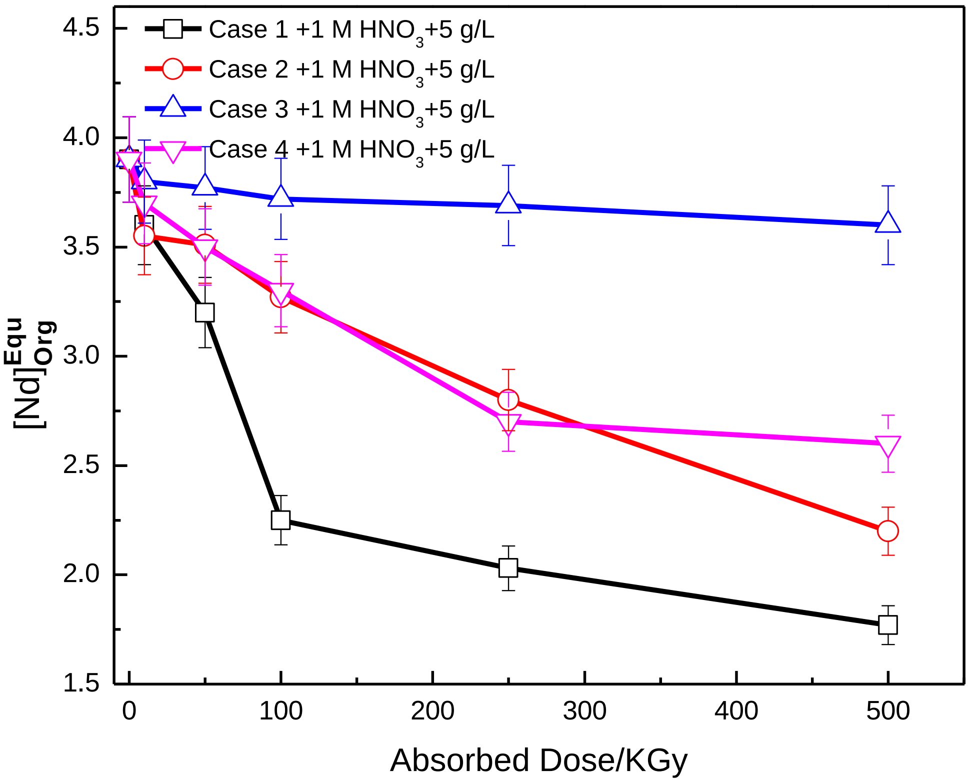

**Figure 5.15.** Variation in the extraction of Nd(III) as a function irradiated absorbed dose rates. Organic phase: Case 1 or case 2 or case 3 or case 4 organic phase, Aqueous phase: 1 M $HNO_3$+ 5 g/L Nd(III).

### 5.3.10 ATR-FTIR spectroscopic studies

To understand the loading behavior observed in different organic phases discussed above, the ATR-FTIR spectra of the irradiated (500 kGy) organic phase was recorded and compared with unirradiated 0.2 M TEHDGA/*n*-DD organic phase in Figure 5.16. It should be noted that the FTIR spectrum of unirradiated 0.2 M TEHDGA/*n*-DD shows a transmittance band at 1663 cm$^{-1}$, which correspond to the amidic carbonyl stretching frequency of TEHDGA (see Part II of chapter 3). When the unirradiated 0.2 M TEHDGA/*n*-DD was contacted with 1 M nitric acid containing 5 g/L $Nd(NO_3)_3$, the resultant organic phase shows a couple of transmittance bands at

1663 cm$^{-1}$, corresponding to the uncoordinated amidic carbonyl stretching frequencies and the red shifted transmittance band at 1610 cm$^{-1}$, corresponding to the amidic carbonyl stretching frequencies of TEHDGA coordinated to $Nd(NO_3)_3$ as described in section 3.5.7 of chapter 3. It is interesting to note that the relative intensity of the transmittance band at 1610 cm$^{-1}$ ($I_{1610}$) more than 1663 cm$^{-1}$ ($I_{1663}$) in this case (unirradiated) indicating that significant amount of Nd(III) is coordinated TEHDGA in the organic phase as compared to the uncoordinated or free TEHDGA present in organic phase. It should be noted that Nd(III) was extracted from1 M nitric acid. Under these conditions, the amount of Nd(III) and nitric acid extracted into organic phase was determined to be 3.2 g/L and 0.1 M respectively. Assuming that TEHDGA forms a 1:3 (Nd:TEHDGA) complex with Nd(III) [13,20] and ~1:1 protonated species with nitric acid, the amount of TEHDGA consumed during the coordination of Nd(III) and protonation of $HNO_3$ is estimated to be ~0.16 M TEHDGA in the organic phase. In view of this, the intensity of 1610 cm$^{-1}$ band is more as compared to 1663 cm$^{-1}$ transmittance band.

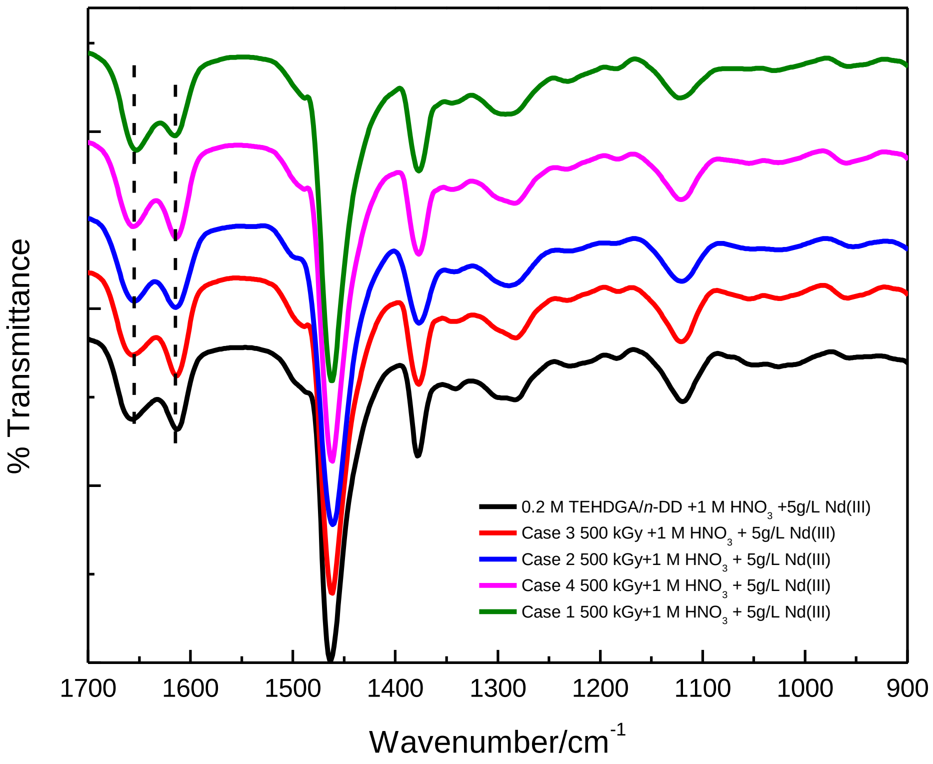

**Figure 5.16.** ATR- FTIR spectra of organic phase recorded after the extraction of Nd(III) from 1 M nitric acid. Absorbed dose 500 kGy. Organic phase: unirradiated 0.2 M TEHDGA/*n*-DD or case 1 or case 2 or case 3 or case 4, Aqueous phase: 1 M $HNO_3$+ 5 g/L Nd(III).

Figure 5.16 also shows that the ATR-FTIR spectrum of the, case 3 organic sample, in which *n*-dodecane alone was irradiated and mixed with TEHDGA. When this organic phase was irradiated to 500 kGy and subjected to the extraction of Nd(III) from 1 M nitric acid solution, the ATR-FTIR spectrum of organic phase shows a couple of bands at 1663 cm$^{-1}$ and 1610 cm$^{-1}$, with $I_{1610} > I_{1663}$ in this case also. The features of case 3, FTIR spectrum are comparable with unirradiated organic phase. When TEHDGA was irradiated alone and mixed with unirradiated *n*-dodecane (case 2), the FTIR spectrum of the organic phase obtained after extraction of Nd(III) from 1 M nitric acid, shows the relative intensity of $I_{1610}$ is marginally higher than $I_{1663}$. In contrast to this, the $I_{1610} < I_{1663}$ in case of organic phase containing 0.2 M TEHDGA/*n*-DD irradiated together (case 1). For the case 4, the behavior of transmittance bands at $I_{1610}$ and $I_{1663}$ are quite similar to that observed in case 2. All these observations indicate that the extraction of Nd(III) in organic phase results in the coordination of $Nd(NO_3)_3$ with amidic carbonyl of TEHDGA. Upon irradiation, the TEHDGA undergoes radiolytic degradation and the concentration of TEHDGA in organic phase decreases with increase of absorbed dose. The degradation is accelerated when TEHDGA is irradiated in the presence of *n*-dodecane. The relative intensity of $I_{1663}$ decreases in the following order case 1 > case 2 ~ case 4 > case 3 ~ unirradiated organic phase, which is the order of the decrease in the degradation of TEHDGA upon irradiation. The decrease is more when TEHDGA is irradiated along with *n*-dodecane, indicating the sensitization effect of *n*-dodecane on TEHDGA, discussed elsewhere [13-15, 21].

### 5.3.11 Aggregation behavior organic phase after Nd(III) extraction

The decrease in the concentration of TEHDGA upon irradiation could alter the aggregation behavior of the irradiated organic phase. Figure 5.17 shows the aggregate distribution of the case 1 organic phase obtained at different absorbed dose levels. It can be seen that the average aggregate size, aggregate distribution and the intensity of aggregates decreases with increase of absorbed dose. Irradiation of case 1 organic phase results in the radiolytic degradation of TEHDGA and it decreases the concentration of TEHDGA, as discussed elsewhere [13, 21]. Since the aggregation is dependent on the concentration of TEHDGA in organic phase, the aggregate size and the distribution of aggregates in organic phase decrease with increase of absorbed dose.

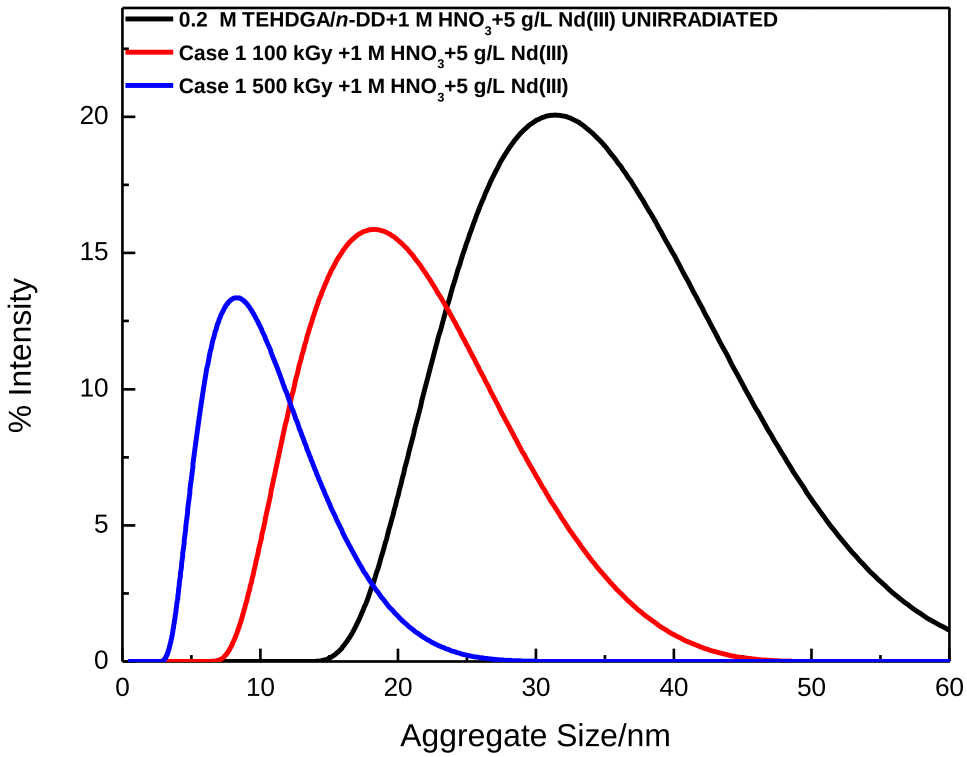

**Figure 5.17.** The aggregation behaviour of the organic phase irradiated at various absorbed dose levels from 0 kGy to 500 kGy. Organic phase: unirradiated 0.2 M TEHDGA/*n*-DD or case 1, Aqueous phase: 1 M $HNO_3$+ 5 g/L Nd(III).

Figure 5.18 shows the comparison of the aggregation behavior of the case 1 organic phase irradiated to 500 kGy with the unirradiated 0.2 M TEHDGA/*n*-DD. The aggregate distribution was recorded after contacting the organic phase with 1 M nitric acid solution containing different amount of Nd(III). It is observed that the aggregate size and their distribution increases with increase in the amount of Nd(III) in aqueous phase for both unirradiated and irradiated organic phases. However, the irradiated case 1 organic phase undergoes organic phase splitting when it was contacted with 1 M nitric acid solution containing above 12 g/L Nd(III). This corresponds to the average aggregate size of 30 nm (see Figure 5.18

a), above which the organic phase undergoes phase splitting. Comparing the aggregation behavior of irradiated (Figure 5.18 a) and unirradiated organic phases (Figure 5.18b), it can be seen that the average aggregate size of the unirradiated organic phase approaches the value of ~ 30 nm, when it was contacted with 1 M nitric acid solution containing 5 g/L Nd(III) as discussed in section 3.5.5 of chapter 3. It is evident from previous chapters, that the unirradiated organic phase undergoes phase splitting when it was contacted with 1 M nitric acid solution containing Nd(III) above 5 g/L. Therefore, in both irradiated and unirradiated organic phases, the phase splitting is observed when the average aggregate size reaches the value of > 30 nm. However, the 30 nm aggregate size was achieved in the irradiated and unirradiated systems at 12 g/L and 5 g/L Nd(III) in 1 M nitric acid, respectively. The organic phase splitting observed at different amount of Nd(III) in aqueous phase in these systems could be due to the requirement of that amount of Nd(III) in aqueous phase for achieving 30 nm aggregate size. The extraction data shown in Figure 5.14 indicates that the unirradiated organic phase and the irradiated organic phase undergoes phase splitting, when the concentration of Nd(III) in organic phase exceeds 3.6g/L. The loading of 3.6 g/L was achieved when the irradiated case 1 organic phase was contacted with 1 M nitric acid containing 12 g/L, whereas the same loading of Nd(III) was achieved when the unirradiated organic phase was contacted with 1 M nitric acid solution containing 5 g/L Nd(III). Higher concentration of Nd(III) (12 g/L) in 1 M nitric acid is required to load equal amount of Nd(III) (3.6 g/L) in the irradiated organic phase could be due to the decrease in the concentration of TEHDGA upon irradiation.

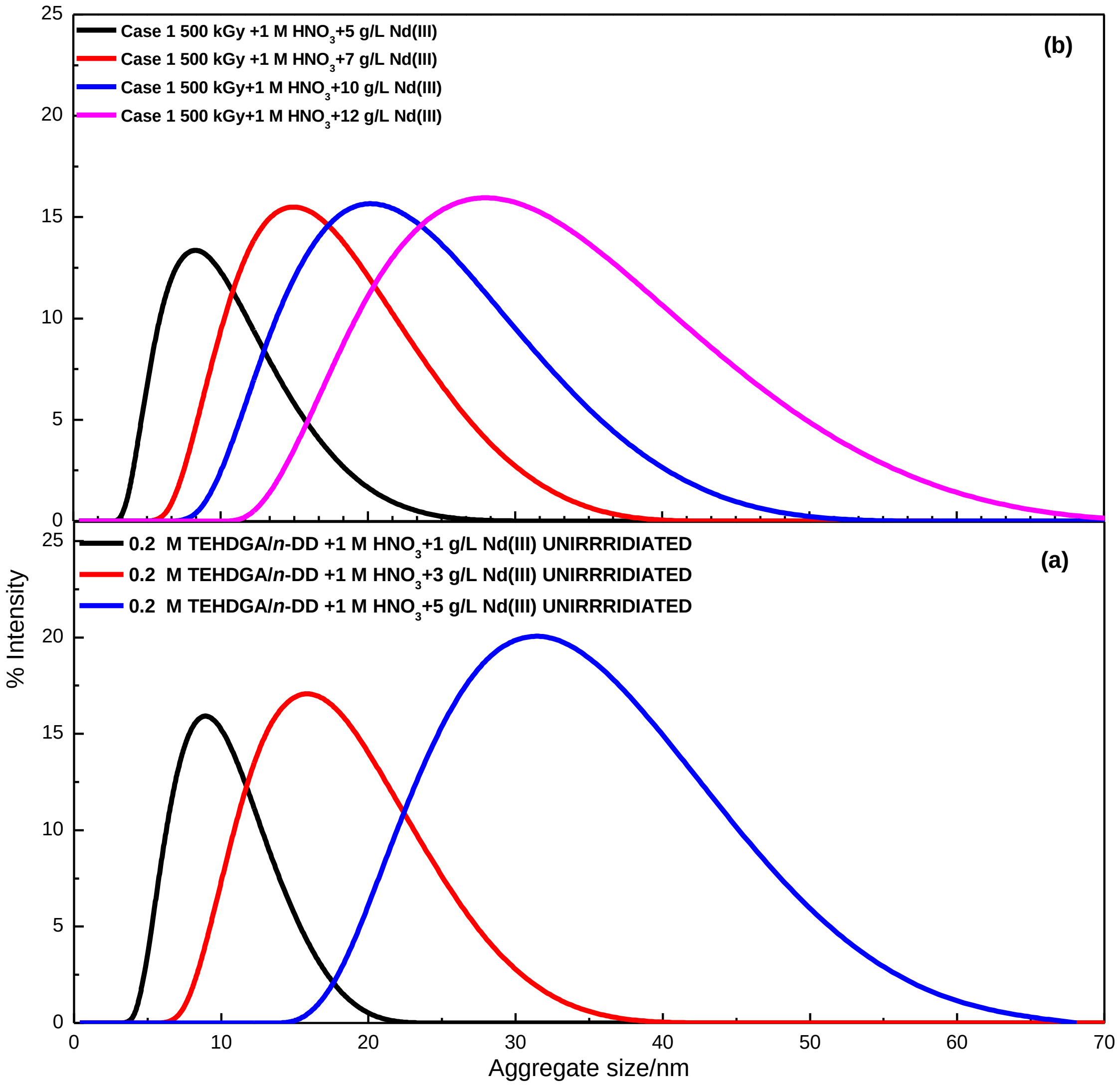

**Figure 5.18.** Aggregate size distribution behaviour of the organic phase containing 0.2 M TEHDGA/*n*-DD unirradiated (plot (a)) or case 1 organic phase (plot (b)) after contacting the organic phase with 1 M nitric acid containing different Nd(III) concentrations.

It is well recognized that the extraction of trivalents increases with increase in the concentration of nitric acid in aqueous phase. Figure 5.19 shows the aggregation behavior of the irradiated (500 kGy) 0.2 M TEHDGA/*n*-DD (case 1) phase recorded after contacting the organic phase with different concentration of nitric acid containing 1 g/L Nd(III). It can be seen that the average aggregate size and the aggregate distribution increases with increase in the concentration of nitric acid. This could be due to the increase in the extraction of Nd(III) and nitric acid in organic phase. This results in the increase in the concentration of reverse micellar aggregates containing TEHDGA….$Nd(NO_3)_3$ and TEHDGA….$HNO_3$ in the organic phase. It should be noted that the unirradiated 0.2 M TEHDGA/*n*-DD forms third phase when the Nd(III) in aqueous phase exceeds 5 g/L and 0.4 g/L Nd(III) in 1 M and 3 M nitric acid respectively as shown in section 3.2.5. However, the case 1 organic phase irradiated to 500 kGy was found to undergo third phase formation when the concentration of Nd(III) in 1 M and 3 M nitric acid exceeds 12 g/L and 2 g/L Nd(III) in aqueous phase respectively. This is due to the increase in the radiolytic degradation of TEHDGA upon irradiation, as discussed above.

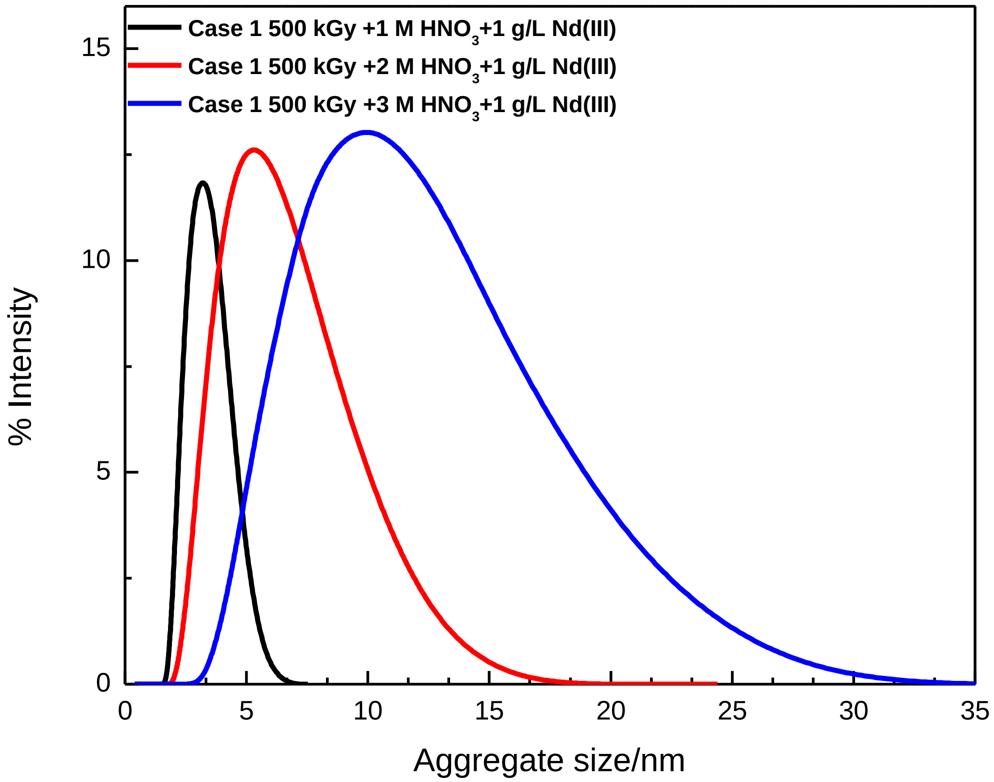

**Figure 5.19.** The aggregation behaviour of the organic phase (500 kGy) as a function of nitric acid concentration in aqueous phase. Organic phase: Case 1, Aqueous phase: $HNO_3$ varied + 5 g/L Nd(III).

The radiolytic degradation of TEHDGA, in case 2 organic phase is lower than that observed for the case 1 organic phase as shown in Figure 5.15. Therefore, it is quite likely that the aggregation behavior of case 2 organic phase could be higher as compared to case 1 organic phase. Figure 5.20 shows comparison in the aggregate distribution of the case 2 organic phase with case 1, and unirradiated 0.2 M TEHDGA/*n*-DD. The aggregate distribution was recorded after contacting the organic phases with 1 M nitric acid solution containing 5 g/L Nd(III). The organic phase was irradiated to 500 kGy. As expected, the average aggregate size and the aggregate distribution is more for case 2 organic phase as compared to case 1 [14, 21]. It is also noted from Figure 5.20 that the aggregate distribution of the organic phase obtained from case 4 under similar conditions is comparable with that obtained in case 2 organic phase. Similarly, *n*-dodecane only was irradiated in case 3 organic phase, the aggregate distribution of case 3 organic phase is comparable with unirradiated 0.2 M TEHDGA/*n*-DD.

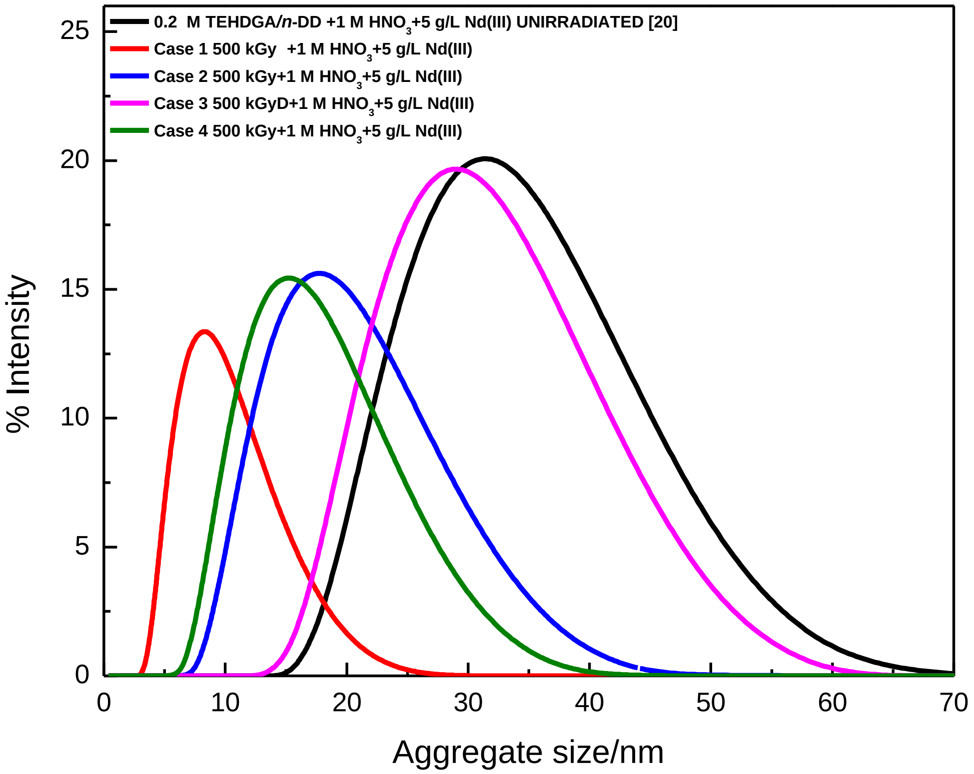

**Figure 5.20**. Comparison in the aggregation behaviour of organic phases irradiated to 500 kGy. Organic phase: unirradaited 0.2 M TEHDGA/*n*-DD or case 1 or case 2 or case 3 or case 4, Aqueous phase: 1 M $HNO_3$+ 5 g/L Nd(III).

## 5.4 Summary

The aggregation behavior of the organic phase containing radiolytically degraded TEHDGA and *n*-DD was studied by dynamic light scattering technique. The organics were irradiated from 10 kGy to 500 kGy absorbed dose in a $^{60}$Co gamma irradiator. The radiolytic degradation of TEHDGA and *n*-DD produced a number of degradation products and the aggregation behavior observed in the radiolytically degraded solution, 0.2 M TEHDGA/*n*-DD, was due to the combined effect of all degradation products present in the degraded solution. The production of polar degradation products minimized the aggregation, and the formation of higher homologs of paraffins enhanced the aggregation. The results revealed the following.

<u>Case 1.</u> The irradiated sample was a solution of 0.2 M TEHDGA dissolved in *n*-dodecane medium. The irradiation of 0.2 M TEHDGA/*n*-DD produced significant amount of radiolytic degradation products resulting from the degradation of TEHDGA due to sensitization effect. The dispersion of aggregates observed in the irradiated solution was attributed predominantly to the formation of smaller homologs of *n*-dodecane and the branched hydrocarbons, confirmed by GC-MS analysis. Even though the tendency of third phase formation could not be avoided in the unirradiated 0.2 M TEHDGA/*n*-DD, when contacted with nitric acid solution of concentration 4 M and above, interestingly no third phase formation was observed in the irradiated solution at the absorbed dose of 50 kGy and above, when contacted with 4 M nitric acid, showing the spin-off merit of gamma irradiation. The absence of third phase formation was due to the decrease in aggregate size upon irradiation, due to the formation of smaller homologs of *n*-dodecane.

<u>Case 2.</u> Since TEHDGA was irradiated alone in this case, the radiolytic degradation of TEHDGA due to sensitization effect was absent. Eventually, the overall degradation of TEHDGA was quite lower than those observed in case 1, and the behavior of aggregation in the organic phase

containing irradiated TEHDGA in unirradiated *n*-dodecane was similar to those observed in the solution containing unirradiated TEHDGA present in unirrdiated *n*-dodecane. However, the aggregation tendency was marginally lower in the irradiated solution. The aggregate size and their distribution in organic phase decreased with increase of absorbed dose.

<u>Case 3.</u> In this case, the *n*-dodecane was irradiated and mixed with TEHDGA for aggregation studies. In contrast to the above two cases, interestingly, the average size of aggregates formed in organic phase at a particular concentration of nitric acid increased with increase of absorbed dose. This behavior was attributed to the formation of the higher homologs of *n*-paraffins, which seems to control the aggregation behavior of the solution containing 0.2 M unirradiated TEHDGA in irradiated *n*-dodecane.

<u>Case 4.</u> This case involved irradiation of TEHDGA and *n*-dodecane independently to various absorbed dose levels and mixed together to obtain 0.2 M solution of irradiated TEHDGA in irradiated *n*-dodecane for DLS measurements. The studies showed that the average aggregate size and their distribution in organic phase in this case were intermediate between the other two organic solutions, discussed in cases 2 and 3. The intermediate behavior of aggregation was found to be applicable at all dose levels and at all nitric acid concentrations.

<u>Case 5.</u> The organic phase composed of 0.19 M extracted nitric acid in 0.2 M TEHDGA/*n*-DD was irradiated to different gamma absorbed dose levels. The aggregate size, aggregate distribution and the intensity of aggregates in the irradiated solution decreased significantly with increase of absorbed dose, in this case. The FTIR analysis of the irradiated organic phase confirmed the presence of strongly polar nitroalkanes, derivatives of alcohol etc., in the irradiated solution that dispersed the aggregates to a significant extent. In view of this, the third

phase formation was not observed in the irradiated organic phase at all absorbed dose levels when contacted with 4 M nitric acid.

In contrast to the assumption of deteriorating effect of gamma radiation on organic phases, the studies showed that the radiolytic degradation of diglycolamide/*n*-dodecane produced polar degradation products, and these polar products benefits the organic phase by preventing the third phase formation. Moreover, since the ligands containing amidic functional group do not produce any deleterious degradation products that hold actinides during recovery, which is in contrast to phosphoryl reagents, the concern associated with the radiolytic degradation of diglycolamides in *n*-dodecane medium is reasonably less.

In the case of the extraction of Nd(III) in organic phase at 1 M nitric acid was lowered leading to the requirement of higher amounts of Nd(III) needed in aqueous phase to achieve the loading of Nd(III) comparable to that of unirradiated organic phase. Therefore, the third phase formation in the irradiated 0.2 M TEHDGA/*n*-DD (500 kGy) was observed above 12 g/L of Nd(III) in aqueous phase as compared to 5 g/L in the unirradiated system, showing the unexpected merit of radiolytic degradation of organic phase. Aggregation results revealed that the phase splitting was observed when the average aggregate size reached the value of ~30 nm in both irradiated and unirradiated organic phases. However, the 30 nm aggregate size was achieved in the irradiated and unirradiated systems at 12 g/L and 5 g/L Nd(III) in 1 M nitric acid. Under these conditions only the critical amount of Nd(III) in organic phase (~3.52 g/L) was achieved, above which the organic phase underwent splitting.

When TEHDGA was irradiated alone the sensitization effect was absent. The loading of Nd(III) in the irradiated organic phase decreased in the order of case 3 > case 2 ~ case 4 > case 1, which was also the order of aggregate distribution in organic phase. When *n*-dodecane was irradiated alone and mixed with an unirradiated TEHDGA (i.e. case 3), the loading behaviour of Nd(III) was nearly comparable with the unirradiated organic phase. As a result, the aggregate distribution of case 3 organic phase was comparable with unirradiated 0.2 M TEHDGA/*n*-DD. However, the irradiation of TEHDGA alone (case 2) showed the Nd(III) loading behavior in between the behavior observed for case 1 and case 3 organic phases. The Nd(III) loading in case 4 was similar to case 2, and therefore, their aggregation distribution in organic phases were comparable. Since the radiolytic degradation of TEHDGA in case 2 was lower than that observed in case 1, the aggregate distribution of case 2 organic phase was more than that observed for case 1.

## References

[1] Y. Sasaki, Y. Sugo, S. Suzuki, S. Tachimori, The novel extractants, diglycolamides, for the extraction of lanthanides and actinides in $HNO_3$–*n*-dodecane system, Solvent Extr. Ion Exch. 19 (2001) 91-103.

[2] S.A. Ansari, P.N. Pathak, P.K. Mohapatra, V.K. Manchanda, Chemistry of diglycolamides: Promising extractants for actinide partitioning, Chem.Rev.112 (2012) 1751-1772.

[3] A. Leoncini, J. Huskens, W. Verboom, 2017. Ligands for f-element extraction used in the nuclear fuel cycle, Chem. Soc. Rev. 46 (2017) 7229-7273.

[4] S.A. Ansari, P.N. Pathak, P.K. Mohapatra, V.K. Manchanda, Aqueous partitioning of minor actinides by different processes, Sep. Purif. Rev. 40 (2011) 43-76.

[5] Emanuel Makrlík, Petr Vaňura, Pavel Selucký, Vasily Babain, Mikhail Alyapyshev, and Dmitriy Dar'in, N, N′-diethyl-N, N′-diphenyl-1, 10-phenanthroline-2, 9-dicarboxamide as an extraordinarily effective extraction agent for trivalent europium and americium, J. Mol. Liq. 237 (2017): 490-495.

[6] P.K. Wattal, Back-end of Indian nuclear fuel cycle-A road to sustainability, Prog. Nucl. Energy. 101 (2017) 133-145.

[7] J.N. Mathur, M.S. Murali, K.L. Nash, Actinide partitioning – a review, Solvent Extr. Ion Exch. 19 (2001) 357-390.

[8] M. Salvatores Nuclear fuel cycle strategies including partitioning and transmutation, Nucl. Eng. Des. 235 (2005) 805-816.

[9] B. J. Mincher, G. Modolo, S.P. Mezyk, The effects of radiation chemistry on solvent extraction 3: a review of actinide and lanthanide extraction, Solvent Extr. Ion Exch. 27 (2009) 579-606.

[10] B. J. Mincher, G. Modolo, S.P. Mezyk, The effects of radiation chemistry on solvent extraction 4: separation of the trivalent actinides and considerations for radiation-resistant solvent systems, Solvent Extr. Ion Exch. 28 (2010) 415-436.

[11] R.B. Gujar, S.A. Ansari, A. Bhattacharyya, A.S. Kanekar, P.N. Pathak, P.K. Mohapatra, V.K. Manchanda, Radiolytic stability of *N, N, N′, N′-t*etraoctyl diglycolamide (TODGA) in the presence of phase modifiers dissolved in *n*-dodecane, Solvent Extr. Ion Exch. 30 (2012) 278-290.

[12] P. Sinharoy, D.P. Nair, J. N. Sharma, K. Banerjee, Effect of degradation products of TEHDGA on actinide partitioning process, Sep. Purif. Technol. 16 (2016) 32-37.

[13] P. Deepika, K.N. Sabharwal, T.G. Srinivasan, P.R. Vasudeva Rao, Studies on the use of *N*, *N*, *N′, N′*-tetra (2-ethylhexyl) diglycolamide (TEHDGA) for actinide partitioning II: Investigation on radiolytic stability, Solvent Extr. Ion Exch. 29 (2011) 230-246.

[14] R. Gujar, S.A. Ansari, A. Bhattacharyya, P.K. Mohapatra, A. Kanekar, P.N. Pathak, V.K. Manchanda, Studies on the radiolytic stability of N, N, N′, N′-tetra-2-ethylhexyl diglycolamide in *n*-dodecane solution containing different phase modifiers, J. Radioanal. Nucl. Chem. 288(2011) 621-627.

[15] J. Ravi, B.R. Selvan, K.A. Venkatesan, M.P. Antony, T.G. Srinivasan, P.V. Rao, Evaluation of radiation stability of N, N-didodecyl N′, N′-di-octyl diglycolamide: a promising reagent for actinide partitioning, J. Radioanal. Nucl. Chem. 299 (2014) 879-885.

[16] Y. Sugo, Y. Sasaki, S. Tachimori, Studies on hydrolysis and radiolysis of N, N, N′, N′-tetraoctyl-3-oxapentane-1, 5-diamide, Radiochim. Acta. 90 (2002) 161-165.

[17] J. Ravi, B.R. Selvan, K.A. Venkatesan, M.P. Antony, T.G. Srinivasan, P.V. Rao, Radiolytic stability of *N*, *N*-didodecyl-*N',N'*-diethylhexyl diglycolamide, J. Radioanal. Nucl. Chem. 300 (2014) 981-986.

[18] J. Ravi, B.R. Selvan, K.A. Venkatesan, M.P. Antony, T.G. Srinivasan, P.V. Rao, Radiolytic stability of di-2-ethylhexyl-dioctyl diglycolamide, Radiochim. Acta. 102 (2014) 451-45.

[19] S.A. Ansari, D.R. Prabhu, R.B. Gujar, A.S. Kanekar, B. Rajeswari, M.J. Kulkarni, M.S. Murali, Y. Babu, V. Natarajan, S. Rajeswari, A. Suresh, Counter-current extraction of uranium and lanthanides from simulated high-level waste using *N,N,N′,N′*-tetraoctyl diglycolamide, Sep. Purif. Technol. 66 (2009) 118-124.

[20] P. Deepika, K.N. Sabharwal, T.G. Srinivasan, P.R. Vasudeva Rao, Studies on the use of *N*, *N*, *N*, *N*-tetra(2-ethylhexyl) diglycolamide (TEHDGA) for actinide partitioning. I: Investigation on third-phase formation and extraction behavior, Solvent Extr. Ion Exch. 28 (2010) 184-201.

[21] J.N. Sharma, R. Ruhela, K.K. Singh, M. Kumar, C. Janardhanan, P.V. Achutan, S. Manohar, P.K. Wattal, A.K. Suri, Studies on hydrolysis and radiolysis of tetra (2-ethylhexyl) diglycolamide (TEHDGA)/isodecyl alcohol/n-dodecane solvent system, Radiochim. Acta. 98 (2010) 485-491.

[22] S. Sarkar, A. Suresh, N. Sivaraman, V.K. Aswal, An insight into third-phase formation in the extraction of thorium nitrate by tris(2-methylbutyl) phosphate and tri-*n*-alkyl phosphates, Sep. Sci. Technol. 54 (2019) 970-984.

[23] L. Berthon, L. Martinet, F. Testard, C. Madic, T. Zemb, Solvent penetration and sterical stabilization of reverse aggregates based on the DIAMEX process extracting molecules: consequences for the third phase formation, Solvent Extr. Ion Exch. 25 (2007) 545-576.

[24] K.B. Rakesh, A. Suresh, N. Sivaraman, V.K. Aswal, P.V. Rao, P.V., 2016. Extraction and third phase formation behaviour of tri-iso-amyl phosphate and tri-*n*-butyl phosphate with Zr (IV) and Hf (IV): a comparative study, J. Radioanal. Nucl. Chem. 309 (2016) 1037-1048.

[25] Y. Sugo, Y. Izumi, Y. Yoshida, S. Nishijima, Y. Sasaki, T. Kimura, T. Sekine, H. Kudo, Influence of diluent on radiolysis of amides in organic solution, Radiat. Phys. Chem. 76(2007) 794-800.

[26] S.C. Tripathi, P. Bindu, A. Ramanujam, Studies on the identification of harmful radiolytic products of 30% TBP-*n*-dodecane-$HNO_3$ by gas liquid chromatography. I. Formation of diluent degradation products and their role in Pu retention behavior, Sep. Sci. Technol. 36 (2001) 1463-1478.

[27] T. Prathibha, K. A. Venkatesan, M. P. Antony, Comparison in the aggregation behaviour of amide extractant systems by dynamic light scattering and ATR-FTIR spectroscopy, Colloids Surf. A. 538 (2018) 651-660.

[28] B. Abécassis, F. Testard, T. Zemb, L. Berthon, C. Madic, Effect of n-octanol on the structure at the supramolecular scale of concentrated dimethyldioctylhexylethoxy malonamide extractant solutions, Langmuir. 19 (2003) 6638-6644.

# Chapter 6: Effect of pKa on the extraction of trivalent actinides in combined solvent system

The present chapter describes the effect of pKa of acidic extractants on the extraction behavior of trivalent actinides in an organic phase composed of TEHDGA+organophosphorus acid in *n*-DD and the spectroscopic investigations on the extracted organic phase to understand the insights of extraction in the binary solvent system. This chapter is divided into three parts. Part I discusses the extraction behavior of Am(III) from nitric acid medium in a solution of tetra TEHDGA and organophosphorous acidic extractant (HA) in *n*-DD to understand role of acidic extractant in the combined solvent formulation. Part II deals with the extraction behavior of Eu(III) in a binary solution of TEHDGA and HA present in *n*-DD. The interaction of Eu(III) with TEHDGA and HA at various acidities was studied by Attenuated Total Reflectance (ATR)-Fourier Transform Infrared (FTIR) spectroscopy. Part III deals with the effect organophosphorous acid on the reverse micellar aggregation behavior of the binary solution containing TEHDGA + HA/*n*-DD.

# Part I: Effect of $pK_a$ on the extraction behavior of Am(III) in organo phosphorus acid and diglycolamide solvent system

## 6.1. Introduction

The long-term radiotoxicity of HLLW generated from reprocessing of spent nuclear fuel is essentially due to the presence of small amount of trivalent actinides such as $^{241}$Am, $^{243}$Cm and $^{244}$Cm. The safe management of HLLW requires partitioning of trivalent actinides (Am and Cm) from HLLW and transmutation into stable or short lived products, as described elsewhere [1, 2]. The separation of trivalent actinides from HLLW is a two-cycle process [3-5]. The first–cycle involves the group separation of trivalent actinides and lanthanides together from HLLW and the second-cycle involves the mutual separation of lanthanides and actinides. A number of methods and ligands have been reported in literature for group separation, as well as for the mutual separation of lanthanides and actinides [3-8]. In contrast to the two-cycle process, single-cycle processing approaches are becoming popular in recent past for the separation of trivalent actinides directly from HLLW [9-21].

It is important to note that the single-cycle methods reported in literature use a combination of neutral and acidic extractants for the separation of actinides from nitric acid medium. Since the concentration of nitric acid in the feed (i.e. HLLW) is usually 3-4 M and the trivalent actinides co-exist with chemically similar lanthanides, the extraction of both these trivalents from the feed solution is predominantly governed by the neutral extractant [9,13,15]. However, the acidic extractant does not play much role during extraction, as the dissociation of proton in acidic extractant is very poor at 3-4 M nitric acid concentration. After extraction, the recovery of actinides alone from the loaded organic phase is carried out by aqueous soluble complexing agents present in dilute nitric acid (< 0.1 M). These reagents selectively co-ordinate with actinides at low nitric acid concentration and facilitate the stripping of actinides alone from organic phase, thus leaving the chemically similar lanthanides in organic phase. Under these low nitric acid conditions, the acidic extractant plays a predominant role in the mutual separation of lanthanides and actinides [9,13,15]. Therefore, it is necessary to understand the role of acidic extractant and its $pK_a$ value on the extraction behaviour of Am(III) and Eu(III) from nitric acid medium in the solvent phase containing neutral and acidic extractants in *n*-DD.

The organic phase was composed of *N,N,N’,N’*-tetra(2-ethylhexyl)diglycolamide (TEHDGA) and organophosphorous acidic extractants such as bis(2-ethylhexyl)phosphoric acid (HDEHP) or bis(2-ethylhexyl)phosphonic acid (PC88A) or bis(2,4,4-trimethylpentyl)phosphinic acid (CYANEX-272) whose pKa values increases in the order 3.24 (HDEHP) < 4.51 (PC88A) < 6.37 (CYANEX-272).

## 6.2 Results and Discussion

### 6.2.1 Kinetics of extraction

The extraction of Am(III) was studied at various intervals of time to obtain the time taken for the establishment of equilibrium. The solvent phase was composed of 0.1 M TEHDGA + 0.25 M HDEHP/*n*-DD or 0.1 M TEHDGA + 0.25 M PC88A/*n*-DD or 0.1 M TEHDGA + 0.5 M CYANEX-272/*n*-DD. It was equilibrated with 3 M nitric acid spiked with $^{241}$Am(III) tracer. Figure 6.1 shows the distribution ratio of Am(III) as a function of equilibration time. It is observed that distribution ratio of Am(III) increases with increase in duration equilibration and attained equilibrium within 2-3 minutes of equilibration for all the systems. After 2-3 minutes of equilibration, the D values reached the plateau and there is no significant change in D values. Therefore, all the experiments, the equilibration was carried out for about 60 minutes to ensure the attainment of equilibrium.

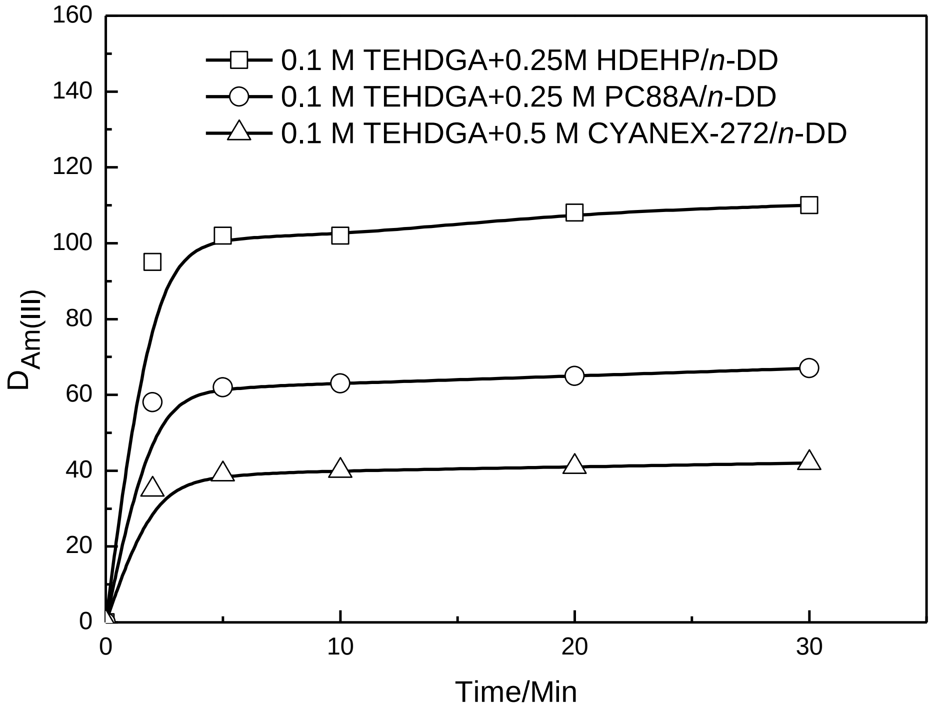

**Figure 6.1.** The variation in the distribution ratio of Am(III) as a function of equilibration time. Organic phase: 0.1 M TEHDGA/*n*-DD or 0.1 M TEHDGA + 0.5 M CYANEX-272/*n*-DD or 0.1 M TEHDGA + 0.25 M PC88A/*n*-DD or 0.1 M TEHDGA + 0.25 M HDEHP/*n*-DD. Aqueous phase: 3 M nitric acid spiked with $^{241}$Am tracer. Equilibration time = 5-30 minutes. Temperature = 298 K.

### 6.2.2 Extraction of Am(III) in TEHDGA +HA/*n*-DD

In combined solvent system, the extraction of both trivalent actinides and lanthanides from HLLW is predominantly controlled by the neutral extractant and the selective stripping of actinides alone from the organic phase is controlled by the nature or pKa value of the acidic extractant. The structure and pKa value of the acidic extractants employed in the present study are shown in Table 6.1 and the pKa increases in the order HDEHP < PC88A < CYANEX-272.

These acidic extractants were combined with a neutral extractant, TEHDGA, and studied for the extraction of Am(III) and Eu(III) from nitric acid medium. The results on the variation in the distribution ratio of Am(III) as function of nitric acid concentration in aqueous phase is shown in Figure 6.2(a). It is observed that the distribution ratio of Am(III) in 0.1 M TEHDGA/*n*-DD increases with increase in the concentration of nitric acid, as expected [18,22]. Addition of any acidic extractant to TEHDGA increases the distribution ratio of Am(III) in the entire acid range. However, the increase in distribution ratio of Am(III) is more at lower acid concentration as compared to those observed at higher nitric acid concentration. The distribution ratio of Am(III) in various combined extraction systems converges at nitric acid concentration beyond 2 M nitric acid. It is observed from Figure 6.2(a) that the distribution ratio of Am(III) observed in all combined extraction systems increase in the order (TEHDGA + CYANEX-272) < (TEHDGA + PC88A) < (TEHDGA + HDEHP). This order is in accordance with the acidity of (Table 6.1) the acidic extractants, CYANEX-272 < PC88A < HDEHP. Since strong acidic (low pKa) extractant dissociates more, it extracts Am(III) efficiently from a particular nitric acid medium. Moreover, it is observed that the distribution ratio of Am(III) in all combined extractant systems initially decrease with increase in the concentration of nitric acid reaches a minimum value at a particular nitric acid concentration followed in increase in distribution ratios. The minimum distribution ratio observed at a particular acidity increase in the order in the extraction systems (TEHDGA + CYANEX-272) < (TEHDGA + PC88A) < (TEHDGA + HDEHP). This indicates that strong acid extractant shifts the minimum distribution ratio to higher aqueous acidities. A similar behaviour was also observed for the extraction of Eu(III) in the combined extraction systems, as shown in Figure 6.2(b). However, the distribution ratio of Eu(III) is more as compared to the distribution ratio of Am(III) at all acidities in all these systems, as excepted for the oxygen donor ligands [3,4]. The concentration of CYANEX-272 employed in the present study was more than that employed in other acidic extractants. About 0.5 M concentration of CYANEX-272 was needed in the combined extractant system to obtain appreciably higher distribution ratios of Am(III) and Eu(III) as compared to 0.1 M TEHDGA /*n*-DD, due to the high pKa value of CYANEX-272.

**Table 6.1.** Structure of extractants and their pKa values.

| **Extractant** | **Structure** | **pK$_a$** |
|---|---|---|
| HDEHP | 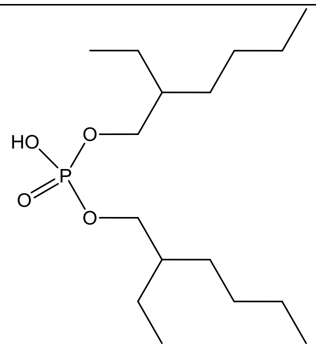 | 3.24 |
| PC88A | 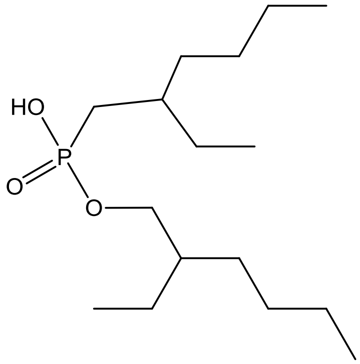 | 4.51 |
| CYANEX-272 | 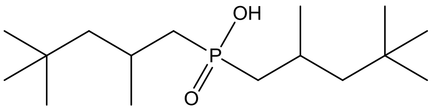 | 6.37 |
| TEHDGA | 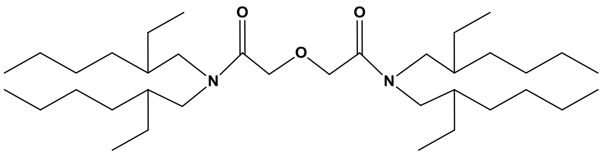 | - |

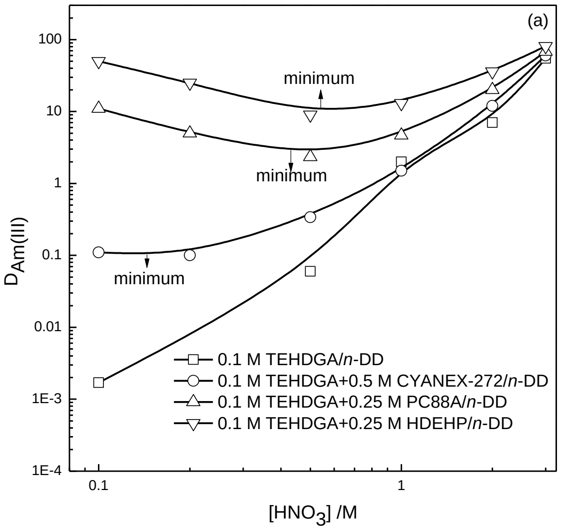

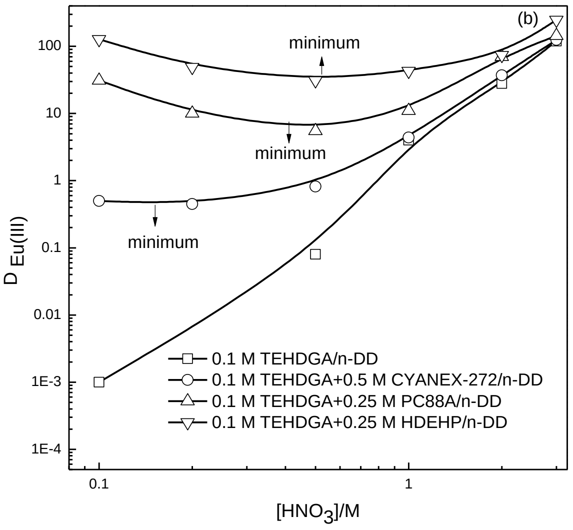

**Figure 6.2(a).** Distribution ratio of Am(III) as a function of nitric acid concentration. Organic phase: 0.1 M TEHDGA/*n*-DD or 0.1 M TEHDGA + 0.5 M CYANEX-272/*n*-DD or 0.1 M TEHDGA + 0.25 M PC88A/*n*-DD or 0.1 M TEHDGA + 0.25 M HDEHP/*n*-DD. Aqueous phase: Various concentrations of nitric acid spiked with $^{241}$Am(III) tracer.

**Figure 6.2(b).** Distribution ratio of Eu(III) as a function of nitric acid concentration. Organic phase: 0.1 M TEHDGA/*n*-DD or 0.1 M TEHDGA + 0.5 M CYANEX-272/*n*-DD or 0.1 M TEHDGA + 0.25 M PC88A/*n*-DD or 0.1 M TEHDGA + 0.25 M HDEHP/*n*-DD. Aqueous phase: Various concentrations of nitric acid spiked with $^{(152+154)}$Eu(III) tracer.

### 6.2.3 Role of acidic extractant

To understand the role and involvement of acidic extractant in the combined extraction system, the distribution ratio of Am(III) as a function of acidic extractant concentration at a fixed concentration of neutral extractant was measured. The variation in the distribution ratio of Am(III) as a function of acidic extractant concentration is shown in Figure 6.3(a). The concentration of nitric acid in aqueous phase in these systems was fixed at different values in order to get reliable and reproducible distribution ratios. It can be seen that the distribution ratio of Am(III) increases with increase in the concentration of acidic extractant in all cases. However, the dependence of acidic extractant on the distribution ratio of Am(III) is quite different. Linear regression of the extraction data results in a slope of 1.2 in case of HDEHP variation, and ~ 2.5 in the case of CYANEX- 272 and PC88A. This shows that the number of acidic extractant molecules involved in the extraction of Am(III) varies with respect to the nature of extracatnt, which in turn depends upon the pKa value of the acidic extractant. Since, the slope obtained using HDEHP variation is only 1.2, the involvement of HDEHP (1-2 molecules) in the extraction of Am(III) using TEHDGA + HDEHP/*n*-DD is low as compared to the involvement of CYANEX-272 and PC88A (about 2-3 molecules, since slope is 2.5). Moreover, since the participation of HDEHP is less it could be expected that the other extractant TEHDGA, could be involved in the extraction of Am(III), as the metal ion, Am(III), is usually coordinated by 3-4 molecules of the extractant present in the solvent phase. This indicates the possibility of synergism when HDEHP is mixed with TEHDGA and employed for the extraction of Am(III).

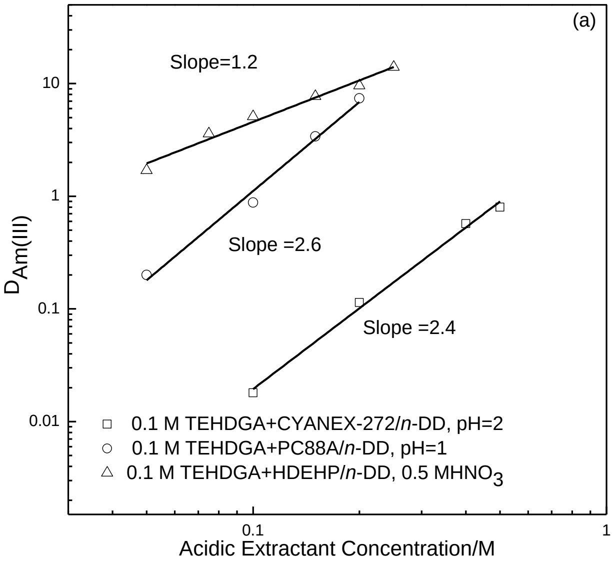

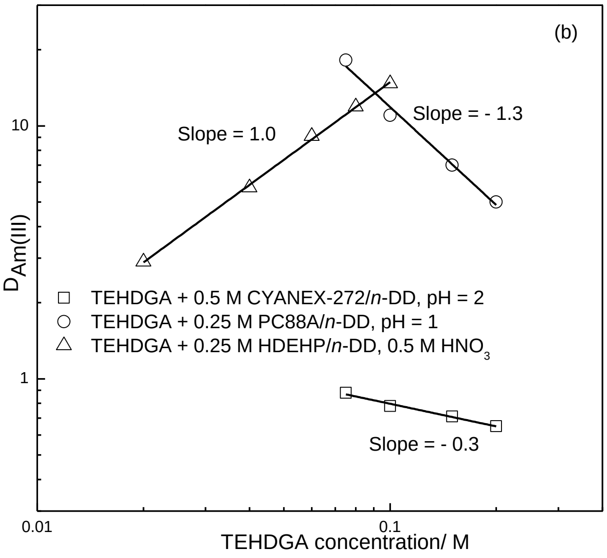

**Figure 6.3(a).** Variation in the distribution ratio of Am(III) as a function of acidic extractant concentration. Organic phase: 0.1 M TEHDGA + CYANEX-272/*n*-DD or 0.1 M TEHDGA + PC88A/*n*-DD or 0.1 M TEHDGA + HDEHP/*n*-DD. Aqueous phase: 0.01 M or 0.1 M or 0.5 M nitric acid spiked with $^{241}$Am(III) tracer.

**Figure 6.3(b).** Variation in the distribution ratio of Am(III) as a function of TEHDGA concentration. Organic phase: TEHDGA + 0.5 M CYANEX-272/*n*-DD or TEHDGA + 0.25 M PC88A/*n*-DD or TEHDGA + 0.25 M HDEHP/*n*-DD. Aqueous phase: 0.01 M or 0.1 M or 0.5 M nitric acid spiked with $^{241}$Am(III) tracer.

### 6.2.4 Synergism in TEHDGA + HDEHP

It is necessary to compare the slope values obtained in the combined extraction system at low acidities (Figure 6.3(a)) with those obtained in the absence of TEHDGA. The variation in the distribution ratio of Am(III) as a function of nitric acid concentration in the solution of acidic extractants present in *n*-DD alone has shown in Figure 6.4. It is observed that the distribution ratio of Am(III) decreases with increase in the concentration of nitric acid. Linear regression analysis of the extraction data results in a slope of ~3 in all cases indicating that three $H^+$ ions are released for the extraction of Am(III) from nitric acid medium. This shows that three molecules of acidic extractants (HA) are involved in the extraction of Am(III) from dilute nitric acid solution as shown in equation 6.1. The acidic extractants (HA) in *n*-dodecane solution exists as dimer [17,47].

$$\mathrm{Am}^{3+} + 3\,(\mathrm{HA})_2 \Leftrightarrow \mathrm{Am(AHA)}_3 + 3\,\mathrm{H}^+ \tag{6.1}$$

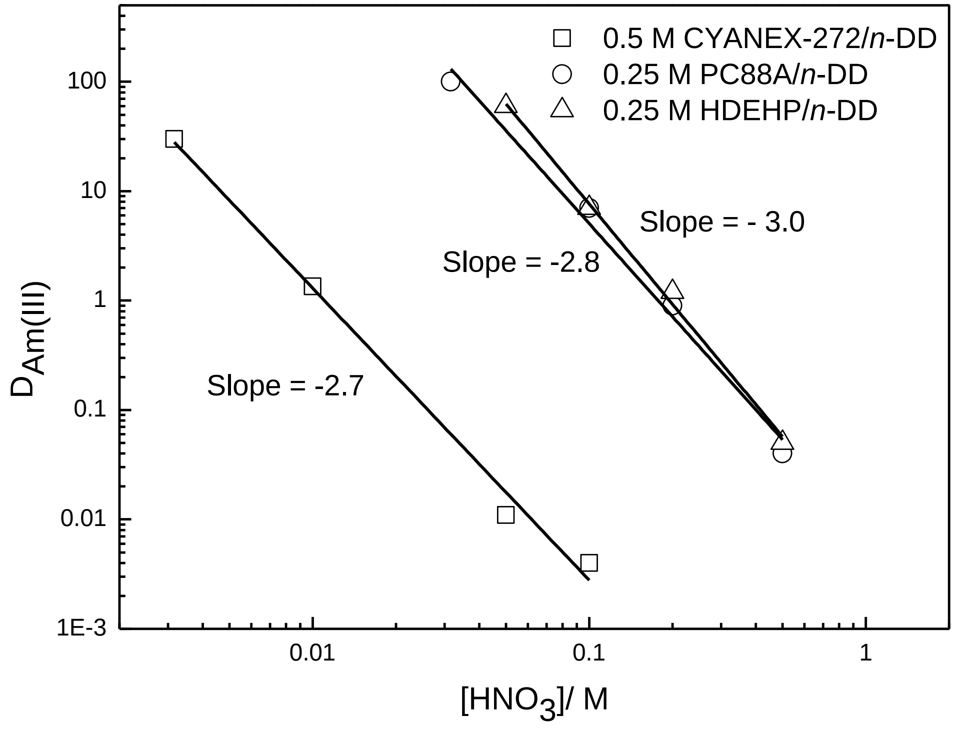

**Figure 6.4.** Distribution ratio of Am(III) as a function of nitric acid concentration. Organic phase: 0.5 M CYANEX-272/*n*-DD or 0.25 M PC88A/*n*-DD or 0.25 M HDEHP/*n*-DD. Aqueous phase: Various concentrations of nitric acid spiked with $^{241}$Am(III) tracer.

In the contrast to this, addition of TEHDGA to the acidic extractant reduced the participation of HDEHP in the extraction of Am(III) (slope of 1.2 from Figure 6.3(a)) and the participation of CYANEX-272 and PC88A are not affected (slope values are similar in Figures 6.3(a) and 6.4 for these extractants) to any significant extent by adding TEHDGA. This indicates that TEHDGA in a solution of CYANEX-272 or PC88A is not playing much role during the extraction of Am(III). However, the lowering of HDEHP participation allows the involvement of TEHDGA in the extraction of Am(III) as the metal ion Am(III) in the combined solvent system is usually coordinated by 3-4 ligands during solvent extraction [3,18, 22].

In order to confirm the degree of participation of TEHDGA in the extraction of Am(III) at low nitric acid concentration, the distribution ratio of Am(III) was measured as a function of TEHDGA concentration in the combined solvent system at a fixed nitric acid concentration. The results on the variation in the distribution of Am(III) as a function of TEHDGA concentration is shown in Figure 6.3(b). It is observed that the distribution ratio of Am(III) in a solution containing TEHDGA+ HDEHP in *n*-DD increased with increase in concentration of TEHDGA, whereas in other cases the distribution ratio of Am(III) decreased with increase in the concentration of TEHDGA. This shows that TEHDGA participates in the extraction of Am(III) when TEHDGA is mixed with HDEHP by synergic extraction. Linear regression of the extraction data results in a slope of +1 indicating that the involvement of about one molecule of TEHDGA in the extraction of Am(III) along with HDEHP (~1-2 molecules from Figure 6.3(a)).

### 6.2.5 Antagonism in TEHDGA-HA/*n*-DD

In contrast to HDEHP system, a negative slope was obtained (Figure 6.3(b)) in the extraction of Am(III) in TEHDGA+PC88A/*n*-DD and TEHDGA+CYANEX-272/*n*-DD systems reveal the antagonistic role of TEHDGA when it was added to CYANEX-272 or PC88A extractants. This observation is in good agreement with the slope value ~3 observed in Figure 6.3(a) for CYANEX-272 and PC88A systems. Literature indicates that Am(III) is generally coordinated to ~3 molecules of acidic extractants in solvent extraction systems [3,22]. Since, three molecules of CYANEX-272 or PC88A are already involved in the extraction of Am(III) at low acidity, the coordinated acidic extractants are not permitting the participation of TEHDGA in the combined solvent system. Perhaps, this could be the reason for the observed antagonism in TEHDGA+ PC88A and TEHDGA + CYANEX-272 systems. Considering all these observations, the study shows that the extraction of Am(III) at low nitric acid concentration in TEHDGA + HDEHP/*n*-DD is governed by synergism and that in TEHDGA + PC88A/*n*-DD or TEHDGA + CYANEX-272/*n*-DD systems are governed by antagonism is established. Moreover, the synergic and antagonistic extraction of Am(III) in the combined extraction is governed by the pKa value of the acidic extractant. Lower pKa value of the acidic extractant favors synergism, and higher favors antagonism.

### 6.2.6 Extraction of Am(III) at higher nitric acid

The extraction behaviour of Am(III) observed at higher nitric acid (> 1M $HNO_3$) concentration is quite different in the combined solvent system than lower nitric acid medium. To understand the involvement of neutral and acidic extractants in the extraction of Am(III) at high nitric acid (above 1M $HNO_3$) concentration, the variation in the distribution ratio of Am(III) as a function of acidic extractant concentration in a solution of 0.1 M TEHDGA + acidic extractant in *n*-DD at 2 M nitric acid was measured and the results are displayed in Figure 6.5(a). It is observed that the distribution ratio of Am(III) in the solvent phase increases with increase in the concentration of acidic extractant in all cases. This showed that all acidic extractants participate in the extraction of Am(III) even at 2 M nitric acid, even though the pKa value for these acidic extractants are in the range 3 to 7 (Table 6.1). This could be possible only when the acidic extractant is involved in the synergic extraction of Am(III) at 2 M nitric acid when they are mixed with TEHDGA in *n*-DD. Figure 6.5(b) shows the variation in the distribution ratio of Am(III) as a function of TEHDGA concentration in the combined solvent extraction system at 2 M nitric acid. It can be seen that the distribution ratio of Am(III) increases with increase in the concentration of TEHDGA in the solvent phase. Linear regression of the extraction data results a slope of 1.2 - 1.7 for all extraction systems. This indicates that about 1-2 molecules of TEHDGA are involved in the extraction of Am(III) at 2 M nitric acid. But, in the absence of acidic extractants, it is observed that 3 - 4 molecules of TEHDGA [3] were involved in the extraction of Am(III) at 1 M to 3 M nitric acid. Reduction in the participation of TEHDGA molecules in the combined extraction system is due to the participation of acidic extractant in the extraction of Am(III) and facilitate synergism, as discussed above.

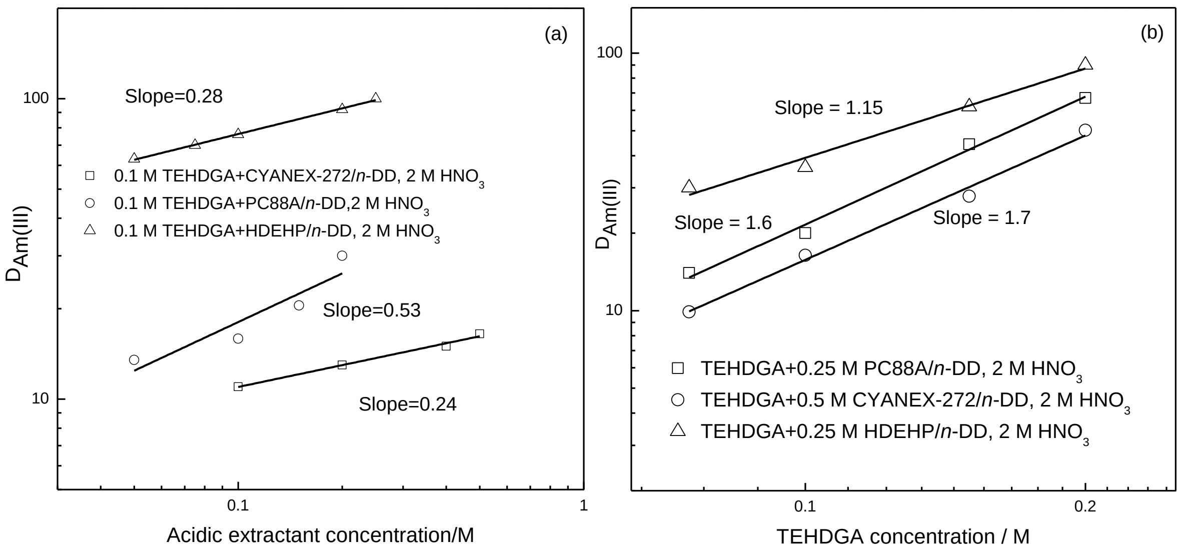

**Figure 6.5(a).** Variation in the distribution ratio of Am(III) as a function of acidic extractant concentration at 2 M nitric acid. Organic phase: 0.1 M TEHDGA + CYANEX-272/*n*-DD or 0.1 M TEHDGA + PC88A/*n*-DD or 0.1 M TEHDGA + HDEHP/*n*-DD. Aqueous phase: 2 M Nitric

acid spiked with $^{241}$Am(III) tracer.

**Figure 6.5(b).** Variation in the distribution ratio of Am(III) as a function of TEHDGA concentration. Organic phase: TEHDGA + 0.5 M CYANEX-272/*n*-DD or TEHDGA + 0.25 M PC88A/*n*-DD or TEHDGA + 0.25 M HDEHP/*n*-DD. Aqueous phase: 2 M Nitric acid spiked with $^{241}$Am(III) tracer.

Figure 6.6 displays the comparison in the extraction behaviour of Am(III) in various systems containing 0.25 M HDEHP/*n*-DD, 0.1 M TEHDGA/*n*-DD and 0.1 M TEHDGA + 0.25 M HDEHP/*n*-DD. It can be seen that the extraction in the combined solvent system is much higher than those observed either in 0.25 M HDEHP/*n*-DD or 0.1 M TEHDGA/*n*-DD at all nitric acid concentrations. These results are in line with the synergic extraction of Am(III) when TEHDGA is mixed in HDEHP in *n*-DD. Based on the above observations, the extraction of Am(III) in the TEHDGA + HDEHP solvent system can be represented by equation 6.2 applicable for all acid concentrations.

$$\mathrm{M}^{3+} + (3-x)\mathrm{TEHDGA} + x\ \mathrm{HDEHP} + (3-x)\ \mathrm{NO}_3^- \Leftrightarrow \mathrm{M\,(DEHP)}_{\mathrm{x}}(\mathrm{NO}_3^-)_{3-x}(\mathrm{TEHDGA}\,)_{3\text{-}\mathrm{x}} + \mathrm{x\ H}^+ \quad (6.2)$$

0 <x < 3 at all nitric acid concentrations, where DEHP is the acid dissociated form of HDEHP

In contrast to HDEHP system, Am(III) extraction in the combined solvent system containing other acidic extractants is lower than those observed either in CYANEX-272/*n*-DD or PC88A/*n*-DD (Figure 6.6). Especially at acidities lower than 0.01 M, the distribution ratio of Am(III) is more in CYANEX-272/*n*-DD as compared to the solution containing TEHDGA+CYANEX-272 in *n*-DD, as shown in Figure 6.6. Similarly, the distribution ratio of Am(III) is more in PC88A/n-DD as compared to those observed in TEHDGA+PC88A/*n*-DD at acidities lower than 0.05 M nitric acid as shown in Figure 6.6. These results clearly indicate the antagonistic role of TEHDGA, when TEHDGA is added to CYANEX-272 or PC88A extractants. However at higher acidities synergism is observed at all nitric acid concentrations investigated in the present study beyond 0.1 M nitric acid.

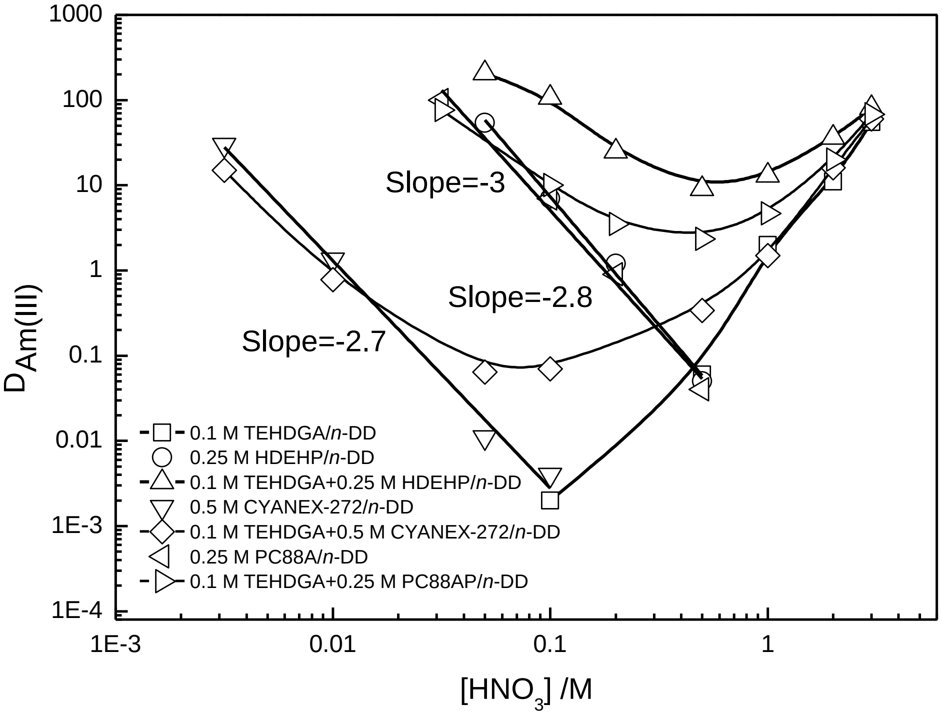

**Figure 6.6.** Variation in the distribution ratio of Am(III) as a function of nitric acid concentration. Organic phase: 0.1 M TEHDGA/*n*-DD or 0.25 M HDEHP/*n*-DD or 0.1 M TEHDGA + 0.25 M HDEHP/*n*-DD or 0.5 M CYANEX-272/*n*-DD or 0.1 M TEHDGA + 0.5 M CYANEX-272/*n*-DD or 0.25 M PC88A/*n*-DD or 0.1 M TEHDGA + 0.25 M PC88A/*n*-DD. Aqueous phase: Nitric acid spiked with $^{241}$Am(III) tracer.

Based on these observations the following plausible mechanism can be proposed for extraction of Am(III) at low nitric concentration and at high nitric acid concentration by equations 6.3 and 6.4 respectively.

$$\mathrm{Am}^{3+} + 3\,(\mathrm{HA})_2 \Leftrightarrow \mathrm{Am(AHA)}_3 + 3\,\mathrm{H}^+ \qquad \text{(At low nitric acid)} \qquad (6.3)$$

$$\mathrm{M}^{3+} + (3-x)\mathrm{TEHDGA} + x\,\mathrm{HA} + (3-x)\,\mathrm{NO_3^-} \Leftrightarrow \mathrm{M\,A_x(NO_3^-)_{3-x}(TEHDGA)_{3-x}} + \mathrm{x\,H^+} \qquad (6.4)$$
$$\mathrm{x} = 0-1 \text{at high nitric acid}$$

### 6.2.7 Extraction of trivalent metal ions from FR-SHLLW

The distribution ratio of various metal ions present in FR-SHLLW was determined using TEHDGA+HA/*n*-DD and the results are tabulated in Table 6.2.

**Table 6.2.** Distribution ratios of metal ions in organic phase determined in the presence and absence of 0.05 M CyDTA in FR-SHLLW. Organic phase: 0.1 M TEHDGA+ 0.25 M HDEHP/*n*-DD or 0.1 M TEHDGA+ 0.25 M PC88A/*n*-DD or 0.1 M TEHDGA+ 0.5 M CYANEX-272/*n*-DD, Aqueous phase: FR- SHLLW in the presence or absence of complexing agent. Organic/Aqueous phase ratio = 1, Temperature = 298 K. Concentration of $HNO_3$ in FR-SHLLW is 3 M.

| **Metals** | **Concentration [g.L$^{-1}$]** | **$D_M$ in 0.1 M TEHDGA+ 0.25 HDEHP/*n*-DD** | | **$D_M$ in 0.1 M TEHDGA+0.25 PC88A/*n*-DD** | | **$D_M$ in0.1 M TEHDGA+0.5 CYANEX-272/*n*-DD** | |
|---|---|---|---|---|---|---|---|
| | | **No CyDTA** | **0.05 M CyDTA** | **No CyDTA** | **0.05 M CyDTA** | **No CyDTA** | **0.05 M CyDTA** |
| Cr | 0.10 | 2.1 | 0.02 | 1.7 | <0.01 | 1.5 | <0.01 |
| Cd | 0.04 | 0.01 | <0.01 | <0.01 | <0.01 | <0.01 | <0.01 |
| Mo | 1.09 | >50 | >50 | >50 | >50 | >50 | >50 |
| Gd | 0.06 | >50 | >50 | >50 | >50 | >50 | >50 |
| La | 0.34 | 1.68 | 2.1 | 0.78 | 1.03 | 0.96 | 1 |
| Ni | 0.12 | <0.01 | <0.01 | <0.01 | <0.01 | <0.01 | <0.01 |
| Sr | 0.14 | 0.02 | 0.015 | 0.006 | 0.006 | <0.01 | <0.01 |
| Dy | 0.01 | >50 | >50 | >50 | >50 | >50 | >50 |
| Fe | 0.51 | 0.08 | <0.01 | 0.06 | < 0.01 | 0.2 | <0.01 |
| Eu | 0.03 | 64 | 63 | 27 | 26 | 28 | 26 |

| | | | | | | | |
|---|---|---|---|---|---|---|---|
| Sm | 0.31 | 55 | 51 | 22 | 21 | 34 | 33.6 |
| Y | 0.07 | >50 | >50 | >50 | >50 | >50 | >50 |
| Nd | 1.12 | 15 | 14 | 6.3 | 6.1 | 8.8 | 8.7 |
| Pr | 0.34 | 14.6 | 14.2 | 6.8 | 3.7 | 10.2 | 6.3 |
| Ce | 0.68 | 4.3 | 5.88 | 2.2 | 2.5 | 2.8 | 2.9 |
| Ba | 0.41 | 0.02 | 0.02 | <0.01 | <0.01 | <0.01 | <0.01 |
| Ru | 0.81 | 0.07 | 0.06 | 0.04 | 0.03 | 0.02 | 0.01 |
| Pd | 0.60 | 1.08 | 0.29 | 1.8 | 0.49 | 0.88 | 0.21 |
| Zr | 0.82 | >50 | 0.1 | >50 | <0.01 | >50 | 0.2 |
| Rh | 0.26 | <0.01 | <0.01 | <0.01 | <0.01 | <0.01 | <0.01 |
| $^{137}$Cs | Tracer | 0.01 | 0.01 | 0.01 | 0.01 | <0.01 | <0.01 |
| $^{241}$Am | Tracer | 28 | 28 | 7.2 | 7.2 | 9.8 | 9.8 |
| $^{152+154}$Eu | Tracer | 64 | 63 | 27 | 26 | 28 | 26 |

It can be seen from Table 6.2 that the distribution ratios of Am(III), Ln(III), and fission products such as Zr(IV), Mo(VI) and Y(III) (D >50) are higher than the distribution ratios observed for other metal ions in all TEHDGA+ HA systems. High extraction of Zr(IV) and Pd(II) in organic phase observed in TEHDGA+HA is likely to create problems during lanthanide -actinide separation as discussed elsewhere [16,17]. Therefore, it is necessary to eliminate or minimize the extraction of unwanted elements in TEHDGA+HA phase. In this context, an aqueous complexing agent 0.05 M trans-1,2-Cyclohexanediaminetetraacetic Acid (CyDTA) was added to the aqueous phase to retain the extraction of unwanted metal ions. Literature indicates that CyDTA is a promising reagent for the retention of Zr(IV) and Pd(II) in aqueous phase that are likely to create problems during Ln-An separation [15]. It can be seen in Table 6.2 that the addition of CyDTA to aqueous phase lowered the extraction of Zr(IV) and Pd(II) in organic phase. However, it is noted that there is no significant change in the distribution values of Am(III) and Ln(III). This indicates that addition of 0.05 M CyDTA prevents the extraction of

Zr(IV) and Pd(II). Therefore, it is recommend adding 0.05 M CyDTA in FR-SHLLW to prevent the extraction of unwanted metal ions. From Table 6.2, it is also noted that the distribution values of Am(III) and Ln(III) are higher in 0.1 M TEHDGA + 0.25 M HDEHP/*n*-DD as compared to 0.1 M TEHDGA +0.25 M PC88A/*n*-DD and 0.1 M TEHDGA + 0.5 M CYANEX-272/*n*-DD system, as expected.

### 6.2.8 Selective stripping of Am(III)

The selective back extraction of Am(III) from loaded organic phase, 0.1 M TEHDGA+ 0.25 M HDEHP/*n*-DD or 0.1 M TEHDGA+ 0.25 M PC88A/*n*-DD or 0.1 M TEHDGA+ 0.5 M CYANEX-272/*n*-DD, was studied using an aqueous phase consisted of 0.05 M DTPA + 0.5 M citric acid at pH 3. The aqueous phase stripping formulation was fixed in the present study based on the studies reported elsewhere [17]. The elements Am(III) and Eu(III) were taken as a representative for An(III) and Ln(III) respectively. Table 6.3 shows the stripping behaviour of Am(III) and Eu(III) from the organic phase (extracted from 3 M $HNO_3$). In case of 0.1 M TEHDGA + 0.25 M HDEHP/*n*-DD system, about 80% of Am(III) was back extracted in 6 contacts, whereas about 12% of Eu(III) was back extracted in 6 contacts. The separation factor of ~10 was achieved [18]. Therefore, the aqueous stripping formulation composed of 0.05 M DTPA + 0.5 M CA at pH 3 could be proposed for the back extraction of Am(III) alone from the organic phase in a single cycle process. It should be noted that the separation factor reported here is based on the batch extraction and stripping mode. However, the separation factor is likely to increase or can be optimized to obtain higher separation factor in continuous counter current extraction mode, which is usually employed for large scale separation.

**Table 6.3.** Stripping behaviour of Am(III) and Eu(III) from the loaded organic phase. Extraction of Am(III) and Eu(III) in 0.1 M TEHDGA + 0.25 M HDEHP/*n*-DD or 0.1 M TEHDGA+ 0.25 M

PC88A/*n*-DD or 0.1 M TEHDGA+ 0.5 M CYANEX-272/*n*-DD from 3 M nitric acid. Stripping formulation was composed of 0.05 M DTPA + citric acid at pH 3.

| Number of contacts (Cumulative stripping %) | 0.1 M TEHDGA+0.25 M HDEHP/*n*-DD | | 0.1 M TEHDGA+0.25 M PC88A/*n*-DD | | 0.1 M TEHDGA+0.5 M CYANEX-272/*n*-DD | |
|---|---|---|---|---|---|---|
| | Am(III) | Eu(III) | Am(III) | Eu(III) | Am(III) | Eu(III) |
| 1 | 13% | 1.5% | 70% | 43% | 79% | 83% |
| 2 | 31% | 5.1% | 81% | 72% | 86% | 92% |
| 3 | 43% | 7.2% | 83% | 84% | 88% | 94% |
| 4 | 55% | 9.5% | 83.2% | 88.5% | 90% | 95% |
| 5 | 62% | 10.6% | 83.5% | 90% | 91% | 96% |
| 6 | 80% | 12.6% | 88% | 93% | 93% | 98% |

On the other hand, in case of 0.1 M TEHDGA + 0.25 M PC88A/*n*-DD and 0.1 M TEHDGA + 0.5 M CYANEX-272/*n*-DD systems it can be seen from Table 6.3 that both Am(III) and Eu(III) are back extracted to aqueous phase to the equal extent. This indicates that the separation Am(III) over Eu(III) achieved in these cases are not adequate for the separation of Am(III) from SHLLW, by a single cycle process. In view this, the single cycle separation studies of Am(III) from FR-SHLLW was restricted only to 0.1 M TEHDGA + 0.25 M HDEHP/*n*-DD system.

Table 6.4 shows the percentage stripping of Am(III) and Eu(III) from the loaded organic phase using 0.05 M DTPA + 0.5 M CA at pH 3. The loaded organic phase was obtained by equilibrating 0.1 M TEHDGA + 0.25 M HDEHP/*n*-DD solution with FR-SHLLW containing 0.05 M CyDTA spiked with $^{241}$Am and $^{(152+154)}$Eu tracer. It can be seen from Table 6.4 that 90% of Am(III) was back extracted within 6 contacts. However, the stripping of Am(III) is also accompanied by the co-stripping of Eu(III) to some extent. Nevertheless, in a counter current mixture-settler, it should be noted that the stripped solution goes for contacting with the fresh organic phase and it is quite likely that the stripped Eu(III) could be extracted in subsequent contacts. Therefore, it is quite possible that the separation factor of Am(III) over Eu(III) expected to be achieved in a counter current or mixture- settler run could be more.

**Table 6.4.** Stripping behaviour of Am(III) and Eu(III) from the loaded organic phase. Extraction of Am(III) and Eu(III) in 0.1 M TEHDGA + 0.25 M HDEHP/*n*-DD from FR-SHLLW. Stripping formulation was composed of 0.05 M DTPA + citric acid at pH 3.

| Number of contacts (Cumulative stripping %) | 0.1 M TEHDGA+0.25 M HDEHP/*n*-DD in SHLLW | |
|---|---|---|
| | Am(III) | Eu(III) |
| 1 | 69% | 10% |
| 2 | 80% | 13.3% |
| 3 | 84% | 14.8% |
| 4 | 86% | 16.3% |
| 5 | 87% | 18.6% |
| 6 | 90% | 21.6% |

## 6.3 Summary

The dependence of the neutral extractant, TEHDGA, and $pK_a$ of the acidic extractants, HDEHP, PC88A and CYANEX-272 on the distribution ratio of Am(III) in the combined solvent system was measured to understand the role of acidic extractant in the extraction of Am(III) from nitric acid medium. The extraction Am(III) in the combined solvent system initially decreased with increase in the concentration of nitric acid reached a minimum value of distribution ratio at a particular aqueous phase acidity followed by increase in distribution value. The $pK_a$ value of the acidic extractant played a profound role in enhancing the distribution ratio of Am(III) especially at lower nitric acid. The distribution ratio of Am(III) increased with decrease with the $pK_a$ value of the acidic extractant in the combined solvent system at a particular acidity. Slope analysis of the extraction data revealed the synergic extraction of Am(III) when TEHDGA was mixed with HDEHP and antagonistic effect when TEHDGA was mixed with PC88A and CYANEX-272 at lower acidities. In contrast to this, synergistic extraction of Am(III) was observed at higher acidity irrespective of the $pK_a$ value of the acidic extractant. Among the various solvent formulations investigated 0.1 M TEHDGA+0.25 M HDEHP/*n*-DD provided appreciable separation of Am(III) over Eu(III) from FR-SHLLW by using DTPA and CA.

# Part II. FTIR spectroscopic investigations on the extraction of Eu(III) in diglycolamide-organophosphorous acid binary solvent system

## 6.4 Introduction

The Fourier Transform Infrared (FTIR) spectroscopy has been utilized as an analytical tool for studying the nature of extracted metal ion complexes formed in organic phase [23-29]. The spectrum can provide information on the coordination behavior of ligand with metal ion and the strength of interaction between ligand and metal etc. For this purpose, the FTIR spectrum of the organic phase obtained after the extraction of Eu(III) in the binary solution containing neutral and acidic extractant in *n*-dodecane was recorded and the results are discussed in this part of the chapter.

## 6.5 Results and discussion

### 6.5.1 Characterization of binary solution by ATR-FTIR spectroscopy

Figure 6.7 shows the ATR-FTIR spectrum of the binary solution composed of TEHDGA and HDEHP or PC88A or CYANEX-272 in *n*-dodecane. The characterization of various transmittance bands in the ATR-FTIR spectrum are shown in Figure 6.7. The neat TEHDGA spectrum shows a strong transmittance bands occurring at 1663 $cm^{-1}$ is due to the amidic C=O stretching frequencies [30, 31]. A weak transmittance bands occurring at 1117 $cm^{-1}$ is due to the etheric C-O stretching of TEHDGA [31]. A solution of 0.1 M TEHDGA in *n*-dodecane also shows the characteristic transmittance bands of amidic C=O (1663 $cm^{-1}$) and etheric C-O groups (1117 $cm^{-1}$). However, the intensities of these bands were significantly reduced, as expected, upon dilution. The neat HDEHP shows the transmittance band of phosphoryl P=O stretching at 1230 $cm^{-1}$ and P-O-C stretching band at 1032 $cm^{-1}$ [27,28]. The literature on the FTIR spectrum of HDEHP reports that weak transmittance bands of P-O-H asymmetric stretching occurs at 2650 cm$^{-1}$, and 2327 cm$^{-1}$. In addition, the O-H bending bands of P(=O)O-H group occurs at 1687 cm$^{-1}$, which is also weak [27,28]. The ATR-FTIR spectrum of neat HDEHP is shown in Figure 6.7, exhibits all these features. It should be noted that the intensities of these weak transmittance bands are further decreased to negligible value upon dilution with *n*-dodecane (0.25 M HDEHP/*n*-DD). The ATR-FTIR spectrum of 0.1 M TEHDGA + 0.25 M HDEHP/*n*-DD is compared with ATR-FTIR spectra of individual solutions shown in Figure 6.7. The spectrum shows a strong transmittance bands occurring at 1663 cm$^{-1}$ due to the amidic C=O stretching and a weak transmittance bands at 1117 cm$^{-1}$ due to the etheric C-O stretching of TEHDGA [28-30]. In addition, the phosphoryl P=O stretching bands of HDEHP occurs at 1230 cm$^{-1}$. Other weak O-H stretching bands of P-O-H and P(=O)O-H groups are not apparent in the ATR-FTIR spectrum of binary solution, suggesting that it is difficult to draw any conclusion regarding the interaction between TEHDGA and HDEHP, based on the spectrum.

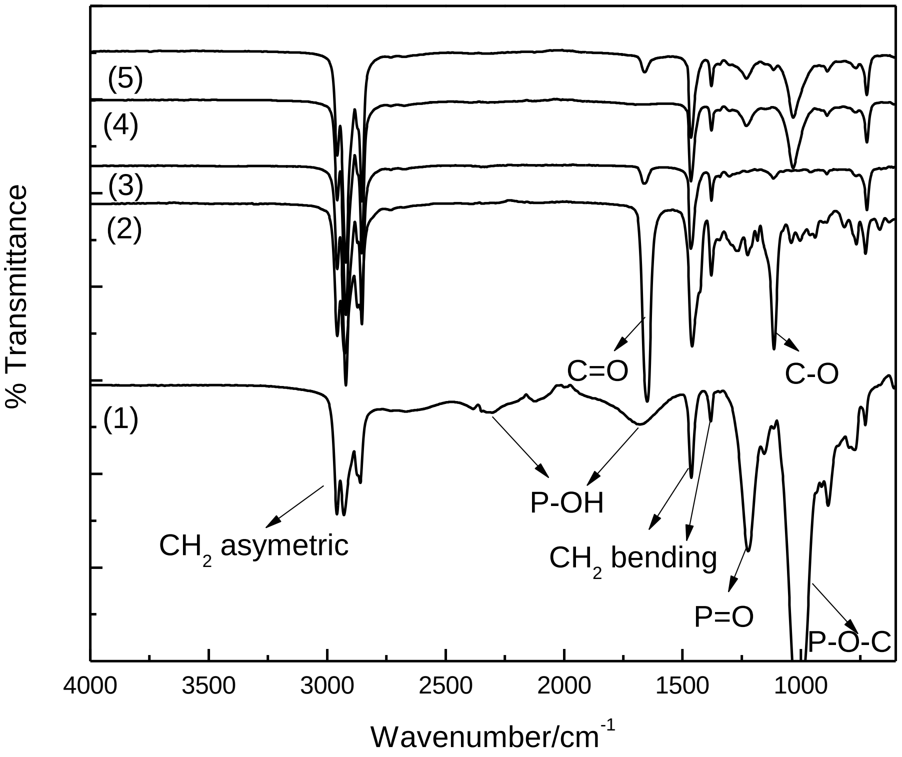

**Figure 6.7**. ATR-FTIR spectra of individual and combined extractants in *n*-dodecane. (1) HDEHP neat, (2) TEHDGA neat, (3) 0.1 M TEHDGA/*n*-DD, (4) 0.25 M HDEHP/*n*-DD, (5) 0.1 M TEHDGA+0.25 M HDEHP/*n*-DD.

Figure 6.8 shows the ATR-FTIR spectra of the binary solution composed of TEHDGA and PC88A or CYANEX-272 in *n*-dodecane. The ATR-FTIR spectrum was compared with the spectrum of TEHDGA+HDEHP solution shown in Figure 6.7. The spectrum shows a strong transmittance bands occurring at 1663 cm$^{-1}$ is due to the amidic C=O stretching frequencies of TEHDGA in all cases [30,31]. A weak transmittance bands occurring at 1117 cm$^{-1}$ is due to the etheric C-O stretching of TEHDGA [30,31]. In addition, the phosphoryl P=O stretching bands PC88A occurs at 1198 cm$^{-1}$ and CYANEX-272 occurs at 1172 cm$^{-1}$ [28]. It should be noted that these bands are likely to be affected by the extraction of nitric acid and Eu(III). Therefore, this particular wave number region of the ATR-FTIR spectrum is henceforth shown in the present work for the clarity, rather than the entire spectrum.

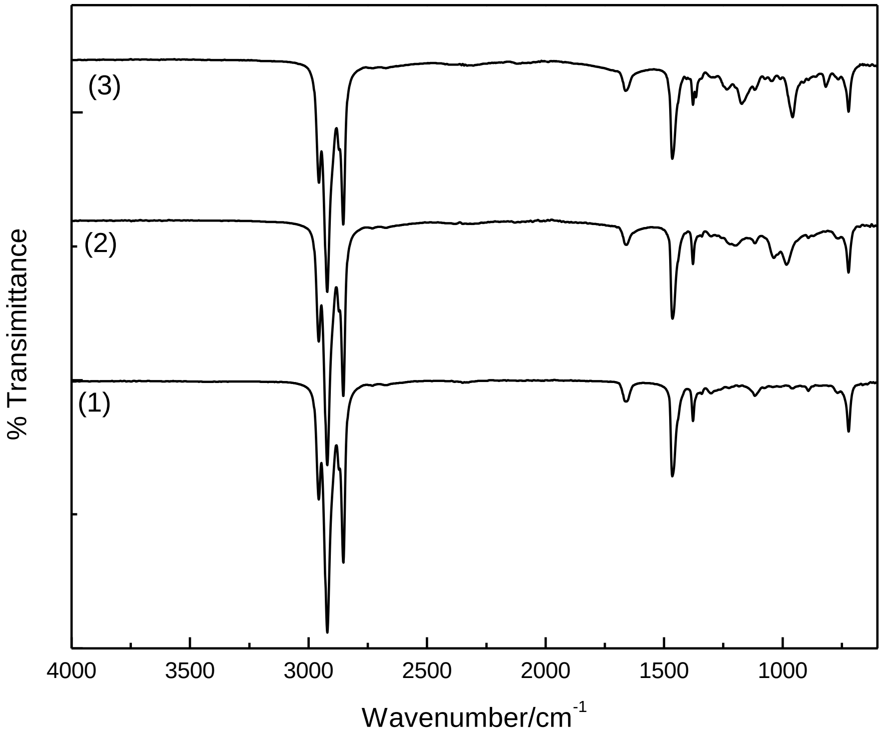

**Figure 6.8.** ATR-FTIR spectra of TEHDGA/*n*-DD or TEHDGA+HA/*n*-DD (1).0.1 M TEHDGA/*n*-DD, (2) 0.1 M TEHDGA+0.25 M PC88A/*n*-DD, (3) 0.1 M TEHDGA+0.5 M CYANEX-272/*n*-DD.

The Figure 6.9 shows the ATR-FTIR spectra of the organic phase (TEHDGA+HA/*n*-DD) recorded after contacting the organic phase with 1 M nitric acid. The extraction of nitric acid by the binary solution phase results in increase in the intensity of band at 1300 cm$^{-1}$ due to N-O stretching of nitrate ions [27].

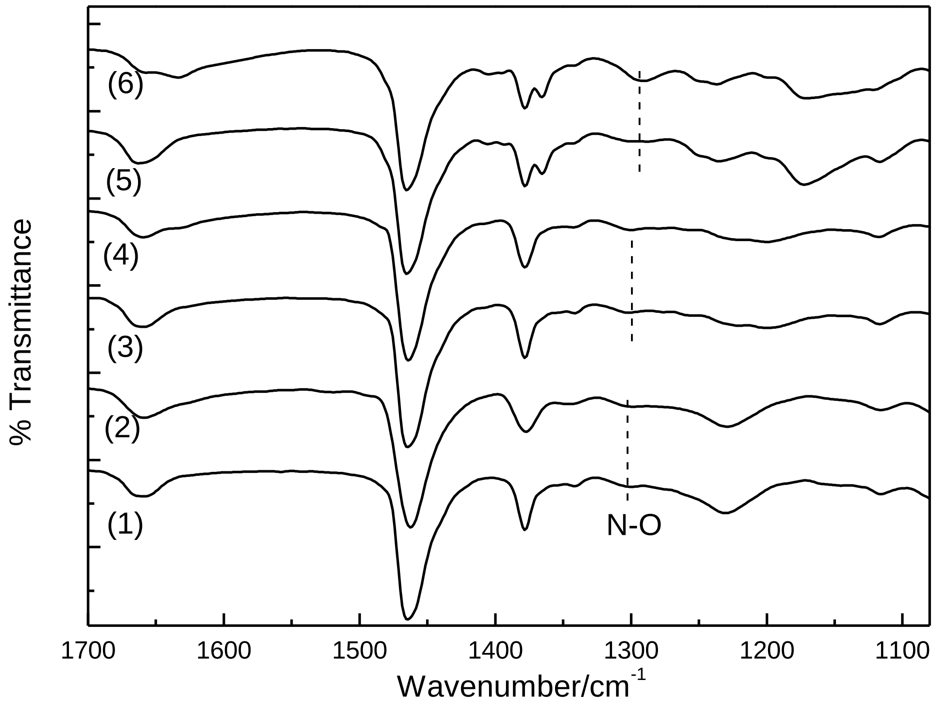

**Figure 6.9.** ATR-FTIR spectra of TEHDGA+HA/*n*-DD recorded after contacting the organic phase with 1 M nitric acid solution. (1) Org: 0.1 M TEHDGA+0.25 M HDEHP/*n*-DD, (2) Org: 0.1 M TEHDGA+0.25 M HDEHP/*n*-DD, Aq: 1 M $HNO_3$, (3) Org: 0.1 M TEHDGA+0.25 M PC88A/*n*-DD, (4) Org: 0.1 M TEHDGA+0.25 M PC88A/*n*-DD, Aq: 1 M $HNO_3$, (5) Org: 0.1 M TEHDGA+0.5 M CYANEX-272/*n*-DD, (6) Org: 0.1 M TEHDGA+0.5 M CYANEX-272/*n*-DD, Aq: 1 M $HNO_3$.

### 6.5.2 Extraction of Eu(III) in TEHDGA/*n*-DD

Figure 6.2 (b) shows that the variation in the distribution ratio of Eu(III) as a function of nitric acid concentration in aqueous phase. It is observed that the distribution ratio of Eu(III) in 0.1 M TEHDGA/*n*-DD increases from $10^{-3}$ to ~ 80 with the increase in the concentration of nitric acid from $10^{-3}$ M to 3 M, as expected [18] for the neutral extractant, TEHDGA. To understand the interaction of Eu(III) with TEHDGA, the ATR-FTIR spectra of extracted organic phase was recorded at various acidities and compared with the spectrum of TEHDGA. The ATR-FTIR spectrum of 0.1 M TEHDGA/*n*-DD phase is shown in Figure 6.10. Only selected wave number region is shown in the ATR-FTIR spectra for clarity. As discussed above, the amidic C=O stretching bands and etheric C-O stretching of TEHDGA occurs at 1663 $cm^{-1}$and 1117 $cm^{-1}$ respectively [30,31] (see the structure of TEHDGA in Table 6.1). It should be noted that these groups (amidic carbonyl and etheric oxygen) are likely to be involved in the extraction of Eu(III) from nitric acid medium. Therefore, it would be interesting to monitor the changes that could occur in these transmittance bands (1663 $cm^{-1}$ and 1117 $cm^{-1}$) upon Eu(III) extraction from nitric acid medium.

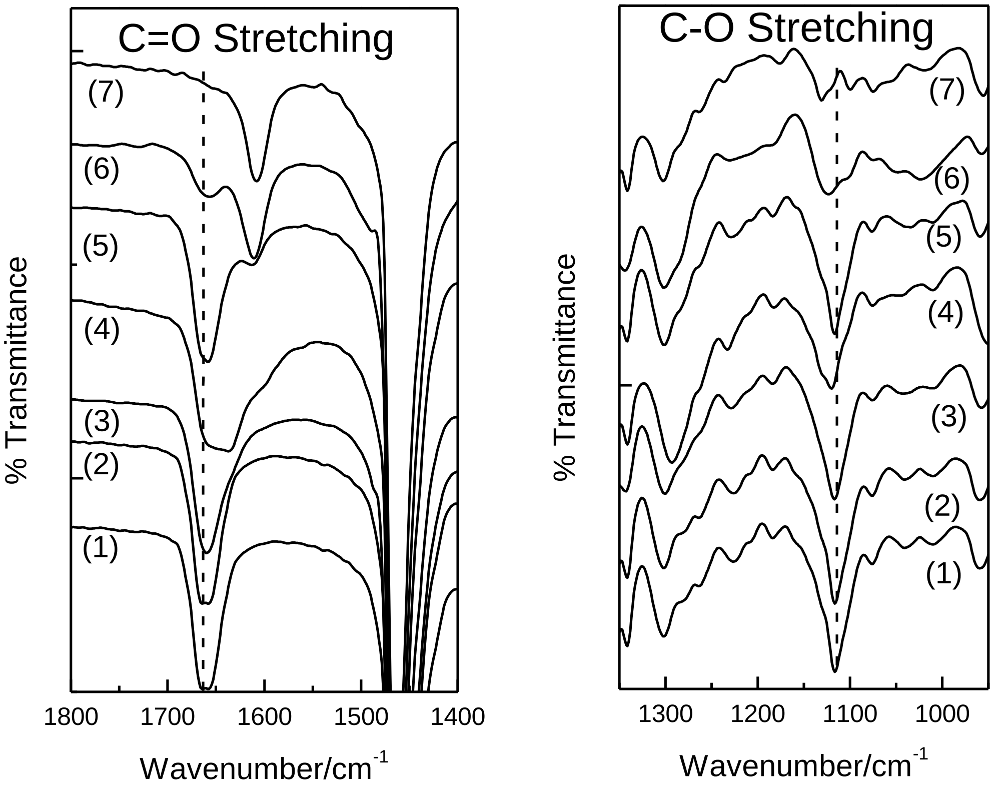

**Figure 6.10**. ATR-FTIR spectra of TEHDGA/*n*-DD recorded after contacting the organic phase with nitric acid solution in the presence and absence of Eu(III). The vertical dash in the figure indicates the initial position of the band. (1) Org: 0.1 M TEHDGA/*n*-DD, (2) Org: 0.1 M TEHDGA/*n*-DD, Aq: 0.1 M $HNO_3$, (3) Org: 0.1 M TEHDGA/*n*-DD, Aq: 1 M $HNO_3$, (4) Org: 0.1 M TEHDGA/*n*-DD, Aq: 3 M $HNO_3$, (5) Org: 0.1 M TEHDGA/*n*-DD, Aq: 0.1 M $HNO_3$+Eu(III), (6) Org: 0.1 M TEHDGA/*n*-DD, Aq:1 M $HNO_3$+Eu(III), (7) Org: 0.1 M TEHDGA/*n*-DD, Aq: 3 M $HNO_3$+Eu(III).

### 6.5.3 ATR-FTIR spectroscopy of TEHDGA/*n*-DD contacted with nitric acid

Figure 6.10 also shows the ATR-FTIR spectra of the organic phase, 0.1 M TEHDGA/*n*-DD, recorded after contacting the organic phase with 0.1 M, 1 M and 3 M nitric acid concentrations. It is observed that there is no change in the position of amidic C=O stretching bands of TEHDGA, when the organic phase was contacted with 0.1 M nitric acid. However, broadening of C=O transmittance bands is observed when the TEHDGA phase was contacted with 1 M and 3 M nitric acid. This can be due to the protonation of amidic carbonyl groups in TEHDGA leading to the extraction of nitric acid in organic phase [30]. Deepika *et al.* reported the extraction of nitric acid in 0.2 M TEHDGA/*n*-DD. The extraction of nitric acid was reported to be negligible, when contacted with 0.1 M nitric acid and significant quantity of nitric acid was extracted in TEHDGA/*n*-DD at 3 M nitric acid [32]. Moreover, there is an increase in the relative intensity of transmittance bands at 1300 $cm^{-1}$ due to nitrate ions in the ATR-FTIR spectra of 0.1 M TEHDGA/*n*-DD when contacted with 1 M and 3 M nitric acid, as shown in Figure 6.10. As far as the etheric C-O transmittance bands are concerned, there is no change in the nature of etheric C-O transmittance bands occurring at 1117 $cm^{-1}$. This indicates that the etheric oxygen does not seem to be protonated, significantly, to cause broadening of C-O stretching bands as compared to the amidic C=O bands of TEHDGA even at 3 M nitric acid.

### 6.5.4 ATR-FTIR spectroscopy of TEHDGA/*n*-DD contacted with Eu(III)

In contrast to broadening of amidic C=O transmittance bands, the ATR-FTIR spectrum of 0.1 M TEHDGA/*n*-DD phase recorded after contacting the organic phase with 3 M nitric acid solution containing Eu(III) ion (see Figure 6.10) shows the shift of transmittance bands from 1663 $cm^{-1}$ to 1610 $cm^{-1}$ [30,31]. This observation can be attributed to the extraction of Eu(III) in 0.1 M TEHDGA/*n*-DD phase at 3 M $HNO_3$. From Figure 6.2(b), it can be seen that the distribution ratio of Eu(III) in 0.1 M TEHDGA/*n*-DD reaches a value of ~ 80 at 3 M nitric acid, indicates that the extraction of Eu(III) was more than 99% in TEHDGA phase. Extraction and efficient co-ordination of amidic C=O groups of TEHDGA with Eu(III) results in weakening of amidic carbonyl double bond and shifting of C=O transmittance bands from 1663 $cm^{-1}$ to lower stretching frequency region, 1610 cm$^{-1}$ in the FTIR spectrum. In addition, the C-O transmittance bands of TEHDGA at 1117 cm$^{-1}$ is shifted to 1125 cm$^{-1}$ upon Eu(III) extraction from 3 M $HNO_3$ (see Figure 6.10) [31]. This could be due to the co-ordination of etheric oxygen with Eu(III) leading to the formation of tridendate complex as reported by Kannan *et al.*[33]. The authors studied the single crystal X-ray crystallography of lanthanum–diglycolamide complexes and reported that Lanthanum(III) was coordinated by three ligands of diglycolamides through tridentate co-ordination [33]. The formation of co-ordinate bond between etheric oxygen and Eu(III) results in the development of partial positive charge on oxygen and increase in the bond order of etheric C-O bands [31]. This leads to the shift of C-O transmittance bands from 1117 cm$^{-1}$ to 1125 cm$^{-1}$. The ATR-FTIR spectrum of 0.1 M TEHDGA/*n*-DD phase recorded after contacting with 1 M nitric acid solution containing Eu(III) ion, shows that the amidic carbonyl C=O transmittance bands of TEHDGA are shifted from 1663 cm$^{-1}$ to 1610 cm$^{-1}$. This indicates the coordination and extraction of Eu(III) by the TEHDGA in to the organic phase, as shown in Figure 6.2 (b). However, a shoulder observed at 1663 cm$^{-1}$ (original position) indicates that Eu(III) is extracted in a lesser extent compared to 3 M nitric acid concentration. In addition, the C-O transmittance bands of TEHDGA are shifted from 1117 cm$^{-1}$ to 1125 cm$^{-1}$ with shoulder at original position at 1117 cm$^{-1}$.

Figure 6.10 also shows the ATR-FTIR spectrum of 0.1 M TEHDGA/*n*-DD phase recorded after contacting with 0.1 M nitric acid solution containing Eu(III) ion. It can be seen that the amidic C=O transmittance bands of TEHDGA at 1663 cm$^{-1}$ are fairly unaffected in 0.1 M nitric acid. This indicates that the amidic carbonyl group is not involved in the coordination of Eu(III) at 0.1 M nitric acid. A weak shoulder observed at 1610 cm$^{-1}$ could be attributed to a very small loading of Eu(III) in 0.1 M TEHDGA/*n*-DD phase at 0.1 M $HNO_3$. A small loading of

Eu(III) invariably occurs in this case owing to the employment of large concentration Eu(III) (15 g/L) in the aqueous phase, which was found to be necessary to obtain a perceptible changes in ATR-FTIR spectra upon extraction. It is also noted that there is no change in the position of transmittance band at 1117 $cm^{-1}$. These observations confirm that Eu(III) is not extracted into organic phase at 0.1 M nitric acid.

Therefore, the study shows that FTIR spectroscopy can be used for monitoring the extraction behavior of Eu(III) in TEHDGA phase. The red shift of amidic carbonyl stretching bands from 1663 $cm^{-1}$ to 1610 $cm^{-1}$ and the blue shift of etheric C-O stretching bands from 1117 $cm^{-1}$ to 1125 $cm^{-1}$ indicates the coordination of these oxygen donor ligands with Eu(III) and extraction of Eu(III) from aqueous phase. This observation is consistent with negligible extraction of Eu(III) at 0.1 M nitric acid (D=0.001) and high extraction of Eu(III) at 3 M $HNO_3$ (D > 80) in 0.1 M TEHDGA/*n*-DD. The extraction of nitric acid, on the other hand, results in the protonation of amidic carbonyl group and broadening of transmittance bands at 1663 $cm^{-1}$.

### 6.5.5 Extraction of Eu(III) in binary solution

It is necessary to understand the extraction behavior of Eu(III) upon adding acidic extractants to 0.1 M TEHDGA/*n*-DD phase. The results on the variation in the distribution ratio of Eu(III) in the combined solvent system as a function of nitric acid concentration in aqueous phase is shown Figure 6.2(b). It can be seen that the addition of any acidic extractant to TEHDGA increases the distribution ratio of Eu(III) in the entire acid range, investigated in the present study. However, the increase is more in the lower acid region. In addition, the distribution ratio of Eu(III) increases in the order of (TEHDGA + CYANEX-272) < (TEHDGA + PC88A) < (TEHDGA + HDEHP) at all nitric acid concentrations. The order of extraction observed in the combined solvent system is in accordance with decrease $pK_a$ value of acidic extractants. However, strong acidic extractants (HDEHP and PC88A) present in the combined solvent system dissociates more and facilitate higher extraction of Eu(III) at a particular nitric acid concentration. This indicates that TEHDGA in the combined solution could be playing a predominant role in deciding the extraction of Eu(III) at higher nitric acid concentration. Therefore, it would be interesting to investigate the FTIR spectrum of TEHDGA present in the combined solvent system upon contacting with 3 M nitric acid containing Eu(III) ion.

### 6.5.6 ATR-FTIR spectroscopy of TEHDGA+HA/*n*-DD at 3 M nitric acid

Figure 6.11 shows the ATR-FTIR spectra of the combined solvent system recorded after contacting the organic phase with 3 M nitric acid. It can be seen that the amidic C=O transmittance bands of TEHDGA at 1663 $cm^{-1}$ are broadened due to protonation of C=O groups by nitric acid, as discussed above. However, the ATR-FTIR spectra of the combined solvent system recorded after contacting with organic phase at 3 M nitric acid phase containing Eu(IIII) ion shows the shift of amidic C=O transmittance bands from 1663 $cm^{-1}$ to 1610 $cm^{-1}$. In addition, a marginal shift of etheric C-O stretching bands from 1117 $cm^{-1}$ to 1125 $cm^{-1}$ is also observed. These observations clearly indicate the participation of TEHDGA in the extraction of Eu(III) at 3 M $HNO_3$, which is not unexpected. However, it should be noted that the distribution ratio of Eu(III) in the combined solvent system at 3 M nitric acid increases in the order (TEHDGA+CYANEX-272) < (TEHDGA+PC88A) < (TEHDGA+HDEHP), as shown in Figure 6.2(b). This observation shows that the acidic extractant added to TEHDGA in the combined solvent might be playing some role in the extraction of Eu(III) even at 3 M nitric acid, which is not expected.

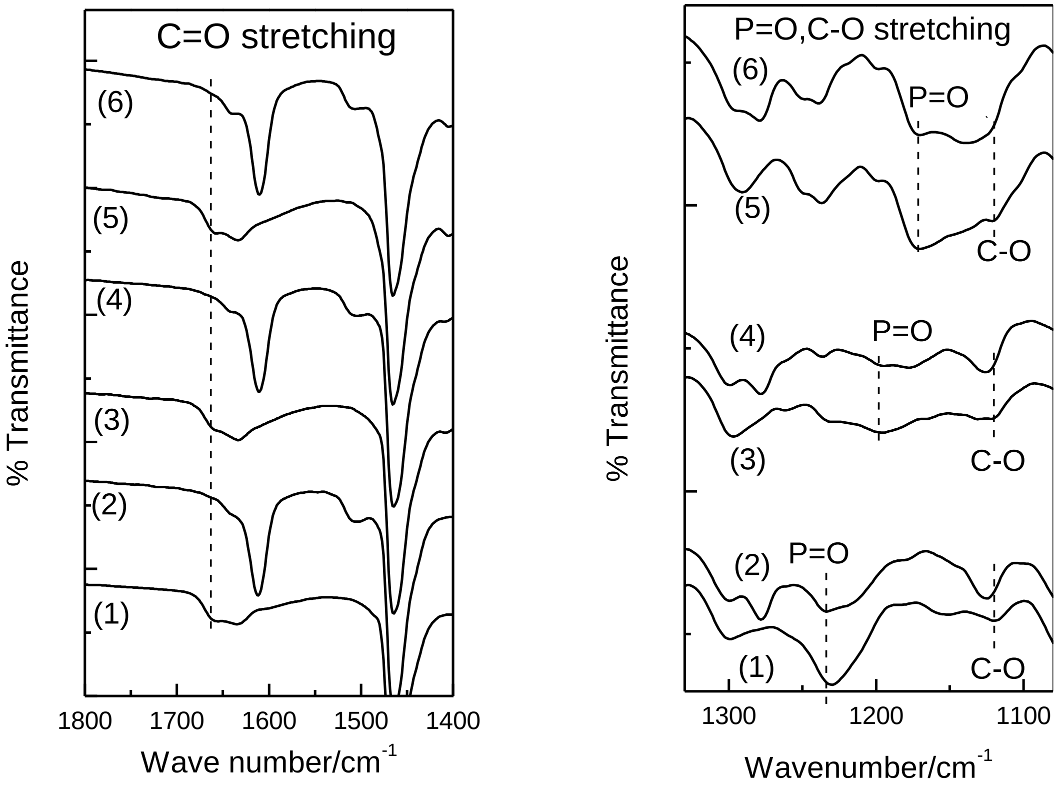

**Figure 6.11.** ATR-FTIR spectra of TEHDGA+HA/*n*-DD recorded after contacting the organic phase with 3 M nitric acid solution in the presence and absence of Eu(III). The vertical dash in the figure indicates the initial position of the band. (1) Org: 0.1 M TEHDGA+0.25 M HDEHP/*n*-DD, Aq: 3 M $HNO_3$, (2) Org: 0.1 M TEHDGA+0.25 M HDEHP/*n*-DD, Aq: 3 M $HNO_3$+ Eu(III), (3) Org: 0.1 M TEHDGA+0.25 M PC88A/*n*-DD, Aq: 3 M $HNO_3$, (4) Org: 0.1 M TEHDGA+0.25 M PC88A/*n*-DD, Aq: 3 M $HNO_3$+Eu(III), (5) Org: 0.1 M TEHDGA+0.5 M CYANEX-272/*n*-DD, Aq: 3 M $HNO_3$, (6) Org: 0.1 M TEHDGA+0.5 M CYANEX-272/*n*-DD, Aq: 3 M $HNO_3$+Eu(III).

In order to understand the role of acidic extractant in the extraction of Eu(III) at 3 M nitric acid, the changes in the phosphoryl (P=O) stretching bands of the acidic extractant in the combined solvent system was monitored in the ATR-FTIR spectra. The results are shown in Figure 6.11 (right side). It can be seen that the phosphoryl P=O stretching bands occurs at 1230 cm$^{-1}$ in case of HDEHP, 1198 cm$^{-1}$ in case of PC88A and 1172 cm$^{-1}$ in case of CYANEX-272. It was noted that the phosphoryl stretching bands of acidic extractant were not affected upon equilibration of the combined solvent with 3 M nitric acid. However, a marginal broadening of P=O stretching bands is observed only in case of HDEHP and PC88A, when the combined solvent system was equilibrated with 3 M nitric acid containing Eu(III) ion. This indicates that HDEHP and PC88A in the combined solvent are also involved in the extraction of Eu(III) even at 3 M nitric acid, This behavior was not expected for acidic extractants, since the acidic extractants alone do not extract Eu(III) from nitric acid solution of concentration more than 1 M.

The ATR-FTIR spectra of organic phase (acidic extractants alone in *n*-dodecane) after contacting with 1 M and 3 M nitric acid solution containing Eu(III) ion is shown in Figure 6.12. It can be seen that the P=O transmittance bands of HDEHP, PC88A, CYANEX-272 are not affected, in all these cases, indicating that these acidic extractants are not involved in the extraction of Eu(III) at 1 M as well as 3 M nitric acid (since distribution ratios are quite less). In contrast to this observation, a marginal broadening of P=O stretching bands of HDEHP and PC88A extractants observed in the combined solvent system, as shown in Figure 6.11, clearly indicates that HDEHP and PC88A in the combined solvent are involved in the extraction of Eu(III) even at 3 M nitric acid. Since this kind of broadening of P=O happens only in the presence of the neutral extractant TEHDGA, it is quite likely that both the extractants (TEHDGA+ HA) are involved in the synergic extraction of Eu(III) from nitric acid medium. Such synergic participation of neutral extractant and acidic extractants in various systems has been reported in literature and discussed in detail elsewhere [9-21].

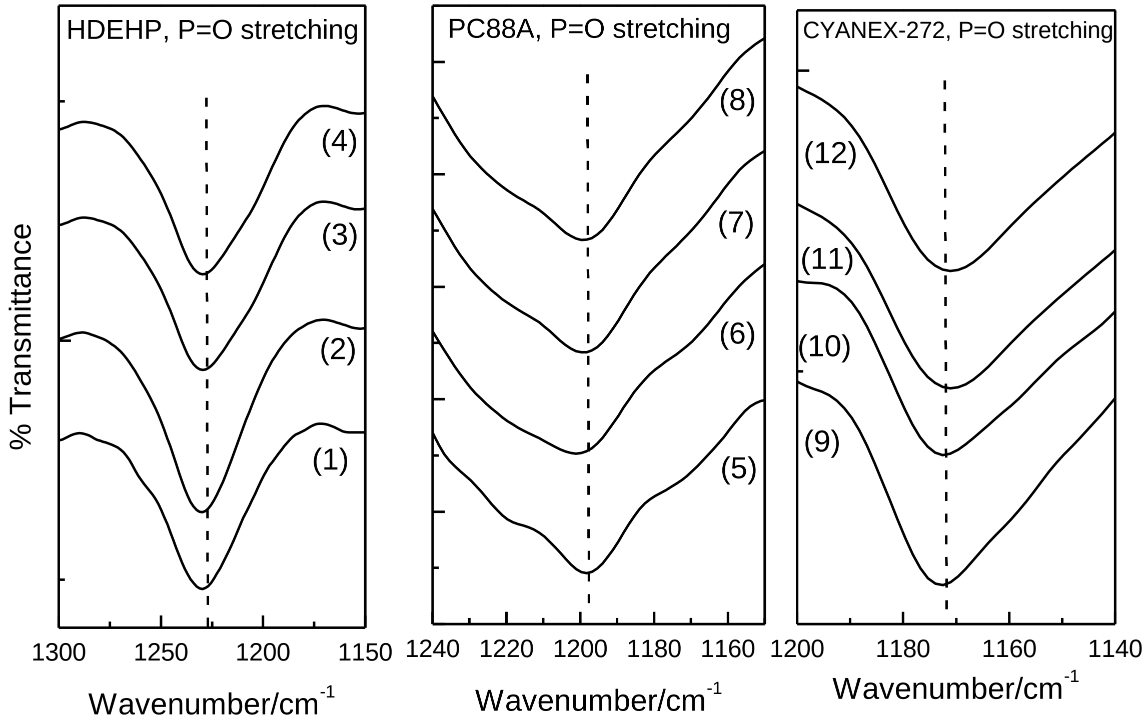

**Figure 6.12.** ATR-FTIR spectra of HA/*n*-DD recorded after contacting the organic phase with nitric acid solution in the presence and absence of Eu(III). The vertical dash in the figure indicates the initial position of the band. (1) Org: 0.25 M HDEHP /*n*-DD, (2) Org: 0.25 M HDEHP/*n*-DD, Aq: 1 M $HNO_3$, (3) Org: 0.25 M HDEHP/*n*-DD, Aq: 1 M $HNO_3$+Eu(III), (4) Org: 0.25 M HDEHP/*n*-DD, Aq: 3 M $HNO_3$+Eu(III), (5) Org: 0.25 M PC88A/*n*-DD, (6). Org: 0.25 M PC88A/*n*-DD, Aq: 1 M $HNO_3$, (7) Org: 0.25 M PC88A /*n*-DD, Aq: 1 M $HNO_3$+Eu(III), (8) Org: 0.25 M PC88A /*n*-DD, Aq: 3 M $HNO_3$+Eu(III) (9) Org: 0.5 M CYANEX-272/*n*-DD, (10) Org: 0.5 M CYANEX-272/*n*-DD, Aq: 1 M $HNO_3$, (11) Org: 0.5 M CYANEX-272/*n*-DD, Aq: 1 M $HNO_3$+Eu(III),(12) Org: 0.5 M CYANEX-272/*n*-DD, Aq: 3 M $HNO_3$+Eu(III).

The above studies indicate that HDEHP and PC88A are involved in the synergic extraction of Eu(III) from 3 M nitric acid when they are mixed in TEHDGA. Figure 6.11 also shows the ATR-FTIR spectrum of the combined solvent TEHDGA + CYANEX-272/*n*-DD recorded after contacting with 3 M nitric acid contacting Eu(III) ion. It shows that there is no change in the nature of P=O stretching bands of CYANEX-272. This indicates that the involvement of CYANEX-272 in the extraction of Eu(III) is negligible as compared to other acidic extractants discussed above, at 3 M nitric acid. In the view of this, the distribution ratio of Eu(III) in the combined solvent system at 3 M $HNO_3$ increases in the order of TEHDGA ~ (TEHDGA + CYANEX-272) < (TEHDGA + PC88A) ~ (TEHDGA + HDEHP).

### 6.5.7 Extraction of Eu(III) in binary solution at 0.01 M nitric acid

In contrast to the extraction observed at 3 M $HNO_3$, the extraction of Eu(III) observed at low nitric acid concentration in the combined solvent system shows a marked difference in the extraction of Eu(III) depending upon the nature of the acidic extractant, as shown in Figure 6.2(b). Since 0.1 M TEHDGA/*n*-DD is not expected to extract Eu(III) at lower acidities (see Figure 6.2(b)), the extraction observed in these combined solvent systems could be, predominantly, due to the involvement of acidic extractants. Therefore, monitoring the changes in the P=O stretching bands of acidic extractant in the combined solvent system at low nitric acid concentration could provide more insights in the observed distribution ratios.

### 6.5.8 ATR-FTIR spectroscopy of HA/*n*-DD and TEHDGA+HA/*n*-DD at 0.01 M nitric acid

Figure 6.13 shows, the ATR-FTIR spectrum of 0.25 M HDEHP/*n*-DD recorded after contacting the organic phase with 0.01 M nitric acid containing Eu(III) ion. The spectrum shows the shift of P=O stretching bands from 1230 $cm^{-1}$ to 1202 $cm^{-1}$, attributed to the extraction of Eu(III) by 0.25 M HDEHP/*n*-DD at 0.01 M nitric acid [27]. Similarly, the Eu(III) extracted phase of 0.25 M PC88A/*n*-DD from 0.01 M nitric acid also shows the shift of P=O stretching bands from 1198 $cm^{-1}$ to 1163 $cm^{-1}$, as shown in Figure 6.12. Since the $pK_a$ of CYANEX-272 is quite high as compared to PC88A and HDEHP, a marginal broadening of P=O stretching bands is observed in the Eu(III) extracted phase of CYANEX-272/*n*-DD from 0.001 M nitric acid, as shown in Figure 6.12.

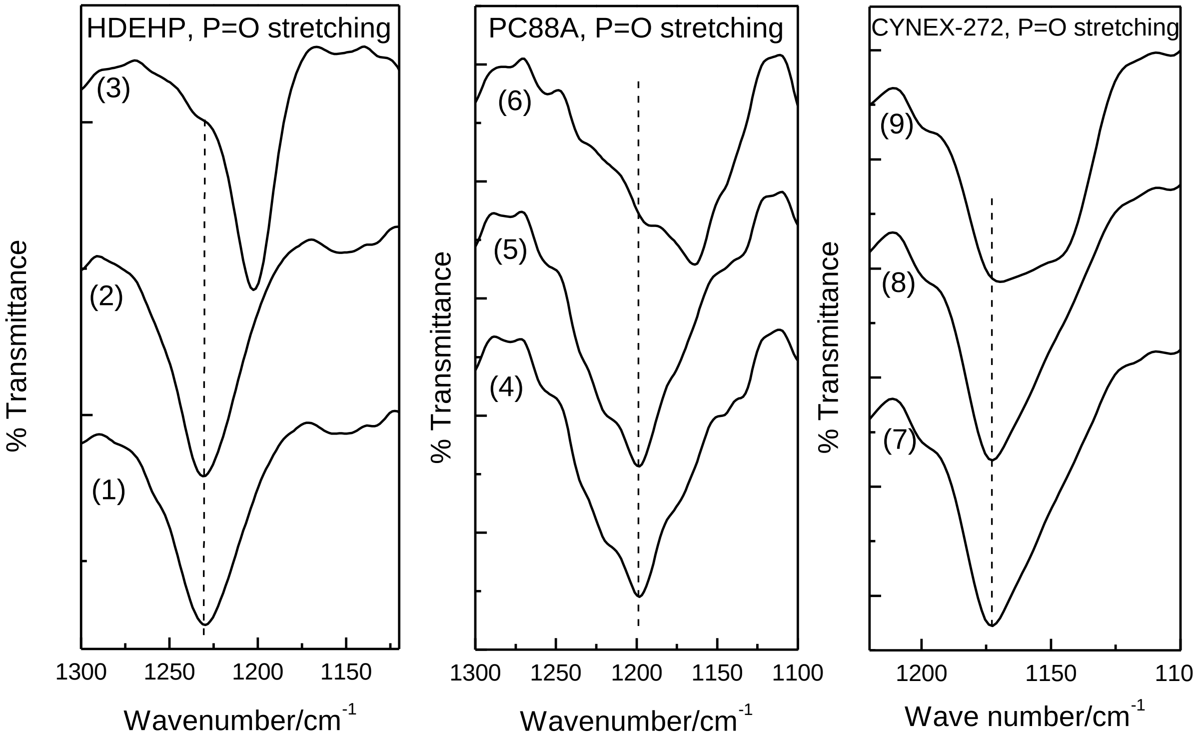

**Figure 6.13.** ATR-FTIR spectra of HA/*n*-DD recorded after contacting the organic phase with nitric acid solution in the presence and absence of Eu(III). The vertical dash in the figure indicates the initial position of the band. (1) Org: 0.25 M HDEHP /*n*-DD, (2) Org: 0.25 M HDEHP/*n*-DD, Aq: 0.01 M $HNO_3$, (3) Org: 0.25 M HDEHP/*n*-DD, Aq: 0.01 M $HNO_3$+Eu(III), (4) Org: 0.25 M PC88A/*n*-DD, (5). Org: 0.25 M PC88A/*n*-DD, Aq: 0.01 M $HNO_3$, (6) Org: 0.25 M PC88A /*n*-DD, Aq: 0.01 M $HNO_3$+Eu(III), (7) Org: 0.5 M CYANEX-272/*n*-DD, (8) Org: 0.5 M CYANEX-272/*n*-DD, Aq: 0.001 M $HNO_3$, (9) Org: 0.5 M CYANEX-272/*n*-DD, Aq: 0.001 M $HNO_3$+Eu(III).

Here, the lower nitric acid (0.001 M) was taken for extraction to achieve perceptible extraction of Eu(III) and changes in FTIR spectrum. The shift of P=O stretching bands to lower wavenumber region observed in case of HDEHP/*n*-DD and PC88A/*n*-DD indicate that these ligands are strongly involved in the extraction of Eu(III). Broadening of P=O stretching bands observed in case of CYANEX-272/*n*-DD shows that CYANEX-272 is weakly involved in the extraction of Eu(III).

A similar shift of P=O stretching bands to lower wavenumber region would be expected in the binary solvent system, when HDEHP and PC88A are strongly involved in the extraction of Eu(III) from 0.01 M nitric acid. Figure 6.14 shows the ATR-FTIR spectrum of TEHDGA+HDEHP/*n*-DD phase recorded after contacting with 0.01 M nitric acid containing Eu(III) ion. It can be seen that the organic phase shows a broadening of P=O transmittance bands instead of the shift. A similar broadening of P=O band is observed in case of PC88A and CYANEX-272 in *n*-DD also. This observation indicates that the involvement of acidic extractants in the extraction of Eu(III) is lowered, in the presence of TEHDGA. Since the involvement of acidic extractants is less, it can be expected that TEHDGA could be participating in the extraction of Eu(III) even at lower nitric acid, which is not expected again (see Figure 6.2 (b)) extraction of Eu(III) in TEHDGA is insignificant at 0.01M nitric acid).

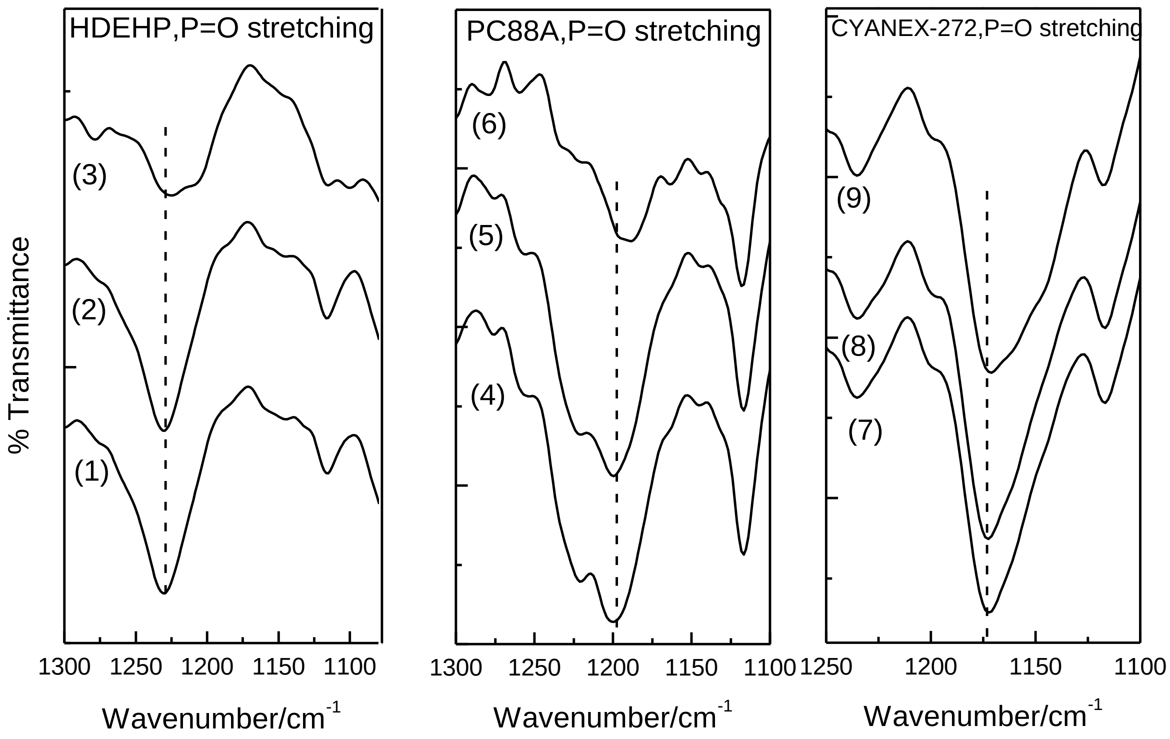

**Figure 6.14**. ATR-FTIR spectra of TEHDGA+HA/*n*-DD recorded after contacting the organic phase with 0.01 M nitric acid solution in the presence and absence of Eu(III). The vertical dash in the figure indicates the initial position of the band. (1) Org: 0.1 M TEHDGA+0.25 M HDEHP/*n*-DD, (2) Org: 0.1 M TEHDGA+0.25 M HDEHP/*n*-DD, Aq: 0.01 M $HNO_3$, (3) Org: 0.1 M TEHDGA+0.25 M HDEHP/*n*-DD, Aq: 0.01 M $HNO_3$+Eu(III), (4) Org: 0.1 M TEHDGA+0.25 M PC88A/*n*-DD, Aq: 0.01 M $HNO_3$, (5) Org: 0.1 M TEHDGA+0.25 M PC88A/*n*-DD, Aq: 0.01 M $HNO_3$, (6) Org: 0.1 M TEHDGA+0.25 M PC88A/*n*-DD, Aq: 0.01 M $HNO_3$+Eu(III), (7) Org: 0.1 M TEHDGA+0.5 M CYANEX-272/*n*-DD, (8) Org: 0.1 M TEHDGA+0.5 M CYANEX-272/*n*-DD, Aq: 0.001 M $HNO_3$, (9) Org: 0.1 M TEHDGA+0.5 M CYANEX-272/*n*-DD, Aq: 0.001 M $HNO_3$+Eu(III).

In order to understand the involvement of TEHDGA in the extraction of Eu(III) at low nitric acid concentration in the combined solvent system, the ATR-FTIR spectrum of TEHDGA+HDEHP/*n*-DD phase was recorded after contacting the organic phase with 0.01 M nitric acid solution containing Eu(III) ion. The results are shown in Figure 6.15. It should be noted that there was no change in the nature C=O stretching bands when the FTIR spectrum was recorded after contacting the combined solvent with 0.01 M nitric acid.

However, upon equilibration of the combined solvent (TEHDGA+HDEHP) with 0.01 M nitric acid containing Eu(III) ion, the position of amidic C=O stretching bands are shifted partially from 1663 $cm^{-1}$ to 1627 $cm^{-1}$. The relative intensity of bands at 1663 $cm^{-1}$ and 1627$cm^{-1}$ are nearly equal in this case. A similar behavior is also observed in the ATR-FTIR spectra of the other combined solvents, as shown in Figure 6.15, recorded after the extraction of Eu(III) from 0.01 M nitric acid in TEHDGA+PC88A and TEHDGA+ CYANEX-272 (extracted from 0.001 M nitric acid in this case). However, the relative intensity of bands at 1663 $cm^{-1}$ and 1627 $cm^{-1}$ are quite different in these cases. The relative intensity of the amidic C=O stretching bands at the shifted position (1627 $cm^{-1}$) is more, when HDEHP acts as acidic extractant. The relative intensity of the band at 1627 $cm^{-1}$ decreases in the order HDEHP > PC88A > CYANEX-272 when HA acts as co-extractant. This observation indicates that the involvement of TEHDGA in the extraction of Eu(III) is more when HDEHP acts as co-extractant and the participation of TEHDGA in the extraction of Eu(III) decreases in the order of HDEHP > PC88A > CYANEX-272.

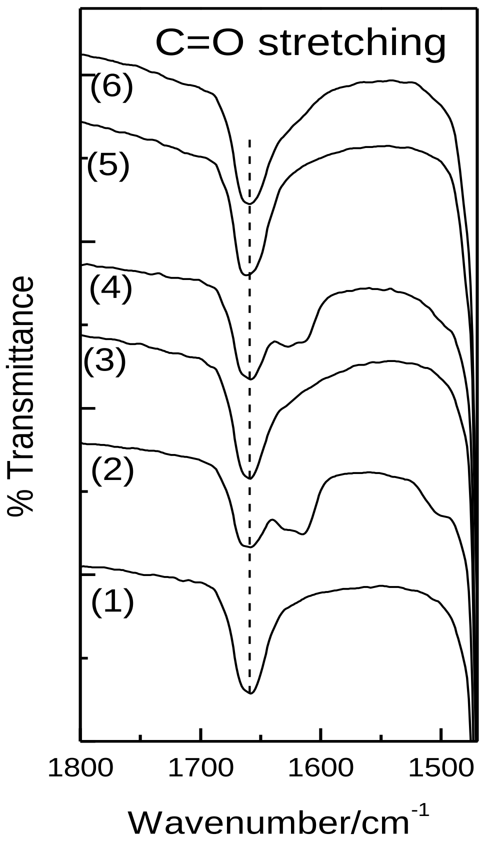

**Figure 6.15.** ATR-FTIR spectra of TEHDGA+HA/*n*-DD recorded after contacting the organic phase with 0.01 M nitric acid solution in the presence and absence of Eu(III). The vertical dash in the figure indicates the initial position of the band. (1) Org: 0.1 M TEHDGA+0.25 M HDEHP/*n*-DD, Aq: 0.01 M $HNO_3$, (2) Org: 0.1 M TEHDGA+0.25 M HDEHP/*n*-DD, Aq: 0.01 M $HNO_3$+Eu(III), (3) Org: 0.1 M TEHDGA+0.25 M PC88A/*n*-DD, Aq: 0.01 M $HNO_3$, (4) Org: 0.1 M TEHDGA+0.25 M PC88A/*n*-DD, Aq: 0.01 M $HNO_3$+Eu(III), (5) Org: 0.1 M TEHDGA+0.5 M CYANEX-272/*n*-DD, Aq: 0.001 M $HNO_3$, (6) Org: 0.1 M TEHDGA+0.5 M CYANEX-272/*n*-DD, Aq: 0.001 M $HNO_3$+Eu(III).

In view of this, the extraction of Eu(III) in combined solvent system at lower nitric acid concentration decreases in the order (TEHDGA + HDEHP) > (TEHDGA + PC88A) > (TEHDGA + CYANEX-272), as shown in Figure 6.2(b). The unexpected participation of TEHDGA at lower acidity indicates the possibility of synergic extraction of Eu(III) when TEHDGA is combined with acidic extractants. Such synergic extraction of various metal ions in several binary solvent systems is well known and they are discussed elsewhere [9-21]. Muller *et al.* studied the extraction behaviour of neodymium in a binary solvent phase composed of DMDOHEMA+HDEHP in TPH and investigated the interaction of Nd(III) with ligands in the organic medium using FT-IR spectroscopy at 0.05 M $HNO_3$ only. Based on the red shift of both carbonyl group stretching frequency (1652 $cm^{-1}$ to 1624 $cm^{-1}$) and P=O stretching frequency of HDEHP (1232 to 1217 $cm^{-1}$), the authors concluded the involvement of both DMDOHEMA and HDEHP during the extraction Nd(III) from lower nitric acid concentrations [34]. Tkac *et al.* studied the interaction between CMPO and HDEHP and its effects on extraction of Ln(III) using FT-IR spectroscopy. A red shift of carbonyl ($\Delta\nu$ = 40-50 $cm^{-1}$) and phosphoryl stretching frequencies ($\Delta\nu$ = 30 $cm^{-1}$) of CMPO was observed upon extraction of Ln(III) from 0.01 M $HNO_3$. Similarly, HDEHP also showed a red shift of P=O transmittance band after the extraction of La(III). These studies clearly suggested the involvement of CMPO and HDEHP in the extraction of La(III) at 0.01 M nitric acid concentration [27].

### 6.5.9 Extraction of Eu(III) in binary solution at 0.5 M nitric acid

It is interesting to note from Figure 6.2(b) that the distribution ratio of Eu(III) in all combined extractant systems initially decrease with increase in the concentration of nitric acid reaches a minimum value at a particular nitric acid concentration followed in increase in distribution ratios as discussed above. In case of PC88A and HDEHP, the minimum occurs at

0.5 M nitric acid, and CYANEX-272 it occurs near 0.1 M nitric acid. It would be worthwhile to check the ATR-FTIR spectrum of the binary solution at 0.5 M nitric acid and compare with results those obtained before and after the minimum.

Figure 6.16 shows the ATR-FTIR spectra of TEHDGA+HDEHP/*n*-DD phase recorded after contacting with various concentrations of nitric acid containing Eu(III) ion. The concentration of nitric acid was varied from 0.1 M to 3 M. At 0.1 M nitric acid, the position of amidic C=O stretching bands are shifted partially from 1663 $cm^{-1}$ to 1627 $cm^{-1}$ with a couple shoulders at the original position and the P=O stretching bands are shifted from 1230 $cm^{-1}$ to 1202 $cm^{-1}$, as expected. The shift of etheric C-O stretching bands of TEHDGA is negligible at 0.1 M nitric acid. This observation indicates that both the extractants are synergistically participating in the extraction of Eu(III), however, the extraction at 0.1 M nitric acid seems to be predominantly governed by HDEHP. At 0.5 M nitric acid, the shift of P=O stretching bands is less and instead a broadening is observed at the P=O position. This indicates the participation of HDEHP in the extraction of Eu(III) is lowered at 0.5 M nitric acid, which seems to be responsible for the local minimum in the extraction of Eu(III) at 0.5 M nitric acid (Figure 6.2(b)). Above 0.5 M nitric acid, the ATR-FTIR spectrum shows the complete shift of amidic C=O stretching bands from 1663 $cm^{-1}$ to 1610 $cm^{-1}$ and the shift of etheric C-O stretching bands from 1117 $cm^{-1}$ to 1125 $cm^{-1}$, indicating the predominant participation of TEHDGA in the extraction of Eu(III) above 0.5 M nitric acid. A broadening of P=O stretching bands above 0.5 M nitric acid indicates the participation of HDEHP in the extraction of Eu(III) also, to some extent. Therefore, the results indicates that the extraction of Eu(III) is predominantly controlled by HDEHP at lower nitric acid and TEHDGA at higher nitric acid concentration and the transfer of control occurs at ~ 0.5 M nitric acid in case of TEHDGA+HDEHP. In view of this, a local minimum is observed at 0.5 M nitric acid in case of TEHDGA+HDEHP. A similar behaviour was also observed in case of TEHDGA+PC88A.

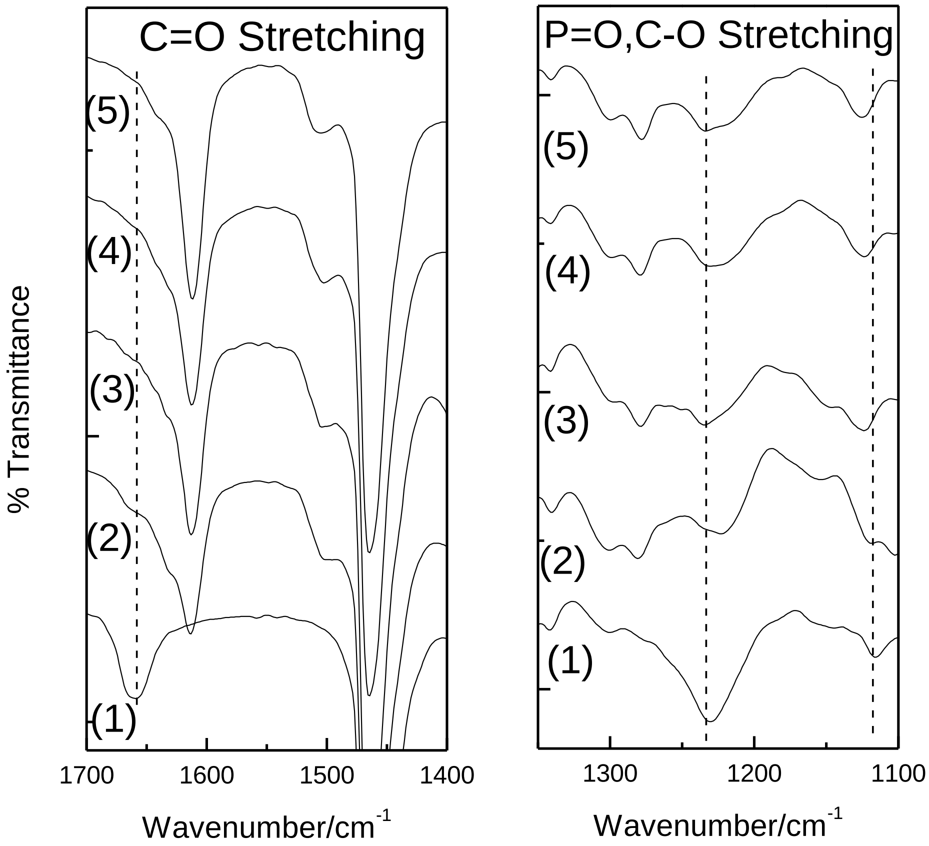

**Figure 6.16.** ATR-FTIR spectra of TEHDGA+HDEHP/*n*-DD recorded after contacting the organic phase with nitric acid solution in the presence of Eu(III). The vertical dash in the figure indicates the initial position of the band. (1) Org: 0.1 M TEHDGA+0.25 M HDEHP/*n*-DD, (2) Org: 0.1 M TEHDGA+0.25 M HDEHP/*n*-DD, Aq: 0.1 M $HNO_3$+Eu(III), (3) Org: 0.1 M TEHDGA+0.25 M HDEHP/*n*-DD, Aq: 0.5 M $HNO_3$+Eu(III), (4) Org: 0.1 M TEHDGA+0.25 M HDEHP/*n*-DD, Aq: 1 M $HNO_3$+Eu(III), (5) Org: 0.1 M TEHDGA+0.25 M HDEHP/*n*-DD, Aq: 3 M $HNO_3$+Eu(III).

## 6.6 Summary

The extraction behavior of Eu(III) from nitric acid medium was studied in a binary solution of TEHDGA and HA present in *n*-DD. The acidic extractants employed in the binary solution were HDEHP, PC88A and CYANEX-272, whose $pK_a$ values were 3.24, 4.51 and 6.37 respectively. The changes in the amidic C=O and etheric C-O stretching bands of TEHDGA and phosphoryl P=O stretching bands of HA were monitored before and after the extraction of Eu(III) from nitric acid medium, and correlated the peak shits observed in the FTIR spectrum to the distribution ratio of Eu(III) as well as to the $pK_a$ value of the acidic extractant. The red shift of amidic carbonyl stretching bands from 1663 $cm^{-1}$ to 1610 $cm^{-1}$ and the blue shift of etheric C-O stretching bands from 1117 $cm^{-1}$ to 1125 $cm^{-1}$ showed the coordination of these oxygen donor ligands with Eu(III) and extraction of Eu(III) from aqueous phase. Similarly, the shift of P=O stretching bands to lower wavenumber region observed only in case of HDEHP/*n*-DD and PC88A/*n*-DD showed that these ligands were strongly involved in the extraction of Eu(III).

At 3 M nitric acid, a binary solution showed a marginal broadening of P=O stretching bands upon Eu(III) extraction when HDEHP and PC88A acted as acidic extractant. This indicated the partial participation of these acidic extractants in the extraction of Eu(III) even at 3 M nitric acid. In view of this, distribution ratio of Eu(III) in the binary solution at 3 M nitric acid increased in the order TEHDGA ~ (TEHDGA + CYANEX-272) < (TEHDGA + PC88A) ~ (TEHDGA + HDEHP). At lower nitric acid concentration, the relative intensity of the amidic C=O stretching bands of TEHDGA at the shifted position (1627 $cm^{-1}$) decreased in the order HDEHP > PC88A > CYANEX-272, when HA acted as co-extractant. Therefore, the extraction of Eu(III) in combined solvent system at lower nitric acid concentration range decreased in the order (TEHDGA + HDEHP) > (TEHDGA + PC88A) > (TEHDGA + CYANEX-272).

# Part III. Effect of pKa of organophosphorus acidic extractant on the aggregation behavior of TEHDGA in *n*-dodecane

## 6.7 Introduction

The present part deals with the extraction behavior of nitric acid and Nd(III) in the binary solvent phase composed of 0.2 M TEHDGA+0.25 M HA in *n*-DD and the reverse micellar aggregation behavior of the binary solution. The organophosphorous acid ligands (HA) investigated were HDEHP, PC88A and CYANEX-272. The results obtained from the extraction studies and DLS measurements are reported in this part.

## 6.8 Results and discussions

### 6.8.1 Extraction of nitric acid in 0.2 M TEHDGA+0.25 M HA/*n*-DD

Figure 6.17 shows the extraction behavior of nitric acid in the binary solution composed of 0.2 M TEHDGA+0.25 M HA in *n*-dodecane. The data was compared with those obtained in 0.2 M TEHDGA/*n*-DD. It can be seen from Figure 6.17 that the extraction of nitric acid in organic phase increases with increase in the initial concentration of nitric acid in aqueous phase, in all cases. The acid extraction in the binary solution increases in the order (TEHDGA + HDEHP) < (TEHDGA + PC88A) < (TEHDGA + CYANEX-272), which is the increasing order of pKa of acidic extractants 3.24 (HDEHP) < 4.57 (PC88A) < 6.37 (CYANEX-272). This indicates that the presence of weaker acidic extractant in organic phase increases the extraction of nitric acid in organic phase.

It was expected that the addition of any extractant (containing polar groups) to TEHDGA/*n*-DD, would increase the extraction of nitric acid in organic phase [35-40]. In contrast to this, the extraction of nitric acid was lowered in all the binary solutions as compared to that observed in TEHDGA/*n*-DD. This could be possible only when the added acidic extractant forms an adduct with TEHDGA, such as TEHDGA….HA, as discussed elsewhere [27, 35-38, 41]. It should be noted that there is a competition between HA and $HNO_3$ for adduct formation and protonation (or acid-solvate formation) of TEHDGA in organic phase. But the adduct formation makes the TEHDGA unavailable for protonation by $HNO_3$. Since the adduct formation depends upon the pKa of acidic extractant, it is quite likely that the formation of an adduct increases in the order TEHDGA….CYANEX-272 < TEHDGA….PC88A < TEHDGA…HDEHP. In view of this, the extraction of nitric acid in organic phase decreases in the order (TEHDGA + CYANEX-272) > (TEHDGA + PC88A) > (TEHDGA + HDEHP) as shown in Figure 6.17.

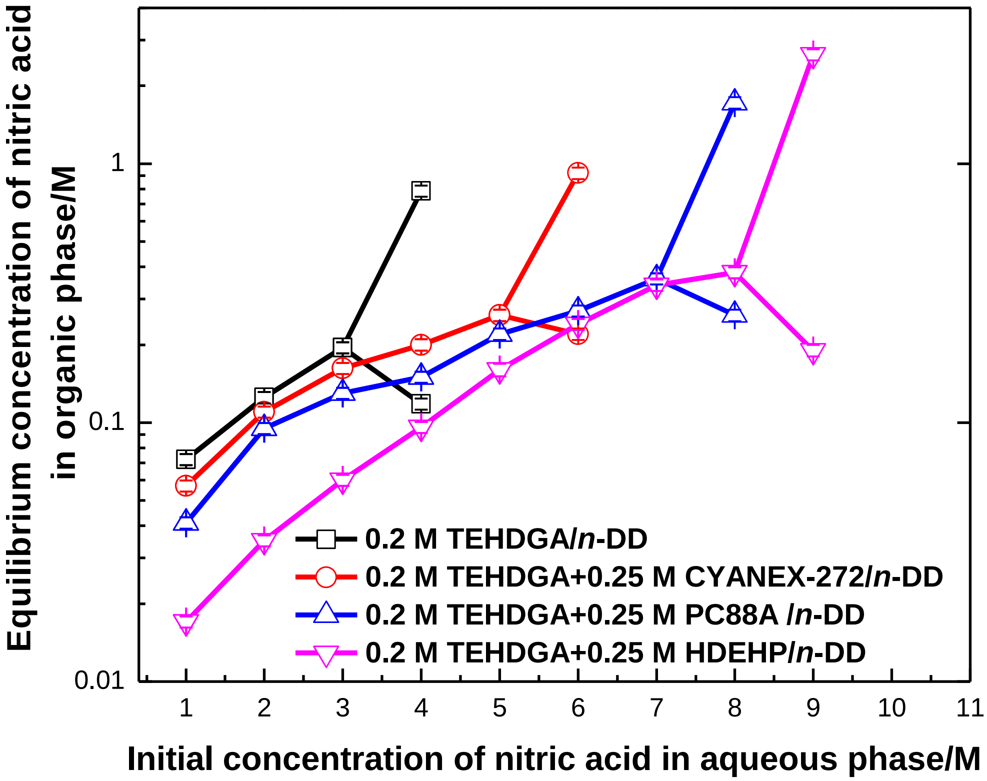

**Figure 6.17.** Variation in the extraction of nitric acid in the organic phase as a function of nitric acid concentration in aqueous phase. Organic phase: 0.2 M TEHDGA/*n*-DD or 0.2 M TEHDGA+0.25 M HDEHP/*n*-DD or 0.2 M TEHDGA+0.25 M PC88A/*n*-DD or 0.2 M TEHDGA+0.25 M CYANEX-272/*n*-DD. Aqueous phase: Nitric acid concentration varied from 1 M to 9 M.

### 6.8.2 Aggregation in 0.2 M TEHDGA+0.25 M HA/*n*-DD

Figure 6.18 shows the variation in the distribution of reverse micellar aggregates obtained after contacting the organic phase with nitric acid. The concentration of nitric acid in aqueous phase was varied from 1 M to 8 M. The distribution data was compared with those obtained in 0.2 M TEHDGA/*n*-DD phase. The aggregation behavior for 0.25 M HA/*n*-DD alone observed that there was no increase in the average aggregate size (~1.6 nm) for 0.25 M HA/*n*-DD upon contacting nitric acid (1-10 M) as well as metal ion of difference concentrations. This was due to poor or negligible extraction of nitric acid by these acidic extractants. Moreover, the acidic extractants does not extract the metal ion above 0.5 M $HNO_3$, since they follow cation exchange mechanism. It can be seen that the average aggregate size and their distribution in organic phase increases with increase in the concentration of nitric acid in aqueous phase, in all cases. The self-aggregate (before contacting with nitric acid) size of the reverse micellar aggregates are in the range of 1.7 to 2.2 nm. The aggregate size then increases upon contacting the organic phase with nitric acid. At a particular concentration of nitric acid (for instance 3 M) in aqueous phase, the average size and the distribution of reverse micellar aggregates in organic phase increases in the order of (TEHDGA + HDEHP) < (TEHDGA + PC88A) < (TEHDGA + CYANEX-272) < TEHDGA, which is the increasing order of pKa of acidic extractants in the binary solution. Since the extraction of nitric acid in organic phase shown in Figure 6.17 increases in the order of TEHDGA+HDEHP) (0.06 M) (< (TEHDGA+PC88A) (0.14 M) < (TEHDGA+CYANEX-272) (0.16 M) < TEHDGA (0.19 M), the average aggregate size observed in the organic phase also increases in same order.

It is important to note that the organic phase containing TEHDGA+CYANEX-272/*n*-DD undergoes splitting, when it was contacted with 6 M nitric acid. Similarly, the organic phase containing TEHDGA+PC88A/*n*-DD and TEHDGA+HDEHP/*n*-DD undergoes splitting when contacted with 8 M and 9 M nitric acid respectively. However, the organic phase containing a solution of TEHDGA in *n*-DD undergoes splitting when contacted with 4 M nitric acid. It is important to recognize from this observation that the addition of acidic extractant to TEHDGA/*n*-DD increases the limiting concentration of nitric acid required for phase splitting.

This is essentially due to the minimization of average aggregate size and their distribution in organic phase, upon adding acidic extractant (which is to be discussed below). The splitting of organic phase leads to the formation of two of phases namely the reverse micellar aggregate-rich third phase, and the diluent-rich phase.

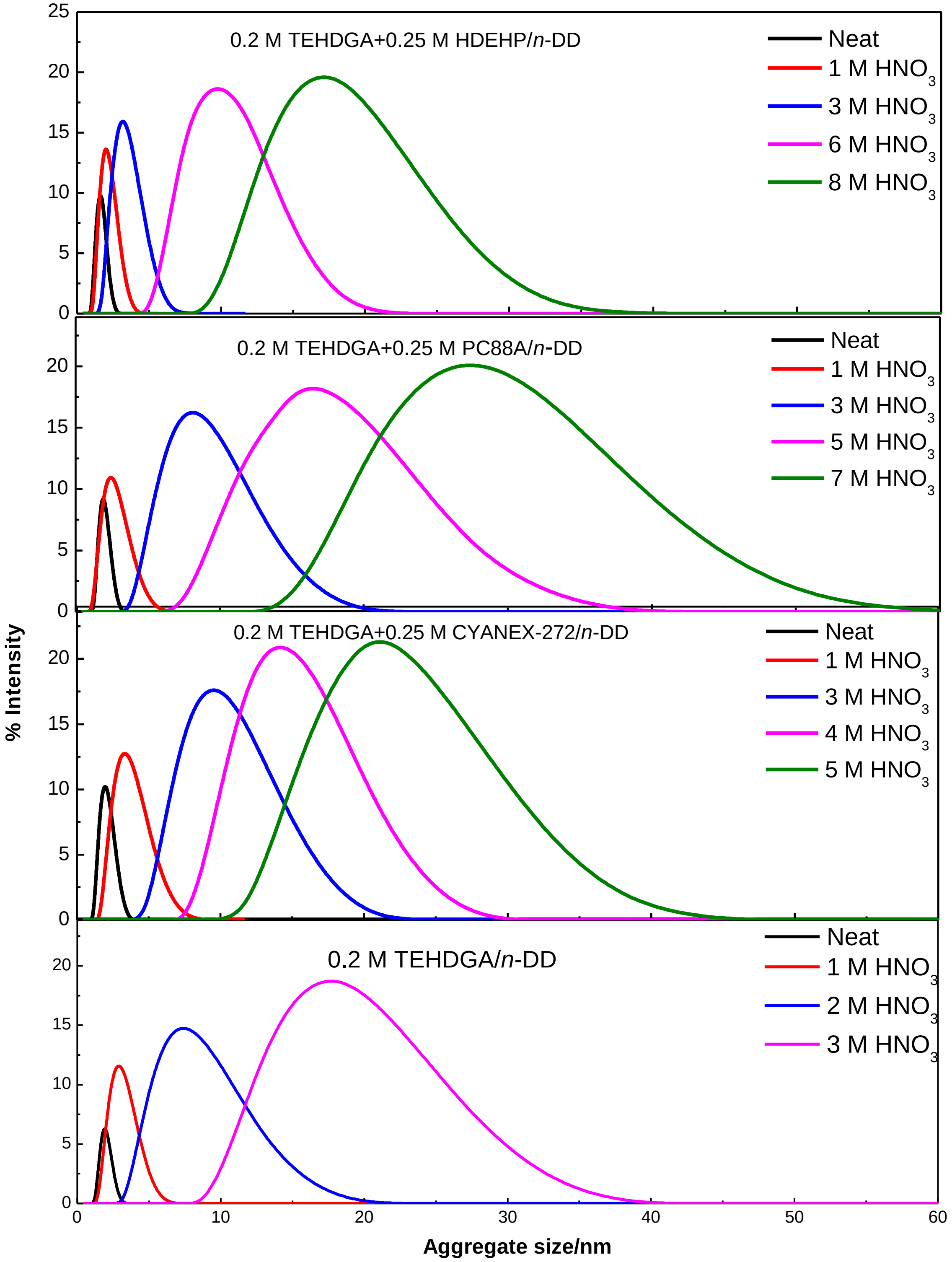
0.2 M TEHDGA+0.25 M HDEHP/n-DD
Neat
1 M HNO3
3 M HNO3
6 M HNO3
8 M HNO3
0.2 M TEHDGA+0.25 M PC88A/n-DD
Neat
1 M HNO3
3 M HNO3
5 M HNO3
7 M HNO3
0.2 M TEHDGA+0.25 M CYANEX-272/n-DD
Neat
1 M HNO3
3 M HNO3
4 M HNO3
5 M HNO3
0.2 M TEHDGA/n-DD
Neat
1 M HNO3
2 M HNO3
3 M HNO3
% Intensity
Aggregate size/nm
0
5
10
15
20
25
0
10
20
30
40
50
60

**Figure 6.18.** Variation in the aggregate size distribution in organic phase as a function of nitric acid concentration in aqueous phase. Organic phase: 0.2 M TEHDGA/*n*-DD or 0.2 M TEHDGA+0.25 M HDEHP/*n*-DD or 0.2 M TEHDGA+0.25 M PC88A/*n*-DD or 0.2 M TEHDGA+0.25 M CYANEX-272/*n*-DD. Aqueous phase: Nitric acid concentration varied from 1 M to 8 M.

### 6.8.3 Limiting aggregate size

Figure 6.19 shows the aggregate distribution of the third phase obtained in all organic solutions. It is observed that the average aggregate size of the third phase is much bigger than that obtained before third phase formation (see Figure 6.18) in all cases. Similarly, the average aggregate size of the diluent-rich phase (Figure 6.19) is much smaller than the aggregate size obtained before third phase formation (Figure 6.18). It is also noted that the intensity of the aggregate distribution observed in third phase is much higher than the diluent-rich phase, indicating that the concentration of aggregates in third phase is much higher than the diluent-rich phase, as discussed in chapters 3 and 4.

The limiting concentration of nitric acid in organic phase (LOC) and aqueous phase (CAC) for third phase formation was determined and the results are displayed in Table 6.5. It can be seen that the LOC of nitric acid for third phase formation increases with decrease in the pKa of the acidic extractant. Figure 6.19 also shows the aggregate distribution of the organic phase determined at LOC. This distribution can be regarded as the limiting aggregate distribution and the average aggregate size can be regarded as the limiting aggregate size (LAS) for third phase formation. It is observed from Table 6.5 that the limiting aggregate size decreases in the order of (TEHDGA + CYANEX-272) > (TEHDGA + PC88A) > (TEHDGA + HDEHP). However, the

LOC and CAC decreases in the opposite direction in the order (TEHDGA+HDEHP) > (TEHDGA+PC88A) > (TEHDGA+CYANEX-272).

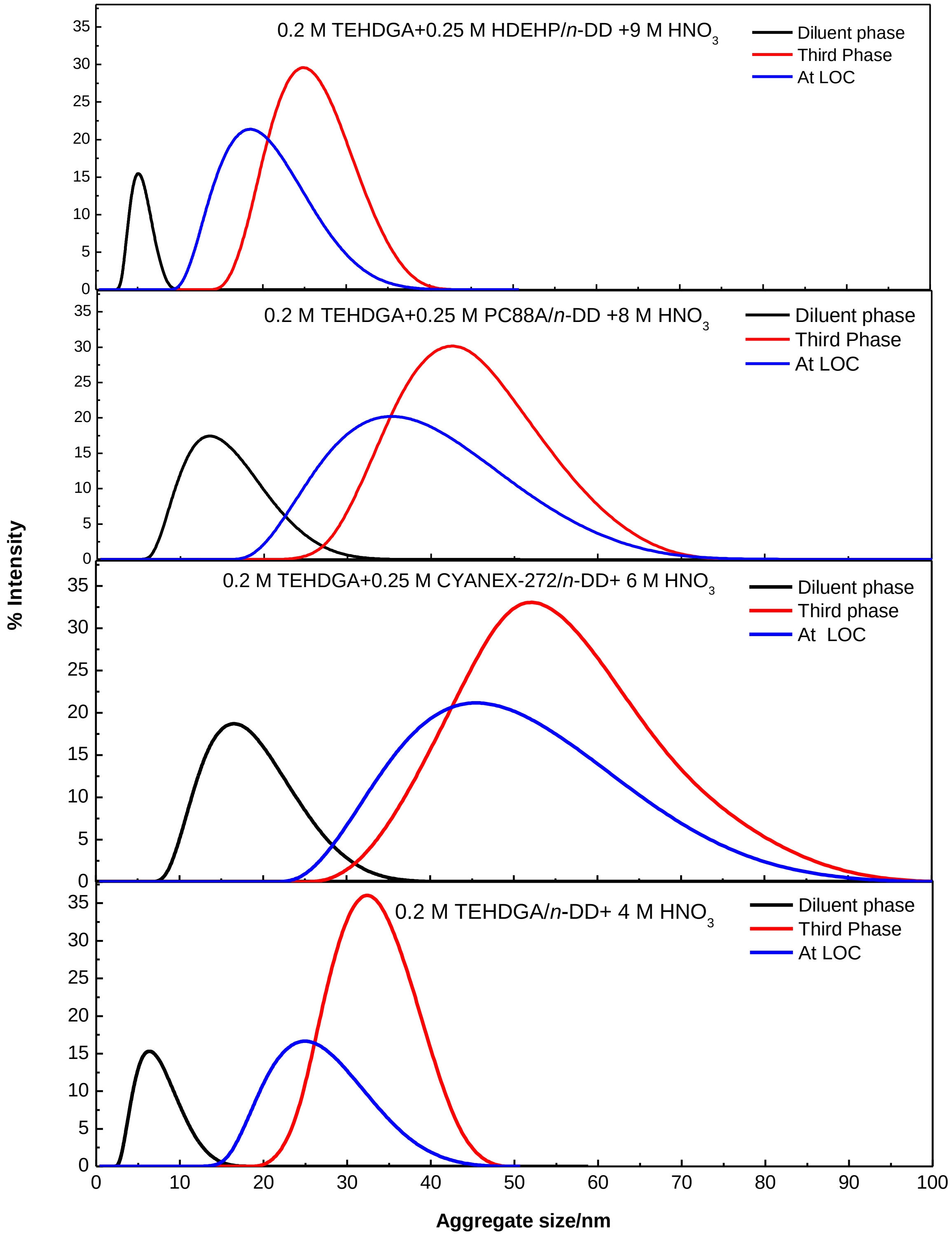
0.2 M TEHDGA+0.25 M HDEHP/*n*-DD +9 M HNO$_3$
Diluent phase
Third Phase
At LOC
0.2 M TEHDGA+0.25 M PC88A/*n*-DD +8 M HNO$_3$
Diluent phase
Third Phase
At LOC
0.2 M TEHDGA+0.25 M CYANEX-272/*n*-DD+ 6 M HNO$_3$
Diluent phase
Third phase
At LOC
0.2 M TEHDGA/*n*-DD+ 4 M HNO$_3$
Diluent phase
Third Phase
At LOC
% Intensity
0
5
10
15
20
25
30
35
0
10
20
30
40
50
60
70
80
90
100
Aggregate size/nm

**Figure 6.19.** Variation in the aggregate size distribution in organic phase obtained after contacting 0.2 M TEHDGA/*n*-DD or 0.2 M TEHDGA+0.25 M HDEHP/*n*-DD or 0.2 M TEHDGA+0.25 M PC88A/*n*-DD or 0.2 M TEHDGA+0.25 M CYANEX-272/*n*-DD with nitric acid concentration ranging from 6 M to 9 M.

**Table 6.5.** The LOC, CAC and LAS values of the binary solution.

| Organic phase/*n*-DD | $pK_a$ of acidic extractant | Initial $[HNO_3]$ / M | LOC/ M | CAC/ M | LAS/nm |
|---|---|---|---|---|---|
| 0.2 M TEHDGA/*n*-DD | - | 4 M | 0.23 | 3.58 | 28.2 |
| 0.2 M TEHDGA+0.25 M CYANEX-272/*n*-DD | 6.37 | 6 M | 0.29 | 5.41 | 38.9 |
| 0.2 M TEHDGA+0.25 M PC88A/*n*-DD | 4.57 | 8 M | 0.41 | 6.72 | 35.5 |
| 0.2 M TEHDGA+0.25 M HDEHP/*n*-DD | 3.24 | 9 M | 0.52 | 8.14 | 19.8 |

### 6.8.4 Extraction behaviour of Nd(III) in 0.2 M TEHDGA+0.25 M HA/*n*-DD

It is learnt from the above discussions that the extraction of nitric acid results in the formation of reverse micellar aggregates and their distribution increased with increase in the concentration of nitric acid. Since TEHDGA coordinates specifically with trivalent metal ion and the presence of an acidic extractant with TEHDGA usually enhances the extraction of trivalent metal ion by synergism [16,17], it can be expected that the aggregate size and the distribution of aggregates in the binary organic phase could increase with increase in the extraction of trivalent metal ion from aqueous phase. To understand this, the extraction behavior of the trivalent metal ion, Nd(III), was studied in the binary solution and the results are discussed below.

The extraction behavior of Nd(III) in the binary solution as a function of Nd(III) concentration in aqueous phase at 1 M nitric acid is shown in Figure 6.20. It is can be seen that the loading of Nd(III) in organic phase increases with increase in the amount of Nd(III) present in aqueous phase. The organic phase containing 0.2 M TEHDGA/*n*-DD undergoes phase splitting when the organic phase was equilibrated with 7g/L Nd(III) in 1 M nitric acid [38]. However, all the binary solutions containing 0.2 M TEHDGA+0.25 M HA/*n*-DD does not undergo any phase splitting even at 7 g/L Nd(III) in 1 M nitric acid. It is also observed from Figure 6.20 that the loading of Nd(III) in organic phase at a particular concentration of Nd(III) in aqueous phase increases in order TEHDGA < (TEHDGA+CYANEX-272) < (TEHDGA+PC88A) < (TEHDGA+HDEHP). The reason for this trend can be attributed to the synergic extraction of Nd(III) in binary solution was discussed in part I of chapter 6.

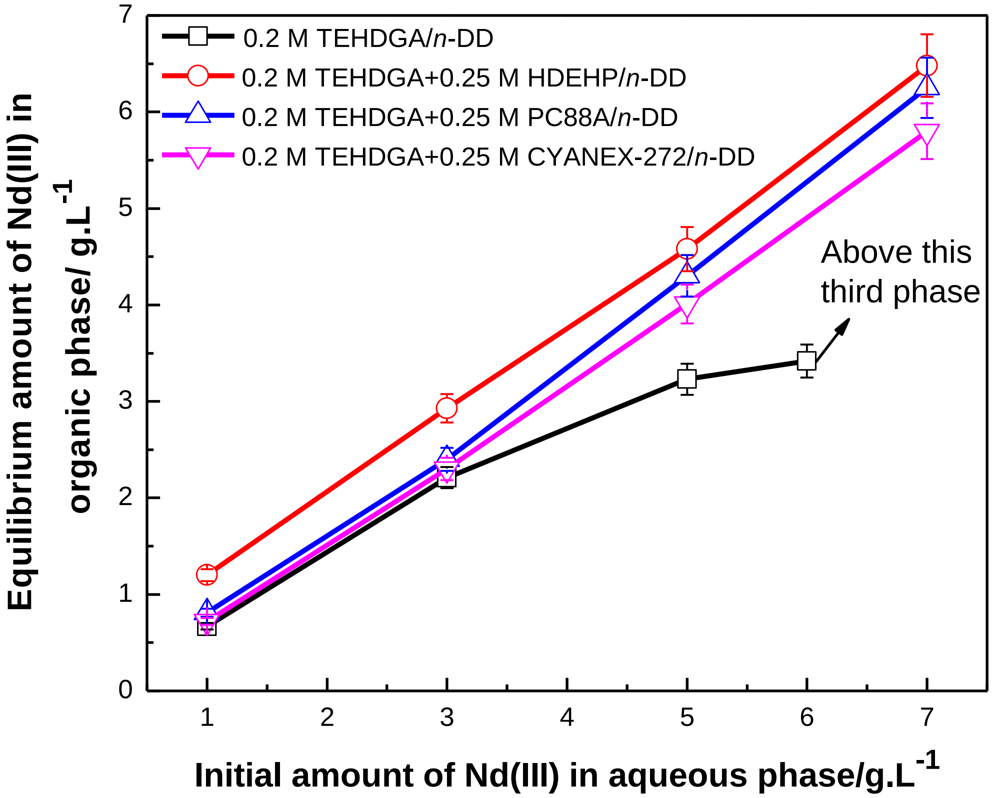

**Figure 6.20.** Variation in the extraction Nd(III) in organic phase as a function of initial amount of Nd(III) in 1 M nitric acid phase. Organic phase: 0.2 M TEHDGA/*n*-DD or 0.2 M TEHDGA+0.25 M HDEHP/*n*-DD or 0.2 M TEHDGA+0.25 M PC88A/*n*-DD or 0.2 M TEHDGA+0.25 M CYANEX-272/*n*-DD. Aqueous phase: $[Nd(III)]_{initial}$ varied from 1 g/L to 7 g/L in 1 M nitric acid.

### 6.8.5 Aggregation in 0.2 M TEHDGA+0.25 M HA/*n*-DD with Nd(III)

Figure 6.21 shows the variation in the average size of reverse micellar aggregates determined in a solution of 0.2 M TEHDGA+0.25 M HA in *n*-DD. The organic phase was contacted with the aqueous solution of Nd(III) in 1 M nitric acid before recording the aggregate distribution. It can be seen from Figure 6.21 that the average aggregate size increases with increase in the amount of Nd(III) in aqueous phase. The average aggregate size at a particular concentration of Nd(III) in aqueous phase increases in the order (TEHDGA+HDEHP) < (TEHDGA+PC88A) < (TEHDGA+CYANEX-272) < TEHDGA, which is the increasing order of the pKa of acidic extractants, 3.24 (HDEHP) < 4.57 (PC88A) < 6.37 (CYNAEX-272). Therefore, the study shows that the presence of an acidic extractant with lower pKa in the binary solution minimizes the average aggregate size to a larger extent.

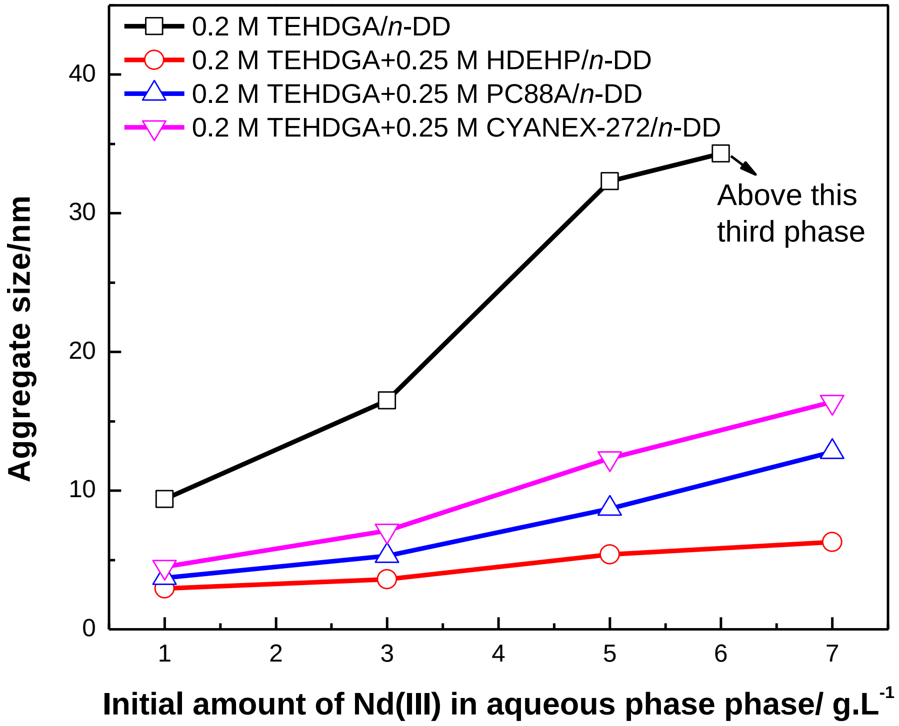

**Figure 6.21.** Variation in the average size of the aggregates produced in organic phase after contacting 0.2 M TEHDGA/*n*-DD or 0.2 M TEHDGA+0.25 M HDEHP/*n*-DD or 0.2 M TEHDGA+0.25 M PC88A/*n*-DD or 0.2 M TEHDGA+0.25 M CYANEX-272/*n*-DD phase with the 1 M nitric acid solution containing Nd(III). The initial amount of Nd(III) in nitric acid was varied from 1 g/L to 7 g/L.

Generally, it is expected that the extraction of nitric acid and Nd(III) in organic phase results in the formation of bigger aggregates in organic phase. In contrast to this, it is observed from Figure 6.21 that the extraction of Nd(III) in binary solution increased in the order (TEHDGA+CYANEX-272) < (TEHDGA+PC88A) < (TEHDGA+HDEHP), whereas average size of reverse micellar aggregates formed in the binary solution decreased in the order (TEHDGA+CYANEX-272) > (TEHDGA+PC88A) > (TEHDGA+HDEHP), as shown in Figure 6.21. This behavior can be attributed to the synergic extraction of Nd(III) in the binary solution. From part I of chapter 6, it is reported that the synergic extraction behavior of Am(III) and Eu(III) in the binary solution containing TEHDGA and HA in *n*-DD, and the involvement of an acidic extractant in the extraction of trivalent metal ion increased in the order of (TEHDGA+CYANEX-272) < (TEHDGA+PC88A) < (TEHDGA+HDEHP). This observation showed that the co-ordination of the acidic extractant molecules with Nd(III) increased in the order of CYNEX-272 < PC88A < HDEHP. Due to the participation of HA, the TEHDGA molecules coordinated to Nd(III) were liberated from the coordination sphere of Nd(III). Since coordination of TEHDGA with Nd(III) was responsible for aggregation in organic phase, the average aggregate size determined in the binary solution decreased in order (TEHDGA+CYANEX-272) > (TEHDGA+PC88A) > (TEHDGA+HDEHP). Moreover, the amount of nitric acid extracted into organic phase is also less in the binary solution containing an acidic extractant having lower pKa values, as shown in Figure 6.17. As a result of lower extraction of nitric acid and higher degree of participation of HA in the extraction of Nd(III) in the binary solution, the average aggregate size decreased in the order of TEHDGA/*n*-DD > (TEHDGA+CYANEX-272)/*n*-DD > (TEHDGA+PC88A)/*n*-DD > (TEHDGA+HDEHP)/*n*-DD. A similar behavior is also observed for the extraction of Nd(III) in the binary solution at 3 M and

5 M nitric acid. The data on the extraction of Nd(III) as a function of Nd(III) aqueous phase and resultant aggregate size are reported in the Figures 6.22 to 6.25, as shown in below.

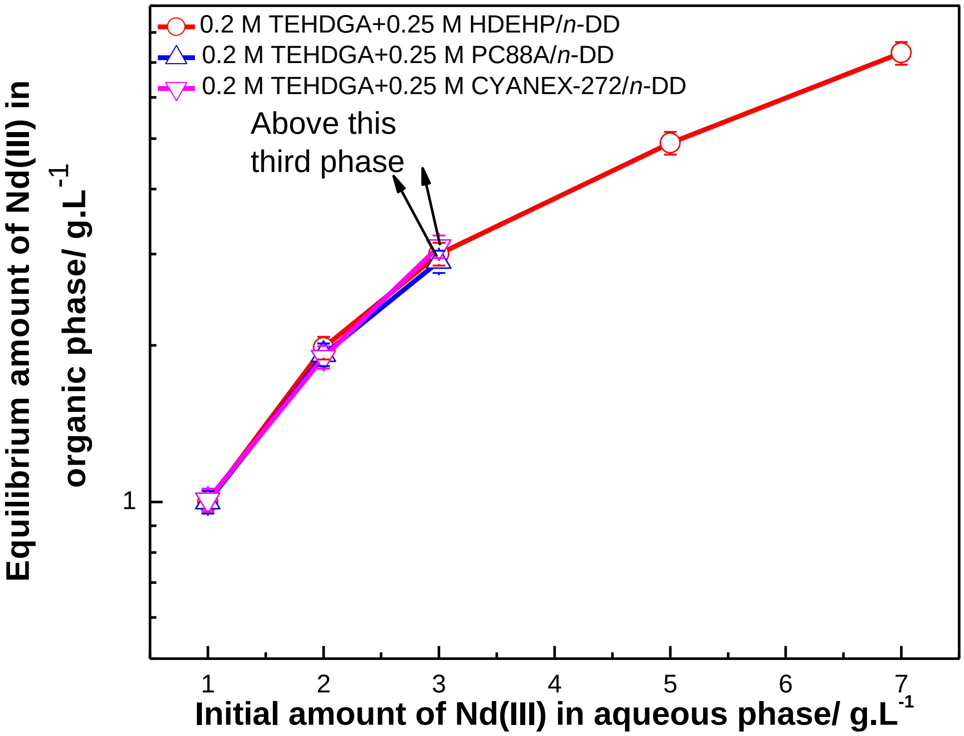

**Figure 6.22.** Variation in the extraction Nd(III) in organic phase as a function of initial amount of Nd(III) in 3 M nitric acid phase. Organic phase: 0.2 M TEHDGA+0.25 M HDEHP/*n*-DD or 0.2 M TEHDGA+0.25 M PC88A/*n*-DD or 0.2 M TEHDGA+0.25 M CYANEX-272/*n*-DD. Aqueous phase: $[\mathrm{Nd(III)}]_{\mathrm{initial}}$ varied from 1 g/L to 7 g/L in 3 M nitric acid.

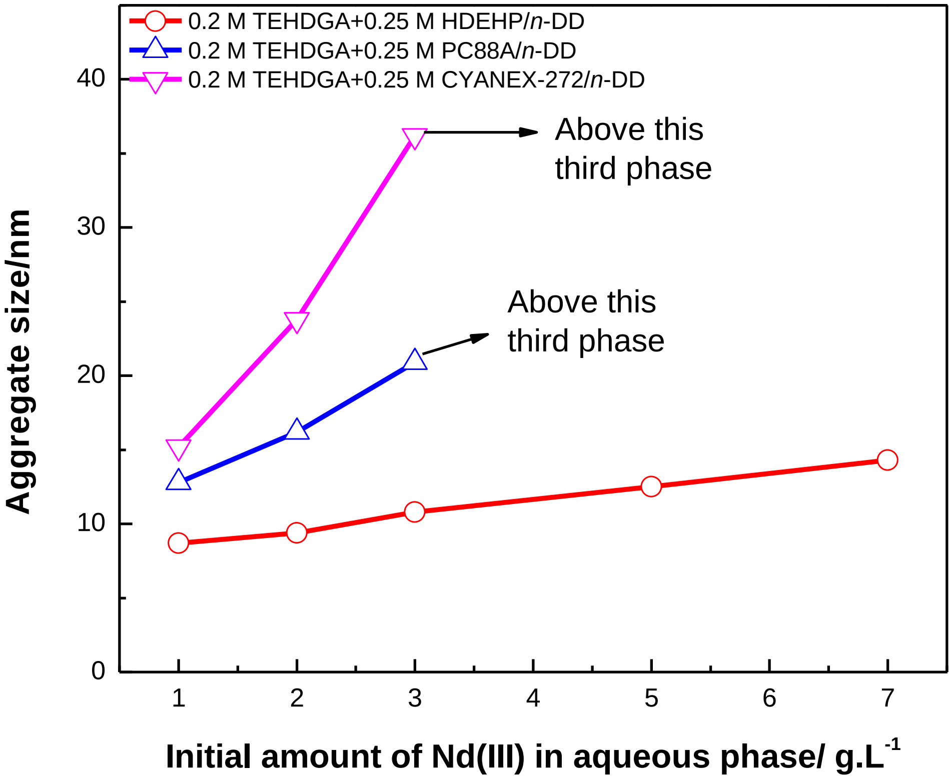

**Figure 6.23.** Variation in the average size of the aggregates produced in organic phase after contacting 0.2 M TEHDGA+0.25 M HDEHP/*n*-DD or 0.2 M TEHDGA+0.25 M PC88A/*n*-DD or 0.2 M TEHDGA+0.25 M CYANEX-272/*n*-DD phase with the 3 M nitric acid solution containing Nd(III). The initial amount of Nd(III) in nitric acid was varied from 1 g/L to 7 g/L.

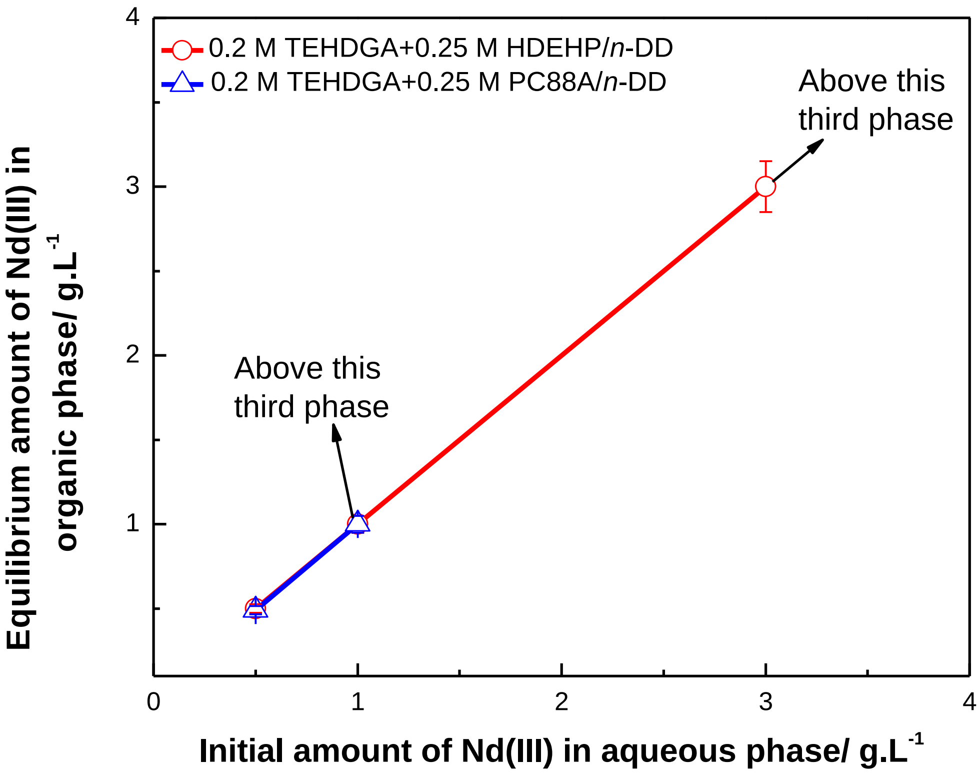

**Figure 6.24.** Variation in the extraction Nd(III) in organic phase as a function of initial amount of Nd(III) in 5 M nitric acid phase. Organic phase: 0.2 M TEHDGA+0.25 M HDEHP/*n*-DD or 0.2 M TEHDGA+0.25 M PC88A/*n*-DD or 0.2 M TEHDGA+0.25 M CYANEX-272/*n*-DD. Aqueous phase: $[\mathrm{Nd(III)}]_{\mathrm{initial}}$ varied from 1 g/L to 3 g/L in 5 M nitric acid.

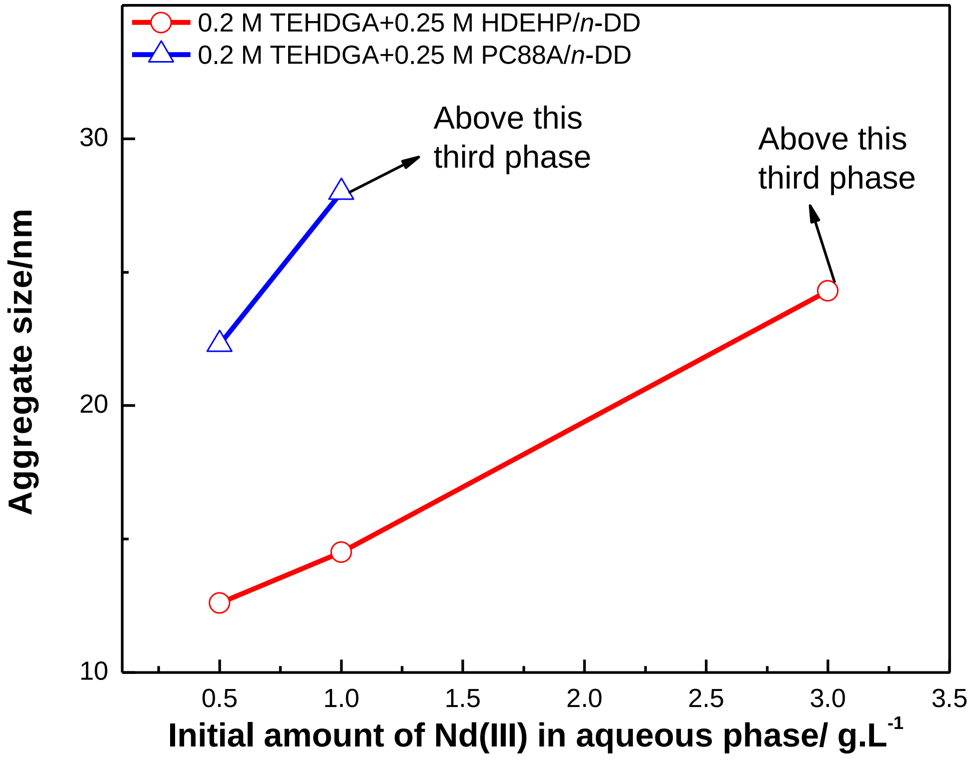

**Figure 6.25.** Variation in the average size of the aggregates produced in organic phase after contacting 0.2 M TEHDGA+0.25 M HDEHP/*n*-DD or 0.2 M TEHDGA+0.25 M PC88A/*n*-DD or 0.2 M TEHDGA+0.25 M CYANEX-272/*n*-DD phase with the 5 M nitric acid solution containing Nd(III). The initial amount of Nd(III) in nitric acid was varied from 1 g/L to 3 g/L.

## 6.9 Summary

The aggregation behavior of the organic phase containing 0.2 M TEHDGA+0.25 M organo phosphorous acid in *n*-DD was investigated by dynamic light scattering technique The added acidic extractant seems to form an adduct with TEHDGA in the order TEHDGA…. CYANEX-272 < TEHDGA…..PC88A < TEHDGA…..HDEHP, which was the decreasing order of the pKa of acidic extractants namely CYNAEX-272 (6.37) < PC88A (4.57) < HDEHP (3.24).

In view of the adduct formation, the extraction of nitric acid in organic phase decreased in the order (TEHDGA+CYANEX-272) > (TEHDGA+PC88A) > (TEHDGA+HDEHP). As a result, the reverse micellar aggregates produced in organic phase increased in the order (TEHDGA+HDEHP) < (TEHDGA+PC88A) < (TEHDGA+CYNEX-272) < TEHDGA.

The addition of acidic extractant to TEHDGA/*n*-DD increased the limiting concentration of nitric acid required for organic phase splitting. The limiting aggregate size determined for phase splitting decreased in the order of (TEHDGA+CYANEX-272) > (TEHDGA+PC88A) > (TEHDGA+HDEHP), which is decreasing order of pKa of acidic extractant. The extraction of Nd(III) in the organic phase increased in the order of TEHDGA < (TEHDGA+CYNEX-272) < (TEHDGA+PC88A) < (TEHDGA+HDEHP), but average aggregate size increased in the reverse order (TEHDGA+HDEHP) < (TEHDGA+PC88A) < (TEHDGA+CYNEX-272) < TEHDGA. The acidic extractant with lower pKa minimized the average size of aggregates produced in the binary solution to a larger extent. The addition of HA to TEHDGA favored synergic extraction of Nd(III) from nitric acid medium and liberated the TEHDGA molecules from coordination sphere of Nd(III). Since coordination of TEHDGA with Nd(III) was responsible for aggregation in organic phase, the average aggregate size decreased in the order TEHDGA > (TEHDGA+CYANEX-272) > (TEHDGA+PC88A) > (TEHDGA+HDEHP).

Therefore, the organic phase composed of a solution of TEHDGA and HDEHP in *n*-DD was found to have several attractive properties suitable for the solvent extraction of trivalent actinides from nuclear waste. They are (a) the presence of HDEHP in organic phase facilitates the extraction of trivalent metal ion from nitric acid medium by synergism, (b) the added HDEHP forms an adduct with TEHDGA to a larger extent and therefore minimizes the protonation of TEHDGA by $HNO_3$. In view of this, the aggregate formation in organic phase was significantly lowered. (c) Due to synergism, the involvement of HDEHP in the extraction of Nd(III) was more as compared to other organo phosphorous acids, and the synergism liberated the co-extractant TEHDGA from the coordination sphere of Nd(III). Since, protonated TEHDGA (acid solvates) or coordinated TEHDGA was responsible for aggregation, the limiting aggregate size (LAS) for third phase formation was significantly reduced in the presence of HDEHP. Therefore, the organic phase composed of TEHDGA and HDEHP in *n*-DD can be regarded as the promising synergic solution for the extraction of trivalent actinides from nuclear waste.

## References

1. J. Veliscek-Carolan, Separation of actinides from spent nuclear fuel: A review, J. Hazard. Mater. 318(2016) 266-281.
2. T. Takeda, Minor actinides transmutation performance in a fast reactor, Ann. Nucl. Energy. 95 (2016) 48-53.
3. S.A. Ansari, P.N. Pathak, P.K. Mohapatra, V.K. Manchanda, Chemistry of diglycolamides: Promising extractants for actinide partitioning, Chem.Rev.112 (2012) 1751-1772.
4. J. N. Mathur, M. S. Murali, K. L. Nash, Actinide partitioning – a review, Solvent Extr. Ion Exch. 19 (2001) 357-390.
5. M. Nilson, K.L. Nash, A review of the development and operational characteristics of the TALSPEAK process, Solvent Extr. Ion Exch. 25 (2007) 665-701.
6. M.J.Zhang, F.W. Lewis, L. M. Harwood, Chapter 6 - The Circuitous Journey from Malonamides to BTPhens: Ligands for Separating Actinides from Lanthanides, In: Michael Harmata, Editor(s), Strategies and Tactics in Organic Synthesis, Academic Press. 9,177-202(2013).
7. A. Zhang, E. Kuraoka, M. Kumagai, Group partitioning of minor actinides and rare earths from highly active liquid waste by extraction chromatography utilizing two macroporous silica-based impregnated polymeric composites, Sep .Purif. Technol. 54 (2007)363-372.
8. S.A. Ansari, D.R. Prabhu, R.B. Gujar, A.S. Kanekar, B. Rajeswari, M.J. Kulkarni, M.S. Murali, Y. Babu, V. Natarajan, S. Rajeswari, A. Suresh, R. Manivannan, M.P. Antony, T.G. Srinivasan, V.K. Manchanda, Counter-current extraction of uranium and lanthanides from simulated high-level waste using N,N,N′,N′-tetraoctyl diglycolamide, Sep. Purif. Technol. 66 (2009) 118-124.

9. G.J. Lumetta, A.V Gelis, F. Vandegrift, Solvent systems combining neutral and acidic extractants for separating trivalent lanthanides from the transuranic elements, Solvent Extr. Ion Exch. 28 (2010) 287-312.
10. G.J. Lumetta, A.V. Gelis, J.C. Braley, J.C. Carter, J.W. Pittman, M.G. Warner, G.F. Vandegrift, The TRUSPEAK concept: combining CMPO and HDEHP for separating trivalent lanthanides from the transuranic elements, Solvent Extr. Ion Exch. 31(2013) 223-236.
11. J.C. Braley, G.J. Lumetta, J.C. Carter, Combining CMPO and HEH [EHP] for separating trivalent lanthanides from the transuranic elements, Solvent Extr. Ion Exch. 31 (2013) 567-577.
12. P.S. Dhami, R.R. Chitnis, V. Gopalakrishnan, P.K. Wattal, A. Ramanujam. A.K. Bauri, Studies on the partitioning of actinides from high level waste using a mixture of HDEHP and CMPO as extractant, Sep. Sci. Technol. 36 (2001) 325-339.
13. B. Gannaz, R. Chiarizia, R.K. Antonio, C. Hill, G. Cote. Extraction of lanthanides(III) and Am(III) by mixtures of malonamide and dialkylphosphoric acid, Solvent Extr. Ion Exch. 25 (2007) 313-337.
14. G. Modolo, R. Odoj. Synergistic selective extraction of actinides(III) over lanthanides from nitric acid using new aromatic diorganyldithiophosphinic acids and neutral organophosphorus compounds., Solvent Extr. Ion Exch.17(1999) 33-53.
15. P.K. Nayak, R. Kumaresan, K.A. Venkatesan, M.P. Antony, P.R. Vasudeva Rao, Extraction behavior of Am (III) and Eu (III) from nitric acid medium in tetraoctyldiglycolamide-bis (2-ethylhexyl) phosphoric acid solution, Sep. Sci. Technol. 49 (2014) 1186-1191.

16. P.K. Nayak, R. Kumaresan, K.A. Venkatesan, S. Rajeswari, G.G.S. Subramanian, M.P. Antony, P.R. Vasudeva Rao, Single-cycle separation of americium (III) from simulated high-level liquid waste using tetra-bis (2-ethylhexyl) diglycolamide and bis (2-ethylhexyl) phosphoric acid solution, J. Environ. Chem. Eng. 1 (2013) 559-565.
17. P.K. Nayak, R. Kumaresan, S. Chaurasia, K.A. Venkatesan, G.G.S. Subramanian, T. Prathibha, K.V. Syamala, B. Robert Selvan, S. Rajeswari, M.P. Antony, P.R. Vasudeva Rao, B.M. Bhanage, Studies on the feasibility of using completely incinerable reagents for the single-cycle separation of americium (III) from simulated high-level liquid waste, Radiochim. Acta. 103 (2015) 265-275.
18. P.K. Nayak, R.Kumaresan, K.A. Venkatesan, M.P. Antony, P.R. Vasudeva Rao, A new method for partitioning of trivalent actinides from high-level liquid waste, Sep. Sci. Technol. 48 (2013) 1409-1416.
19. G.J. Lumetta, A.V. Gelis, J.C. Carter, C.M. Nilver, M.R. Smoot. The Actinide-Lanthanide Separation Concept, Solvent Extr. Ion Exch. 32 (2014) 333-347.
20. A.V. Gelis, G.J. Lumetta. Actinide Lanthanide Separation Process—ALSEP, Ind. Eng. Chem. Res. 53 (2014) 1624-1631
21. J. Ravi, K. A. Venkatesan, M. P. Antony, T. G. Srinivasan, P. R. Vasudeva Rao, Single-cycle method for partitioning of trivalent actinides using completely incinerable reagents from nitric acid medium, Radiochimi. Acta. 102 (2014) 599–607.
22. R.B. Gujar, P.N. Pathak, G.B. Dhekane, P.K. Mohapatra, Extraction of some Hexavalent Actinide Ions from Nitric Acid Medium using Several Substituted Diglycolamides, Solvent Extr. Ion Exch. 32 (2014) 637-649.

23. I. Georgieva, N. Trendafilova, W. Kiefer, V. K. Rastogi, I. Kostova, Vibrational and theoretical study of coumarin-3-carboxylic acid binding mode in Ce (III) and Nd (III) complexes, Vib. Spectrosc. 44 (2007) 78-88.
24. G Świderski,. M. Kalinowska, J. Malejko, W. Lewandowski, Spectroscopic (IR, Raman, UV and fluorescence) study on lanthanide complexes of picolinic acid, Vib. Spectrosc. 87(2016) 81-87.
25. Y. Liu, M. S. Lee, Effect of the diluents on the interaction between components in the binary mixtures of organophosphorus acid and tertiary amine J. Mol. Liq. 220 (2016) 41-48.
26. H. G. M. Edwards, E. Hickmott, M. A. Hughes, Vibrational spectroscopic studies of potential amidic extractants for lanthanides and actinides in nuclear waste treatment. Spectrochim. Acta A.1 (1997) 43-53.
27. P. Tkac, G. F. Vandegrift, G. J. Lumetta, A. V. Gelis,. Study of the interaction between HDEHP and CMPO and its effect on the extraction of selected lanthanides, Ind. Eng.Chem. Res. 51 (2012) 10433-10444.
28. Y. Liu, M. S. Lee, Analysis of the interaction between organophosphorus acid and tertiary amine extractants in the binary mixtures by Fourier Transform Infrared Spectroscopy (FT-IR), Solvent Extr. Ion Exch. 34 (2016) 74-85.
29. C. Musikas, H. Hubert, Extraction by N,N'-Tetraalkylmalonamides II. Solvent Extr. Ion Exch. 5 (1987) 877-893.
30. T. Prathibha, K. A. Venkatesan, B. Robert Selvan, M. P. Antony, P.R. Vasudeva Rao, Anomalous extraction behavior of americium (III) in some diglycolamide isomers present in ionic liquid medium, Radiochim. Acta. 100 (2012) 907-914.

31. Y. Cui, J. Yang, G. Yang, G. Xia, Y. Nie, G. Sun, Effect of diluents on extraction behavior of rare earth elements with N, N, N′, N′-tetrabutyl-3-oxy-glutaramide from hydrochloric acid, Hydrometallurgy. 121 (2012) 16-21.
32. P. Deepika, K.N. Sabharwal, T.G. Srinivasan, P.R. Vasudeva Rao, Studies on the use of N,N,N’N’-tetra(2-ethylhexyl) diglycolamide (TEHDGA) for actinide partitioning I: Investigation on third-phase formation and extraction behavior, Solvent Extr. Ion Exch. 28 (2010) 184–201.
33. S. Kannan, M.A. Moody, C.L. Barnes, P.B. Duval, Lanthanum (III) and uranyl (VI) diglycolamide complexes: synthetic precursors and structural studies involving nitrate complexation, Inorg. Chem.47 (2008) 4691-4695.
34. J. M. Muller, C. Berthon, L. Couston, N. Zorz, J.P. Simonin, L. Berthon, Extraction of Lanthanides (III) by a Mixture of a Malonamide and a Dialkyl Phosphoric Acid, Solvent Extr. Ion Exch. 2(2016)141-160.
35. G.J. Lumetta, D. Neiner, S.I. Sinkov, J.C. Carter, J.C. Braley, S.L. Latesky, A.V. Gelis, P. Tkac, and G.F. Vandegrift, Proceedings of the 19th International Solvent Extraction Conference, Gecamin Ltda, Santiago, Chile, Paper No. 68, 2011.
36. P. Calandra, M. Passarello, A. Ruggirello, V.T. Liveri, Fast proton conduction in hydrogen bonded microheterogeneous systems: Bis (2-ethylhexyl) phosphoric acid/N-methyl formamide liquid mixtures, J. Colloid. Interface. Sci. 343 (2010)149-154.
37. A. Paulenova, Organic Speciation and Interactions in ALSEP. One Step Partitioning Process of Minor Actinides, Lanthanides, and Fission Products, 2018 (No. DOE/NEUP-13-5124). Oregon State Univ., Corvallis, OR (United States); Argonne National Lab.(ANL), Argonne, IL (United States).

38. P. Deepika, K.N. Sabharwal, T.G. Srinivasan, P.R. Vasudeva Rao, Studies on the use of N, N, N, N-tetra(2-ethylhexyl) diglycolamide (TEHDGA) for actinide partitioning. I: Investigation on third-phase formation and extraction behavior, Solvent Extr. Ion Exch. 28 (2010) 184-201.
39. R.B. Gujar, S.A. Ansari, A. Bhattacharyya, A.S. Kanekar, P.N. Pathak, P.K. Mohapatra, V.K. Manchanda, Radiolytic stability of N, N, N′, N′-tetraoctyl diglycolamide (TODGA) in the presence of phase modifiers dissolved in *n*-dodecane, Solvent Extr. Ion Exch. 30 (2012) 278-290.
40. D. Whittaker, A. Geist, G. Modolo, R. Taylor, M. Sarsfield, A. Wilden, Applications of diglycolamide based solvent extraction processes in spent nuclear fuel reprocessing, part 1: TODGA, Solvent Extr. Ion Exch. 36(2018) 223-256.
41. P.W. Huang, C.Z. Wang, Q.Y. Wu, J.H. Lan, G. Song, Z.F. Chai, W.Q. Shi, Theoretical studies on the synergistic extraction of $Am^{3+}$ and $Eu^{3+}$ with CMPO–HDEHP and CMPO–HEH [EHP] systems, Dalton Trans. 47 (2018) 5474-5482.

# Chapter 7: Single-cycle separation of trivalent actinides from nitric acid medium using hydoxyacetamide-acidic extractant solvent system and the aggregation behavior of organic phase

Partitioning of trivalent actinides (An(III) = Am(III) and Cm(III)) from high-level liquid waste followed by transmutation (P&T strategy) of them into stable or short-lived products in accelerated driven systems or fast-reactors is a viable option for minimizing the radiotoxicity of HLLW [1,2]. However, the partitioning procedure involves a challenging job of separating trivalent actinides from chemically similar lanthanides present in 3-4 M nitric acid medium of HLLW [3,4]. The current approach for partitioning of trivalent actinides involves a two-cycle procedure. The first-cycle is the group separation of trivalent lanthanides and actinides from HLLW, and second-cycle aims at the mutual separation of lanthanides and actinides from the product of the first-cycle [4-9]. In the recent past, research in this area is focused on the development of single-cycle approaches for partitioning of trivalent actinides directly from HLLW for minimizing the waste generation [10-12].

A couple of single-cycle methods have been reported in literature for the separation of trivalent actinides. The first method involves the direct separation of trivalent actinides from HLLW using a polydentate nitrogen donor ligands [10] and S-donor ligands [11,12]. The details of direct separation of trivalent actinides from HLLW using soft donor ligands were discussed in chapter-1. The other method involves group separation of lanthanides and actinides together from 3-4 nitric acid solution using a combination of extractants composed of neutral and acidic extractants followed by selective stripping of actinides alone from the loaded organic phase [13-19]. The details of experimental systems containing TEHDGA and acidic extractants and the results on the separation of Am(III) from Eu(III) have been discussed in chapter-6.

In continuation of this method, the present chapter deals with the employment of *N*,*N*-dioctyl-2-hydroxyacetamide (DOHyA) as neutral extractant and various acidic extractants in *n*-DD for the single-cycle separation of trivalent actinides from nitric acid solution containing Eu(III). This chapter is divided into three parts (Part I, Part II and Part III). Part I discusses the extraction behaviour of Am(III) and Eu(III) in DOHyA+HDEHP/*n*-DD. Part II describes the extraction behavior of Am(III) and Eu(III) in a solvent phase containing completely incinerable ligands such as DOHyA+HDEHDGA in *n*-DD and part III discusses the aggregation behavior of the organic phase containing DOHyA and HDEHDGA in *n*-DD and the acid and extracted organic phase.

# Part I. The extraction behavior of Am(III) and Eu (III) in DOHyA-HDEHP solvent system

## 7.1 Introduction

Several combinations of neutral and acidic extractants have been reported in the literature for the single-cycle separation of trivalent actinides from HLLW. Most of the neutral extractants employed in single-cycle methods suffered from the limitations of third phase formation and extraction of unwanted metal ions from HLLW. The neutral extractants such as diglycolamides (DGA) also showed good extraction of trivalent metal ions even at 0.1 M nitric acid, which causes problems during stripping of the metal ions [20,21]. To resolve these issues, *N*,*N*-dioctyl-2-hydroxyacetamide (DOHyA) has been identified as a neutral ligand for the extraction of trivalent metal ions [20,21]. The major advantage of hydroxyacetamide as compared to TODGA and TEHDGA is that DOHyA does not require any phase modifier for the separation of trivalent metal ions from nitric acid medium. Moreover, it was possible to recover the extracted metal ions even at 1 M nitric acid in this case. The advantages of using DOHyA from trivalent group (Ln and An) is described elsewhere [20]. In the present chapter, a binary solution composed of DOHyA and HDEHP has been evaluated for the separation of Am(III) from nitric acid solution containing Eu(III) ion. The extraction behavior of Am(III) and Eu(III) in a binary solution phase composed of 0.2 M DOHyA + 0.25 M HDEHP/*n*-DD as well as in the individual solutions 0.2 M DOHyA/*n*-DD and 0.25 M HDEHP/*n*-DD was studied as a function of nitric acid concentration. The structure of the extractants used in the present study is shown in Figure 7.1.

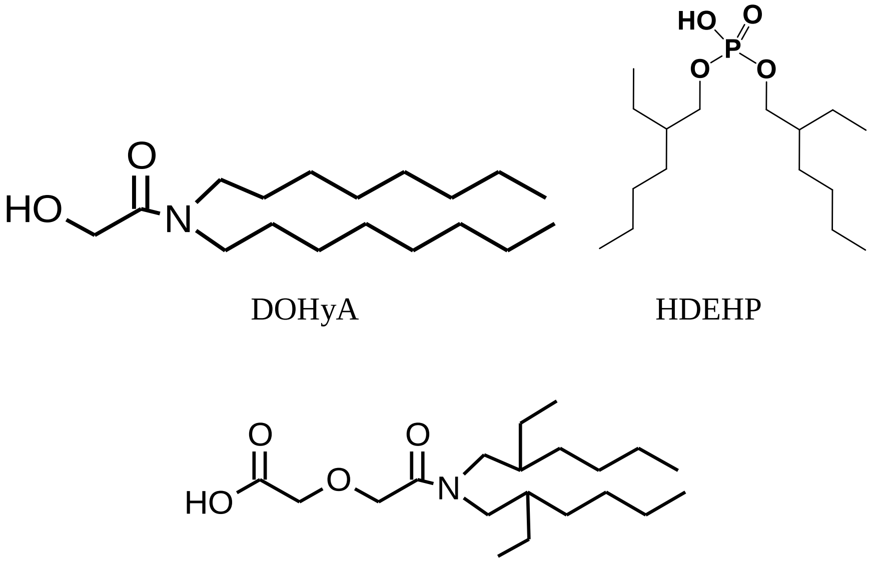

DOHyA HDEHP

HDEHDGA

**Figure 7.1.** Structures of DOHyA, HDEHP and HDEHDGA.

## 7.2 Results and discussion

### 7.2.1 Synergistic extraction of Am(III) and Eu(III)

The variation in the distribution ratio of Am(III) and Eu(III) in 0.2 M DOHyA/*n*-DD studied as a function of nitric acid concentration in aqueous phase is shown in Figures 7.2 and 7.3, respectively. It is observed that the distribution ratio of Am(III) and Eu(III) increases with increase in the concentration of nitric acid. To understand the number of molecules of DOHyA involved in the extraction of Am(III) and Eu(III) in organic phase at 3 M nitric acid, the variation in the distribution ratio of these metal ions as a function of DOHyA concentration in organic phase was studied and the logarithmic plot of distribution ratio against DOHyA concentration is shown in Figure 7.4. It can be seen that the distribution ratio increases with increase in the concentration of DOHyA. Linear regression analysis of the extraction data results in the slope of 5 to 6. This indicates that 5-6 molecules of DOHyA are involved in the extraction of Am(III) and Eu(III) from nitric acid medium. Previously, Prathibha *et al.*, and Kannan *et al.*, independently studied the extraction of Am(III) in dialkyl-hydroxyacetamide and reported a similar metal – solvate stoichiometry of 1:5 and 1:6 [20,21]. The number of nitrate ions involved in the extraction was determined by variation of concentration of nitrate at 3 M nitric acid. The logarithmic plot of distribution ratio of Am(III) and Eu(III) against nitrate concentration yielded a slope of 3.3 and 3.2 respectively as shown in Figure 7.5. This indicated that about three nitrate ions participated in the extraction of Am(III) and Eu(III) in DOHyA/*n*-DD system. In view of this, the extraction of trivalent metal ion ($M^{3+}$= $Am^{3+}$and $Eu^{3+}$) in DOHyA/*n*-DD can be described by the equation 7.1.

$$\mathrm{M}_{\mathrm{aq}}^{3+} + 3(\mathrm{NO}_3^-)_{aq} + 5-6\,\mathrm{DOHyA}_{\mathrm{org}} \Leftrightarrow (\mathrm{M}(\mathrm{NO}_3)_3(\mathrm{DOHyA})_{5\text{-}6})_{org} .......(7.1)$$

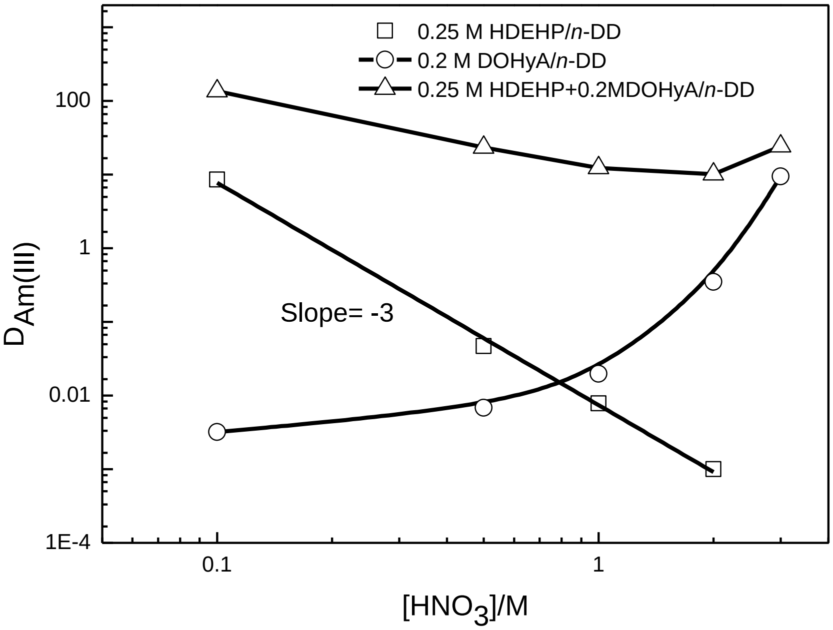

**Figure 7.2.** Variation in the distribution ratio of Am(III) as a function of nitric acid concentration. Organic phase: 0.2 M DOHyA/*n*-DD or 0.25 M HDEHP/*n*-DD or 0.2 M DOHyA + 0.25 M HDEHP/*n*-DD. Aqueous phase: Nitric acid spiked with $^{(241)}$Am(III).

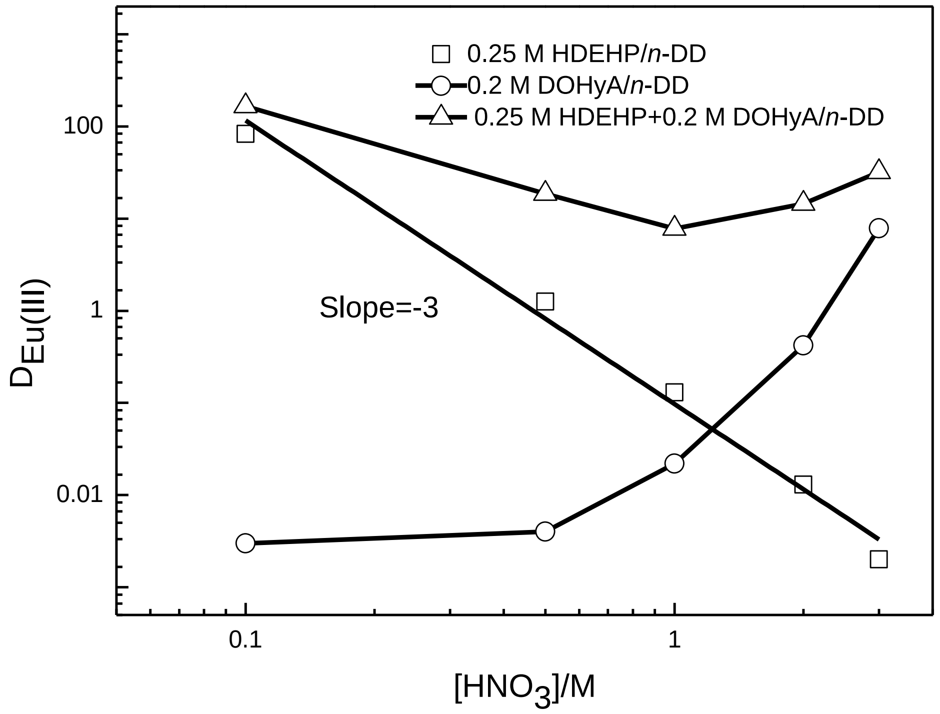

**Figure 7.3.** Variation in the distribution ratio of Eu(III) as a function of nitric acid concentration. Organic phase: 0.2 M DOHyA/*n*-DD or 0.25 M HDEHP/*n*-DD or 0.2 M DOHyA + 0.25 M HDEHP/*n*-DD. Aqueous phase: Nitric acid spiked with $^{(152+154]}$ Eu(III) tracer.

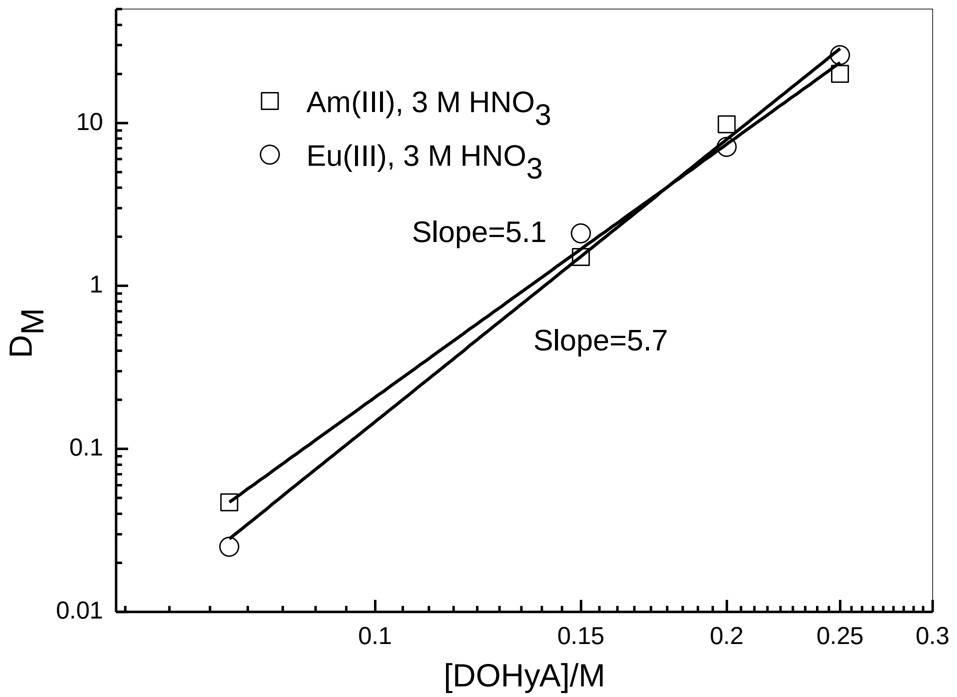

**Figure 7.4.** Variation in the distribution ratio of Am(III) and Eu(III) as a function of DOHyA concentration. Organic phase: DOHyA/*n*-DD. Aqueous phase: 3 M Nitric acid spiked with $^{(241)}$Am(III) or $^{(152+154)}$Eu(III) tracer. [DOHyA] varied from 0.075 M to 0.25 M.

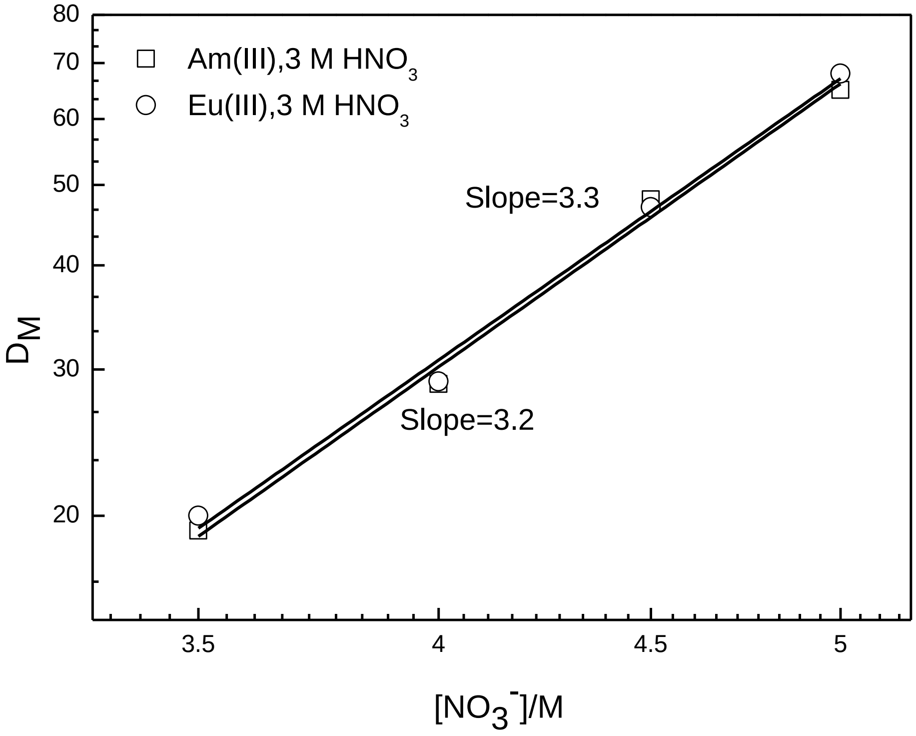

**Figure 7.5**. Variation in the distribution ratio of Am(III) and Eu(III) as a function of nitrate ion concentration. Organic phase: 0.2 M DOHyA /*n*-DD. Aqueous phase: $NaNO_3$ present in 3 M nitric acid spiked with $^{(241)}$Am(III) or $^{(152+154)}$Eu(III) tracer. [$NaNO_3$] varied from 0.5 M to 2 M.

Bis(2-ethylhexyl)phosphoric acid (HDEHP) is a well-known acidic extractant employed for the mutual separation of Am(III) and Eu(III) from dilute nitric acid medium as discussed in chapter 1and chapter 6. The logarithmic plots of variation in the distribution ratio of Am(III) and Eu(III) in HDEHP as a function of nitric acid concentration in the aqueous phase are shown in Figures 7.2 and 7.3 respectively. It can be seen that the distribution ratio decreases with increase in the concentration of nitric acid in both cases, as expected. Linear regression of the extraction data resulted in a slope of -3 for the both Am(III) and Eu(III), indicating the involvement of three molecules of HDEHP in the extraction of three trivalent metal ion is shown in equation 7.2

as discussed in chapter 6. Since HDEHP exists as dimer in aliphatic diluents it is represented in dimeric [22,23] form in equation 7.2

$$\mathrm{M_{aq}}^{3+} + (3\,(\mathrm{HDEHP})_2)_{org} \Leftrightarrow (\mathrm{M(DEHP.\,HDEHP)}_3)_{org} + 3\mathrm{H^+}_{aq} \qquad \text{………} \ (7.2)$$

The extraction behavior of Am(III) and Eu(III) in the combined solvent system composed of 0.2 M DOHyA and 0.25 M HDEHP in *n*-DD was studied and results are displayed in Figures 7.2 and 7.3. It is observed that the distribution ratio of Am(III) and Eu(III) decreases with increase in the concentration of nitric acid reaches a minimum value of distribution ratio at 1-2 M nitric acid followed by increase in distribution ratios. It should be noted that the distribution ratio of Am(III) and Eu(III) achieved in the combined solvent system is higher than that achieved in individual solvents. The degree of synergism can be expressed using synergic coefficient (SC) shown in equation 7.3.

$$\text{Synergistic Coefficient (SC)} = \frac{\text{D of Metal in (0.25 M HDEHP+ 0.2 M DOHyA/}n\text{-DD)}}{\text{D of Metal in 0.25 M HDEHP/}n\text{-DD+ D of Metal in 0.2 M DOHyA/}n\text{-DD}} \qquad \text{……….} \ (7.3)$$

Table 7.1 shows the synergic coefficient of Am(III) and Eu(III) calculated using equation 7.3. It can be seen that the SC increases with increase in concentration of nitric acid and decreases beyond 1 M $HNO_3$. A maximum SC of 62 and 50 are obtained for Am(III) and Eu(III) respectively at 1 M nitric acid concentration. It should be noted that SC is higher for Am(III) than Eu(III) at all nitric acid concentration. The synergism observed in the present study indicates the participation of both ligands in the extraction of Am(III) and Eu(III) at all nitric acid concentrations. Therefore, it is essential to determine the possible metal-solvate complexes in the combined solvent systems. Several methods have been reported in literature for determining the composition of metal-solvates in the organic phase in combined solvent systems [22,23]. However, slope-analysis method is the one of the simple methods for examining the composition of metal complexes.

**Table 7.1.** Calculated synergistic coefficient (SC) for Am(III) and Eu(III) in 0.2 M DOHyA + 0.25 M HDEHP/*n*-DD at various nitric acid concentration.

| $[HNO_3]$/M | Synergistic coefficient for Am(III) | Synergistic coefficient for Eu(III) |
|---|---|---|
| 0.1 | 15.9 | 2.0 |
| 0.5 | 48.8 | 14.7 |
| 1 | 61.5 | 50.0 |
| 2 | 29.3 | 22.1 |
| 3 | 2.6 | 4.1 |

### 7.2.2 Extraction mechanism

#### 7.2.2.1 Extraction mechanism at 0.5 M nitric acid

The synergism observed in the combined solvent system can be investigated by the slope analysis of the extraction data and nature of metal-solvate complex at three different acidities, one at lower acidity (0.5 M nitric acid) and the other at higher acidity (1M and 3.0 M nitric acid). Since the extraction of Am(III) and Eu(III) at lower nitric acid concentration is significantly low in DOHyA/*n*-DD as compared to that observed in HDEHP/*n*-DD, as shown in Figure 7.2, the acidic extractant seems to play a predominant role in the extraction of Am(III) and Eu(III) at low nitric acid concentration. To understand the role of HDEHP in the combined extractant system at 0.5 M nitric acid concentration, the distribution ratio of Am(III) and Eu(III) was measured at various concentration of HDEHP in the binary solvent 0.2 M DOHyA + HDEHP/*n*-DD. The results are shown in Figure 7.6. The concentration of HDEHP was varied from 0.05 M to 0.25 M. It can be seen that the distribution ratio of Am(III) and Eu(III) increases with increase in the concentration of HDEHP. Slope analysis of the extraction data gave a slope of about 1.7 for both Am(III) and Eu(III).

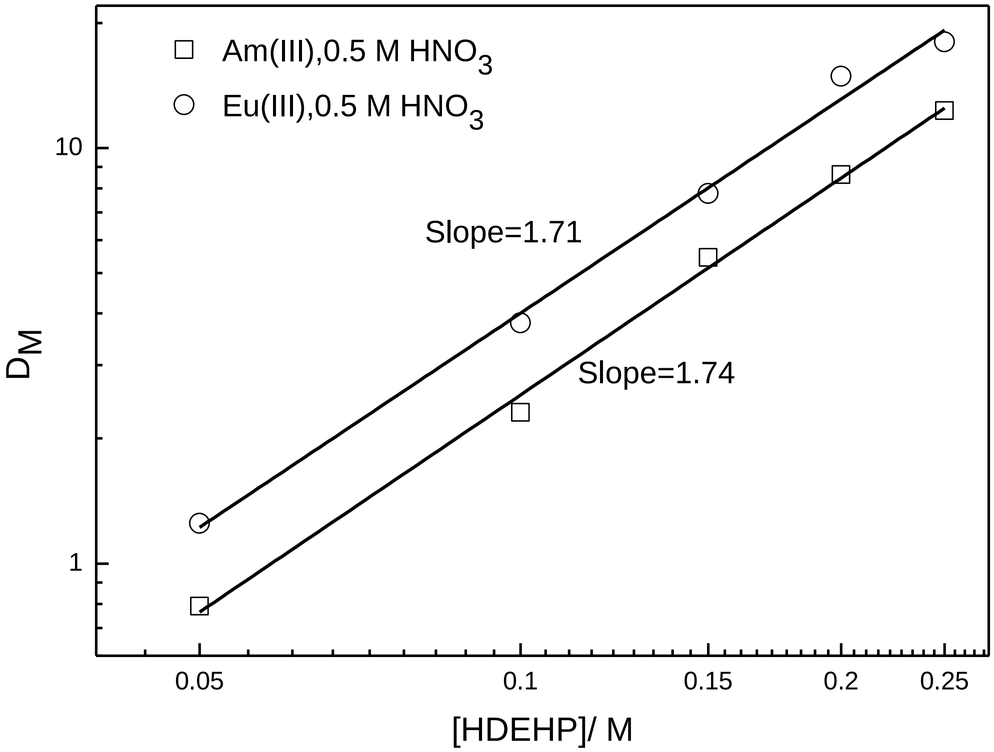

**Figure 7.6.** Variation in the distribution ratio of Am(III) and Eu(III) as a function of HDEHP concentration. Organic phase: 0.2 M DOHYA+ HDEHP/*n*-DD. Aqueous phase: 0.5 M Nitric acid spiked with $^{(241)}$Am(III) or $^{(152+154)}$Eu(III) tracer. [HDEHP] varied from 0.05 M to 0.25 M.

This indicates that the extraction of Am(III) and Eu(III) was accompanied by the release of two protons (approximately 1:2 metal stoichiometry) from the combined extractants system. This value is lower than the metal- solvate stoichiometry of 1:3, when HDEHP alone was used for extraction (see Figures 7.2 and 7.3). In synergism, it can be expected that both extractants can coordinate with the metal ion leading to the formation of mixed species. Therefore, it is necessary to understand the role of DOHyA at low nitric acid concentration in the combined solvent system. This can be studied by keeping the concentration of HDEHP (0.25 M HDEHP/*n*-DD) constant in the combined solvent and varying the DOHyA concentration. Figure 7.7 shows the variation in the distribution ratio of Am(III) and Eu(III) as a function of DOHyA concentration in the combined solvent at 0.5 M nitric acid concentration. The concentration of DOHyA was varied from 0.05 M to 0.25 M in the combined solvent system. The D value increases linearly with increase in the concentration of DOHyA.

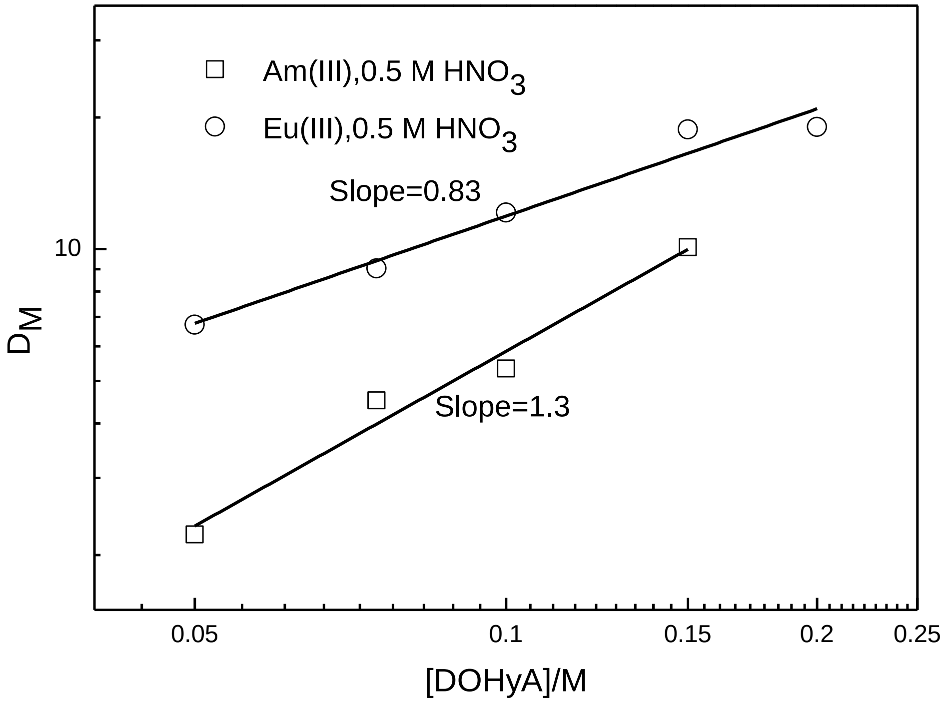

**Figure 7.7.** Variation in the distribution ratio of Am(III) and Eu(III) as a function of DOHyA concentration. Organic phase: DOHyA +0.25 M HDEHP/*n*-DD. Aqueous phase: 0.5 M Nitric acid spiked with $^{(241)}$Am(III) or $^{(152+154)}$Eu(III) tracer. [DOHyA] varied from 0.05 M to 0.2 M.

A slope value of 1.3 is observed for Am(III) and 0.85 for Eu(III). This result clearly shows the involvement or participation of the neutral extractant (DOHyA) even at low nitric acid concentration (0.5 M) in a combined extraction system. Based on this result the equilibrium reaction for the extraction of trivalent metal ions at low nitric acid concentration in the combined solvent can be given by equation 7.4. To maintain the electro-neutrality of the extracted species, a nitrate ion was included in the equation 7.4. The involvement of nitrate ion in the extraction of Am(III) and Eu(III) was also confirmed by studying the effect of nitrate ion concentration on the extraction of Am(III) and Eu(III) in the combined solvent system at 0.5 M nitric acid. The total nitrate ion concentration was varied from 1 M to 2.5 M using sodium nitrate solution. The results are shown in Figure 7.8. It is observed that the D values increases with increase in the concentration of nitrate ion in aqueous phase. A slope of ~ 0.5 is obtained from the plot indicates the involvement of nitrate ion in the extraction of Am(III) and Eu(III) in the binary solution at low nitric acid concentration.

$$\mathrm{M^{3+} + DOHyA} + x\,\mathrm{HDEHP} + (3-x)\,\mathrm{NO_3^-} \Leftrightarrow \mathrm{M(DEHP)_x(NO_3^-)_{3-x}(DOHyA) + x\,H^+} \quad \textit{at low acidity}.\ \mathrm{x = 1\text{-}2}. \qquad (7.4)$$

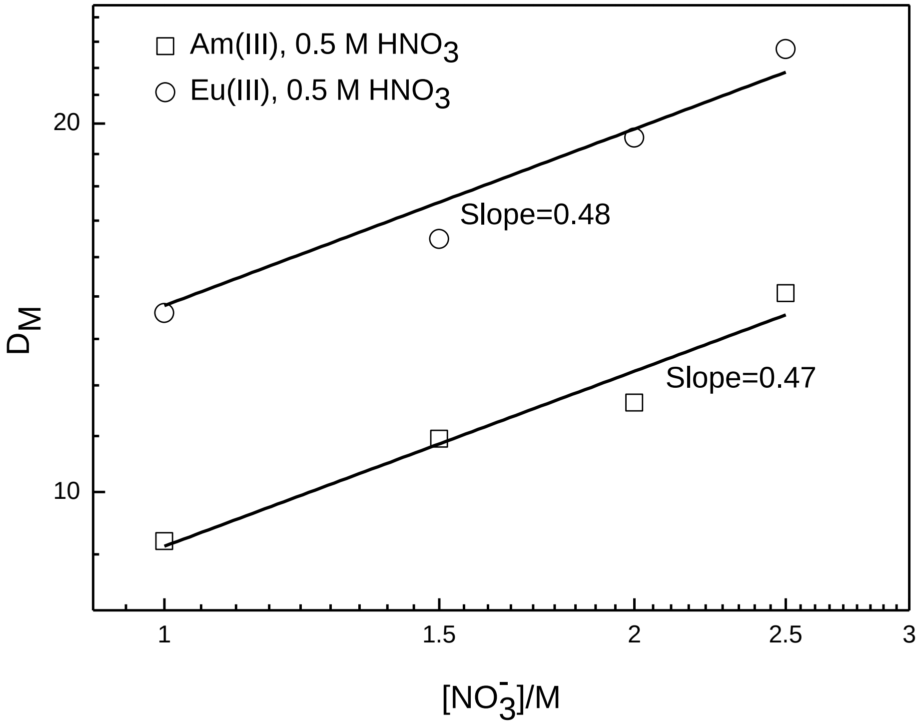

**Figure 7.8.** Variation in the distribution ratio of Am(III) and Eu(III) as a function of nitrate ion concentration. Organic phase: 0.2 M DOHyA +0.25 M HDEHP/*n*-DD. Aqueous phase: $NaNO_3$ present in 0.5 M nitric acid spiked with $^{(241)}$Am(III) or $^{(152+154)}$Eu(III) tracer. [$NaNO_3$] varied from 0.5 M to 2 M.

### 7.2.2.2 Extraction mechanism at 1 M and 3 M nitric acid

The dependency of DOHyA on the extraction of Am(III) and Eu(III) in the binary extractant system at 1 M and 3 M nitric acid concentration was studied by measuring the D value of Am(III) and Eu(III) as a function of DOHyA concentration in DOHyA+0.25 M HDEHP/n-DD. The concentration of DOHyA was varied from 0.05 M to 0.25 M. The results are presented in Figure 7.9. It is observed that the distribution ratio of Am(III) and Eu(III) increases with increase in the concentration of DOHyA concentration. A slope value of 2.0 and 1.6 was obtained for the extraction of Am(III) and Eu(III) respectively in the combined solution at 1 M

$HNO_3$. At 3 M nitric acid, a slope value of 2.7 and 2.4 was obtained for Am(III) and Eu(III) respectively. Higher slope value obtained at 3 M nitric acid as compared to 1 M nitric acid indicates the involvement of DOHyA in the extraction of Am(III) and Eu(III) is more at 3 M nitric acid. However, a slope of 5-6 was obtained for the extraction of Am(III) and Eu(III) in DOHyA/*n*-DD (Figure 7.4). A lower slope value obtained in a combined extractant system at 1 and 3 M nitric acid concentration as compared to the individual extractant system (5 to 6 molecules) indicates that the number of DOHyA molecules involved in the extraction decreases with the addition of HDEHP. It also indicates that HDEHP could be participating in the extraction of Am(III) and Eu(III) due to synergism.

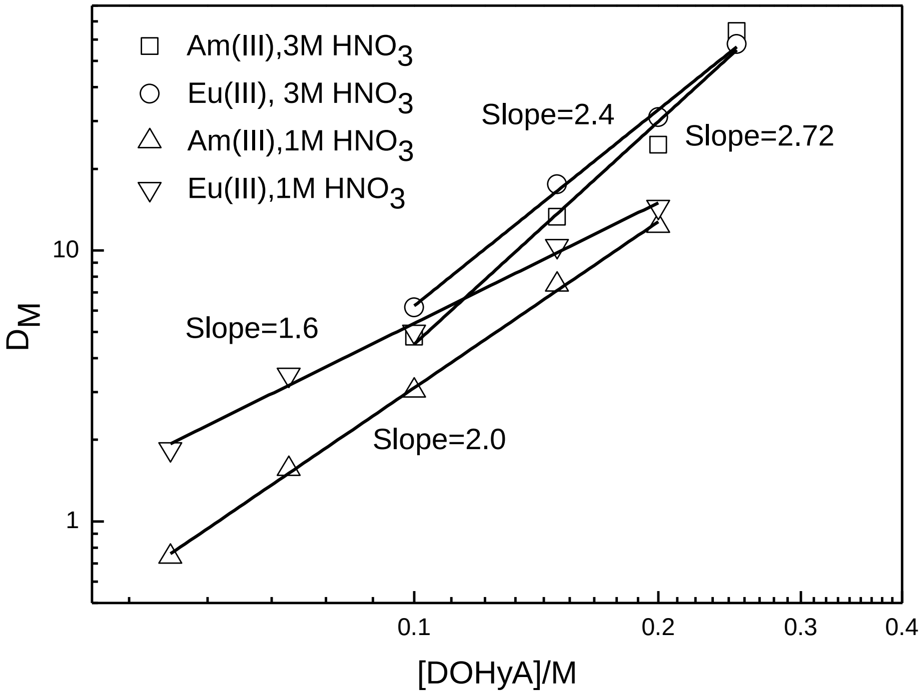

**Figure 7.9.** Variation in the distribution ratio of Am(III) and Eu(III) as a function of DOHyA concentration. Organic phase: DOHYA +0.25 M HDEHP/*n*-DD. Aqueous phase: 1 M and 3 M Nitric acid spiked with $^{(241)}$Am(III) or $^{(152+154)}$Eu(III) tracer. [DOHyA] is varied from 0.1 M to 0.25 M.

To confirm the participation of HDEHP in the combined system, the dependency of HDEHP in the extraction of trivalent metal ion at 1 M and 3 M nitric acid was studied. Figure 7.10 shows the variation in distribution ratio value of Am(III) and Eu(III) as a function of HDEHP concentration in 0.25 M DOHyA +HDEHP/*n*-DD at 1 M and 3 M nitric acid concentration. Increasing the concentration of HDEHP in the combined solvent increases the D value. This observation confirms the participation of HDEHP in the extraction of Am(III) and Eu(III), even at 1 M and 3 M nitric acid concentration. Therefore, the equilibrium reaction for the extraction of Am(III) and Eu(III) in DOHyA-HDEHP mixture can be given by equation 7.5. The equations 7.4 and 7.5 thus represents the equilibrium reaction involved in the extraction of Am(III) and Eu(III) at low and high nitric acid concentration, respectively. It should be noted that both the extractants are participating in the extraction of trivalent metal ion at all nitric acid concentrations.

$$\mathrm{M^{3+}} + y\ \mathrm{DOHyA} + z\ \mathrm{HDEHP} + (3-z)\ \mathrm{NO_3^-} \Leftrightarrow \mathrm{M(DEHP)_z(NO_3^-)_{(3-z)}(DOHyA)}_y + z\ \mathrm{H^+}$$

$$\textit{at higher acidity}.\ \mathrm{z = 0.5\text{-}1,\ y = 2\text{-}3.} \qquad (7.5)$$

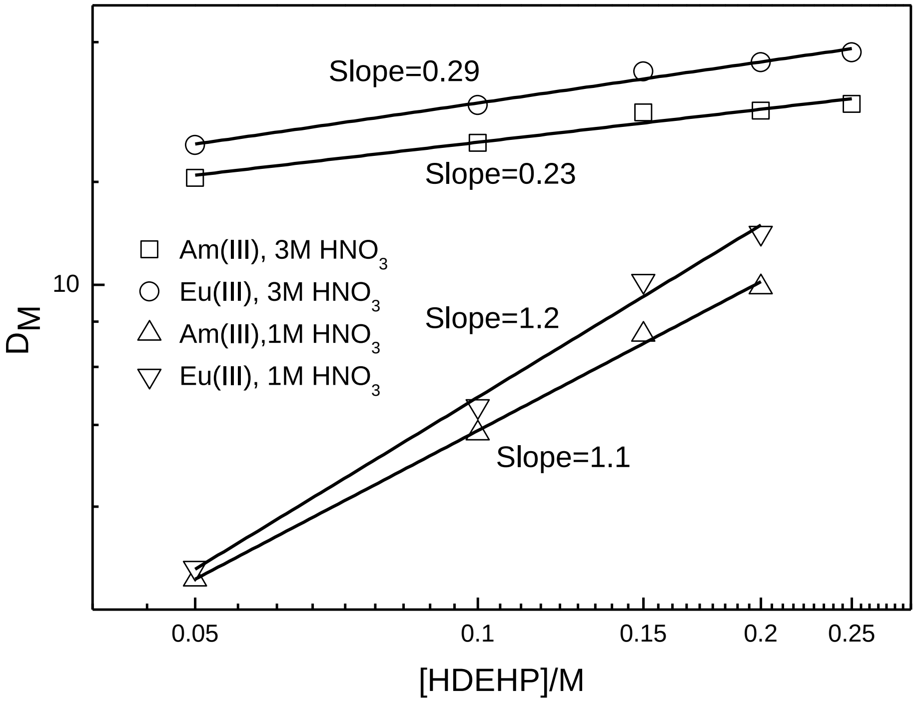

**Figure 7.10**. Variation in the distribution ratio of Am(III) and Eu(III) as a function of HDEHP concentration. Organic phase: 0.2 M DOHyA + HDEHP/*n*-DD. Aqueous phase: 3 M, 1 M Nitric acid spiked with $^{(241)}$Am(III) or $^{(152+154)}$Eu(III) tracer. [HDEHP] varied from 0.05 M to 0.25 M.

Table 7.2 shows the number of molecules of DOHyA and HDEHP participated in the extraction of Am(III) and Eu(III) in the combined extraction system at various nitric acid concentration studied. The data was derived from the slope analysis of the extracted data as discussed above. It can be seen that the number of DOHyA molecule involved in the extraction increased and the number of HDEHP molecules involved in the extraction decreased with increase in concentration of nitric acid. This observation confirms the involvement of both the extractant molecules for the extraction of Am(III) and Eu(III) in entire range (from 0.1 to 3 M) investigated in the present study, according to equations 7.4 and 7.5.

**Table 7.2**. The number of molecules of DOHyA and HDEHP participated in the extraction of Am(III) and Eu(III) in the combined extraction system at various nitric acid concentration.

| Combined System | Metal Ions | 0.5 M $HNO_3$ | 1 M $HNO_3$ | 3 M $HNO_3$ |
|---|---|---|---|---|
| HDEHP variation | Eu(III) | 1.7 | 1.2 | 0.29 |
| | Am(III) | 1.7 | 1.1 | 0.23 |
| DOHyA variation | Eu(III) | 0.8 | 1.6 | 2.4 |
| | Am(III) | 1.3 | 2.0 | 2.7 |

### 7.2.3 FT- IR spectroscopy

FTIR spectroscopy can be employed for monitoring the synergic extraction of Eu(III) in the binary solvent system. The FT-IR spectra of organic phase containing individual extractants namely 0.25 M DOHyA/*n*-DD and 0.25 M HDEHP/*n*-DD loaded with Eu(III) from 3 M and 0.1 M nitric acid respectively are shown in Figure 7.11. After the extraction of europium, the amidic C=O transmittance bands of 2-hydroxyacetamide and phosphoryl P=O transmittance bands of HDEHP were monitored. The spectrum was compared with the FTIR spectrum of organic phase recorded after contacting the organic phase with nitric acid solution without Eu(III) ion. As shown in Figure 7.11, the amidic C=O transmittance bands occurs at 1658 $cm^{-1}$. Upon equilibrating the 0.2 M DOHyA/*n*-DD with 0.1 M Eu(III) ion in 3 M nitric acid, the amidic C=O bands are shifted from 1658 $cm^{-1}$ to 1614 $cm^{-1}$. This indicates the co–ordination of amidic C=O groups of DOHyA with Eu(III) ion. In view of this, the strength of C=O bond was weakened and shifted the transmittance bands to lower stretching frequency region. However, the presence of a less intense band at 1658 $cm^{-1}$ indicates the existence of residual un-complexed C=O groups in DOHyA. In case of HDEHP, the phosphoryl P=O stretching bands are shifted from 1230 $cm^{-1}$ to 1203 $cm^{-1}$ [23], after the extraction of Eu(III) from 0.1 M nitric acid concentration. This shift is again attributed to weakening of P=O bonds due the complexation of phosphoryl group with Eu(III) ion.

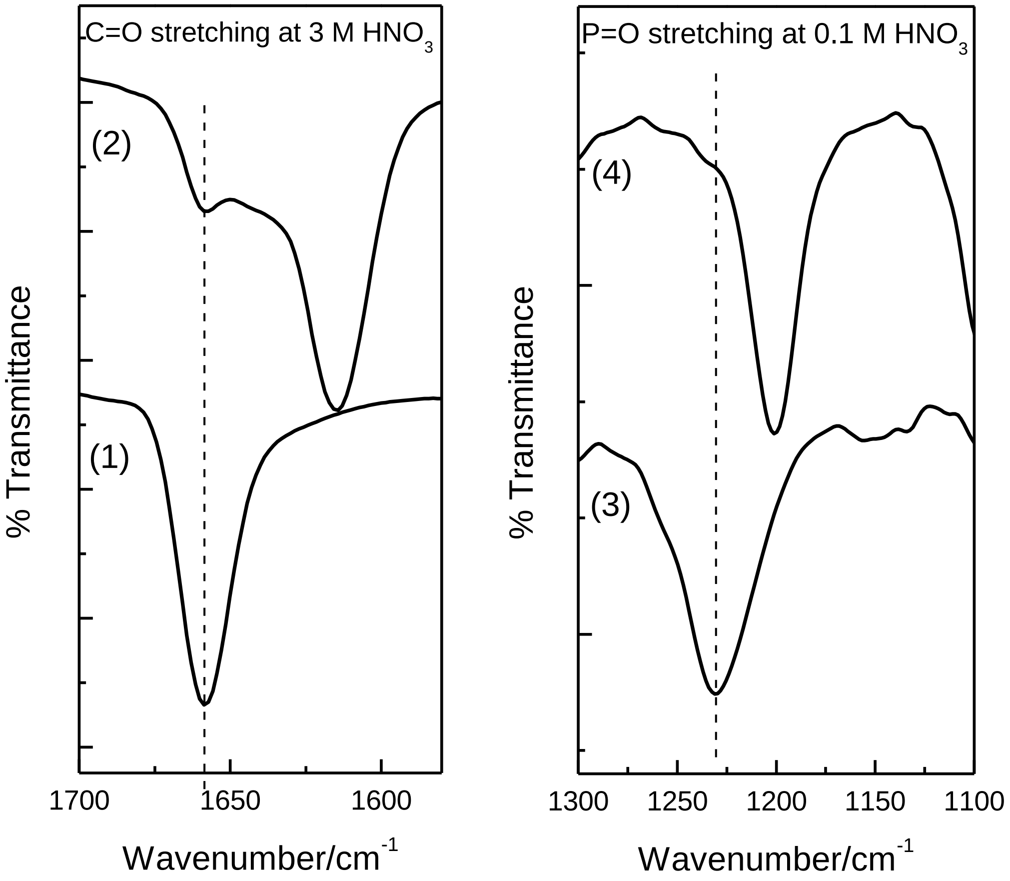

**Figure 7.11.** ATR-FTIR spectrum of DOHyA/*n*-DD, HDEHP/*n*-DD recorded after contacting the organic phase with nitric acid solution in the presence and absence of Eu(III). The vertical dash in the figure indicates the initial position of the band. (1) Org: 0.2 M DOHyA/*n*-DD, Aq: 3 M $HNO_3$, (2) Org: 0.2 M DOHyA/*n*-DD, Aq: 3 M $HNO_3$+Eu(III), (3) Org: 0.25 M HDEHP/*n*-DD, Aq: 0.1 M $HNO_3$, (4) Org: 0.25 M HDEHP/*n*-DD, Aq: 0.1 M $HNO_3$+Eu(III).

Figure 7.12 shows the ATR-FTIR spectrum of the combined solvent system obtained after the extraction of Eu(III) from 0.1 M and 3 M $HNO_3$. At 0.1 M nitric acid the P=O transmittance band of HDEHP is shifted from 1230 $cm^{-1}$ to 1203$cm^{-1}$ [23] after equilibrating with Eu(III). The participation of DOHyA in the extraction of Eu(III) even at low nitric acid concentration (0.1 M) can be confirmed by the partial shift of amidic C=O transmittance bands from 1658 $cm^{-1}$ to 1627 $cm^{-1}$. Similarly, at 3 M nitric acid, the amidic C=O transmittance bands are shifted significantly from 1658 $cm^{-1}$ to 1614 $cm^{-1}$ with a weak shoulder at the original position 1658 $cm^{-1}$ upon Eu(III) extraction. In addition, the phosphoryl transmittance bands at 1230 $cm^{-1}$ are broadened due to the complexation of Eu(III) with HDEHP even at 3 M $HNO_3$. The study, therefore, confirms the participation of both the extractants at low and high nitric acid concentrations leading to the formation of mixed metal-solvate species in organic phase.

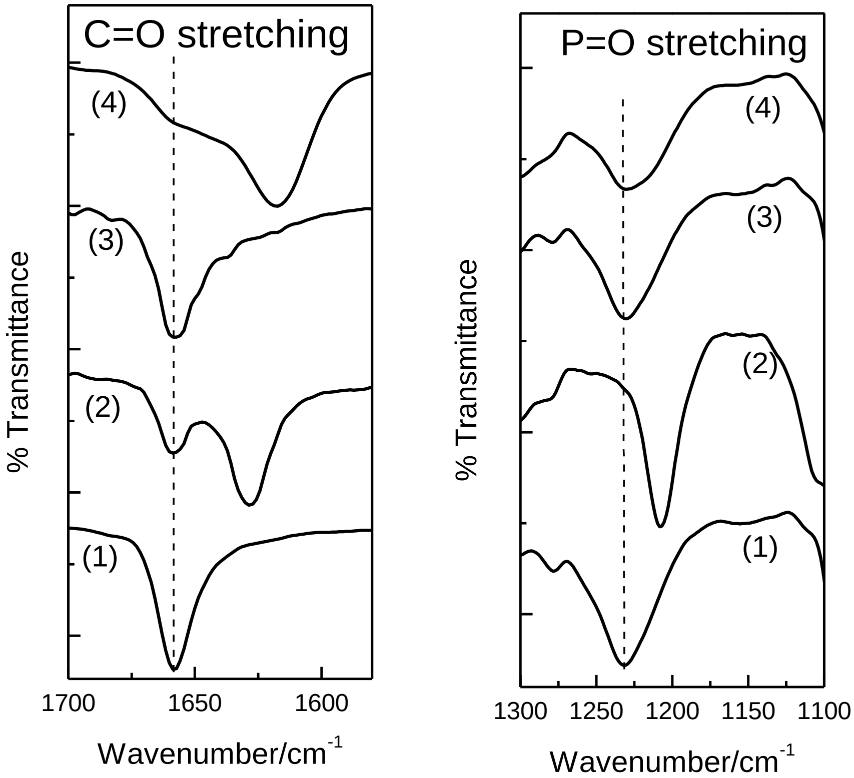

**Figure 7.12**. ATR-FTIR spectrum of DOHyA+ HDEHP/*n*-DD recorded after contacting the organic phase with nitric acid solution in the presence and absence of Eu(III). The vertical dash in the figure indicates the initial position of the band. (1) Org: 0.2 M DOHyA+0.25 M HDEHP/*n*-DD, Aq: 0.1 M $HNO_3$, (2) Org: 0.2 M DOHyA+0.25 M HDEHP/*n*-DD, Aq: 0.1 M $HNO_3$+Eu(III), (3) Org: 0.2 M DOHyA+0.25 M HDEHP/*n*-DD, Aq: 3 M $HNO_3$, (4) Org: 0.2 M DOHyA+0.25 M HDEHP/*n*-DD, Aq: 3 M $HNO_3$+Eu(III).

### 7.2.4 Extraction from metal ions from FR-SHLLW

When the combined extractant system is proposed for the separation of Am(III) from high- level liquid waste (HLLW), it is necessary to study the extraction behavior of other metal ions present in HLLW. Therefore, the extraction of behavior of various elements present in the fast reactor-simulated high level liquid waste (FR-SHLLW) was studied by using 0.2 M DOHyA+ 0.25 M HDEHP/*n*-DD. The composition of fast reactor simulated HLLW (burn up 80,000 MWd/Te) used in the present study is shown in Table 7.3 [18]. The nitric acid concentration of FR-SHLLW was 3 M. Table 7.3 shows the distribution ratio of various metal ions present in the FR-SHLLW. It is observed that the distribution ratio of trivalent metal ions (lanthanides and Am(III)) are quit high as compared to other metal ions, except molybdenum, iron and zirconium. Among the lanthanides, the D values increased with increase in atomic number or decrease in the atomic radii of the lanthanides. Mo(VI) and Zr(IV) showed very high D values as compared to Ln(III). However, the extraction of Zr(IV) and Mo(VI) in the binary solvent phase was undesirable owing to their hydrolysable nature during stripping and third phase formation during extraction. Therefore, an aqueous soluble reagent trans-1,2-diaminocyclohexane-N,N,N,N'-tetraaceticacid (CyDTA) was added to FR-SHLLW to eliminate the extraction of these metal ions. The distribution ratio of various metal ions determined in the presence of CyDTA in FR-SHLLW is shown in Table 7.3. It can be seen that the addition of CyDTA to FR-SHLLW eliminated the extraction of Zr(IV), and lowered the D value of Mo(VI). However the extraction of Fe(III) in the binary solution was unaffected. Moreover, there is no significant change in D values of trivalent metal ions in presence of CyDTA. The D value of Am(III) observed was 4.34, which is quite adequate for the quantitative extraction of Am(III) in the binary solution in few contacts.

**Table 7.3.** Distribution ratios of metal ions present in organic phase determined in the presence and absence of 0.05 M CyDTA in FR-SHLLW.Organic phase: 0.2 M DOHyA + 0.25 M HDEHP/*n*-DD, Aqueous phase: FR- SHLLW in the presence or absence of complexing agent. Organic/Aqueous phase ratio = 1, Temperature = 298 K. Concentration of HNO3 in FR-SHLLW is 3 M.

| Metals | Concentration[g/L] | $D_M$ in the absence of 0.05 M CyDTA | $D_M$ in the presence of 0.05 M CyDTA |
|---|---|---|---|
| Cr | 0.10 | 0.14 | 0.23 |
| Te | 0.16 | 0.13 | 0.25 |
| Cd | 0.04 | 0.05 | 0.06 |
| Mo | 1.09 | 606 | 35.7 |
| Gd | 0.06 | 4.72 | 5.14 |
| La | 0.34 | 0.84 | 0.97 |
| Ni | 0.12 | 0.06 | 0.11 |
| Sr | 0.14 | 0.11 | 0.17 |
| Dy | 0.01 | 7.04 | 7.72 |
| Fe | 0.51 | 5.70 | 4.41 |
| Eu | 0.03 | 6.34 | 6.34 |
| Sm | 0.31 | 3.72 | 4.21 |
| Y | 0.07 | 5.77 | 6.09 |
| Nd | 1.12 | 2.44 | 2.64 |
| Pr | 0.34 | 2.12 | 2.10 |
| Ce | 0.68 | 1.45 | 1.58 |
| Ba | 0.41 | 0.05 | 0.11 |
| Ru | 0.81 | <0.01 | <0.01 |
| Pd | 0.60 | 0.03 | <0.01 |
| Zr | 0.82 | 241 | 0.15 |

| | | | |
|---|---|---|---|
| Rh | 0.26 | <0.01 | <0.01 |
| $^{241}$Am | Tracer | 4.74 | 4.74 |
| $^{152+154}$Eu | Tracer | 6.34 | 6.34 |

### 7.2.5 Selective stripping of Am(III)

As indicated above, the extraction of Am(III) from FR-SHLLW in 0.2 M DOHyA +0.25 M HDEHP/*n*-DD results in co-extraction of lanthanides. The mutual separation of lanthanides from actinides is necessary for the transmutation of actinides. The TALSPEAK process developed for the mutual separation of lanthanides (Ln(III)) and actinides (An(III)) exploits the differential complexing ability of Ln(III) and An(III) towards HDEHP present in organic phase and DTPA present in aqueous phase [5]. Therefore, in the present study also the mutual separation of Am(III) and Eu(III) from 0.2 M DOHyA +0.25 M HDEHP/*n*-DD phase was performed using 0.5 M citric acid +0.05 M DTPA solution at various pH. As shown in Table 7.4, the separation factor increases with increase in pH. A separation factor of ~10 was obtained with 0.05 M DTPA+0.5 M CA stripping formulation at pH 4. Further increase in the pH or the aqueous phase results is the lowering of distribution ratio of Eu(III) which is not desirable for the retention of Eu(III) in organic phase and stripping of Am(III) alone to aqueous phase.

**Table 7.4.** Distribution ratio of Am(III) and Eu(III) in the binary solution extracted from the proposed stripping formulation. Organic phase: 0.2 M DOHyA + 0.25 M HDEHP/*n*-DD, Aqueous phase: Stripping formulation composed of 0.05 M DTPA +0.5 M citric acid at different pH.

| pH | Distribution Values | | Separation factor (SF) |
|---|---|---|---|
| | Am(III) | Eu(III) | |
| pH = 2 | 30 | 77 | 2.5 |
| pH = 2.5 | 17 | 43 | 2.5 |
| pH = 3 | 5.7 | 28 | 4.9 |
| pH = 3.5 | 0.7 | 4.8 | 6.8 |
| pH = 4 | 0.3 | 2.5 | 8.4 |

### 7.3 Summary

The extraction behavior of Am(III) and Eu(III) from nitric acid medium was studied in a binary solution composed of 0.2 M DOHyA+0.25 M HDEHP in *n*-DD and the results were compared with those obtained in the individual solvent system. Synergic extraction of Am(III) and Eu(III) was observed in the binary extractant system and the number of molecules of DOHyA and HDEHP involved in the extraction of Am(III) and Eu(III) in the combined solvent decreased (as compared to the individual solvent system) to accommodate to the involvement of the other extractant in the binary solution. The synergic coefficient obtained in the binary solution increased with increase in the concentration of nitric acid reached a maximum at 1 M nitric acid. The synergic participation of both extractants in the binary solution was confirmed by the slope analysis of the extraction data and ATR-FTIR spectroscopy. The extraction behavior of

Am(III), lanthanides and other metal ions present in the FR-SHLLW was studied to understand the feasibility of using the combined solvent for single-cycle separation of Am(III) from FR-SHLLW. The results revealed the possibility of such separations with a separation factor of ~10 for Am(III) over Eu(III).

## Part II. The extraction behavior of Am(III) and Eu(III) in DOHyA-HDEHDGA solvent system

### 7.4 Introduction

The part II of this chapter deals with the extraction behavior of Am(III) and Eu(III) in a binary solution composed of 0.2 M DOHyA+0.1 M HDEHDGA in *n*-dodecane. The extraction data was compared with those obtained in the individual extractant present in *n*-DD under similar conditions. It should be noted that the extractants present in binary solution are made up of CHON-atoms and therefore the organic phase is completely incinerable. The structure of DOHyA and HDEHDGA is shown in Figure 7.1.

### 7.5 Results and discussion

#### 7.5.1 Extraction behavior of Am(III) and Eu(III) in binary solution

The binary solution was composed of a solution of 0.2 M DOHyA+0.1 M HDEHDGA in *n*-dodecane. The extraction behavior of Am(III) and Eu(III) in the binary solution is shown in Figure 7.13. It is observed that the distribution ratio of Am(III) and Eu(III) in the binary solution decreases with increase in the concentration of nitric acid, reaches a minimum value of distribution ratio at 0.5 to 0.6 M nitric acid followed by increase in distribution ratios. To understand the extraction trend observed in the binary solution, it is necessary to study the behavior of Am(III) and Eu(III) extraction in the individual extractant present in *n*-dodecane. The extraction behaviour of Am(III) and Eu(III) in 0.1 M HDEHDGA/*n*-DD and 0.2 M DOHyA/*n*-DD was studied as function of nitric acid concentration and the results are displayed in the same Figure 7.13. It can be seen that the distribution ratio of Am(III) and Eu(III) in 0.1 M HDEHDGA/*n*-DD decreases with increase in the concentration of nitric acid, as expected. The distribution ratio of Am(III) and Eu(III) was about 0.01 at 1 M nitric acid [19, 24]. In contrast, the distribution ratio of Am(III) and Eu(III) in 0.2 M DOHyA/*n*-DD increases abruptly from the value of 0.01 at 0.5 M nitric acid, reaches a value of ~ 100 at 4 M nitric acid, as discussed in previous part [20, 21].

Comparing the extraction trend observed in the binary solution and individual extractants, the results indicate that the extraction of Am(III) and Eu(III) in the binary solution at lower nitric acid concentration range (< 0.5 M) is governed predominantly by the cation exchange mechanism controlled by HDEHDGA. At higher nitric acid concentrations (> 0.5 M) the extraction is governed by a solvation type of mechanism, controlled predominantly by DOHyA. Nevertheless, it should be noted that the distribution ratio of Am(III) and Eu(III) observed in the binary solution in the lower nitric acid range is lower than those observed for an acidic extractant, whereas the distribution ratios are more for the binary solution at the higher nitric acid concentration range (> 0.5 M) as compared to those observed for the neutral extractant present in *n*-dodecane. A similar behavior was also reported in several other extraction systems [13-19]. This indicates that the addition of DOHyA to HDEHDGA in *n*-dodecane lowers the extraction of Am(III) and Eu(III) in the lower nitric acid concentration range due to antagonistic effect [24], and the addition of HDEHDGA to DOHyA in *n*-DD enhances the extraction of Am(III) and Eu(III) in the higher nitric acid concentrations due to synergism.

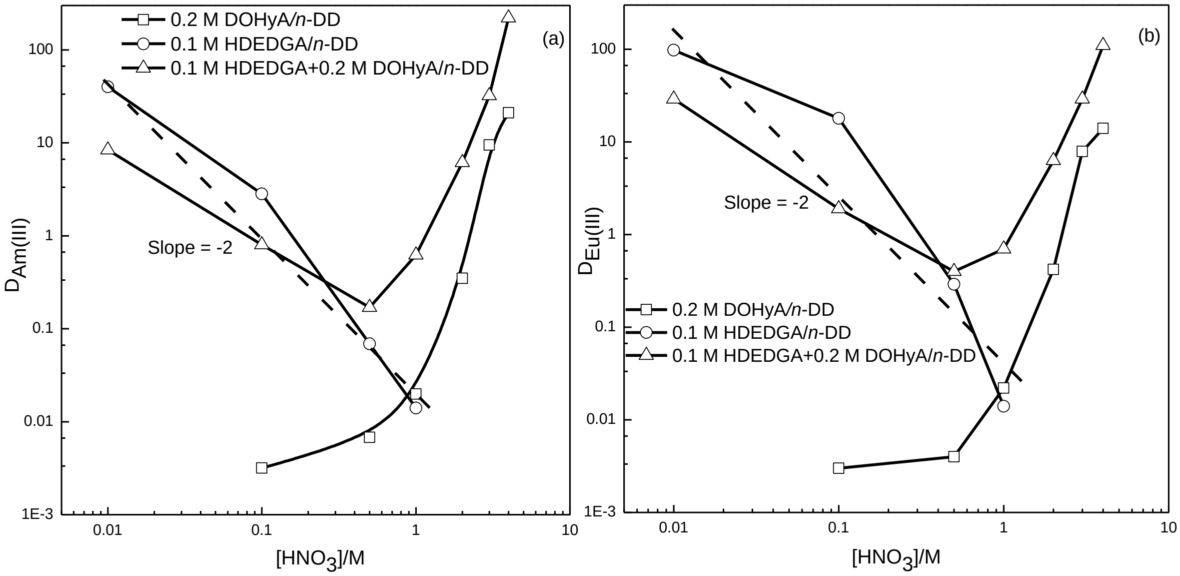

**Figure 7.13(a).** Variation in the distribution ratio of Am(III) as a function of nitric acid concentration. Organic phase: 0.2 M DOHyA/*n*-DD or 0.1 M HDEHDGA/*n*-DD or 0.1 M HDEHDGA + 0.2 M DOHyA/*n*-DD. Aqueous phase: Various concentrations of nitric acid spiked with $^{241}$Am(III) tracer.

**Figure 7.13(b).** Variation in the distribution ratio of Eu(III) as a function of nitric acid concentration. Organic phase: 0.2 M DOHyA/*n*-DD or 0.1 M HDEHDGA/*n*-DD or 0.1 M HDEHDGA + 0.2 M DOHyA/*n*-DD. Aqueous phase: Various concentrations of nitric acid spiked with $^{(152+154)}$Eu(III) tracer.

### 7.5.2 Extraction mechanism

#### 7.5.2.1 Extraction behavior at 3 M nitric acid

To understand the synergic and antagonistic effects exhibited by these ligands, the extraction stoichiometry of metal-ligand complexes in organic phase was determined in a similar way as describe in the previous part of this chapter. The mechanism of extraction of trivalent metal ions with DOHyA was studied by slope analysis of the extraction data showing variation of DOHyA (Figure 7.4) and $NO_3^-$ (Figure 7.5) concentrations confirming the validity of extraction mechanism shown in equation 7.1.

At 3 M nitric acid, the extraction behavior of Am(III) and Eu(III) in the binary solution was studied as function of DOHyA concentration and the results are shown in Figure 7.14. It is observed that the extraction of both these metal ions, obviously increases with increase in the concentration of DOHyA. However, it is observed that the dependence of distribution ratio of Am(III) and Eu(III) on DOHyA concentration decreased significantly, by half, as the slope value of ~2.3 (see in Figure 7.14) was obtained for the binary solution as compared to the slope value of ~5 in case of the DOHyA alone in *n*-DD (see in Figure 7.4). The decrease in the involvement of DOHyA in the binary solution could be due to the participation of HDEHDGA, which is also present in the binary solution. In order to confirm the involvement of HDEHDGA in the extraction of these trivalent metal ions at 3 M nitric acid, the extraction behavior of Am(III) and Eu(III) from 3 M nitric acid was studied in the solution of 0.2 M DOHyA+ HDEHDGA/*n*-DD at various concentrations of HDEHDGA. The results are depicted in Figure 7.15. Interestingly, the distribution ratios of Am(III) and Eu(III) increased with increase in the concentration of HDEHDGA in the binary solution. However, it should be noted that HDEHDGA alone does not extract these metal ions at nitric acid concentration above 0.5 M, as shown in Figure 7.13 [24]. Linear regression analysis of the extractant data (Figure 7.15) yielded a slope value of ~ 0.5 for the both Am(III) and Eu(III) at 3 M nitric acid. This confirms the synergic participation of HDEHDGA in the extraction of Am(III) and Eu(III) even at 3 M nitric acid.

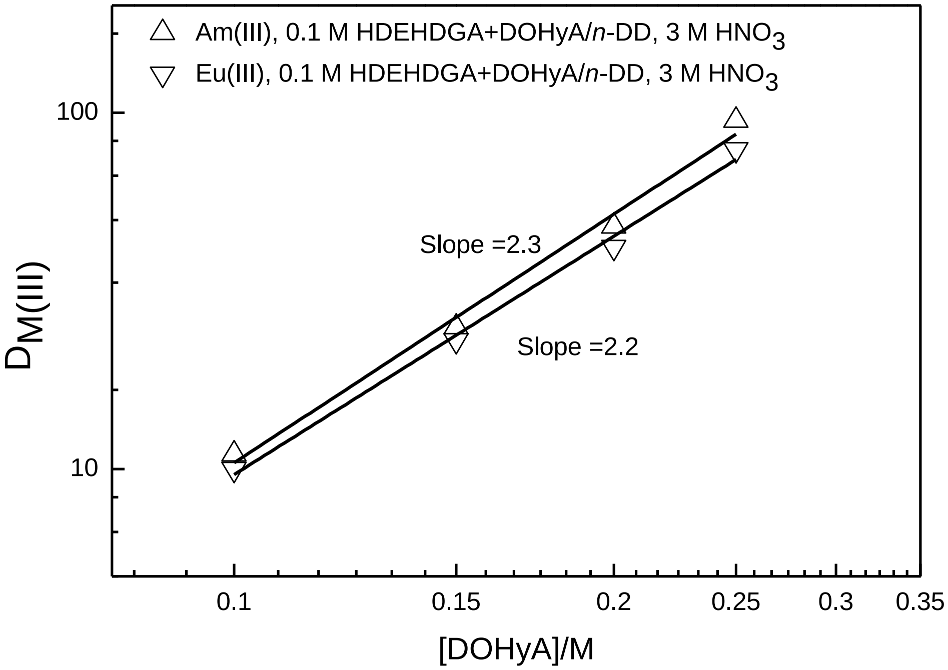

**Figure 7.14.** Variation in the distribution ratio of Am(III) and Eu(III) as a function of DOHyA concentration. Organic phase: DOHyA/*n*-DD or 0.1 M HDEHDGA+ DOHyA/*n*-DD. Aqueous phase: 3 M Nitric acid spiked with $^{(241)}$Am(III) or $^{(152+154)}$Eu(III) tracer. [DOHyA] varied from 0.075 M to 0.25 M.

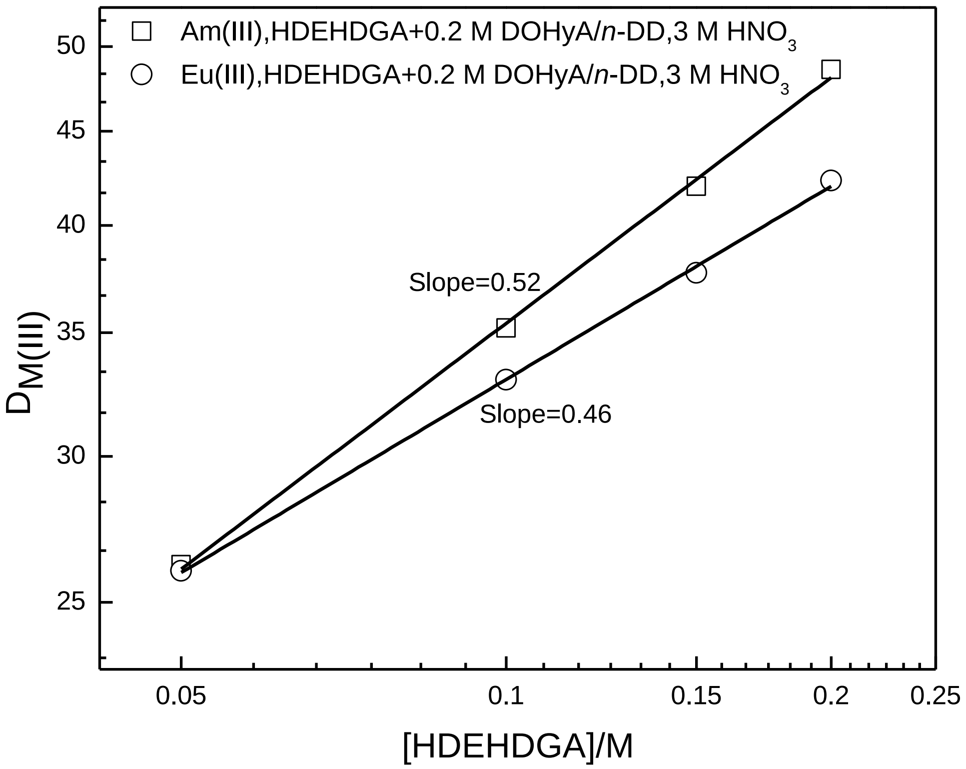

**Figure 7.15.** Variation in the distribution ratio of Am(III) and Eu(III) as a function of HDEHDGA concentration. Organic phase: HDEHDGA+ 0.2 M DOHyA/*n*-DD. Aqueous phase: 3 M nitric acid spiked with $^{(241)}$Am(III) or $^{(152+154)}$Eu(III) tracer. [HDEHDGA] varied from 0.05 M to 0.2 M.

It would be interesting to understand coordination behaviour of HDEHDGA in the binary solution at higher nitric acid concentration. The ligand, HDEHDGA is as an acidic extractant, wherein the conjugate base of HDEHDGA, namely bis(2-ethyhexyl) glycolamate (DEHDGA) would be coordinating to the trivalent metal ion during synergic extraction. This can happen only when the nitrate ion coordinated to the trivalent metal ion, shown in equation 7.1, is partially substituted by DEHDGA anion. From Figure 7.15, the number of molecules of HDEHDGA (slope =0.5) involved in the extraction of Am(III) and Eu(III) in the binary solution was already established. Therefore, it is now necessary to obtain number of molecules of nitrate ions involved in the extraction of Am(III) and Eu(III) in the binary solution at 3 M nitric acid. To obtain the number of molecules of nitrate ion coordinated to the trivalent metal ion in the binary solution, the effect of nitrate ion concentration in aqueous phase on the extraction of Am(III) and Eu(III) in the binary solution was studied and the results are displayed in Figure 7.16. It is observed that the extraction of Am(III) and Eu(III) increased with increase with concentration of nitrate ion aqueous phase. However, it is important to note that the slope of ~2.5 was obtained upon linear regression of the extraction data obtained in a binary solution. This value is lower than the value of 3 obtained in case of nitrate variation in 0.2 M DOHyA alone in *n*-DD (Figure 7.4). This shows that the participation of nitrate ion in the extraction of Am(III) and Eu(III) is lowered by the addition of HDEHDGA to 0.2 M DOHyA/*n*-DD. It should be noted that the trivalent metal ion requires three molecules of anion for the formation of a neutral complex in organic phase, for its extraction in DOHyA/*n*-DD as shown in equation 7.1. The reduction in the participation of nitrate ion molecules for the extraction of trivalent metal ion in the binary solution indicates that the conjugate base of HDEHDGA namely DEHDGA could be coordinating to the trivalent metal ion, as a substitute to nitrate ion for charge compensation. Table 7.5 shows the magnitude of slope obtained for the dependence of HDEHDGA and DOHyA on the extraction of Am(III) and Eu(III) at various nitric acid concentrations in the binary solution. It is observed that the dependence of DOHyA on the extraction of Am(III) and Eu(III) increases, whereas the dependence of HDEHDGA decreases with increase in concentration of nitric acid in aqueous phase.

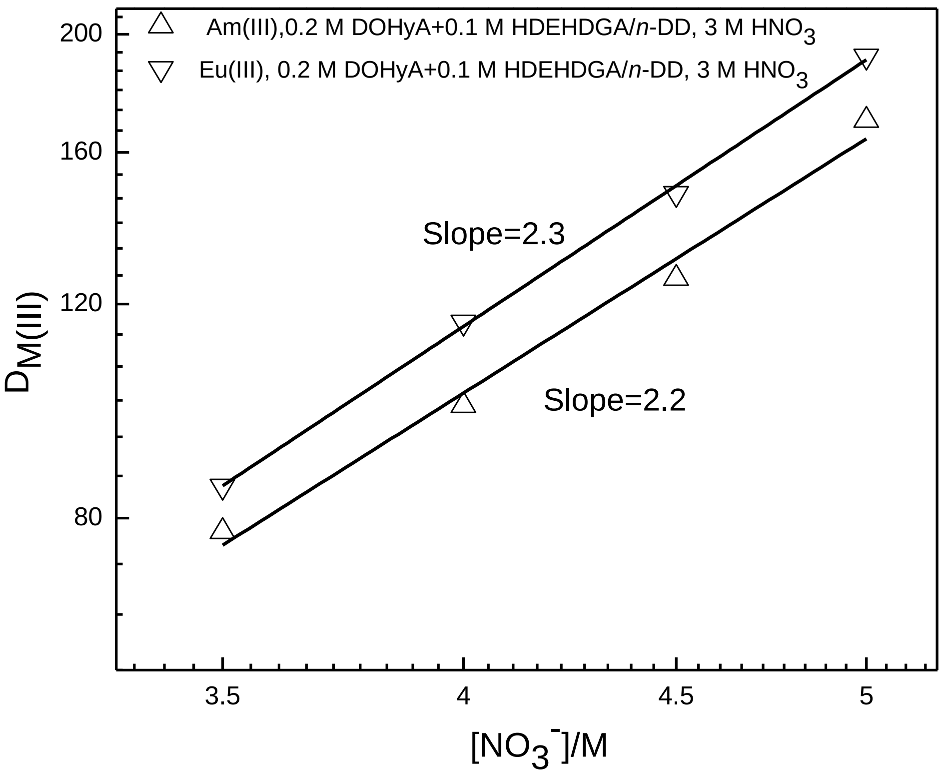

**Figure 7.16.** Variation in the distribution ratio of Am(III) and Eu(III) as a function of nitrate ion concentration. Organic phase: 0.2 M DOHyA/*n*-DD or 0.2 M DOHyA +0.1 M HDEHDGA/*n*-DD. Aqueous phase: [$NaNO_3$] present in 3 M nitric acid spiked with $^{(241)}$Am(III) or $^{(152+154)}$Eu(III) tracer. [$NaNO_3$] varied from 0.5 M to 2 M.

**Table 7.5.** Magnitude of slope obtained for the effect of HDEHDGA and DOHyA concentration on the extraction of Am(III) and Eu(III) in the binary solution at various nitric acid concentrations.

| Binary solution | Metal Ions | 0.1 M $HNO_3$ | 1 M $HNO_3$ | 3 M $HNO_3$ |
|---|---|---|---|---|
| HDEHDGA variation | Eu(III) | 2.1 | 1.1 | 0.49 |
| | Am(III) | 1.8 | 1.0 | 0.52 |
| DOHyA variation | Eu(III) | -1.5 | 1.6 | 2.2 |
| | Am(III) | -1.4 | 1.7 | 2.3 |

This shows that the stoichiometry of the solvent system changes with respect to nitric acid owing to the change in the participation of both acidic and neutral extractant with nitric acid. Based on these dependencies, the extraction of Am(III) and Eu(III) in the binary solution at higher nitric acid concentration range, where synergism is observed, can be represented by the following equation 7.6.

$$M^{3+} + x\,\mathrm{DOHyA} + y\,\mathrm{HDEHDGA} + (3-y)\,\mathrm{NO_3^-} \Leftrightarrow \mathrm{M(DEHDGA)}_y\,(\mathrm{NO_3^-})_{3-y}(\mathrm{DOHyA})_x + y\,\mathrm{H}^+ \text{......(7.6)}$$

where 1 < x < 5 and 0 < y < 2 depending upon the concentration of nitric acid in the synergic extraction regime.

#### 7.5.2.2 Extraction at lower nitric acid region

In contrast to the synergic extraction observed at higher nitric acid concentration (> 0.5 M), antagonistic extraction of Am(III) and Eu(III) is observed in the binary solution at lower nitric acid concentration region. This shows that the addition of DOHyA to HDEHDGA in *n*-DD reduces the distribution ratio Am(III) and Eu(III). Figure 7.17 shows the variation in the distribution ratio of Am(III) and Eu(III) observed in a binary solution composed of DOHyA+0.1

M HDEHDGA/*n*-DD at 0.1 M nitric acid. The concentration of DOHyA was varied in this experiment. It is observed that the distribution ratio of Am(III) and Eu(III) decreases with increase in the concentration of DOHyA in the binary solution. This observation confirms the antagonistic effect of DOHyA on the extraction of these metal ions by the binary solution at lower nitric acid concentrations.

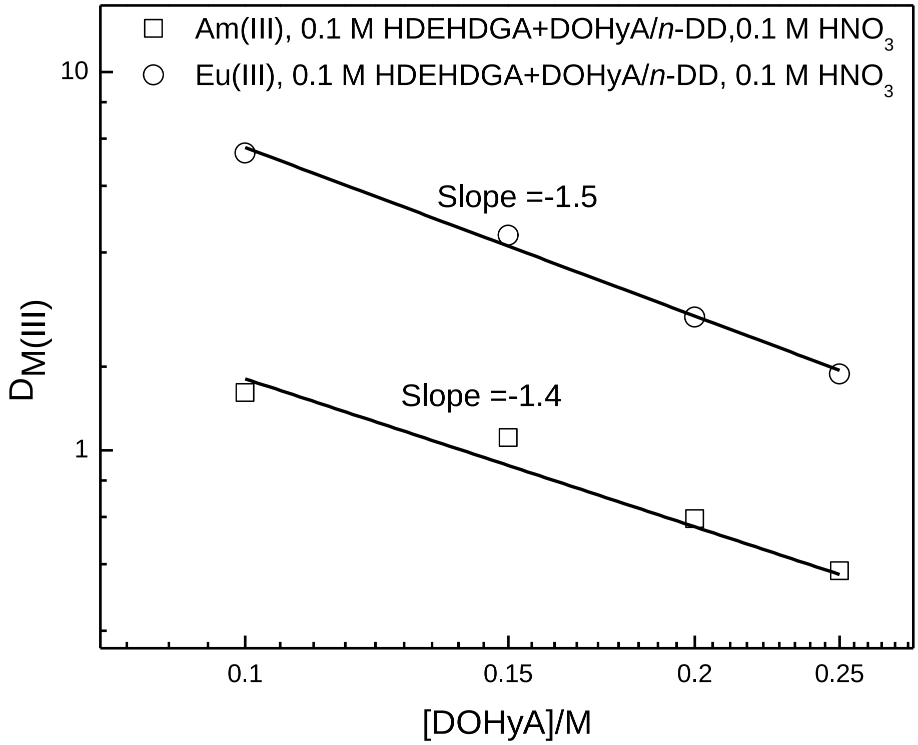

**Figure 7.17.** Variation in the distribution ratio of Am(III) and Eu(III) as a function of DOHyA concentration. Organic phase: 0.1 M HDEHDGA +DOHyA /*n*-DD. Aqueous phase: 0.1 M nitric acid spiked with $^{(241)}$Am(III) or $^{(152+154)}$Eu(III) tracer. [DOHyA] varied from 0.1 M to 0.25 M.

Figure 7.18 shows the effect of HDEHDGA concentration in the binary solution on the distribution ratio of Am(III) and Eu(III) at 0.1 M nitric acid. The data were compared with the results obtained in HDEHDGA/*n*-DD, where in the concentration of HDEHDGA was varied. The distribution ratio of Am(III) and Eu(III) in both cases increased with increase in the concentration of HDEHDGA. Interestingly and unlike the results observed in synergic extraction, linear regression of extraction data obtained in both binary and individual solution gave a slope of ~2. This shows that the involvement of HDEHDGA in the binary solutions is not altered even in the presence of DOHyA. Based on this observation as well as on the antagonistic effect observed in Figure 7.17, the following extraction mechanism shown in equation 7.7, could be proposed for the extraction of Am(III) and Eu(III) in the lower nitric acid concentration range.

$$M^{3+} + NO_3 + 2\,HDEHDGA \Leftrightarrow M(NO_3)(DEHDGA)_2 + 2\,H^{+} \text{......(7.7)}$$

The equation described above shows that the extraction of trivalent metal ion varies directly with nitrate ion concentration in aqueous phase and inversely with the equilibrium $H^+$ ion concentration in aqueous phase. The inverse dependence of $H^+$ ion concentration in aqueous phase on the extraction of Am(III) and Eu(III) can be seen in Figure 7.13, in the lower nitric acid range for binary solution. Linear regression of the extraction data gave a slope of -2 in the lower nitric acid region confirm the validity of equation 7.5. The direct dependence of nitrate ion concentration on the extraction of Am(III) and Eu(III) with a slope value of 1 has been reported elsewhere [19,24]. Those results confirmed the validity of equation 7.5 for the extraction of Am(III) and Eu(III) at lower nitric acid concentration range .

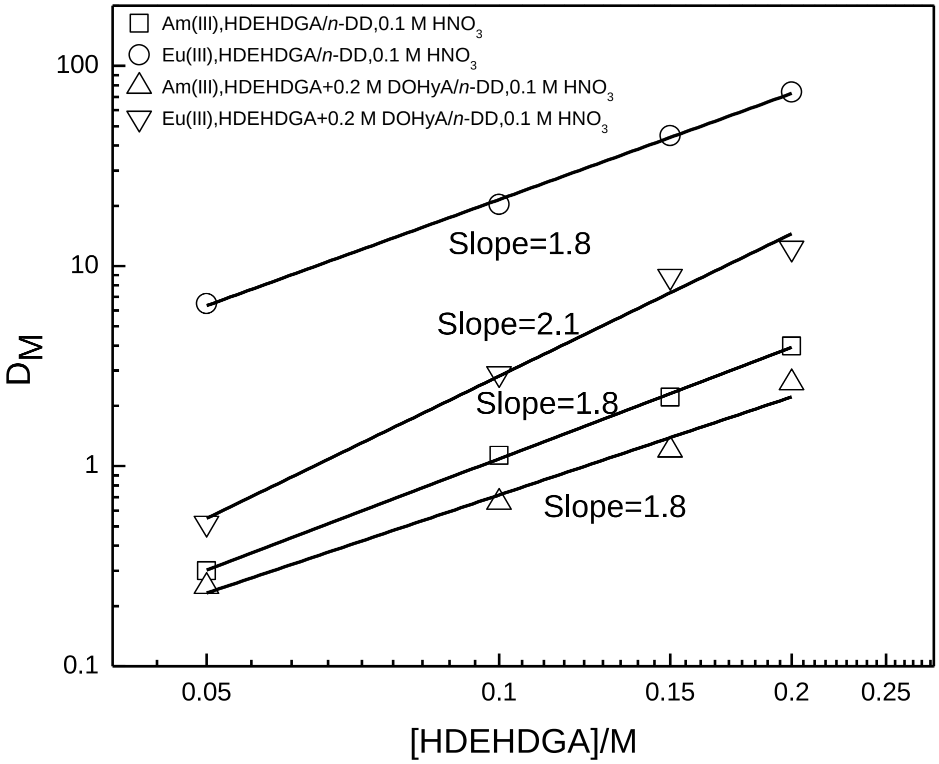

**Figure 7.18.** Variation in the distribution ratio of Am(III) and Eu(III) as a function of HDEHDGA concentration. Organic phase: HDEHDGA+ 0.2 M DOHyA /*n*-DD or HDEHDGA/*n*-DD. Aqueous phase: 0.1 M nitric acid spiked with $^{(241)}$Am(III) or $^{(152+154)}$Eu(III) tracer. [HDEHDGA] varied from 0.05 M to 0.2 M.

### 7.5.3 Stripping studies

After the extraction of lanthanides and actinides from 3 M nitric acid, stripping of actinides alone from the organic phase needs to be achieved in a single-cycle separation process. Since the stripping of trivalent metal ion is controlled by an acidic extractant, namely HDEHDGA in this case, it is necessary to play with the aqueous phase conditions for achieving higher separation factor of Am(III) over trivalent lanthanides. To improve the stripping of

Am(III) from organic phase, the aqueous complexing reagents such as diethylenetriamine tetra acetic acid (DTPA) and citric acid (CA) have been employed so far by several authors [13-19]. Table 7.6 shows the distribution ratio of Am(III), Eu(III) and Nd(III) in 0.2 M DOHyA+0.1 M HDEHDGA/*n*-DD measured under the stripping condition, that is at nitric acid concentrations lower than 0.1 M, in the presence of DTPA and citric acid. It is observed that the distribution ratio of Am(III), Eu(III) and Nd(III) decrease with increase in the pH of the aqueous solution. This could be due to the dissociation of polycarboxylic acid and citric acid, facilitating the coordination of these metal ions, thereby stripping them to the aqueous phase. Since Am(III) is coordinated efficiently by DTPA as compared to Eu(III) or Nd(III), a separation factor of about 10 is achieved for Eu(III) and a separation of 25 is achieved for Nd(III) at pH 2.

**Table 7.6.** Distribution ratio of Am(III), Nd(III) and Eu(III) and the separation factor (SF= $D_{Eu(III)}/D_{Am(III)}$ *or* $D_{Nd(III)}/D_{Am(III)}$) as a function of HDEHDGA concentration in organic phase, and aqueous phase conditions, at 298 K.

| | pH | Distribution Values | | | Separation factor * | |
|---|---|---|---|---|---|---|
| | | Am(III) | Eu(III) | Nd(III) | $D_{Eu(III)}/D_{Am(III)}$ | $D_{Nd(III)}/D_{Am(III)}$ |
| 0.2 M DOHyA+0.1M HDEHDGA/*n*-DD | 0.01 M DTPA +0.1 M citric acid at pH = 2 | 0.06 | 0.6 | 1.5 | 10 | 25 |
| | 0.01 M DTPA +0.1 M citric acid at pH = 2.5 | 0.009 | 0.1 | 0.38 | 12 | 42 |
| | 0.01 M DTPA +0.1 M citric acid at pH = 3 | 0.002 | 0.03 | 0.07 | 15 | 34 |
| 0.2 M DOHyA+0.3M HDEHDGA/*n*-DD | 0.003 M DTPA at pH = 2 | 0.41 | 5.1 | 35 | 13 | 86 |
| | 0.003 M DTPA at pH = 2.5 | 0.08 | 0.86 | 0.9 | 11 | 11 |
| | 0.003 M DTPA at pH = 3 | 0.06 | 0.64 | 0.6 | 10 | 10 |

* Separation factor is the ratio of distribution ratio of Eu(III) over Am(III) or Nd(III) over Am(III).

It should be noted that at pH 2, the distribution ratio of Am(III) and Eu(III) are quite less. This renders that both these metal ions are strippable to aqueous phase, even though separation factor of 10 was achieved for Eu(III). However, it is necessary to retain all the lanthanides including Eu(III) in organic phase and strip only Am(III) into aqueous phase during recovery. To improve the retention of Eu(III) in organic phase, the concentration of HDEHDGA was increased to 0.3 M in the binary solution and the concentration of DTPA was lowered in aqueous phase. The distribution ratios of Am(III), Eu(III) and Nd(III) achieved under such condition in 0.2 M DOHyA+0.3 M HDEHDGA/*n*-DD are also shown in Table 7.6. It is observed that the distribution of Am(III), Nd(III) and Eu(III) is increased some extent. However, the distribution ratio of Am(III) is quite less as compared to the lanthanides and the separation factors of 13 and 86 are achieved for Eu(III) and Nd(III) respectively. Therefore, it can be concluded that the organic phase having 0.2 M DOHyA+0.3 M HDEHDGA/*n*-DD and the aqueous phase having 0.003 M DTPA at pH = 2 seems to be favourable for the mutual separation of trivalent actinides from lanthanides present in 3-4 M nitric acid medium.

## 7.6 Summary

The extraction behaviour of Am(III) and Eu(III) in a completely incinerable binary solution of DOHyA + HDEHDGA in *n*-DD was studied to explore the possibility of single-cycle separation of Am(III) from Eu(III) present in 3 M nitric acid medium. The method involved the group extraction of both Am(III) and Eu(III) in a binary solution from 3 M nitric acid medium followed by selective stripping of Am(III) from organic phase. Comparing the extraction of Am(III) and Eu(III) in the binary solution with those obtained in the individual extractants, the group extraction of Am(III) and Eu(III) was controlled by DOHyA present in organic phase and the stripping of Am(III) was controlled by the differences in the coordinating ability of HDEHDGA present in organic phase and DTPA present in aqueous phase.

The mechanism of Am(III) and Eu(III) extraction in the binary solution was determined by the slope analysis of the extraction data. Interestingly, synergic extraction of Am(III) and Eu(III) was observed at nitric acid concentrations above 0.5 M, where both the ligands present in organic phase co-ordinate to trivalent metal ion for facilitating the extraction of Am(III) and Eu(III). However, the stoichiometry of the ligand coordinated to Am(III) and Eu(III) was dependent on the aqueous phase nitric acid concentration. Even though HDEHDGA did not extract Am(III) and Eu(III) at nitric acid concentration above 0.5 M, HDEHDGA participated in the extraction of these metal ions when combined with DOHyA in the binary solution. The participation of HDEHDGA in the extraction of Am(III) and Eu(III) decreased, whereas the participation of DOHyA increased with increase in the concentration of nitric acid. In contrast to the synergic extraction of Am(III) and Eu(III) observed at nitric acid concentrations above 0.5 M nitric acid, antagonistic extraction of Am(III) and Eu(III) was observed at lower acidities.

The selective stripping of Am(III) from loaded organic phase was facilitated by the adding DTPA to aqueous phase. A separation factor of ~ 13 and 86 were respectively obtained for the mutual separation of Eu(III) over Am(III) and Nd(III) over Am(III). Even though the separation factor achieved in batch mode was not very high, but it would be quite sufficient for the separation of Am(III) from other lanthanides when a continuous counter current mixer-settler was employed for mutual separations.

# Part III. Aggregation and organic phase splitting behavior in DOHyA-HDEHDGA synergistic system

## 7.7 Introduction

A binary solution of DOHyA + HDEHDGA in *n*-dodecane has been suggested for the single cycle separation of Am(III) and Cm(III) from high-level liquid waste in part II of chapter 7. In part III, the reverse micellar aggregation behavior of the binary solution composed of DOHyA and HDEHDGA in *n*-dodecane is discussed. In these studies, the organic phase was contacted with an aqueous solution containing Nd(III) in nitric acid and the aggregate distribution in organic phase was recorded using DLS spectroscopy The LOC, CAC and limiting aggregate size (LAS) for third phase formation was determined, and the results are reported in this chapter.

## 7.8 Results and discussion

### 7.8.1 Self-aggregation of neat organics in *n*-dodecane

The aggregation behavior of the binary solution composed of 0.2 M DOHyA+0.1 M HDEHDGA in *n*-dodecane is shown in Figure 7.19. The aggregate distribution observed in the binary solution has been compared with that obtained in the individual extractant present in *n*-dodecane. It can be seen that the average aggregate size observed for 0.2 M DOHyA/*n*-DD is 1.6 nm. This aggregate size is smaller than the aggregate size of 2.1 nm reported for 0.2 M tetraoctyl diglycolamide (TODGA) in *n*-dodecane (see part I of chapter 3). Since, the structure of DOHyA is half the molecular size of TODGA. As a result, the polar-polar interaction among the reverse micellar aggregates is more in TODGA and therefore, the average aggregate size formed in the solution of 0.2 M TODGA/*n*-DD is more as compared to that observed for 0.2 M DOHyA/*n*-DD. In contrast to this, the acidic ligand HDEHDGA contains an amidic, etheric as well as a carboxylic acid functional group, which has the pKa of 5.08 [24]. It is regarded as more polar than DOHyA. Therefore, the average size of the aggregate formed in a solution of 0.1 M HDEHDGA/*n*-DD is more (2.5 nm), and the aggregate distribution in *n*-dodecane is also higher than DOHyA. Combining these two ligands in *n*-dodecane results in a solution with the average aggregate size of 2.2 nm and the aggregate distribution similar to 0.1 M HDEHDGA/*n*-DD, as shown in Figure 7.19.

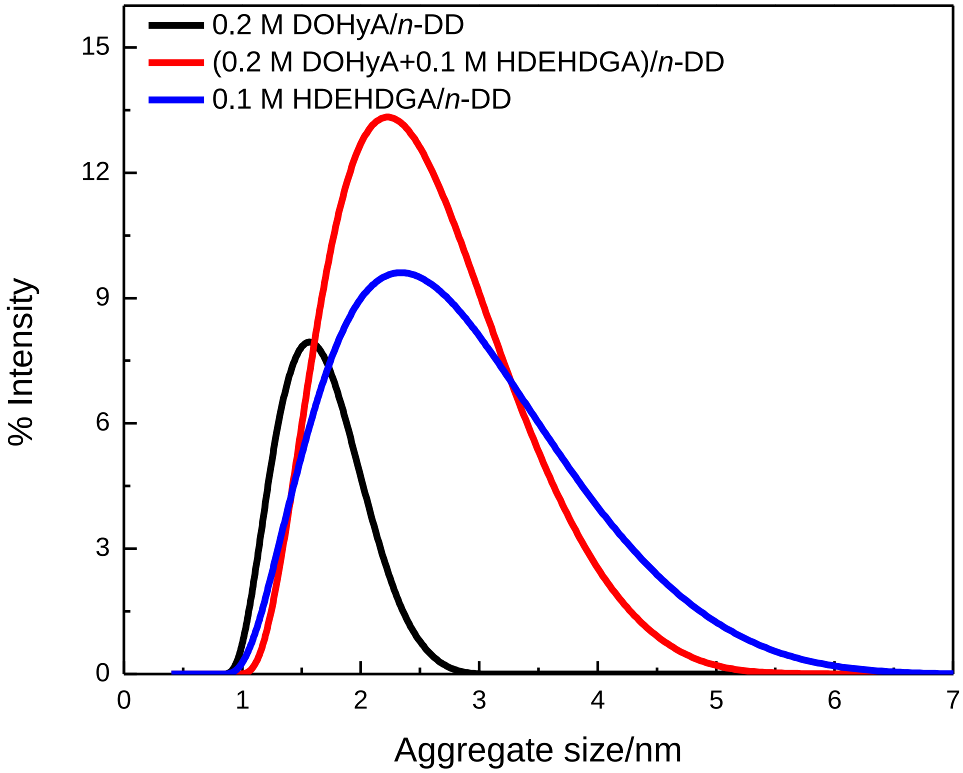

**Figure 7.19.** The aggregation behaviour of neat 0.2 M DOHyA/*n*-DD, 0.1 M HDEHDGA/*n*-DD and 0.2 M DOHyA+0.1 M HDEHDGA/*n*-DD.

### 7.8.2 Extraction of nitric acid

The extraction behavior of nitric acid in the individual and binary solution in *n*-dodecane is shown in Figure 7.20. It can be seen that the extraction of nitric acid in 0.2 M DOHyA/*n*-DD and 0.2 M DOHyA+0.1 M HDEHDGA/*n*-DD increases with increase in the initial concentration of nitric acid in aqueous phase in this case also. It should be noted that the organic phase undergoes splitting into two phases, when the initial concentration of the nitric acid in aqueous phase is 8 M in case of binary solution and 10 M in case of 0.2 M DOHyA/*n*-DD. The splitting of organic phase observed in these solutions could be attributed to the aggregation of reverse micelles beyond the limiting aggregate size for third phase formation, to be discussed below.

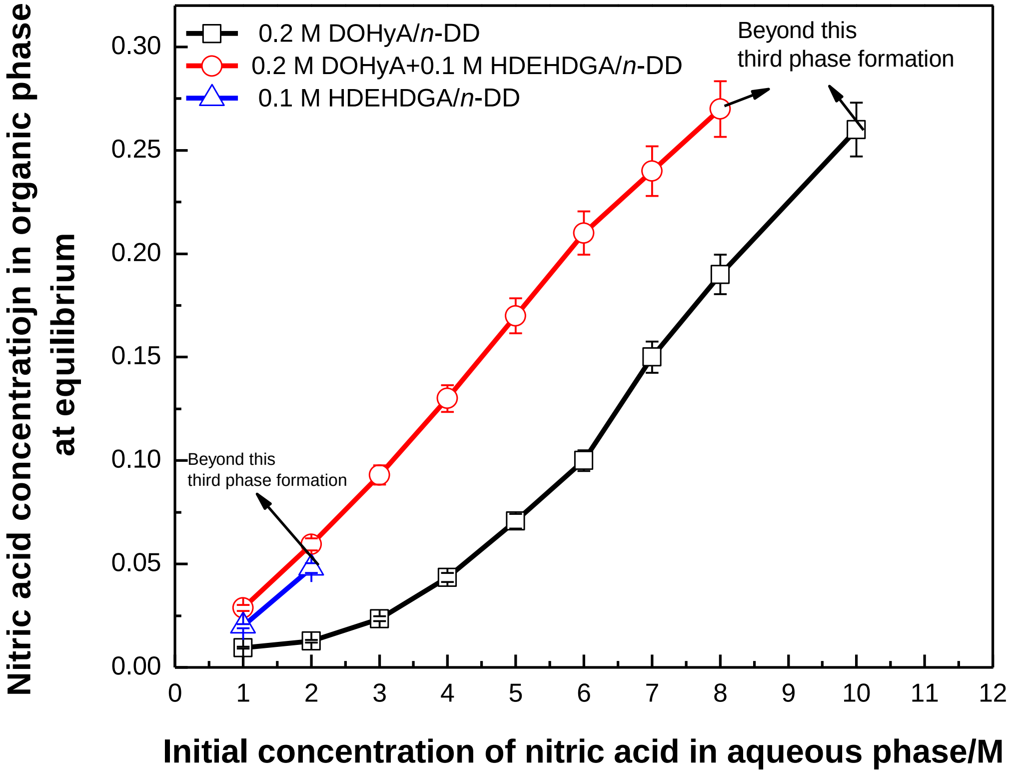

**Figure 7.20.** The extraction behavior of nitric acid in organic phase as a function of the initial

concentration of nitric acid in aqueous phase. Organic phase: 0.2 M DOHyA/*n*-DD or 0.1 M HDEHDGA/*n*-DD or 0.2 M DOHyA+0.1 M HDEHDGA/*n*-DD. Aqueous phase: Nitric acid concentrations varied from 1M to 10 M.

### 7.8.3 Aggregation and third phase formation

Extraction of nitric acid in organic phase results in the protonation of amidic and etheric functional moieties by nitric acid. The polarity of the ligand increases upon protonation and facilitates the aggregation of protonated ligands or acid-solvates due to polar-polar interactions in *n*-dodecane phase [25,26]. Figure 7.21 shows the comparison in the aggregation behavior of the organic phase containing DOHyA or HDEHDGA or the binary extractants in *n*-dodecane at different concentrations of nitric acid. It can be seen that the average aggregate size and the aggregate distribution in organic phase increases with increase in the concentration of nitric acid in aqueous phase. At 10 M nitric acid, the organic phase composed of 0.2 M DOHyA/*n*-DD underwent splitting into two phases namely, the "diluent-rich" phase and "third phase." The aggregate distribution of the third phase is also shown in Figure 7.21. The Figure also compares the aggregate distribution of other organic solutions namely HDEHDGA/*n*-DD, and binary solution. It can be seen that the average aggregate size of the third phase in all cases is much higher than the average aggregate size of the organic phase obtained before third phase formation as discussed in chapter 3. Moreover, the intensity of the third phase is much higher than that obtained for the organic phase before third phase formation. This indicates that the concentration of polar aggregates in third phase is higher, as compared to the organic phase before third phase formation as discussed in chapter 3.

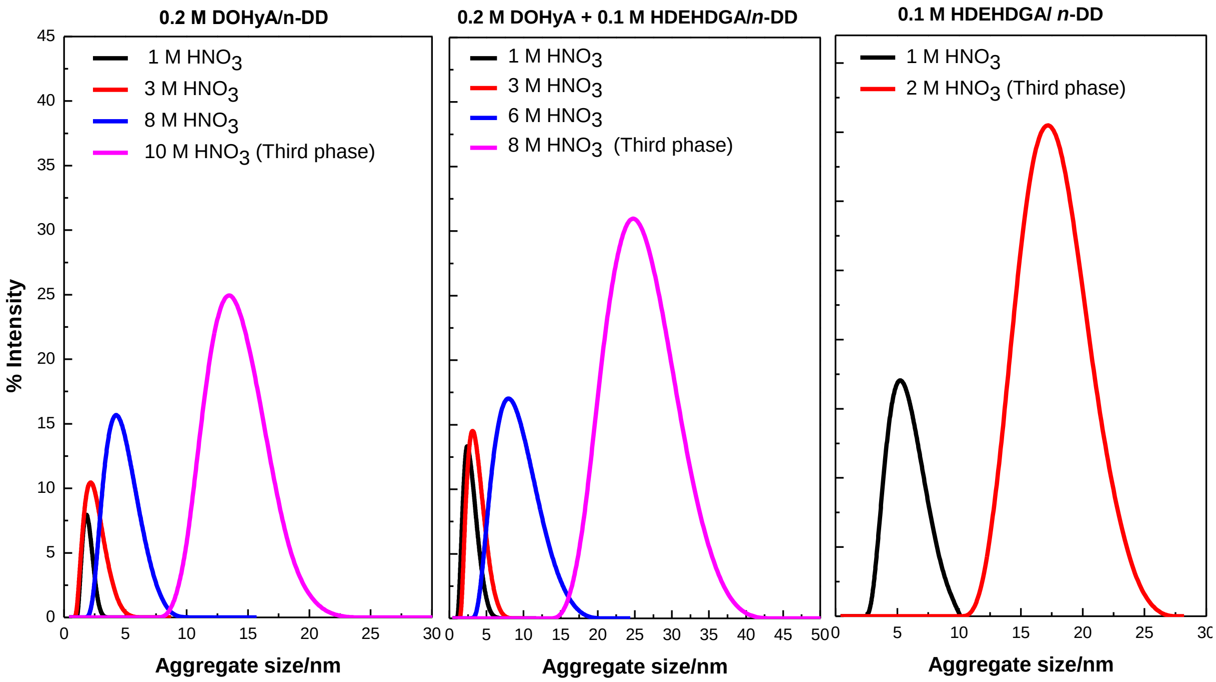

**Figure 7.21.** The variation in the aggregate distribution of the organic phase obtained after contacting 0.2 M DOHyA/*n*-DD or 0.1 M HDEHDGA/*n*-DD or 0.2 M DOHyA+0.1 M HDEHDGA/*n*-DD phases with nitric acid solution, whose concentration varied from 1 M to 10 M.

### 7.8.4 Limiting aggregate size

Figure 7.22 compares the aggregate distribution of the third phase with “diluent-rich” phase obtained after phase splitting. It can be seen that the aggregate distribution and the intensity of aggregates in the “diluent-rich” phase is much lower than the third phase, as discussed earlier chapters. The limiting organic phase concentration (LOC) of nitric acid for third phase formation was determined and the values for various organic phases are tabulated in Table 7.7. It can be seen that the LOC of nitric acid increases in the order of 0.1 M HDEHDGA/*n*-DD << 0.2 M DOHyA+0.1 M HDEHDGA/*n*-DD ~ 0.2 M DOHyA/*n*-DD.

The aggregation behavior of the organic phase at LOC was recorded for all organic solutions, and they are displayed in Figure 7.22. It can be seen that the average limiting aggregate size (LAS) for third phase formation is in the range of 10 to 15 nm. This indicates that the organic phase is likely to undergo splitting when the average aggregate size exceeds 10-15 nm in the present systems. It is interesting to compare the limiting aggregate size observed in case of DOHyA with that of TODGA reported elsewhere [26]. At LOC, the limiting concentration of nitric acid in the organic phase was determined to be 0.24 and 0.29 for 0.2 M DOHyA/*n*-DD and 0.2 M TODGA/*n*-DD, respectively (see Part I of chapter 3). However, the limiting aggregate size (that is at LOC) is 11 nm for 0.2 M DOHyA/*n*-DD, and 27 nm for 0.2 M TODGA/*n*-DD. The aggregate size observed for TODGA is about three times higher than that observed for DOHyA, even though the amount of nitric acid extracted into organic phase is nearly same. This could be due to the bigger molecular size of TODGA as compared to DOHyA (see Figure 7.1) that leads to the formation of bigger aggregates. In addition, the number of alkyl groups attached to the TODGA is more, and these alkyl groups interact efficiently with *n*-dodecane, as compared to DOHyA. These dispersive or Van der Waals interactions seem to stabilize the bigger aggregates without undergoing any phase splitting, even though the amount of nitric acid extracted into organic phase is quite similar in both the cases.

**Table 7.7.** The LOC and CAC of nitric acid in the individual and binary solutions.

| Organic phase | $[HNO_3]$ / M | LOC / M | CAC / M |
|---|---|---|---|
| 0.2 M DOHyA/*n*-DD | 10 M | 0.24 | 9.52 |
| 0.1 M HDEHDGA/*n*-DD | 2 M | 0.043 | 1.42 |
| 0.2 M DOHyA+0.1 M HDEHDGA/*n*-DD | 8 M | 0.27 | 6.78 |

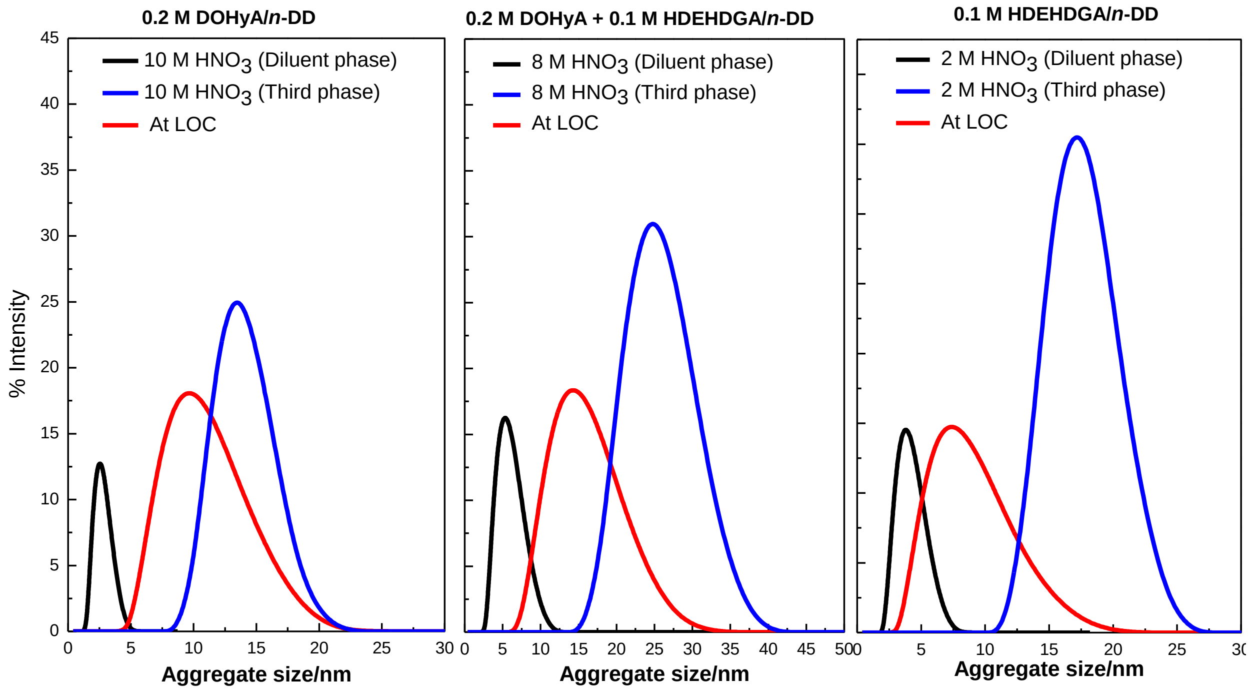

**Figure 7.22.** The variation in the average aggregate size of the organic phase obtained after contacting 0.2 M DOHyA/*n*-DD or 0.1 M HDEHDGA/*n*-DD or 0.2 M DOHyA+0.1 M HDEHDGA/*n*-DD with nitric acid concentration ranging from 1 M to 10 M.

### 7.8.5 Aggregation behavior upon Nd(III) extraction

Figure 7.23a shows the aggregation behavior of the 0.2 M DOHyA/*n*-DD phase recorded after contacting the organic phase with an aqueous phase containing Nd(III) in 3 M nitric acid. The concentration of Nd(III) in aqueous phase was varied from 1 g/L to 7 g/L. The aggregate distribution has been compared with the aggregation behavior of 0.2 M DOHyA+0.1 M HDEHDGA/*n*-DD under similar conditions in Figure 7.23b. It can be seen that the average aggregate size and their distribution in organic phase increases with increase in the amount of Nd(III) in nitric acid phase in both cases. However, the aggregate size and their distribution in 0.2 M DOHyA/*n*-DD phase are smaller than that observed for the binary extractants in *n*-

dodecane. This shows that the presence of HDEHDGA increases the aggregation behavior of the organic phase, as expected.

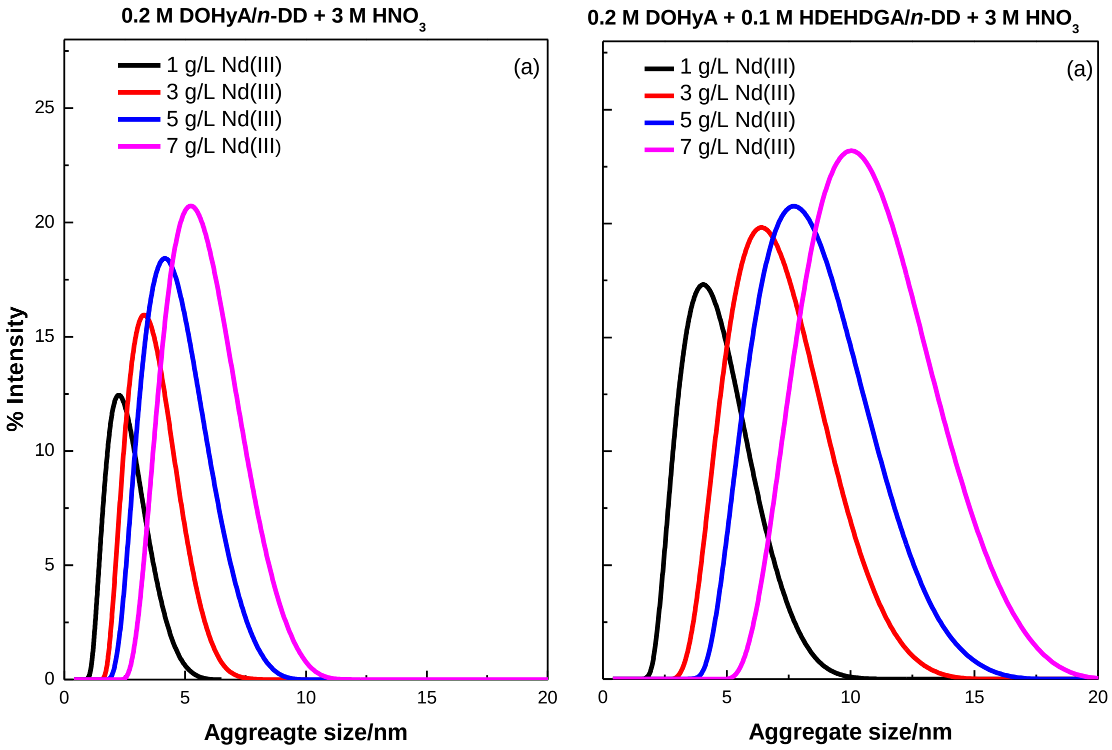

**Figure 7.23.** The variation in the average aggregate size of the organic phase obtained after contacting 0.2 M DOHyA/*n*-DD or 0.2 M DOHyA+0.1 M HDEHDGA/*n*-DD phase with 3 M nitric acid solution containing Nd(III) varied from 1 g/L to 7 g/L.

### 7.8.6 Effect of Nd(III) and nitric acid

Figure 7.24 shows the variation in the average aggregate size of the organic phase as a function of the initial amount of Nd(III) in aqueous phase (in g/L) at different concentrations of nitric acid. The aggregate size was recorded after contacting the organic phase, both 0.2 M DOHyA/*n*-DD and the binary solution, with an aqueous phase containing Nd(III) in 1 M to 5 M nitric acid. It can be seen that the aggregate size obtained in both cases increase with increase in the amount of Nd(III) in aqueous phase, as well as with nitric acid concentration. Increasing the concentration of nitric acid in aqueous phase increases the extraction of nitric acid (see Figure 7.20) and Nd(III). The coordination of Nd(III) and protonation of nitric acid on the ligand increases the polarity of the ligand in organic phase. Therefore, the polar-polar interaction increases in organic phase, and the aggregate size increases with increase in the concentration of nitric acid and Nd(III). The loading behavior of Nd(III) in 0.2 M DOHyA/*n*-DD and in binary solution, as a function of the initial amount of initial Nd(III) in aqueous phase is shown in Figure 7.25 a. It is obvious from the figure that loading of Nd(III) increases with increase in the amount of Nd(III) in aqueous phase. The increase in the loading of Nd(III) observed at higher nitric acid concentration is due to higher distribution ratio of Nd(III) achieved at higher nitric acid concentration, as discussed elsewhere [26-28].

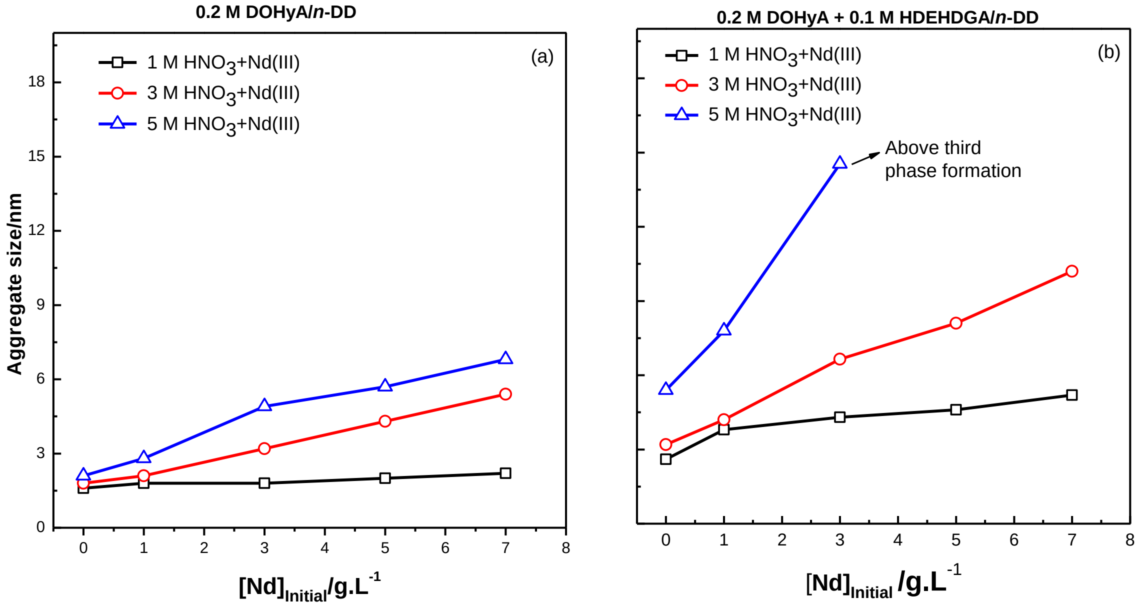

**Figure 7.24.** The variation in the average aggregate size of the organic phase obtained after contacting 0.2 M DOHyA/*n*-DD or 0.2 M DOHyA+0.1 M HDEHDGA/*n*-DD phase with the nitric acid solution containing Nd(III). The initial amount of Nd(III) in nitric acid was varied from 1 g/L to 7 g/L and the concentration of nitric acid in aqueous phase was varied from 1 M to 5 M.

It is important to note from Figure 7.25 b that the loading of Nd(III) is more in the binary solution than that observed for 0.2 M DOHyA/*n*-DD, under similar condition. At 5 M nitric acid, the third phase formation was observed when the binary solution was contacted with 4 g/L Nd(III) in 5 M nitric acid (Figure 7.25b). However, it was also noted from the Figure 7.25b that there was no third phase formation at 3 M and 1 M nitric acid even at the initial amount of Nd(III) was 7 g/L. In addition, the amount of Nd(III) loaded in the organic phase at 3 M nitric acid is more as compared to the loading of Nd(III) at 5 M nitric acid. The absence of third phase formation at lower nitric acid (1-3 M nitric acid) and the observation of phase splitting at 5 M nitric acid could be attributed to the variations in the reverse micellar aggregate size of the binary solution upon Nd(III) loading at 5 M nitric acid. Figure 7.24b shows the variation in the average aggregate size determined for the binary solution at different initial amounts of Nd(III) in aqueous phase. It can be seen that the average aggregate size of 15 nm is observed at 3 g/L Nd(III) in 5 M nitric acid. Since this aggregate size appears to be the limiting value for phase splitting in organic phase, the third phase formation was observed at 5 M nitric acid solution containing Nd(III) more than 3 g/L. However, the aggregate size was lower than 15 nm for 1 M and 3 M nitric acid solutions containing Nd(III) ranging from 1 g/L to 7 g/L (see Figure 7.24b). Therefore, the third phase formation was not observed in those systems, even at high loading of Nd(III) achieved in organic phase, as shown in Figure 7.25.

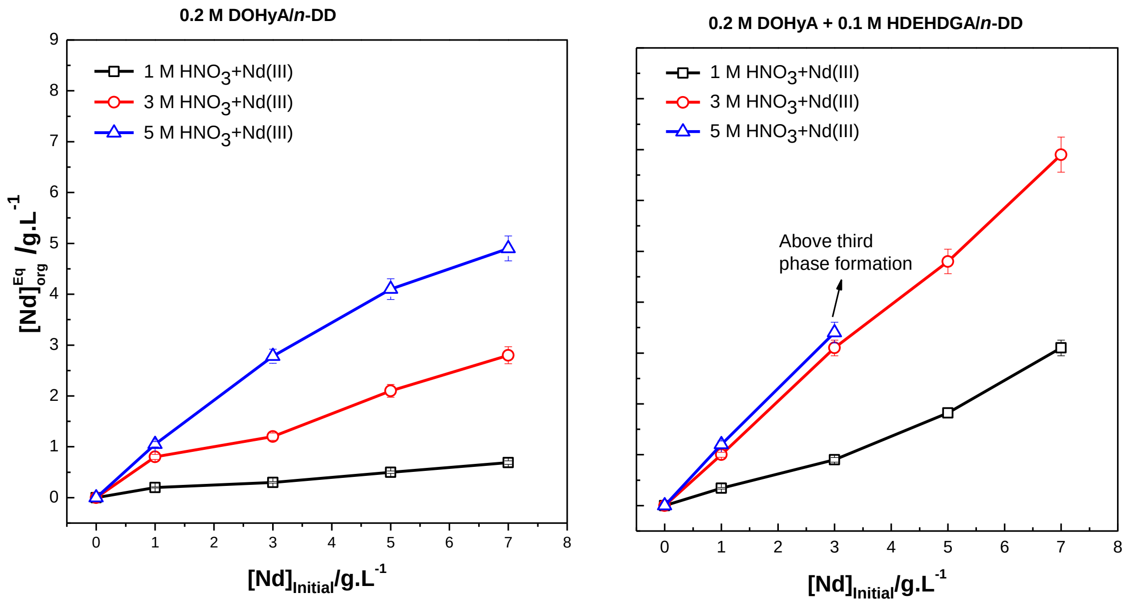

**Figure 7.25.** The extraction behavior of Nd(III) in organic phase as a function of initial amount of Nd(III) in nitric acid. Organic phase: 0.2 M DOHyA/*n*-DD or 0.2 M DOHyA+0.1 M HDEHDGA/*n*-DD. Aqueous phase: $[Nd(III)]_{initial}$ varied from 1 g/L to 7 g/L in 1 M to 5 M nitric acid.

### 7.8.7 Aggregation behavior with simulated waste

The binary solution composed of 0.2 M DOHyA+0.1 M HDEHDGA/*n*-DD has been proposed for the extraction of trivalent metal ions from high-level liquid waste (HLLW) solution, which is composed of multi component metal ions dissolved in 3-4 M nitric acid medium as described previous chapters. The aggregation behavior of the binary solution was recorded after contacting the binary solution with fast reactor simulated high-level liquid waste (SHLLW), and the results are shown in Figure 7.26. It can be seen that the aggregate size increases after contacting the organic phase with SHLLW. However, the average aggregate size is lower than the limiting aggregate size of 15 nm for third phase formation. Therefore, the third phase formation was not observed in the binary solution after contacting with simulated waste.

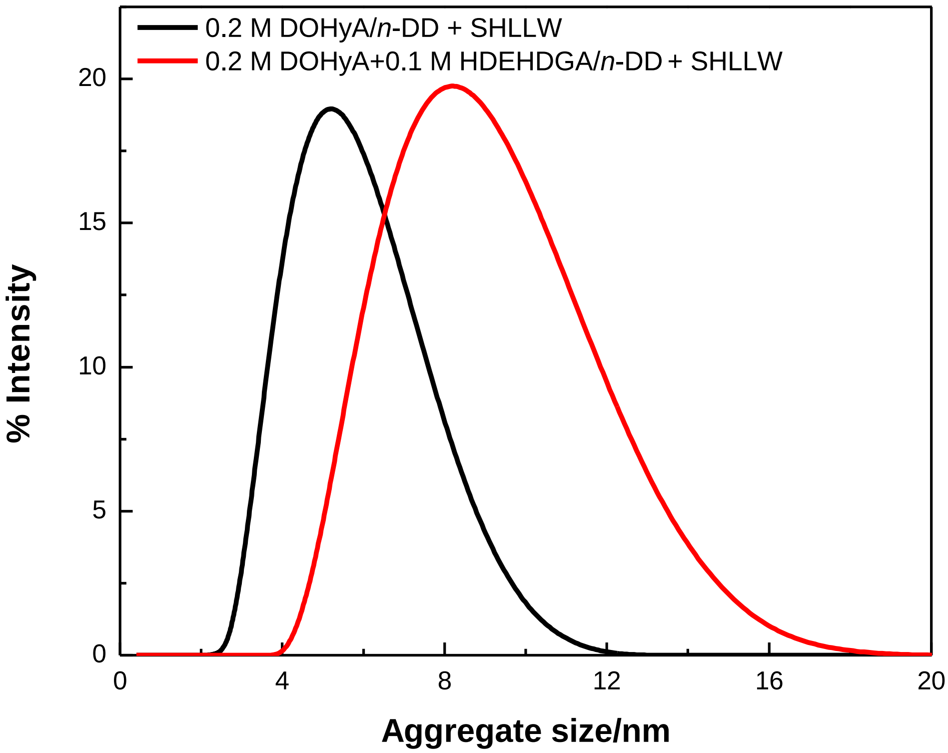

**Figure 7.26.** The variation in the aggregate distribution of the organic phase obtained after contacting 0.2 M DOHyA/*n*-DD or 0.2 M DOHyA+0.1 M HDEHDGA/*n*-DD with simulated HLLW.

## 7.9 Summary

The ligands, DOHyA and HDEHDGA, undergo reverse micellar aggregation in *n*-dodecane and the self- aggregate size increased in the order DOHyA< DOHyA + HDEHGA < HDEHDGA in *n*-dodecane medium. The extraction of nitric acid in organic phase containing either DOHyA or HDEHDGA or the binary ligands in *n*-dodecane increased with increase in the concentration of nitric acid and the average size of aggregates formed in organic phase at a particular concentration of nitric acid increased in the order DOHyA < DOHyA + HDEHGA <<

HDEHDGA. As a result, the tendency of third phase formation increased in the same order when the organic phase was contacted with nitric acid. Interestingly, all these ligands in *n*-dodecane resulted in a third phase when the average aggregate size exceeded the limiting value of about 10-15 nm. However, the limiting aggregate size (LAS) was achieved at different concentrations of nitric acid in aqueous phase for these organic solutions. For instance, 0.1 M HDEHDGA/*n*-DD acquired the LAS after contacting with 2 M nitric acid whereas 0.2 M DOHyA + 0.1 M HDEHDGA/*n*-DD and 0.2 M DOHyA/*n*-DD acquired LAS above 8 M and 10 M nitric acid, respectively.

Similarly, the extraction of Nd(III) in DOHyA or a binary solution in *n*-dodecane increased with increase in the concentration of Nd(III) and nitric acid in aqueous phase. The average aggregate size and their distribution in organic phase was significantly more in case of binary solution as compared to that observed in DOHyA/*n*-DD. The aggregates formed in binary solution easily exceeded the LAS of 15 nm at 5 M nitric acid solution containing 4 g/L of Nd(III). However, at 1 M and 3 M nitric acid, the aggregate size was much lower than the LAS, even at higher Nd(III) loadings. As a result, the third phase formation was not observed in the binary solution at 1 M and 3 M nitric acid. Moreover, the binary solution did not form third phase when it was contacted with simulated waste containing ~4 g/L of trivalents (lanthanides and actinides) in 3 M nitric acid in addition to other metal ions. In all the cases discussed above, the aggregate size and distribution was much lower in DOHyA as compared to the binary solution. Finally, the binary solution composition 0.2 M DOHyA+0.1 M HDEHDGA/*n*-DD was suitable for the extraction of trivalent metal ions from SHLLW without third phase formation.

**References**

[1] R.R.J.M. Konings, J.L. Kloosterman, A view of strategies for transmutation of actinides, Prog Nucl. Energ. 38 (2001) 331-334.

[2] T. Takeda, Minor actinides transmutation performance in a fast reactor, Ann. Nucl. Energy. 95 (2016) 48-53.

[3] S.A. Ansari, P.N. Pathak, P.K. Mohapatra, V.K. Manchanda, Chemistry of diglycolamides: Promising extractants for actinide partitioning, Chem. Rev. 112 (2012) 1751-1772.

[4] J.N. Mathur, M.S. Murali, Nash, K.L.: Actinide partitioning – a review, Solvent Extr. Ion Exch.19, 357-390(2001).

[5] M. Nilson, K.L. Nash, A review of the development and operational characteristics of the TALSPEAK process, Solvent Extr. Ion Exch. 25 (2007) 665-701.

[6] M.J. Zhang, F.W. Lewis, L. M. Harwood, Chapter 6 - The Circuitous Journey from Malonamides to BTPhens: Ligands for Separating Actinides from Lanthanides, In: Michael Harmata, Editor(s), Strategies and Tactics in Organic Synthesis, Academic Press. 9,177-202(2013).

[7] J. Veliscek-Carolan, Separation of actinides from spent nuclear fuel: A review, J. Hazard. Mater. 318(2016) 266-281.

[8] S.A. Ansari, D.R. Prabhu, R.B. Gujar, A.S. Kanekar, B. Rajeswari, M.J. Kulkarni, M.S. Murali, Y. Babu, V. Natarajan, S. Rajeswari, A. Suresh, R. Manivannan, M.P. Antony, T.G. Srinivasan, V.K. Manchanda, Counter-current extraction of uranium and lanthanides from simulated high-level waste using N,N,N’,N’-tetraoctyl diglycolamide, Sep. Purif. Technol. 66 (2009) 118-124.

[9] S.A. Ansari, P.N. Pathak, P.K. Mohapatra, V.K. Manchanda, Chemistry of diglycolamides: Promising extractants for actinide partitioning, Chem.Rev.112 (2012) 1751-1772.

[10] P.J. Panak, A. Geist, Complexation and Extraction of Trivalent Actinides and Lanthanides by Triazinylpyridine N‑Donor Ligands, Chem. Rev. 113 (2013) 1199−1236

[11] A. Wilden, C. Schreinemachers, M. Sypula, G. Modolo, Direct Selective Extraction of Actinides (III) from PUREX Raffinate using a Mixture of CyMe4BTBP and TODGA as 1-cycle SANEX Solvent, Solvent Extr. Ion Exch. 29 (2011) 190-212.

[12] A. Bhattacharyya, P. K. Mohapatra. Separation of trivalent actinides and lanthanides using various 'N','S'and mixed 'N, O'donor ligands: a review, Radiochimica Acta.

[13] G.J. Lumetta, A.V Gelis, F. Vandegrift, Solvent systems combining neutral and acidic extractants for separating trivalent lanthanides from the transuranic elements, Solvent Extr. Ion Exch. 28 (2010) 287-312.

[14] G.J. Lumetta, A.V. Gelis, J.C. Braley, J.C. Carter, J.W. Pittman, M.G. Warner, G.F. Vandegrift, The TRUSPEAK concept: combining CMPO and HDEHP for separating trivalent lanthanides from the transuranic elements, Solvent Extr. Ion Exch. 31 (2013) 223-236.

[15] J.C. Braley, T.S. Grimes, K.L. Nash, Alternatives to HDEHP and DTPA for simplified TALSPEAK separations, Ind. Eng. Chem. Res. 2 (2011) 629-638.

[16] P.K. Nayak, R.Kumaresan, K.A. Venkatesan, M.P. Antony, P.R. Vasudeva Rao, A new method for partitioning of trivalent actinides from high-level liquid waste, Sep. Sci. Technol. 48 (2013) 1409-1416.

[17] P.K. Nayak, R. Kumaresan, K.A. Venkatesan, M.P. Antony, P.R. Vasudeva Rao, Extraction behavior of Am (III) and Eu (III) from nitric acid medium in

tetraoctyldiglycolamide-bis (2-ethylhexyl) phosphoric acid solution, Sep. Sci. Technol. 49 (2014) 1186-1191.

[18] P.K. Nayak, R. Kumaresan, K.A. Venkatesan, S. Rajeswari, G.G.S. Subramanian, M.P. Antony, P.R. Vasudeva Rao, Single-cycle separation of americium (III) from simulated high-level liquid waste using tetra-bis (2-ethylhexyl) diglycolamide and bis (2-ethylhexyl) phosphoric acid solution, J. Environ. Chem. Eng. 1 (2013) 559-565.

[19] J. Ravi, K. A. Venkatesan, M. P. Antony, T. G. Srinivasan, P. R. Vasudeva Rao, Single-cycle method for partitioning of trivalent actinides using completely incinerable reagents from nitric acid medium, Radiochimi. Acta. 102 (2014) 599–607.

[20] S. Kannan, B.G. Vats, I.C. Pius, D.M. Noronha, P.S. Dhami, P.W. Naik, M. Kumar, Extraction and structural studies of an unexplored monoamide, N, N′-dioctyl, α-hydroxy acetamide with lanthanide (iii) and actinide (iii) ions, Dalton Trans. 43 (2014) 5252-5255.

[21] T. Prathibha, R. Kumaresan, B. R. Selvan, K.A. Venkatesan, M. P Antony, P. R. Vasudeva Rao, N, N-dialkyl-2-hydroxyacetamides for modifier-free separation of trivalent actinides from nitric acid medium, Radiochimi. Acta. 104 (2016) 173-181.

[22] V.V. Ramakrishna, S.K. Patil, Synergic extraction of actinides. In New Developments, Springer Berlin Heidelberg, (1984) 35-90.

[23] P. Tkac, G. F. Vandegrift, G. J. Lumetta, A. V. Gelis, Study of the interaction between HDEHP and CMPO and its effect on the extraction of selected lanthanides, Ind. Eng. Chem. Res. 51 (2012) 10433-10444.

[24] A. S. Suneesh, K. A. Venkatesan, K. V. Syamala, M. P. Antony P. R. Vasudeva Rao, Mutual separation of americium(III) and europium(III) using glycolamic acid and thioglycolamic acid, Radiochim. Acta. 100 (2012) 425-430.

[25] L. Berthon, L. Martinet, F. Testard, C. Madic, T. Zemb, Solvent penetration and sterical stabilization of reverse aggregates based on the DIAMEX process extracting molecules: consequences for the third phase formation, Solvent Extr. Ion Exch. 25 (2007) 545-576.

[26] T. Prathibha, K. A. Venkatesan, M. P. Antony, Comparison in the aggregation behaviour of amide extractant systems by dynamic light scattering and ATR-FTIR spectroscopy, Colloids Surf. A 538 (2018) 651-660.

[27] T. Yaita, A. W. Herlinger, P.Thiyagarajan, M. P. Jensen, Influence of extractant aggregation on the extraction of trivalent f-element cations by a tetraalkyldiglycolamide, Solvent Extr. Ion Exch. 22 (2004) 553-571.

[28] M. P. Jensen, T. Yaita, R. Chiarizia, Reverse-micelle formation in the partitioning of trivalent f-element cations by biphasic systems containing a tetraalkyldiglycolamide, Langmuir 234 (2007) 4765-4774.

# Homi Bhabha National Institute

## SYNOPSIS OF Ph. D. THESIS

1. **Name of the Student: KANTAMANI RAMA SWAMI**
2. **Name of the Constituent Institution: INDIRA GANDHI CENTRE FOR ATOMIC RESEARCH**
3. **Enrolment No. : CHEM02201504004**
4. **Title of the Thesis: Solvent extraction of some trivalent lanthanides and actinides in alkyldiglycolamides and the aggregation and spectroscopic investigations on the extracted phase**
5. **Board of Studies: CHEMICAL SCIENCES**

## SYNOPSIS

Electricity is required for the welfare of human beings. The generation of electricity is largely dependent on the availability of fossil fuels such as coal, oil and natural gas. The use of fossile fuels for the production of electricity releases considerable amount of green house gases, which are identified to be the major factor for global warming and climate changes happening all over the world. Moreover, the consumption of these non-renewable fossil fuels for the production of electricity decreases the availability of valuable energy resources in the earth crust. Therefore, there is a need to look for alternative resources that supply electricity without emitting the green house gases. In this context, the production of energy from renewable resources and nuclear fission reaction have evolved as promising alternatives to fossil fuels.

Currently, the global contribution of nuclear energy for the production of electricity is about 18% and in India it is 4% [1]. The nuclear reactors employ uranium (natural or enriched) oxide and uranium-plutonium mixed oxide as a fuel for the generation of nuclear power. The fuel discharged from the reactor after the production of energy is known as the spent nuclear fuel. It contains depleted uranium, significant amount of plutonium, fission product elements and activation products. The concept of closed nuclear fuel cycle envisages reprocessing of the spent nuclear fuel which is aimed at the recovery of useful fissile elements such as uranium and plutonium from the spent fuel. The fissile elements thus recovered can be employed as a fuel in other/future nuclear reactors for the sustainable growth of nuclear power.

PUREX (Plutonium Uranium Recovery by EXtraction) process has been adopted for reprocessing of spent nuclear fuels. The process involves the dissolution of spent nuclear fuel in nitric acid medium followed by the solvent extraction of uranium and plutonium from the dissolver solution into the organic phase containing 1.1 M tri-*n*-butyl phosphate (TBP) present in *n*-dodecane (*n*-DD) [2]. The aqueous raffinate rejected after the separation of uranium and plutonium is concentrated to obtain "high-level liquid waste" (HLLW). The HLLW is a complex mixture of several elements such as the radioactive actinides, short and long-lived fission products, stable fission products and corrosion products present in 3-4 M nitric acid medium. Since the half-lives of the radionuclides present in HLLW are in the range varying from few years to several hundred years, the HLLW poses a long-term risk to the human health and safety of the environment [3]. Among the radionuclides, the radiotoxicity of HLLW is essentially governed by the alpha-emitting long-lived actinides such as $^{241}$Am ($t_{1/2}$ = 433 y), $^{237}$Np ($t_{1/2} = 2.14\times10^6$ y) and $^{244}$Cm ($t_{1/2}$ = 18 y) and fission products such as $^{137}$Cs ($t_{1/2}$ = 30 y) and $^{90}$Sr ($t_{1/2}$ = 28.8 y).

Partitioning of trivalent actinides (An(III) = Am(III) and Cm(III)) from high-level liquid waste followed by transmutation of them into stable or short-lived products in accelerated driven systems or fast-reactors is a viable option for minimizing the radiotoxicity of HLLW [4]. However, the partitioning procedure is not simple. It is a challenging job of separating the trivalent actinides from chemically similar lanthanide fission products present in 3-4 M nitric acid medium of HLLW. Currently, the separation of trivalent actinides from HLLW is a two-cycle process. The first–cycle involves the group separation of trivalent actinides (An) and lanthanides (Ln) together from HLLW, followed by the mutual separation of lanthanides and actinides in the second-cycle. A number of methods and extractants have been reported in literature on group separation (Ln and An) as well as the mutual separation of lanthanides and actinides [5-7].

In contrast to the two-cycle approach, the single-cycle approaches are also becoming popular in recent past, for the separation of trivalent actinides alone from HLLW. In this context, several nitrogen containing polydendate donors have been developed for selective binding of Am(III) alone present in aqueous nitric acid. Since the nitrogen containing ligands are classified as soft base donors, they interact efficiently with actinides as compared to lanthanides. For instance, the 1-cycle SANEX method developed for the direct separation of Am(III) alone from nitric acid medium employed a polydendate nitrogen donor, namely 6,6'-bis(5,5,8,8-tetramethyl-5,6,7,8-tetrahydro-benzotriazin-3-yl)-[2,2'] bipyridine ($CyMe_4$-BTBP) in a solution containing *N,N,N',N'*-tetra-octyldiglycolamide (TODGA) in TPH/1-octanol[8]. However, the diluent used in the study, TPH/1-octanol, was not a conventional diluent, *n*-dodecane, which is usually employed for reprocessing applications. In addition to this, another variant of the single-cycle method uses a combination of a neutral and acidic extractants for the separation of trivalent actinides. In this approach, the trivalent actinides and lanthanides are extracted together from HLLW using a binary solvent formulation and the recovery of actinides alone from the loaded solvent phase was carried out using aqueous soluble complexing agents [9].

One of the major concern associated with the extraction of trivalent actinides and lanthanides from HLLW is the third phase formation. It is the splitting of organic phase into two phases namely the "diluent rich phase" and "third phase" during the course of solvent extraction. This happens at a particular loading of nitric acid and metal ions in organic phase. The concentration of nitric acid or metal ion in organic phase above which the organic phase splits into two phases is called as limiting organic phase concentration (LOC), and the corresponding aqueous phase concentration is known as the critical aqueous phase concentration (CAC) [10]. The occurrence of third phase formation is due to the extensive reverse micellar aggregation of polar ligands present in a non-polar diluent ,*n*-dodecane [11]. The third phase formation or organic phase splitting causes large variations in the physicochemical properties of the solvent phase, such as changes in density, poor phase disengagement accompanied by flooding etc., during the industrial scale solvent extraction procedure. Moreover, the third phase can cause uncontrolled fission reaction when the fissile elements are accumulated at the third phase [12]. All these limitations call for the development of advanced solvent systems for preventing the third phase formation or procedures to minimise third phase formation.

## 2. Scope of the present study

Diglycolamides (DGAs) are regarded as promising reagents for the separation of trivalent actinides and lanthanides from the nitric acid solution. The alkyl group attached to DGA plays a pivotal role in deciding the extraction and third phase formation behavior of trivalents in organic phase. However, the exact role of the alkyl group attached to DGA in deciding the third phase formation is not known, unambiguously. To prevent this undesirable third phase formation during the course of solvent extraction, the organic phase modifiers have been usually added to the organic solvent phase. For instance, the phase modifiers such as tri-*n*-butyl phosphate (TBP), or dihexyloctanamide (DHOA), or long chain alcohols have been added as phase modifiers during the extraction of trivalent actinides in a solution of tetra octyl diglycolamides in *n*-dodecane. However, the knowledge on how the addition of phase modifiers controls the aggregation and third phase formation are very limited. Moreover, the behavior of reverse micellar aggregation of the radiolytically degraded diglycolamides in *n*-DD is not known so far, even though the effect of degradation products on the solvent extraction of actinides is well documented.

A combination of neutral and acidic extractants has been proposed for the single-cycle separation of trivalent actinides from HLLW. The neutral extractant in the binary solution governs the extraction of lanthanides and actinides as a group, and the acidic extractant controls the stripping of actinides alone from the organic phase. For efficient separation of lanthanides and actinides, it is necessary to understand the role of acidic extractant and its pKa value on the extraction and stripping behaviour of lanthanides and actinides from the binary solvent system. Apart from this, the behavior of acidic extractants in controlling the third phase formation and the mechanism of aggregation in the presence of acidic extractant have not been reported so far.

In view of the absence of vital information on the issues discussed above, it is proposed to address them in the present thesis. Therefore, the objective of the thesis is many fold and they are highlighted in below.

1. The role of alkyl chain length attached to DGA (varied from hexyl to dodecyl derivatives) in determining the tendency of aggregation and third phase formation of alkyl diglycolamides in *n*-DD was investigated by dynamic light scattering technique. The aggregation behavior of a particular alkyl diglycolamide in different *n*-paraffins was also investigated. The extraction behavior of nitric acid in various organic phases was studied

and the organic phase obtained after extraction was subjected to dynamic light scattering and MD simulations to understand the aggregation and organic phase splitting behaviour.

2. To examine the role of phase modifiers, the solvent extraction of Nd(III) from nitric acid medium was carried out in a solution of tetra(2-ethylhexyl)diglycolamide (TEHDGA) dissolved in *n*-dodecane in the presence of TBP, DHOA and long chain alcohols. The organic phase obtained after extraction was again subjected to dynamic light scattering studies to bring out the role of these modifiers in minimizing the third phase formation.
3. Similarly, the role of degradation products on the aggregation behavior of organic phase containing tetra(2-ethylhexyl) diglycolamide and *n*-dodecane was studied by irradiating the organic liquid to various absorbed dose levels in a gamma irradiation chamber. The irradiated organic phases were subjected to solvent extraction and the organic phase obtained after the extraction of nitric acid and Nd(III) was investigated by dynamic light scattering. The results were compared with those obtained for the unirradiated organic phases.
4. Towards the development of single-cycle separations, the effect of pKa of the acidic extractant in the binary solution was investigated by studying the extraction behavior of Am(III) in a solution of tetra(2-ethylhexyl)diglycolamide and acidic extractant (HA) present in *n*-dodecane. The acidic extractants investigated were bis(2-ethylhexyl)phosphoric acid (HDEHP), bis(2-ethylhexyl)phosphonic acid (PC88A) and bis(2,4,4-trimethylpentyl)phosphinic acid (CYANEX-272) and whose pKa values decreased in the order CYANEX-272 (6.37) > PC88A (4.51) > HDEHP (3.24). The extraction results obtained in the combined solvent system was further probed by ATR-FTIR spectroscopy to understand the interactions between metal ion and solvent system. Moreover, the organic phase was probed by dynamic light scattering to examine the reverse micellar aggregation in the binary solution.

5. Similarly, a binary solution composed of *N,N*-2-dioctylhydroxyacetamide (DOHyA) and HDEHP or bis(2-ethylhexyl)diglycolamic acid (HDEHDGA) was evaluated for the mutual separation of Am(III) from Eu(III) containing nitric acid solution for the development of a method for single-cycle separation. The feasibility of selective stripping of Am(III) alone from loaded solvent system containing both Am(III) and Eu(III) was investigated. In addition, the reverse micellar aggregation behavior of the binary solution containing DOHyA+ HDEHDGA dissolved in *n*-dodecane was also studied.

The results obtained from all the investigations discussed above are described in this thesis.

## 3. Organization of the thesis

This thesis comprises of eight chapters. A brief discussions on the contents of the chapters are described below.

### 3.1. Chapter 1: Introduction

The introduction chapter starts with the significance of nuclear energy in the current scenario, resources for the production of nuclear power, reprocessing of spent nuclear fuel and safe management of high-level liquid waste (HLLW) generated during the reprocessing. The importance of trivalent actinide partitioning from HLLW and the methods and materials developed so far for partitioning of Am(III) are described in detail. In addition, this chapter also discusses the third phase formation behavior of the solvent systems employed for the extraction of trivalent metal ion, nitric acid and the literature survey on various approaches for preventing third phase formation. A short note on the scope of the present work is enumerated at the end of this chapter.

### 3.2. Chapter 2: Experimental

The second chapter deals with the description of materials, methods and instruments employed in the present study. The synthesis of the extractants and characterization techniques for confirming the structure and purity of extractants are discussed. A brief principle of instrumental and spectroscopic methods employed in the present study such as dynamic light scattering (DLS), ATR-FTIR, Raman, GC-MS and molecular dynamic (MD) simulation studies are explained. The solution preparation for liquid-liquid extraction and fast reactor (FR) - simulated high-level liquid waste (SHLLW) are described in detail.

### 3.3. Chapter 3: Aggregation behaviour of tetraalkyl diglycolamides in *n*-paraffins

This chapter deals with the extraction behavior of nitric acid and Nd(III) in various tetraalkyl diglycolamides dissolved in different *n*-paraffins. The extracted organic phase was subjected to dynamic light scattering, ATR-FTIR and MD simulations to understand the aggregation behavior of the organic phase. The chapter was divided into two parts.

The first part of the chapter describes the extraction behavior of nitric acid and Nd(III) in a solution of 0.2 M tetraalkyl diglycolamide dissolved in *n*-dodecane (*n*-DD). The alkyl moiety in DGA was varied from hexyl to dodecyl. The results showed that the extraction of nitric acid into organic phase was similar in all cases. However, the dynamic light scattering studies revealed that the diglycolamides with longer alkyl chain showed a lesser tendency to form bigger aggregates and third phase owing to the predominant dispersive interaction of the aggregates with *n*-DD. A similar aggregation trend was also observed during the extraction of Nd(III). In addition, the extraction behavior of nitric acid in a alkyl diglycolamide dissolved in different *n*-paraffins (varied from *n*-octane to *n*-tetradecane) was also reported in this chapter. The extraction of nitric acid into organic phase was similar in all solvent phases in this case also. However, the DLS results showed that the aggregates size increased with increasing alkyl chain length of *n*-paraffin, which in turn led to early third phase formation in organic phase containing longer alkyl chain *n*-paraffins. The aggregation data was validated by molecular dynamic simulations and radial distribution analysis.

The second part of the chapter deals with the aggregation behaviour of 0.2 M TEHDGA dissolved in *n*-dodecane, probed by DLS, ATR-FTIR spectroscopic methods. The results revealed that the extraction of nitric acid and Nd(III) into organic phase increased with increase in the aqueous phase concentration of nitric acid and Nd(III). The limiting organic phase concentration (LOC) of nitric acid and Nd(III) for third phase formation was reported. The DLS studies revealed that a large number of aggregates of different sizes were formed in organic phase and reached a maximum aggregate size at LOC. Upon organic phase splitting, a significant increase in the concentration of nitric acid and Nd(III) in third phase was observed. In contrast to this, the aggregate size was lower in the diluent rich phase. The aggregation results obtained from DLS were corroborated to the ATR-FTIR spectroscopy results of the organic phase obtained after the extraction.

### 3.4. Chapter 4: Role of phase modifiers in controlling the third phase formation

This chapter deals with the role of phase modifiers in controlling the third phase formation of the solvent phase composed of 0.2 M TEHDGA/*n*-DD. The organic phase obtained after the extraction of trivalent metal ion and nitric acid was probed by dynamic light scattering and FTIR spectroscopy. This chapter was divided into two parts.

The Part I describes the results on the investigations aimed at the role of neutral extractants namely TBP and DHOA as phase modifiers in maneuvering the third phase formation. The extraction behaviour of nitric acid and Nd(III) was studied in a binary solution of 0.2 M TEHDGA + TBP/ DHOA in *n*-dodecane and the results were compared with the individual solvent systems. The extraction results showed that the LOC and CAC of nitric acid in 1.1 M TBP/*n*-DD and 0.5 M DHOA/*n*-DD were significantly higher than that obtained in 0.2 M TEHDGA/*n*-DD. The DLS studies showed that the average size of aggregates and the aggregate distribution in organic phase increased with increase in the concentration of nitric acid in aqueous phase in all cases. The addition of phase modifier was found to reduce the average size of aggregates below the limiting aggregate size for third phase formation, which in turn increased the dispersion of aggregates in *n*-dodecane phase.

Part II discusses the effect of long-chain alcohols on the third phase formation behavior of 0.2 M TEHDGA/*n*-DD. The long chain aliphatic alcohols chosen were *n*-octanol, *n*-decanol and isodecanol. The results showed that the extraction of Nd(III) or $HNO_3$ in all organic phases (0.2 M TEHDGA/*n*-DD+alcohol) increased with increase in the initial amount of Nd(III) and $HNO_3$ in aqueous phase. The DLS results revealed that addition of alcohol phase modifiers controlled the aggregate size to a much lower value than the limiting aggregate size needed for third phase formation. This was due to the polar nature of alcohols that did not allow the aggregation of reverse micelles in organic phase and prevented the third phase formation during extraction.

### 3.5. Chapter 5: Effect of gamma irradiation on aggregation

This chapter describes about results on the aggregation behavior of the organic phase containing radiolytically degraded TEHDGA and *n*-dodecane. The solvent system was classified into four different categories of liquids comprising of (1) 0.2 M solution of TEHDGA present in *n*-DD, (2) TEHDGA alone, (3) *n*-dodecane alone, and (4) 0.2 M TEHDGA/*n*-DD in the presence of extracted nitric acid. The liquids were irradiated to a specified absorbed dose levels (10 kGy to 500 kGy) in a $^{60}$Co gamma irradiator. The irradiated liquids were made to a solution containing 0.2 M TEHDGA in *n*-dodecane, if required. The extraction of nitric acid in the irradiated organic phase was and the organic phase obtained after extraction was investigated by dynamic light scattering technique. The results showed that the extraction of nitric acid into the irradiated organic phase was quite similar for all the irradiation systems. However, the third phase formation behavior was different. The DLS results revealed that the average aggregate size obtained in the organic phase decreased with increase of the absorbed dose for all irradiated systems due to the decrease in the concentration of TEHDGA. However, the decrease in the average size and their distribution was dependent on the nature of the solution. The presence of *n*-DD along with TEHDGA during irradiation enhanced the degradation of TEHDGA, due to sensitization effect. In such cases the aggregate size was lowered to a significant extent. Irradaition of the organic phase with extracted nitric acid produced nitration products and other polar radiolytic degradation products in organic phase. The presence such products minimized the aggregation and prevented the third phase formation to a significant extent.

### 3.6. Chapter 6: The role of pKa on single-cycle separations

This chapter desribes the role of organo phosphorous acidic extractants (HA) on the extraction, third phase formation and single cycle separation of Am(III) from Eu(III) present in the nitric acid solution. The speciation of the ligands with metal ions in the organic phase was also probed by different spectroscopic techniques. The results obtained from these studies were reported in three parts.

Part I of this chapter deals with the single-cycle separation of Am(III) using a binary solution composed of *N,N,N',N'*-tetra(2-ethyl hexyl) diglycolamide and various acidic extractants (HA). The acidic extrctants employed were HDEHP, PC88A and CYANEX-272 and whose pKa values were 3.24, 4.51, 6.37 respectively. The distribution ratio of Am(III) was measured as a function of various parameters. The slope analysis of the extraction data showed the synergic participation of both TEHDGA and HDEHP in the extraction of Am(III) at all acidities. However, antagonistic effect was observed at lower acidity when TEHDGA was mixed with PC88A or CYANEX-272 present in *n*-DD. Above 1 M nitric acid, the synergic extraction of Am(III) was observed in all systems. The distribution ratio of various metal ions present in simulated waste was measured in a solution composed of 0.1 M TEHDGA- 0.25 M HA/*n*-DD. The stripping studies showed that about 90% of Am(III) and 10 % Eu (III) was back extracted from the loaded organic phase using 0.05 M DTPA + 0.5 M CA at pH 3.

Part II discusses the extraction behavior of Eu(III) from nitric acid medium in the binary solution of TEHDGA+HA in *n*-DD. The interaction of Eu(III) with TEHDGA and HA at various acidities was studied by ATR-FTIR spectroscopy. The changes in the characteristic transmittance bands of extractants were monitored in the organic phase, which was obtained after the extraction of Eu(III) from nitric acid. The results were correlated to the distribution ratio of Eu(III) as well as to the pKa value of the acidic extractant. The FTIR studies revealed the partial participation of HDEHP, PC88A and CYANEX-272 in the extraction of Eu(III) at higher nitric acid (> 1M ) concentrations, which in turn led to the synergic extraction of Eu(III) in the binary solvent system. Whereas at lower nitric acid (< 0.1 M), the antagonistic behavior was observed in case of the acidic extractants having higher pKa (PC88A, CYANEX-272). This behavior was also confirmed well by the FTIR spectroscopic results, where in the intensity of amidic carbonyl bands in shifted position (after extraction) decreased in the order of HDEHP> PC88A> CYANEX-272.

Part III describes aggregation behavior of the organic phase composed of 0.2 M TEHDGA+0.25 M HA in *n*-DD and extracted nitric acid and Nd(III) ion. The results revealed that the extraction of nitric acid into the organic phase decreased with decrease in the pKa of acidic extractant. As a result, the aggregate size distribution and tendency of organic phase splitting also decreased in the same order. The addition of HA to TEHDGA favored synergic extraction of Nd(III) and the synergism increased in the order of TEHDGA < (TEHDGA+CYNEX-272) < (TEHDGA+PC88A) < (TEHDGA+HDEHP). However, the average aggregate size obtained from dynamic light scattering studies increased in the reverse order of (TEHDGA+HDEHP) < (TEHDGA+PC88A) < (TEHDGA+CYNEX-272) < TEHDGA. The studies thus showed that the acidic extractant with lower pKa minimized the average size of aggregates produced in the binary solution and shifted the third phase formation limits to higher nitric acid and Nd(III) concentrations.

### 3.7. Chapter 7: Single-cycle separation using hydoxyacetamide-acidic extractant system

This chapter deals with single-cycle separation of Am(III) from Eu(III) using a combined solvent system containing *N,N*-dioctyl-2-hydroxyacetamide as neutral extractant and HDEHP or HDEHDGA as acidic extractant. The results on the aggregation behavior of the binary solution containing extracted nitric acid and trivalent metal ion were reported. This chapter was divided into three parts.

Part I deals with the extraction behavior of Am(III) and Eu(III) from nitric acid solution into the binary solution composed of 0.2 M DOHyA+0.25 M HDEHP in *n*-DD and the results were compared with those observed in the individual solvent system. The extraction studies were performed as a function of various parameters. The results revealed that the synergic extraction of Am(III) and Eu(III) in DOHyA-HDEHP was observed at all nitric acid concentrations. The extraction mechanism was confirmed by the slope analysis of the extraction data and ATR-FTIR spectroscopy. The extraction behavior of Am(III), lanthanides and other metal ions present in the simulated waste was also reported. A separation factor (SF) of Eu(III) over Am(III) of about 10 was achieved.

Part II discusses the results on the extraction of behaviour of Am(III) and Eu(III) in a completely incinerable binary solution composed of 0.2 M DOHyA + 0.1 M HDEHDGA in *n*-DD. The results showed the synergic extraction of Am(III) and Eu(III) observed at nitric acid concentrations above 0.5 M and antagonistic extraction observed at lower acidities. The mechanism of Eu(III) and Am(III) extraction in the binary solution was determined by the slope analysis of the extraction data at various acidities. The results revealed the possibility of single-cycle separation of Am(III) from Eu(III) with a separation factor ~13.

Part III of this chapter deals with the aggregation behavior of the organic phase containing 0.2 M DOHyA+0.1 M HDEHDGA/*n*-DD. The results revealed that the extraction of nitric acid and Nd(III) ion in the binary solution increased with increase in the initial concentration of nitric acid and Nd(III) in aqueous phase. DLS studies showed that the average size of aggregates formed in organic phase upon nitric acid extraction increased in the order DOHyA < DOHyA + HDEHGA << HDEHDGA, and the tendency of third phase formation also increased in the same order. Studies with simulated nuclear waste revealed that the binary solution did not undergo organic phase splitting as the aggregate size formed in organic phase was much lower than the limiting aggregate size.

### 3.8. Chapter 8: Conclusions and future directions

This chapter summarizes the conclusions of the present investigations and scope of the future work.

**Publications in Refereed Journal:**

a. Published

1. **K. Rama Swami**, R. Kumaresan, K. A. Venkatesan, and M. P. Antony. "Synergic extraction of Am (III) and Eu (III) in *N,N*-dioctyl-2-hydroxyacetamide-bis (2-ethylhexyl) phosphoric acid solvent system." Journal of Molecular Liquids, 232 (2017) 507-515.
2. **K. Rama Swami**, R. Kumaresan, P. K. Nayak, K. A. Venkatesan, and M. P. Antony. "Extraction of Eu (III) in diglycolamide- organophosphorous acid and the interaction of binary solution with Eu (III) studied by FTIR spectroscopy." Vibrational Spectroscopy, 93 (2017) 1-11.
3. **K. Rama Swami**, R. Kumaresan, P. K. Nayak, K. A. Venkatesan, and M. P. Antony. "Effect of pKa on the extraction behavior of Am (III) in organo phosphorus acid and diglycolamide solvent system." Radiochimica Acta, 106 (2018) 107-118.

4. **K. Rama Swami**, A.S. Suneesh, R. Kumaresan, K. A. Venkatesan, and M. P. Antony. "Dynamic Light Scattering and FTIR Spectroscopic Investigations on the Reverse Micelles Produced During the Extraction of Nd(III) and nitric Acid in Tetra Ethylhexyl Diglycolamide." ChemistrySelect, 2 (2017) 11177-11186.
5. **K. Rama Swami**, R. Kumaresan, K. A. Venkatesan, and M. P. Antony. "Minimizing the aggregation of diglycolamide reverse micelles in the *n*-dodecane phase with bis-(2-ethylhexyl) phosphoric acid "reactive" phase modifier." New Journal of Chemistry, 42(2018) 8891-8899.
6. **K. Rama Swami,** K. A. Venkatesan, and M. P. Antony. "Aggregation behavior of alkyldiglycolamides in *n*-dodecane medium during the extraction of Nd(III) and nitric acid." Industrial and Engineering Chemistry Research, 57 (2018) 13490-13497.
7. **K. Rama Swami**, T. Prathibha, K. A. Venkatesan and M. P. Antony. "Separation of Am(III) from Eu(III) present in 3 M nitric acid medium using completely incinerable binary extractants." Journal of Molecular Liquids, 279 (2019) 427-433.
8. **K. Rama Swami**, K. A. Venkatesan, and M. P. Antony. "Role of phase modifiers in controlling the third phase formation during the solvent extraction of trivalent actinides." Solvent Extraction and Ion Exchange, 37 (2019) 500-517.
9. **K. Rama Swami**, T. Prathibha and K. A. Venkatesan. "Aggregation and organic phase splitting behavior of a synergic extractant system probed by dynamic light scattering spectroscopy." Journal of Molecular Liquids, 291(2019) 111320.
10. **K. Rama Swami** and K. A. Venkatesan. "Effect of pKa of organophosphorous acidic extractants on the aggregation behavior of diglycolamide in *n*-dodecane." Journal of Radio analytical and nuclear chemistry, 322 (2019) 1055-1064.
11. **K. Rama Swami** and K. A. Venkatesan. "Unraveling the role of phase modifiers in the extraction of Nd(III) from nitric acid medium in tetra-bis(2-

ethylhexyl)diglycolamide in *n*-dodecane containing long chain aliphatic alcohols." Journal of Molecular Liquids, 296 (2019)111741.

12. **K. Rama Swami,** K.A. Venkatesan and B. Robert Selvan, "The studies on the aggregation behaviour of radiolytically degraded tetra(2-ethyhexyl)diglycolamide in *n*-dodecane medium during the extraction of trivalent metal ions ." Journal of Radio analytical and nuclear chemistry, 325 (2020) 283-291.
13. **K. Rama Swami**, K. A. Venkatesan, Pooja Sahu, Sk. Musharaf Ali. "The effect of chain length attached to the diglycolamides and *n*-paraffins on the aggregation behaviour during nitric acid extraction in symmetrical diglycolamides probed by using dynamic light scattering and MD simulations." Journal of Molecular Structure, 1221 (2020) 128795.
14. **K. Rama Swami,** K.A. Venkatesan, B. Robert Selvan, Dattatraya vasant Hase and R. V. Jayaram. "Investigation on the unusual aggregation behavior of TEHDGA upon gamma irradiation." Journal of Molecular Liquids, 319 (2020) 114177.

b. Accepted:

c. Communicated:

15. **K. Rama Swami**, T. Prathibha, A.S. Suneesh, B Robert Selvan, G.G.S Subramanian and K.A. Venkatesan. "Batch optimization studies for the single cycle separation of Am(III) from simulated high level waste using hydroxyacetamide-diglycolamic acid combined extractant system." (Manuscript under correction and not included in thesis).
16. **K. Rama Swami**, K. A. Venkatesan. "The studies on the aggregation behaviour of tetra-ethyl hexyl diglycolamide in various polar diluents during the extraction of nitric acid and trivalent metal ions" (Manuscript under preparation and not included in thesis).

**Other Publications**

17. T. Prathibha, **K. Rama Swami**, S. Sriram and K.A. Venkatesan. "Interference of Zr(IV) during the extraction of trivalent Nd(III) from the aqueous waste generated from metallic fuel reprocessing". Radiochimica Acta, 108 (2020) 543–554.
18. Parvathy Narayanan, **K. Rama Swami**, T. Prathibha and K. A. Venkatesan. "Antagonism in the aggregation behaviour of *N,N,N',N'*-tetraoctyldiglycolamide upon adding the reactive organic phase modifier N,N-dioctylhydroxyacetamide". Journal of Molecular Liquids, 317 (2020) 113940.
19. Parvathy Narayanan, **K. Rama Swami**, T. Prathibha, K. A. Venkatesan. "FTIR Spectroscopic Investigations on the Aggregation Behaviour of *N,N,N',N'*-tetraoctyldiglycolmide and *N,N*-dioctylhydroxyacetamide in *n*-Dodecane during the Extraction of Nd(III) from Nitric Acid Medium". Journal of Molecular Liquids, 314 (2020) 113685.
20. T. Prathibha, **K. Rama Swami**, A.S. Suneesh, B. Robert Selvan, S. Sriram, K.A. Venkatesan. "Extraction and aggregation of Zr(IV) in diglycolamide extractants during the treatment of high-level liquid waste solutions from metallic fuel reprocessing", Radiochimica Acta (Under Review).
21. Parvathy Narayanan, **K. Rama Swami**, T. Prathibha, K. A. Venaktesan. "The extraction and Aggregation behaviour of trivalent metal ions in *N,N,N',N'*-tetraoctyldiglcolmide in *n*-dodecane medium in the presence of *N,N,N',N'*-tetradodecyldiglcolmide (Manuscript under preparation)

d. Book/Book Chapter : Nil

e. Conference/Symposium

1. **K. Rama Swami**, R. Kumaresan, P. K. Nayak, K. A. Venkatesan, and M. P. Antony. "Effect of p$K_a$ on the extraction behavior of Am (III) in organophosphorous acid and

diglycolamide solvent system." In Proceedings of the thirteenth DAE-BRNS nuclear and radiochemistry symposium. 2017.

2. R. Kumaresan, **K. Rama Swami**, A.S.Suneesh, K.A. Venkatesan, M.P Antony. "Investigations on the reverse micelles produced during the extraction of Nd(III) and nitric acid in tetra-bis(2-ethylhexyl) diglycolamide using ATR-FTIR and photon correlation spectroscopy." International Conference on Molecular Spectroscopy, 6-8 Dec 2017, Kottayam.
3. **K. Rama Swami,** R. Kumaresan, K.A. Venkatesan, M.P Antony. "Synergistic extraction behaviour of Am(III) and Eu(III) from nitric acid medium by using DOHyA-HDEHP system." In Proceedings of the Eighth DAE-BRNS biennial symposium on emerging trends in separation science and technology 2018, BITS-Goa, Goa.
4. **K. Rama Swami**, A.S.Suneesh, R. Kumaresan, K.A. Venkatesan, M.P Antony. "Investigations on third phase formation in diglycolamide system by using dynamic Light Scattering and FTIR Spectroscopy." In Proceedings of the Eighth DAE-BRNS biennial symposium on emerging trends in separation science and technology 2018, BITS-Goa, Goa.

K. RamaSwamy
Signature of Student:

Date: 11.12.2020

**Doctoral Committee**:

| S. No. | Name | Designation | Signature | Date |
|---|---|---|---|---|
| 1. | Prof. N. Sivaraman | Chairman | N. Sivaraman | 11.12.2020 |
| 2. | Prof. K. A. Venkatesan | Guide/ Convener | K.A. Venkatesan | 11/12/20 |
| 3. | Prof. V. Jayaraman | Co-guide (if any) | V. Jayaraman | 11/12/20. |
| 4. | Prof. S. Jeyakumar (BARC) | Member | HBNI-BARC | 11/12/2020 |
| 5. | Prof. A. Suresh | Member |  | 11/12/2020 |
| 6. | Prof. R.V. Subba Rao | Member | RVRao | 11/12/2020 |
| 7. | Prof. K. Ananthasivan | Member |  | 11/12/20 |

Brahmananda Rao

**Dean-Academic, CI**

15/12/2020

C.V.S. BRAHMANANDA RAO
Dean-Academic
Chemical Sciences
HBNI-IGCAR
Kalpakkam-603102.

**Dean, HBNI**

## References

1. http://www.world-nuclear.org/info/Current-and-Future-Generation/World-Energy-Needs-and-Nuclear-Power/
2. H.A.C. Mckay, J.H. Miles, J.L. Swanson, The PUREX Process. In: W.W. Schulz, J.D. Navratil, K.P. Bender (eds) Science and technology of tributyl phosphate vol III, CRC Press, Boca Raton Florida. (1990).
3. K. Raj, K.K. Prasad, N.K. Bansal, Radioactive waste management practices in India. Nuclear Engineering and Design, 236 (2006) 914-930.
4. J.C. Veliscek, Separation of actinides from spent nuclear fuel: A review, J. Hazard. Mater. 318 (2016) 266-281.
5. S.A. Ansari, P.N. Pathak, P.K. Mohapatra, V.K. Manchanda, Aqueous partitioning of minor actinides by different processes, Sep & Purif.Rev.40 (2011) 43-76.
6. J. N. Mathur, M. S. Murali, K. L. Nash. Actinide partitioning-a review, Solvent Extr. Ion Exch. 19 (2001) 357-390.
7. S.A. Ansari, P.N. Pathak, P.K. Mohapatra, V.K. Manchanda, Chemistry of diglycolamides: Promising extractants for actinide partitioning, Chem.Rev.112 (2012) 1751-1772.
8. A. Bhattacharyya, P.K. Mohapatra, Separation of trivalent actinides and lanthanides using various 'N','S'and mixed 'N, O'donor ligands: a review, Radiochim. Acta. 107(2019) 931-949.
9. G. J. Lumetta, A.V. Gelis, F. Vandegrift. Solvent systems combining neutral and acidic extractants for separating trivalent lanthanides from the transuranic elements, Solvent Extr. Ion Exch. 28 (2010) 287-312.

10. P.R. Vasudeva Rao, Z. Kolarik, A review of third phase formation in extraction of actinides by neutral organophosphorus extractants, Solvent Extr. Ion Exch. 14 (1996) 955-993.

11. T. Yaita, A. W. Herlinger, P. Thiyagarajan M.P. Jensen, Influence of extractant aggregation on the extraction of trivalent f-element cations by a tetraalkyldiglycolamide, Solvent Extr. Ion Exch. 22 (2004) 553-571.

12. L. Berthon, L. Martinet, F. Testard, C. Madic, T. Zemb, Solvent penetration and sterical stabilization of reverse aggregates based on the DIAMEX process extracting molecules: Consequences for the third phase formation, Solvent Extr. Ion Exch. 2007, 25 (2007) 545-576.

**Abbreviations**

| | |
|---|---|
| An(III) | Trivalent Actinides |
| ATR | Attenuated Total internal Reflectance |
| CA | Citric Acid |
| CAC | Critical Aqueous Concentration |
| CyDTA | Trans-1,2-Cyclohexanediamine-*N,N,N',N'*-tetraacetic acid |
| CyMe4-BTBP | 2,6-bis-(5,5,8,8-tetramethyl-5,6,7,8-tetrahydro-benzo [1,2,4]triazy-3-yl)-[2,2']bipyridine |
| CYANEX-272 | Bis(2,4,4-trimethylpentyl)phosphinic acid |
| DGAs | Diglycolamides |
| DHOA | *N,N* –diHexyl OctanAmide |
| DLS | Dynamic Light Scattering |
| DOHyA | *N,N*-2-hydroxy acetamide |
| DTPA | Diethylenetriamine pentaacetic acid |
| FPs | Fission Products |
| FR | Fast Reactor |
| FTIR | Fourier Transform Infra Red |
| HA | Acidic extractants |
| HDEHDGA | *N,N*-di-2-ethylhexyl diglycolamic acid |
| HDEHP | Di(2-ethylhexyl) Phosphoric Acid |
| HLLW | High Level Liquid Waste |
| Ln(III) | Trivalent Lanthanides |
| LAS | Limiting Aggregate Size |
| LOC | Limiting Organic Concentration |
| MAs | Minor Actinides |

| | |
|---|---|
| MD | Molecular Dynamics |
| *n*-DD | *n*-Dodecane |
| PC88A | Bis(2-ethylhexyl)phosphonic acid |
| PUREX | Plutonium Uranium Recovery by Extraction process |
| SHLLW | Simulated High Level Liquid Waste |
| TBP | Tri-*n*-Butyl Phosphate |
| TEHDGA | *N,N,N',N'*-tetra-2-ethylhexyl diglycolamide |
| TODGA | *N,N,N',N'*-tetra-octyl-3-oxapentane-1,5-diamide or<br>*N,N,N',N'*-tetra-octyl diglycolamide |
| TPH | Hydrogenated tetrapropylene |
| SANEX | Selective ActiNide Extraction |
| SF | Separation Factor |

**Name of the Student:** K. Rama Swami

**Name of the CI/OCC:** HBNI-IGCAR Kalpakkam **Enrolment No.:** CHEM02201504004

**Thesis Title:** Solvent extraction of some trivalent lanthanides and actinides in alkyldiglycolamides and the aggregation and spectroscopic investigations on the extracted phase

**Discipline:** Chemical Sciences **Sub-Area of Discipline:** Separation Science

**Date of viva voce:** 27-04-2021

---

## Highlights

Solvent extraction of trivalent actinides (An(III) = Am(III) and Cm(III)) from high-level liquid waste (HLLW) followed by transmutation of them into stable or short-lived products in accelerated driven systems or fast-reactors is a viable option for safe management of HLLW. Among the various ligands, diglycolamides (DGAs) are regarded as promising compounds for the separation of trivalent actinides from the nitric acid solution. However, one of the major drawbacks associated with the solvent phase composed of diglycolamide ligand present in the diluent, n-dodecane, is the undesirable third phase formation, that is the splitting of solvent phase into two phases namely the “diluent rich phase” and “metal-solvate rich phase (third phase)” during the course of solvent extraction from HLLW.

In the present study, the role of alkyl chain length attached either to DGA or n-paraffin in determining the tendency of aggregation leading to third phase formation was studied by using dynamic light scattering, ATR-FTIR and MD simulation studies. The role of phase modifiers such as TBP, DHOA, long chain alcohols, HDEHP, PC88A, CYANEX-272 in controlling the third phase formation in tetra(2-ethylhexyl) diglycolamide in *n*-dodecane system was investigated during the solvent extraction of Nd(III) from nitric acid. The radiolytic degradation products affecting the aggregation behavior of TEHDGA in *n*-dodecane phase was explored by subjecting the irradiated solvent to dynamic light scattering studies. Towards the development of single-cycle separation of minor actinides from HLLW, various neutral and acidic ligands were employed for the extraction of Am(III) and Eu(IIII) from nitric acid solutions. The neutral ligands explored were TEHDGA or DOHyA in combination with acidic ligands such as HDEHP or PC88A or CYANEX-272 or HDEHDGA. The mechanistic aspects of extraction and conditions needed for efficient separation of Am(III) from Eu(III) was identified.

The results revealed that the average aggregate size has been brought down by increasing the alkyl chain length of DGA and addition of significant quantity of phase modifiers to the solvent phase by increasing the dispersion of aggregates or decreasing the protontation of ligand in the organic phase. The formation of polar degradation products upon gamma irradiation led to decrease the aggregate size and shifts the third phase formation to higher limits. The single-cycle studies results showed that the combined solvent system containing lower pKa acidic extractant system is suitable for selective separation of trivalent actinides from HLLW.